

George WYPYCH

HANDBOOK *of*
MATERIAL
WEATHERING

2nd Edition

ChemTec Publishing

Copyright © 1995 by ChemTec Publishing
ISBN 1-895198-12-7

All rights reserved. No part of this publication may be reproduced, stored or transmitted in any form or by any means without written permission of copyright owner. No responsibility is assumed by the Author and the Publisher for any injury or/and damage to persons or properties as a matter of products liability, negligence, use, or operation of any methods, product ideas, or instructions published or suggested in this book.

Printed in Canada

ChemTec Publishing
38 Earswick Drive
Toronto-Scarborough
Ontario M1E 1C6
Canada

Canadian Cataloguing in Publication Data

Wypych, George
Handbook of material weathering

2nd ed.

First ed. published 1990 under title: Weathering handbook
Includes bibliographical references and index.
ISBN 1-895198-12-7

1. Materials--Deterioration. 2. Environmental testing.
3. Accelerated life testing. 4. Polymers--Testing. 5. Polymers--
Effect of radiation on. I. Title. II. Title: Weathering handbook.

TA418.74.W96 1995

620.1'122

C95-900814-4

PREFACE

For centuries, the durability of products has been controlled by the properties of naturally occurring materials. The human skills to process them, experience gained over long periods of observation, and local availability were the major factors in the selection of a material. Rapid development of polymer synthesis in this century produced a great variety of new materials which were attractive for producers of finished goods. These materials offered repeatable quality, ease of processing, and cost effectiveness. The first trials of these new materials did not include much durability testing because, even if the natural products had not been very durable, there were many ways available to improve or protect them.

It was soon discovered that the new materials were substantially different and, although they had excellent initial properties, they usually suffered from limited durability. This has triggered an interest in the prediction of a material's lifetime.

Each new branch of applied science suffers from the same problem of choice in its infancy stage. This choice is always between the art and the science. The "art" approach is always attractive because it makes room for immediate activity but seldom offers permanent solutions. The "scientific" approach is slow but fundamental and only on such a proper foundation can a durable structure be built.

After several decades of fascination with new possibilities and randomly discovered good solutions, it becomes clear that the scientific approach is required. Materials should not only be durable but also recyclable and these, sometimes conflicting, requirements produce an equation which cannot be solved by simple mathematics.

With this background, it appeared that this book could contribute only through arranging the existing information in some orderly fashion. It is always easier to improve something if some milestones are properly selected and their position is known. On the other hand, it is equivalently important to indicate the essential skills required to solve the problem and this must be done by dividing the multidisciplinary field to its component subjects. Finally, it seemed, at the time of writing, that a good inventory of knowledge and methods would also help in the iterative improvement of the current information by those who are willing to read this book and develop the field further.

This has been the approach of the author. In addition, the precision of studies and their speed were also important considerations. Were the approaches correct? Was their execution successful? It will always be difficult to know the answer because many aspects in science are a matter of opinion, and the unsurpassed advantage of science is the variety of these opinions. Their challenge is what makes science prevail.

In selecting topics, every effort was made to emphasize the practical aspects of current efforts to produce materials according to agreed expectations. This is why there are several chapters designed to help the study of currently produced materials in a re-

sult-oriented fashion. Where these two streams meet is the place in which this book wants to be - to bring both sides (practice and theory) together.

The author of a book can only deliver information which is already available. Therefore, I would like to thank the authors of published information for their valuable input based on which this book was built. Most authors are cited in the book. Also, I would like to thank many people in Atlas Electric Devices Company who gave me encouragement, data, and information used throughout the book. Some (but not all) are Randy Bohman, Margaret MacBeth, and Rudolph Leber who were kind enough to help me in finding required information and who also offered their knowledge and assistance in development of some new methods of testing.

My two friends: Dr. Robert Fox and John Paterson devoted substantial amount of time to read this book on various stages and offered invaluable suggestions which immensely improved the content.

George Wypych
Toronto
September, 1995

TABLE OF CONTENTS

Chapter 1

PHOTOPHYSICS - ENERGY ABSORPTION, DISSIPATION, AND CONVERSION	1
1.1 Absorption of Radiation by Materials	1
1.1.1 Radiative Energy	1
1.1.2 Radiation Intensity	3
1.1.3 Radiation Incidence	4
1.2 Absorption of Radiation	6
1.2.1 General Principles	6
1.2.2 General Model of Molecular Excitation	10
1.3 Radiative Processes	12
1.4 Non-radiative Conversions	22
<i>References</i>	23

Chapter 2

PHOTOCHEMISTRY	25
2.1 General Principles	25
2.2 Primary Photoreactions	26
2.2.1 Cleavage into Free Radicals	26
2.2.2 Abstraction of Hydrogen	28
2.2.3 Photoaddition Reactions	30
2.2.4 Photoisomerism	30
2.2.5 Intramolecular Rearrangement	32
2.2.6 Photodimerization	34
2.2.7 Photoreactions	35
2.3 Secondary Photoreactions	35

Chapter 3

ENVIRONMENTAL CONDITIONS	39
3.1 Solar Radiative Emission	39
3.2 Effect of Orbital Variations on Energy Supply	41
3.3 Scattering of Solar Radiation	42
3.4 Absorption of Solar Radiation	43
3.5 Variations in the Radiative Fluxes	44
3.6 Temperature and Moisture	46
3.7 Atmosphere Composition	47
3.8 Nitrogen Compounds	50
3.9 Oxygen Species	52
3.10 Hydrogen Species	53
3.11 Carbon Oxides	55

3.12	Sulfur-containing Components	56
3.13	Chlorine-containing Components	57
3.14	Particulate Materials	58
	<i>References</i>	59
Chapter 4		
CLIMATIC CONDITIONS		61
Chapter 5		
ARTIFICIAL WEATHERING EQUIPMENT		95
5.1	Light Sources	95
5.2	Filters	103
5.3	Specimen Racks and Holders	104
5.4	Artificial Weathering Equipment	105
	<i>References</i>	107
Chapter 6		
MEASUREMENTS IN ASSESSMENT OF WEATHERING CONDITIONS		121
Chapter 7		
SAMPLE PREPARATION FOR WEATHERING STUDIES		125
	<i>References</i>	139
Chapter 8		
NATURAL WEATHERING CONDITIONS		141
8.1	General Description	141
8.2	Methods of Sample Exposure	149
8.2.1	Exposure Site	149
8.2.2	Exposure Racks	149
8.2.2.1	Standard Rack	150
8.2.2.2	Under Glass Exposure	150
8.2.2.3	Black Box Exposure	150
8.2.2.4	Exposure with Spray	151
8.2.2.5	Dry Exposure	151
8.2.2.6	Sun-Tracking Devices	152
8.2.2.7	Light Concentrating Devices	152
8.3	Standards	152
	<i>References</i>	153

Chapter 9	
TYPICAL WEATHERING CYCLES	155
<i>References</i>	161
Chapter 10	
ARTIFICIAL WEATHERING VERSUS NATURAL EXPOSURE	165
<i>References</i>	179
Chapter 11	
IMPORTANT VARIABLES OF WEATHERING	181
11.1 Stress	181
11.2 Molecular Stress	184
11.3 Molecular Mobility	188
11.4 Diffusion, Free-volume, Permeability, Sorption, Density	191
11.5 Chemical Reactivity	194
11.6 Other Variables in Photodegradation	199
<i>References</i>	200
Chapter 12	
COLOR FADING IN TEXTILE MATERIALS	203
<i>References</i>	214
Chapter 13	
METHODS OF WEATHERED SPECIMEN EVALUATION	217
13.1 Visual Evaluation	218
13.2 Gloss Retention and Surface Roughnes	219
13.3 Surface Morphology and Imaging Techniques	220
13.4 Color Changes	223
13.5 Spectroscopic Methods	225
13.5.1 Visible Spectrophotometry	225
13.5.2 UV Spectrophotometry	226
13.5.3 Infrared Spectrophotometry	228
13.5.4 Nuclear Magnetic Resonance	235
13.5.5 Electron Spin Resonance	236
13.5.6 Chemiluminescence, Fluorescence, and Phosphorescence	239
13.5.7 Reflectance Spectrophotometry	240
13.5.8 Mass Spectrometry	241
13.5.9 Atomic Absorption Spectroscopy	242
13.6 X-ray Analysis	242
13.6.1 WAXS and SAXS	242
13.6.2 X-ray Photoelectron Spectroscopy	243

13.7	Physical Properties of Materials	245
13.7.1	Mass Change	245
13.7.2	Density	246
13.7.3	Contact Angle	247
13.7.4	Diffusion of Gases and Water Transport in Polymers	248
13.7.5	Electrical Properties	249
13.7.6	Other Physical Parameters	249
13.8	Thermal Methods	250
13.9	Rheological Properties of Materials	251
13.10	Mechanical Properties	252
13.10.1	Tensile Strength	252
13.10.2	Elongation	254
13.10.3	Flexural Strength	255
13.10.4	Other Mechanical Properties	255
13.11	Other Methods of Analysis	258
13.11.1	Molecular Weight Analysis	258
13.11.2	Gas and Liquid Chromatography	260
13.11.3	Titrimetry	261
13.11.4	Dehydrochlorination Rate	261
13.11.5	Gel Fraction	261
13.11.6	Oxygen Uptake	262
	<i>References</i>	263

Chapter 14

DATA ON SPECIFIC POLYMERS		275
14.1	Poly(vinyl chloride)	275
14.1.1	Mechanism of Degradation	276
14.1.1.1	Models	276
14.1.1.2	Polymers	276
14.1.2	Effect of Thermal History	280
14.1.3	Characteristic Changes and Properties	281
14.1.4	Data	284
14.2	Poly(vinyl alcohol)	284
14.2.1	Mechanism of Degradation	284
14.2.2	Effect of Thermal History	286
14.2.3	Characteristic Changes and Properties	286
14.2.4	Data	286
14.3	Polystyrenes	288
14.3.1	Mechanism of Degradation	288
14.3.1.1	Models	288
14.3.1.2	Polymers	288
14.3.2	Effect of Thermal History	294
14.3.3	Characteristic Changes and Properties	294

14.3.4	Data	298
14.4	Polyacrylonitrile	299
14.4.1	Mechanism of Degradation	299
14.5	Acrylic Resins	300
14.5.1	Mechanism of Degradation	300
14.5.2	Effect of Thermal History	303
14.5.3	Characteristic Changes and Properties	303
14.5.4	Data	304
14.6	Polyamides	305
14.6.1	Mechanism of Degradation	305
14.6.1.1	Models	305
14.6.1.2	Polymer	306
14.6.2	Effect of Thermal History	310
14.6.3	Characteristic Changes and Properties	310
14.6.4	Data	312
14.7	Polyurethanes	312
14.7.1	Mechanism of Degradation	313
14.7.1.1	Models	313
14.7.1.2	Polymers	313
14.7.2	Effect of Thermal History	318
14.7.3	Characteristic Changes and Properties	319
14.7.4	Data	319
14.8	Epoxy Resins	322
14.8.1	Mechanism of Degradation	322
14.8.2	Effect of Thermal History	326
14.8.3	Characteristic Changes and Properties	326
14.8.4	Data	328
14.9	Polyethylene	328
14.9.1	Mechanism of Degradation	329
14.9.1.1	Models	329
14.9.1.2	Polymers	330
14.9.3	Effect of Thermal History	333
14.9.4	Characteristic Changes and Properties	334
14.9.5	Data	337
14.10	Polypropylene	338
14.10.1	Mechanism of Degradation	338
14.10.1.1	Model	338
14.10.1.2	Polymers	338
14.10.2	Effect of Thermal History	340
14.10.3	Characteristic Changes and Properties	340
14.10.4	Data	340
14.11	Polyoxymethylene	343
14.11.1	Mechanism of Degradation	343
14.11.2	Effect of Thermal History	345

14.11.3	Characteristic Changes and Properties	345
14.12	Poly(phenylene oxide)	346
14.12.1	Mechanism of Degradation	346
14.12.1.1	Models	346
14.12.1.2	Polymer	347
14.12.2	Effect of Thermal History	349
14.12.3	Characteristic Changes and Properties	349
14.12.4	Data	350
14.13	Polycarbonates	351
14.13.1	Mechanism of Degradation	351
14.13.1.1	Models	351
14.13.1.2	Polymers	351
14.13.2	Effect of Thermal History	354
14.13.3	Characteristic Changes and Properties	354
14.13.4	Data	357
14.14	Polyesters	357
14.14.1	Mechanism of Degradation	357
14.14.2	Effect of Thermal History	360
14.14.3	Characteristic Changes and Properties	361
14.14.4	Data	361
14.15	Phenoxy Resins	363
14.15.1	Mechanism of Degradation	363
14.16	Polysulfones and Polysulphides	366
14.16.1	Mechanism of Degradation	367
14.16.2	Effect of Thermal History	368
14.16.3	Characteristic Changes and Properties	368
14.16.4	Data	369
14.17	Silicones	371
14.17.1	Mechanism of Degradation	371
14.17.2	Characteristic Changes and Properties	373
14.18	Polyimides	374
14.18.1	Mechanism of Degradation	374
14.18.1.1	Models	374
14.18.1.2	Polymers	375
14.18.2	Characteristic Changes and Properties	375
14.18.3	Data	377
14.19	Polytetrafluoroethylene	377
14.19.1	Mechanism of Degradation	377
14.20	Acrylonitrile Copolymers	378
14.20.1	Mechanism of Degradation	378
14.20.2	Characteristic Changes and Properties	380
14.21	Ethylene-Propylene Copolymers	382
14.21.1	Mechanism of Degradation	382
14.21.2	Characteristic Changes and Properties	383

14.22	Polymer Blends	385
14.23	Rubbers	391
14.23.1	Mechanism of Degradation	391
14.23.2	Effect of Thermal History	394
14.23.3	Characteristic Changes and Properties	394
14.23.4	Data	395
	<i>References</i>	396
 Chapter 15		
	EFFECT OF POLYMER MORPHOLOGY ON PHOTODEGRADATION KINETICS	411
	<i>References</i>	422
 Chapter 16		
	EFFECT OF ADDITIVES ON WEATHERING	425
	<i>References</i>	434
 Chapter 17		
	WEATHERING OF COMPOUNDED PRODUCTS	437
17.1	Coatings	437
17.2	Paints	444
17.3	Textile Materials	447
17.4	Upholstery Fabrics	450
17.5	Museum Textiles	452
17.6	Coated Fabrics	453
17.7	Geosynthetics	454
17.8	Composites	456
17.9	Space Applications	459
17.10	Building Materials	463
17.11	Sealants	468
17.12	Plastic Pipes	471
17.13	Bituminous Products	472
17.14	Cover Plates for Solar Collectors	475
17.15	Automotive Materials	477
17.16	Vinyl Siding	478
17.17	Films, Cables, and Tapes	479
17.18	Wood	480
17.19	Paper	485
17.20	Data from Medical Applications	485
17.21	Weathering Studies of Other Materials	488
	<i>References</i>	490

Chapter 18

STABILIZATION AND STABILIZERS	497
18.1 Limiting the Incoming Radiation	498
18.2 Deactivation of Excited States and Free-radicals	506
18.3 Elimination of Singlet Oxygen, Peroxide Decomposition, Limiting Oxidative Changes	510
18.4 Defect Removal	513
18.5 Stability of UV Stabilizers	514
18.6 Effect of Stabilization	519
<i>References</i>	520

Chapter 19

BIODEGRADATION	523
19.1 Biodegradation Environment	523
19.2. Enzymatic Reactions	524
19.3 Biodegradation of Materials	526
19.4 Biocides	531
19.5 Methods of Testing	532
<i>References</i>	533

International Abbreviations for Polymers	535
---	------------

Index	547
--------------	------------

1

PHOTOPHYSICS - ENERGY ABSORPTION, DISSIPATION, AND CONVERSION

1.1 ABSORPTION OF RADIATION BY MATERIALS

Grotthus-Draper Principle:

Absorption of radiation by any component of the system is the first necessary event for photo-chemical reaction occurrence.

The Grotthus-Draper Principle established the essential relationship between the cause and the result. The following points illustrate various fundamental limitations of the fact that some specimen was found in the pathway of a particular radiation.

1.1.1 RADIATIVE ENERGY

Visible light, infrared, UV, and γ -rays are each a distinct form of electromagnetic radiation. Each propagate in space as waves of electronic and magnetic fields. This is based on the fundamental Maxwell's theory of electromagnetic radiation.

Frequently, it is convenient to use a corpuscular description of electromagnetic radiation, as given below. Electromagnetic waves carry a discrete amount of energy depending on their frequency, as stated by Planck's Law:

$$E = h\nu \quad [1]$$

where	E	energy of radiation
	ν	frequency of radiation
	h	Planck's constant.

The frequency of radiation depends on the conditions in which this radiation was formed. For the sake of convenience, a perfect black body was introduced (and used by

Table 1.1: Physical constants

Constant	Symbol	Value	Unit
Avogadro's number	N	6.022×10^{23}	mol^{-1}
Boltzmann's constant	k	1.38×10^{-23}	J K^{-1}
Gas constant	R	8.31	$\text{J mol}^{-1} \text{K}^{-1}$
Planck's constant	h	6.63×10^{-34}	J s
Speed of light in <i>vacuo</i>	c	2.998×10^8	m s^{-1}

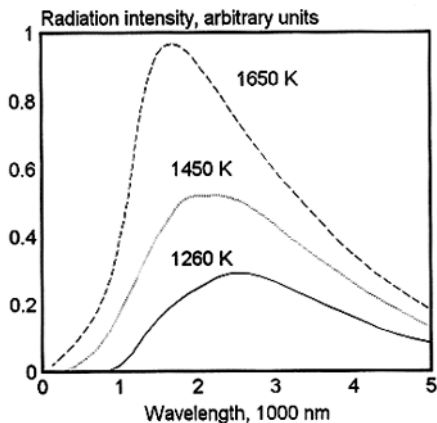


Fig. 1.1. Radiation intensity vs. wavelength for blackbody radiation at varying temperature.

Planck for the development of his law). A black body can absorb and emit radiation at all wavelengths. Such a hypothetical black body has radiation characteristics as shown by Fig. 1.1.

With a temperature increase, the light spectrum is shifted to the left, meaning that more UV and visible light is emitted. Fig. 1.1 illustrates the point that the frequency of radiation depends on the conditions of emission, mainly temperature. Eq 2 can be expressed in a form useful for calculating energy of radiation of known wavelength. The excitation energy per mole can be obtained by multiplying molecular excitation energy by Avogadro's number. Based on a linear relationship between energy and

frequency, one arrives at this equation (see Table 1.1 for values of constants needed for calculations):

$$E = Nh\nu = \frac{Nhc}{\lambda} = \frac{119627}{\lambda} \text{ [kJ/mol]} \quad [2]$$

where
 c velocity of light
 λ wavelength of radiation in nm.

Table 1.2: Energy of radiation

Type	λ , nm	Energy, kJ/mol
Far UV	100	1196
Vacuum UV	200	598
UV	300	399
	350	341
	390	306
Blue-green	500	239
Red	700	171
Near IR	1000	120
IR	5000	24
Hard X-rays, soft γ -rays	0.05	2.4×10^6
Hard γ -rays	0.005	2.4×10^7
Laser	matching λ (see Eq 2)	

Table 1.3: Intensity of radiation

Quantity	Unit
Radiant energy	J
Radiant density	J/m^3
Radiant flux	W
Irradiance	W/m^2

Energy calculated from Eq 2 can be used to evaluate the probability of a photochemical reaction. Table 1.2 gives the energy of radiation for some common energy sources used in photochemical studies and shows the energy level difference between γ -rays irradiation, laser etching, UV degradation by mercury lamp, and UV degradation by sun's rays.

1.1.2 RADIATION INTENSITY

Table 1.2 indicates that the energy of laser light is the same as the energy of visible light or UV (depending on wavelength). But the fact that laser light is substantially more intense is central to the following discussion.

Table 1.3 shows some of the quantities which characterize radiation intensity. Laser radiation can emit radiation in the range of 1 mW (lasers frequently used in optical experiments) to 10 W (moderately powerful argon laser) and more. At the same time, this power is emitted onto a very small surface area (laser light has high coherence, monochromacity and small beam width) such as $10 \mu\text{m}^2$ or 1mm^2 . If one calculates the value of irradiance, it is in the range of 10^7 - 10^8W/m^2 respectively, for given conditions (in fact the surface area is limited by and equal to the wavelength of radiation, and power can be as large as 100 W giving an irradiance of 10^{13}W/m^2). If one compares these values with the mean intensity of sunlight on the Earth's surface, which is in the range of 10^3W/m^2 , it is easy to understand the difference between these two sources of radiation and to explain the differences in the results of their action (surface etching versus minor changes or no changes at all).

The above example illustrates the importance of the conditions under which the experiment is run and reported. We can use the laser example to elaborate further. Laser light delivers 10^{12} to 10^{17} photons/ cm^3 . At this intensity, several photons will react with a

single atom readily causing high levels of excitation. Also, laser light creates very strong electric fields often as much as 100 gigavolts per meter, which inevitably creates conditions for orientation, dipole formation, ionization, etc.

The use of pulsed radiation showed that lasers, with their highly ordered (polarized) beams, can selectively excite the single isomer (in the mixture) which has the right configuration for energy absorption. This means that irradiation by chaotic radiation (e.g., sunrays) will produce totally different results from radiations of different intensities (e.g., lasers).

From Table 1.2, it is also evident that irradiation by high energy radiation, such as γ -rays, will produce different results than irradiation by xenon lamp. The xenon lamp does not have enough energy to propagate through the entire thickness of a material nor can it excite so many atoms at once. The consequence of increasing irradiance in a Weather-O-Meter from 0.35 W/m^2 , typical of UV radiation in daylight, to higher values is difficult to predict because the change in irradiance does not simply increase the number of excited molecules but also causes the random formation of higher excited states. The proportion of both is difficult to predict even though the magnitude of change is lower than that between γ -rays and a xenon lamp.

1.1.3 RADIATION INCIDENCE

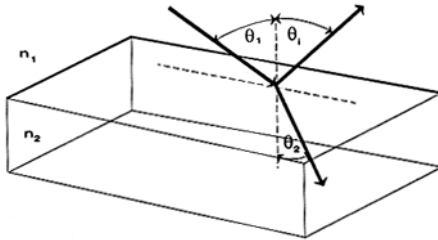


Fig. 1.2. Reflection/refraction of radiation.

$$n_2 \sin \theta_2 = n_1 \sin \theta_1 \quad [3]$$

where n_1 and n_2 refractive indices
 θ_1 and θ_2 the angles illustrated in Fig. 1.2.

Two processes, reflection and scattering, determine the amount of energy which crosses the surface of a specimen exposed to radiation. Each affect the amount of energy transmitted through the material and returned to it because of reflection from backing material or internal reflection.

The geometrical relationship between incident, transmitted, and reflected beams is given by Snell's law:

Table 1.4: Refractive index

Material	n
Air	1.00
Glass	1.50-1.95
Polymers	1.34-1.65
Water	1.34

It should be noted that $\theta_i = -\theta_r$ because the angle of incidence and the angle of reflection are equal. Table 1.4 gives refractive indices for some common materials. From Snell's equation we can calculate that if the incoming beam has an incidence angle of 30° , it has an angle of transmission, θ_t , of 19.5° (if n_1 equals 1 (for air), and n_2 is assumed equal to 1.5). For any other angle of incidence the transmission angle is smaller than the incidence angle if $n_2 > n_1$. If $n_2 < n_1$, there always exists some critical angle of incidence

above which the beam is internally reflected. The first condition ($n_2 > n_1$) exists when the material surface is exposed to radiation through air, because some portion of the beam energy will be transmitted (considering refraction/reflection only). In practice, specimens are frequently exposed through glass or plastic and/or have backup of metal, plastic, glass, or other materials. In such cases, refractive indices must be carefully considered to evaluate the possibility of the internal reflection of covering materials or of the energy retention in the material backing the specimen. It should be noted that the refractive index depends on radiation wavelength (refractive index generally decreases with the increase in wavelength from UV to IR).

It would be helpful to know what proportion of light is reflected from the specimen surface and what proportion is transmitted into the specimen. Unfortunately, such a universal relationship does not exist. Some guidance can be obtained from Rayleigh (particle size \ll than wavelength) and Mie scattering (particle size \approx wavelength), although, these relationships were developed for particles of very small size (totally different from the materials dealt with in degradation studies). According to Rayleigh theory, scattering is proportional to λ^{-4} , meaning that shorter wavelengths are preferentially scattered and longer wavelengths are transmitted.

The character of the surface causes the most difficulty in developing a theory to relate refraction and reflection. With a complex surface, it is very difficult to predict scattering because of the complex geometries involved. Large particles attached to the surface (typical of exposed specimens) make the modelling virtually impossible.

This brings us to scattering which also diminishes the energy which can be transferred to the material. In situations where the energy loss cannot be predicted similar specimens must be analyzed. It is essential that specimens are produced with similar surface structure and angle of exposure. The wavelength of incident radiation must also be the same for each set of samples compared within the range of the experiment. Comparing degradation under varying condition will introduce so many variables that the real changes cannot be distinguished.

1.2 ABSORPTION OF RADIATION

1.2.1 GENERAL PRINCIPLES

The absorption of radiation by materials obeys the principles of the Beer-Lambert Law:

$$\log_{10} I_0/I = \epsilon c l \quad [4]$$

where	I_0	intensity of incident beam
	I	intensity of transmitted beam
	ϵ	molar decadic extinction coefficient
	c	concentration of absorbing species
	l	path length.

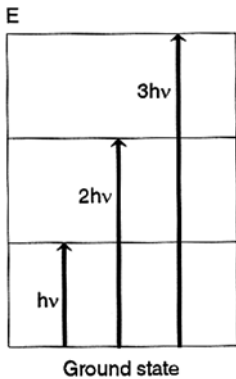


Fig. 1.3. Allowed energy levels of oscillator (nuclei and electrons).

The Beer-Lambert Law implies that both the type and the concentration of the molecules play an important role in the process of radiation absorption. There is no information in this law about the nature of light. Also, the law does not consider the properties of the material nor the angle of incident beam which together determine the actual amount of beam energy used (absorbed and transmitted) within the borders of the material exposed to radiation (see the above discussion).

Planck's Law states that energy can be emitted only in portions called discrete energy levels (Fig. 1.3). Einstein extended Planck's Law to postulate that each photon with an energy of $h\nu$ is transported as corpuscles or quanta of electromagnetic radiation. Further works by de Broglie showed that there is no contradiction between corpuscular and wave forms of energy:

$$\lambda = h/mv \quad [5]$$

where	λ	wavelength of radiation
	h	Planck's constant
	m	particle mass
	v	particle velocity.

With this background, we can now study how the emitting material effects the radiation emitted. Emission spectra of elements have long been known to contain certain spectral lines. The positions of these lines were expressed by mathematical formula based on empirical data:

$$\nu = R_H(1/n^2 - 1/m^2) \quad [6]$$

where	ν	wavelength of spectral line
	R_H	Rydberg's constant
	n	integral constant - 1,2,3,....
	m	integral constant - (n+1),(n+2),....

Thirty years later, Bohr explained these observations when he postulated a model for the hydrogen atom. He stated that, when an electron makes a transition from an initial to a final energy state, the approximate amount of emitted energy is given by the following formula:

$$E_i - E_f = h\nu \quad [7]$$

where	E_i	initial energy state
	E_f	final energy state
	h	Planck's constant
	ν	wavelength emission.

If energy is absorbed by an electron, the same relationship must apply. Two important conclusions are included in Bohr's statement:

- there is no difference between the process of energy absorption and energy emission
- lines are related to the different energy levels at which the electrons are absorbed or emitted

The absorption of energy occurs in a single step therefore final and initial energy levels differ by the energy of photon. The process of adsorption causes a gradual decrease in the electromagnetic radiation intensity and a corresponding increase in absorbed energy by irradiated species. There is also a converse process in which excited molecules return their energy in electromagnetic radiation which increases in intensity. Such a process is called stimulated emission and it is derived from the fact that there is an interaction between existing radiation and energy-rich species which stimulates energy transfer from energy-rich species. In addition to stimulated emission, there also exists a process of spontaneous emission in which excited species may lose their energy in the absence of radiation and reach a lower energy state.

Bohr's theory was later replaced by quantum mechanics, which differs from previous theories in its perception of particle movement control. In the classical theory, the electron trajectory can be followed, whereas in quantum mechanics, Heisenberg's uncertainty principle applies, as given by the formula:

$$\Delta x \Delta p_x = nh \quad [8]$$

where	Δx	uncertainty in position of particle
	Δp_x	uncertainty of momentum of particle
	n	value of quantum state
	h	Planck's constant.

When a particle is in the ground state ($n = 1$), the product of uncertainties in position and in momentum is at a minimum and equals Planck's constant. When separation of particles approaches infinity (uncertainty in position approaches infinity, uncertainty in momentum approaches zero), the particle behavior approaches that of a free particle. In other words, between the ground state and the infinity position there is a place where a particle is no longer part of the system, and to reach this point, the particle must obtain a sufficient amount of energy. This shows the difference between an excited molecule ready to dissociate and an excited molecule which survives radiation without dissociating because the energy absorbed can be safely emitted.

Between the two extreme points there are various energy levels, each corresponding to the transfer of electrons from one electronic level to the other, which should result in an electronic spectrum consisting of one or more sharp peaks. In practice, the peaks are seldom sharp because the molecules are constantly vibrating and rotating and these motions are also quantified:

$$\Delta E = \Delta E_{el} + \Delta E_{osc} + \Delta E_v \quad [9]$$

where	ΔE	total change of molecule energy on photon absorption
	ΔE_{el}	change in electron energy
	ΔE_{osc}	change in oscillation
	ΔE_v	change in vibration.

The molecule, at any given time, is not only in a given electronic state but also in a given vibrational and rotational state. A sample of material contains a large number of molecules which differ in vibrational and rotational states. Thus, not just one wavelength of radiation is absorbed but a number of them in the same vicinity. The most probable transition causes the most intense peak. The amount of energy required for the transition depends on the nature of the two orbitals involved in the bonding, and that is why a simple functional group always causes absorption in the same general area. A group which causes absorption is called a chromophore.

The theory of absorption was further developed based on the Schrödinger equation, quantum mechanics principles, and the assumption that the motion of electrons, due to their mass difference, is much faster than their nuclear motion. Electrons are considered moving in the potential field of static nuclei. Application of the Born-Oppenheimer

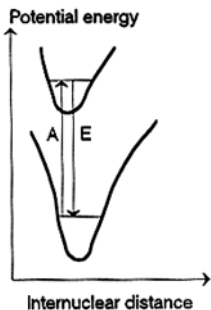


Fig. 1.4. Franck-Condon Principle.

approximation results in factorizing the entire wavefunction into nuclear (vibrational) and electronic wavefunctions. Three terms (treated separately and based on the Born-Oppenheimer approximation) describe absorption. They are: vibrational overlap integral (Franck-Condon principle), spin overlap integral, and electronic transition moment.

The Franck-Condon principle states that an electronic transition, compared with vibration, occurs so rapidly that there is no change in internuclear separation and nuclear kinetic energy. Figure 1.4 illustrates this principle. This implies that the transition might be represented by a vertical line connecting two potential energy levels. The most probable transition involves states having the same internuclear distance.

Spin overlap integral determines allowed transitions. Because singlet to triplet transitions have transition moments equal to zero such transitions are strongly forbidden. Only singlet to singlet and triplet to triplet transitions are allowed.

Electronic transition moment is related to the symmetry of orbitals. From studies on polarization of emission, it is known that polarization frequently occurs along a particular molecular axis.

With these factors selected, the use of the Born-Oppenheimer approximation led to the formation of selection rules based on the fact that if any of the terms of the equation equals zero then the transition moment also equals zero, meaning that the transition has a zero probability. Such a transition is called forbidden transition. The allowed transition is one which has a transition moment different from zero. Although the selection rules were specified above in the discussion of equation terms, let us spell them out in a different form. Vibrational overlap depends on the proportions of energies involved. If a nucleus has very high mass (e.g., in heavy metals) spin-orbit coupling occurs which causes singlets and triplets to have mixed characters. The most important rule governs spin multiplicity (second term). This rule says that spin must not change during transition (absorption or emission). The electronic transition moments can cause forbidden transitions based on symmetry grounds, and this can only happen if all of Cartesian components equal zero. Eq 9 above characterizes these forms of energy.

The type of electronic excitation depends on the type of electrons available in the molecule and the amount of energy which can be supplied by a particular wavelength, as illustrated in Fig. 1.5. From a combination of two adjacent atomic orbitals, two molecular orbitals are produced, one of higher and one of lower energy than the original orbitals. The lower energy orbital is called a bonding orbital where two electrons will typically occupy the bonding orbital in ground-state electronic configuration. The higher

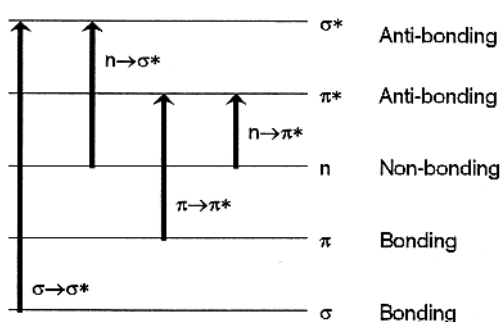


Fig. 1.5. Relative energies of molecular orbitals and transitions between them.

energy orbital is called an antibonding orbital, where one electron in electronically excited molecule occupies orbital. A star symbol is used to indicate an antibonding orbital.

The $\sigma \rightarrow \sigma^*$ excitation demands the highest energy for excitation, only available in the far UV range. This explains the high durability of alkanes to UV radiation. They do not have n and π electrons, and thus $\sigma \rightarrow \sigma^*$ excitation is the only one possible if no sensitizer is present. For $n \rightarrow \pi^*$ excitation, a much lower energy difference is needed; therefore such excitation can be caused by ordinary UV radiation. It is true that the relationship between bonding type and energy needed for excitation is not as simple as pictured by Fig. 1.5 which is further discussed below.

energy difference is needed; therefore such excitation can be caused by ordinary UV radiation. It is true that the relationship between bonding type and energy needed for excitation is not as simple as pictured by Fig. 1.5 which is further discussed below.

1.2.2 GENERAL MODEL OF MOLECULAR EXCITATION

Principle of Degradation

The amount of energy absorbed by a molecule must exceed the bond energy to cause degradation.

Under normal conditions, most organic molecules are in the ground state (S_0). The lowest energy state for these molecules is a singlet state in which electrons with opposing spins are paired in the molecular orbitals.

The frequently-used Jablonski diagram shows the possible outcomes when molecules absorb energy (Fig. 1.6). There are two states called singlet and triplet. Singlet states have opposing electron spins as depicted by arrows in the boxes which illustrate molecular orbitals. Triplet states have parallel spins (Pauli's exclusion principle applies only when electrons occupy the same molecular orbital). Promotion from the ground state (S_0) to any triplet state is forbidden for the reason outlined above (Born-Oppenheimer approximation), and a triplet state can only be initiated from an excited singlet state by the process called intersystem crossing. This is a two stage process of electronic relaxation followed by collisional vibrational relaxation. In the course of these processes, spin inversion is produced.

Depending on the energy absorbed by the molecule, the electrons are promoted from ground state, S_0 , to higher energy state levels S_1 , S_2 , or S_3 . Regardless of the energy

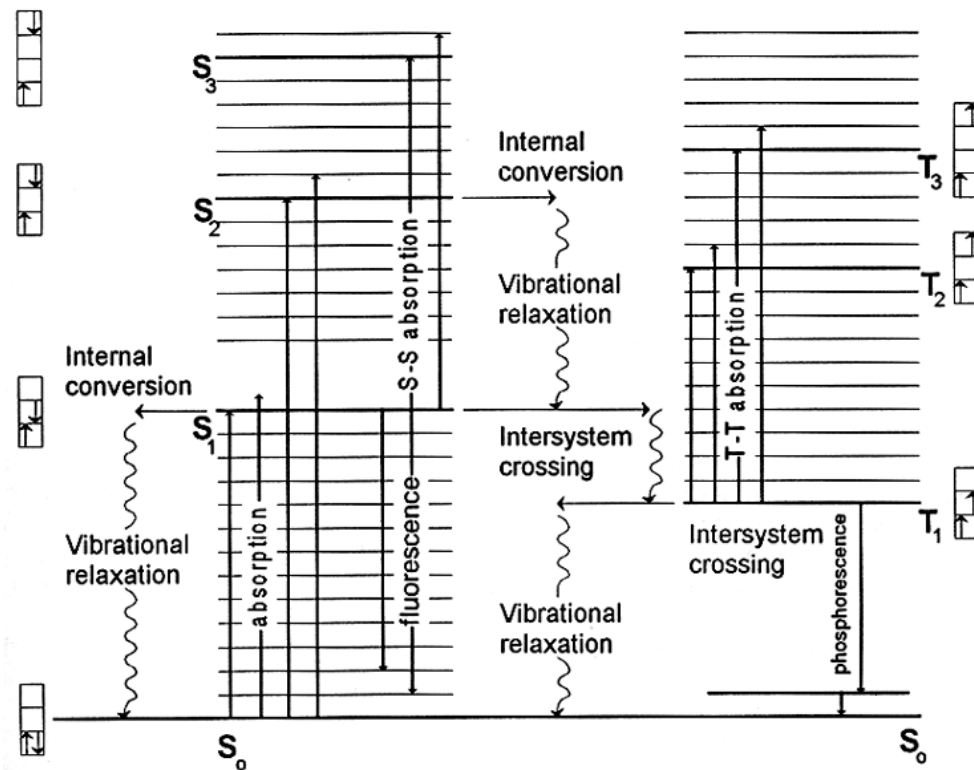
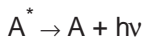


Fig. 1.6. Jablonski's diagram.

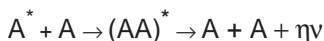
state level, molecular dissociation or isomerization or both are possible, but at higher state levels (S_2 or S_3) molecules are so susceptible to radiationless conversion that fluorescent energy dissipation is very unlikely. Similarly, a triplet state formed from intersystem crossing can still be promoted to higher energy levels on further absorption of radiative energy. Triplet states dissociation or isomerization are possible regardless of the energy state. Internal conversion is another alternative to the non-radiative process of energy dissipation.

1.3 RADIATIVE PROCESSES

Both the act of radiative energy absorption followed by promotion of a molecule to a higher energy singlet state level, S_1 , and a triplet state, T_1 , formed from a singlet in intersystem crossing, may result in emission:

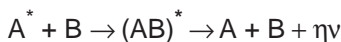


Apart from these simple processes, a polymer may emit radiation from an excimer or an exciplex. Excimer emission occurs when an excited species forms an excited complex with a ground state species of the same kind:



An excimer is a molecular dimer formed from a molecule in its lowest excited state (S_1) and a molecule in its ground state (S_0) or from two lowest excited triplets (T_1). During singlet excimer decomposition, excimer fluorescence occurs which differs from "normal" fluorescence because it lies in a region of longer wavelength, has no vibrational structure and is affected by temperature. Excimers formed from triplet states produce delayed fluorescence on decomposition. The delayed fluorescence is different from "normal" fluorescence because it has a longer decay time, depends on light intensity, and is sensitive to oxygen.

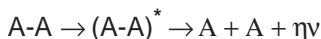
The exciplex emission has a similar origin but results from the complex formed by an excited species and a species in the ground state:



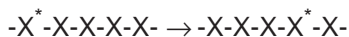
An exciplex, formed from an excited donor with an acceptor in the ground state, produces a fluorescent emission which depends on solvent polarity (fluorescent yield decreases with increasing solvent polarity).

There are other possibilities:

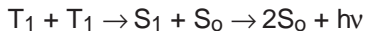
The dimeric excited species can be formed:



Energy can be transferred along the chain by a migrating exciton:



Delayed fluorescence might be formed from triplet states:



Unlike normal fluorescence, the delayed fluorescence is long lived (it lasts from milliseconds to seconds) because it originates from a triplet state.

To simplify further, we may consider all of the above reactions as reactions between an excited molecule (frequently called a sensitizer) and a molecule in the ground state (often called a quencher). The excited state may transfer energy to the ground state (if the quencher has lower energy than the sensitizer) producing the quencher molecule in the excited state at the expense of the sensitizer molecule returning to its ground state. Also, a singlet is produced from a singlet and a triplet from a triplet. These reactions may involve formation of ionized molecules because an electron-rich donor may transfer electrons to an electron-deficient acceptor. In this reaction, a charge separated pair of ions is formed. Depending on charge transfer it can be either hole or electron transfer. Primary processes might be followed by secondary (or chain) processes leading to energy or charge migration or to chemical reaction or to recombination.

Table 1.5: Energies of singlet and triplet states

	Excited state	Singlet, kJ/mol	Triplet, kJ/mol
Acetone	n,π^*	365	325
Benzophenone	n,π^*	320	290
Benzene	π,π^*	460	350

Table 1.6: Lifetimes of singlet and triplet states

	Singlet, s	Triplet, s
Acetone	2×10^{-9}	6×10^{-4}
Benzophenone	5×10^{-12}	6×10^{-3}
Benzene	3×10^{-8}	6.3

Table 1.5 shows energies of singlet and triplet states. Triplet energies are always considerably smaller than singlet energies. Table 1.6 shows lifetimes of singlet and triplet states. Triplet state lifetimes are considerably longer than singlet lifetimes. Recent studies show that singlet and triplet energies can be transferred over a distance as large as 20 Å. The maximum distance depends on orientation, polarity of solvent, and bonding type.

Three mechanisms are believed to operate in energy transfers involving polymer molecules. These are space transfer, bond interaction (through bonds forming main chain), and collisions between sensitizer and quencher (either residing in different segments of the chain or present in two different molecules). The last mechanism (collision) acts frequently in solution where molecules have more freedom to move. Space transfer and bond interaction are more complex. If the emission spectrum of the sensitizer overlaps with quencher absorption, the energy can be transferred by radiative transfer.

Main chain properties play also a role here. If a polymer backbone is conductive, then charge can be transferred if the distance is not large. If the backbone is non-conductive, space energy transfer will prevail. If the polymer can fold in a time shorter than its excited state lifetime then intramolecular collision is a probable mechanism of energy transfer. If polymers have numerous sensitizer groups (energy absorbing side groups), the energy can be transferred by energy exchange between neighboring sensitizers until the final transmission to the quencher occurs. This energy transmission can proceed along the chain but the distance of energy transfer can also be shortened in flexible polymers because of chain bending and the involvement of sensitizers from different segments of the chain.

Energy transfer can involve additives such as solvents, plasticizers, etc. First, it should be understood that chain flexibility influences the photochemical reaction. It should also be understood that chain flexibility can be due either to chain structure or to the molecule's interaction with other components of the mixture which are also exposed to radiation. This illustrates the importance of the interplay between chemical and physical phenomena in the utilization of absorbed energy.

Experience has shown that these energy transfers can be described, using Monte Carlo simulation, as a random walk processes in which the energy migrates without directional control and with no preference for either space transfer or transfer along the chain. Energy transfer depends only on the distance involved and the amount of energy available. The energy transfer mechanism also depends on the density of excited states. If only a few excited states exist, then energy transfer is most likely to occur between a sensitizer and the closest quencher. When there is a high density of excited states, energy migrates through a series of donors. The probability of this mechanism change is important because it indicates that the mechanism of energy utilization depends on the intensity of radiation applied to the sample.

Studies of quenchers and sensitizers of different form, conducted in model systems, make it apparent that energy transfer along the chain is faster (an intramolecular process) than between a sensitizer and a quencher from different molecules. It is especially interesting that this can be demonstrated in solution where the mobility of molecules is enhanced. This evidence seem to indicate that there is a similarity of behavior no matter whether studies are conducted in solid materials or in solution. But the results from both studies are usually a matter of controversy and these data seem to show that the

structure of matter has a prevailing effect on the sequence of events after energy absorption. At the same time, this observation does not change the fact that in solution, rates of changes will differ and the actual locations of energy quenching may also differ because of increased chain flexibility and molecular mobility.

Intersystem crossing is other route of energy conversion. Existing data seem to indicate that it differs from the above described energy conversion mechanism, in the sense that formation of a triplet from an existing singlet occurs more easily between a low molecular weight sensitizer and a quencher in a chain (intermolecular process) than in an intramolecular process. This observation suggests that most polymer degradation occurs in the presence of low molecular weight admixtures, which act as sensitizers because the ease of formation of relatively stable triplet states may contribute to more intense photochemical conversions.

Energy transfer to a terminal location - a quencher - may cause either formation of radicals or of pairs of ions which are precursors of macroscale chemical reactions or degradation processes. Fortunately and importantly most of these species recombine. Recombination efficiency depends on several factors such as pH, solvent, and structure of

involved species. Therefore, the role of chain flexibility is more complex than described by single factor (energy transfer, recombination rate, etc.). All the processes occurring within the material exposed to radiation are in dynamic equilibrium, and the final effect depends not only on the initial structure of the material but also on the modifications introduced into the material during the photolytic process.

Chromophores within the molecule are the main centers of absorption but the rest of the molecule also participates in the process. For example, double bond conjugation causes a dramatic shift in wavelength absorption, as seen from Fig. 1.7.

The effects discussed above and bathochromic and hypsochromic shifts

leave sufficient finger-prints to identify composition. The opposite also holds true - known composition allows one to predict the properties of the product. Table 1.7 shows absorption maxima for some typical chromophores.

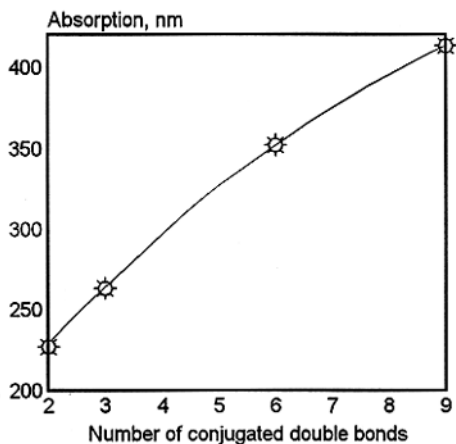
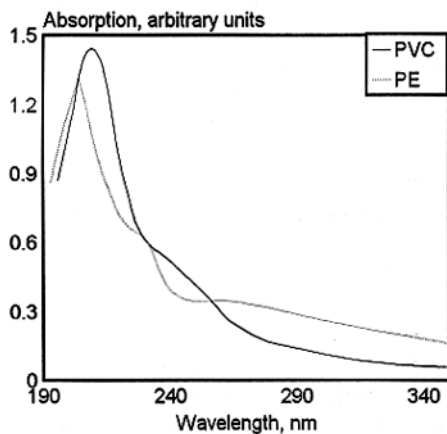


Fig. 1.7. Effect of number of conjugated double bonds, n , on UV absorption.

Table 1.7: Absorption wavelength of chromophores

Chromophore	Molecule	λ_{\max} , nm
Cl	CH ₃ Cl	173
OH	H ₂ O	166
OCH ₃	CH ₃ OH	184
NH ₂	CH ₃ NH ₂	215
C=C	CH ₂ =CH ₂	162
C≡C	CH≡CH	220,182
C≡N	CH ₃ CN	167
C=O	H ₂ C=O	295
N=O	(CH ₃) ₃ CNO	665
Ar	benzene	255
CH	CH ₄	150



[Data from J. F. McKellar and N. S. Allen, *Photochemistry of Man-Made Polymers*. Applied Science Publishers, London, 1979.]

Generally, polymers can be divided into two groups:

- those which absorb radiation through isolated impurities
- polymers which are built from monomers having chromophoric properties.

Fig. 1.8 shows the UV absorption spectra of polymers belonging to the first group. Although, these polymers contain bonds which should not absorb in near ultraviolet light, according to the data included in Table 1.7, Fig. 1.8 shows the existence of absorption throughout the UV range. It is also known that these three polymers are not weather resistant. Small amounts of admixtures found as end-groups or in the middle of the chain contribute to the initial absorption. Fig. 1.9 shows another group of polymers which contain light absorbing chromophores because part of their structure is derived from particular monomers.

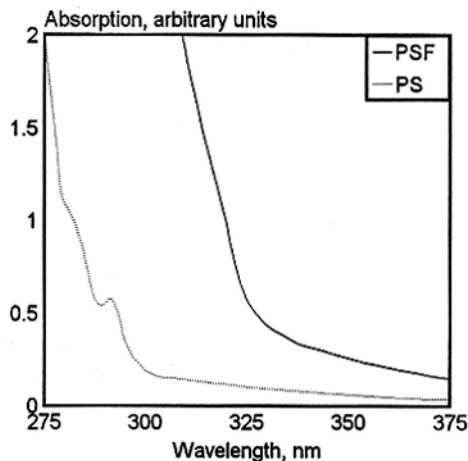


Fig. 1.9. UV absorption spectra of polymer films. [Data from J. F. McKellar and N. S. Allen, *Photochemistry of Man-Made Polymers*. Applied Science Publishers, London, 1979.]

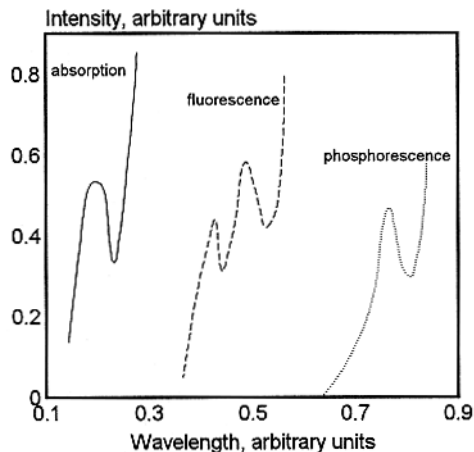


Fig. 1.10. Absorption, fluorescence, and phosphorescence spectra.

The presence of chromophores, such as an the aromatic ring or a carbonyl group, cause intensive absorption in the ultraviolet region. Major light-absorbing groups include the carbonyl group, hydroperoxide group, double bonds, oxygen-polymer charge transfer complexes, metallic impurities, and residual catalysts. It is also evident from the examples discussed above that absorption does not implicate or preclude polymer degradation by UV radiation.

The general relationship between absorption, fluorescence, and phosphorescence is illustrated by Fig. 1.10. Quite frequently, fluorescence, and phosphorescence form mirror-images of the absorption spectrum with a shift to a longer wavelength. One important difference between fluorescence and phosphorescence is that phosphorescence is even more red-shifted than fluorescence. The other important difference is in the time scale. Fluorescence is a short-lived process lasting only 10^{-12} - 10^{-6} seconds. Phosphorescence originates from the forbidden transition $T_1 \rightarrow S_0$ and is therefore long-lived, lasting from 10^{-4} to 100 seconds. Afterglow is a typical feature of phosphorescence, and is frequently observed in highly crystalline polymers which emit energy long after the exciting radiation has been removed.

From the point of view of material durability, the long lifetime of excited species is a negative feature because these molecules have a high probability of participating in collisions which will lead to their degradation. On the other hand, the shorter wavelength

of emission and the higher concentration of energy in fluorescence may initiate further excitation of molecules present in the system. The energy of fluorescent emission can best be quantified using the primary quantum yield:

$$\Psi_F = k_F / (k_F + k_{isc} + k_{ic} + k_D) \quad [10]$$

where	Ψ_F	primary quantum yield
	k_F	rate constant of fluorescence
	k_{isc}	rate constant of intersystem crossing
	k_{ic}	rate constant of internal conversion
	k_D	rate constant of reaction.

Fluorescence quantum yield is seldom equal to one, even when a molecule is isolated in a gaseous state or frozen in a rigid, inert matrix. The quantum yield depends first of all on the excitation type then on the amount of energy involved in such excitation. For example, the transitions $n \rightarrow \sigma^*$ and $\sigma \rightarrow \sigma^*$ are transitions of high energy difference, as seen from Fig. 1.5, and they seldom result in fluorescence which is too slow a process to effectively compete with non-radiative conversions (reactions). The energy dependence can also be explained in a different manner, by the Beer-Lambert Law:

$$A = \epsilon cL \quad [11]$$

where	A	absorbance
	ϵ	molar decadic extinction coefficient
	c	concentration
	L	path length.

Fig. 1.11 gives data which confirm the relationship between the source wavelength and the emission spectrum. Temperature also affects the quantum yield of fluorescence because an increase in the Brownian motion of particles increases the probability of a non-radiative process (reaction) and thus decreases the probability of radiative energy dissipation. In a similar manner, the quantum yield is affected by the concentration, pressure, and viscosity of medium because all of these affect reactivity. The above criteria for fluorescent emission would be incomplete without including the participation of more than one molecule. In polymer systems such a simplistic mechanism is rarely possible because real materials are densely packed and concentrated and most of them are solids. Energy migration in such a system is a common phenomenon, although still not well studied (see discussion above). Despite the fact that theoretical solutions are not final, experience shows that energy migration occurs in such common polymers as polystyrene, polyvinyltoluene, polyvinylcarbazole, etc.

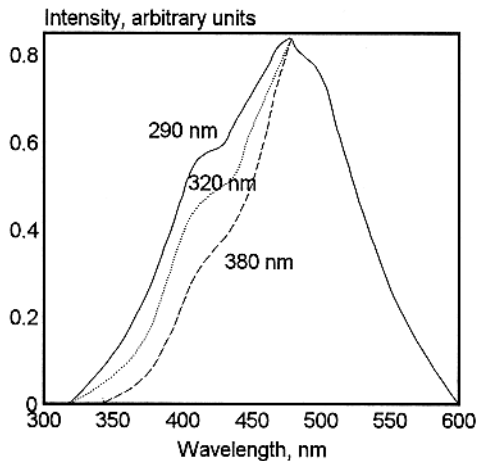


Fig. 1.11. SPA emission spectra at different excitation wavelengths. [Data from J. E. Guillet, C. E. Hoyle, and J. R. McCallum, *Chem. Phys. Lett.*, 54(1978)337.]

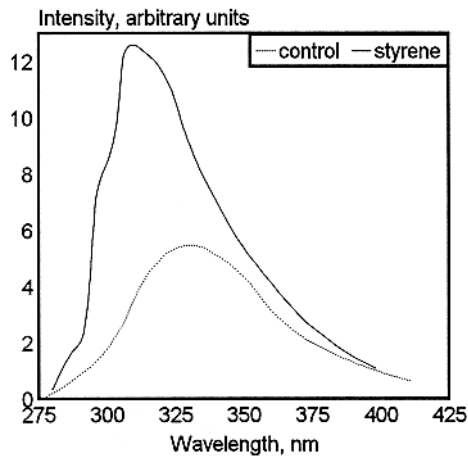


Fig. 1.12. PS fluorescence spectra (control and film containing 1% styrene). [Data from F. Heisel and G. Laustriat, *J. Chim. Phys.*, 66(1969)1895.]

The most simple case occurs when sensitizers and quenchers are too distant from each other for energy migration or excimer formation. The energy can only be transferred by radiative exchange or dipole-dipole interaction.

Polymer formed from neighboring chromophores, which are unable to form excimers but are able to transfer energy on collision, is another theoretical possibility. Iinuma¹ studied polymer containing 1,3,5-triphenyl-2-pyrazoline as a pendant unit which cannot form excimers and confirmed this theory. That energy is also transferred by collisions and that excimers are formed by energy migration is shown by other models. Polyvinyl naphthalene, polyvinyl carbazole, and some copolymers are thought to react due to collisions and excimer formation. The process depends strongly on the concentration of excimer-forming sites and on the concentration of guest molecules.

Another possibility includes energy transfer by collision following excimer migration. This has a very low probability because the excimer sites are not sufficiently numerous to allow migration of excimer energy. Studies on polystyrene reveal that long-range dipole-dipole transfer from the excimer is another credible mechanism (Fig. 1.12). When polystyrene contains free monomer, the emission occurs through the free monomer. If there is no free monomer, excimer emission is observed.

There are two practical reasons to review some of the mechanisms of energy transfer:

- they contribute to our understanding of the quenching effect
- they help us to understand the properties of polymer blends.

Perrin's model is the simplest model of quenching:

$$\Psi_0/\Psi = \exp(VN[A]) \quad [12]$$

where	Ψ_0	luminescence quantum efficiency in the absence of acceptor
	Ψ	luminescence quantum efficiency in the presence of acceptor
	V	volume of quenching sphere
	N	constant= 6.02×10^{20}
	$[A]$	concentration of acceptor.

This model implies that a molecule is activated when an excited molecule is within a specific distance from a quencher. It is obvious from this model that quenching efficiency depends on the concentration of the quencher (acceptor). More elaborate theories connect quenching efficiency with the diffusion rate of the quencher and require a more exact description of Perrin's volume of a quenching sphere. Doped polymer films are convenient models for studies of energy migration. Values of diffusion length derived from studies of doped polymers are still disputable but it seems that a distance of 100 nm is realistic. Compatibility of polymer blends is important for their properties, including weatherability, but it is difficult to study. The measurement of excimer and exciplex fluorescence helps to measure the compatibility of polymers in blends at levels much below those at which phase separation occurs. The phosphorescence follows principles given in the fluorescence discussion, but lifetime difference between singlet and triplet states changes the proportions between the modes of energy utilization. Triplet state formation is a two-stage process and, thus, phosphorescence quantum yield, Ψ_p , is a composite of triplet formation and decay:

$$\Psi_p = \Psi_{isc}\Psi_d \quad [13]$$

where	Ψ_{isc}	quantum yield of intersystem crossing
	Ψ_d	quantum yield of triplet decay

$$\Psi_p = [k_{isc}/(k_F + k_{isc} + k_{ic} + k_D)] \times [k_p/(k_p' + k_{isc}' + k_D')] \quad [14]$$

where	Ψ_p	phosphorescence quantum yield
	k_{isc}	rate constant of intersystem crossing ($S_1 \rightarrow T_1$)
	k_F	rate constant of fluorescence (S_1)
	k_{ic}	rate constant of internal conversion ($S_1 \rightarrow S_0$)
	k_D	rate constant of reaction (S_1)
	k_p'	rate constant of phosphorescence ($T_1 \rightarrow S_0$)
	k_{isc}'	rate constant of intersystem crossing ($T_1 \rightarrow S_1$)
	k_D'	rate constant of reaction (T_1).

The long-lived triplet state can be upgraded to the singlet state by the acquisition of thermal energy, but the energy gap between the singlet and the triplet states is in the order of kT .

The triplet state has an unpaired electron spin which contributes to the long lifetime of the triplet state. Also, many reaction pathways are available for a triplet state because of the unpaired electrons state which are not available in a singlet state. Therefore, the triplet state dominates the photochemistry of many organic molecules. Its radiative processes also have more competition from other processes. The long lifetime of triplet states, related to the high probability of triplet reaction, causes serious problems for those studying phosphorescence. Their results are affected by small amounts of impurities which act as quenchers of excited states.

Phosphorescence is studied more easily in solid samples because collision-induced quenching is eliminated. In solutions, the viscosity of the solvent, the temperature, and other parameters related to molecular collision have substantial effects on phosphorescence quantum yield. Energy transfer from an excited triplet differs essentially from that of a singlet. The probability of an energy transfer falls off exponentially and approaches zero when the distance is greater than 1.5 nm. This is because the mechanism of energy transfer, resembling electron exchange between the pair of molecules, requires intermolecular overlap of molecular orbitals.

The delayed fluorescence, originating from a triplet upgrading to a singlet by thermal energy absorption or from triplet-triplet annihilation, has the same wavelength as normal fluorescence because it begins from the same energy level (S_1) but it is delayed by the time used for $S_1 \rightarrow T_1 \rightarrow S_1$ conversions. This helps us understand why phosphorescence is more red-shifted than fluorescence. It is due to the fact that the triplet state (T_1) has a lower energy level than the singlet state (S_1) and thus the energy gap ($S_1 - S_0 > T_1 - S_0$) is also smaller.

Finally, because of triplet formation and as a result of intersystem crossing, the factors affecting the rate constants of intersystem crossing, k_{isc} and $k_{isc'}$, also affect the concentration of triplet states. It has also been found that in the proximity of a molecule containing an atom of high molecular charge (e.g., a heavy metal), spin-selection rules break down. This results in the enhancement of intersystem crossing rates and diminishes the quantum yields of singlet state processes such as fluorescence at the expense of the formation of more triplet states. Molecular oxygen can induce a similar effect by increasing the values of the following rate constants: k_{isc} , $k_{isc'}$, and k_p . When the rates of non-radiative conversions are increased, the reactivity of molecules in the triplet state increases.

1.4 NON-RADIATIVE CONVERSIONS

Non-radiative conversions are less relevant in this context (photophysics) because they lead mostly to changes in the chemical structure of molecules, and this subject is discussed broadly in later chapters of this book.

Internal conversion is a process of non-radiative energy dissipation which, like radiative conversion, does not lead to chemical conversion. The high energy of the molecule is dissipated by going through series of vibrational states. Vibrations are slow compared with promotions, which is known as the Franck-Condon Principle, and vibrational energy dissipation is also a rather slow process. Depending on the amount of energy absorbed and the distribution of this energy in the molecule, the energy is either safely dissipated by this slow vibrational process or bonds might be broken in an outward surge, recovering from compressed condition.

Large molecules in their higher states (S_n) undergo transition to a S_1 state before luminescing. This transition is radiationless, and it is represented by a horizontal line on Jablonski's diagram, similar to intersystem crossing. Observation that similar conversions occur in low pressure gases seems to indicate that the transition is intramolecular rather than collisional. Internal conversion arises from electrostatic interactions between the electrons and their nuclei unlike intersystem crossing which is related to spin-orbit interaction. Based on the Born-Oppenheimer approximation, two factors determining internal conversion may be selected namely the electronic matrix element

and the vibrational overlap integral (Franck-Condon factor). The electronic matrix element is a function of nuclear kinetic operator which dictates that only states of the same symmetry can convert internally due to vibronic coupling. From the vibrational overlap integral, it can be deduced that the energy gap determines the rate of the process. If the energy gap between states (initial and final) is low, the rate of internal conversion is high (and *vice versa*).

Based on the above discussion on internal conversion and the Principle of Degradation (section 1.2.2), one can easily see that in the process of energy dissipation there is no special reason for any particular conversion to occur. The final result of energy absorption depends on the balance of

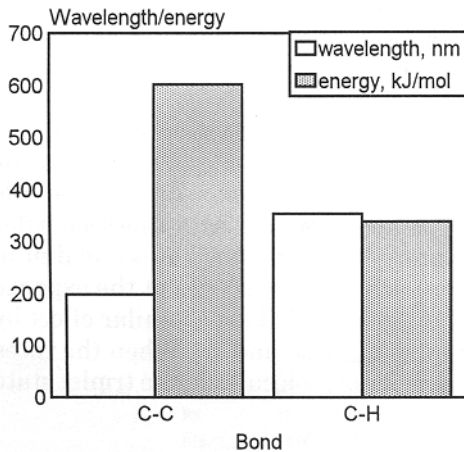


Fig. 1.13. Quantum energy related to bond strength vs. radiation wavelength.

energy available in a particular molecule and the chemical structure of the excited molecule as is documented in Fig. 1.13. When conditions favor chemical conversion, one of the primary photochemical reactions can take place:

- cleavage into free radicals
- abstraction of hydrogen atom
- photosensitization
- decomposition with formation of two or more molecules
- photodimerization or crosslinking
- intramolecular rearrangement
- photoisomerization.

Which reaction type predominates partly depends on the environment. The presence of other molecules in the neighborhood and the state of matter also favor a particular type of conversion. If primary photochemical reactions are followed by secondary reactions, general solutions are not likely to be found; instead, the analysis should include all the conditions relevant to the understanding the ways in which energy is absorbed by materials is utilized.

REFERENCES

1. F. Inuma, H. Mikawa, and R. G. Aviles, *Macromolecules*, 12(1979)1078.
2. F. Heisel and G. Laustriat, *J. Chim. Phys.*, 66(1969)1895.
3. M. A. Fox, W. E. Jones, and D. M. Watkins, *Chem. Eng. News*, 71(1993)11,38.

2

PHOTOCHEMISTRY

2.1 GENERAL PRINCIPLES

An excited molecule may:

- change into a different electronic state (see Chapter 1)
- absorb more energy
- change into a different compound (photochemical reaction)
- transfer energy to another molecule or segment of the excited molecule (sensitizer→quencher)

A discussion of photophysical changes is included in Chapter 1. Absorption of additional energy is governed by principles similar to absorption of the first quantum (there are some exceptions). Two different mechanisms exist in multiphoton excitation. In one, a species may absorb the energy of one photon, and during the lifetime of excitation (10^{-4} to 10^{-9} s) may absorb the energy of a second photon or more photons. Such excitation is called resonant excitation. The other excitation process is called non-resonant excitation; in this process a second photon must arrive almost simultaneously (within the time frame of one cycle of electromagnetic radiation or 10^{-15} s). The intensity of radiation must be very high for any reasonable probability of such sequential acts. When resonant excitation occurs, the molecule in an excited state may change its properties which determine its capability to further absorb radiation of a particular wavelength (its absorption may differ from the wavelength absorbed by the molecule in its original state). In both cases the Beer-Lambert Law does not hold.

Electronically excited species (single or multiphoton) may possess sufficient energy to dissociate. In complex molecules, the optical dissociation usually does not play an essential role because such molecules are populated by a large number of electronic states and vibrational modes which favor radiational transitions between the states. Fig. 2.1 shows the various states of molecules. Horizontal lines show quantized vibrational energy levels. At the minimum potential energy level (minimum on graph) bond distances

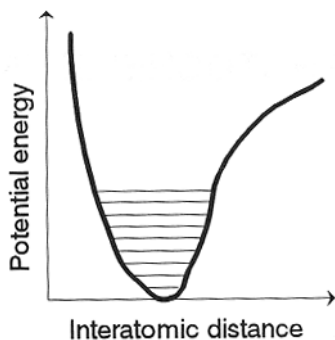


Fig. 2.1. Energy states of molecule.

are normal. Moving towards the left from the minimum (towards y axis) the molecular bond becomes compressed (the bond is under compressive stress), and, moving towards the right from the minimum, the bond becomes extended (the bond is under extension stress). Bonds which are either extended or compressed have an increased probability of undergoing a chemical conversion. This is especially true when the bond is excessively extended (the nuclear distance is large) and the bond is broken.

In the absence of molecular collisions or internal conversion, excited organic molecules will remain in an excited state for a particular time (radiative lifetime) and then dispose of their energy through spontaneous emission. The prevalent reactions are those which lead to configurational changes or those which involve several molecules or groups in one segment of a molecule.

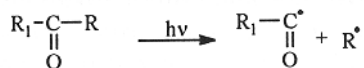
2.2 PRIMARY PHOTOREACTIONS

2.2.1 CLEAVAGE INTO FREE RADICALS

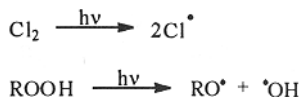
A species containing one or more unpaired electrons is called a free radical. The stability of free radicals varies and includes some very stable species such as the oxides of nitrogen. The stability of radicals can be increased by resonance, hyperconjugation, steric hindrance, etc. Another distinctive feature of free radicals is their paramagnetic property. According to Pauli's Principle, any two electrons occupying the same orbital must have opposite spins in order to maintain a total magnetic moment of zero. Free radicals, however, have one or more unpaired electrons therefore, their net magnetic moment is different from zero. This property is important because it allows us to detect and distinguish free radicals by electron spin resonance, ESR, measurement. Free radicals are the only species giving ESR spectrum which might be used for both quantitative and qualitative studies. UV radiation present in sunrays has enough energy to cause bond cleavage and generate free radicals.

Several mechanisms of bond cleavage are known, but Norrish type cleavages of type I and II are the ones most applicable to macromolecular materials. The $n \rightarrow \pi^*$ singlet-singlet transitions (forbidden) in aldehydes and ketones are responsible for their UV absorption in the 230 to 330 nm region. The absorption band lies near 290 nm for aliphatic aldehydes and near 280 nm for ketones. In aromatic substitution, this band is shifted to longer wavelengths (in benzophenone near 340 nm). This helps to explain the

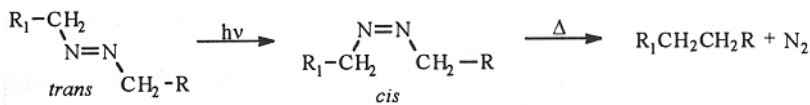
properties of some materials. For example, aliphatic polyurethanes are known to degrade rather rapidly with a simultaneous decrease in carbonyl absorption whereas aromatic polyurethanes exposed to UV radiation, accumulate carbonyl groups but do not degrade (apparently the energy at the shifted wavelength (340 nm) is not sufficient to cause bond cleavage). The cleavage of ketones to two radicals, called Norrish type I cleavage, is explained by the following equation:



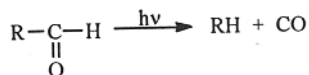
The secondary process of this cleavage yields carbon monoxide and R· radical. Norrish type I reactions occur with aldehydes and ketones as well as carboxylic acids, their esters, and their amides. Several other bonds cleave according to the Norrish type I mechanism:



Aliphatic azo compounds degrade according to the same mechanism, sometimes called photoextrusion:



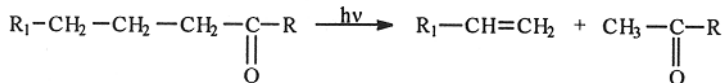
The first step is *trans* to *cis* isomerization, followed by elimination of nitrogen from the compound. The other extrusion reaction involves aldehydes:



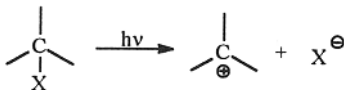
causing carbon monoxide to be lost by the molecule. This reaction applies only to aldehydes. Although the ketone reaction gives the same result, ketones require the formation of two radicals which then can recombine, whereas in the case of aldehydes the first step requires proton migration followed by expulsion of CO. These reactions are temperature dependent. At lower temperatures, less vibrational energy is available, therefore

the efficiency of decarbonylation is greatly reduced. In solution, vibrational energy dissipates rapidly, consequently, decarbonylation is reduced.

The Norrish type II cleavage involves abstraction of γ -hydrogen and bond cleavage:



This mechanism applies to aldehydes and ketones of both singlet and triplet $n \rightarrow \pi^*$ states having γ -hydrogen. Esters, anhydrides and other carbonyl compounds can also follow this path. Aliphatic ketones undergo reactions from both singlet and triplet states, whereas the reactions of aromatic ketones may start from triplet state only. Both Norrish type I and II mechanisms depend on radiation wavelength. As wavelength decreases, most ketones produce an increasing amount of CO. Both Norrish mechanisms involve the homolytic cleavage which results in a radical pair or, if a cyclic compound is involved, a diradical. Heterocyclic cleavage produces an ion pair or a zwitterion:



2.2.2 ABSTRACTION OF HYDROGEN

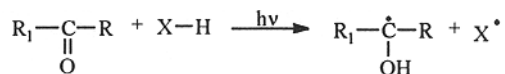
The Norrish type II mechanism occurs in the first stage of the reaction. The intermolecular Norrish type II hydrogen abstraction occurs easily when a cyclic six-membered transition state is not precluded by transition states, whereas three- and four-membered transition states are highly unfavorable.

The hydrogen abstraction can be an intramolecular or an intermolecular processes. Both processes are typical of molecules in the two lowest excited states (n, π^*). Aryl ketones normally react through a triplet state, and such reactions are not stereospecific. Alkyl ketones react via both singlet and triplet states, and only the singlet reaction is stereospecific. In their excited state, ketones act as if they were radicals, and thus they are capable of very effective hydrogen abstraction.

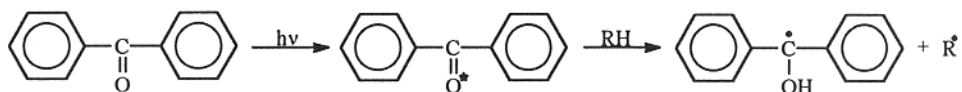
In an intramolecular abstraction route, similar to the Norrish type II mechanism, a biradical is generated which may recombine forming the cyclic compound. This reaction is typical of many photochemical processes which lead to degradation or synthesis of materials. The efficiency of intermolecular abstraction of hydrogen depends on steric hindrance.

Many photochemical reactions occur through an intramolecular route. Here, a good donor of hydrogen must be present (saturated hydrocarbons are not efficient donors be-

cause slightly weaker hydrogen bonding is required in the donor - this exists in compounds which have electron-withdrawing groups in the α -position). The irradiation of ketones in the presence of hydrogen donors, such as amines, alcohols, hydrocarbons, etc., results in hydrogen abstraction:

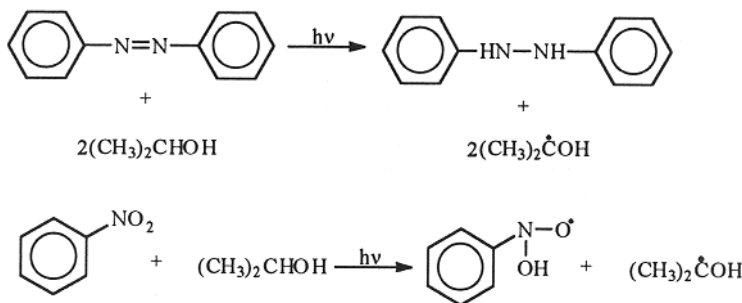


Benzophenone is a well known photosensitizer:

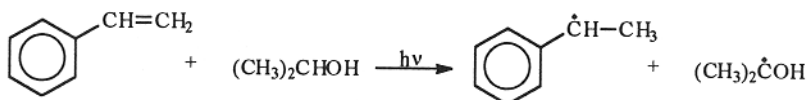


The efficiency of this reaction decreases as temperature increases. Ketyl radicals formed in this process can participate in secondary recombination reactions leading to pinacols (see below under photodimerization).

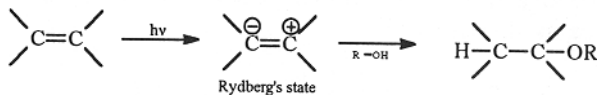
Ketones are not the only compounds able to abstract hydrogen. Other examples include azobenzene and nitrobenzene, both of which can abstract hydrogen from isopropyl alcohol:



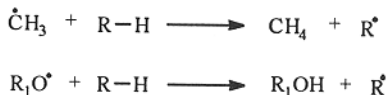
The presence of a double bond in the molecule contributes to hydrogen abstraction:



Alkenes, on photoexcitation, form a 'Rydberg state'. In this state, they are able to abstract hydrogen:



Finally, hydrogen can be easily abstracted by free radicals:



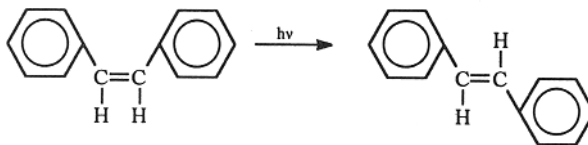
2.2.3 PHOTODDITION REACTIONS

In photoaddition reactions, the Woodward-Hoffmann rule of conservation of orbital symmetry applies. According to this rule, no change of orbital symmetry occurs on transiting from reactants to products. In other words, during the adiabatic transformation of the molecular orbitals of reactants to the molecular orbitals of products, no change in symmetry occurs. Based on this rule, photochemical reactions differ from reactions which are thermally induced. In thermally induced reactions, the conrotatory mode is more energetically favored. But in photochemical reactions the disrotatory mode is more favored. In most cases, this rule is confirmed by experiment. However, some exceptions are known.

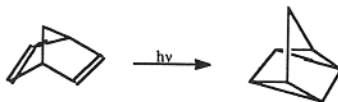
Numerous reactions are typical; some of the most common involve a condensation mechanism forming cyclic compounds, hydroperoxides, dioxetanes, and addition of aldehydes and ketones (some are reported under photodimerization, e.g., Diels-Adler reaction). Some of these routes might be useful in explaining crosslinking and secondary mechanisms of radical degradation.

2.2.4 PHOTOISOMERISM

Two types of photochemical rearrangements cause isomerism: formation of structural isomers and formation of valence-bond isomers. The first group is discussed in the next section, and here we are concerned with formation of isomers without an actual displacement of atoms or groups. The isomers are formed by the movement of electrons and the change in the position of some nuclei. Photochemical changes of this nature can be reversed by thermal energy. One example of photoisomerism for azo compounds appears above. Others are important in the understanding of the changes occurring in the molecules during the photolytic process. *Cis-trans* isomerization is the most common example. *Cis-stilbene* is an example of *cis-trans* isomerization:



followed by *cis*-octyloctene:



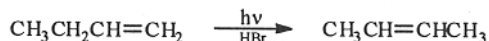
Cis-trans conversions involve triplet states which are different for the *cis* and the *trans* forms (there is no common intermediate for *cis*→*trans* and *trans*→*cis* conversions). In the case of stilbene the *trans*→*cis* conversion is temperature and solvent dependent whereas the *cis*→*trans* conversion is independent of these. There is also a difference in the amount of longer wave radiation that each isomer can absorb (*trans*-stilbene absorbs more energy). In photochemical isomerization, substantially more *cis*-stilbene is formed. For conjugated dienes, these relationship will be reversed (the photochemical conversion produces less of the *cis* form). One explanation is that the *cis* triplet state has a lower energy than the *trans* triplet state (opposite to stilbene). The direction of isomerization also depends on an absorbed wavelength (the amount of energy in the absorbed radiation) and on whether the process occurs directly or through a sensitizer (if a sensitizer is involved, its type will affect the ratio of isomers).

These principles are important when considering photolytic changes. The nuclear shape or geometry of electronically excited species are frequently different than that of the ground state. This is not surprising, because the energy, the electronic configuration, and possibly the electronic spin of an excited state, are different from those of a ground state. These differences also exist between triplet and singlet states in the same excited molecule. An excited molecule of *cis*-stilbene has perpendicular geometry, as compared to the planar geometry of the *cis-trans* isomers. When an excited molecule returns to the ground state, it can form either of the two isomers. The probability of one being formed is determined by the above considerations. This helps us to realize that molecules in excited states have properties which differ from those of their ground state. Therefore, a reaction which would not be possible in the ground state, because of the steric hindrance, may occur in the excited state. On the other hand, one should also take into consideration the Franck-Condon Principle:

“Since electronic motions are much faster than nuclear motions, electronic transitions occur most favorably when the nuclear structure of the initial and final states are most similar”.

When an electron is in a lower vibrational level than that which can cause cleavage, bond scission can still occur because the bond finds itself in a compressed position and, when retracted by an outward surge, the bond may break.

Double bond isomerization also occurs. In the case of olefins, double bond migration



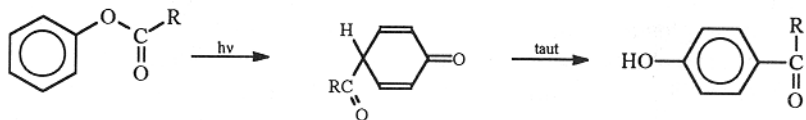
was observed when UV radiation was employed in the presence of hydrogen bromide:

The possible mechanism of double bond migration involves a free-radical process. The photo-Fries rearrangement discussed below can also be treated as a particular case of photoisomerization.

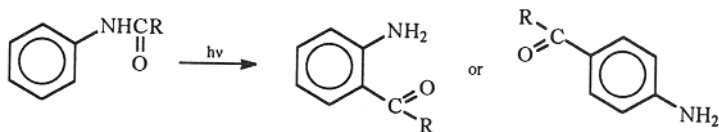
2.2.5 INTRAMOLECULAR REARRANGEMENT

When a molecule absorbs radiation it changes geometry, as explained above, and this creates conditions for many possible rearrangements to occur. If an excited molecule loses its natural rigidity, it becomes more flexible which results in a higher probability that its structural element could come into sufficient proximity to exchange elements of their structure. This is the reason for numerous rearrangements occurring - some of them discussed above as photoisomerization.

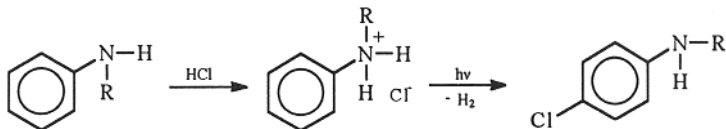
The photo-Fries rearrangement explains photolytic changes in several polymers. The reaction is predominantly a free-radical process described by the following equation:



tion:



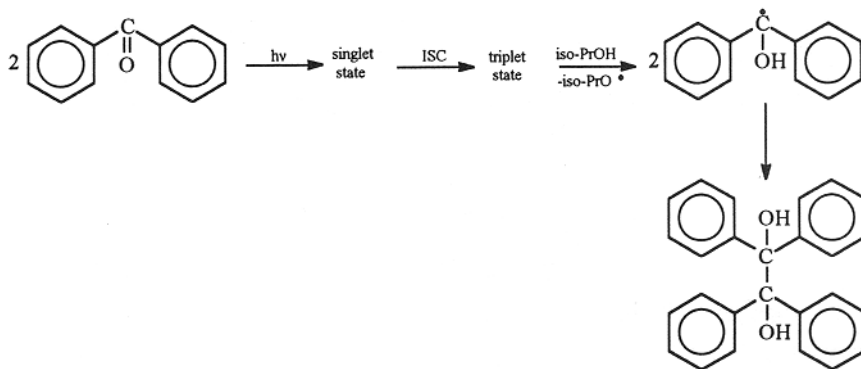
It can be seen that the reaction changes the structure of the backbone of polymers and forms reactive groups which did not exist before. A similar reaction occurs when acylated arylamines are exposed to UV radiation:



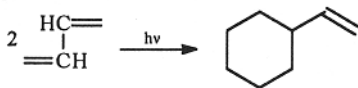
which in turn releases a free amine group - changes relevant in the case of polyamides and polyurethanes. Many other similar reactions are possible. In some, halogen-containing protonic acids participate:

which introduces a new substituent to the aromatic structure.

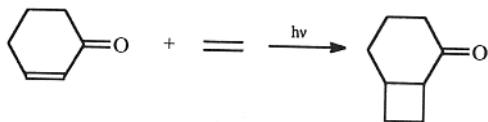
Intermolecular rearrangement reactions, when divided into sigmatropic, electrocyclic, and structural rearrangements help to explain the formation of conjugated segments and various cyclic compounds found in degradation products of polymeric materials.



2.2.6 PHOTODIMERIZATION

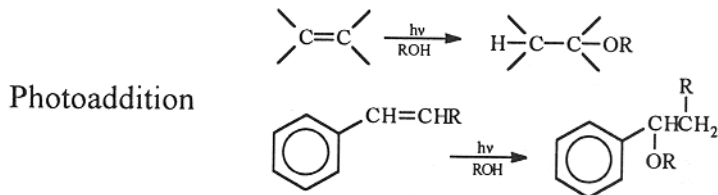
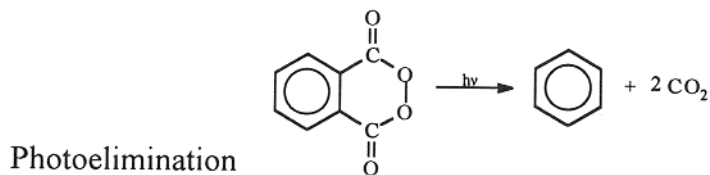
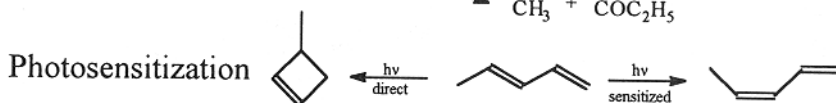
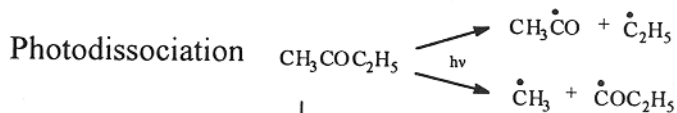
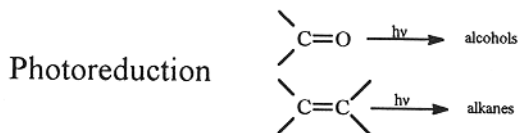


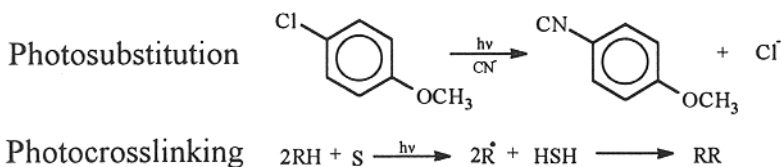
A well-known sensitizer - benzophenone - when irradiated in the presence of a hydrogen



donor (e.g., alcohol), dimerizes according to the following reaction:

A reaction of a similar type may lead to Diels-Adler condensation products: or other structures of unusual geometries: some of which are useful in explaining the peculiarities of various degradation mechanisms.





2.2.7 PHOTOREACTIONS

The list below includes some common photolytic reactions:

2.3 SECONDARY PHOTOREACTIONS

From the brief discussion of primary photoreactions above, one may deduce that they multiply into a wide variety of secondary processes which are material specific which should be discussed as specific cases. One type of reaction (primary or secondary) is common for all materials - namely, photooxidation - and this reaction is the only one discussed here. Molecular oxygen normally exists in its triplet state ($^3\Sigma_g^-$). Of the two singlet

Table 2.1: Sources of singlet oxygen

Electrical discharge

Microwave discharge

Chemical sources - reactions:

hydrogen peroxide and hypochlorite ion

alkaline hydroperoxide

decomposition of sec-butylperoxy radicals

decomposition of superoxide ion

decomposition of transition-metal-oxygen complexes

decomposition of products reacted with ozone

Photolysis:

direct formation

heating of peroxides formed during photolysis

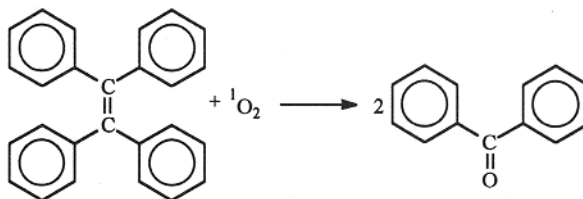
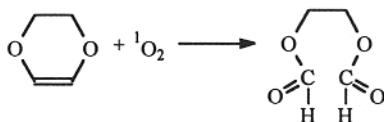
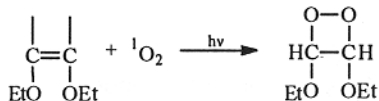
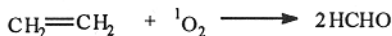
Table 2.2: Lifetime of singlet oxygen, $^1\Delta_g$, in various solvents

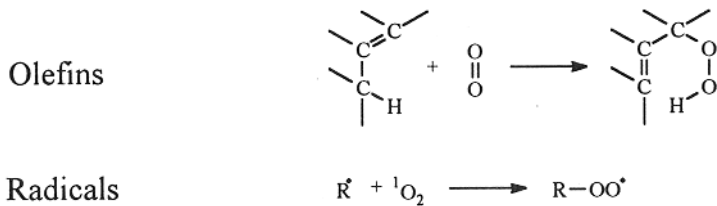
Solvent	Lifetime, μs
H ₂ O	2
CH ₃ OH	7
benzene	24
CH ₃ COCH ₃	26
CHCl ₃	60
CS ₂	200
CCl ₄	700

states, ($^1\Delta_g$ and $^1\Sigma_g^+$), only one, ($^1\Delta_g$), is in a highly reactive form but the second, ($^1\Sigma_g^+$), may rapidly relax to $^1\Delta_g$ with the liberation of 15 kcal/mol energy. Sources of singlet oxygen are given in Table 2.1.

The lifetime of singlet oxygen is relatively long because the conversion to its ground state triplet requires spin change. Temperature has some effect on singlet oxygen lifetime but it is most dependent on the environment (Table 2.2). The presence of hydrogen in the solvent molecule considerably reduces singlet oxygen lifetime. Singlet oxygen is an important factor in the photooxidative process of polymer films because of its large mean diffusion path (115 Å)

and its relatively long lifetime (half-life of 5×10^{-2} s at atmospheric pressure).

Sulfides**Tetraphenyl ethylene****Phenols****1,4-dioxene****Diethoxyethylene****Ethylene**



Singlet oxygen reactivity is characterized by the following reactions:

The most important species which can react with singlet oxygen are unsaturations, aromatic rings, and radicals.

3

ENVIRONMENTAL CONDITIONS

Radiative flux determines the conditions under which materials function and degrade. The effect of temperature on degradation rate must also be considered since heat is another form of energy which acts simultaneously on materials. The composition of the atmosphere, including the moisture component, affect radiative flux but moisture, in particular, and other atmospheric components initiate changes, often corrosive in exposed materials. Volcanoes, on eruption, produce gaseous and particulate pollutants. Winds contribute to the transportation of matter and thus to the residence time of pollutants in the atmosphere and to climate formation. Winds also affect temperature distribution in samples during exposure. Clouds produce precipitation but also absorb sun radiation and reflect or absorb re-radiated energy. Lightning produces energy utilized for chemical reactions in the atmosphere. All of these, due to general circulation and transport processes, contribute to the climatic or environmental conditions which affect exposed material and in which they must be designed to work. The following analysis outlines important features and relations of these environmental conditions.¹⁻¹²

3.1 SOLAR RADIATIVE EMISSION

Outer space surrounding the Earth does not contain material particles; therefore the only form in which energy can be supplied to our planet is by radiation. Radiation is emitted by all matter having temperature higher than absolute zero. The energy of emitted radiation is described by Planck's Law:

$$E_{\lambda} = c_1[\lambda^5(\exp c_2/\lambda T) - 1] \quad [1]$$

where

E_{λ} amount of energy emitted at a specific wavelength, λ
 T absolute temperature
 c_1, c_2 constants.

The Stefan-Boltzmann Law:

$$E^* = \sigma T^4 \quad [2]$$

where E^* total energy emitted by a body
 σ the Stefan-Boltzmann constant
 T absolute temperature

shows that the total energy emitted by a body depends on its temperature as does its wavelength of maximum emission, according to Wien's Law:

$$\lambda_{\max} = 2897T \quad [3]$$

where λ_{\max} wavelength of maximum emission
 T absolute temperature.

Rydberg's Law specifies the radiation wavelength:

$$1/\lambda = R[1/(n+a)^2 - 1/(m+b)^2] \quad [4]$$

where λ radiation wavelength
 n, m integers, $m > n$
 a, b constants for particular series
 R Rydberg constant.

According to this equation, each element is capable of emitting radiation at several specific lines restricted by the values of constants included in the equation. Solar radiation does not depend on just one element; rather, the spectrum of light emitted results from a combination of component spectra and their relative concentrations. Evidently, the radiative emission of the sun depends on the combination of elements involved in the energy generation process and on the temperature at which radiation occurs. This should then tell us that the radiative emission of the sun should be constant if both temperature and the concentration of elements involved are also constant.

The sun was formed 4.6 billions years ago and it is composed of 74% hydrogen and 25% helium by mass. The remaining 1% comprises elements, such as oxygen, carbon, silicon, iron, magnesium, and calcium. The sun emits energy generated by the thermonuclear fusion of hydrogen into helium at a temperature of around 1.5 million degrees K. This thermonuclear fusion process occurs in the core of the sun and energy is passed to the photosphere. The core contains more helium (65%) than hydrogen. Hydrogen is deficient because of its conversion in the thermonuclear fusion process. It is estimated that

the remaining hydrogen should last for another 4 billion years at the sun's recent level of luminosity.

The photosphere does not have a uniform temperature; it varies between 4000 and 8000 K, depending on the distance from the core. The radiation spectrum of the sun, when fitted to the black body curve, gives an average temperature of 5800 K. The main difference between the prediction model and the real emission spectra of the sun is in the UV region, which suggests a lower temperature of emission. UV emissions may originate close to the lower chromosphere which has a temperature between 2000 and 4000 K. Above the chromosphere in the corona, the temperature increases to about 1 million K, but, because of a low concentration of gas in this region, the radiation from the chromosphere and the corona amounts to only 0.1% of the total output of solar radiation.

In order to understand temperature uniformity, and thus radiation, one should mention sunspots, which appear in the photosphere. Sunspots can have diameters of 10,000-150,000 km and may last for a few weeks. The radiation in the sunspot area is reduced, due to the suppression of convection heat transfer from the core to the photosphere. Horizontal temperature variations of up to 2000 K are not unusual, but because sunspots occupy only up to 1% of total surface area of the sun, the total solar output is within 0.1% of constant. The distribution of emitted energy is such that 9% is in the UV region, 45% is in the visible range, and the remaining 46% is in the infrared. The above data are based on continuous satellite observations over 10 years. The errors of measurements are in the range of 5-15%, depending on radiation wavelength.

3.2 EFFECT OF ORBITAL VARIATIONS ON ENERGY SUPPLY

The eccentricity of the Earth's orbit causes the distance between the Earth and the sun to change between perihelion (the closest distance) and aphelion (the farthest distance). This causes the radiation received by the Earth, at aphelion, to be 3.5% lower than the average radiation. Moreover, during the last 110,000 years, the Earth's orbit changed from more circular to more elliptical, which produced changes in incident radiation in the order of 10%. The Earth's axis (the line which joins two poles through the Earth's center) is tilted at present at 23.5° . During the last 1 million years, this tilt varied from 22 to 24.5° with a variation period of 41,000 years. The obliquity change affects seasonal variations but does not influence the total radiation intercepted by the Earth.

Finally, due to interaction with other planets, particularly Jupiter, the elliptical orbit is distorted. Full rotation of the ellipse takes 21,000 years and changes the distribution of radiation on the Earth's surface. For example, the perihelion now occurs in January but 11,000-15,000 years from now it will happen in July. This will mean warmer summers and colder winters at that future time.

Solar radiation cannot be measured directly at the sun but can be measured by satellites above the Earth's atmosphere. From these measurements, we know that the

range in radiation flux between perihelion and aphelion is at present in the range of 1411 to 1329 W/m². The energy which the Earth intercepts is only a small fraction of the total energy emitted by the sun. Still, the amount of energy intercepted by the Earth in 10 days is equivalent to the total energy derived from the combustion of all fossil fuels available on the Earth or a million times larger than the amount of electrical energy produced in the world in the same period.

3.3 SCATTERING OF SOLAR RADIATION

Two theories give us a fundamental understanding of the phenomenon of light scattering by particles found in the path of the sun's rays as they travel to Earth. The Rayleigh Law defines the conditions of scattering for particles much smaller in diameter than the wavelength of radiation they scatter:

$$I_o = [9\pi^2 V^2 (m^2 - 1)^2 (1 + \cos^2 \Theta)] / 2d^2 \lambda^4 (m^2 + 2)^2 \quad [5]$$

where	I_o	intensity of scattered radiation
	V	$= 4\pi r^3 / 3$
	r	radius of the particle
	m	refractive index
	d	distance
	λ	light wavelength
	Θ	incident ray angle.

This law implies that the scattered intensity increases as the sixth power of particle radius and decreases as the fourth power of wavelength. Therefore, light of shorter-wavelength is scattered more than longer-wavelength light. Gas molecules are atmospheric particles which are much smaller than the wavelength of the sun's radiation thus the Rayleigh Law is followed. Contaminant particles are outside the size criteria and their scattering effect does not follow the Rayleigh Law. Rayleigh scattering is responsible for the blue sky, because blue light is scattered about 10 times more than red light. Scattered light beams are not necessarily lost but rather diverted from their normal course, which also means that they stand a higher chance of being absorbed, since they normally travel longer distances.

Bigger particles, such as clouds, water droplets, and pollutant particles also scatter sunlight based on Mie scattering:

$$I_0 = \lambda^2(i_1+i_2)/8\pi^2d^2 \quad [6]$$

where I_0 intensity of scattered radiation
 λ light wavelength
 d distance
 i_1, i_2 coefficients of the electric and magnetic waves.

Mie scattering is less wavelength dependent, and, in fact, radiation of longer wavelength is preferentially scattered. The effects are slightly more complex because scattering occurs in areas where particles are concentrated causing mainly a multiple scattering. The question, now, is how much of the energy arriving at the top of the Earth's atmosphere is scattered? In a clear atmosphere, the molecules scatter about 6.3% of incident solar radiation back to space. This means that 11.7% of ultraviolet and visible light is scattered, whereas IR radiation is not affected by Rayleigh scattering.

3.4 ABSORPTION OF SOLAR RADIATION

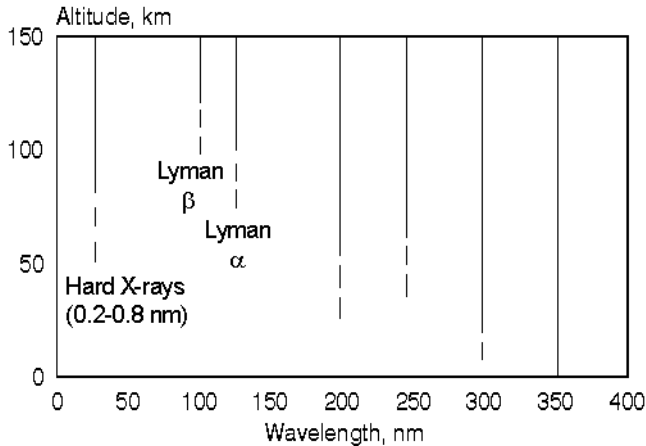


Fig. 3.1. The absorption altitude of incoming solar radiation.

The principles of energy absorption by chemical molecules are outlined in Chapter 1. The effects of energy absorption by molecules contained in the atmosphere are discussed later in this chapter. Here, we deal first with quantitative and qualitative energy loss due to absorption. Fig. 3.1 shows the altitudinal absorption of incoming solar radiation. Two observations can be made: ultraviolet radiation is readily absorbed in the upper layers of the atmosphere; the absorption is wavelength-specific. Therefore, adsorption depends on the composition of

the atmosphere in a particular layer. The visible and infrared components of the sun's radiation are not affected by the upper layers of atmosphere. Absorption of infrared occurs in the troposphere, due mainly to clouds and pollutants. Fig. 3.2 provides more data on the effect of clouds on radiation transmittance.

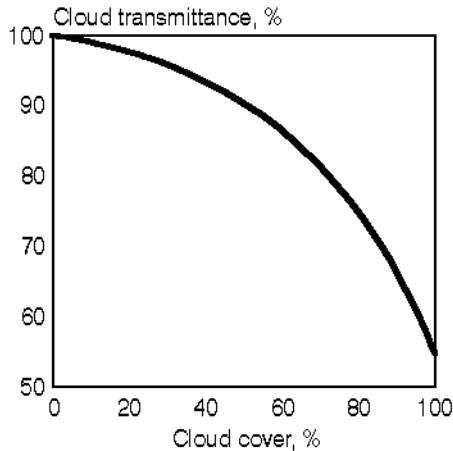


Fig. 3.2. Cloud transmittance vs. cloud cover.

When spectral distribution of incoming solar radiation is compared with outgoing terrestrial radiation, it is evident that the energy absorbed is converted to a higher wavelength (infrared). The shift in radiation wavelength, the negative heat balance at long-wavelength radiation, and, in particular, the energy re-radiation cause the temperature distribution in the troposphere, shown in Fig. 3.3.

Temperature in the troposphere decreases with altitude at a rate of 6.5 K/km. The temperature of the stratosphere increases with altitude at a rate of approximately 2 K/km because of the absorption of short-wavelength radiation. Temperature increase in the thermosphere results from high absorption of energy which causes photo-ionization.

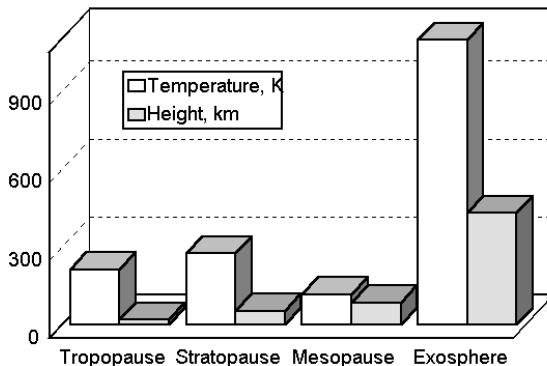


Fig. 3.3. Height in the atmosphere vs. temperature.

3.5 VARIATIONS IN THE RADIATIVE FLUXES

Data on the sun's radiation and its scattering and absorption are summarized in Fig. 3.4. The solar spectrum is modified in both the ultraviolet and the infrared range much more than it is in the visible range. The most important changes occur in the UV range

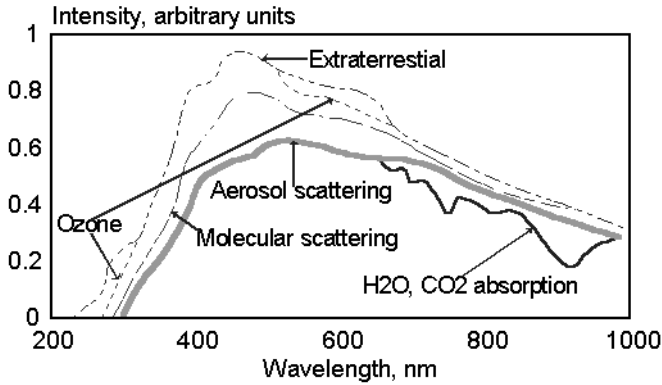


Fig. 3.4. Sunlight spectrum as modified by the presence of various components.

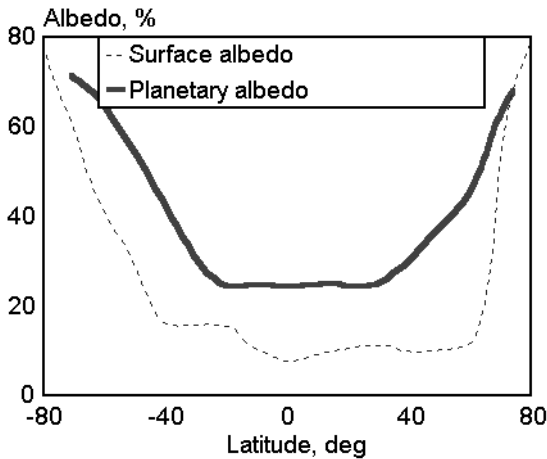


Fig. 3.5. Planetary and surface albedo vs. latitude.

where the ultrashort wavelengths are virtually eliminated. A discussion on radiation intensity is not complete without covering latitudinal, seasonal, geographical, and daily variations in radiative fluxes.

Latitudinal variations in the radiation flux depend on the elevation of the sun, the distribution and type of clouds, and the surface albedo. As the sun's zenith angle increases, the absorption and scattering of radiative energy increases as a result of the longer path it must take through the atmosphere and the higher chance of photon absorption. Fig. 3.2 contains data explaining the reasons for the cloud effect. The surface albedo is the ratio of reflected (scattered) solar radiation to incident solar radiation measured above the atmosphere. Fig. 3.5 presents data on the surface albedo as a function of latitude. The surface albedo of each hemisphere is not the same, due to different cloud distribution. Geographical, seasonal, and daily variations also occur as a result of variations in cloud cover and surface reflectivity as seen from Fig. 3.6.

Snow and ice-cover variations cause the albedo curve in the Northern Hemisphere to reach its maximum in winter. Additionally, one has to consider the effect of the seasonal changes in the sun's zenith angle on the radiative energy supply. If we consider urban climatic conditions and plot the daily radiation flux, we find that the relationship is complicated by an additional parameter - the daily rate of pollution affecting radiation flux by the amount of energy absorbed.

Snow and ice-cover variations cause the albedo curve in the Northern Hemisphere to reach its maximum in winter. Additionally, one has to consider the effect of the seasonal changes in the sun's zenith angle on the radiative energy supply. If we consider urban climatic conditions and plot the daily radiation flux, we find that the relationship is complicated by an additional parameter - the daily rate of pollution affecting radiation flux by the amount of energy absorbed.

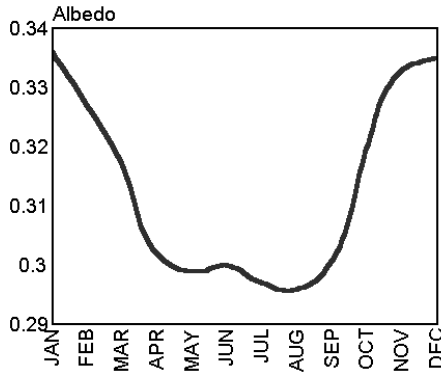


Fig. 3.6. Seasonal variation of albedo.

3.6 TEMPERATURE AND MOISTURE

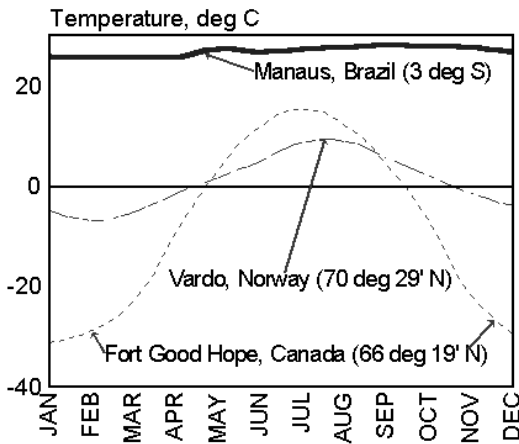


Fig. 3.7. Seasonal temperature variations and latitude.

An effort was made to show what may influence the natural radiation level to which materials are exposed. The value of this data is in the awareness it creates rather than its usefulness as a base material for comparative study. Data clearly indicate that in a natural environment, materials are subjected to a great variety of effects. It is, therefore, essential to develop a data base which characterizes the conditions of degradation if the results of studies are to be used in comparative evaluations.

Seasonal variations of air temperature depend on latitude (Fig. 3.7). Close to the equator, temperatures do not vary much and the radiative flux is uniform. The temperature distribution for Vardo, Norway is characteristic of a coastal location. Large temperature variations occur in a continental interior (Fort Good Hope). The surface temperature of materials is greatly affected by the absorption of radial energy (Fig. 3.8). Material type and color determine surface temperature. The rate of heat penetration depends on the thermal diffusivity of the material, on its heat capacity, and on its thermal conductivity. All three factors

together determine surface temperature. Absorption of solar radiation depends on the surface finish. A polished surface reflects more radiation than unpolished surface. Lighter colored materials reflect more than darker. Wind speed has considerable effect on surface temperature increasing the rate of heat exchange.

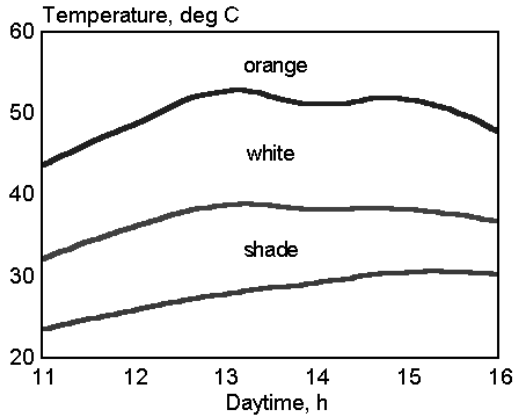


Fig. 3.8. Air temperature behind awning material on sunny days. [Data from E. Hilscher, *Problems with coated polyester fabrics*, *Ann. Conf. Ind. Text. Group, Text. Inst., Manchester, 1975.*]

The examples discussed above show that temperature control in weathering studies might be more complex than simple measurement of air temperature. Real temperatures, frequently higher than ambient by as much as 30 degrees, are sufficiently high to have a considerable effect on the degradation rate of many materials.

The atmosphere is the smallest reservoir of water of the Earth, containing only 0.001% of the total water mass. Still, this relatively small amount of water is responsible for scattering and absorption of the sun's energy. Slightly less

than one-quarter of the solar influx is used for water evaporation, which is an important regulator of the Earth's temperature.

The molecular weight of water is about 40% lower than the average molecular weight of atmospheric components, which is one of the reasons that a water molecule is very mobile. The average lifetime of a water molecule from evaporation to condensation is about 9 days, which is a sufficient length of time for a water molecule to be carried around the globe by the tropospheric wind system before being precipitated. This explains the considerable latitudinal difference between evaporation and precipitation. Humidity and the amount of precipitation are more local than global climatic phenomena, and, as an important factors in weathering studies, should be carefully monitored.

3.7 ATMOSPHERE COMPOSITION

The total mass of air surrounding the Earth is 5.1×10^{18} kg. Atmospheric density changes exponentially with altitude. About 80-85% of the total atmospheric mass resides in the troposphere, extending from the Earth's surface up to 8-12 km at high latitudes and up to 16 km in the tropics. Most of the water available in the atmosphere is found in the troposphere (the region adjacent to the Earth's surface), which is a region of an active vertical motion due to its negative temperature gradient (almost linear decrease in temperature with increasing altitude). The remaining mass of the atmosphere is found in the next layer the stratosphere. The stratosphere contains about 90% of all atmospheric ozone and controls much of the solar UV radiation reaching the surface and the climate of our planet. The temperature of the stratosphere rises to a maximum at about 50 km due to absorption of UV by oxygen and ozone. The ozone layer has its highest den-

sity at altitudes of 20-25 km. The proportion of nitrogen and oxygen is almost constant up to 100 km. Also, carbon dioxide is fairly evenly distributed throughout the atmosphere, presently at the level of 350 ppm (CO₂ concentration has increased in last 100 years by 70 ppm). Water vapor concentration depends on its saturation vapor pressure and thus, on temperature. It therefore decreases with altitude from about 7% over tropical oceans to 3 ppm in the stratosphere. The mesosphere, thermosphere, and ionosphere, the layers above the stratosphere combined, contain only about 0.1% of the total atmosphere mass.

Gas molecules in the atmosphere are continuously exchanged by the interaction of different sources and sinks. The residence time of molecule in the system is given by the formula:

$$F_i = F_o = A/\tau$$

where	F_i	flux of substance into the system
	F_o	flux of substance out of the system
	A	amount of substance in the reservoir
	τ	residence time.

Vertical mixing occurs up to about 50 km and thus occurs faster compared with horizontal mixing (interhemispheric) because the distance from equator to poles is much larger (10,000 km). An exchange of air between the hemispheres takes about a year. This exchange becomes even slower in the stratosphere therefore the southern and the northern stratospheres are practically decoupled.

Based on residence time, the components of the atmosphere were divided into three groups:

quasi-permanent gases	1000 years
<i>variable gases</i>	<i>a few years</i>
<i>highly variable gases</i>	<i>1 year</i>

This classification is used in grouping the components of the atmosphere, as seen in Table 3.1. Stratospheric composition differs essentially in water and in ozone concentration. Water concentration is on average about 100 times lower and ozone about 100 times higher in the stratosphere than in the troposphere. Ozone concentration in the stratosphere reaches 10 ppm compared to 10-40 ppb at ground level. The similar composition of other components in troposphere and stratosphere suggests that effective exchange mechanisms exist. The tropopause forms a pronounced stability barrier between the troposphere and the stratosphere but it is highly variable in position. Sometimes the tropopause may extend down to 6 km and stratospheric air may be drawn into the tropo-

Table 3.1: Composition of atmosphere

Component	Unit	Concentration	Residence time
Quasi-permanent			
Oxygen	%	20.964	
Nitrogen	%	78.084	
Argon	%	0.934	
Neon	ppm	18.18	
Helium	ppm	5.24	
Krypton	ppm	1.14	
Xenon	ppm	0.087	
Variable			
Carbon dioxide	ppm	330	
Methane	ppm	1.5	9 years
Hydrogen	ppm	0.5	2 years
Nitrous oxide	ppm	0.3	30 years
Highly variable			
Water	ppm	20,000	10 days
Ozone	ppm	0.03	up to 2 months
Carbon monoxide	ppm	0.15	3 months
Nitrogen dioxide	ppm	0.003	1 day
Ammonia	μg	5	5 days
Sulfur dioxide	μg	5	4 days
Hydrogen sulfide	μg	0.5	
Organic carbon	μg	25	less than a day

sphere. In the upper layers of the atmosphere (mesosphere, thermosphere), composition does not differ much except for higher concentrations of elemental hydrogen, helium, and fast oxygen. Except for hydrogen and helium, the components of the atmosphere are relatively constant because they are seldom lost to space.

The components of the atmosphere, which contribute to pollution or interfere with radiative fluxes by participation in photochemical reactions, are discussed below.

3.8 NITROGEN COMPOUNDS

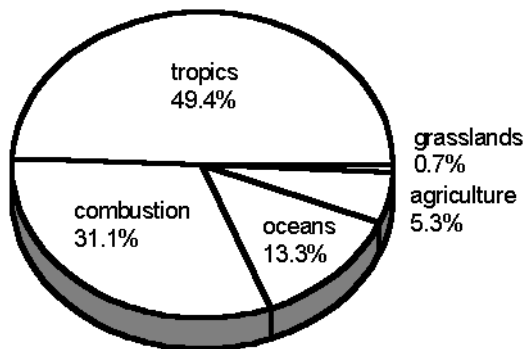
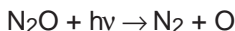


Fig. 3.9. Sources of nitrous oxide.

This group of compounds includes: nitrous oxide, other oxides of nitrogen, and ammonia. Table 3.1 shows their average concentrations and lifetimes. All but nitrous oxide are contained in the group of atmosphere components having highly variable concentrations and short lifetimes. Nitrous oxide has a very long atmospheric lifetime of about 150 years and has very little geographic variation in concentration (<1%). Fig. 3.9 gives information on the sources of nitrous oxide emission, although the presently available data do not account for all

nitrous oxide and do not explain its increase. Until recently, combustion, biomass burning, and the use of fertilizers were regarded the most important sources of nitrous oxide. Now, it is known that the influence of biomass burning was overestimated. Currently, the atmospheric concentration of nitrous oxide is 0.31 ppm and growing by 0.3% per year (about 150 years ago it was 0.285 ppm).

The tropical forests produce by far the greatest amount of nitrous oxide followed by world wide combustion of fossil fuels and biomass in the tropics. Nitrous oxide is produced in nature by bacterial denitrification processes which can be decreased by conversion of tropical forest into farmlands and by reducing the use of ammonium salt and urea fertilizers. Nitrous oxide is removed from the atmosphere mainly by photolysis in the stratosphere and by reaction with elemental oxygen:



Presently, its total rate of destruction is about 30% lower than its production and this results in an increase in concentration of nitrous oxide by 0.3% per year. The above reactions show that nitrous oxide, by reacting with elemental oxygen, affects the formation of ozone, the concentration of ozone in the atmosphere, and indirectly, the intensity of UV radiation.

Oxides of nitrogen (NO and NO₂) are decomposed in the atmosphere in a few days and have an important indirect influence on the concentration of tropospheric radicals.

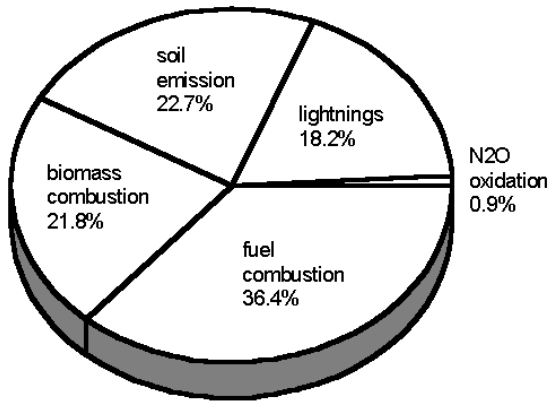


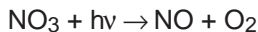
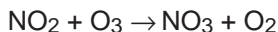
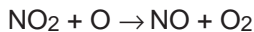
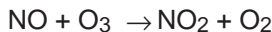
Fig. 3.10. Sources of nitrogen oxides (NO_x).

The short lifetime causes the concentration of nitrogen oxides to be linked geographically to the sources thus the concentration of nitrogen oxides varies in a broad range. Fig. 3.10 shows the sources of nitrogen oxides formation.

Combustion of fuels by vehicle engines, power stations, and industry contribute heavily to the overall emission of nitrogen oxides. In large cities, NO_x is produced by car emission. It is considered that 75% of NO_x emission in Athens, Greece (about 40 kt/year) is automobile

emission related. Morning traffic increases the concentration by factor of 3. Nitric oxide is produced from the reaction between molecular nitrogen and oxygen in a lightning flash. The discharge channel may reach a temperature as high as 4000 K. Since there is, on average, about hundred bolts of lightning a second around the globe, the estimated output of nitrogen oxide is not high. The denitrification process in acidic soil also results in the production of nitric oxide, which is then easily oxidized to nitrogen dioxide in the atmosphere. Biomass burning (mostly in tropical countries) produces large quantities of nitrogen oxides steaming from the high nitrogen content of the biomass and the low temperature required for its oxidation.

Nitrogen oxides participate in several chain reactions:



These reactions decrease ozone concentration, reduce the UV filtration barrier in the stratosphere, and contribute to increased UV radiation on the Earth. Additionally, NO_x species interfere with the formation of hydrogen- and chlorine-containing radicals, which, in turn, affects ozone concentration.

The ammonia cycle in the atmosphere is quite simple and short. Its very short lifetime of 2 days is due to its high solubility and reactivity with sulphur-containing compounds. Most ammonia is produced by denitrification with small amounts emitted from coal combustion. Pollution is local, little is oxidized in the troposphere, and most ammonia is returned to the Earth's surface dissolved in water or in the form of ammonium sulphate.

3.9 OXYGEN SPECIES

Oxygen species include atomic (elemental) oxygen, the excited singlet states of molecular oxygen, and ozone. Formation of odd oxygen in the stratosphere and mesosphere starts from the photodissociation of molecular oxygen, which is a two-stage process. Molecular oxygen, on absorption of UV radiation, is transformed into excited singlet oxygen, which dissociates, forming two oxygen atoms. The photodissociation process is followed by a secondary thermal reaction with molecular oxygen in the presence of a neutral body (oxygen or nitrogen) and ozone is produced. Molecular oxygen absorbs solar radiation in the range of 176-210 nm. Ozone has maximum absorption in the range of 280-320 nm.

Ozone decay is also a two-step process. In the first step, ozone absorbs UV radiation and dissociates to molecular and atomic oxygen. Atomic oxygen reacts further with another molecule of ozone and two molecules of molecular oxygen are formed. Ozone absorbs in the UV between 200 and 320 nm and also in the visible range at 450 and 700 nm. Absorbing in the UV range, ozone converts the UV radiation to heat, which causes the stratosphere to have a positive temperature gradient. If the above reactions were the only once occurring, the thermal and radiative balance would be constant. In reality, there are more reactions competing for ozone and atomic oxygen. These have received much public attention since the processes involved could have dramatic effect on life on Earth. It is believed that three reactions have almost equivalent effect on ozone destruction: reaction with NO_x , reaction with chlorine, and recombination with molecular oxygen.

There are two anomalies which may affect the results of weathering studies. One is the drastic increase in ozone concentration at the Earth's surface and the other is the formation of ozone holes. The change in the position of the tropopause causes stratospheric air to be drawn into the troposphere and this causes a major increase in ozone concentration close to the Earth's surface, possibly altering weathering behavior. There are two typical latitudes where such events are more likely to occur: in the proximity of 30° where air masses of tropical origin meet the colder mid-latitude air and at 60° where polar air contacts warmer air. These two latitudes in Northern Hemisphere are known to have higher ozone concentrations. The latitudes between 42° and 45° , where the tropopause folds between polar and tropical air masses, also have an unusually high ozone concentration. Ozone holes, which form mostly above the poles, can drift to other

locations; these, in turn, may facilitate degradative processes by allowing more UV radiation to reach the Earth.

Two separate processes should be considered in weathering studies. One is related to the above discussed ozone depletion which increases UV radiation. The other is related to the ozone concentration at ground level. Ozone has very short lifetime (about 2 min), therefore the processes of formation and degradation of ozone in the stratosphere are not related to ozone formation at ground level. Similarly, ozone in the stratosphere does not directly contribute to ozone concentration at ground level. Ground level of ozone, because it is so reactive, affects the degradation of materials in its surrounding. Ozone on the Earth surface is produced by industry and transportation. Concentrations are 2-3 times higher in summer than in winter. During the day, peak concentrations follow morning and afternoon peak traffic volumes. Ozone is formed indirectly from nitrous oxide which on absorption of UV forms molecular oxygen which then reacts with molecular oxygen to form ozone. It is therefore not surprising that ozone concentration trails concentration profile of oxides of nitrogen. In Europe, WHO quality guidelines set ozone level at 150-200 $\mu\text{g}/\text{m}^3$ (1 h average) and 100-120 $\mu\text{g}/\text{m}^3$ (8 h average). Recorded values in Mexico City are in the range of 300-900 $\mu\text{g}/\text{m}^3$.

3.10 HYDROGEN SPECIES

The group discussed here includes hydrogen, hydroxyl, hydroperoxyl, peroxide, water, and methane. Hydrogen is not particularly important in weathering studies. It may be appropriate to mention that the concentration of hydrogen is higher in a polluted area because it is a component of automotive exhaust gases (1-5% by volume). Hydrogen is also produced from oceanic sources and soils due to microbiological activities. Altitudinal concentration of hydrogen is constant and it is detected in all layers of the atmosphere. Hydrogen can react with OH radicals, producing water and atomic hydrogen.

Hydroxyl radical generation is mostly due to the reaction between water and atomic oxygen but other pathways are also known:

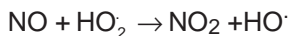
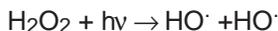
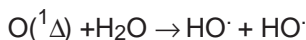
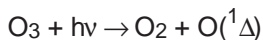


Fig. 3.11 shows that the highest OH radical concentration occurs when the sun is at its zenith. These data are in accordance with the photochemical theory of hydroxyl radical formation. The concentration of hydroxyl radical is higher by 28% in winter, than in

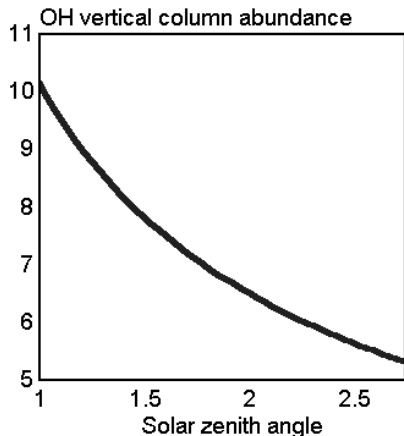
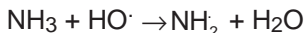
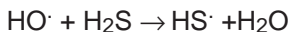
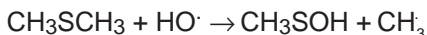
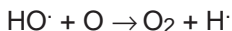
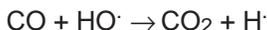
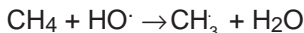


Fig. 3.11. OH vertical column abundance vs. solar zenith angle.

the summer, which is due to seasonal temperature changes. It is difficult to measure hydroxyl radical concentration. Its concentration based on model calculations is 5×10^5 molecules per cm^3 . In the tropics, this value is larger by factor of 2. The concentration of hydroxyl radical changes throughout the day and it is at its peak at noon.

The hydroxyl radical concentration is very low because the highly reactive radical has a residence time of less than 1 s. It occupies a special place in atmospheric chemistry because it is reactive to most trace gases. Some of the examples of reactions are given below:



Accordingly, the hydroxyl radical initiates a chain of oxidation reactions with many components in the atmosphere. The most important reaction concerns the oxidation of methane, which controls the concentration of methane in the atmosphere. Hydroperoxyl radical and hydrogen peroxide both participate in oxidation reactions in a way similar to the hydroxyl radical. Their importance is in balancing the trace components and by indirectly preventing the loss of ozone due to reactions with pollutants.

Methane has had a constant concentration of 0.7 ppm for about 10,000 years (found by testing polar ice). About 150 years ago, its concentration began to rise by 1% per year due to the increase in the area given to agriculture. An increase in methane causes a decrease in the concentration of hydroxyl radical.

3.11 CARBON OXIDES

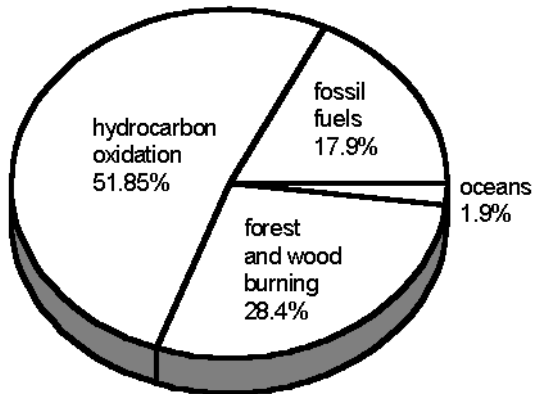


Fig. 3.12. Sources of carbon monoxide.

Carbon monoxide's role in atmospheric chemistry is extremely important because it tends to suppress the atmospheric levels of hydroxyl radicals, leading to longer lifetimes and higher concentrations of methane and the trace components of the atmosphere. Fig. 3.12 gives data on carbon monoxide sources.

Two human activities play a major role in carbon monoxide emission: the use of automotive engines in the Northern Hemisphere and land clearing and savanna burning in the tropics. But both activities produce less carbon monoxide than the oxidation of methane, which is related to natural processes not as much related to human activities. It is estimated that carbon monoxide concentration increases in the Northern Hemisphere by about 1% per year. In the

Southern Hemisphere, there is little evidence of increase. Because of its rather short lifetime (2-3 months), carbon monoxide is concentrated close to its emission sites. Its concentration is highly variable (short lifetime) and it is estimated at 0.2 ppm in the Northern Hemisphere and 0.06 ppm in the Southern Hemisphere.

Carbon dioxide is not photochemically active but it is the single most important greenhouse gas in the atmosphere. Because of this, it also has an influence on photochemistry in the stratosphere. Because it is so much related to its uptake by vegetation, the concentration of carbon dioxide is dependent on season and latitude. The Northern Hemisphere has higher concentration because of greater fuel combustion. Sedimentary rocks are the largest reservoir of carbon dioxide. Dissolved calcium and magnesium carbonates are flushed into the oceans by rain, surface and ground water to form new carbonate sediments. A surplus of bicarbonate ion is returned to the atmosphere as carbon dioxide. It is estimated that the concentration of carbon dioxide grows in the Northern Hemisphere by 4% yearly. Other data show that the increase in carbon

dioxide concentration is less than this. Carbon dioxide concentration in 1958 was 315 ppm. By 1988 it has risen to 350 ppm which is an annual growth rate of 0.4%. Doubling the concentration of carbon dioxide in the atmosphere would increase the average temperature by 2.5 K. The process of carbon dioxide removal from the atmosphere takes a long time (lifetime of 250 years or longer) because the amount of carbon dioxide in the atmosphere is large compared to what can be consumed by vegetation. In turn, the excessive removal of carbon dioxide may have adverse consequences as lower concentration would lower the temperature on Earth. Too high a concentration would result in excessive ice melting and an increase of the sea level on Earth. This shows that it is highly desirable to maintain the concentration of all atmospheric components in fine balance.

3.12 SULFUR-CONTAINING COMPONENTS

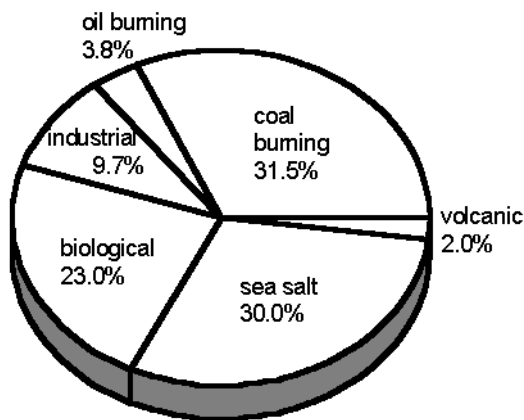


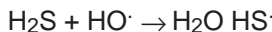
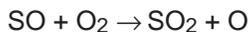
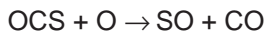
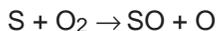
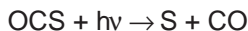
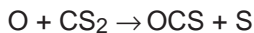
Fig. 3.13. Sources of sulfur-containing compounds.

Several compounds are included in this group: sulfur dioxide, hydrogen sulfide, carbonyl sulfide, and carbon disulfide. Fig. 3.13 presents data on sulfur emission from various sources. Sulfur-containing components of the atmosphere have a short lifetime in the atmosphere - sulfur dioxide 2 days, hydrogen sulfide 0.5 days, carbonyl sulfide more than 1 year, and carbon disulfide, a few weeks. These short lifetimes contribute to local pollution. This agrees with observations of volcanic eruptions which contribute to increases in regional concentration by 20-40%.

Half of all emissions of sulfur dioxide comes from burning of fossil fuels. Other sources include: biomass burning, volcanic eruptions, oxidation of dimethyl sulfide (from the oceans) and oxidation of hydrogen sulfide in the atmosphere. The sulfur dioxide formed is

eventually converted to aerosol particles as it combines with water droplets in the clouds. In volcanic eruptions, sulfur dioxide is directly injected into the stratosphere where it has long lifetime. Current theory suggests that aerosols which end up in the troposphere produce a cooling effect in the Northern Hemisphere.

The conversion of original pollutants is explained below:



One look at the products of these reactions shows that the final product will be acid rain. As it is produced, the valuable resource of hydroxyl radicals is consumed. Acid rain and sulfur dioxide are very aggressive, corrosive materials. For example, books and leather bindings deteriorate in library environments because of the presence of these contaminants. Building materials suffer from reactions with sulfur-containing compounds. A typical reaction between sulfuric acid and calcium carbonate produces gypsum which is subsequently washed out. This deterioration process is usually attributed to acid rain but many buildings are in places where pollution is produced therefore reactions may simply occur with gaseous products coming directly from those local sources. This has a high probability given the short lifetime of sulfur dioxide in the atmosphere.

3.13 CHLORINE-CONTAINING COMPONENTS

Chlorinated fluorocarbons have become a subject of particular interest because of their effect on ozone concentration in the atmosphere. Their long lifetime and their direct consumption of ozone pose a threat to the future energy balance. Chlorinated fluorocarbons absorb UV radiation at a wavelength below 300 nm and dissociate to free radicals or react with singlet oxygen, producing more free radicals. Further steps in the chain reaction include ozone, and the reaction cycle may occur hundreds of times before a Cl atom (a product of the primary reaction) is recycled into an inert HCl. This scheme of reactions has been developed after intensive studies of these components. Two compounds are the most common: CFCl_3 and CF_2Cl_2 . There is 0.28 ppb of CFCl_3 in the atmosphere and it has a lifetime of 65 years. The concentration of CF_2Cl_2 is 0.48 ppb and its lifetime is 120

years. Although they do not contain fluorine, carbon tetrachloride and methylene chloride have similar photochemical properties.

Very few studies on hydrogen chloride have been carried out and the results to date are not conclusive. Hydrogen chloride originates from two main sources - photochemical decomposition of other chlorine-containing compounds (mostly methylene chloride) and from volcanic deposition. Other sources include coal burning, incineration (mostly due to the combustion of PVC) and the alkali industry. Hydrogen chloride is widely distributed and present throughout all layers of the atmosphere. It must, therefore, be an important reactive component of the chemical activity in the atmosphere.

3.14 PARTICULATE MATERIALS

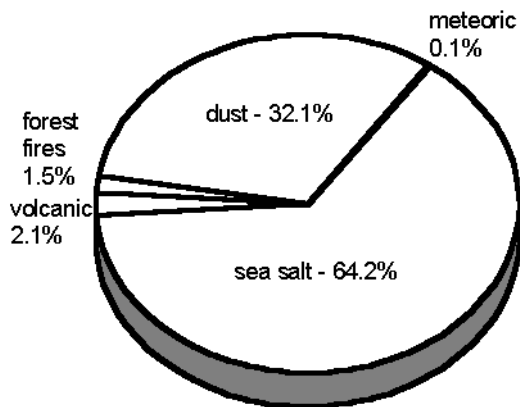


Fig. 3.14. Particles released to the atmosphere.

There are two sources of particulate materials in the atmosphere: particles formed on the Earth's surface and particles formed from chemical reactions in the atmosphere. Global release of particles to the atmosphere is summarized by Fig. 3.14. Forest fires produce small particles (50 nm) with a very high yield of up to several tones per hectare. In tropical areas, land-clearing and savanna-burning continues to be carried out routinely. The largest dust-producing areas include the Sahel, the deserts of Asia, and some parts of the USA. Winds can carry particles to very far; for example, the Harmattan can carry particles from the Sahara desert to England, about 3000 miles away.

Volcanoe eruptions create enormous uplift forces which cause particles to travel great distances because of high ejection velocities. These particles have very large diameters - up to 10,000 nm - and the aerosol is highly concentrated. Sea salt particles are also of relatively large dimensions. These are produced by bubbles of sea breaking into small droplets, which, after evaporation, produce small particles of salt.

Secondary particulate material, formed in the atmosphere, consists of sulfates (mostly ammonium sulfate) and nitrates. The composition of aerosols is usually determined by local conditions, but particles need not have a simple composition related to their source of origin. For example, elements such as mercury, cadmium, and selenium are found in atmospheric particulates in concentrations much higher than are found in

seawater. This shows that particles undergo an enrichment process which changes their composition. Such processes may include the volatilization of metals through methylation, deposition of surface-active organic species, and biological processes which modify the aerosol composition. Finally, gas molecules may be absorbed followed by thermal and photochemical reactions. Many of these processes may continue to be active at high altitudes.

Deposition of suspended particles depends on their size. Particles having diameter 20 μm can be easily lifted into the troposphere and can be transported over large distances. Their lifetime can be very long (1 year and more). Smaller particles have almost infinite lifetimes. Larger particles fall back with a rate which increases exponentially with their weight and diameter. The mass of all particles returning to the Earth's surface is estimated to be 4 g/m^2 year. Particulate materials have two effects on the weathering process of materials: they can be deposited on the sample surface (most likely by impaction) and also they absorb part of radiant energy from sun. The absorption is more pronounced in the UV and visible regions than in the infrared.

REFERENCES

1. J. S. Levine, *The Photochemistry of Atmospheres*, Academic Press, Orlando 1985
2. N. Wells, *The Atmosphere and Ocean: a Physical Introduction*. Taylor & Francis, London, 1986.
3. A. Henderson-Sellers and P. J. Robinson, *Contemporary Climatology*, Longman, Harlow, 1986.
4. *Atmospheric Ozone 1985*, World Meteorological Organization, Global Ozone Research and Monitoring Project, Vol. I and II.
5. H. Schmetz, *Phil. Trans. Roy. Soc.*, A308 (1983)382.
6. G. Ohring and A. Gruber, *Adv. Geophys.*, 25(1983).
7. E. Hilscher, *Problems with coated polyester fabrics*, Ann. Conf. Ind. Textile Group, Textile Inst., Manchester, 1975.
8. P. Brimblecombe, *Air. Composition & Chemistry*, Cambridge University Press, Cambridge, 1986.
9. E. Meszaros, *Atmospheric Chemistry, Fundamental Aspects*, Elsevier, Amsterdam, 1981.
10. A. Henderson-Sellers and K. McGuffie, *A Climate Modelling Primer*, Wiley, Chichester, 1987.
11. C. N. Hewitt and W. T. Sturges, Eds. *Global Atmospheric Chemical Change*, Elsevier, Applied Science, Barking, 1993.
12. P. Zannetti, C. A. Brebbia, J. E. Garcia Gardea, and G. Ayala Milian, Eds. *Air Pollution, Computational Mechanics Publications*, Boston, 1993.

4

CLIMATIC CONDITIONS

Table 10.1: Conditions of exposure in South Florida Test Service in Miami (average data for the four years - 1989, 1992, 1993, and 1994) [Data from South Florida Test Service, Miami, USA]

Month	Radiation energy MJ/m ² at 45°			Radiation energy MJ/m ² at 5°			Temperature °C			RH %	Wet time h
	Total	UV	%UV	Total	UV	%UV	ambient	under glass	black panel		
JAN	516.00	21.48	4.16	407.05	19.10	4.69	20	26	27	83	445.3
FEB	530.66	23.38	4.41	458.58	21.22	4.63	22	26	24	81	357.6
MAR	610.36	29.33	4.81	583.31	28.22	4.84	21	28	25	81	321.5
APR	538.73	30.85	5.73	624.07	31.16	4.99	23	29	30	79	286.3
MAY	520.17	29.79	5.73	680.87	33.97	4.99	25	29	29	77	261.3
JUN	392.25	24.18	6.16	421.15	28.89	6.86	27	33	31	82	395.7
JUL	430.32	24.70	5.74	584.49	29.99	5.13	28	34	33	81	381.7
AUG	445.10	22.24	5.00	539.22	27.36	5.07	27	34	35	82	367.5
SEP	475.93	23.61	4.96	471.06	25.69	5.45	28	34	32	79	404.0
OCT	539.39	24.76	4.59	487.04	24.39	5.00	25	32	33	80	354.0
NOV	497.08	20.09	4.04	398.26	18.69	4.69	24	29	29	81	377.1
DEC	503.90	19.95	3.96	399.74	17.72	4.43	19	24	23	81	364.6
Total	6000	294.36		6055	306.36						4316.6
Ave.	500.00	24.53	4.91	504.57	25.53	5.06	24	30	29	81	359.7

Tables 10.1 to 10.4 contain reference data on conditions of weathering. These data should be compared with weather data given for numerous locations around the world in the following part of this chapter. The data in Tables 10.1 and 10.2 contain information

on UV radiation in two reference locations: Florida and Arizona. Industry most frequently uses these sites to test durability of materials. The data on UV radiation in Tables 10.1 and 10.2 were obtained from wide band measurement in the range of 290 to 385 nm. The data in Table 10.4 were collected for band between 300 and 400 nm.

Table 10.2: Conditions of exposure in South Florida Test Service in Wittmann, Arizona (average data for the four years - 1989, 1992, 1993, and 1994) [Data from South Florida Test Service, Wittman, USA]

Month	Radiation energy MJ/m ² at 45°			Radiation energy MJ/m ² at 5°			Temperature °C			RH %	Wet time h
	Total	UV	%UV	Total	UV	%UV	ambient	under glass	black panel		
JAN	573.20	20.60	3.59	415.72	18.21	4.38	11	15	21	49	84.10
FEB	547.48	20.69	3.78	466.24	20.43	4.38	13	17	22	50	56.15
MAR	660.43	29.39	4.45	657.08	29.11	4.43	17	21	26	52	62.48
APR	706.75	32.86	4.65	801.58	36.76	4.58	22	26	29	34	8.23
MAY	679.79	33.64	4.95	896.67	41.32	4.61	26	29	31	32	16.63
JUN	643.84	34.54	5.36	910.22	42.08	4.62	31	34	36	25	0
JUL	649.87	33.00	5.08	863.10	39.89	4.62	33	35	39	33	13.48
AUG	680.91	35.16	5.16	727.16	39.75	5.47	32	34	38	42	26.10
SEP	728.43	32.20	4.42	686.71	33.82	4.92	30	32	37	29	5.7
OCT	678.79	27.58	4.06	581.80	27.15	4.66	22	25	29	34	11.2
NOV	641.96	20.46	3.19	467.20	18.59	3.98	14	17	22	36	11.1
DEC	573.42	17.29	3.02	391.52	15.05	3.84	11	14	18	47	66.9
Total	7764.8	337.44		7865	362.16						361.97
Ave.	647.07	28.12	4.35	655.42	30.18	4.60	22	25	29	39	30.16

When we compare the data in Tables 10.1 and 10.2 with the data in Table 10.4, we see that for most of the year in Florida and for the entire year in Arizona, the percentage of radiation was lower than the world standard UV radiation (6.07%). The percentage of UV in both Florida and Arizona varies throughout the year (at a maximum in Florida during June and in Arizona during August). The angle of inclination of the plane on which radiation is measured also influences the percentage UV energy of the total radiation. Florida measurements show a very interesting anomaly: the radiation peak is

Table 10.3: Mean values of irradiation at 340 nm in MJ/m²

Month	Miami, FL (1983)	Whittmann, AZ (1983)	Toronto, Canada (average for 1989-95)
JAN	0.3436	0.2381	0.0902
FEB	0.3516	0.2435	0.1406
MAR	0.4563	0.3369	0.1931
APR	0.4830	0.4355	0.2406
MAY	0.4961	0.3947	0.3227
JUN	0.4148	0.3786	0.3375
JUL	0.4619	0.3575	0.3658
AUG	0.3593	0.3527	0.3094
SEP	0.2866	0.2988	0.2196
OCT	0.3336	0.2651	0.1609
NOV	0.2808	0.2085	0.0840
DEC	0.2698	0.1740	0.0732
TOTAL	4.5372	3.6839	2.5376

higher than the percentage of radiation given in the CIE Publication # 20 (Table 10.4). This difference may have several causes, including the conditions of measurement, the specific conditions in Florida in which more radiation may be absorbed in wavelengths other than UV (see Chapter 3), and because the amount of UV radiation in daylight recently may have increased due to changes in the atmosphere.

Data included in Tables 10.1 and 10.2 confirm that Arizona exposure is characterized by a higher energy of UV radiation. The UV exposure dose in Arizona is higher by 14.6-18.2% (depending on the angle of inclination) than in Florida. Exposure at 5° gives a more uniform distribution of energy throughout the year than exposure at 45°.

When we compare the data from Tables 10.1 and 10.2 with the data in Table 10.3 which was measured by a narrow band (340 nm) instrument, we see that Florida readings at 340 nm are 23.2% higher than Arizona readings which is just the reverse of the wide band readings. The data in Table 10.3 for the three locations correlated very well with their latitudes (correlation coefficient: -0.999). In the literature, there is no reasons given for these differences. They may be due to different absorptions by clouds of different wavelengths or due to measurement. From this data alone, it can be concluded that the regression equation:

Table 10.4: Global radiation [Data from CIE Publication # 20]

Wavelength, nm	Irradiance, W/m ²	Percentage of total radiation	Percentage of total radiation in each range, %
<280	0	0	0
280-320	5	0.45	
320-360	27	2.41	6.07
360-400	36	3.21	
400-440	56	5.00	
440-480	73	6.52	
480-520	71	6.34	
520-560	65	5.80	
560-600	60	5.36	51.79
600-640	61	5.45	
640-680	55	4.91	
680-720	52	4.64	
720-760	46	4.11	
760-800	41	3.66	
800-1000	156	13.93	
1000-1200	108	9.64	29.37
1200-1400	65	5.80	
1400-1600	44	3.93	
1600-1800	29	2.59	
1800-2000	20	1.78	12.77
2000-2500	35	3.13	
2500-3000	15	1.34	
>3000	0	0	0
Total	1120	100	100

$$(\text{Radiation energy}) = 0.118(\text{latitude}) + 7.63$$

predicts data for the three locations with less than 1% error. Also, correlation between UV energy and latitude agrees with theory. But the question remains: why is data obtained from broader band measurements different?

It is useful to compare temperature data between Florida and Arizona. A black panel system was chosen by the automotive industry to increase the temperature of exposure. The data show that in Florida, where the humidity is higher and wet time longer, the black panel temperature is almost identical to the exposure under glass. This is probably caused by the evaporation of water from the sample surface which has cooling effect helping to hold the temperature from rising higher. In Arizona, where there is a lower humidity and shorter wet time there is little evaporative cooling and the black panel temperature is consistently higher than the temperature of exposure under glass which is even higher than the ambient temperature.

In conclusion, the data for global radiation in different locations (presented in this chapter below) give only a partial indication of the severity of exposure because the most important information - UV radiation energy - is not available. The percentage of UV varies between locations along with other parameters, such as temperature, humidity, wet time, length of cloudless exposure period, wind direction and speed, latitude, and angle of exposure. Since some of these parameters influence percentage of UV radiation in a complex way, it is not possible to estimate amount of UV radiation based on global radiation data. The best practice is to measure radiation in the exposure location. This is often not possible so the data on global radiation given below should be used cautiously, knowing that they offer only crude approximation of energy which can be utilized for chemical conversions. The other possible solution would be to expose samples only in locations where full data are available.

Tables below give the data characterizing climatic conditions in 79 locations from 19 countries. For some locations data on pollutant concentrations were also available. Station *Baseline* in Australia provides data for an environment known to have very low pollution and is frequently used as a point of reference.

The numbers in parentheses give the hour at which temperature or relative humidity was measured. The abbreviation (av) means “mean” temperature or relative humidity. Values for “year” are either average values or a sum, as in the case of “Total precipitation”, “Mean rainfall”, “Mean snowfall”, or “Total bright sunshine”. “Period” means the length of observation time.

Data were kindly supplied by the following organizations:

Bureau of Meteorology, Melbourne, Australia
Bureau of Meteorology, Tasmania, Australia
Department of Meteorology, Colombo, Sri Lanka
Directorate General of Civil Aviation, Kuwait
Environment Canada, Toronto, Canada
Environment Protection Authority, Melbourne, Australia
Environment Protection Authority, Perth, Australia
Environment Protection Department, Hong Kong
Federal Ministry of Civil Aviation, Lagos, Nigeria
Government of India, Meteorological Department, New Delhi, India
Government of Singapore, Singapore
Institut National de la Meteorologie, Tunis, Republique Tunisienne
Japan Meteorological Agency, Tokyo, Japan
Meteorological Department, The Republic of Sudan, Khartoum, Sudan
Meteorological Office, London, Great Britain
Ministry of Environment and Physical Planning, Athens, Greece
Ministry of Defense, Athens, Greece
Royal Observatory, Kowloon, Hong Kong
South Florida Test Service, Miami, USA
Sweizerische Meteorologische Anstalt, Zürich, Switzerland
Turkish State Meteorological Service, Ankara, Turkey
US Department of Commerce, Asheville, USA
Zentralanstalt für Meteorologie und Geodynamik, Vienna, Austria

Location: Alert, NWT, Canada

Latitude: 82 30N

Longitude: 62 20W

Altitude: 62 m

Parameter	JAN	FEB	MAR	APR	MAY	JUN	JUL	AUG	SEP	OCT	NOV	DEC	YEAR
Temperature, °C (13)	-31	-33	-32	-23	-12	0	5	1	-9	-19	-25	-30	-17
Relative humidity, % (13)	70	62	60	63	73	80	78	84	83	76	69	62	72
Mean rainfall, mm	0	0	0	0	0	3	8	7	0.2	0	0	0	18
Mean snowfall, cm	7	6	7	8	13	10	11	21	33	16	9	8	148
Total precipitation, mm	7	5	7	8	10	12	20	28	28	14	8	8	154
Total bright sunshine, h	0	0	67	390	410	304	299	207	83	9	0	0	1767
Global radiation, MJ m ⁻²	0	0	2	12	23	25	19	11	4	0	0	0	8
Net radiation MJ m ⁻²	-1	-1	-1	-1	0	6	11	4	-1	-2	-1	-1	1

Location: Eureka, NWT, Canada

Latitude: 80 00N

Longitude: 85 56W

Altitude: 10 m

Parameter	JAN	FEB	MAR	APR	MAY	JUN	JUL	AUG	SEP	OCT	NOV	DEC	YEAR
Temperature, °C (13)	-36	-38	-37	-26	-10	2	6	4	-7	-22	-32	-35	-19
Relative humidity, % (13)	68	79	64	73	79	77	76	81	84	78	74	73	76
Mean rainfall, mm	0	0	0	0	0	3	11	9	0	0	0	0	23
Mean snowfall, cm	3	3	2	3	4	2	1	3	10	8	3	3	44
Total precipitation, mm	3	2	2	3	3	5	12	12	10	7	3	2	64
Total bright sunshine, h	0	0	118	355	521	405	341	240	102	9	0	0	2091
Global radiation, MJ m ⁻²	0	0	3	12	23	25	19	11	4	1	0	0	8
Net radiation MJ m ⁻²	-2	-1	-2	-1	4	13	10	4	-1	-2	-2	-1	2

Location: Resolute A, NWT, Canada

Latitude: 74 43N

Longitude: 94 59W

Altitude: 67 m

Parameter	JAN	FEB	MAR	APR	MAY	JUN	JUL	AUG	SEP	OCT	NOV	DEC	YEAR
Temperature, °C (13)	-32	-33	-31	-22	-9	0	5	3	-4	-15	-25	-29	-16
Relative humidity, % (13)	68	67	67	71	81	84	81	85	87	82	72	69	76
Mean rainfall, mm	0	0	0	0	0	5	19	25	4	0	0	0	53
Mean snowfall, cm	3	3	3	7	9	7	3	7	15	15	6	5	84
Total precipitation, mm	3	3	3	6	8	12	23	31	18	14	6	5	131
Total bright sunshine, h	0	18	146	276	292	256	274	159	59	24	0	0	1505
Global radiation, MJ m ⁻²	0	1	5	15	23	25	19	11	5	1	0	0	9
Net radiation MJ m ⁻²	-2	-2	-2	-1	2	8	9	5	0	-2	-2	-2	1

Location: **Baker Lake, NWT, Canada**

Latitude: 64 18N

Longitude: 96 00W

Altitude: 18 m

Parameter	JAN	FEB	MAR	APR	MAY	JUN	JUL	AUG	SEP	OCT	NOV	DEC	YEAR
Temperature, °C (13)	-32	-31	-27	-15	-4	6	14	12	4	-6	-20	-28	-11
Relative humidity, % (13)	66	66	66	74	80	71	63	67	76	82	75	69	71
Mean rainfall, mm	0	0	0	0	6	18	38	37	31	8	0	0	138
Mean snowfall, cm	8	5	8	14	6	3	0	0	6	23	17	9	100
Total precipitation, mm	7	5	8	14	12	21	38	37	37	31	17	8	235
Total bright sunshine, h	36	107	190	235	264	262	301	211	107	72	51	7	1843
Global radiation, MJ m ⁻²	1	3	10	18	22	22	19	13	8	4	1	0	10
Net radiation MJ m ⁻²	-2	-2	-2	0	6	11	9	6	2	-1	-2	-2	2

Location: **Edmonton Stony Plain, Alberta, Canada**

Latitude: 53 33N

Longitude: 114 06W

Altitude: 767 m

Parameter	JAN	FEB	MAR	APR	MAY	JUN	JUL	AUG	SEP	OCT	NOV	DEC	YEAR
Temperature, °C (13)	-14	-9	-3	7	15	18	20	19	14	10	-2	-11	5
Relative humidity, % (13)	71	72	69	53	43	51	57	58	57	53	67	73	60
Mean rainfall, mm	1	1	3	12	45	99	96	74	44	12	4	3	391
Mean snowfall, cm	25	19	18	15	3	0	0	0	1	9	18	25	131
Total precipitation, mm	27	21	21	26	48	99	96	74	45	20	23	29	529
Total bright sunshine, h	98	119	172	233	284	287	313	284	183	163	103	78	2315
Global radiation, MJ m ⁻²	4	7	12	18	20	22	22	18	12	8	4	3	12
Net radiation MJ m ⁻²	-2	-1	1	6	9	10	11	8	4	1	-2	-2	4

Location: **Sandspit A, BC, Canada**

Latitude: 53 15N

Longitude: 131 49W

Altitude: 8 m

Parameter	JAN	FEB	MAR	APR	MAY	JUN	JUL	AUG	SEP	OCT	NOV	DEC	YEAR
Temperature, °C (13)	3	5	6	8	10	13	15	16	15	11	7	4	9
Relative humidity, % (13)	84	82	77	76	76	77	78	77	78	80	82	84	79
Mean rainfall, mm	113	98	89	82	52	52	43	50	90	194	176	162	1200
Mean snowfall, cm	34	16	11	2	0	0	0	0	0	0	5	17	85
Total precipitation, mm	144	113	100	84	52	52	43	50	90	194	181	178	1281
Total bright sunshine, h	58	82	121	155	210	175	187	175	139	91	64	40	1496
Global radiation, MJ m ⁻²	2	5	9	14	18	18	17	15	11	6	3	2	10

Location: Goose UA, Newfoundland, Canada

Latitude: 53 18N

Longitude: 60 22W

Altitude: 36 m

Parameter	JAN	FEB	MAR	APR	MAY	JUN	JUL	AUG	SEP	OCT	NOV	DEC	YEAR
Temperature, °C (13)	-15	-12	-6	1	8	15	19	17	12	5	-2	-11	3
Relative humidity, % (13)	71	69	67	66	58	56	59	60	61	66	75	73	65
Mean rainfall, mm	2	4	4	14	45	89	105	103	85	52	21	6	529
Mean snowfall, cm	80	61	75	49	18	4	0	0	4	25	57	74	445
Total precipitation, mm	74	60	72	61	64	93	105	103	89	77	75	80	946
Total bright sunshine, h	88	117	129	140	176	187	196	176	121	94	66	73	1565
Global radiation, MJ m ⁻²	3	7	12	16	18	19	18	14	10	6	3	3	11
Net radiation, MJ m ⁻²	-2	-2	-1	1	7	8	8	6	3	0	-1	-2	2

Location: Nichequon, Quebec, Canada

Latitude: 53 12N

Longitude: 70 54W

Altitude: 536 m

Parameter	JAN	FEB	MAR	APR	MAY	JUN	JUL	AUG	SEP	OCT	NOV	DEC	YEAR
Temperature, °C (13)	-20	-18	-10	-2	5	12	16	14	8	1	-7	-17	-2
Relative humidity, % (13)	78	78	77	73	67	61	64	68	69	75	81	84	80
Mean rainfall, mm	0	0	3	8	37	80	107	111	88	45	14	3	496
Mean snowfall, cm	39	32	34	30	16	3	0	1	10	39	51	42	296
Total precipitation, mm	37	29	36	37	53	84	107	112	99	83	63	43	783
Total bright sunshine, h	79	124	151	187	216	216	203	182	99	55	34	59	1604
Global radiation, MJ m ⁻²	4	8	13	19	20	19	17	14	9	5	3	3	11

Location: Kapuskasing, Ontario, Canada

Latitude: 49 25N

Longitude: 82 28W

Altitude: 226 m

Parameter	JAN	FEB	MAR	APR	MAY	JUN	JUL	AUG	SEP	OCT	NOV	DEC	YEAR
Temperature, °C (13)	-16	-13	-5	4	12	18	21	19	13	7	-2	-13	4
Relative humidity, % (13)	76	69	64	59	54	55	59	61	66	70	79	79	66
Mean rainfall, mm	1	1	10	29	64	84	96	93	92	57	20	3	552
Mean snowfall, cm	55	44	48	25	10	1	0	0	2	21	62	53	320
Total precipitation, mm	54	43	55	53	74	85	96	93	94	77	80	53	858
Total bright sunshine, h	81	111	142	466	201	221	239	215	121	84	47	58	1687
Global radiation, MJ m ⁻²	5	9	14	17	20	23	21	16	12	7	4	4	13

Location: Vancouver, BC, Canada

Latitude: 49 15N

Longitude: 123 15W

Altitude: 87 m

Parameter	JAN	FEB	MAR	APR	MAY	JUN	JUL	AUG	SEP	OCT	NOV	DEC	YEAR
Temperature, °C (13)	4	7	8	11	15	17	20	20	17	12	8	5	12
Relative humidity, % (13)	80	78	72	68	65	66	65	68	72	78	79	83	73
Mean rainfall, mm	304	253	226	159	120	99	72	97	149	304	323	389	2494
Mean snowfall, cm	47	21	11	1	0	0	0	0	0	0	6	37	123
Total precipitation, mm	351	271	236	160	120	99	72	97	149	304	328	426	2612
Total bright sunshine, h	55	83	129	168	240	236	297	244	181	123	69	49	1872
Global radiation, MJ m ⁻²	3	5	10	15	20	22	23	19	13	7	4	2	12

Location: Toronto, Ontario, Canada

Latitude: 43 48N

Longitude: 79 33W

Altitude: 194 m

Parameter	JAN	FEB	MAR	APR	MAY	JUN	JUL	AUG	SEP	OCT	NOV	DEC	YEAR
Temperature, °C (13)	-5	-4	2	9	16	22	25	24	20	13	6	-2	11
Relative humidity, % (13)	76	74	70	59	55	57	54	57	60	63	72	78	65
Mean rainfall, mm	23	20	36	60	63	65	70	75	62	57	55	35	619
Mean snowfall, cm	28	23	20	6	0	0	0	0	0	1	7	34	120
Total precipitation, mm	53	45	61	66	63	65	70	75	62	58	62	68	747
Total bright sunshine, h	94	123	144	194	230	273	296	247	184	142	79	77	2083
Global radiation, MJ m ⁻²	6	9	13	17	20	22	22	19	14	9	5	4	13
Net radiation, MJ m ⁻²	-1	0	3	8	10	11	11	9	6	3	1	-1	5

Location: Korrør Island, Pacific, USA

Latitude: 7 20N

Longitude: 134 29E

Altitude: 33 m

Parameter	JAN	FEB	MAR	APR	MAY	JUN	JUL	AUG	SEP	OCT	NOV	DEC	YEAR
Temperature, °F (15)	81	81	81	82	82	82	81	81	82	82	82	82	82
Relative humidity, % (15)	76	75	74	74	77	78	78	77	77	77	77	77	77
Total precipitation, in	11	8	8	10	13	15	16	15	13	14	11	13	148
Precipitation >0.1 in, days	22	19	20	19	24	25	24	23	21	23	22	24	267
Possible sunshine, %	56	58	66	64	57	47	49	47	55	49	54	51	54
Global radiation, MJ m ⁻²	16	18	19	19	18	17	16	17	17	17	16	15	17

Location: San Juan, Puerto Rico, USA

Latitude: 18 26N

Longitude: 66 00W

Altitude: 19 m

Parameter	JAN	FEB	MAR	APR	MAY	JUN	JUL	AUG	SEP	OCT	NOV	DEC	YEAR
Temperature, °F (14)	77	77	78	79	80	82	82	82	82	81	80	78	80
Relative humidity, % (14)	63	62	60	61	65	66	66	66	67	66	66	66	65
Total precipitation, in	3	2	2	4	6	5	5	6	6	6	6	4	54
Precipitation >0.1 in, days	16	13	12	13	17	16	19	19	17	17	18	20	196
Possible sunshine, %	67	69	74	68	60	62	67	66	61	61	59	59	64
Global radiation, MJ m ⁻²	15	17	20	21	21	21	21	21	19	17	16	14	19

Location: Wake Island, Pacific, USA

Latitude: 19 17N

Longitude: 166 39E

Altitude: 4 m

Parameter	JAN	FEB	MAR	APR	MAY	JUN	JUL	AUG	SEP	OCT	NOV	DEC	YEAR
Temperature, °F (12)	77	77	78	78	80	82	83	83	83	82	80	78	80
Relative humidity, % (12)	65	65	67	68	69	68	70	71	71	71	69	67	68
Total precipitation, in	1	1	2	2	2	2	4	5	6	5	3	2	35
Precipitation >0.1 in, days	11	10	12	14	15	16	19	19	19	19	15	13	181
Possible sunshine, %	69	74	77	72	74	76	72	70	70	69	63	66	71
Global radiation, MJ m ⁻²	15	18	21	22	23	23	22	21	20	18	16	15	20

Location: Honolulu, Hawaii, USA

Latitude: 21 20N

Longitude: 157 55W

Altitude: 5 m

Parameter	JAN	FEB	MAR	APR	MAY	JUN	JUL	AUG	SEP	OCT	NOV	DEC	YEAR
Temperature, °F (14)	73	73	74	76	78	79	80	81	81	80	77	74	77
Relative humidity, % (14)	63	59	58	57	54	53	52	53	52	55	59	61	56
Total precipitation, in	4	3	3	1	1	1	1	1	2	3	3	23	46
Precipitation >0.1 in, days	10	9	9	9	7	6	7	6	7	9	9	10	100
Possible sunshine, %	62	64	68	66	68	70	73	75	75	68	61	59	67
Global radiation, MJ m ⁻²	13	16	18	20	22	23	23	22	21	17	14	13	19

Location: Miami, Florida, USA

Latitude: 25 48N

Longitude: 80 16W

Altitude: 2 m

Parameter	JAN	FEB	MAR	APR	MAY	JUN	JUL	AUG	SEP	OCT	NOV	DEC	YEAR
Temperature, °F (13)	67	68	72	75	79	81	83	83	82	78	73	69	76
Relative humidity, % (13)	59	57	56	55	60	66	63	65	67	64	61	59	61
Total precipitation, in	2	2	2	3	7	9	6	7	8	7	3	2	58
Precipitation >0.1 in, days	7	6	6	6	10	15	16	16	17	15	8	7	129
Possible sunshine, %	68	66	77	77	70	74	76	75	72	71	66	66	72
Global radiation, MJ m ⁻²	12	15	18	21	21	19	20	18	17	15	13	12	17

Location: Tampa, Florida, USA

Latitude: 27 58N

Longitude: 82 32W

Altitude: 3 m

Parameter	JAN	FEB	MAR	APR	MAY	JUN	JUL	AUG	SEP	OCT	NOV	DEC	YEAR
Temperature, °F (13)	60	61	66	72	77	81	82	82	81	74	67	61	72
Relative humidity, % (13)	59	56	55	51	53	60	63	64	62	57	57	59	58
Total precipitation, in	2	3	3	2	3	5	7	8	6	2	2	2	47
Precipitation >0.1 in, days	6	7	7	5	6	12	16	17	13	7	5	6	107
Possible sunshine, %	64	66	71	74	75	67	61	60	61	65	65	62	66
Global radiation, MJ m ⁻²	11	14	18	22	23	21	20	19	17	15	13	11	17

Location: New Orleans, Louisiana, USA

Latitude: 29 59N

Longitude: 90 15W

Altitude: 3 m

Parameter	JAN	FEB	MAR	APR	MAY	JUN	JUL	AUG	SEP	OCT	NOV	DEC	YEAR
Temperature, °F (12)	52	55	61	69	75	80	82	82	79	69	60	55	68
Relative humidity, % (12)	66	63	60	60	60	62	66	66	65	59	61	66	63
Total precipitation, in	5	5	5	5	5	5	7	6	6	3	4	5	60
Precipitation >0.1 in, days	10	9	9	7	8	10	15	13	10	6	7	10	114
Possible sunshine, %	48	52	57	63	62	67	61	61	63	66	55	54	59
Global radiation, MJ m ⁻²	9	13	16	20	22	23	21	19	17	15	11	9	16

Location: Houston, Texas, USA

Latitude: 29 59N

Longitude: 95 22W

Altitude: 33 m

Parameter	JAN	FEB	MAR	APR	MAY	JUN	JUL	AUG	SEP	OCT	NOV	DEC	YEAR
Temperature, °F (12)	51	55	61	69	75	81	83	83	78	70	60	54	68
Relative humidity, % (12)	64	60	60	59	59	59	58	59	61	57	59	61	60
Total precipitation, in	3	3	3	4	5	4	3	4	5	4	3	4	45
Mean snowfall, in	0.2	0.2	0	0	0	0	0	0	0	0	0	0	0.4
Precipitation >0.1 in, days	10	8	10	7	8	8	10	10	10	8	9	8	105
Possible sunshine, %	43	50	47	51	58	64	66	64	62	59	52	55	56
Global radiation, MJ m ⁻²	9	12	15	17	20	22	21	19	17	14	10	8	15

Location: Tallahassee, Florida, USA

Latitude: 30 23N

Longitude: 84 22W

Altitude: 21 m

Parameter	JAN	FEB	MAR	APR	MAY	JUN	JUL	AUG	SEP	OCT	NOV	DEC	YEAR
Temperature, °F (13)	52	54	60	67	74	80	81	81	78	68	59	53	67
Relative humidity, % (13)	59	54	52	48	51	55	62	63	59	53	55	58	56
Precipitation >0.1 in, days	10	9	9	7	9	12	17	15	9	5	7	8	116
Global radiation, MJ m ⁻²	10	13	17	21	22	21	20	19	17	15	11	9	16

Location: Mobile, Alabama, USA

Latitude: 30 41N

Longitude: 88 15W

Altitude: 67 m

Parameter	JAN	FEB	MAR	APR	MAY	JUN	JUL	AUG	SEP	OCT	NOV	DEC	YEAR
Temperature, °F (12)	51	54	60	68	75	81	82	82	78	69	59	53	68
Relative humidity, % (12)	61	55	55	53	54	54	60	61	59	53	57	61	57
Total precipitation, in	5	5	6	6	5	5	8	7	7	3	4	5	67
Mean snowfall, in	0.1	0.1	0	0	0	0	0	0	0	0	0	0.1	0.3
Precipitation >0.1 in, days	11	10	11	8	8	11	16	14	10	6	8	10	123
Global radiation, MJ m ⁻²	9	12	16	20	21	21	19	19	16	15	11	9	16

Location: El Paso, Texas, USA

Latitude: 31 48N

Longitude: 106 24W

Altitude: 1194 m

Parameter	JAN	FEB	MAR	APR	MAY	JUN	JUL	AUG	SEP	OCT	NOV	DEC	YEAR
Temperature, °F (17)	44	48	55	64	72	81	83	80	74	64	51	44	63
Relative humidity, % (17)	36	26	21	16	16	18	28	32	34	30	33	36	27
Total precipitation, in	0.4	0.5	0.3	0.2	0.2	0.6	2	1	1	1	0.3	0.4	8
Mean snowfall, in	1	1	0.5	0.4	0	0	0	0	0	0	1	1	5
Precipitation >0.1 in, days	4	3	2	2	2	3	8	7	5	4	3	4	47
Possible sunshine, %	77	82	85	87	89	89	80	81	82	83	82	78	83
Global radiation, MJ m ⁻²	13	17	22	27	30	30	28	26	23	19	14	12	22

Location: Savannah, Georgia, USA

Latitude: 32 08N

Longitude: 81 12W

Altitude: 16 m

Parameter	JAN	FEB	MAR	APR	MAY	JUN	JUL	AUG	SEP	OCT	NOV	DEC	YEAR
Temperature, °F (13)	49	52	58	66	73	79	81	81	77	67	58	51	66
Relative humidity, % (13)	54	49	48	46	52	57	59	61	60	54	51	54	54
Total precipitation, in	3	3	4	3	5	6	7	7	5	2	2	3	50
Precipitation >0.1 in, days	9	9	9	7	9	11	14	12	10	6	6	8	111
Possible sunshine, %	55	58	62	70	67	65	62	62	57	63	62	55	62
Global radiation, MJ m ⁻²	9	12	16	20	21	21	20	18	15	14	11	9	15

Location: Yuma, Arizona, USA

Latitude: 32 40N

Longitude: 114 36W

Altitude: 63 m

Parameter	JAN	FEB	MAR	APR	MAY	JUN	JUL	AUG	SEP	OCT	NOV	DEC	YEAR
Temperature, °F (17)	56	60	64	71	78	87	94	92	87	76	64	57	74
Relative humidity, % (17)	28	24	21	17	15	13	22	24	24	23	27	32	23
Total precipitation, in	0.4	0.3	0.2	0.1	0	0	0.2	0.4	0.3	0.3	0.2	0.3	3
Precipitation >0.1 in, days	3	2	2	1	0	0	1	2	1	1	2	3	17
Possible sunshine, %	83	87	90	94	96	97	90	91	93	92	86	82	90
Global radiation, MJ m ⁻²	12	16	22	27	31	32	28	26	23	18	14	11	22

Location: Phoenix, Arizona, USA

Latitude: 33 26N

Longitude: 112 01W

Altitude: 339 m

Parameter	JAN	FEB	MAR	APR	MAY	JUN	JUL	AUG	SEP	OCT	NOV	DEC	YEAR
Temperature, °F (17)	52	56	61	68	77	87	92	90	85	73	61	53	71
Relative humidity, % (17)	32	27	24	16	13	12	20	23	23	23	28	34	23
Total precipitation, in	0.7	0.6	0.8	0.3	0.1	0.2	0.7	1	0.6	0.6	0.5	0.8	7
Precipitation >0.1 in, days	4	4	4	2	1	1	4	5	3	3	3	4	36
Possible sunshine, %	78	80	83	88	93	94	85	85	89	88	83	77	85
Global radiation, MJ m ⁻²	12	16	21	27	30	31	28	26	23	18	13	11	21

Location: Birmingham, Alabama, USA

Latitude: 33 34N

Longitude: 86 45W

Altitude: 192 m

Parameter	JAN	FEB	MAR	APR	MAY	JUN	JUL	AUG	SEP	OCT	NOV	DEC	YEAR
Temperature, °F (12)	43	46	54	63	70	77	80	79	74	63	52	46	62
Relative humidity, % (12)	62	55	53	52	56	57	61	61	59	55	57	60	57
Total precipitation, in	5	5	7	5	5	4	5	4	4	3	4	5	55
Mean snowfall, in	0.6	0.2	0.1	0	0	0	0	0	0	0	0	0.4	1
Precipitation >0.1 in, days	11	10	11	9	10	10	13	10	8	6	9	11	117
Possible sunshine, %	42	50	55	63	66	65	59	63	61	66	55	46	58
Global radiation, MJ m ⁻²	8	11	15	19	21	22	21	20	17	14	10	8	15

Location: Los Angeles, California, USA

Latitude: 33 56N

Longitude: 118 24W

Altitude: 32 m

Parameter	JAN	FEB	MAR	APR	MAY	JUN	JUL	AUG	SEP	OCT	NOV	DEC	YEAR
Temperature, °F (16)	56	57	57	60	62	66	69	70	70	66	61	57	63
Relative humidity, % (16)	59	62	65	63	65	67	67	68	66	64	62	61	64
Total precipitation, in	3	2	2	1	0	0	0	0	0.2	0.3	2	2	12
Precipitation >0.1 in, days	6	6	6	4	1	1	1	0	1	2	4	5	36
Possible sunshine, %	69	72	73	70	66	65	82	83	79	73	74	71	73
Global radiation, MJ m ⁻²	11	14	18	22	23	24	26	23	19	14	11	10	18

Location: Memphis, Tennessee, USA

Latitude: 35 03N

Longitude: 89 59W

Altitude: 87 m

Parameter	JAN	FEB	MAR	APR	MAY	JUN	JUL	AUG	SEP	OCT	NOV	DEC	YEAR
Temperature, °F (12)	40	44	52	63	71	79	82	81	74	63	51	43	62
Relative humidity, % (12)	63	59	56	54	55	56	57	57	56	51	56	61	57
Total precipitation, in	5	4	5	6	5	4	4	4	4	2	4	5	52
Mean snowfall, in	3	2	1	0	0	0	0	0	0	0	0.1	0.7	6
Precipitation >0.1 in, days	10	10	11	10	9	8	9	8	7	6	9	10	107
Possible sunshine, %	50	54	56	64	69	74	74	75	69	70	58	50	64
Global radiation, MJ m ⁻²	8	11	15	19	21	23	22	21	17	14	9	7	16

Location: Albuquerque, New Mexico, USA

Latitude: 35 03N

Longitude: 106 37W

Altitude: 1619 m

Parameter	JAN	FEB	MAR	APR	MAY	JUN	JUL	AUG	SEP	OCT	NOV	DEC	YEAR
Temperature, °F (17)	35	39	46	55	64	75	79	76	69	57	44	36	56
Relative humidity, % (17)	41	32	25	18	18	17	27	30	31	30	36	43	29
Total precipitation, in	0.4	0.4	0.5	0.4	0.5	0.5	1	2	0.9	0.9	0.4	0.5	8
Mean snowfall, in	3	2	2	0.5	0	0	0	0	0	0	1	3	11
Precipitation >0.1 in, days	4	4	5	3	4	4	9	9	6	5	3	4	60
Possible sunshine, %	72	73	73	77	80	83	76	76	79	79	77	72	76
Global radiation, MJ m ⁻²	12	15	20	25	29	30	28	26	22	18	13	11	21

Location: Cape Hatteras, North Carolina, USA

Latitude: 35 16N

Longitude: 75 33W

Altitude: 2 m

Parameter	JAN	FEB	MAR	APR	MAY	JUN	JUL	AUG	SEP	OCT	NOV	DEC	YEAR
Temperature, °F (13)	45	46	51	59	67	74	78	78	74	65	56	49	62
Relative humidity, % (13)	68	64	62	59	65	68	70	69	67	66	64	66	66
Total precipitation, in	5	4	4	3	4	4	5	6	6	5	5	4	56
Mean snowfall, in	0.5	0.7	0.6	0	0	0	0	0	0	0	0	0.1	2
Precipitation >0.1 in, days	11	10	10	8	11	9	12	10	9	9	9	10	119
Possible sunshine, %	49	53	60	66	62	62	62	63	62	58	56	48	58
Global radiation, MJ m ⁻²	8	11	15	20	22	23	22	19	17	13	10	7	16

Location: Fort Smith, Arkansas, USA

Latitude: 35 20N

Longitude: 94 22W

Altitude: 141 m

Parameter	JAN	FEB	MAR	APR	MAY	JUN	JUL	AUG	SEP	OCT	NOV	DEC	YEAR
Temperature, °F (12)	38	42	51	61	70	77	82	81	74	63	50	41	61
Relative humidity, % (12)	60	57	53	52	57	57	54	53	55	51	56	60	55
Total precipitation, in	2	3	4	4	5	4	3	3	3	3	4	3	40
Mean snowfall, in	3	2	1	0	0	0	0	0	0	0	0.5	1	7
Precipitation >0.1 in, days	8	8	9	10	10	8	8	7	7	7	7	7	96
Possible sunshine, %	50	55	56	59	63	69	73	72	66	65	55	51	61
Global radiation, MJ m ⁻²	8	11	15	18	22	24	23	21	17	14	10	8	16

Location: Las Vegas, Nevada, USA

Latitude: 36 05N

Longitude: 115 10W

Altitude: 664 m

Parameter	JAN	FEB	MAR	APR	MAY	JUN	JUL	AUG	SEP	OCT	NOV	DEC	YEAR
Temperature, °F (14)	45	50	55	64	73	84	90	88	80	68	54	45	66
Relative humidity, % (14)	31	26	22	15	13	10	15	17	17	19	27	33	20
Total precipitation, in	0.5	0.5	0.4	0.2	0.2	0.1	0.5	0.5	0.3	0.3	0.4	0.3	4
Mean snowfall, in	1	0	0	0	0	0	0	0	0	0	0.1	0.1	1
Precipitation >0.1 in, days	3	3	3	2	1	1	3	3	2	2	2	3	26
Possible sunshine, %	77	81	83	87	88	93	87	88	91	87	80	78	85
Global radiation, MJ m ⁻²	11	15	21	26	30	31	29	27	23	17	12	10	21

Location: San Francisco, California, USA

Latitude: 37 37N

Longitude: 122 23W

Altitude: 5 m

Parameter	JAN	FEB	MAR	APR	MAY	JUN	JUL	AUG	SEP	OCT	NOV	DEC	YEAR
Temperature, °F (16)	49	52	53	55	58	61	62	63	64	61	55	49	57
Relative humidity, % (16)	66	65	63	60	60	59	59	61	58	59	64	68	62
Total precipitation, in	5	3	3	2	0.3	0.1	0	0	0.2	1	2	4	20
Precipitation >0.1 in, days	11	10	10	6	3	1	0	0	1	4	7	10	63
Possible sunshine, %	56	62	69	73	72	73	66	65	72	70	62	53	66
Global radiation, MJ m ⁻²	8	11	17	22	25	27	27	24	20	14	9	7	18

Location: Sacramento, California, USA

Latitude: 38 31N

Longitude: 121 30 W

Altitude: 8 m

Parameter	JAN	FEB	MAR	APR	MAY	JUN	JUL	AUG	SEP	OCT	NOV	DEC	YEAR
Temperature, °F (16)	45	50	53	58	65	71	76	75	72	64	53	46	61
Relative humidity, % (16)	71	61	53	44	35	31	28	29	32	39	60	71	46
Total precipitation, in	4	3	2	1	0.3	0.1	0.1	0.1	0.3	1	2	3	17
Precipitation >0.1 in, days	10	9	9	6	3	1	0	0	1	3	7	9	58
Possible sunshine, %	44	62	72	81	89	93	97	96	93	85	63	46	77
Global radiation, MJ m ⁻²	7	11	17	23	28	30	31	27	22	15	9	6	19

Location: Washington, DC, USA

Latitude: 38 57N

Longitude: 77 27W

Altitude: 88 m

Parameter	JAN	FEB	MAR	APR	MAY	JUN	JUL	AUG	SEP	OCT	NOV	DEC	YEAR
Temperature, °F (13)	31	34	42	53	62	71	76	74	67	55	45	35	54
Relative humidity, % (13)	59	55	52	48	56	58	56	56	56	56	56	58	56
Total precipitation, in	3	3	3	3	4	4	4	4	3	3	3	3	40
Mean snowfall, in	7	7	3	0.2	0	0	0	0	0	0.1	1	4	23
Precipitation >0.1 in, days	10	9	10	10	12	10	10	10	8	8	9	10	117
Possible sunshine, %	48	52	55	58	59	64	64	63	63	58	51	47	57
Global radiation, MJ m ⁻²	6	9	13	17	19	22	21	18	15	11	7	5	14

Location: Denver, Colorado, USA

Latitude: 39 45N

Longitude: 104 52W

Altitude: 1625 m

Parameter	JAN	FEB	MAR	APR	MAY	JUN	JUL	AUG	SEP	OCT	NOV	DEC	YEAR
Temperature, °F (17)	30	33	38	47	57	67	73	71	63	52	39	33	50
Relative humidity, % (17)	49	43	41	35	38	35	34	35	34	35	49	51	40
Total precipitation, in	0.5	0.7	1	2	2	2	2	2	1	1	0.8	0.6	15
Mean snowfall, in	8	7	13	9	2	0	0	0	2	4	8	7	60
Precipitation >0.1 in, days	6	6	9	9	11	9	9	9	6	5	5	5	88
Possible sunshine, %	71	71	70	67	64	71	71	73	74	72	64	67	70
Global radiation, MJ m ⁻²	10	13	17	21	24	27	26	23	20	15	10	8	18

Location: Philadelphia, Pennsylvania, USA

Latitude: 39 53N

Longitude: 75 15W

Altitude: 9 m

Parameter	JAN	FEB	MAR	APR	MAY	JUN	JUL	AUG	SEP	OCT	NOV	DEC	YEAR
Temperature, °F (13)	31	33	42	53	63	72	77	75	68	56	46	36	54
Relative humidity, % (13)	59	56	53	48	53	54	54	55	55	54	56	59	55
Total precipitation, in	3	3	4	3	3	4	4	4	3	3	3	3	41
Mean snowfall, in	7	7	4	0.3	0	0	0	0	0	0	0.6	4	22
Precipitation >0.1 in, days	11	9	11	11	11	10	9	9	8	8	9	10	117
Possible sunshine, %	50	53	55	56	56	62	62	62	60	59	52	49	56
Global radiation, MJ m ⁻²	6	9	13	16	19	21	20	18	15	11	7	5	13

Location: New York City, New York, USA

Latitude: 40 46 N

Longitude: 73 54W

Altitude: 16 m

Parameter	JAN	FEB	MAR	APR	MAY	JUN	JUL	AUG	SEP	OCT	NOV	DEC	YEAR
Temperature, °F (13)	32	33	41	52	62	71	76	75	68	57	47	36	54
Relative humidity, % (13)	57	55	54	50	53	55	52	55	56	55	58	60	55
Total precipitation, in	3	3	4	4	3	3	4	4	3	3	4	4	43
Mean snowfall, in	7	8	5	1	0	0	0	0	0	0	0	5	26
Precipitation >0.1 in, days	11	10	11	11	11	10	9	9	8	8	10	11	119
Possible sunshine, %	6	9	13	17	19	20	20	18	15	11	7	5	13

Location: Salt Lake City, Utah, USA

Latitude: 40 46N

Longitude: 111 58W

Altitude: 1288 m

Parameter	JAN	FEB	MAR	APR	MAY	JUN	JUL	AUG	SEP	OCT	NOV	DEC	YEAR
Temperature, °F (17)	29	34	41	49	59	68	77	75	65	53	40	30	52
Relative humidity, % (17)	69	59	47	39	33	26	21	23	29	41	59	71	43
Total precipitation, in	1	1	2	2	1	1	1	1	1	1	1	1	15
Mean snowfall, in	13	10	10	5	1	0	0	0	0	1	7	12	59
Precipitation >0.1 in, days	10	9	10	10	8	6	5	6	5	6	8	9	91
Possible sunshine, %	45	54	63	67	72	79	83	83	82	72	53	42	66
Global radiation, MJ m ⁻²	7	11	17	21	27	29	29	26	21	15	9	6	18

Location: Cleveland, Ohio, USA

Latitude: 41 24N

Longitude: 81 51W

Altitude: 245 m

Parameter	JAN	FEB	MAR	APR	MAY	JUN	JUL	AUG	SEP	OCT	NOV	DEC	YEAR
Temperature, °F (13)	26	27	37	48	58	68	72	70	64	53	42	31	50
Relative humidity, % (13)	70	68	63	56	57	57	57	60	60	59	66	70	62
Total precipitation, in	2	2	3	3	3	3	3	3	3	2	3	3	35
Mean snowfall, in	12	12	10	2	0	0	0	0	0	0	5	12	54
Precipitation >0.1 in, days	17	14	16	14	13	11	10	10	10	11	15	16	156
Possible sunshine, %	31	37	44	52	58	65	67	63	60	53	31	26	49
Global radiation, MJ m ⁻²	4	7	10	15	19	21	21	18	14	10	5	4	12

Location: Chicago, Illinois, USA

Latitude: 41 47 N

Longitude: 87 45W

Altitude: 190 m

Parameter	JAN	FEB	MAR	APR	MAY	JUN	JUL	AUG	SEP	OCT	NOV	DEC	YEAR
Temperature, °F (12)	21	26	36	49	59	69	73	72	65	54	40	28	49
Relative humidity, % (12)	67	66	61	55	54	55	57	57	58	56	64	70	60
Total precipitation, in	2	1	3	4	3	4	4	4	3	2	2	2	33
Mean snowfall, in	11	8	7	2	0.1	0	0	0	0	0.3	2	9	40
Precipitation >0.1 in, days	11	10	13	13	11	10	10	9	10	9	10	12	127
Possible sunshine, %	45	44	50	47	60	69	68	64	57	49	33	43	52
Global radiation, MJ m ⁻²	6	9	13	17	20	23	22	20	15	11	6	5	14

Location: Boston, Massachusetts, USA

Latitude: 42 22N

Longitude: 71 02W

Altitude: 5 m

Parameter	JAN	FEB	MAR	APR	MAY	JUN	JUL	AUG	SEP	OCT	NOV	DEC	YEAR
Temperature, °F (13)	30	31	38	49	59	68	74	72	65	55	45	34	52
Relative humidity, % (13)	57	56	57	53	59	59	56	59	60	58	60	60	58
Total precipitation, in	4	4	4	4	4	3	3	4	3	3	4	4	44
Mean snowfall, in	13	12	8	1	0	0	0	0	0	0	1	8	42
Precipitation >0.1 in, days	12	11	12	11	12	11	9	10	9	9	11	12	127
Possible sunshine, %	53	57	57	57	59	63	66	65	64	60	50	52	59
Global radiation, MJ m ⁻²	5	8	12	15	18	21	20	17	14	10	6	5	13

Location: Medford, Oregon, USA

Latitude: 42 22N

Longitude: 122 52W

Altitude: 396 m

Parameter	JAN	FEB	MAR	APR	MAY	JUN	JUL	AUG	SEP	OCT	NOV	DEC	YEAR
Temperature, °F (10)	38	42	46	50	58	65	73	71	65	54	44	38	54
Relative humidity, % (10)	88	84	73	63	56	48	44	48	54	72	87	89	67
Total precipitation, in	3	2	2	1	1	0.7	0.3	0.5	0.8	2	3	3	20
Precipitation >0.1 in, days	14	11	12	9	8	5	2	2	4	8	12	15	102
Global radiation, MJ m ⁻²	5	8	13	19	23	26	28	24	18	11	6	4	15

Location: Detroit, Michigan, USA

Latitude: 42 25N

Longitude: 83 01W

Altitude: 191 m

Parameter	JAN	FEB	MAR	APR	MAY	JUN	JUL	AUG	SEP	OCT	NOV	DEC	YEAR
Temperature, °F (13)	23	26	35	47	58	68	72	71	63	52	40	29	49
Relative humidity, % (13)	69	65	61	55	53	54	53	56	57	57	66	71	60
Total precipitation, in	2	2	3	3	3	3	3	3	2	2	2	3	31
Mean snowfall, in	10	9	7	2	0	0	0	0	0	0.1	3	11	41
Precipitation >0.1 in, days	13	11	13	13	11	11	9	9	10	9	12	14	134
Possible sunshine, %	40	46	51	55	61	67	70	69	61	50	34	30	53
Global radiation, MJ m ⁻²	5	8	11	16	19	21	21	18	14	10	5	4	13

Location: Sioux Falls, South Dakota, USA

Latitude: 43 34N

Longitude: 96 44W

Altitude: 435 m

Parameter	JAN	FEB	MAR	APR	MAY	JUN	JUL	AUG	SEP	OCT	NOV	DEC	YEAR
Temperature, °F (12)	12	19	30	46	58	68	74	72	61	49	33	20	45
Relative humidity, % (12)	67	68	64	56	53	56	53	55	57	56	65	71	60
Total precipitation, in	0.5	1	2	2	3	4	3	3	3	2	1	0.7	24
Mean snowfall, in	7	8	10	2	0	0	0	0	0	0.5	0.5	8	41
Precipitation >0.1 in, days	6	7	9	9	10	11	9	9	8	6	6	6	97
Global radiation, MJ m ⁻²	6	9	13	18	21	24	24	21	16	11	7	5	15

Location: Portland, Maine, USA

Latitude: 43 39N

Longitude: 70 19W

Altitude: 19 m

Parameter	JAN	FEB	MAR	APR	MAY	JUN	JUL	AUG	SEP	OCT	NOV	DEC	YEAR
Temperature, °F (13)	22	23	32	43	53	62	68	67	59	49	38	26	45
Relative humidity, % (13)	61	59	59	54	58	61	59	59	60	59	63	62	59
Total precipitation, in	4	4	4	4	3	3	3	3	3	4	5	5	44
Precipitation >0.1 in, days	11	10	11	12	13	11	10	9	8	9	12	12	128
Possible sunshine, %	56	59	56	55	55	59	64	64	62	58	48	52	57
Global radiation, MJ m ⁻²	5	8	11	15	18	19	19	17	13	9	5	4	12

Location: Lewiston, Idaho, USA

Latitude: 46 23N

Longitude: 117 01W

Parameter	JAN	FEB	MAR	APR	MAY	JUN	JUL	AUG	SEP	OCT	NOV	DEC	YEAR
Temperature, °F (16)	32	39	43	50	58	66	75	72	64	52	40	35	52
Relative humidity, % (16)	72	63	50	42	40	36	24	25	32	50	70	75	48
Total precipitation, in	1	1	1	1	1	1	0.5	0.8	0.8	1	1	1	13
Mean snowfall, in	7	3	1	0.1	0	0	0	0	0	0.1	2	5	17
Precipitation >0.1 in, days	12	10	11	10	9	8	4	5	6	8	10	12	104
Global radiation, MJ m ⁻²	4	7	12	16	21	23	27	22	16	10	5	3	14

Location: Seattle, Washington, USA

Latitude: 47 27N

Longitude: 122 18W

Altitude: 122 m

Parameter	JAN	FEB	MAR	APR	MAY	JUN	JUL	AUG	SEP	OCT	NOV	DEC	YEAR
Temperature, °F (16)	39	43	44	49	55	60	65	64	60	52	45	41	51
Relative humidity, % (16)	74	67	62	57	54	53	49	51	58	67	74	77	62
Total precipitation, in	6	4	4	2	2	1	1	1	2	3	6	6	39
Mean snowfall, in	6	2	1	0.1	0	0	0	0	0	0	1	3	13
Precipitation >0.1 in, days	19	16	17	14	10	9	5	7	9	14	18	20	157
Possible sunshine, %	25	37	49	52	56	54	65	64	59	43	29	21	46
Global radiation, MJ m ⁻²	3	6	10	15	19	20	26	18	13	7	4	2	12

Location: Athens, Nea Filadelfia, Greece

Latitude: 38 03N

Longitude: 23 40E

Altitude: 138 m

Parameter	JAN	FEB	MAR	APR	MAY	JUN	JUL	AUG	SEP	OCT	NOV	DEC	YEAR
Temperature, °C (av)	9	9	11	15	21	25	28	27	23	18	14	11	18
Relative humidity, % (av)	74	73	70	62	54	46	44	46	54	66	74	75	62
Total precipitation, mm	57	49	43	31	23	12	6	5	15	56	60	67	422
Precipitation >0.1 in, days	16	11	11	9	8	4	2	3	4	8	12	15	103
Total bright sunshine, h	115	122	171	218	288	323	351	337	274	204	146	120	2672
Possible sunshine, %	40	48	48	58	63	73	82	85	76	60	47	40	62
Global radiation, MJ m ⁻²	6	7	11	15	18	20	18	17	14	9	6	4	12
Carbon monoxide, mg m ⁻³	1.3	1.2	0.7	0.8	0.9	0.9	0.8	0.9	1.4	1.2	2.6	2.8	1.3
Nitrogen dioxide, mg m ⁻³	40	62	52	55	57	57	52	50	61	57	76	75	53
Sulfur dioxide, µg m ⁻³	12	16	9	29	30	23	17	19	15	24	29	38	22
Ozone, µg m ⁻³	15	29	17	34	75	80	97	85	66	37	18	15	47

Location: Thessaloniki, Greece

Latitude: 40 31N

Longitude: 22 58E

Altitude: 5 m

Parameter	JAN	FEB	MAR	APR	MAY	JUN	JUL	AUG	SEP	OCT	NOV	DEC	YEAR
Temperature, °C (av)	5	7	10	14	20	24	26	26	22	16	11	7	16
Relative humidity, % (av)	77	74	74	69	65	57	54	56	63	71	78	79	68
Total precipitation, mm	38	41	44	38	45	31	24	20	29	49	65	55	448
Precipitation >0.1 in, days	11	8	9	9	10	7	4	3	5	8	11	11	96
Total bright sunshine, h	94	95	139	202	254	296	326	294	229	162	116	103	2310

Location: Piarco, Trinidad

Parameter	JAN	FEB	MAR	APR	MAY	JUN	JUL	AUG	SEP	OCT	NOV	DEC	YEAR
Temperature, °C (av)	25	25	26	26	27	26	26	26	26	26	26	25	26
Relative humidity, % (av)	82	80	78	77	80	84	85	85	85	85	86	85	83
Total precipitation, mm	72	48	36	50	112	254	264	234	185	166	214	150	1783
Precipitation >0.1 in, days	11	9	6	7	13	20	20	19	15	15	18	15	168
Total bright sunshine, h	236	230	250	239	239	187	214	215	202	204	198	207	2620
Possible sunshine, %	64	66	67	65	60	50	55	57	55	56	56	57	59
Global radiation, MJ m ⁻²	17	19	21	21	19	17	17	18	17	17	15	15	18

Location: Nagasaki, Japan

Latitude: 32 44N

Longitude: 129 52E

Altitude: 27 m

Parameter	JAN	FEB	MAR	APR	MAY	JUN	JUL	AUG	SEP	OCT	NOV	DEC	YEAR
Temperature, °C (av)	6	7	10	15	19	23	26	27	24	19	14	9	17
Relative humidity, % (av)	67	65	69	69	73	80	83	78	76	70	69	68	72
Total precipitation, mm	62	79	151	168	197	358	428	224	161	109	71	52	1950
Precipitation >0.1 in, days	11	9	10	11	11	13	12	9	11	7	7	10	119
Total bright sunshine, h	127	110	137	169	200	138	171	208	164	182	134	118	1858
Possible sunshine, %	36	42	48	48	47	40	48	61	50	57	54	41	48
Global radiation, MJ m ⁻²	8	10	12	16	18	15	17	18	15	13	9	7	13

Location: Fukuoka, Japan

Latitude: 33 55N

Longitude: 130 23E

Altitude: 4 m

Parameter	JAN	FEB	MAR	APR	MAY	JUN	JUL	AUG	SEP	OCT	NOV	DEC	YEAR
Temperature, °C (av)	6	6	10	15	19	23	27	28	24	19	13	8	20
Relative humidity, % (av)	64	64	68	68	70	77	78	75	75	70	69	65	70
Total precipitation, mm	51	64	130	122	150	311	342	237	165	90	77	54	1794
Precipitation >0.1 in, days	10	9	11	10	9	11	11	9	11	7	8	10	116
Total bright sunshine, h	102	114	140	174	203	144	167	194	155	177	132	114	1817
Possible sunshine, %	35	40	46	48	47	41	47	57	45	54	51	39	46
Global radiation, MJ m ⁻²	8	10	13	16	18	16	16	17	14	12	9	7	13

Location: Tokyo, Japan

Latitude: 35 41N

Longitude: 139 46E

Altitude: 6 m

Parameter	JAN	FEB	MAR	APR	MAY	JUN	JUL	AUG	SEP	OCT	NOV	DEC	YEAR
Temperature, °C (av)	5	6	9	14	19	22	25	27	23	18	13	8	16
Relative humidity, % (av)	50	51	58	63	65	73	77	74	74	65	61	54	64
Total precipitation, mm	35	53	122	113	123	180	138	153	190	158	85	40	1390
Precipitation >0.1 in, days	5	6	9	10	10	11	9	9	12	11	8	5	104
Total bright sunshine, h	185	163	150	167	190	134	125	168	97	141	134	177	1830
Possible sunshine, %	60	54	48	46	44	34	41	49	36	39	47	56	45
Global radiation, MJ m ⁻²	9	10	12	15	16	14	13	14	10	10	8	8	12

Location: Singapore, Singapore

Latitude: 1 21N

Longitude: 103 54E

Altitude: 10 m

Parameter	JAN	FEB	MAR	APR	MAY	JUN	JUL	AUG	SEP	OCT	NOV	DEC	YEAR
Temperature, °C (av)	26	27	27	27	27	27	27	27	27	27	26	26	27
Relative humidity, % (av)	85	83	84	85	85	83	83	83	84	85	87	87	85
Total precipitation, mm	242	171	188	182	172	167	158	179	173	200	254	280	2367
Precipitation >0.1 in, days	15	11	11	11	12	11	11	13	11	13	16	15	150
Total bright sunshine, h	165	182	192	175	182	180	193	184	161	160	133	137	2043
Possible sunshine, %	42	52	50	49	49	50	52	49	46	43	39	38	46
Global radiation, mW day cm ⁻²	452	478	481	443	416	412	417	433	435	428	376	377	429

Location: Royal Observatory, Hong Kong

Latitude: 22 18N

Longitude: 114 10E

Altitude: 33 m

Parameter	JAN	FEB	MAR	APR	MAY	JUN	JUL	AUG	SEP	OCT	NOV	DEC	YEAR
Temperature, °C (av)	16	16	19	22	26	28	29	28	28	25	21	18	23
Relative humidity, % (av)	71	78	82	83	83	84	81	83	79	72	69	69	78
Total precipitation, mm	27	42	55	139	298	432	317	413	320	121	35	25	2225
Precipitation >0.1 in, days	4	5	6	8	13	17	15	15	13	5	3	3	107
Total bright sunshine, h	153	109	101	120	163	159	231	206	189	210	192	179	2012
Possible sunshine, %	43	35	25	32	39	39	56	50	53	64	61	54	46
Global radiation, MJ m ⁻²	12	11	11	14	16	17	19	18	17	16	14	12	15
Sulfur dioxide, µg m ⁻³	31	24	22	29	26	28	47	46	27	19	20	27	29
Nitrogen oxides, µg m ⁻³	133	129	130	123	114	110	110	131	109	106	121	126	120
Suspended particulates, µg m ⁻³	117	95	101	91	64	61	62	71	71	96	89	108	86

Location: Colombo, Sri Lanka

Latitude: 6 54N

Longitude: 79 52E

Parameter	JAN	FEB	MAR	APR	MAY	JUN	JUL	AUG	SEP	OCT	NOV	DEC	YEAR
Temperature, °C (av)	26	27	28	28	28	28	27	27	27	27	27	28	27
Relative humidity, % (av)	76	77	78	79	81	80	80	79	79	81	80	78	79
Total precipitation, mm	88	96	118	260	353	212	140	124	153	354	324	175	2396
Precipitation >0.1 in, days	8	7	11	18	23	22	15	15	17	21	19	12	188
Total bright sunshine, h	232	232	273	237	192	198	189	202	192	192	204	214	2557
Possible sunshine, %	67	75	67	59	51	43	49	51	51	54	54	67	57

Location: **Kuwait International Airport, Kuwait**

Parameter	JAN	FEB	MAR	APR	MAY	JUN	JUL	AUG	SEP	OCT	NOV	DEC	YEAR
Temperature, °C (av)	13	15	19	25	31	36	37	37	33	27	20	14	26
Relative humidity, % (av)	63	55	48	41	30	18	19	21	28	40	52	62	40
Total precipitation, mm	26	15	13	15	4	0	0	0	0	3	14	18	109
Total bright sunshine, h	220	219	241	239	302	322	327	340	307	287	239	218	3261
Possible sunshine, %	67	69	63	62	69	75	76	79	83	79	73	67	72
Global radiation, MJ m ⁻²	13	17	21	23	27	29	28	28	25	19	14	12	21

Location: **Jungfrauoch Sphinx, Switzerland**

Latitude: 46 33N

Longitude: 7 59E

Altitude: 3580 m

Parameter	JAN	FEB	MAR	APR	MAY	JUN	JUL	AUG	SEP	OCT	NOV	DEC	YEAR
Temperature, °C (13)	-14	-14	-13	-9	-6	-3	1	-4	-1	-4	-9	-11	-7
Relative humidity, % (13)	73	68	76	72	80	76	70	69	63	66	64	67	70
Total bright sunshine, h	88	118	127	162	130	150	201	196	190	147	131	110	1749
Possible sunshine, %	33	34	42	40	35	38	43	45	46	41	36	34	39
Global radiation, MJ m ⁻²	5	9	13	20	21	23	23	20	16	10	7	5	14

Location: **Davos, Switzerland**

Latitude: 46 49N

Longitude: 9 51E

Altitude: 1590 m

Parameter	JAN	FEB	MAR	APR	MAY	JUN	JUL	AUG	SEP	OCT	NOV	DEC	YEAR
Temperature, °C (13)	-3	-3	1	5	9	12	16	15	13	10	3	-1	7
Relative humidity, % (13)	67	51	51	48	53	56	52	55	54	51	56	63	55
Total precipitation, mm	105	39	63	44	100	117	124	133	101	48	47	59	981
Total bright sunshine, h	86	126	135	138	125	139	186	170	171	154	118	93	1640
Global radiation, MJ m ⁻²	5	10	14	19	19	20	20	17	14	10	6	4	13

Location: Zürich, Switzerland

Latitude: 47 23N

Longitude: 8 34E

Altitude: 556 m

Parameter	JAN	FEB	MAR	APR	MAY	JUN	JUL	AUG	SEP	OCT	NOV	DEC	YEAR
Temperature, °C (13)	1	1	6	11	15	18	21	20	18	12	6	3	11
Relative humidity, % (13)	78	72	64	57	60	57	57	59	64	70	74	78	66
Total precipitation, mm	92	53	77	83	116	127	109	130	114	79	71	80	1130
Precipitation >0.1 in, days	12	10	9	11	13	13	13	13	10	10	10	10	135
Total bright sunshine, h	45	68	109	150	145	149	219	192	156	101	68	51	1452
Possible sunshine, %	17	27	41	42	44	46	49	49	44	32	18	14	38
Global radiation, MJ m ⁻²	3	6	9	14	16	18	19	16	12	7	4	3	11

Location: Madras, India

Latitude: 13 00N

Longitude: 80 11E

Altitude: 16 m

Parameter	JAN	FEB	MAR	APR	MAY	JUN	JUL	AUG	SEP	OCT	NOV	DEC	YEAR
Temperature, °C (av)	21	22	24	26	26	24	24	24	25	25	24	22	24
Relative humidity, % (av)	83	80	77	72	63	58	65	69	73	81	83	84	74
Total precipitation, mm	24	7	15	25	52	53	84	124	118	267	309	139	1215
Precipitation >0.1 in, days	1	1	1	1	2	4	7	8	7	10	10	5	57
Total bright sunshine, h/day	9	10	10	10	9	7	5	6	6	6	7	7	8
Possible sunshine, %	75	85	79	77	68	52	42	47	52	54	58	61	63
Global radiation, cal cm ⁻²	440	532	582	585	548	489	456	474	479	412	366	362	477

Location: Goa, India

Latitude: 15 25N

Longitude: 73 47E

Altitude: 62 m

Parameter	JAN	FEB	MAR	APR	MAY	JUN	JUL	AUG	SEP	OCT	NOV	DEC	YEAR
Temperature, °C (av)	24	28	25	27	29	29	28	27	27	26	27	26	27
Relative humidity, % (av)	66	72	73	72	73	83	86	87	87	82	69	62	76
Total precipitation, mm	2	0	0	20	81	778	905	413	226	139	43	5	2611
Precipitation >0.1 in, days	0	0	0	1	4	22	27	22	15	7	2	0	100
Total bright sunshine, h/day	10	10	9	10	9	4	3	4	6	8	9	9	8
Possible sunshine, %	84	85	77	76	70	33	25	34	47	64	82	82	63
Global radiation, cal cm ⁻²	487	543	576	589	577	412	351	412	454	478	490	470	487

Location: Calcutta, India

Latitude: 22 32N

Longitude: 88 20E

Altitude: 6 m

Parameter	JAN	FEB	MAR	APR	MAY	JUN	JUL	AUG	SEP	OCT	NOV	DEC	YEAR
Temperature, °C (av)	17	21	26	30	31	30	29	29	29	28	23	18	26
Relative humidity, % (av)	78	75	71	71	74	80	84	85	84	80	74	76	78
Total precipitation, mm	14	24	27	43	121	259	301	306	290	160	35	3	1582
Precipitation >0.1 in, days	1	2	2	3	6	12	17	18	14	8	1	0	84
Total bright sunshine, h/day	8	9	8	9	8	4	4	4	5	7	8	8	7
Possible sunshine, %	74	75	68	69	63	31	29	29	37	56	73	74	56
Global radiation, cal cm ⁻²	356	423	490	535	550	423	389	376	379	386	377	350	419

Location: Lagos, Nigeria

Latitude: 6 27N

Longitude: 3 24E

Altitude: 3 m

Parameter	JAN	FEB	MAR	APR	MAY	JUN	JUL	AUG	SEP	OCT	NOV	DEC	YEAR
Temperature, °C (12)	29	30	30	30	29	28	27	26	27	28	30	29	29
Relative humidity, % (12)	62	64	63	65	67	78	79	78	78	75	71	70	71
Total precipitation, mm	32	43	95	148	274	458	278	81	151	193	67	23	1842
Total bright sunshine, h/day	6	7	7	7	6	4	3	4	4	6	7	6	6

Location: Ibadan, Nigeria

Latitude: 7 26N

Longitude: 3 54E

Altitude: 227 m

Parameter	JAN	FEB	MAR	APR	MAY	JUN	JUL	AUG	SEP	OCT	NOV	DEC	YEAR
Temperature, °C (12)	30	32	31	30	29	28	26	26	27	28	30	30	29
Relative humidity, % (12)	51	51	57	64	68	73	77	78	76	71	61	55	65
Total precipitation, mm	8	24	87	136	152	181	156	100	178	162	40	10	1235
Total bright sunshine, h/day	6	6	6	6	6	5	3	2	3	5	7	7	5

Location: **Zaria, Nigeria**

Latitude: 11 08N

Longitude: 7 41E

Altitude: 654 m

Parameter	JAN	FEB	MAR	APR	MAY	JUN	JUL	AUG	SEP	OCT	NOV	DEC	YEAR
Temperature, °C (12)	27	31	34	34	31	29	27	26	28	30	30	28	29
Relative humidity, % (12)	16	12	19	31	49	57	68	71	66	45	21	18	39
Total precipitation, mm	0	1	8	44	99	150	228	283	199	40	2	0	1054
Total bright sunshine, h/day	9	10	9	8	8	8	6	10	7	9	10	10	8

Location: **Khartoum, Sudan**

Parameter	JAN	FEB	MAR	APR	MAY	JUN	JUL	AUG	SEP	OCT	NOV	DEC	YEAR
Temperature, °C (12)	31	35	38	39	41	41	40	39	38	39	35	31	38
Relative humidity, % (12)	25	20	14	13	20	30	40	42	37	28	24	32	27
Total precipitation, mm	0	0	0	0	5	7	22	60	16	2	0	0	112
Total bright sunshine, h/day	10	10	9	10	9	9	9	9	9	9	10	10	9
Global radiation, MJ m ⁻²	19	21	23	25	24	21	23	23	20	20	19	19	22

Location: **Tunis-Carthage, Tunisia**

Parameter	JAN	FEB	MAR	APR	MAY	JUN	JUL	AUG	SEP	OCT	NOV	DEC	YEAR
Temperature, °C (av)	11	12	13	16	20	24	27	27	25	21	16	12	19
Relative humidity, % (av)	78	76	74	72	68	64	62	65	69	74	68	75	70
Total precipitation, mm	52	48	46	37	20	7	2	4	53	56	55	71	541
Total bright sunshine, h	144	153	202	225	281	325	357	332	271	222	162	152	2829
Global radiation, MJ m ⁻²	9	11	15	19	24	27	27	24	19	14	10	8	17

Location: **Ankara, Turkey**

Parameter	JAN	FEB	MAR	APR	MAY	JUN	JUL	AUG	SEP	OCT	NOV	DEC	YEAR
Temperature, °C (av)	3	4	5	12	15	19	23	22	19	12	6	2	11
Relative humidity, % (av)	77	71	69	61	58	53	48	43	44	60	73	76	62
Total precipitation, mm	56	41	37	47	43	46	14	4	5	32	32	39	396
Precipitation >0.1 in, days	14	10	16	13	15	9	3	1	2	10	11	14	118
Global radiation, cal cm ² min ⁻¹	132	211	281	368	467	528	525	490	416	269	161	114	325

Location: **Izmir, Turkey**

Parameter	JAN	FEB	MAR	APR	MAY	JUN	JUL	AUG	SEP	OCT	NOV	DEC	YEAR
Temperature, °C (av)	10	10	11	15	21	25	27	28	24	18	13	10	18
Relative humidity, % (av)	74	68	68	58	58	52	47	52	53	62	69	69	61
Total precipitation, mm	186	89	103	38	13	5	4	0	0	12	108	100	844
Precipitation >0.1 in, days	16	11	9	6	3	1	0	0	0	3	11	10	70
Global radiation, cal cm ² min ⁻¹	171	244	320	462	531	594	596	554	457	329	193	164	392

Location: **London, Great Britain**

Parameter	JAN	FEB	MAR	APR	MAY	JUN	JUL	AUG	SEP	OCT	NOV	DEC	YEAR
Temperature, °C (av)	4	5	6	10	12	16	18	17	15	11	7	5	11
Relative humidity, % (av)	81	73	63	63	59	56	58	60	64	70	77	82	67
Total precipitation, mm	50	40	40	42	48	51	58	62	54	55	60	52	612
Total bright sunshine, h	36	53	99	151	191	204	185	172	134	95	49	33	1401
Global radiation, MJ m ⁻²	3	4	7	13	15	16	16	14	10	5	3	2	9

Location: **Dundee, Great Britain**

Parameter	JAN	FEB	MAR	APR	MAY	JUN	JUL	AUG	SEP	OCT	NOV	DEC	YEAR
Temperature, °C (av)	3	3	5	7	10	13	15	14	12	9	6	4	9
Relative humidity, % (av)	82	76	70	69	73	70	69	73	74	77	80	83	75
Total precipitation, mm	60	47	44	41	61	52	70	78	63	62	66	63	707
Total bright sunshine, h	51	81	102	151	169	168	157	138	118	91	61	45	1331
Global radiation, MJ m ⁻²	2	4	7	12	16	17	16	13	9	5	2	1	9

Location: **Vienna, Austria**

Latitude: 48 14N

Longitude: 16 21E

Altitude: 202 m

Parameter	JAN	FEB	MAR	APR	MAY	JUN	JUL	AUG	SEP	OCT	NOV	DEC	YEAR
Temperature, °C (13)	2	4	9	15	20	23	25	24	20	14	8	2	14
Relative humidity, % (13)	74	67	58	50	52	55	53	54	57	64	73	75	61
Total precipitation, mm	37	38	46	57	59	79	74	61	37	44	50	44	626
Precipitation >0.1 in, days	14	12	13	12	13	14	13	12	10	10	14	15	152
Total bright sunshine, h	55	75	125	175	226	232	247	235	181	138	60	49	1798
Global radiation, MJ m ⁻²	3	5	9	14	18	19	19	16	12	7	3	2	11
Ozone, ppb	11	16	27	32	40	40	49	42	29	18	12	14	28
Nitrogen dioxide, ppb	20	14	15	16	19	13	16	17	21	32	28	17	19
Sulfur dioxide, µg m ⁻³	90	72	43	21	17	14	14	14	20	35	51	56	37

Location: **Innisfail, Australia**

Latitude: 17 31S

Longitude: 146 02E

Altitude: 4 m

Parameter	JAN	FEB	MAR	APR	MAY	JUN	JUL	AUG	SEP	OCT	NOV	DEC	YEAR
Temperature, °C (15)	29	29	28	26	25	23	23	24	25	27	28	29	26
Relative humidity, % (15)	74	76	75	75	75	71	68	68	66	67	69	71	71
Total precipitation, mm	578	647	709	490	329	196	132	120	94	85	156	277	3813
Total bright sunshine, h/day	7	6	6	6	5	6	6	7	8	8	9	8	7
Global radiation, MJ m ⁻²	19	17	16	14	12	16	13	16	16	20	21	20	17

Location: Townsville, Australia

Latitude: 19 15S

Longitude: 146 46E

Altitude: 4 m

Parameter	JAN	FEB	MAR	APR	MAY	JUN	JUL	AUG	SEP	OCT	NOV	DEC	YEAR
Temperature, °C (15)	30	30	29	28	26	24	24	25	26	28	29	30	27
Relative humidity, % (15)	65	67	65	60	57	51	51	51	52	55	57	60	58
Total precipitation, mm	297	300	212	62	36	21	14	13	11	25	54	116	1161
Precipitation >0.1 in, days	14	16	13	7	6	5	3	2	2	4	6	8	86
Total bright sunshine, h	236	196	226	231	226	237	264	282	282	301	282	276	3038
Possible sunshine, %	55	56	56	73	65	73	79	80	78	76	71	63	68
Global radiation, MJ m ⁻²	21	20	20	17	15	15	16	18	22	24	25	24	20

Location: Perth, Australia

Latitude: 31 56S

Longitude: 115 58E

Altitude: 20 m

Parameter	JAN	FEB	MAR	APR	MAY	JUN	JUL	AUG	SEP	OCT	NOV	DEC	YEAR
Temperature, °C (15)	23	24	22	19	16	14	13	14	15	16	19	22	18
Total precipitation, mm	7	12	22	52	125	192	183	135	69	54	23	15	889
Precipitation >0.1 in, days	3	3	5	8	15	17	19	19	15	12	7	5	128
Total bright sunshine, h	322	277	270	222	177	144	167	186	210	245	288	326	2833
Possible sunshine, %	74	74	58	52	44	55	59	62	69	72	79	74	64
Global radiation, MJ m ⁻²	29	26	21	15	11	9	10	12	17	22	25	28	19
CO, ppm	0.7	0.8	0.8	0.8	1.2	1.2	1.1	1	1	0.7	0.7	0.6	0.9
NO _x , µg m ⁻³	38	34	38	51	67	69	66	61	50	39	38	35	49
O ₃ , ppm	1	0.9	0.8	0.6	0.5	0.6	0.6	1.1	1.2	1.8	1.8	1.6	1.1
SO ₂ , µg m ⁻³	18	14	16	7	5	1	5	5	6	7	12	16	9
Particulates, µg m ⁻³	52	63	58	53	57	47	47	45	48	48	55	58	53

Location: Melbourne, Australia

Latitude: 37 49S

Longitude: 144 58E

Altitude: 123 m

Parameter	JAN	FEB	MAR	APR	MAY	JUN	JUL	AUG	SEP	OCT	NOV	DEC	YEAR
Temperature, °C (15)	20	20	18	15	12	10	10	10	12	14	16	18	15
Total precipitation, mm	45	59	50	69	54	52	54	50	58	74	70	58	691
Precipitation >0.1 in, days	9	8	9	13	14	16	17	17	15	14	13	11	156
Total bright sunshine, h	252	211	200	144	118	95	109	139	161	179	186	229	2023
Possible sunshine, %	56	55	52	43	38	33	36	42	45	44	44	50	46
Global radiation, MJ m ⁻²	24	22	16	11	8	6	7	9	13	18	21	24	15

Location: Baseline, Tasmania, Australia

Latitude: 40 41S

Longitude: 144 41E

Altitude: 94 m

Parameter	JAN	FEB	MAR	APR	MAY	JUN	JUL	AUG	SEP	OCT	NOV	DEC	YEAR
Temperature, °C (av)	15	15	15	13	12	10	10	11	11	11	13	14	13
Relative humidity, % (av)	78	77	80	81	83	79	79	82	80	81	81	80	80
Total precipitation, mm	36	27	69	58	78	100	92	108	75	63	54	36	794
Global radiation, MJ m ⁻²	22	20	14	10	6	5	5	9	13	17	23	22	14
UV radiation, MJ m ⁻²	0.7	0.6	0.4	0.3	0.2	0.15	0.16	0.26	0.38	0.53	0.7	0.7	0.43
CO ₂ , ppb	29	29	31	31	38	40	44	43	45	48	46	39	39
CO ₂ , ppm	335	335	335	335	335	336	336	336	337	337	336	336	336
O ₃ , ppb	15	16	21	25	28	31	32	32	31	29	23	18	25
CCl ₃ F, ppt	196	197	196	196	197	198	199	201	203	204	204	205	200
N ₂ O, ppb	334	334	334	334	335	336	336	336	336	337	337	337	335

5

ARTIFICIAL WEATHERING EQUIPMENT

5.1 LIGHT SOURCES

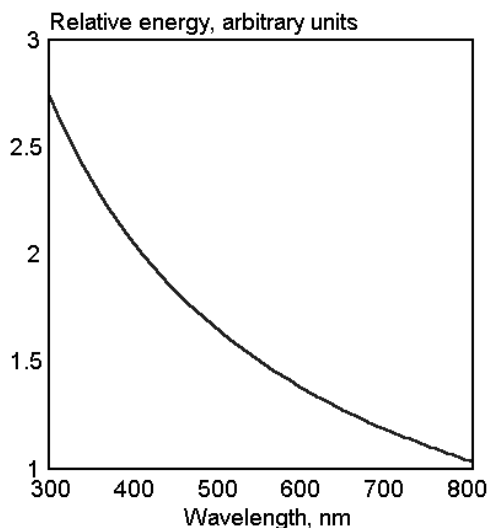


Fig. 5.1. Relative photon energy vs. radiation wavelength. [Adapted, by permission, from G. L. Comerford, *Sun Spots*, 15(1985).]

Relative photon energy vs. wavelength is shown in Fig. 5.1. The most important parameter of weathering studies is explained by this data. Photon energy increases as wavelength decreases therefore photoreactions which require a particular amount of energy only occur at a certain wavelength. It is therefore imperative to assure that there is no wavelength in the radiation used in artificial weathering equipment which is lower than any wavelength in the daylight spectrum. This is the most important criterion used in the evaluation of light sources discussed below, since we seldom want to monitor reactions which cannot occur in service conditions. Fig. 5.2 compares conditions of natural weathering in winter and summer to provide a background for choosing the energy level required in simulating

natural conditions. The intensity of UV radiation at 320 nm is reduced by factor of 8 in winter, as compared to summer, and the short wavelength solar cut-off shifts from about 295 nm in summer to about 310 nm in winter. Materials sensitive to radiation in the range of 295-310 nm do not degrade in winter.

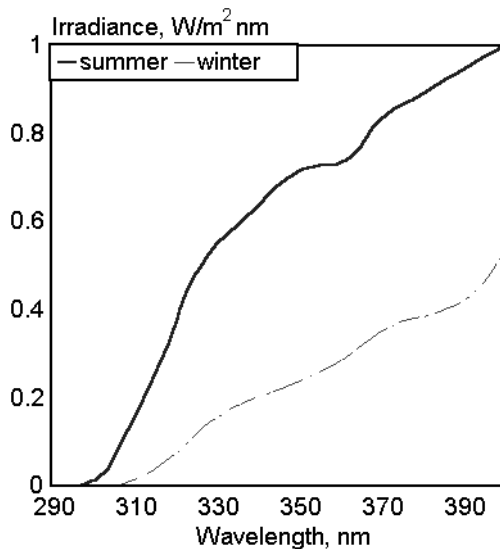


Fig. 5.2. Solar spectrum in summer and winter. [Adapted, by permission, from P. Brennan, *Kunststoffe*, 78(1988)323.]

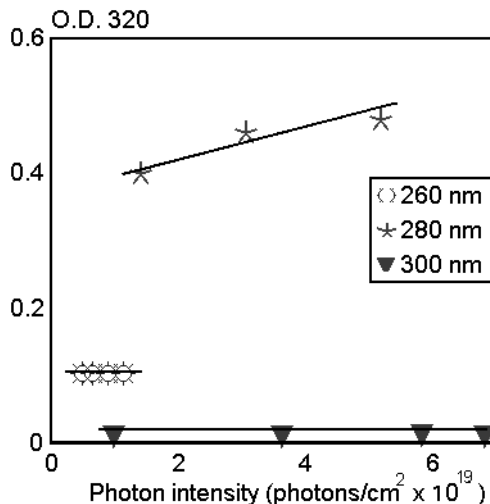


Fig. 5.3. Optical density at 320 nm of polycarbonate vs. photon intensity. [Adapted, by permission, from A. Torikai, T. Mitsuoka, and K. Fueki, *J. Appl. Polym. Sci.*, 31(1993)2785.]

Several examples from the current literature¹⁻¹⁰ are given below to substantiate these statements and to allow the reader to choose the appropriate equipment.

Fig. 5.3 shows the changes in optical density of polycarbonate exposed to different wavelengths of monochromatic light.¹ If this polycarbonate is exposed to UV radiation, which exists in daylight, no changes in optical density are observed. It is also interesting to note that absorption of radiation by a material and degradation of such a material are wavelength specific since the less energetic radiation at 280 nm is more destructive to polycarbonate than the more energetic radiation at 260 nm. This difference is because the photo-Fries rearrangement (one of the major mechanisms of degradation of this polymer) has a high efficiency due to better absorption at this wavelength (efficiency of photo-Fries rearrangement at 260 nm is 1.2×10^{-20} and 1.7×10^{-20} at 280 nm). The same study contains data on quantum yields of main-chain scission for different wavelengths: 260 nm - 7.5×10^{-4} , 280 nm - 2.9×10^{-4} , 300 nm - 1.3×10^{-4} , 320 nm - 0. Main chain scission depends on the radiative energy and, as the energy decreases with wavelength, the rate of chain scission decreases until, at 320 nm, this reaction is virtually eliminated. If unfiltered radiation at 254 nm from a mercury lamp was used in polycarbonate studies and the results extrapolated to the natural conditions, the conclusions will be misleading because 254 nm radiation is not present in natural daylight.

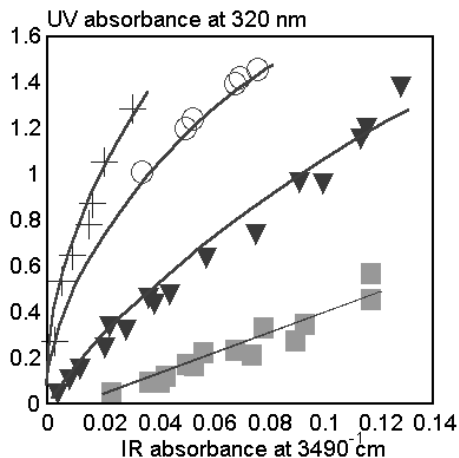


Fig. 5.4. UV vs. IR absorbance of PVC films. + irradiation at 254 nm, ○ irradiation with unfiltered xenon light, ▼ irradiation with filtered xenon light, ■ outdoor exposure. [Adapted, by permission, from A. Rivaton, *Angew. Makromol. Chem.*, 216(1994)147.]

The results of Rivaton's studies² on polycarbonate are depicted in Fig. 5.4. The curves obtained from irradiation at 254 nm by an unfiltered xenon lamp are distinctly different from those from a filtered xenon lamp or from natural exposure. Also, a comparison of the results of exposure to filtered xenon arc radiation and natural conditions shows the extent of acceleration due to the energy level received by the samples. There is a good correlation between results.

Fukuda and Osawa³ studied polycarbonate/polymethylmethacrylate blends and their results for one of the blend participants (polycarbonate) are given in Fig. 5.5. It is again clear that the exposure of this polymer to radiation beyond the normal range leads to false conclusions. A fundamental understanding of the behavior of blends requires not only information about the individual components but also knowledge of the fate of formed radicals. Radicals formed in one polymer may initiate degradation of the other. Polymethylmethacrylate is a very durable polymer and it degrades only when the radiation wavelength is below 260 nm. If an unfiltered mercury lamp were used, both polymers would degrade and would contribute to formation of radicals affecting both components. From the studies discussed above, it is seen that polycarbonate can degrade at 300 nm (the radiation wavelength available in daylight) and that free radicals formed in this process can become the cause of degradation of the blend.

An important contribution to the subject comes from studies conducted in Germany.^{4,5} A new method of testing was developed in which radicals formed are measured

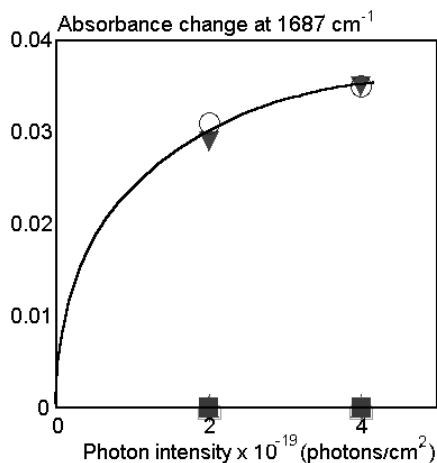


Fig. 5.5. PC absorbance at 1687 cm^{-1} vs. photoirradiation in air at different wavelengths. ○ 260 nm, ▼ 280 nm, □ 300 nm, ◆ 320, ▽ 340 nm, ■ 360 nm, ● 400 nm. [Adapted, by permission, from Y. Fukuda and Z. Osawa, *Polym. Deg. Stab.*, 34(1991)75.]

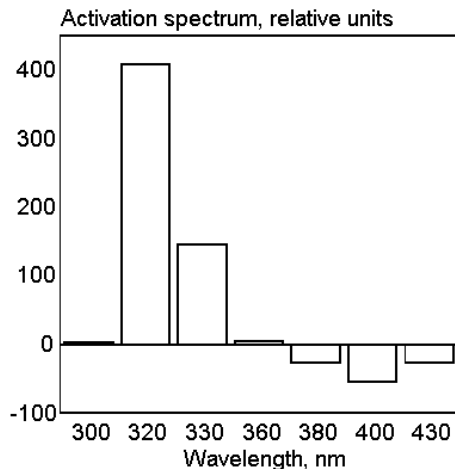


Fig. 5.6. The spectral sensitivity and activation spectrum of polyamide-6 as measured by yellowing. [Adapted, by permission, from G. Kämpf, K. Sommer, and E. Zirngiebl, *Prog. Org. Coat.*, 19(1991)69.]

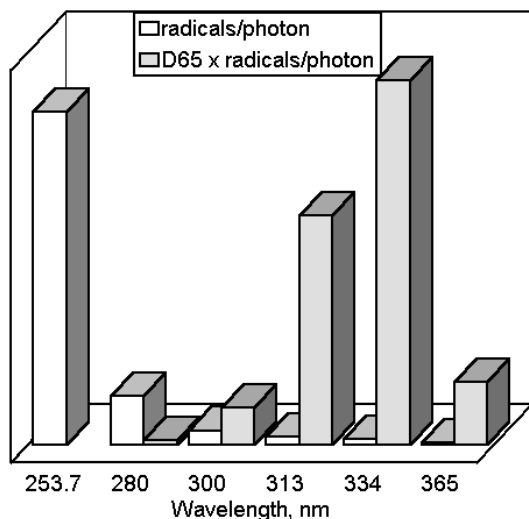


Fig. 5.7. The number of radicals per photon formed in PA-6 and activation spectrum. [Adapted, by permission, from G. Kämpf, K. Sommer, and E. Zirngiebl, *Prog. Org. Coat.*, 19(1991)69.]

directly in the samples as they are exposed to radiation. ESR direct measurement was used and samples were exposed to radiation in instrument. Fig. 5.6 shows “the activation spectrum” (the spectral sensitivity measured by the effect of a particular wavelength on the yellowness index, multiplied by the radiation distribution in daylight spectrum) of polyamide-6. Fig. 5.7 explains the difference between the absorption of UV radiation by the polymer and the practical implication of this absorption. Polyamide-6 absorbs UV radiation intensively at 254 nm and produces a great number of radicals per photon absorbed. At the same time, because this wavelength is not available in the daylight spectrum, this radical formation is irrelevant. In contrast, the production of radical per photon is relatively low at 334 nm but it can cause polymer degradation. In practice, maximum damage occurs in polyamide-6 at 330 nm. These interesting studies provide us with another essential piece of information illustrated in Fig. 5.8. It may appear trivial but it is frequently forgotten. The atmosphere surrounding the specimen plays an essential role. More radicals are detected in nitrogen because they have longer life in nitrogen. In the presence of oxygen, radicals immediately form peroxides.

The influence of radiation wavelength on the mechanism

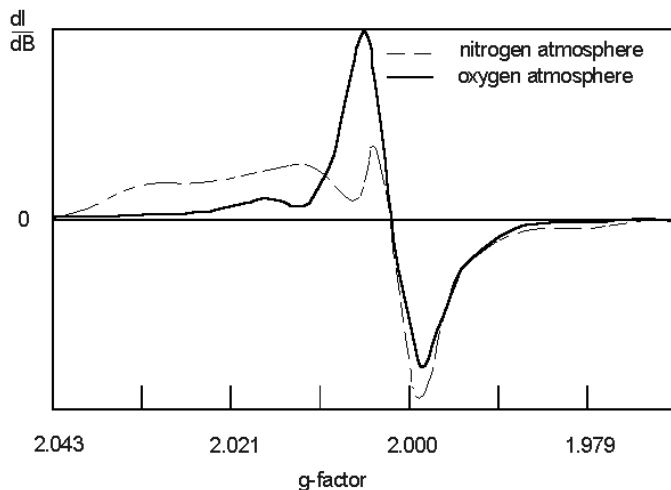


Fig. 5.8. Typical radical signal measured in PU during weathering. [Adapted, by permission, from G. Kämpf, K. Sommer, and E. Zirngiebl, *Prog. Org. Coat.*, 19(1991)79.]

of degradation is not a new discovery. More than a decade ago, Gardette and Lemaire⁶ demonstrated this effect in their work on polyurethanes. They have constructed sets of equipment which allow them to expose specimens to different radiation wavelength and they have skillfully adapted this technique to distinguish among various mechanisms. In their earlier paper,⁶ they showed that preradiation of some polyurethanes at low wavelength (254 nm) may be used to increase their overall stability. They also used this method to demonstrate the difference in behavior between aliphatic and aromatic polyurethanes. The photooxidation of aliphatic polyurethanes is not dependent on radiation wavelength. Their vulnerability is related to a radical-triggered photooxidative processes.

The same authors (Gardette and Lemaire⁷) studied PVC photodegradation using various ranges of radiation wavelength. Their account contains a long sequence of conversions. When PVC was exposed to radiation of 254 nm, two products were formed one absorbing at 270 nm, the other at 284 nm. Subsequently, the products of the photolytic reactions were exposed to radiation at 365 nm which transformed the product absorbing at 284 nm to a product absorbing at 270 nm but on exposing the samples once more to radiation at 254 nm, the initial concentration of the product absorbing at 284 nm was restored. Most conversions would not occur if photodegradation was conducted by exposure to daylight radiation. A variety of abnormal exposure conditions can be used to increase our understanding of degradation mechanisms. Gardette and Lemaire

derivatized degradation products by reaction with ammonia, sodium hydroxide, or water for their subsequent analysis by IR. Such methodology helps in identifying the photoproducts formed and permits a precise description of the reaction mechanisms. One must have a full understanding of the purpose of research. Simple use of multi-range radiation or radiation having a wavelength range or other conditions substantially different from that existing in natural environment will not allow the correlation of data with the performance of the product in outdoor exposure. The majority of studies are conducted to develop materials which are made more stable or more durable due to changes in structure or chemical composition. In such studies, a consistent model (point of reference) and set of experimental conditions are required which should closely imitate the conditions to which product will be exposed.

The above remarks concentrate on only one (although the most important) parameter of degradation conditions. Several other parameters are also essential and they are discussed in other chapters of this book.

Five major light sources were used in studies referred to in other parts of this monograph:

- carbon arc
- xenon arc
- fluorescent UV lamps
- mercury lamps
- indoor actinic source

Carbon arc lamps are historically the oldest source of artificial radiation. The enclosed carbon arc was introduced in 1918 and it is still specified for some test methods. In 1934, the Sunshine carbon arc, which was an improvement over the enclosed carbon arc, was introduced. Fig. 5.9 (at the end of this chapter) compares the output of a Sunshine carbon arc lamp used with Corex D filters with the daylight spectrum and xenon arc spectrum. Fig. 5.10 shows similar comparison for the enclosed carbon arc.

Much of the wavelengths produced by the Sunshine carbon arc are not found in daylight radiation at the Earth's surface. The radiation spectra of these carbon arcs are very different from daylight spectra. Enclosed carbon arc has two strong peaks at 358 and 386 nm which are respectively 4 and 20 times stronger than daylight at the same wavelengths. In other ranges of UV, radiation is substantially lower than in daylight. Sunshine carbon arc offers a substantial improvement over enclosed carbon arc but it has a stronger radiation below 300 nm than daylight. This radiation can cause an unrealistic degradation of materials.

Xenon arc was adapted for accelerated weathering in 1954 in Germany. Initially, there were several problems with the source stability over time and with the choice of proper filters, but, after these were overcome, the xenon arc lamp emerged as the source

most closely resembling UV radiation in the daylight spectrum (Fig. 5.11). Two facts are pertinent: its light does not contain radiation below daylight cut-off; its radiation intensity is similar to that of daylight radiation. It is possible to increase the radiation output by selecting the appropriate filters and by increasing the energy supplied to the burner. The results obtained with different filters and lamp energies are given in Figs. 5.12 - 5.16 at the end of this chapter. In 1979, the light monitor control system was introduced to monitor and adjust the radiative energy output delivered to the sample. This system further improved the reliability of the source by providing a constant repeatable output. The lamp cooling system is another important refinement. The burner has temperature of about 1000°C. It is enclosed in a double wall quartz cylinder. Water or air flow between the walls to reduce temperature. Water has an advantage as a cooling medium because it also eliminates part of infrared radiation above 1200 nm. There is no doubt that xenon arc is the artificial radiation source closest to natural daylight.

Several fluorescent UV lamps are used by industry. FS-40 was the first lamp introduced in the 1970's. UVB-313, introduced in 1984, is essentially a second generation of FS-40. UVA-340 was introduced in 1987 in order to achieve better correlation with natural weathering. Fig. 5.17 compares emissions of FS-40 and UVA-340 lamps with the daylight spectrum at the Earth's surface.

There is no question that the radiation output of FS-40 and UVB-340 is not comparable with natural conditions. Studies using these lamps were severely criticized and there is basically no rationale behind using such a source. In spite of this, some industries, attracted by the possibility of obtaining fast results (using less expensive equipment), spent a considerable amount of resources on such testing. UVA-340 simulates daylight radiation well in a certain range but does not produce the acceleration caused by higher temperatures. Some wavelengths in the UV range, which are known to degrade materials, are missing or have negligible intensity.

Heraeus developed a metal halide lamp (so-called Ultratest radiation).^{13,14} This lamp has output similar to the xenon arc lamp up to 340 nm but a much stronger radiation in the remaining UV and visible region (Fig. 5.18). The main application of this lamp is in studies where degradation is accelerated by substantially increased temperature. So far, the automotive industry has shown an interest in studies under these conditions (temperatures up to 100°C).

Unfiltered radiation of a high-pressure mercury lamp is also used in some studies. A mercury lamp has its main emission at 254, 290, and 365 nm, which excludes it from the sources which simulate natural conditions.

Fig. 5.19 shows the spectral output of HPUV lamp used in indoor actinic exposure systems.

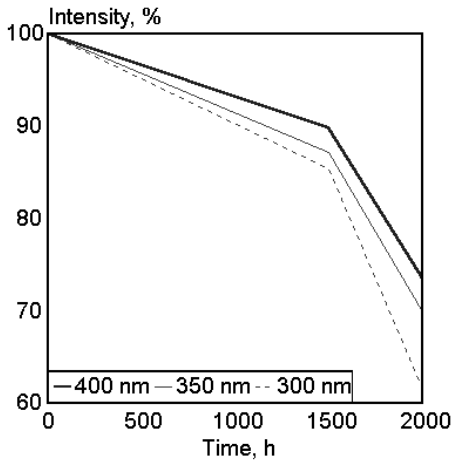


Fig. 5.20. Average drop in intensity of the filtered xenon radiation as a result of burner aging. [Adapted, by permission, from *Xenotest 150S. Light and Weatherfastness Tester. Heraeus, 1988.*]

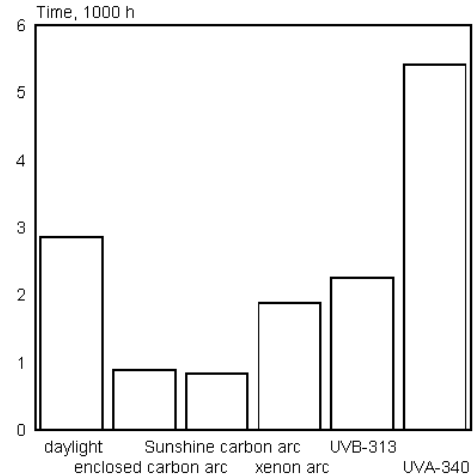


Fig. 5.21. Time to total radiant exposure of 275 MJ/m². [Data from R. A. Kinmonth and J. L. Scott, *Sun Spots*, 14(1984).]

Table 5.1: Spectral power distribution with carbon arc sources [Data from C Series Weather-O-Meter, Bull. 1400, Atlas Electric Devices Company, Chicago, 1987]

Filter		Irradiance, W/m ²		
		<300 nm	300-400 nm	400-800 nm
Single enclosed	Borosilicate	0	85	95
Twin enclosed	Borosilicate	0	85	95
Sunshine	Soda lime	0	90	250
Sunshine	Corex	0.5	90	250
Sunshine	none	3.8	110	275
Daylight	-	0	30	280

Artificial sources have a limited output stability (Fig. 5.20). Xenon arcs are extremely stable compared with carbon arcs, which have to be replaced every day, but it is important to replace the source according to manufacturer recommendation and to use weathering equipment which controls the output.

Finally, Fig. 5.21 compares the time required to produce a total ultraviolet radiant exposure of 275 MJ/m^2 , using typical radiation sources. It is interesting to note in this comparison that xenon arc gives a reasonably good acceleration factor, compared with other sources whose spectra do not resemble natural conditions.

5.2 FILTERS

Light source output can be corrected by filter(s) in order to eliminate UV below 300 nm and excess IR radiation. This situation is characterized by data obtained by Atlas (Tables 5.1 and 5.2).

Table 5.2: Spectral power distribution with xenon arc source [Data from C Series Weather-O-Meter, Bull. 1700, Atlas Electric Devices Company, Chicago, 1989]

Filter		Wattage	Irradiance range, W/m^2			
			<300 nm	300-400 nm	400-800 nm	340 nm
Borosilicate	Borosilicate	2500	0.1	24.4	232.7	0.20
		7000	0.3	122.6	992.2	1.01
Type "S"	Type "S"	2500	0.2	25.6	236.5	0.22
		7000	0.75	133.6	1039.0	1.18
Quartz	Type "S"	2500	0.8	30.3	233.4	0.27
		7000	4.0	146.2	987.2	1.33
Quartz	Quartz	2500	6.1	33.3	227.8	0.29
		7000	36.1	163.9	985.5	1.49
Borosilicate	Soda lime	2500	0	22.4	219.5	0.17
		7000	0	115.4	962.1	0.91
IR absorbing	Borosilicate	2500	0	19.0	181.8	0.13
		7000	0	94.6	839.6	0.64
IR absorbing	IR absorbing	2500	0	17.6	164.1	0.12
		7000	0	79.7	703.1	0.54
CIRA	Type "S"	2500	0.6	33.3	271.6	0.31
		7500	3.2	168.4	1228.3	1.57
CIRA	Soda lime	2500	0	31.3	282.2	0.28
		7500	0.1	151.3	1231.8	1.40
Natural daylight 26° Florida			0	33.0	309.0	0.35
Peak natural daylight			0.1	66.2	617.0	0.69

Table 5.3: Application of various combinations of filters [Data from Ci35A Weather-Ometer, Atlas Electric Devices Company, Bull. 1700, 1989]

Inner filter	Outer filter	Common applications
Borosilicate	Borosilicate	Most common combination used in weathering tests
Type "S"	Type "S"	Weathering tests with higher irradiance level
Quartz	Type "S"	Lightfastness and weathering tests with slightly more intensive and shorter UV
Quartz	Quartz	Lightfastness and weathering tests with much more intensive and shorter UV
Borosilicate	Soda lime	Most common combination for lightfastness tests behind window glass
IR Absorbing	Borosilicate	Lightfastness with slightly lower black panel temperature
IR Absorbing	IR Absorbing	Lightfastness with substantially lower black panel temperature
CIRA	Type "S"	Weathering which requires full spectrum match and/or lower temperature
CIRA	Soda lime	Weathering which requires precise match for solar cut-off, full spectrum match, and lower temperature

With an IR inner filter, black panel temperature can be in the range of 38-60°C, whereas without this filter, the black panel temperature will be above 60°C. The most common applications of various combinations of filters are given in Table 5.3.

A study of one filter system¹⁷ shows that after 400 h of use, an inner borosilicate filter lost about 10% of its transmission. From this data, it appears that the loss of transmission is not wavelength specific therefore it can be compensated by instruments with controlled irradiance (approximately about 50% of the change can be compensated). Instruments without this control do not give repeatable values because of both burner and filter aging.

5.3 SPECIMEN RACKS AND HOLDERS

Depending on the design of the weathering device, specimens may be exposed in the vertical or in the horizontal position, with vertical systems prevailing. In fact, the most recent developments are a two- and three-tier inclined specimen racks which contribute to further improvement of irradiance uniformity. Atlas offers a great variety of rack designs with specimen holders and self-supporting panels. Heraeus offers racks for alternative operating modes with and without turning sample holders, which allows the sample capacity to be increased from 10,000 cm² to 20,000 cm² with some compromise in irradiance uniformity. For better uniformity and when other functions are required (e.g., spraying), the entire rack is driven by a gear motor at a speed of one revolution per minute.

Atlas developed numerous sample holders. 16 different designs allow installation of specimens of various shapes and thicknesses and also permit studies on materials under tension. Heraeus supplies three types of sample holders: with a mask, a thick sample holder, and a holder with a closed back.

It should be noted that the rack is also one of the most essential parts of any weathering equipment. Fischer et al.¹⁷ present data for films exposed in a normal vertical sample drum which allow one to see differences in the irradiation of these samples by the unaided eye. It is obvious that due to the geometry of both the rack and the burner, the intensity of radiation varies up the height of the rack when the rack has a simple cylindrical form. There are racks available which were designed to limit this effect (e.g., three-tier geometry) and information about intensity of radiation distribution can be obtained from the manufacturers. But there is no universal rack and the rack should be chosen according to the required light distribution for a particular weathering device.

5.4 ARTIFICIAL WEATHERING EQUIPMENT

Modern accelerated weathering equipment allows control of the following parameters of testing:

- wavelength of radiation
- radiation intensity
- irradiance uniformity
- energy dosage and exposure time
- temperature
- rain
- humidity

Radiation wavelength is controlled by the choice of source and filters; remarks included in sections 5.1 and 5.2 apply here. Radiation dosage and temperature are micro-processor controlled. Two major producers of weathering equipment, Atlas and Heraeus, offer wavelength control. Atlas controls the intensity of radiation in most instruments at 340 nm (other options such as control at 295-400 nm or 420 nm and sometimes dual measurements are also available), whereas Heraeus controls radiation in the range of 300-400 nm. Radiation intensity at a particular wavelength or in a particular range are continuously controlled by radiometry, comparing and, if needed, adjusting to a preset value.

Artificial weathering instruments differ in size. This has a bearing on the type of source used and their range of irradiance. Sources in small (benchtop) units are lamps of 1500 W which can be continuously regulated in the range of 1000 to 3200 W by adjusting the supply current. In larger units, light sources of 3000, 4500 or 6500 W are used. In

these units, light sources are automatically regulated to provide the required irradiance. Depending on the instrument, irradiance can be regulated in a range of 0.2 to 2.0 W/m² for irradiance measured at 340 nm. Irradiance uniformity on the samples face is typically rated at $\pm 4\%$.

The temperature is monitored using black-panel control and is automatically adjusted to a required preset value. Black-panel temperature combines the effects of air temperature and radiation on the specimen surface temperature and this causes specimen always to be at higher temperature than air in the inside the chamber. Due to the fact that radiation source increases temperature in the chamber, there is always a difference in the accessible temperature range in the light and dark cycles. In instruments designed for extreme conditions (including freeze/thaw conditions), temperature can be regulated between -15 and 95°C in the light cycle and between -55 and 45°C in the dark cycle with a precision of $\pm 2^\circ\text{C}$. Usually, with standard instruments, only black panel temperature can be selected within the range of 40-120°C (the actual instrument range varies). The lower limit of temperature control depends also on the type of filter chosen. With an IR absorbing filter, a lower minimum temperature can be attained.

Humidity can also be controlled in a broad range but its adjustment depends on the temperature selection. In an extreme conditions instrument, the relative humidity can be controlled between 5 and 60% in the light cycle and between 5 and 95% in the dark cycle with a precision of $\pm 5\%$. In standard instruments, the relative humidity can be controlled within the range of 10 to 75% but the actual range available depends on equipment, filters, and operating temperature.

Atlas offers a set of cams, which, mounted in weathering equipment, allow preset duration of time intervals. There are at least 13 cams available. These provide a standardized set of procedures for regulating the duration of light and dark cycles, whether or not rain will be simulated and when, and for how long, the rain condition will occur. This applies only to the earlier instruments. Several currently produced models have rain intervals controlled by computer. This process is also programmable in some Heraeus equipment, such as Xenotest 1200 CPS. In all cases, the above approaches result in reliable repeatable conditions of weathering. There are a few other options on the available equipment, including separate temperature control in the dark cycle, sample back cooling, spray water temperature control, gas heaters, water purification systems, gas composition control (to study pollutants effect), printers, diagnosis programs, data acquisition and transfer to a remote computer. A broad range of data display and inputting is available using a microprocessor controlled functions. The amount of controls depends on the equipment type and its cost. The range of controls available is practically unlimited.

Each company produces a broad range of equipment varying in size, level of controls, type of samples which can be used, sample position, etc. Heraeus is committed to one radiation source, xenon arc, and has the approval of many standards organizations

in Europe and in USA to use their equipment for standard testing of textiles, plastics, printing inks, paints, electronic parts, pharmaceuticals, food, and laminates. Atlas provides equipment using xenon arc, carbon arc, and fluorescent sources. They also have equipment to study the performance of materials in indoor conditions. Atlas is active in supplying equipment for testing the effect of gas exposure on material degradation. Both companies can supply chambers for large scale testing, e.g., for the automotive industry, which can house one or more automobiles fully exposed to weathering conditions. With recent acquisition of Heraeus production of testing machines by Altas, both lines of testing machines will be most likely consolidated. Suga Test Instruments Co., Ltd. offers weathering equipment in Japan.

Literature also offers other alternative solutions which are used in some laboratories. One of them is SEPAP system developed in France^{2,6,7,9} some information about this system is available in Section 5.1. There is also a unique instrument in Japan³ (Okazaki Large Spectrograph) which allows one to expose samples to monochromatic light. Sophisticated controls allow for precise experiment but this necessarily limits the number of studies that can be done. Unique instrument has the disadvantage in real applications that it does not allow one to compare results from various sources. With the two existing lines of instruments there are already questions regarding repeatability and various methods used to verify results. It is therefore probably more efficient to concentrate on improving repeatability of the existing lines of instruments rather than developing brand new techniques which may contribute to further confusion.

In summary, one may say that all required equipment is available, and it is up to the individual to choose one that meets his or her needs. The best basic technology is the xenon arc filtered with borosilicate/soda lime (borosilicate) filters and fully equipped with irradiance and temperature controlling devices. In order to achieve better efficiency in testing, one should find more efficient methods of weathered specimen evaluation, rather than altering the conditions of irradiation such as wavelength or temperature.

REFERENCES

1. A. Torikai, T. Mitsuoka, and K. Fueki, *J. Polym. Sci., Polym. Chem.*, 31(1993)2785.
2. A. Rivaton, *Angew. Makromol. Chem.*, 216(1994)147.
3. Y. Fukuda and Z. Osawa, *Polym. Deg. Stab.*, 34(1991)75.
4. G. Kämpf, K. Sommer, and E. Zirngiebl, *Prog. Org. Coat.*, 19(1991)69.
5. G. Kämpf, K. Sommer, and E. Zirngiebl, *Prog. Org. Coat.*, 19(1991)79.
6. J. -L. Gardette and J. Lemaire, *Polym. Deg. Stab.*, 6(1984)135.
7. J. -L. Gardette and J. Lemaire, *Polym. Deg. Stab.*, 34(1991)135.
8. K. M. Dyumayev, N. P. Kuzmina, V. V. Lobko, G. A. Matyushin, V. S. Nechitailo, and A. V. Chadov, *Intern. J. Polym. Mater.*, 17(1992)121.
9. Y. Isreali, J. Lacoste, J. Lemaire, R. P. Singh, and S. Sivaram, *J. Polym. Sci., Polym. Chem.*, 32(1994)485.
10. J. W. Martin, *Prog. Org. Coat.*, 23(1993)49.

11. G. L. Comerford, *Sun Spots*, 15(1985).
12. P. Brennan and C. Fedor, *Kunststoffe*, 78(1988).
13. J. Boxhammer, *Angew. Makromol. Chem.*, 114(1983)59.
14. J. Boxhammer and T. Rudzki, *Angew. Makromol. Chem.*, 137(1985)15.
15. *Xenotest 150S*, Heraeus.
16. R. A. Kinmonth and J. L. Scott, *Sun Spots*, 14(1984).
17. R. M. Fischer, W. D. Ketola, and W. P. Murray, *Prog. Org. Coat.*, 19(1991)165.

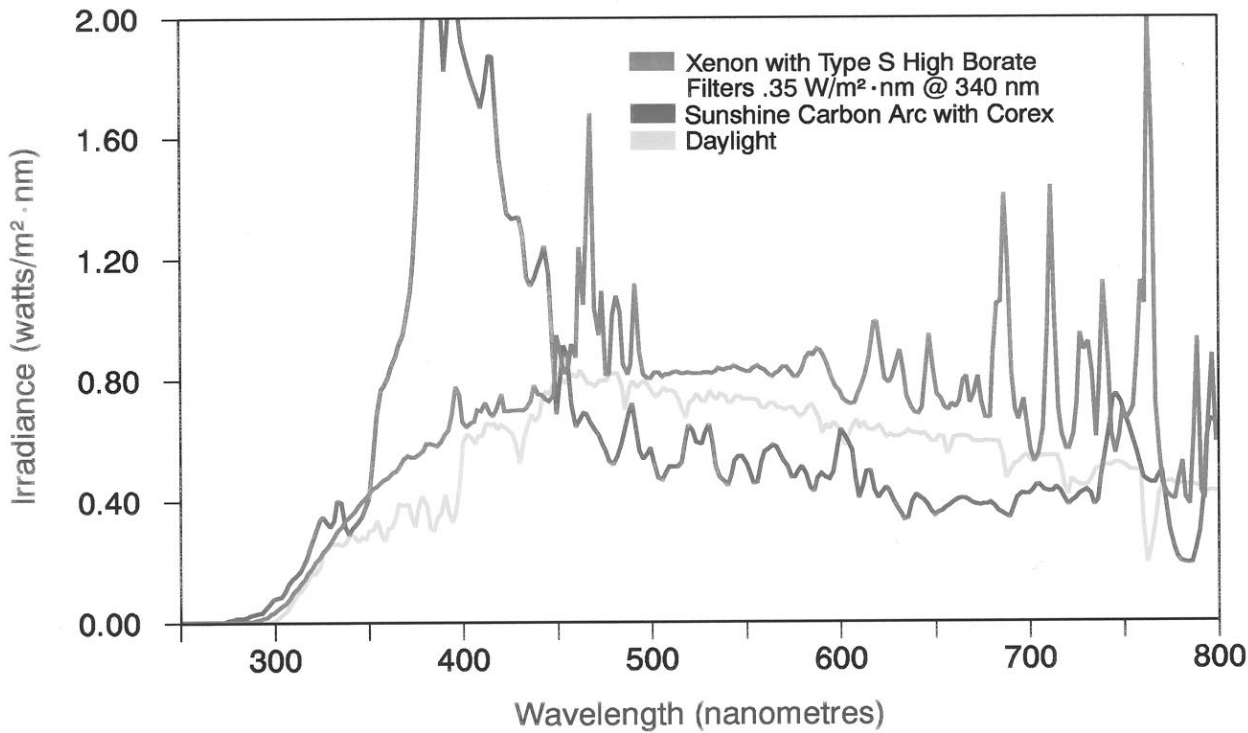


Fig. 5.9. Xenon arc vs. Sunshine carbon arc vs. Miami average 45°S daylight. [Adapted by permission from Atlas Electric Devices Company.]

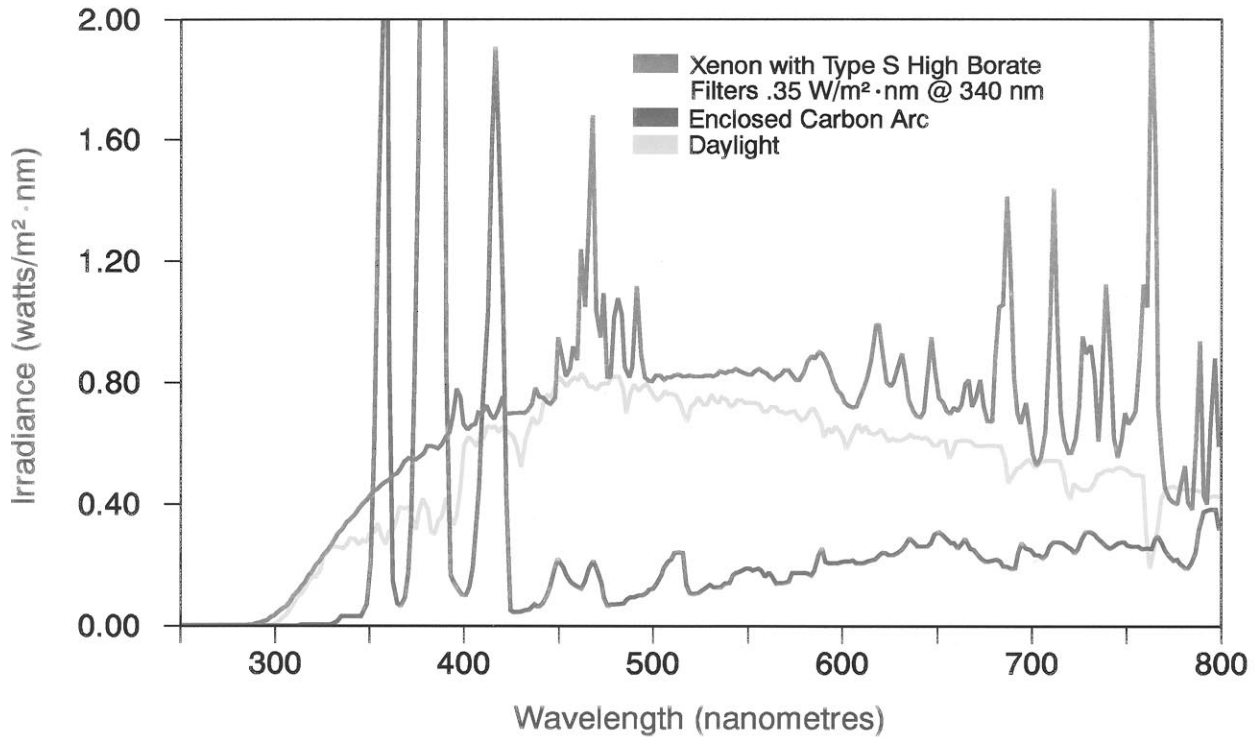


Fig. 5.10. Xenon arc vs. enclosed carbon arc vs. Miami average 45°S daylight. [Adapted by permission from Atlas Electric Devices Company.]

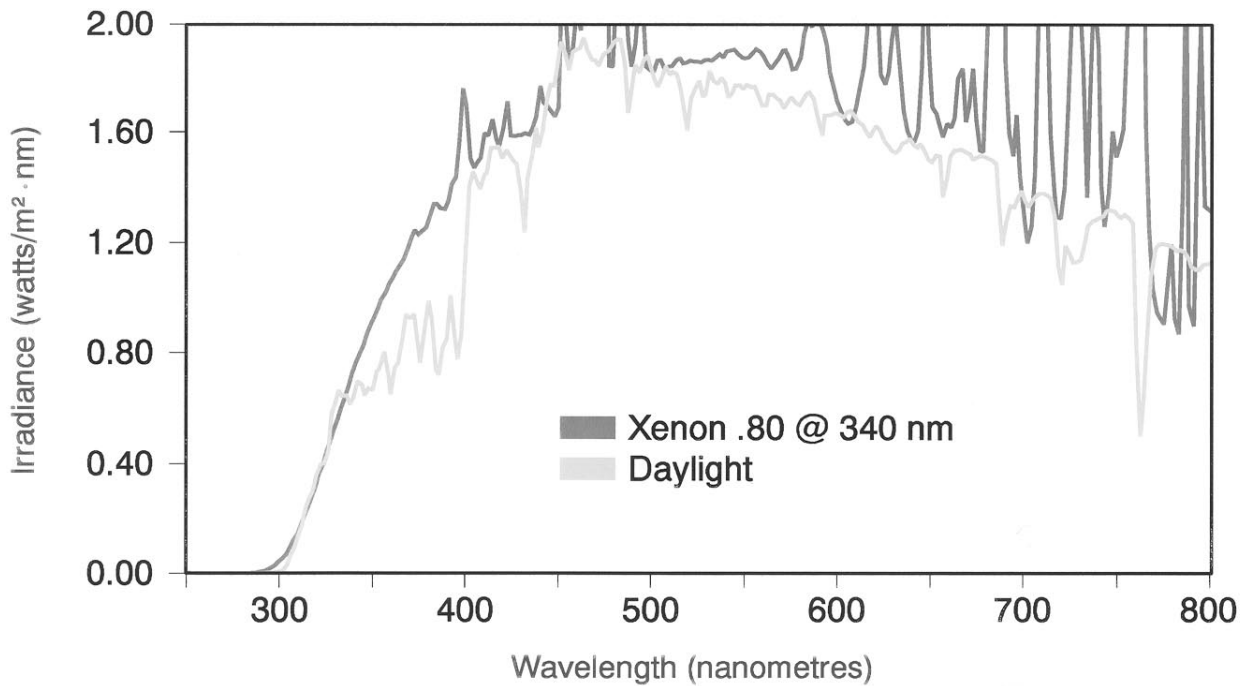


Fig. 5.11. Xenon arc with type S filter vs. Miami "peak" global radiation. [Adapted, by permission, from Atlas Electric Devices Company.]

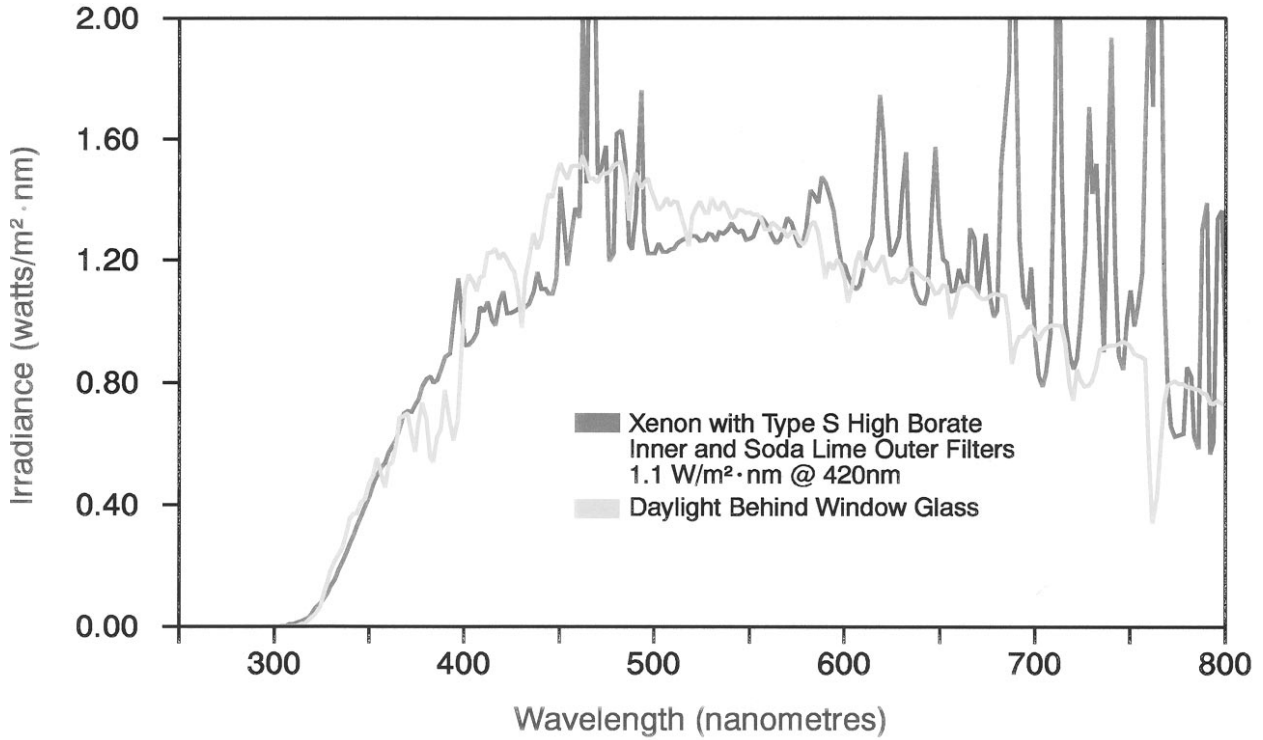


Fig. 5.12. Xenon arc vs. daylight behind window glass daylight. [Adapted, by permission, from Atlas Electric Devices Company.]

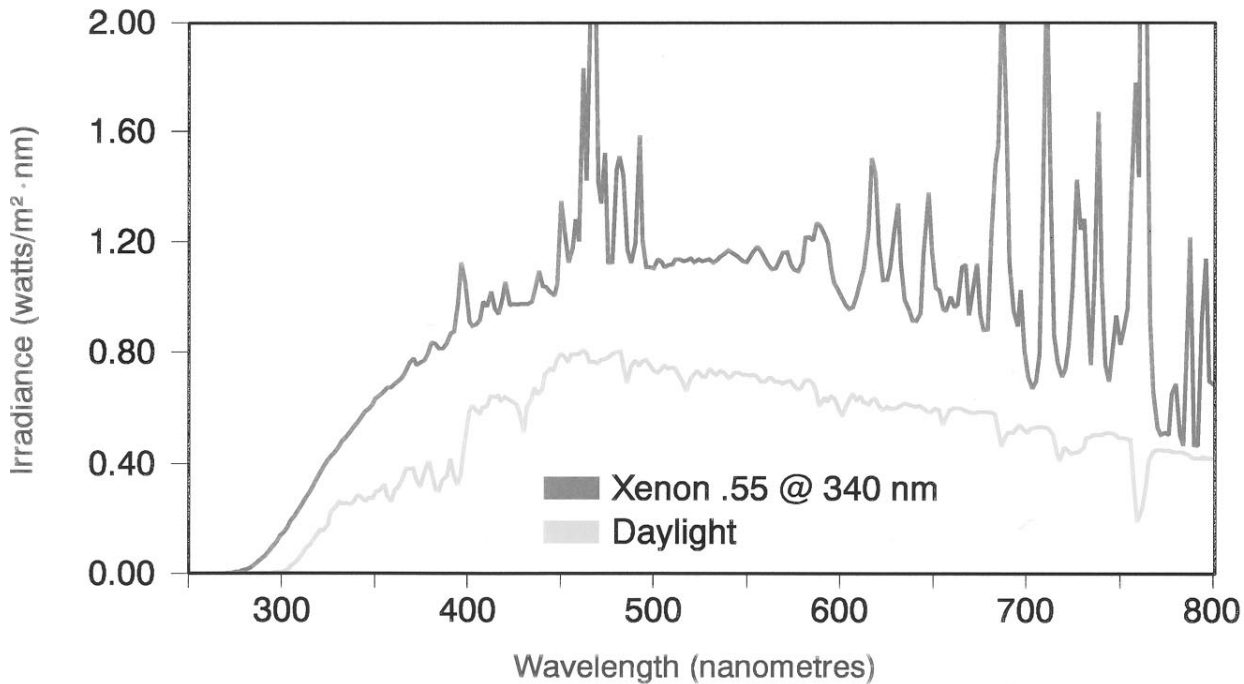


Fig. 5.13. Xenon arc with quartz inner/type S outer filters vs. Miami average 45°S daylight. [Adapted, by permission, from Atlas Electric Devices Company.]

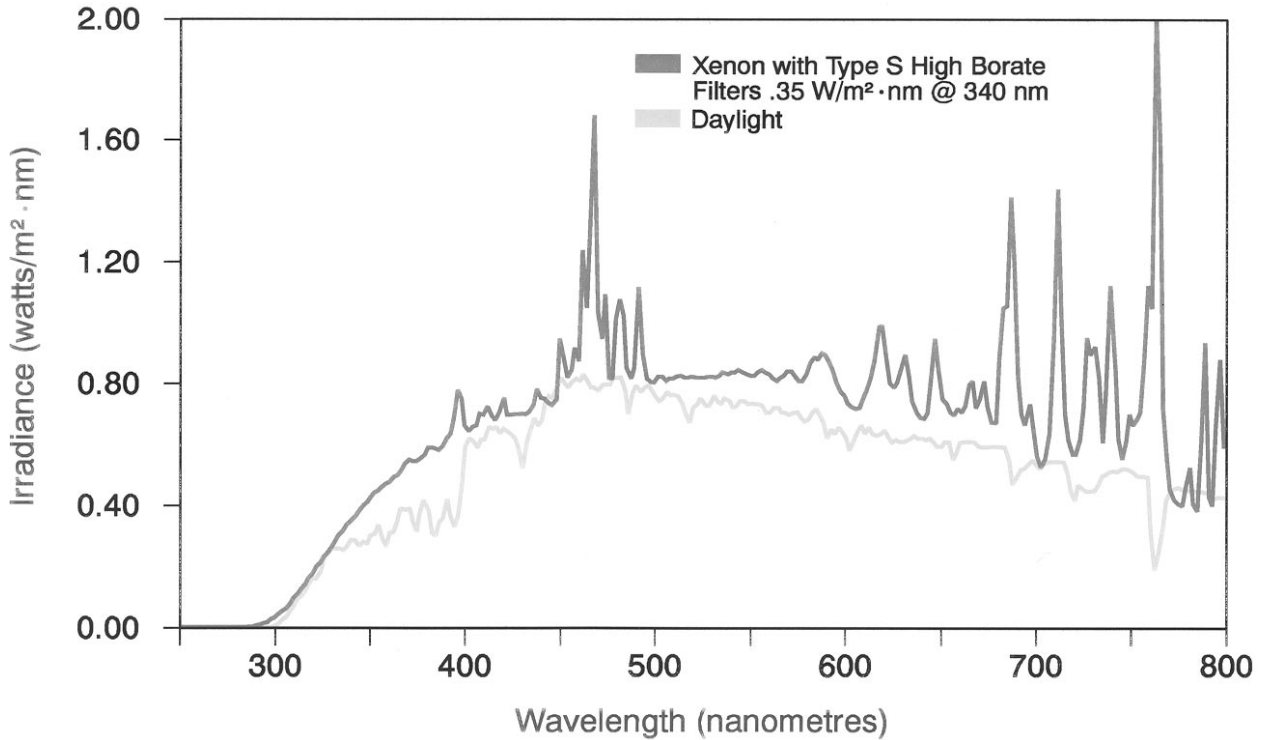


Fig. 5.14. Xenon arc with type S filter vs. Miami average 45°S daylight. [Adapted, by permission, from Atlas Electric Devices Company.]

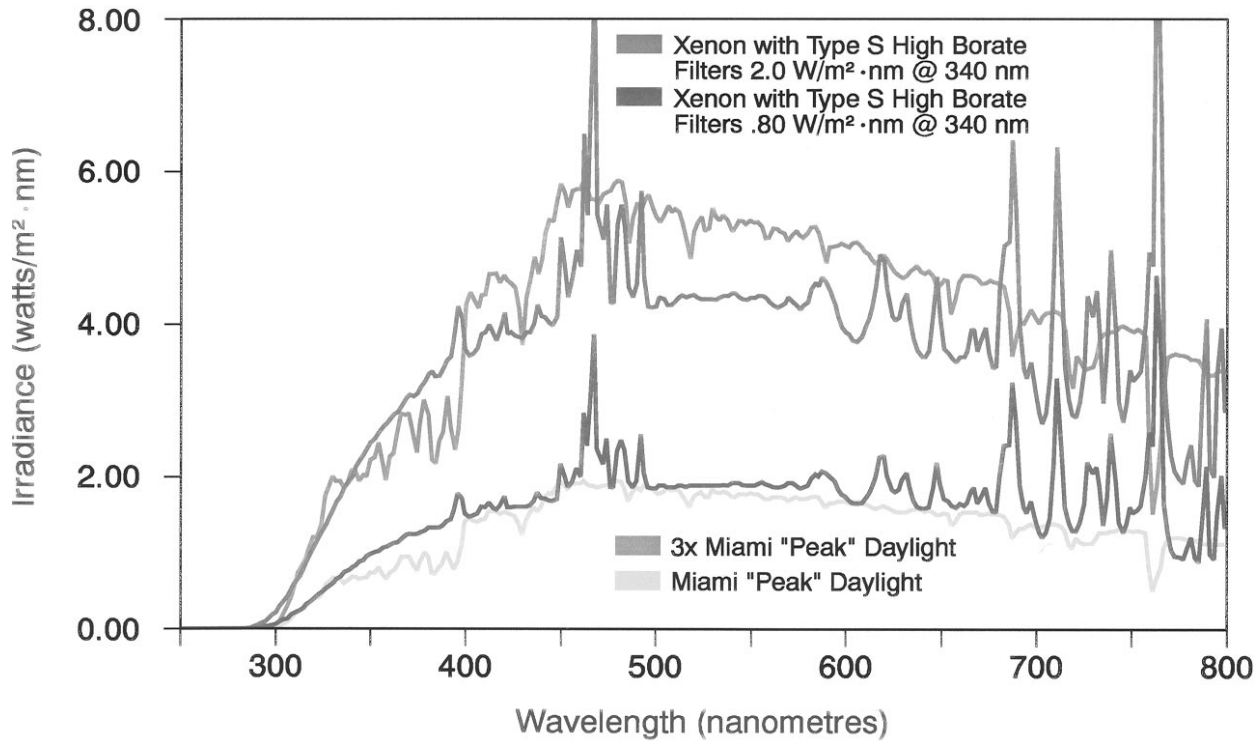


Fig. 5.15. Xenon arc with type S filter vs. Miami average 45°S daylight. [Adapted, by permission, from Atlas Electric Devices Company.]

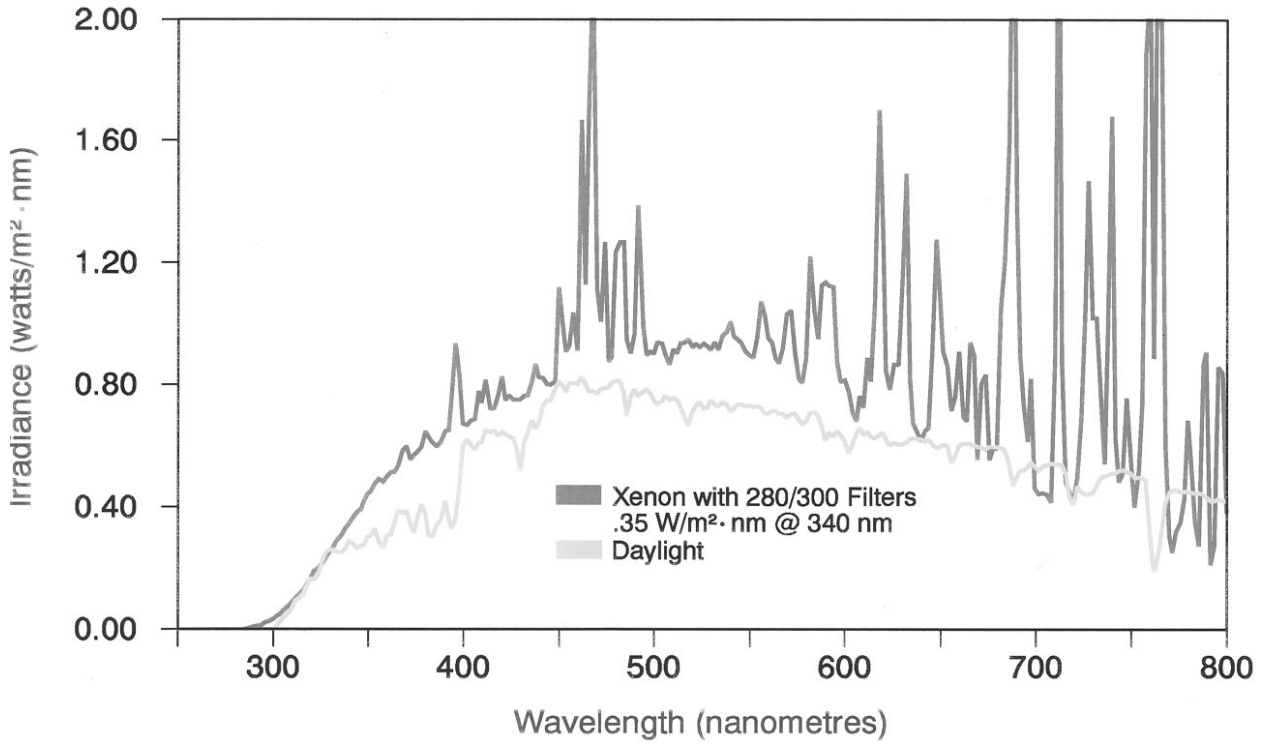


Fig. 5.16. Xenon arc with 280/300 filters vs. Miami average 45°S daylight. [Adapted, by permission, from Atlas Electric Devices Company.]

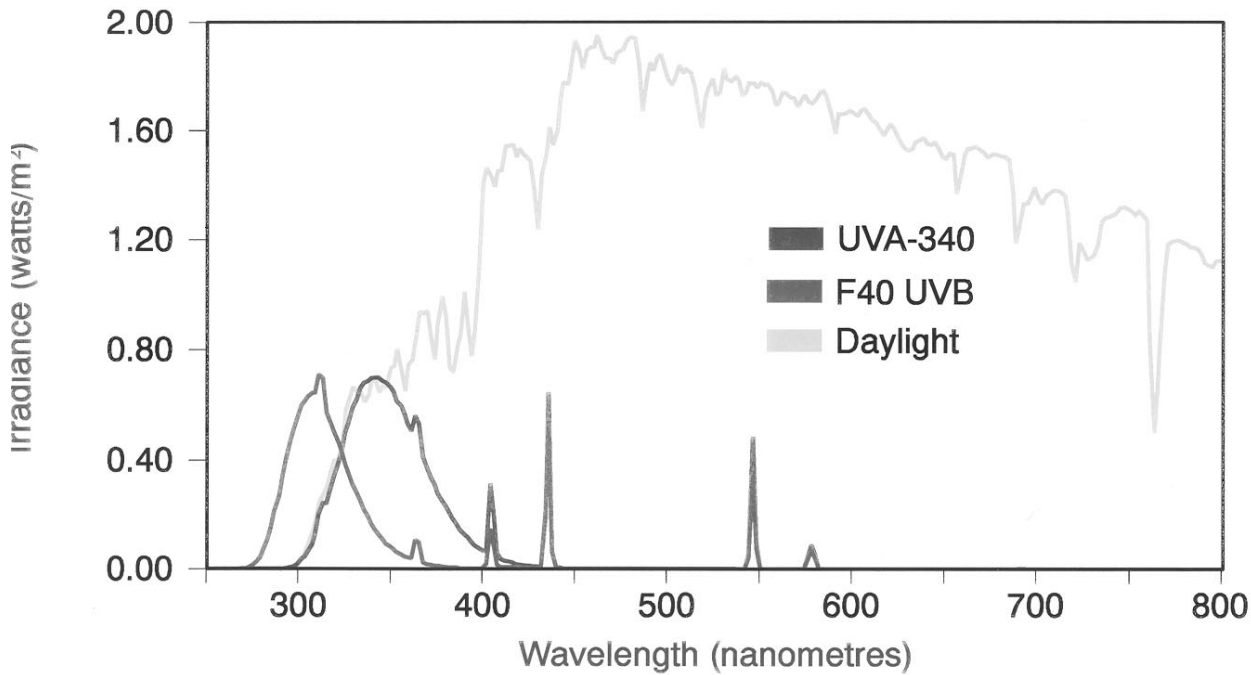


Fig. 5.17. Fluorescent lamps vs. Miami peak daylight. [Adapted, by permission, from Atlas Electric Devices Company.]

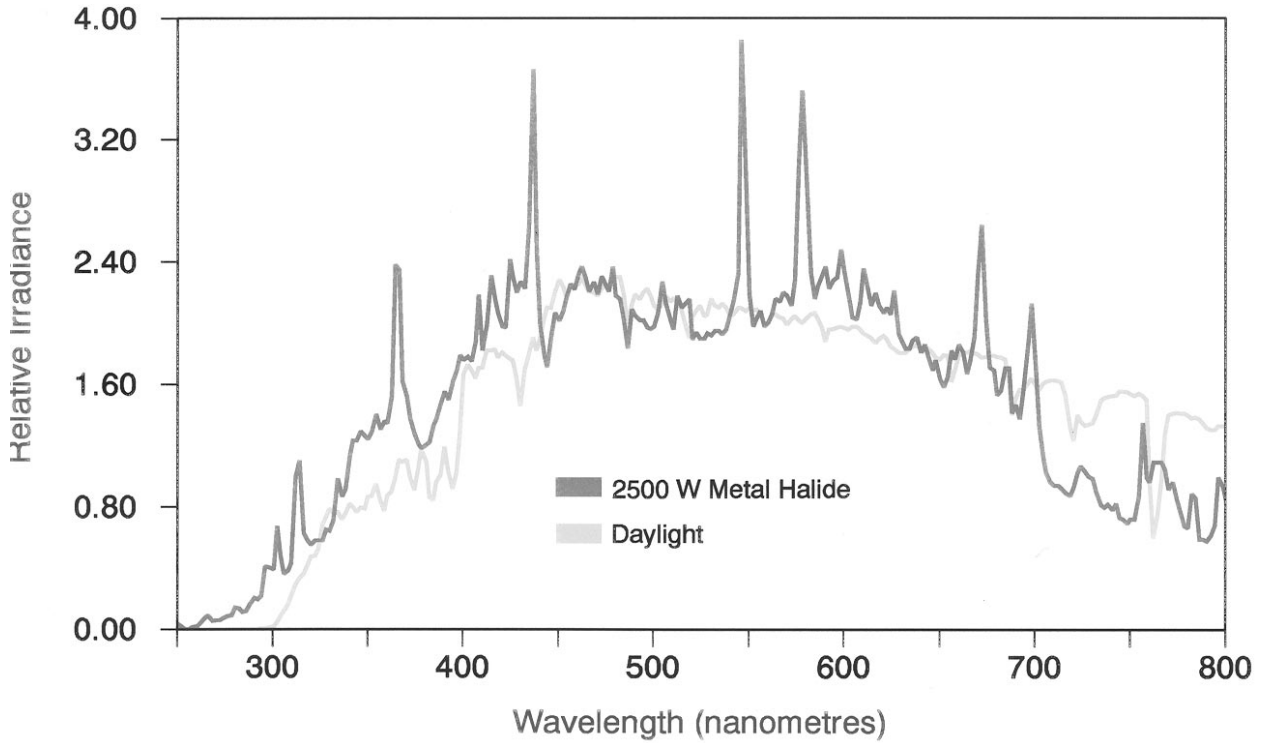


Fig. 5.18. Metal halide lamp vs. Miami average 45°S daylight. [Adapted, by permission, from Atlas Electric Devices Company.]

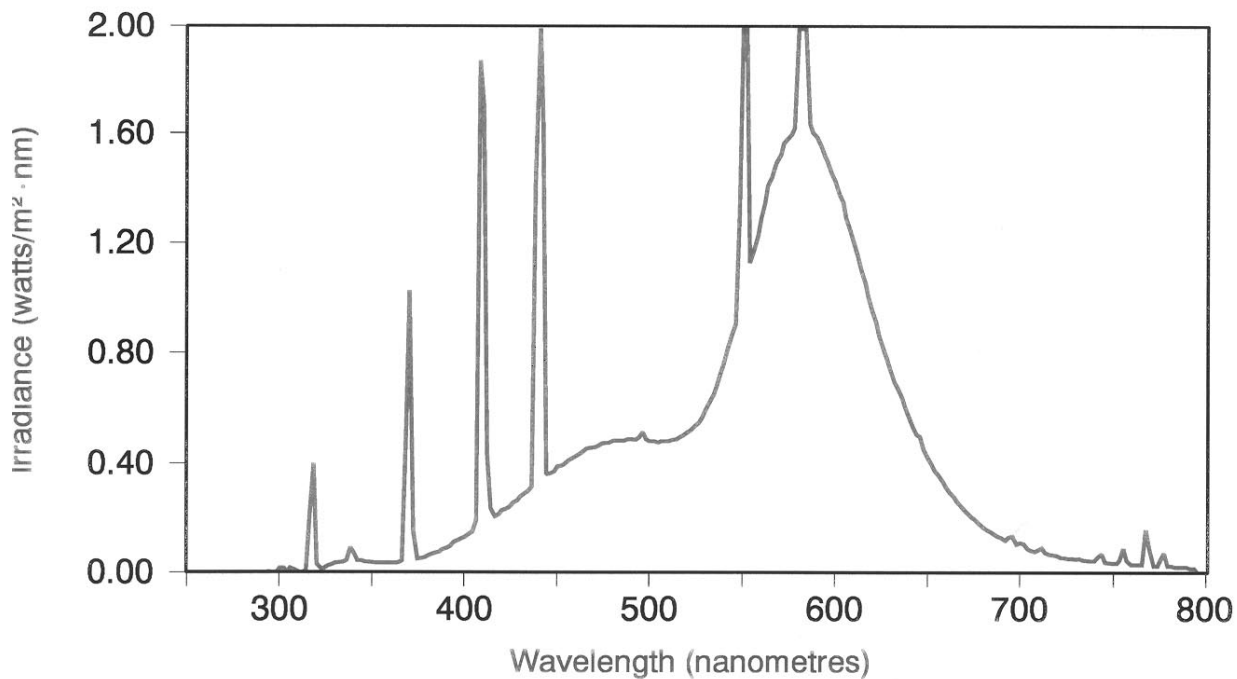


Fig. 5.19. HPUV indoor actinic exposure system. [Adapted, by permission, from Atlas Electric Devices Company.]

6

MEASUREMENTS IN ASSESSMENT OF WEATHERING CONDITIONS

Seasonal and latitudinal variations, sun elevation, pollutant composition, cloudiness, scattering by particles, etc. cause the composition of solar radiation reaching the Earth surface to vary. This, in turn, shows the relevance of data collected under actual weather conditions. Radiation intensity and dose in both natural and accelerated weathering must be known if the effect of each type of exposure is to be compared. On the other hand, all radiation bands are not equal either in their energy or in their effect on materials subjected to weathering. Radiation in the wavelength range of 300-320 nm is usually the most destructive to the majority of materials studied, and thus it is important to know the intensity of radiation in this range as well as in the entire UV range.

Meteorological services throughout the world are the institutions responsible for the systematic collection and exchange of data on climate and weather. Studies are also conducted locally by universities, industry, and various other institutes, but these studies involve only small geographic areas; they are not systematic, and in most cases they are not readily accessible. This tells us that the information on most local conditions can be obtained only from meteorological services of the individual countries. These data contain at best:

- Global solar radiation
- Sky radiation
- Reflected radiation
- Net radiation
- Daylight illumination

and they are available for only a limited number of locations in the world. Radiometers used in these studies (discussed below) belong to the general group of pyranometers, which collect the data of a broad spectrum of the sun's energy, not specifically in the UV

region. Since these data are frequently the only available information on radiative energy at specific points of the globe, this method of measurement is discussed below.

Pyranometry is the older technology of indirect measurement of light which is based on the temperature difference between a black and a white plate. The most important part of a pyranometer is the thermopile made from chromel-constantan wire arranged either in a circular form or in a multijunction linear surface. The surface of the thermopile is blackened with a specially designed durable lacquer which allows the detector element (the thermopile) to absorb almost all of the radiation and approach absorption of a perfect black body. An active thermopile exposed to radiation attains an equilibrium temperature with reference to the thermojunction, resulting in the generation of an emf. The voltage response of the instrument is proportional to the solar radiation flux density through the plane of the sensing element. The detector (thermopile) can convert all wavelengths of radiative energy into an electric signal. Detectors are covered by a filter or filters which are provided to eliminate the infrared part of the spectrum. Usually, a pyranometer has a glass cover which is transparent to radiation between 285 and 3000 nm. These instruments have very good linearity (0.5%) and are not wavelength specific but they are sensitive to temperature. They have a broad range of designs and manufacturers and are made to precise specifications which are usually set by the particular country conducting studies.

Global Solar Radiation is the total incoming shortwave (usually <3000 nm) solar radiation coming from the entire dome of the sky as received on a flat, horizontally-mounted thermopile surface. Sky Radiation is that portion of the total incoming radiation received on a flat, horizontally-mounted thermopile surface which is shielded from the direct rays of the sun by a shade ring. Reflected Radiation is that portion of the total radiation which has been reflected from the Earth's surface and received on a flat, horizontally-mounted, downward-faced thermopile surface. Net Radiation is the net difference between incoming and outgoing radiation. Daylight Illumination is the total visible radiation measured in the range between 510 and 610 nm. Radiation data for selected locations are given in the tables included in Chapter 4.

The above data, although important because of their availability, consist of only approximate information on weathering conditions. More precise information on the energy delivered in the UV range is needed. In order to obtain readings of UV energy, the instrument must consist of three basic elements: the collector, the wavelength selector, and the signal producing element. Mirrors or lenses are usually used to collect sunrays, gratings or filters are used to select wavelengths, and photo-electron or photo-ionization detectors are used to produce signals. The spectral response of a radiometer depends on detector sensitivity and on filter transmittance. Depending on the type of filter used, radiometers can be narrow band (these measure light of only a narrow spectral range or ideally of a single wavelength) or wide band systems. The most frequently used detectors are either silicon photodiodes or photomultipliers.

Spectrographs or spectroradiometers are the most sophisticated and thus the most expensive measuring devices. They demand constant attention during use and are not designed for continuous use. They differ from other radiometers in that they can scan a broad range of radiation wavelengths and thus can provide precise information on radiation composition. But, because of their cost and the difficulty in using them, these instruments are seldom used. They differ from radiometers in that they use a monochromator instead of a filter. Light, before reaching the monochromator, is depolarized and integrated. Monochromators use either ruled or holographic gratings. More sophisticated instruments have double grating to eliminate noise. Rotation of gratings allows one to scan the entire spectrum and determine its composition precisely. Detectors may be either Si photodiodes or photomultipliers. Photodiodes have lower responsiveness to UV radiation (which is their drawback). Photomultipliers have a very wide range but are very sensitive to temperature variations and to variations in the supplied high voltage.

Only a few UV radiometers are available and some of these are discussed in more detail below. The Ultraviolet Radiometer produced by Eppley Laboratory, Inc. has a specially designed disc receiver of opaque quartz which reduces the radiant flux to an acceptable level and permits close adherence to the Lambert cosine law. An encapsulated, narrow band, pass (interference) filter limits incoming radiation to the 295-385 nm range. Incoming radiation is measured by a hermetically-sealed selenium barrier-layer photoelectric cell protected by a quartz window. This instrument has the following specification:

Sensitivity:	150 V per W/m^2
Temperature dependence:	0.1%/deg C in the range of -40 to 40°C
Linearity:	2% (0-70 W/m^2)
Response time:	milliseconds
Cosine response:	±2.5% from normalization at 0-70° Zenith angle
Orientation:	no effect on instrument performance

These limitations exist:

- Spectral sensitivity of the selenium barrier-layer photocell to UV is lower than its peak sensitivity to visible light, meaning that it might be more sensitive to variations in the visible range than to variations in the UV range.
- It is not thermoregulated, which may cause a shift in peak response to longer wavelengths as temperature increases.

The Radialux UV-measuring device is a radiometer produced by Heraeus, who also produces weathering equipment. The advantage of this instrument lies in the fact that the radiation dose is measured in both natural and accelerated conditions using the same instrument. Because Radialux has two sensors, a UV sensor for the 300-400 nm range and a global sensor for 300-800 nm range, it can be used with all of the weathering

equipment manufactured by Heraeus. Incoming radiation enters the instrument through a Teflon diffusion disc which gives true cosine sensing, then passes through a variable filter which permits wavelength selection. The signal is measured by a Si photodiode with the largest available dynamic range of radiation measurement which extends through 10 orders of electric current magnitude. The control panel display shows: irradiance (W/m^2), radiation dosage (Wh/m^2), last reading, and battery capacity. The instrument has the following specification:

Sensitivity:	0.65 nA to 3.25 mA
Temperature drift:	$\pm 2.5\%/10$ deg C
Cosine response:	$\pm 2\%$ (0-60° Zenith angle)

The instrument has these limitations:

- Silicon photodiodes have their sensitivity peak in the near IR, which limits their operation at temperatures below 40°C.
- The sensitivity of the Si photodiode depends on wavelength therefore the result depends on the spectral distribution of the measured beam
- It is not thermoregulated.

The Atlas Model LM3A offers an advantage to Weather-O-Meter users in that the same measuring device is used for both outdoor and for indoor energy dose monitoring. The principle of design differs from the other two instruments. Atlas chose a narrow band filter design. The instrument consists of two elements: a detector (placed on the sample rack) and an electronic processor (usually located inside the laboratory facilities) connected by cable. The detector contains an UV-transmitting, cosine diffuser, narrow-band, interference filter (usually 340 nm, but 420 and 580 nm filters are available). Light energy is converted to an electric signal by a thermomechanically cooled photodiode. The display of the electronic processor shows: spectral irradiance, spectral irradiation, and total operating time. The instrument's performance can be restricted when narrow-band sensors are used for control, especially when there is a significant spectral shift.

From the above discussion, we can see that this area of radiation measurement technology is still in the development stage and requires further efforts and studies.

7

SAMPLE PREPARATION FOR WEATHERING STUDIES

There are two main reasons for testing the weather stability of materials:

- product evaluation
- the study of degradation principles.

The rationale for sample choice and preparation is different in each case. The evaluation of material produced according to a particular technology requires that the specimen conforms as closely as possible to the typical properties of material from normal production. Such a sample should, at best, be composed of regular production material, having in mind that several important factors, as discussed below, will affect the results of the study.

In order to study degradation principles, the researcher should first assure that the material studied is:

- well-defined
- prepared under conditions which can always be repeated
- uniform in structure and composition
- representative of the particular group of materials, processes, etc.
- not contaminated
- permits the drawing of adequate conclusions.

Well-defined material means that its properties, such as chemical composition, molecular weight distribution, conformation, configuration, crystalline structure, etc., have been studied and are well-defined prior to photochemical experiments. Specimens should always be prepared under standard, ideally uncomplicated, conditions from components which are also well-defined to allow other researchers to repeat the experiment and to compare data from different studies. The method of specimen preparation should

assure that the thickness, concentration of components, morphology, thermal treatment, physical-mechanical properties, etc. are uniform throughout the cross-section of the material used for studies.

The composition of the studied specimen should be chosen in such a way that not only reflects the most frequently-used components but also gives consideration to the fact that each component in the material plays a discrete role in degradative changes and may introduce several new variables into the study.

Materials should be prepared in form, composition, and manner which conform to real-life situations. For example, the annealing of samples which are normally cured at room temperature does not generate an acceptable sample. Neglecting to control or specify conditions of the thermal processes involved in specimen preparation undermines the relevance of such studies. It is important that the raw materials and method of preparation do not introduce contaminants, as, even in small quantities, they can act so efficiently that their influence may supersede the relationships studied. Above all, the experimental plan should be evaluated before starting and an assessment should be made as to whether the study as planned can deliver valuable conclusions.

It seems almost trivial to outline guidelines for sample preparation but analysis of research papers¹⁻⁶⁴ shows that adequate information about the studies conducted is not always included and, in some cases, it is evident that evaluation of the method of specimen preparation was simply never an important part of the agenda. For example, in the study of polyurethanes, the authors cast films from DMF solution on glass plates, dried the film at 60°C in a vacuum for 1.5 h, then immersed specimens in water for a prolonged period of time to separate them from the glass. Several errors were made in this sample preparation, most important being the fact that samples should simply have been cast on release paper or on teflon plate, either of which method would have eliminated water immersion. Water immersion is likely to cause hydrolytic changes in the material which would make its composition different from the actual material to be studied. The authors of a paper on polycarbonates manually shaved samples with a scalpel, referring to the material collected as a 10 µm thick layer; material taken from the center of a 3 mm thick specimen was treated as a control neglecting evidence that shows that degradative changes frequently extend more than 1.5 mm below the material surface (see discussion below). There are many such examples. It is important to review the existing procedures and information in order to postulate a more systematic approach to these very expensive and important studies which must be as precise as existing techniques permit.

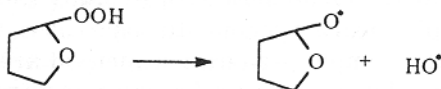
Let us analyze, first, the information on specimen preparation available in the literature in order to summarize the status quo and propose solutions when needed. The samples of materials studied are either liquid or solid. Those that are liquid are usually solutions of materials used as solids. A study using liquid solutions is unusual and it has been often questioned mostly on two grounds:

- polymeric materials behave differently when exposed to radiation in solution than they do when exposed in the solid state
- solvent introduces new mechanisms by quenching excited states or by undergoing its own photolytic changes.

The differences in behavior of polymeric materials, when photolyzed in solution and solid state, are principally related to the differences in chain mobility even at very low concentrations. Solvents increase chain mobility and facilitate conversions which do not normally occur in the solid state. Photochemical reactions are conformation specific. One conformation has a specific reaction mechanism. If conformation changes, that reaction mechanism may not apply. In solution, conformation change is much easier than in the solid state. Also, excited states may transfer an amount of energy adequate for chain or segmental mobility in solution but inadequate for similar mobility in the highly restricted solid state. Radical processes may lead to recombination when chain mobility is low or radicals may react differently, depending on their environment. In general, studies in solution should be discouraged as they may lead to invalid conclusions. On the other hand, introduction of solvent into the system causes that additional low molecular weight material is present. Solvent presence may change the course of photochemical reactions. Solvents participate in excited state quenching by:

- the external heavy atom effect
- energy transfer
- exciplex formation.

Carbon tetrachloride is believed to quench excited states according to an external heavy atom effect mechanism (methylene dichloride does not quench). Exciplex formation quenching is associated with solvents containing cyano, amino, or aromatic ester groups. Dimethylformamid also quenches according to this mechanism. Energy transfer is less probable because the excited state of the solvent is usually below that of the polymer chromophore. Monomers in samples also produce a solvent effect. Styrene in polystyrene is an excimer-forming site. Solvents are also able to form free radicals when exposed to radiation. Fig. 7.1 shows the rate of photooxidized product formation from tetrahydrofuran. Tetrahydrofuran-hydroperoxide is a very photolytically active impurity, which readily produces free radicals:



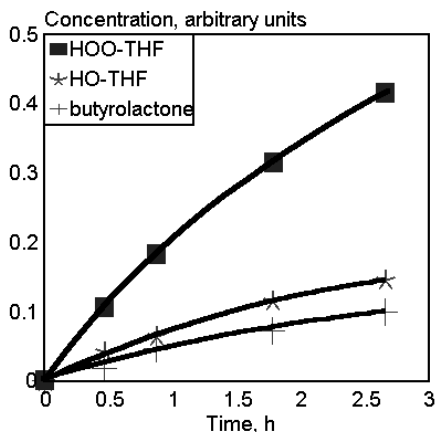


Fig. 7.1. Kinetic curves of tetrahydrofuran oxidation product formation during irradiation at 254 nm. [Adapted, by permission, from J. F. Rabek, T. A. Skowronski, and B. Ranby, *Polymer*, 21(1980)226.]

Many other solvents may absorb radiation and interact with the components of polymer chains to cause mechanism change. Ketones are particular example. It should be taken into account that the removal of traces (the last 2-3%) of solvent from polymer film is very difficult to accomplish even under vacuum and when assisted by extraction with methanol.

Solvents may be used in extraction of components or be used to disperse minor additive. An example of extraction can be taken from PVC or PBT studies.^{61,62} Prior to sample exposure, a thermal stabilizer was extracted by solvent to avoid its contribution to polymer degradation. In some cases, polymers are also precipitated prior to forming.⁶³

UV stabilizers are frequently introduced after predispersing them in solvent.

Solid samples are prepared for most materials either by substrate coating from solution or melting the material. Both methods have disadvantages. The negative effects of solvent presence have been discussed above. Heating of polymeric materials, especially in the presence of air, introduces thermal changes leading to the formation of groups which absorb radiation and form radicals. There is no easy answer as to whether specimens should be exposed to heat or obtained from solution. Some researchers are fortunate enough to be able to prepare a specimen without using either solvent or heating. If this is not possible, the least damaging method should be used, depending on the material's thermal stability and solubility. If it is not clear which is the least damaging, the method selected should be the one closest to that used in normal processing of the material. In some research, it is customary to follow the procedures used in the production method religiously when the studies are geared to gathering background information on the weather stability. This results in a complex regime of heating (1 h - 60°C followed by 1 h at 80°C and 0.5 h at 130°C) for polyester resin studies or (3 h at 135°C followed by 3 h at 180°C and 3 h at 220°C) for epoxy resins, as quoted in the recent literature. Unless researchers wish to study thermal degradation, they would do well to select simpler heating regime. In some cases, temperature effects and potential changes due to the sample preparation method are carefully considered.⁵⁸ Polyolefin tapes having two different regimes of processing were compared in the study. In order to eliminate the effect of sample preparation on results, two sets of samples were heated prior to exposure

at 100°C in sealed ampoules to eliminate persistent radicals then the samples were cooled at fixed rate before exposing them to atmosphere to prevent their oxidation and assure that each experienced the same thermal history (one which was thermally treated and other which was not under normal conditions of processing).

The composition of the specimen is usually meticulously determined. In many research papers, the methods of purification of solvents and other components are given. There are also examples of studies where samples are 'used as received', sometimes referring to polymer samples, but also to sheets of material bought from the nearest dealer, who obviously cannot identify the conditions of sample preparation as they are simply unknown. Rare attempts have been made to study such samples by analytical techniques.

Some authors studied a very well-defined polymer, consisting of analytical standards coming from reputable vendors or materials which had been studied for molecular weight distribution, purified by numerous precipitations, prepared with known thermal stabilizers, which, after thermal processing, were extracted from the material, then checked to determine the extent of the degradative processes. In some cases, an attempt was made to eliminate thermally induced changes from the material. Stabilizers, initiators, metal catalysts, heavy-metal-containing additives should all be controlled in specimens because of their very powerful effect on photolytic reaction kinetics. In Chapter 14 of this book, there is available information on known impurities which are photochemically active. This information should be consulted to evaluate the composition of a specimen used in a study.

Very few researchers consider the morphological character of their specimens. There is sufficient data available (see Chapter 15) to be concerned about the effect of sample morphology on photodegradation. In one study on polyesters, the degree of crystallinity, gauche/trans ratio, orientation, and birefringence were carefully evaluated. Morphological studies are included in less than 5% of the papers and these are usually papers discussing fibers, as, in this field, there is sufficient experience to treat such studies as routine. Recent paper⁵⁷ is a very good example of such an approach. Fibers were not only characterized by their crystalline structure but an elaborate method of specimen preparation was used to test the material under stress. In most other papers, the authors neglect the fact that cooling rate during sample preparation may decrease or increase the reaction rate of the photochemical process by a factor of two, three or more, which makes it impossible to draw correct conclusions. Again, before a proper choice of sample preparation method is made, it would be beneficiary to consult these chapters which discuss the effect of crystallinity and stress on the rates of the degradative processes. This has not been included here to avoid repetition.

Samples may be coated on various substrates. Substrates include molds which have release properties (release paper, teflon, glass, etc.), crystals used for material support in analytical methods (salt, quartz, etc.), and substrates which are typically used in

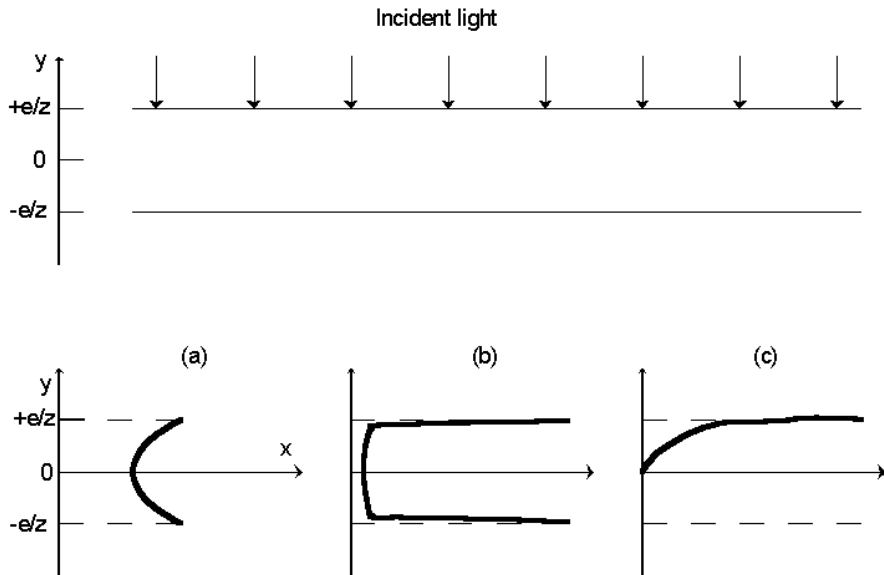


Fig. 7.2. Repartition of photochemical degradation vs. depth. Symbols: x - degree of degradation, y - distance to the center of sample. (a) Material transparent to UV and permeable to O_2 , (b) transparent to UV and not permeable to O_2 , (c) slightly transparent to UV. [Adapted, by permission, from P. Eurin, *Durability Building Mater.*, 1(1983)161.]

coatings (aluminum, steel, etc.). In some cases, the authors take great care not to contaminate the studied material with substrate material by using gold-plated glass or sapphire. In coating studies, great attention is given to the surface finish - steel might be diamond paste polished to remove oxidation and material imperfections, aluminum panels are phosphated and chromated. But there are also papers where no indication is given that the surface of substrate was of concern.

Contamination from the substrate surface is a major concern, and must be taken into consideration along with the sample characteristics. Eurin⁴ prepared an interesting diagram which adequately characterizes the situation (Fig. 7.2). He clearly shows that in the case of transparent samples both surfaces are affected and the bottom surface may have a considerably increased level of radiation if the substrate has reflective properties.

The other aspect of substrate choice relates to its expansion coefficient which, in conjunction with the expansion coefficient of the specimen itself, decides the amount of stress introduced to the specimen when the sample temperature changes. This factor is not always considered. Paint specimens⁵⁴ studied in laboratory were coated on galvanized steel and outdoor exposure studies were done on red cedar.⁵⁴ The expansion coefficients of these two substrates are quite different and this makes a successful comparison

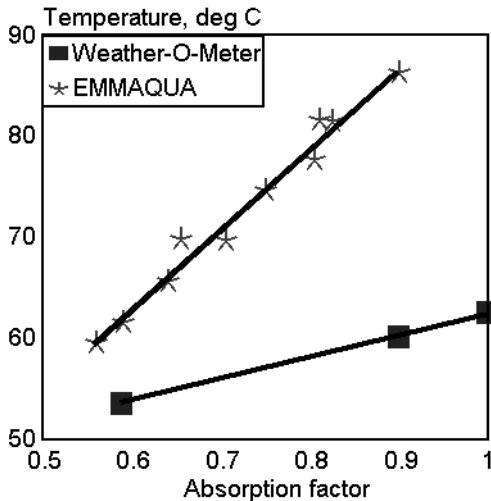


Fig. 7.3. Correlation between color and specimen temperature during exposure. [Adapted, by permission, from E. Takeshima, T. Kawano, H. Takamura, and S. Kato, *Shikizai Kyokaishi*, 56(1983)457.]

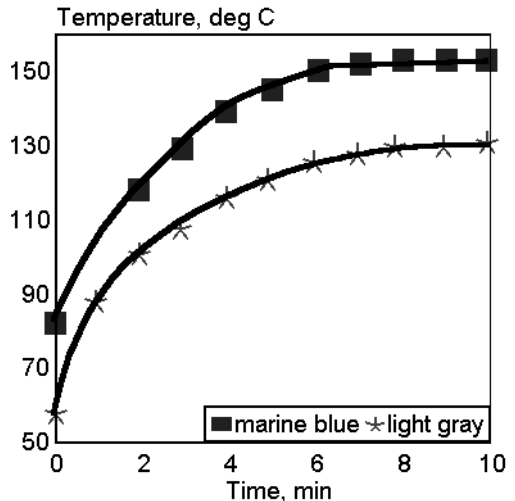


Fig. 7.4. Temperature rise after stopping of cooling blower on EMMAQUA tester for samples of different colors. [Adapted, by permission, from E. Takeshima, T. Kawano, H. Takamura, and S. Kato, *Shikizai Kyokaishi*, 56(1983)457.]

of the results impossible. It was also discovered in this study that zinc from the galvanized steel leached through the specimen. Authors of another paper⁵⁵ on paint testing prepared the wood substrate by splitting panel to obtain two their mirror-image surfaces thus reducing variability of the substrate to minimum.

Specimen color is another important consideration (Figs. 7.3 and 7.4). The rate of photochemical reaction depends not only on the energy of radiation but also on the temperature, and on other parameters; therefore, the higher the temperature of specimen, the higher the degradation rate. When samples of different colors are compared, a substantial error might be introduced due to greater heat absorption by darker colors. Fig. 7.4 shows that the cooling rate (e.g., wind) can also cause different reactions in samples of different color.

On the pages to follow one of the more important parameters of a specimen - thickness - will be discussed. Since such a discussion is not presented in other parts of this book a full account of available details is given. Comparing various studies, one may conclude that two different thicknesses of samples are predominant. For analytical studies by FTIR, UV, NMR, ESR, etc., sample thickness is most frequently in the 15-35 μm range. Microtoming techniques are used for sample preparation in experiments where degradation depth is analyzed.⁵⁹ Samples used for tensile or other physical-mechanical

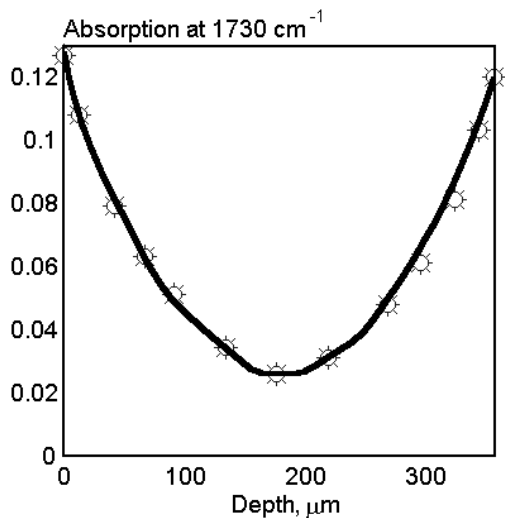


Fig. 7.5. $D_{1730\text{cm}^{-1}}$ vs. depth from specimen surface. [Adapted, by permission, from X. Jouan and J.-L. Gardette, *Polym. Commun.*, 28(1987)329.]

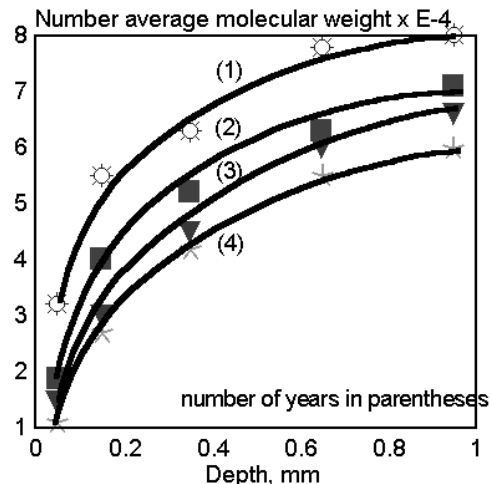


Fig. 7.6. Change in number average molecular weight with depth. Polystyrene sheet exposed outdoors for varying time. [Adapted, by permission, from Y. Watanabe and T. Shirota, *Kenkyu Hokoku-Kogyo Gijutsuin*, 2(1981)149.]

testing are usually thicker, in the range of 0.2-1 mm. There are also specimens used outside this range - the thinnest being 50 nm and the thickest over 3 mm. Frequently, the results with specimens of different thickness are compared in the scope of the same work (e.g., chemical changes versus tensile properties). It is therefore very important to analyze the implications of such treatment of data. Fig. 7.5 shows the carbonyl distribution versus PVC sample thickness.⁶ A sample was irradiated through the thickness, then scanned at various depths. There was no backing on the sample yet the degradative changes still formed a mirror image about mid depth because carbonyl group formation is an oxygen diffusion controlled process.

Polystyrene samples were exposed for various times in natural and in artificial conditions and their average molecular weight analyzed versus sample thickness (Figs. 7.6 and 7.7). Similar dependence can be seen for polydispersity (Figs. 7.8 and 7.9). The depth of sampling has a more pronounced effect on the molecular weight than the period of exposure. Both degradation degree and apparent diffusion coefficient for oxygen vary with thickness (Figs. 7.10 and 7.11). Polyethylene behaves in a manner similar to polystyrene (Figs. 7.12 and 7.13). The rates of carbonyl group formation were drastically different at various depths, suggesting the possibility that here, the mechanism of carbonyl formation may be different. Chemical changes were accompanied by physical-mechanical changes in the material (Figs. 7.14-7.16).

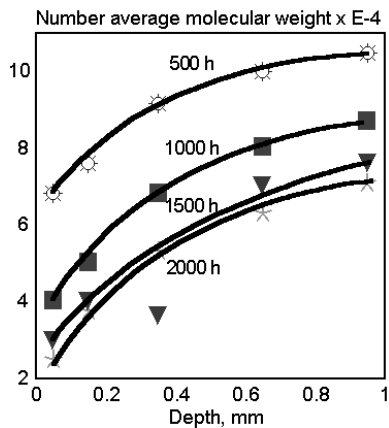


Fig. 7.7. Change in number average molecular weight with depth. Polystyrene sheet exposed to carbon arc radiation for varying time. [Adapted, by permission, from Y. Watanabe and T. Shirota, *Kenkyu Hokoku-Kogyo Gijutsuin*, 2(1981)149.]

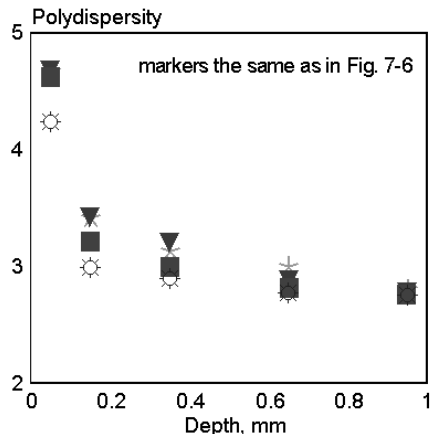


Fig. 7.8. Depth dependence of M_w/M_n for outdoors exposed polystyrene sheet. [Adapted, by permission, from Y. Watanabe and T. Shirota, *Kenkyu Hokoku-Kogyo Gijutsuin*, 2(1981)149.]

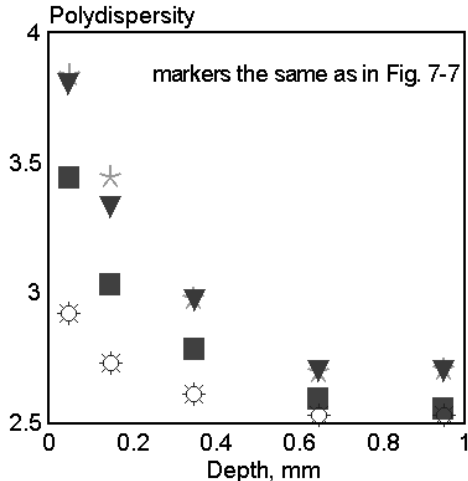


Fig. 7.9. Depth dependence of M_w/M_n for polystyrene sheet exposed to carbon arc. [Adapted, by permission, from Y. Watanabe and T. Shirota, *Kenkyu Hokoku-Kogyo Gijutsuin*, 2(1981)149.]

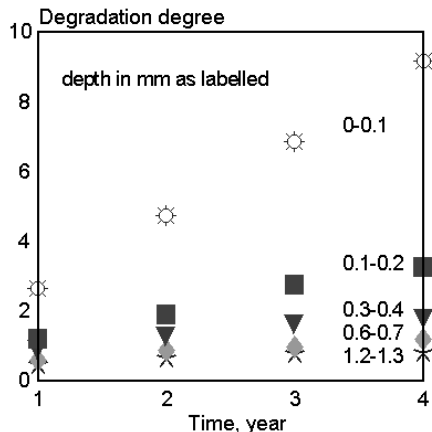


Fig. 7.10. Degradation degree $[(1/DP_n - 1/DP_{n0}) \times 10^3]$ at various depths vs. outdoors exposure time of polystyrene sheet. [Adapted, by permission, from Y. Watanabe and T. Shirota, *Kenkyu Hokoku-Kogyo Gijutsuin*, 2(1981)149.]

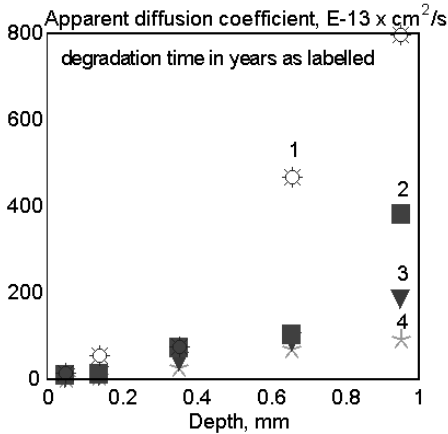


Fig. 7.11. Apparent diffusion coefficient of oxygen vs. depth from surface of polystyrene sheet exposed outdoors for varying time. [Adapted, by permission, from Y. Watanabe and T. Shiota, *Kenkyu Hokoku-Kogyo Gijutsuin*, 2(1981)149.]

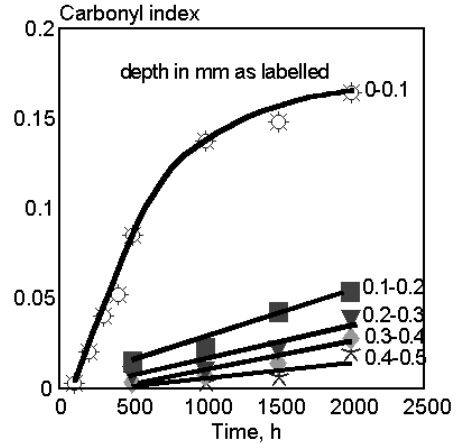


Fig. 7.12. Change in carbonyl index at various depths vs. exposure time of PE sheet. [Adapted, by permission, from Y. Watanabe and T. Shiota, *Kenkyu Hokoku-Kogyo Gijutsuin*, 2(1981)141.]

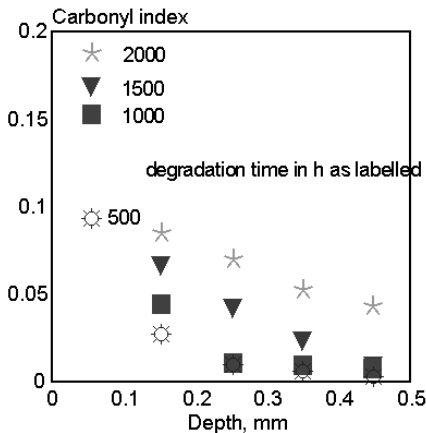


Fig. 7.13. Carbonyl index vs. depth from the surface of weathered PE sheet for different times. [Adapted, by permission, from Y. Watanabe and T. Shiota, *Kenkyu Hokoku-Kogyo Gijutsuin*, 2(1981)141.]

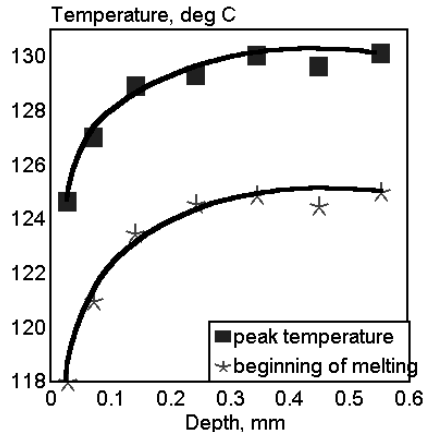


Fig. 7.14. DSC melting peak temperature (T_{m2}) and starting temperature of melting (T_{m1}) vs. depth from the surface of PE sheet exposed for 2000 h. [Adapted, by permission, from Y. Watanabe and T. Shiota, *Kenkyu Hokoku-Kogyo Gijutsuin*, 2(1981)141.]

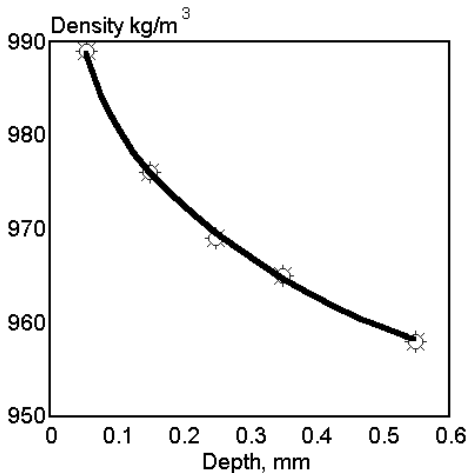


Fig. 7.15. Density change vs. depth from surface of PE sheet exposed for 2000 h. [Adapted, by permission, from Y. Watanabe and T. Shirota, *Kenkyu Hokoku-Kogyo Gijutsuin*, 2(1981)141.]

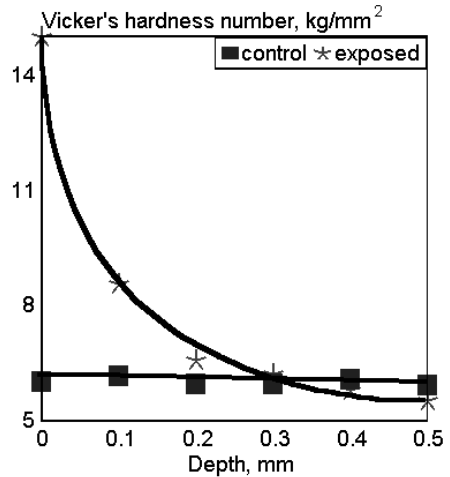


Fig. 7.16. Vicker's hardness number vs. depth from surface of polyethylene sheet exposed for 2000 h. [Adapted, by permission, from Y. Watanabe and T. Shirota, *Kenkyu Hokoku-Kogyo Gijutsuin*, 2(1981)141.]

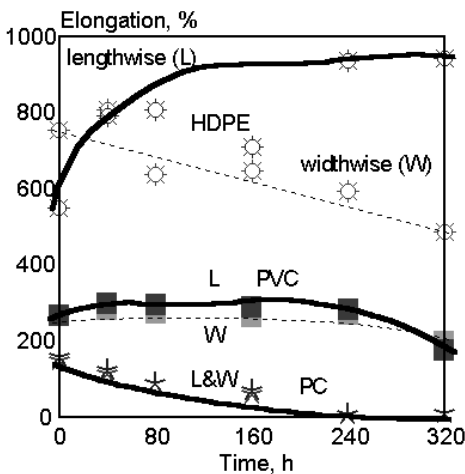


Fig. 7.17. Lengthwise (L) and widthwise (W) elongation of various polymers vs. exposure time in Sunshine Weatherometer. [Adapted, by permission, from O. Nishimura, S. Suzuki, H. Kubota, and K. Yoshikawa, *Hokkaido Kogyo Kaihatsu Shikensho Hokoku*, 24(1981)193.]

Since increasing crystallinity is a typical photodegradative change in polyethylene, both density and Vicker's hardness were higher in surface layers. Nishimura⁹ studied several polymers and he commented not only on the depth of degradation but also on the variation in properties across the width and along the length of the sample (Figs. 7.17 and 7.18).

In his study of HDPE, he reported substantial differences in elongation retention for specimens tested widthwise and lengthwise. Sample thickness affected the degradation of all polymers except polyamide. Figs. 7.19 and 7.20 summarizes this data. Evaluation of results for polymer durability or lifetime would be severely affected if sample thickness was not considered.

The strategy of how the sample should be treated after its exposure must be care-

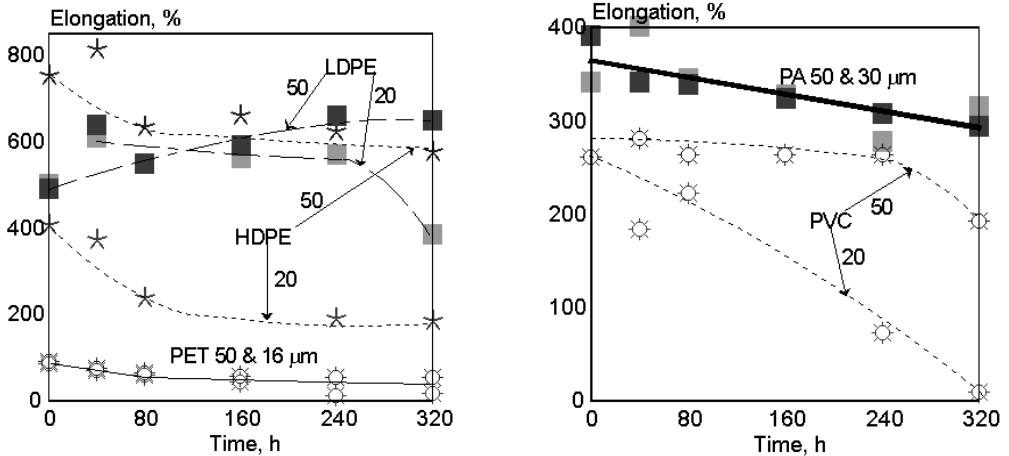


Fig. 7.18. Elongation of polymer films of different thickness vs. irradiation period in Sunshine Weatherometer. [Adapted, by permission, from O. Nishimura, S. Suzuki, H. Kubota, and K. Yoshikawa, *Hokkaido Kogyo Kaihatsu Shikensho Hokoku*, 24(1981)193.]

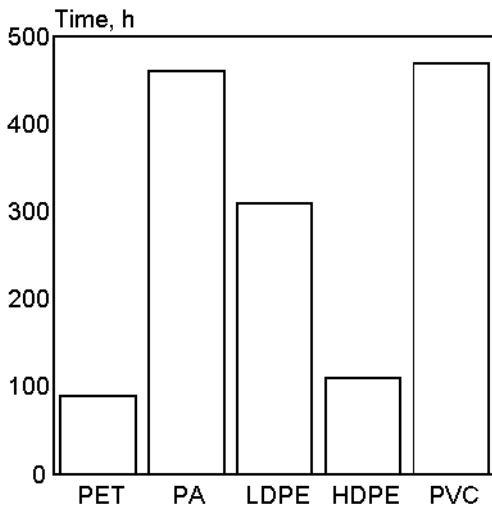


Fig. 7.19. Exposure period in Fadeometer required to reduce ultimate elongation of 50 μm film by half. [Data from as Fig. 8.18.]

fully worked out. How the sample should be processed after it is taken out from exposure field for evaluation is always open to question. Pitfalls that may occur in resolving this question are exemplified by the space program experience.⁵⁶ Due to the conditions in space, samples were returned with a surface heavily contaminated by a dark smoke-like material and inorganic particles such as silica and heavily eroded in a complex, non-uniform surface pattern. Instrumental surface analysis of these samples will determine the composition of the deposit but will not yield any information on the changes that have occurred in the sample itself. Similar situation can occur with samples exposed in natural conditions, even though the effects might be slightly different. The most common contamination

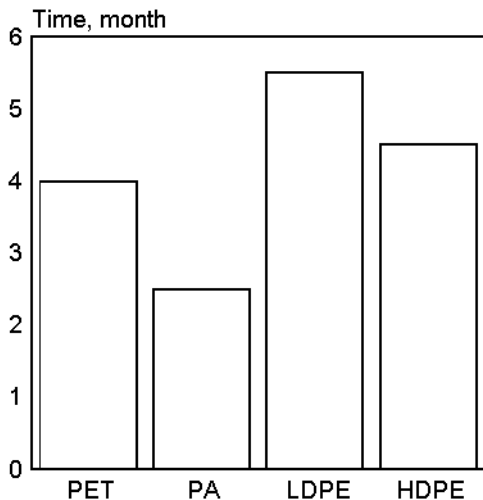


Fig. 7.20. Outdoor exposure time to reduce elongation by half. [Data from as Fig. 8.18.]

effective method has been used in some laboratories where samples have been exposed in sealed quartz containers. This eliminates surface contamination but at the same time several parameters of natural weathering conditions (oxygen, pollutants, wet/dry cycle) are also eliminated.

In some cases,⁶⁰ samples for weathering are prepared by mechanical abrading of the surface to obtain a roughened surface. This allows a visual observation of the surface changes brought about by weathering. Formation of low molecular weight substances, which can melt or flow during degradation, can be thus observed.

The method of samples storage, prior to their weather exposure, is also of concern in some studies. Frequently samples are prepared in advance and, in order to avoid oxidation, they are stored in a dessicator. Some researchers protect their samples from the laboratory radiation by wrapping them in thick, black film (usually polyethylene).

We have pointed out several important sources of errors in weathering studies which might be specimen-related. The list below summarizes the most important variables which should be evaluated in order that the sample studied is a valid and representative material (Table 7.1).

These conditions deal with the most common situations. The conditions available may not always be ideally suited for generating the required information, but attempts must be made to improve the existing practice of providing only a fragmentary descrip-

is from dust particles. Some of these particles are attached to the surface only by static electricity forces, and these can be removed by washing. Many particles are embedded in the sample by attractive forces such as van der Waals forces. These particles cannot be removed without damaging the sample surface. If vigorous action (e.g., brushing) is taken to remove these particles, scratches result which affect sample performance on subsequent exposure. Also, washing the specimen may deposit foreign substances such as detergent on it which may interfere with readings and affect sample performance on subsequent exposure. There is no general rule which can be applied to surface cleaning. The method chosen will depend on the sample and on the method of testing but its selection is an essential factor in research planning. One ef-

Table 7.1: Important considerations regarding specimens for weathering studies

Composition

- small amount of components
- purity of components
- detailed characteristics of polymer
- photoactivity of components
- close to real material

Method of specimen processing

- processing additives (solvents, stabilizers, initiators, etc.)
- processing conditions (time, temperature, pressure, etc.)
- cooling rate
- solvent removal
- effect on composition

Substrate

- contaminating elements
- photocatalytic effect
- radiation reflectance versus specimen transparency

Specimen thickness

- repeatability
- uniformity

Morphology

- crystallinity
- orientation
- configuration, conformation
- surface roughness

Stress

- initial
- change during exposure

Change of specimen properties in the course of exposure

tion of experimental conditions. Specimen definition is an important factor in determining the success of studies and the comparability of results.

In order to reinforce the believe that a need for improvement is real and that it can be achieved by simple means, several experiences from South Florida Test Service are quoted. It was observed that some samples shipped were not flat when prepared. Subsequently, attempts were made to flatten them by force which resulted in stress formation, loss of adhesion, cracks, and development of crazes. Coated samples were packaged for shipment before they were dry and some of them arrived glued to neighboring samples. Some samples were not separated from each other and had visible signs of mechanical wear which affects their degradation. Samples of plastic materials and textile materials were folded for shipment forming creases which, again, contribute to different behavior

during weathering. Surfaces of samples were frequently contaminated by dust during their preparation. Also some shipment containers are unable to withstand impact during transportation and not designed to separate samples from one another.⁶⁴ Most samples are well prepared but it is important that these essential prerequisites of sample handling are remembered to avoid recording results which depend not on the material itself but on the sample preparation.

REFERENCES

1. K. Esumi, K. Meguro, A. M. Schwartz, and A. C. Zettlemoyer, *Bull. Chem. Soc. Jpn.*, 55(1982)1649.
2. E. Takeshima, T. Kawano, H. Takamura, and S. Kato, *Shikizai Kyokaishi*, 56(1983)457.
3. S. Yajima, Y. Togawa, S. Matsushita, T. Suzuki, and T. Okada, *Kinzoku Hyomen, Gijutsu*, 37(1986)718.
4. P. Eurin, *Durability Building Materials*, 1(1982)161.
5. S. G. Croll, *Prog. Org. Coat.*, 15(1987)223.
6. X. Jouan and J. -L. Gardette, *Polym. Commun.*, 28(1987)329.
7. A. Charlesby, *J. Radioan. Nucl. Chem.*, 101(1986)401.
8. V. Rek, H. J. Mencer, and M. Bravar, *Polym. Photochem.*, 7(1986)273.
9. O. Nishimura, S. Suzuki, H. Kubota, and K. Yoshikawa, *Hokkaido Kogyo Kaihatsu Shikensho Hokoku*, 24(1981)193.
10. Y. Watanabe and T. Shirota, *Kenkyu Hokoku-Kogyo Gijutsuin*, 2(1981)149.
11. Y. Watanabe and T. Shirota, *Kenkyu Hokoku-Kogyo Gijutsuin*, 2(1981)141.
12. B. S. Rao and M. R. Murthy, *J. Polym. Sci., Polym. Phys.*, 25(1987)1897.
13. Z. Osawa, E. -L. Chen, and K. Nagashima, *J. Polym. Sci., Polym. Chem.*, 15(1977)445.
14. V. Rek and M. Bravar, *J. Elastom. Plast.*, 12(1980)245.
15. M. Igarashi and K. L. DeVries, *Polymer*, 24(1982)769.
16. E. Baimuratov, B. N. Narzullayev, I. Ya. Kolontarov, and A. W. Zakcharchuk, *Dokl. Akad. Nauk Tadzh. CCR*, 27(1984)204.
17. W. P. Yartsev, *Plast Massy*, 1986,12,16.
18. A. Torikai, A. Takeuchi, and K. Fueki, *Polym. Degrad. Stab.*, 14(1986)367.
19. S. W. Addy, D. W. Clegg, A. A. Collyer, G. C. Corfield, and P. Crum, *J. Rheol.*, 31(1987)297.
20. C. L. Bauer, R. J. Farris, and M. S. Vratsanos, *Polym. Mat. Sci. Eng.*, 56(1987)560.
21. R. Gooden, D. D. Davis, M. Y. Hellman, A. J. Lovinger, and A. F. Winslow, *Macromolecules*, 21(1988)1212.
22. J. -L. Philippart and J. -L. Gardette, *Makromol. Chem.*, 187(1986)1639.
23. R. Geetha, A. Torikai, S. Nagaya, and K. Fueki, *Polym. Degrad. Stab.*, 19(1987)279.
24. L. H. Garcia-Rubio, *Macromolecules*, 20(1987)3070.
25. J. Stumpe and K. Schwetlick, *Polym. Degrad. Stab.*, 17(1987)103.
26. K. Kikkawa, Y. Nakahara, and Y. Ohkatsu, *Polym. Degrad. Stab.*, 18(1987)237.
27. S. E. Webber, *New Trends in the Photochemistry of Polymers*. Elsevier, 1985.
28. R. Gooden, M. Y. Hellman, D. A. Simoff, and F. H. Winslow, *New Trends in the Photochemistry of Polymers*. Elsevier, 1985.
29. N. S. Allen, *New Trends in the Photochemistry of Polymers*, Elsevier, 1985.
30. T. Gantcheva, A. Marinova, and P. Genova, *Angew. Makromol. Chem.*, 137(1985)49.
31. H. N. Neidlinger, M. R. Steffek, and R. Goggin, *Polym. Prep.*, 28(1987)205.

32. D. R. Bauer, M. J. Dean, and J. L. Gerlock, *Polym. Mat. Sci. Eng.*, 55(1986)443.
33. S. Okamoto, H. Hikita, and H. O. Nishiguchi, *Polym. Paint. Colour J.*, 177(1987)683.
34. G. Geuskens, G. Delaunois, Q. Lu-Vinh, W. Piret, and C. David, *Eur. Polym. J.*, 18(1982)387.
35. J. D. Webb and A. W. Czanderna, *Macromolecules*, 19(1986)2810.
36. S. J. Valenty, J. J. Chara, W. Katz, D. R. Olson, and G. Smith, *Polym. Mat. Sci. Eng.*, 53(1985)288.
37. I. Mita, T. Takagi, K. Horie, and Y. Shindo, *Macromolecules*, 17(1984)2256.
38. H. S. Munro, D. T. Clark, and J. Peeling, *Polym. Degrad. Stab.*, 9(1984)185.
39. Z. Osawa, F. Konoma, S. Wu, and J. Cen, *Polym. Photochem.*, 7(1986)337.
40. K. Nate, M. Ishikawa, N. Imamura, and Y. Murakami, *J. Polym. Sci., Polym. Chem.*, 24(1986)1551.
41. M. Ishikawa, *Polym. Prep.*, 28(1987)426.
42. Yu. I. Dorofeev, *Dokl. Akad. Nauk CCCR*, 292(1987)654.
43. T. M. Wilson, R. E. Fornes, R. D. Gilbert, and J. D. Memory, *Poly. Mat. Sci. Eng.*, 56(1987)105.
44. J. M. Augl, *J. Rheol.*, 31(1987)1.
45. M. E. Abu-Zeid, *J. Appl. Polym. Sci.*, 32(1986)2875.
46. H. J. Bowley, D. L. Gerrard, K. J. P. Williams, and I. S. Biggin, *J. Vinyl Technol.*, 8(1986)176.
47. M. H. Tabankia and J. -L. Gardette, *Polym. Degrad. Stab.*, 14(1986)351.
48. A. Ram, O. Zilber, and S. Kenig, *Polym. Eng. Sci.*, 25(1985)535.
49. P. L. Beltrame, E. Dubini-Paglia, B. Marcandalli, P. Sadocco, and A. Seves, *J. Appl. Polym. Sci.*, 33(1987)2965.
50. S. C. Lin, B. J. Bulkin, and E. M. Pearce, *J. Polym. Sci., Polym. Chem.*, 17(1979)3121.
51. T. Nguyen and E. Byrd, *Polym. Mat. Sci. Eng.*, 56(1987)584.
52. A. Factor, W. V. Ligon, and R. J. May, *Macromolecules*, 20(1987)2461.
53. J. F. Rabek, T. A. Skowronski, and B. Ranby, *Polymer*, 21(1980)226.
54. E. O. Edney, *Report*, EPA/600/3-89/032.
55. J. W. Hook, P. J. Jacox, and J. W. Spence, *Prog. Org. Coat.*, 24(1994)175.
56. A. F. Whitaker and J. Gregory, Eds., *NASA Conf. Publ. no. 3257*, NASA 1994.
57. M. C. Perry, M. A. Vail, and K. L. DeVries, *Polym. Eng. Sci.*, 35,(1995)411.
58. W. Ken Busfield and M. J. Monteiro, *Mater. Forum*, 14(1990)218.
59. A. Murase, Y. Esaki, M. Sugiura, and T. Araga, *Anal. Sci.*, 7(1991)1597.
60. G. Zhang, W. G. Pitt, S. R. Goates, and N. L. Owen, *J. Appl. Polym. Sci.*, 54(1994)419.
61. J. -L. Gardette and J. Lemaire, *Polym. Deg. Stab.*, 34(1991)135.
62. A. Rivaton, *Polym. Deg. Stab.*, 41(1993)283.
63. T. Yamashita, H. Tomitaka, T. Kudo, K. Horie, and I. Mita, *Polym. Deg. Stab.*, 39(1993)47.
64. *A Guide to product durability testing and research. South Florida Test Service, R/5/5/89.*

8

NATURAL WEATHERING CONDITIONS

8.1 GENERAL DESCRIPTION

Chapter 7 discussed important factors in sample preparation for weathering studies. This chapter is designed to analyze the exposure conditions that are important for a successful study of specimen degradation in natural weathering conditions. Most attention is given to the sample exposure conditions rather than to radiation intensity and climate variations, which are discussed in Chapter 4. Similarly, the effect of stress is omitted here, since it is discussed in detail in Chapter 11.

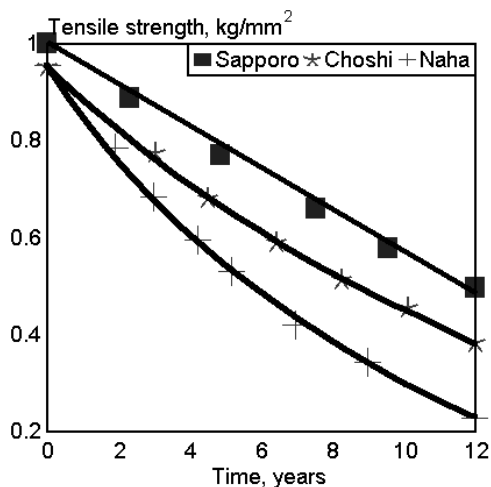


Fig. 8.1. ABS tensile strength vs. outdoor exposure in different sites. [Adapted, by permission, from H. Kubota, S. Suzuki, O. Nishimura, K. Yoshikawa, and T. Shiota, *Kenkyu Hokoku-Kogyo Gijutsuin*, 1981(2)49.]

Degradation studies leave little doubt that the amount of radiative energy is an essential factor in determining the rate of a degradation process (Fig. 8.1). In Japan, Sapporo has an annual UV radiation equal to $6,127 \text{ cal/cm}^2$, followed by Choishi - $8,303 \text{ cal/cm}^2$, and Naha - $10,654 \text{ cal/cm}^2$, and samples of ABS degrade with a rate relative to the energy of radiation.¹ Studies of a broad range of polymers conducted in these locations show that the relationship between tensile strength retention and energy of radiation is not always strictly followed (Figs. 8.2 and 8.3). According to the data given by Yajima,² there is no difference in the amount of energy between Choishi and Naha (Table 8.1). The main dif-

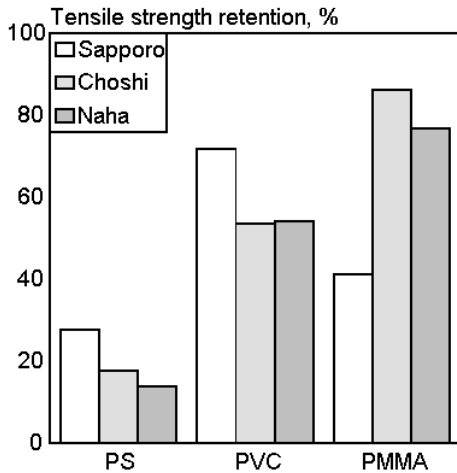


Fig. 8.2. Tensile strength retention of various polymers exposed in three locations for four years. [Data from Y. Nagatsuka, T. Shirota, K. Fukuta, K. Yoshikawa, S. Suzuki, H. Kubota, and O. Nishimura, *Kenkyu Hokoku-Kogyo Gijutsuin*, 1981(2)79.]

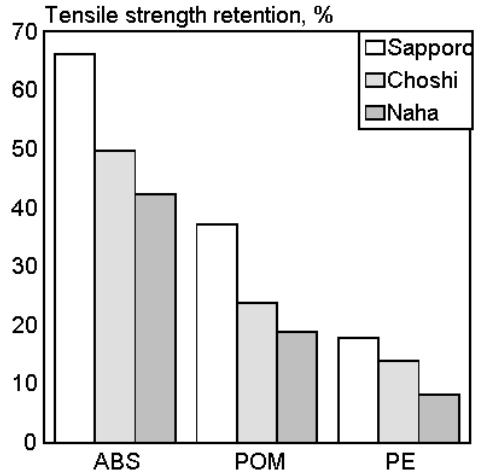


Fig. 8.3. Tensile strength retention of various polymers exposed in three locations for four years. [Data from Y. Nagatsuka, T. Shirota, K. Fukuta, K. Yoshikawa, S. Suzuki, H. Kubota, and O. Nishimura, *Kenkyu Hokoku-Kogyo Gijutsuin*, 1981(2)79.]

Table 8.1: Climatic indicators of some locations in Japan [Data from S. Yajima, Y. Togawa, S. Matsushita, T. Suzuki, and T. Okada, *Kinzoku Hyomen Gijutsu*, 37(1986)718.]

	Unit	Tsukuba	Choshi	Naha
UV radiation	MJ/m ² year	362.8	361.9	359
Mean temperature (A)	°C	12.2	12.7	22
Mean absolute humidity (B)	g/m ³	9.7	10.4	15.7
A x B		118.3	132.1	345.4

ference between Tsukuba and Naha is in temperature and relative humidity. Fig. 8.4 shows the ratio of carbon to oxygen for samples weathered in the two locations. Regardless of polymer type, the different temperature and humidity in each location affects the degradation rate of coatings.

In the discussion below, we will attempt to establish how these three factors - radiation energy, temperature, and humidity - will change depending on the sample exposure method. Trubiroha⁴ explains the physical principles governing light absorption and reflection when a light beam meets the polymer surface. The radiance refracted into the

polymer does not obey Lambert's Law because the radiation is partially reflected to a degree which depends on the refractive index of material and the angle of incidence of the radiation (Fig. 8.5). The individual components of energy distribution are given by the equations:

reflected radiance:	$I_1 = I_0\rho(\alpha)$
refracted radiance:	$I_2 = [1-\rho(\alpha)]I_0\cos\alpha/\cos\beta$
backside radiance:	$I_3 = I_2\exp(-\mu d/\cos\beta)$
absorbed radiance:	$I_{\text{abs}} = I_2[1-\exp(-\mu d/\cos\beta)]$

where μ coefficient of absorption
 $\cos\beta = [1-(\sin\alpha/n_2)^2]^{0.5}$

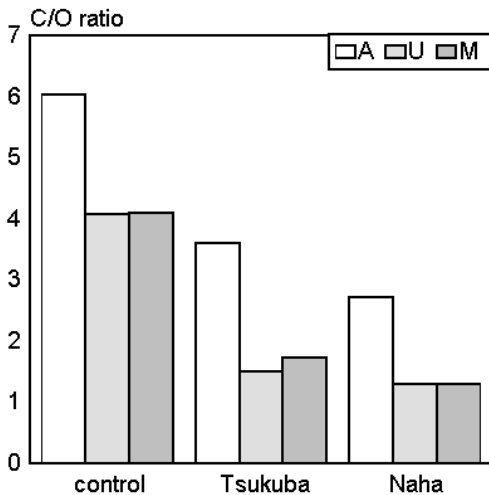


Fig. 8.4. The ratio of carbon to oxygen in weathered coatings from acrylic resins, A, polyurethane, U, and melamine, M. [Data from S. Yajima, Y. Togawa, S. Matsushita, T. Suzuki, and T. Okada, *Kinzoku Hyomen Gijutsuin*, 37(1986)718.]

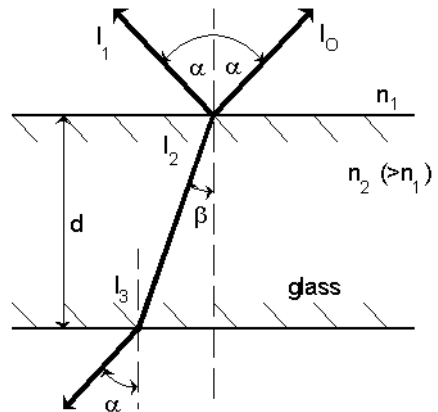


Fig. 8.5. Beam of radiation radiance I_0 striking a glass plate. [Adapted, by permission, from P. Trubiroha, *Angew. Makromol. Chem.*, 137(1985)29.]

Figs. 8.6 and 8.7 show the relative values of absorbed radiance for $n_2 = 1.7$, and two values of internal transmission for normal incidence ($\tau = 0.1\%$ and $\tau = 90\%$). These figures show that the most effective radiation should be at a normal incidence angle ($\alpha = 0$) and that the parameters of the above equation play an essential role.

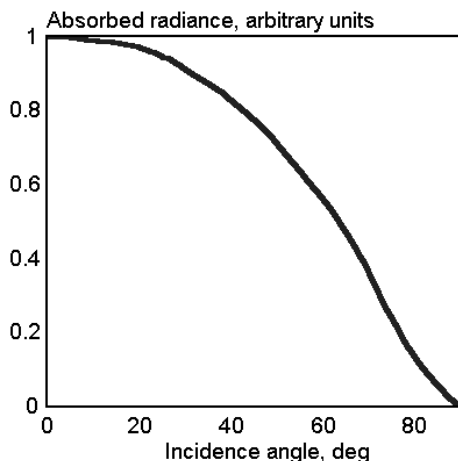


Fig. 8.6. Absorbed radiation as function of incidence angle (internal transmission of polymer film equals 0.1%). [Adapted, by permission, from P. Trubiroha, *Angew. Makromol. Chem.*, 137(1985)29.]

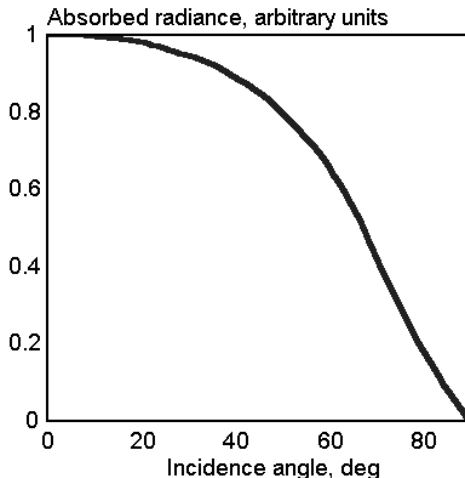


Fig. 8.7. Absorbed radiation as function of incidence angle (internal transmission of polymer film equals 90%). [Adapted, by permission, from P. Trubiroha, *Angew. Makromol. Chem.*, 137(1985)29.]

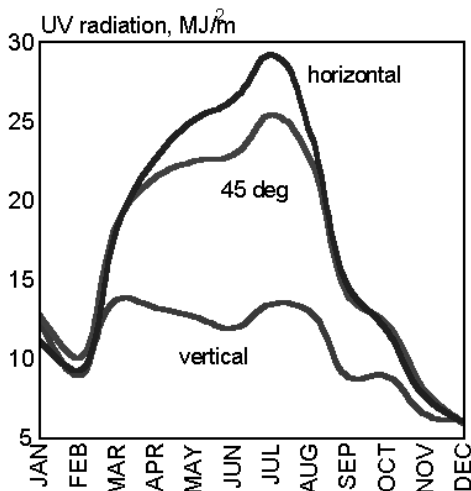


Fig. 8.8. Monthly UV radiation incident on horizontal, 45°, and vertical surfaces. [Adapted, by permission, from R. S. Yamasaki, *Durability Building Mater.*, 2(1983)17.]

To best control conditions of irradiation, samples should be changed in position to follow the sun (sun tracking). This is an expensive solution in terms of equipment and is less frequently used. Another alternative is to choose an efficient angle of exposure which best utilizes light energy and is similar to normal conditions of material service. Yamasaki⁵ studied the effect of varying the southern exposure angle, among horizontal, vertical, and 45° inclination, on the amount of energy reaching the surface of the sample (Fig. 8.8). Total radiation reaching the surface is given by proportion: horizontal/45° inclination/vertical = 96/100/64. The vertical specimen position received a much smaller amount of radiation.

The seasonal distribution of UV radiation is given by Fig. 8.9. Although it receives

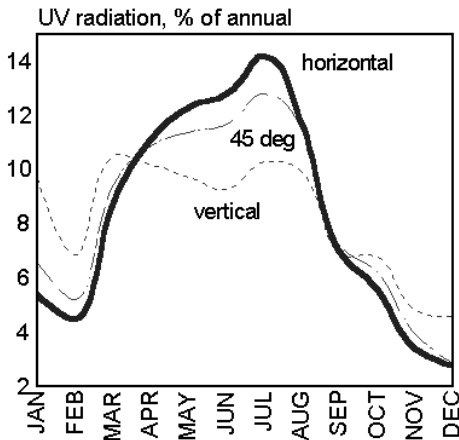


Fig. 8.9. Seasonal distribution of UV radiation on surfaces varying in inclination to horizontal. [Adapted, by permission, from R. S. Yamasaki, *Durability Building Mater.*, 2(1983)17.]

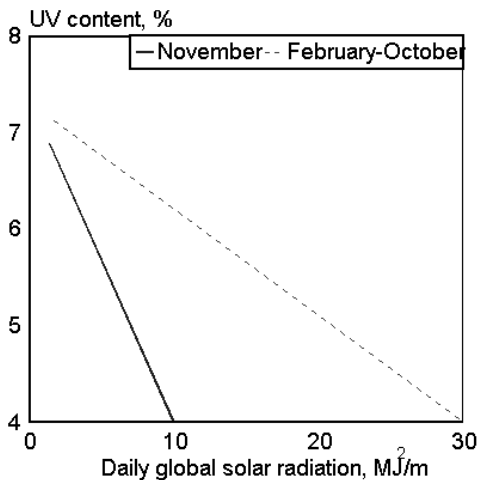


Fig. 8.10. Percent UV radiation vs. daily global radiation on a horizontal surface. [Adapted, by permission, from R. S. Yamasaki, *Durability Building Mater.*, 2(1983)17.]

the least amount of radiation, a vertical surface receives the most uniform amount of radiative energy throughout the year. The horizontal surface has a strong peak in July. Frequently, local stations are only able to offer data on global solar radiation. Note that UV radiation is more influenced by clouds, haze and moisture than the rest of the daylight spectrum, so that the UV content is a complex function of daily global radiation (Figs. 8.10 and 8.11).

The relationship between UV and other radiation components differ depending on latitude and climate. Studies on polycarbonates provide data on the dependence of predicted lifetime on exposure site latitude (Fig. 8.12). The prediction of polymer lifetime is based on a 25% reduction of polymer molecular weight in the surface layers.

There is an additional factor involved in the seasonal distribution of radiation (Fig. 8.13). Depending on the month in which exposure begins, different tensile strength results were obtained. This can be explained by the fact that a sample exposed in winter is in an almost virgin condition and therefore absorbs a much smaller amount of the energy available during the winter period. On the other hand, if a specimen has already undergone the summer cycle of intensive radiation, it will contain more chromophore groups, which increases the probability of energy absorption and thus reaction, even during winter conditions.

We can see that specimen exposure arrangement and timing have an important effect on the exposure results obtained. The most common practice calls for southern ex-

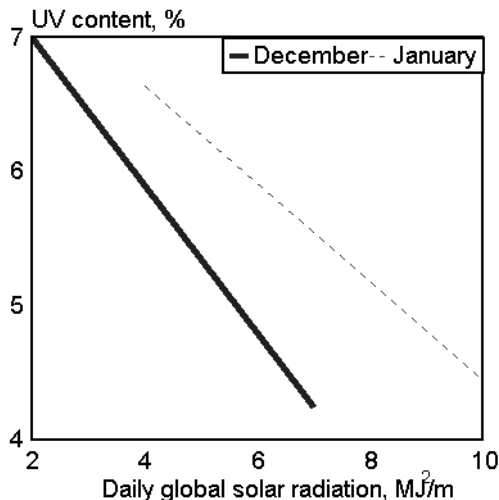


Fig. 8.11. Percent UV radiation vs. daily global radiation on a horizontal surface. [Adapted, by permission, from R. S. Yamasaki, *Durability Building Mater.*, 2(1983)17.]

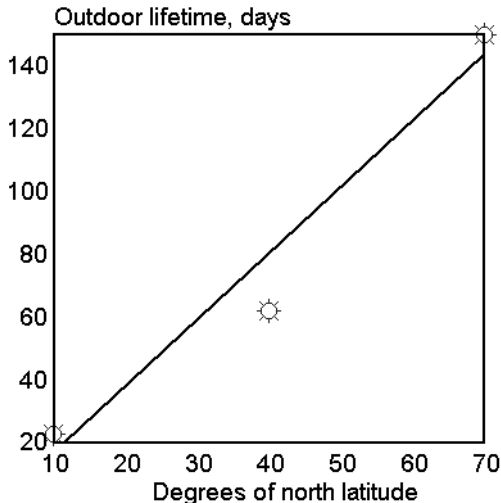


Fig. 8.12. PC outdoor lifetime as a function of northern latitude. [Adapted, by permission, from J. D. Webb and A. D. Czanderna, *Sol. Energy Mater.*, 15(1987)1.]

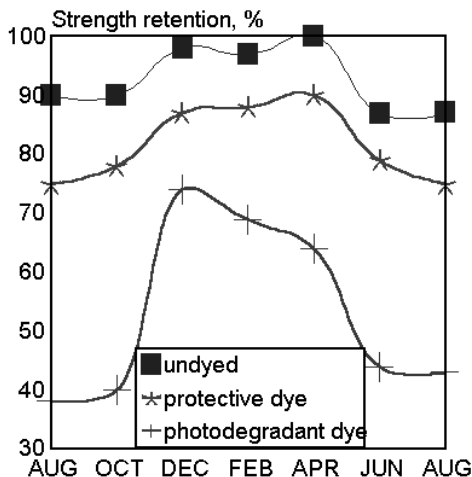


Fig. 8.13. Strength retention vs. month in which polyamide-6 exposure to 21,000 Langley begins. [Adapted, by permission, from G. A. Horsfall, *Text. Res. J.*, 52(1982)197.]

posure at a 45° inclination. A group of researchers disagree with this practice based on the results which they obtained for plasticized PVC.⁸ Fig. 8.14 shows data for PVC dehydrochlorination rate, including various plasticizers (specimens exposed horizontally and at 45° inclination). The authors⁸ explain the results by suggesting that UV radiation is strongly scattered by the atmosphere and therefore the UV reaching the surface at 90° to horizontal ($\alpha=0$) gives a higher probability of absorption. It is possible that this conclusion was reached without evaluation of other factors which may have been involved, namely moisture and temperature. Moisture can extract stabilizers and cause exudation of plasticizer from PVC; temperature affects reaction rate. If the moisture content and

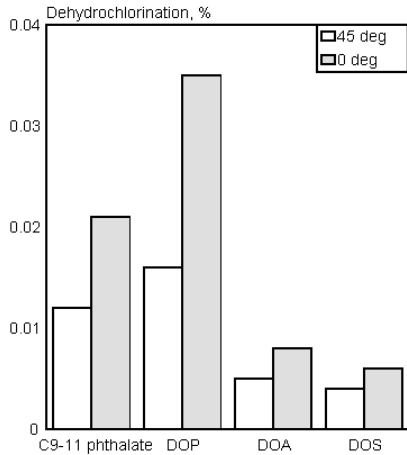


Fig. 8.14. Dehydrochlorination of PVC plasticized with various plasticizers exposed horizontally and at 45°. [Data from H. J. Bowley, D. L. Gerrard, K. J. P. Williams, and I. S. Biggin, *J. Vinyl Technol.*, 8(1986)176.]

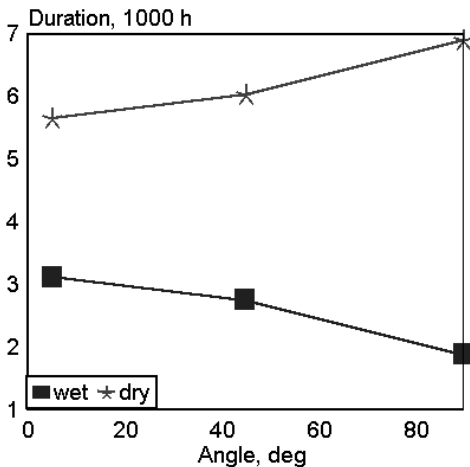


Fig. 8.15. Duration of wet and dry periods for specimens exposed facing south at varying angle to horizontal position. [Data from R. S. Yamasaki, *Durability Building Mater.*, 2(1984)155.]

the temperature of a specimen can be affected by exposure angle, then conclusion is disputable.

Yamasaki⁹ published data on the effect of the exposure angle on specimen temperature during wet and dry periods. Fig. 8.15 shows the duration of wet and dry cycles for specimens exposed at different inclinations. A longer wet cycle contributes to moisture uptake by the sample and to changes related to the presence of moisture, such as hydrolysis, embrittlement, discoloration, swelling and shrinkage of material (causing stress and porosity), interface delamination, extraction of emulsifiers, etc. (in addition to other factors discussed previously). The temperature of the specimen also depends on the duration of the wet cycle (Fig. 8.16). A horizontal panel has the lowest temperature due to a moisture cooling effect. The phenomenon is complex, as suggested by Rogers,¹⁰ because water sorption and desorption also depends on the properties of the material. For example, silicone would retain moisture longer than polyethylene; thus the duration of hydrolytic activity is prolonged in the case of silicone.

Higher static moisture content associated with high relative humidity affects the radiative chalking mass loss in paints, which increases dramatically at 100% RH.¹¹ Mostovaya¹² proposes a mathematical solution for the calculation of polymer photooxidation kinetics in conditions of periodically changing reaction rates.

An additional factor in natural exposure, and probably the most difficult to measure, is related to wind. Wind pressure

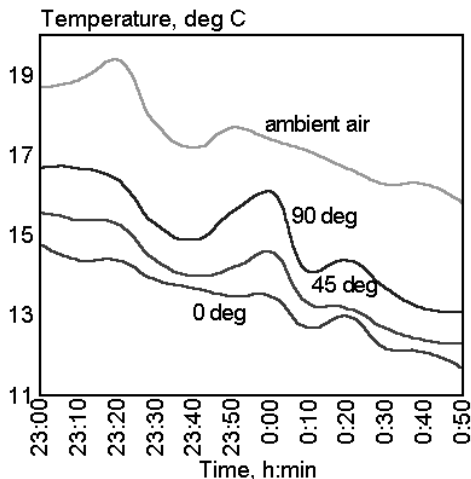


Fig. 8.16. Effect of exposure angle on radiative cooling of grey PVC surface. [Data from R. S. Yamasaki, *Durability Building Mater.*, 2(1984)155.]

exerted on a sample induces stress and thus changes the kinetics of degradation. Winds may cause alterations in specimen surface, affect moisture concentration and dust deposition, and may remove a degraded layer, which all affect the degradation rate. A very broad review of this factor is given by Fischer *et al.*¹³ Numerous samples of coatings were exposed in South Florida and Arizona Test Service Stations (Florida - 5° racks; Arizona 45° racks). Both open and plywood-backed (plywood painted on both sides with black paint) racks were used. In order to estimate temperature and its effect on coating degradation, 20 thermocouples were mounted in the rack. In Arizona, during calm periods, the temperature of specimens was between 55.5 and 58.9°C (ambient temperature 17.2°C) with the hottest area at the rack center. With an east wind the temperature varied between 50 and 57.7°C (ambient temperature 17.2°C) and the “hot spot” shifted to the west end of rack. With a west wind, the temperature range was similar but the “hot spot” moved to the east side of the rack. There were similar observations in Florida but with a somewhat broader range (50-62°C), perhaps because the ambient air temperature was higher (27.7°C). If one compares two different racks (open and plywood-backed), one finds that an open rack has the more uniform temperature but the “hot spot” in the open rack has temperature equivalent to the edge temperature in a plywood-backed rack (specimens exposed in an open rack are exposed to lower temperatures). Plywood-backed and black box exposures give quite similar conditions.

The effect of temperature on other properties of exposed films was measured. It was confirmed that variations in temperature corresponds to gloss changes which is least severe at the rack edge. It was suggested that elimination of the two outside sample positions reduces the error of determination (standard deviation was reduced from 12.3 to 4.4).

Several current papers consider conditions of outdoor exposure, in their respective locations, which include UV radiation, temperature and pollutant concentration.¹⁴⁻¹⁷

8.2 METHODS OF SAMPLE EXPOSURE

8.2.1 EXPOSURE SITE

Conditions of exposure should always attempt to simulate the conditions under which the product is expected to perform. In this, and other chapters of this book, numerous data are presented to illustrate the fact that the result of sample exposure depends on exposure conditions. If the product is only used locally, the best practice would suggest in-plant studies, although it should be taken into consideration that sample exposure is not just a matter of putting the sample outside. Samples must be exposed according to one of the suggested exposure standards (more precisely, the standard suggested for particular material). Exposed samples and the exposure site should be maintained systematically to assure that exposure conditions do not change due to dust coverage, change of sample position, changes in surrounding (e.g., a new structure in the neighborhood shadows the specimens, air-conditioner on the roof blows hot air on the samples, etc.). Often, these conditions, referred to as “standard conditions” of outdoor exposure, are *not standard* at all. It is imperative to have accurate information on these conditions (UV irradiance, temperature, relative humidity, concentration of pollutants, etc.). Some of these data can be obtained from the local weather monitoring station (statistical data are usually expensive) but UV irradiance is less frequently available and must be measured by the experimenter. These requirements are usually taken into account in studies conducted by stations providing a natural exposure service for customers.

Often, products must be designed for worldwide use which implies that samples should be exposed to varying climatic conditions. Several climatological categories are considered typical: subtropical (e.g., Florida), desert (e.g., Arizona), seashore (e.g., Florida, Netherlands), industrial, and temperate.¹⁸ In order to obtain meaningful data for worldwide performance, materials should be exposed in each of these climatic conditions. Frequently, experiments are set up in such a manner that the acceleration effect of certain conditions (e.g., Florida or Arizona) can be utilized. This should begin with an analysis of the mechanisms of degradation because high irradiance is not always a necessary accelerating factor (demonstrated by a vinyl siding study in Chapter 17). In order to select an exposure station, the researcher should contact service providers such as South Florida Test Service or DSET Laboratories to obtain a list of existing sites and their climatic conditions (data in Chapter 4 can also be consulted for this purpose).

8.2.2 EXPOSURE RACKS

It is essential to make a decision on how samples should be exposed. This decision can sometimes be simple because a standardized method for a particular material may exist and exact exposure conditions may be given. Otherwise, one of the racks discussed below

can be selected, providing the specific application for which each rack was designed is taken into account.

8.2.2.1 Standard Rack

Standard racks are made from anodized aluminum and face directly south at a fixed angle (typical sample size 150 x 305 mm or 6 x 12"). The most typical angles of exposure are: 0 (horizontal), 5, 45, 90° (vertical), and equal to a station latitude (e.g., in Florida 26°). Conditions depend on the angle of exposure. Exposure at 0° is very popular for roofing materials because it provides a longer wet period. Irradiation is lower than maximum (the highest irradiation is in sun tracking devices). There is a high degree of dirt accumulation. Exposure at 5° allows for some drainage of water (but the time of surface wetness is also significantly longer than for other angles discussed below) and reduction in dirt accumulation (most experiments for the automotive industry are run under these conditions). Exposure at 45° is the most popular method because time of wetness, temperature, dirt pick up, and mildew are at approximately average values between the two extreme methods of exposure (0 and 90°). Exposure at 90° is typically used to test construction materials. Temperature, irradiation, and wet time are lower in this type of exposure. The racks are designed in such a manner that wash-down from samples in the upper positions does not contaminate samples below. Specimens can also be exposed at a variable angle which compensates for seasonal differences in the sun's position. The schedule of change of exposure angle is given in ASTM E 782. Table 8.2 compares UV energy for different exposure angles.

Measurement of exposure conditions (such as, irradiance, temperature, and wet time) must be done for the configuration chosen. Racks are either open or have a backing. The backing increases the temperature of exposure and slightly increases temperature uniformity.

8.2.2.2 Under Glass Exposure

Test specimens are placed behind 2.5-3 mm window glass which absorbs radiation below 310 nm and transmits 77% of UV radiation and 85% of daylight. Test specimens are placed 75 mm from glass surface. Application of this method is for materials which are not exposed to direct sun light. Temperature of exposure is increased.

8.2.2.3 Black Box Exposure

Samples form the top cover of a black box. All spaces between samples are filled with black-painted metal panels. Black boxes are either closed or opened at the bottom and usually tilted by 5 or 45°. These samples are exposed to higher temperatures than they are in other methods. Many automotive application tests use this method (e.g., coatings, exterior trim, side moldings, etc.). These boxes are sometimes modified to maintain an increased temperature (most frequently 55°C, but also 100°C and sometimes much

Table 8.2: Comparison of UV energy received by samples exposed at different angles in Miami, Florida in 1992

Month	Exposure at 5°		Exposure at 26°		Exposure at 45°	
	TUVR	% TR	TUVR	% TR	TUVR	% TR
JAN	21.98	5.39	23.57	4.76	24.87	4.97
FEB	25.09	5.43	25.90	4.95	27.21	5.36
MAR	28.21	4.99	28.57	4.83	29.06	5.35
APR	32.58	5.09	31.46	5.12	30.73	5.83
MAY	38.74	4.93	36.47	5.14	34.27	5.90
JUN	26.58	5.41	25.04	5.61	23.02	6.06
JUL	34.76	5.21	31.39	5.17	27.15	5.51
AUG	25.54	5.27	24.22	5.25	21.11	5.12
SEP	26.08	5.22	26.32	5.16	23.32	4.85
OCT	25.80	5.21	26.54	4.81	25.39	4.46
NOV	18.92	5.07	20.16	4.62	19.93	4.37
DEC	17.31	4.79	18.91	4.25	19.47	4.02
TOTAL	321.59	5.16	318.55	4.98	305.53	5.15

TUVR - total UV radiation in the range of 290-385 nm in MJ/m²

% TR - UV percent of total radiation

higher). This box is used to simulate conditions in tropical climates. Car interior materials are tested in black boxes under glass. Some of these have a controlled temperature (typically, 90-100°C) and a variable angle to increase irradiance. Car upholstery materials are typical of the type of samples tested.

8.2.2.4 Exposure with Spray

There are racks designed to perform cyclical sprays on exposed samples. Spray can be either distilled water or salt water (5% NaCl solution). Salt spray is applied to increase corrosion rate; water spray is usually applied to cause a change in the sample temperature which will induce rapid mechanical stress.

8.2.2.5 Dry Exposure

A special automatic rack was designed to study the effect of dry deposition of contaminants on coatings.^{19,20} A sensor monitors relative humidity and moisture on the sample

surface to predict rain fall. A rack is driven under shelter before rain falls. Another part of this rack is equipped to spray the sample surface with water and to collect runoff for testing.

8.2.2.6 Sun-Tracking Devices

Between 7 a.m. and 6 p.m., sun tracking devices follow the movement of sun to assure that sun rays are normal to the surface of exposed samples. At other times and during strong winds, the rack remains in a fixed position. Samples in these racks are exposed to about 35% more radiation than the same samples exposed at 45°. Because the samples are always normal to the sun rays, the sample temperature is higher than ambient but always within the temperature range recorded for a particular day, material color, and type.

8.2.2.7 Light Concentrating Devices

In order to obtain higher acceleration, light concentrating devices were developed. The first such device was developed by Desert Sunshine Exposure Tests and it is known as EMMAQUA. These devices are operated by DSET Laboratories, Inc. Also, Atlas offers exposure in concentrating devices known as SUN¹⁰. In both machines, 10 flat mirrors concentrate the sun's light on the surface of specimens. Additionally, the sun is continuously tracked by the machine to further increase the amount of energy collected. Samples are cooled by forced air which keeps the temperature of the sample within 5 to 10°C of an identical sample exposed on a plywood backing without energy concentration. In both devices, a light concentration factor of 8 is given as typical.

8.3 STANDARDS

Table 8.3 gives general information on the existing standards which suggest methods of studying properties of materials exposed to natural weathering.

Table 8.3: Natural weathering standards

Standard number	Application	References
ASTM D1435	plastics	21
ASTMD4141	coatings	22
ASTM D4364	plastics in concentrated natural sunlight	28
ASTM G7	non-metallic materials	23
ASTM G24	non-metallic materials exposed through glass	24
ASTM G90	non-metallic materials exposed to concentrated sunlight	25
BS 2782 Method 540A	plastics exposed under glass	28
BS 4618 Section 4.2	plastics (data presentation)	28
DIN 53386 06.82	plastics	28
DIN 53388	plastics exposed under glass	28
ISO 877	plastics exposed under glass	28
ISO 2810	paints and varnishes	26
ISO 4582	plastics (determination of color changes)	28
ISO 4607	plastics	27
ISO 4665 Part 1	rubber (change of properties assessment)	28
ISO 4665 Part 2	rubber (methods of exposure)	28
ISO 4665 Part 3	rubber (methods of exposure)	28
NF T46 040, 041, & 042	equivalents to ISO 4665 Parts 1 to 3	28
NF T51 055	natural weathering (equivalent to ISO 877)	28
NF T51 165	plastics (equivalent to ISO 4607)	28
NF T51 185 & 058	equivalent to ISO 4582	28

REFERENCES

1. H. Kubota, S. Suzuki, O. Nishimura, K. Yoshikawa, and T. Shiota, *Kenkyu Hokoku-Kogyo Gijutsuin*, 1981,2,49.
2. Y. Nagatsuka, T. Shiota, K. Fukuta, K. Yoshikawa, S. Suzuki, H. Kubota, and O. Nishimura, *Kenkyu Hokoku-Kogyo Gijutsuin*, 1981, 2, 79.
3. S. Yajima, Y. Togawa, S. Matsushita, T. Suzuki, and T. Okada, *Kinzoku Hyomen Gijutsu*, 37(1986)718.

4. P. Trubiroha, *Angew. Makromol. Chem.*, 137(1985)29.
5. R. S. Yamasaki, *Durability Building Mater.*, 2(1983)17.
6. J. D. Webb and A.W. Czanderna, *Sol. Energy Mater.*, 15(1987)1.
7. G. A. Horsfall, *Text. Res. J.*, 52(1982)197.
8. H. J. Bowley, D. L. Gerrard, K. J. P. Williams, and I. S. Biggin, *J. Vinyl Technol.*, 8(1986)176.
9. R. S. Yamasaki, *Durability Building Mater.*, 2(1984)155.
10. C. E. Rogers, *ACS Symp. Ser.*, 220(1983)231.
11. K. G. Martin and R. E. Price, *Durability of Building Mater.*, 1(1982)127.
12. E. M. Mostovaya, *Sov. J. Chem. Phys.*, 1(1984)1886.
13. R. M. Fischer, W. P. Murray, and W. D. Ketola, *Prog. Org. Coatings*, 19(1991)151.
14. J. W. Martin, *Prog. Org. Coat.*, 23(1993)49.
15. P. Genova-Dimitrova, *Polym. Deg. Stab.*, 33(1991)355.
16. M. Just, *Kunststoffe*, 80(1990)1303.
17. E. W. Brand and P. L. R. Pang, *J. Geotechn. Eng.*, 117(1991)979.
18. J. L. Scott, *Real time weathering as a test for evaluating materials*, South Florida Test Service, 1995.
19. J. W. Hook, P. J. Jacox, and J. W. Spence, *Prog. Org. Coat.*, 24(1994)175.
20. E. O. Edney, *Report*, EPA/600/3-89/032.
21. ASTM D1435. *Outdoor weathering of plastics.*
22. ASTM D4141. *Conducting accelerated outdoor exposure tests of coatings.*
23. ASTM G7. *Atmospheric environmental exposure testing of nonmetallic materials.*
24. ASTM G24. *Conducting exposures to daylight filtered through glass.*
25. ASTM G90. *Performing accelerated outdoor weathering of nonmetallic materials using concentrated natural sunlight.*
26. ISO 2810. *Paints and varnishes - Notes for guidance on the conduct of natural weathering tests.*
27. ISO 4607. *Plastics - Methods of exposure to natural weathering.*
28. R. P. Brown, *Polym. Test.*, 10(1991)3.

9

TYPICAL WEATHERING CYCLES

Table 9.1: Standards discussing principles of operation of weathering devices

Standard	Source	Reference
ASTM G23	carbon arc	3
ASTM G26	xenon arc	4
ASTM G53	fluorescent lamp	5
ASTM D4364	concentrated daylight	6
ASTM E838	concentrated daylight	7
ISO 4892	xenon and carbon arcs	51

Research papers rarely describe conditions used to operate equipment for accelerated weathering. Only standardized methods are precise. Several standards give general conditions which should be set for typical accelerated weathering apparatus (Table 9.1). ASTM standards are given in Table 9.1. Some corresponding national standards are given in the references. These standard methods are frequently referred to provide testing standards for typical industrial products and materials.

Table 9.2: Methods of exposure

Method	G23	G26
Continuous exposure to light and intermittent exposure to water spray	1	A
Alternative exposure to light and darkness and intermittent exposure to water spray	2	B
Continuous exposure to light without water spray	3	C
Alternative exposure to light and darkness without water spray	4	D

None of these standards imposes rigid conditions on how an accelerated test should be performed. This is left to the parties involved, although there are some suggestions regarding important test parameters. Both ASTM G23 and ASTM G26 suggest the use of one of four possible methods of exposure (Table 9.2). The exposure parameters suggested in G23 and G26 are given in Table 9.3.

Table 9.3: Parameters of exposure

Parameter	Value
Black panel temperature, °C	63+ \3
Water temperature, °C	16+ \5
Water pH	6-8
Water solids, ppm	<20
Light duration in cycle, min.	102
Spray duration in cycle, min.	18
Relative humidity, %	
light cycle	30+ \5
dark cycle	90+ \5
Temperature during dark cycle, °C	35+ \5
Duration of light cycle (carbon arc only), h	3.8
Duration of darkness (carbon arc only), h	1

Xenon arc apparatus can be equipped with one of five filters specified in G26. When operated with a borosilicate glass inner and outer filter, the suggested minimum of spectral irradiance level should be as follows:

Irradiance, W/m ² /nm	Wavelength, nm
.2	320
.35	340
.5	380
.75	420

When carbon arc is used, it is not possible to regulate irradiance; radiation intensity is achieved by the proper maintenance and control of the parameters given in Table 9.3 and by the acceleration factor controlled by dosimeters.

The ISO standard is even more flexible. The parameters may have any of the values listed below:

temperature, °C	45, 55, 63+ \3
relative humidity, %	35, 50, 65, 90+ \5
cycle time, min.	
spraying	3, 5, 12, 18
dry interval	17, 25, 48, 102

or they can be agreed upon between parties. Other parameters are not specified.

The fluorescent UV-condensation apparatus gives a choice of five types of radiant sources of different spectral characteristics (see ISO-4892). The suggested conditions of operation are given in Table 9.4. Other proportions of light/condensations cycles can also be used (e.g., 8/4), but the duration of condensation cycle should be at least 2 h. Other temperatures (50, 60, 70°C) are also permitted.

Table 9.4: Conditions of operation of fluorescent UV condensation apparatus

Parameter	Value
Light cycle, h	4
Temperature of light cycle, °C	60
Condensation cycle, h	4
Temperature of condensation cycle, °C	50

Concentrated natural sunlight equipment depends on natural conditions. Standards^{6,7} give detailed instruction which only specify spray cycles during the day and night.

These standards give general guidelines for the conditions of the experiment but the conditions can be changed to suit a particular application. Table 9.5 gives examples of the some common standards including the standard conditions of weathering for specific products. The operation parameters suggested in standards included in Table 9.5 frequently differ from the parameters of exposure given in Table 9.3. The black-panel temperature varies from 24-63°C, with 60°C the most frequently used. The temperature of water spray is in the range of 7-23°C. Dry/wet cycle time is usually 51/9 or 102/18, but 1/1 and 18/6 are also suggested. Some standards suggest a day and night cycle (D822 - 18/6 h; D3361 - 1/1 h; D4028 - 5/2 days; D4303 - 8/4 h). Generally, there is a freedom of choice. This does not seem to be dictated by some logical relation between conditions of material performance and material ability to withstand environmental condition. It is rather the reflection of the opinion of a particular standard committee on what is possible to achieve and test in existing equipment. For example, the dry/wet cycle 102/18 min was chosen, not because it is the most typical in nature (Central European conditions have 10-16% of rain), but because of the constraints of the instrument in the past (carbon arc). These constraints are long removed but the 102/18 min cycle remains and it is even used in other pieces of equipment (xenon arc) which never had this constraint.

In addition to national and international standards, there are some other sources of information on weathering cycles used by some industries. The paint industry evaluated three weathering cycles for paint testing.⁵² The most degrading weathering method was suggested by the National Coil Coaters' Association. Here, specimens are irradiated in an open flame carbon arc for a period of 1 h at 50% relative humidity and at a 65°C

Table 9.5: Examples of application standards

Standard	Application	Weathering device	Reference
ASTM C718	solvent release sealants	SN	8
ASTM C732	latex sealants	CA & XA	9
ASTM C734	latex sealants	CA & XA	10
ASTM C1087	glazing sealants	SN	11
ASTM D529	bituminous materials	CA	13
ASTM D822	paints and coatings	CA	14
ASTM D2053	zippers	CA & XA	17
ASTM D2249	bedding compounds	CA	18
ASTM D2565	plastics	XA	19
ASTM D3218	monofilaments	XA	20
ASTM D3334	fabrics	XA	21
ASTM D3361	paints, varnishes, and lacquers	CA	22
ASTM D3424	printed matter	CA & XA	23
ASTM D3583	sealants	CA	24
ASTM D4028	screening	CA	25
ASTM D4303	artists' paints	XA	26
ASTM D4325	rubber tapes	CA	27
ASTM D4459	plastics for indoor use	XA	30
ASTM D4585	coatings	FC	31
ASTM D4587	paints and coatings	FC	32
ASTM D4674	color of plastics	F	33
ASTM F520	aerospace transparencies	CA	34
ISO 2809	paints and varnishes	CA & XA	46
ISO 4582	plastics		48

CA - carbon arc, XA - xenon arc, F(C), fluorescent tube (condensation), SN - sun lamp

black-panel temperature, followed by 1 h dark cycle at 100% relative humidity at 30°C with a continuous spraying of the back of the panels with water at 7°C. The second most degrading method was a typical cycle according to ASTM G23 (see Table 9.3), and the

third followed BS3900 Part F3 which includes the following 24 h cycle in a carbon arc apparatus:

Duration, h	Water spray	Fan
4	on	off
2	off	on
10	on	off
2	off	on
5	on	off
1	apparatus stopped	

The British procedure (BS3900 Part F3) and ASTM G23 gave low acceleration but more adequately simulated the degradation of paints in natural conditions. Carbon arc used without filters degraded samples very rapidly but the results did not correlate with field performance. Scott⁵³ discussed studies by the National Coil Coaters' Association in which two cycles were used in a xenon arc Weather-O-Meter: one, the typical 102/18 min. light/dark cycle, the other, the 1/1 h cycle (light cycle - 63°C, 65% RH; dark cycle - 38°C, 100% RH). The author suggests that studies should be conducted under conditions closely simulating the natural conditions where the products are used.

Recently, one observes a tendency to accelerate the degradation by harsher regimes of equipment operation. A Volkswagen plant operates weathering equipment for simulating "dashboard cracking". Conditions are: 120°C during the light cycle and 20°C during the dark cycle. The big temperature difference between the cycles is designed to create an internal stress in the material.

The Society of Automotive Engineers suggests using the following conditions for testing the interior trim components:

	light cycle	dark cycle
Irradiance, W/m ²	.55	
Black-panel temperature, °C	89	38
Relative humidity, %	50	100
Water temperature, °C	63	40
Duration, h	3.8	1

The use of controlled radiation wavelength (filtered xenon arc) at almost twice the normal irradiance and at a high temperature are the significant features of this test.

These practices do not provide satisfactory artificial weathering conditions and serious efforts are required to improve the existing situation. A variety of new standard methods have been developed recently which contribute to an increasingly complex system. These not always take into account the real reason why standards should be developed. This is to measure and improve existing materials. Following the needs of special interest groups does not contribute to achieving this goal. The following suggestions are offered for consideration:

- instruments should be operated at irradiance which does not exceed the highest values measured in the natural environment (0.8 W/m^2 at 340 nm - "Miami peak")
- preference should be given to methods which suggest operation of the instrument at the irradiance of normal daylight conditions (0.35 W/m^2 at 340 nm)
- wavelength distribution of artificial radiation should be chosen to imitate the exact proportions found in the daylight spectrum
- moisture, temperature, and irradiance should be maximized only to a level which does not alter typical degradation mechanisms (parameters can be set at measured maxima for the conditions at which a particular material performs)
- development of the standard method and conditions should be in relationship to other existing methods for specific products
- each test method for a particular product should have a severity which corresponds to the severity of actual application
- all standards for products testing should have consistent requirements so that all test methods are uniform
- new standard methods for products should be more specific regarding the choice of parameters and should follow guidelines of the current reference standards (see Tables 9.1 to 9.3)
- industry standards and national standards should correspond to each other and should follow the principles of the current international standards or standards in common use (e.g., ASTM)
- methods under development should include the effect of pollutants and mechanical stress whenever appropriate.

A recent review paper⁵⁶ gives a broad outline of the problems facing those who would like to use standard methods. The above points reflect what is being said in the literature and in discussions with users of standard methods. If there is a large variety of imprecise procedures, this opens the door for abuse by suppliers and special interest groups and does not protect the user or customer. Testing one specific product should generate knowledge which can be universally applied in other fields. This is not possible if methods are designed for the sake of uniqueness rather than uniformity. Finally, in the global economy, and, taking into account that we all share the same sun, it is impossible to suggest that each product will be tested according to several different methods

which, for all the possible products, would result in thousands of different methods. Economic reality must prevail.

REFERENCES

1. ASTM G21. Determining the resistance of synthetic polymeric materials to fungi.
2. ASTM G22. Determining the resistance of plastics to bacteria.
3. ASTM G23. Operating light-exposure apparatus (carbon-arc type) with or without water for exposure of nonmetallic materials.
4. ASTM G26. Operating light-exposure apparatus (xenon-arc type) with or without water for exposure of nonmetallic materials.
5. ASTM G53. Operating light- and water-exposure apparatus (fluorescent UV-condensation type) for exposure of nonmetallic materials.
6. ASTM D4364. Performing accelerated outdoor weathering of plastics using concentrated natural sunlight.
7. ASTM E838. Performing accelerated outdoor weathering using concentrated natural sunlight.
8. ASTM C718. Ultraviolet (UV) - Cold box exposure of one part, elastomeric, solvent-release type sealants.
9. ASTM C732. Aging effect of artificial weathering on latex sealants.
10. ASTM C734. Test method for low-temperature flexibility of latex sealants after artificial weathering.
11. ASTM C1087. Determining compatibility of liquid-applied sealants with accessories used in structural glazing systems.
12. ASTM D518. Rubber deterioration - surface cracking.
13. ASTM D529. Accelerated weathering test of bituminous materials.
14. ASTM D822. Operating light- and water-exposure apparatus (carbon-arc type) for testing paint and related coatings and materials.
15. ASTM D1435. Outdoor weathering of plastics.
16. ASTM D1499. Operating light and water exposure apparatus (carbon arc type) for exposure of plastics.
17. ASTM D2053. Colorfastness of zippers to light.
18. ASTM D2249. Predicting the effect of weathering on face glazing and bedding compounds on metal sash.
19. ASTM D2565. Operating xenon-arc type (water cooled) light exposure apparatus with or without water for exposure of plastics.
20. ASTM D3218. Polyolefin monofilaments.
21. ASTM D3334. Fabrics woven from polyolefin monofilaments.
22. ASTM D3361. Operating light- and water-exposure apparatus (unfiltered carbon-arc type) for testing paint varnish, lacquer, and related products using the dew cycle.
23. ASTM D3424. Evaluating the light fastness of printed matter.
24. ASTM D3583. Testing joint sealants, hot-applied, elastomeric type, for Portland cement concrete pavements, or joint sealant, hot-applied, elastomeric, jet-fuel-resistant type, for Portland cement concrete pavements.
25. ASTM D4028. Solar screening woven from vinyl-coated fiber glass yarn.

26. ASTM D4303. Lightfastness of pigments used in artists' paints.
27. ASTM D4325. Nonmetallic conducting and electrically insulating rubber tapes.
28. ASTM D4329. Operating light and water exposure apparatus (fluorescence UV condensation type) for exposure of plastics.
29. ASTM 4364. Performing accelerated outdoor weathering of plastics using concentrated natural sunlight.
30. ASTM D4459. Operating and accelerated lightfastness xenon-arc type (water cooled) light-exposure apparatus for the exposure of plastics for indoor applications.
31. ASTM D4585. Testing water resistance of coatings using controlled condensation.
32. ASTM D4587. Conducting tests on paint and related coatings and materials using a fluorescent UV condensation light- and water-exposure apparatus.
33. ASTM D4674. Accelerated testing for color stability of plastics exposed to indoor fluorescent lighting and window-filtered daylight.
34. ASTM F520. Environmental resistance of aerospace transparencies.
35. BS 2782 Method 540A. Plastics determination of resistance to change upon exposure under glass to daylight. Method 540B. Plastics - method of exposure to laboratory light sources. Method 540C. Determination of ultraviolet radiation intensity using polysulfone film
36. BS 4618 Section 4.2. Recommendation for the presentation of plastics design data - resistance to natural weathering. Section 4.3. Recommendations for the presentation of plastic design data - resistance to color change produced by exposure to light.
37. DIN 53384 10. Artificial weathering or exposure in laboratory Apparatus; exposure to UV radiation.
38. DIN 53386 06. Exposure to natural weathering.
39. DIN 53387 06. Weathering in laboratory apparatus, exposure to filtered xenon arc radiation and periodic wetting.
40. DIN 53388. Testing of plastics -testing of stability under natural light.
41. DIN 53389. Testing of plastics and elastomers - light exposure apparatus.
42. ISO 105/A. Textiles - test for color fastness - general principles.
43. ISO 846. Determination of behavior under the action of fungi and bacteria - evaluation by visual examination or measurement of change in mass or physical properties.
44. ISO 877. Plastics - determination of resistance to change upon exposure under glass to daylight natural weathering.
45. ISO 2579. Plastics - instrumental evaluation of color differences.
46. ISO 2809. Paints and varnishes - Determination of light fastness of paints for interior use.
47. ISO 3557. Plastics - recommended practice for spectrophotometry and calculation of color in CIE systems.
48. ISO 4582. Plastics - Determination of changes in color and variations in properties after exposure to daylight under glass, natural weathering or artificial light.
49. ISO 4607. Plastics - methods of exposure to natural weathering.
50. ISO 4665. Part 1. Assessment of change in properties after exposure to natural weathering or artificial light. Part 2. Methods of exposure to natural weathering. Part 3. Methods of exposure to natural weathering.

-
51. ISO 4892. Plastics - methods of exposure to laboratory light sources.
 52. M. Camina, Evaluation of some artificial weathering cycles. Report, PAINTRA-8207.
 53. J. Scott, Sun Spots, 9(1979/80)21.
 54. J. Boxhammer and T. Rudzki, Angew. Makromol. Chem., 137(1985)15.
 55. SAE-J-1885. Accelerated exposure of automotive interior trim components using a controlled irradiance water cooled xenon arc-apparatus.
 56. R. P. Brown, Polym. Testing, 10(1991)3.

10

ARTIFICIAL WEATHERING VERSUS NATURAL EXPOSURE

How many hours of natural weathering equal one year of natural exposure? This is one of the most frequently asked questions a person working on weathering is asked. Is there any answer to this question? Think of the question: “What is the durability of your product?” If you say, “I do not know”, one starts to wonder why you spend money to conduct weathering studies. If you say, “Because this product withstands 2000 hours in a Weather-O-Meter and its going to last 5 years”, many people will question your truthfulness and perhaps even your qualifications. Endless discussions continue; every participant has some reason for his point of view, but the fact is that some products available in the market today, are expected to last a minimum of 20 years and nobody is willing to wait for another quarter of a century to approve an updated versions of the product.

Several groups of factors determine the result of weathering studies in natural conditions and accelerated tests. These groups are discussed in individual chapters of this book (chapters 4, 5, 7 through 11 and 13). If the conditions of each experiment are well defined and, if the mechanism and kinetics of degradation are well understood, then there is a high probability that the results of various experiments will correlate with each other. The use of artificial weathering is feasible when it offers:

- acceleration
- control over conditions.

We want to perform studies in the minimum possible time and in well controlled, repeatable conditions. It is not reasonable to expect that accelerated weathering conditions will simulate natural weathering conditions. Similarly, testing materials in a tropical climate (Florida) does not expose them to the proper natural conditions if the material will be used in Alaska. The accelerated weathering conditions should be selected to give the highest possible accelerating factor. However, the conditions selected must produce degradation mechanisms which are as similar as possible to the way in

which the material would degrade in natural conditions. The method of evaluating degradation in these conditions must also be chosen carefully to ensure identification of the same factors that are changed in natural exposure.

This discussion was intended to deflect any further debate as to whether or not there is correlation between the data obtained under natural and under artificial weathering conditions and to help the reader to remain objective as he or she reads the following literature review. If there is no correlation, the experiment was not designed properly or the details of experiment are not known or the tools used in the experiment were not adequate and so on. As we look at the data, we should try to determine if the modes of acceleration selected actually prevent correlation with the changes that occur under natural conditions.

Part of the data presented in this chapter comes from a series of Japanese publications.¹⁻⁸ A large group of scientists dedicated their efforts to a coordinated study of six of the most commonly used polymers. These were exposed to natural weather conditions in four Japanese locations and also subjected to artificial weathering in seven test units. The progress of degradation was monitored by measuring the basic physical-mechanical properties of the polymers. These efforts created a broad base of data, which was obtained in comparable conditions and is worthy of more extensive attention (these studies provided additional information for other parts of this book).

Figs. 10.1 to 10.6 show the thickness of the degraded layer versus time for both natural and artificial weathering. Samples exposed in a dew-cycle weathering tester have completely different degradation characteristics from that generated by other accelerated tests. The degradation of PVC, PMMA, ABS in a dew-cycle tester occurs much faster than in other testers. But three other polymers (PS, POM, PE), initially degrade as fast in the dew-cycle tester as they do in other testers and it is only in the last 1000 hours that the degradation of POM and PE is accelerated. This shows that the acceleration factor of dew-cycle weathering apparatus is higher for some materials than for others when compared with natural weathering or with other testers. In most cases, the xenon arc weatherometer and the fadeometer give a lower degradation rate than do any of the four carbon arc units used in the experiments. Comparison of the microphotographs of surface deterioration of specimens weathered both outdoors and in test equipment shows that the crack pattern of specimens exposed outdoors most closely resembles the crack pattern produced in a xenon arc weatherometer. When specimens weathered in a xenon arc weatherometer are ranked according to their degree of degradation, the order is closer to the rankings of specimens weathered outdoors than it is to the ranking of specimens weathered in most of the carbon arc units (Table 10.1). Ranking by the thickness of the degraded layer shows that, as is known from practice, PMMA is the clearly superior polymer. Both natural and artificial exposures confirm its stability.

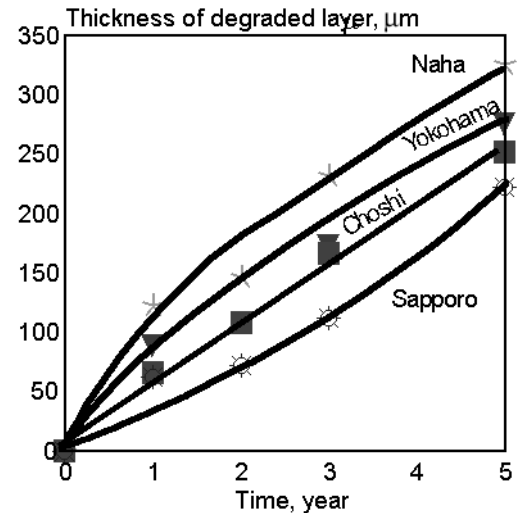
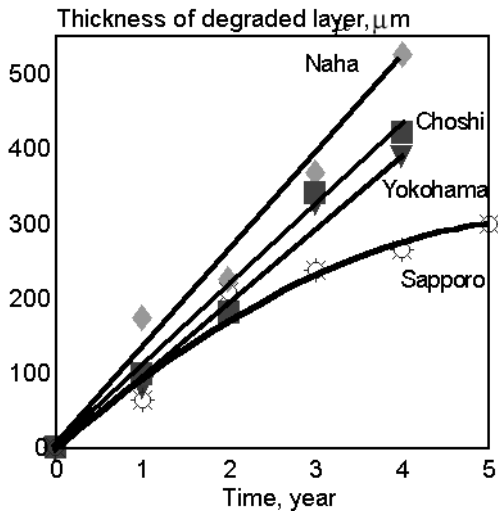
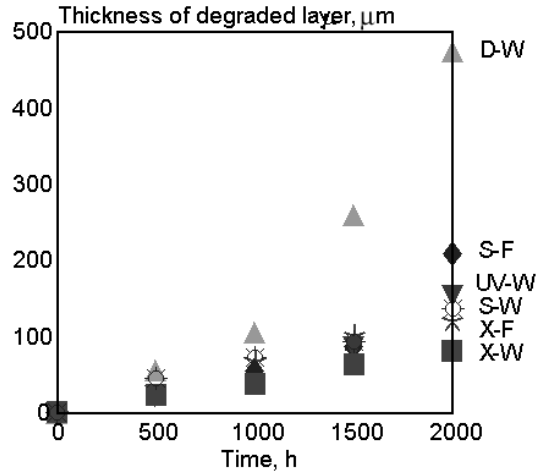
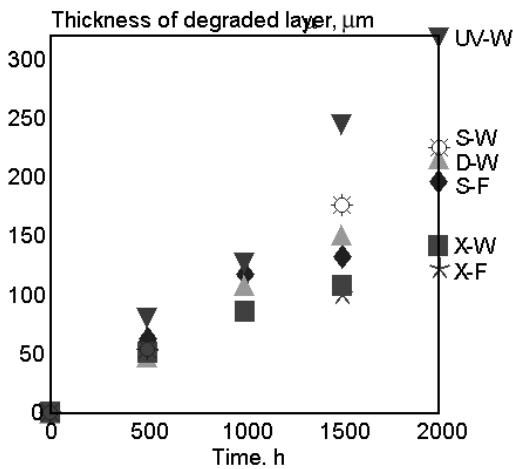


Fig. 10.1. PS. Thickness of degradation layer vs. exposure time. [SW-Sunshine weatherometer, XW-xenon weatherometer, UVW-UV-carbon weatherometer, UVW-UV-carbon weatherometer, DW-dewcycle weatherometer, SF-Sunshine fadeometer, XF-xenon fadeometer]. [Adapted, by permission, from O. Nishimura, H. Kubota, and S. Suzuki, *Kenkyu Hokoku-Kogyo Gijutsuin*, 1981(2)115.]

Fig. 10.2. PVC. Thickness of degradation layer vs. exposure time. [SW-Sunshine weatherometer, XW-xenon weatherometer, UVW-UV-carbon weatherometer, UVW-UV-carbon weatherometer, DW-dewcycle weatherometer, SF-Sunshine fadeometer, XF-xenon fadeometer]. [Adapted, by permission, from O. Nishimura, H. Kubota, and S. Suzuki, *Kenkyu Hokoku-Kogyo Gijutsuin*, 1981(2)115.]

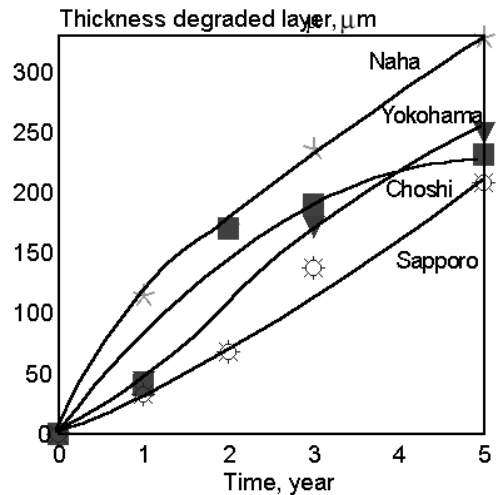
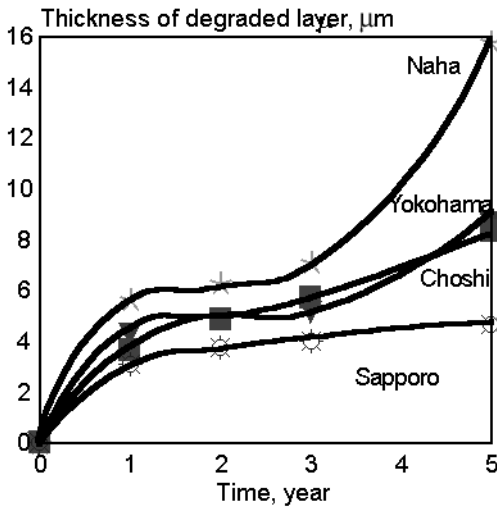
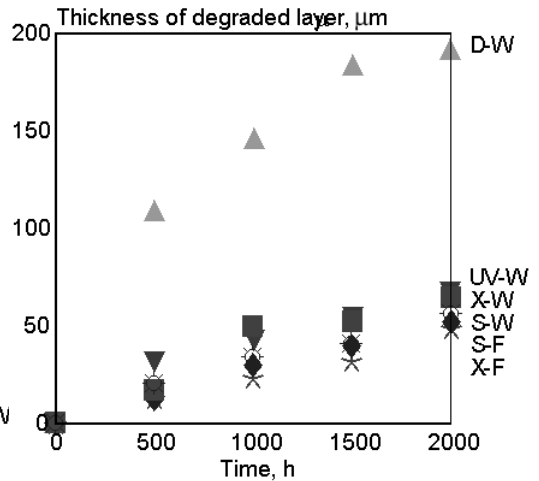
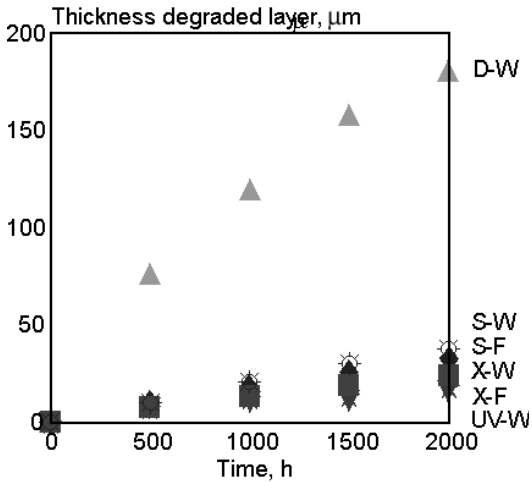


Fig. 10.3. PMMA. Thickness of degradation layer vs. exposure time. [SW-Sunshine weatherometer, XW-xenon weatherometer, UVW-UV-carbon weatherometer, DW-dewcycle weatherometer, SF-Sunshine fadeometer, XF-xenon fadeometer]. [Adapted, by permission, from O. Nishimura, H. Kubota, and S. Suzuki, *Kenkyu Hokoku-Kogyo Gijutsuin*, 1981(2)115.]

Fig. 10.4. ABS. Thickness of degradation layer vs. exposure time. [SW-Sunshine weatherometer, XW-xenon weatherometer, UVW-UV-carbon weatherometer, DW-dewcycle weatherometer, SF-Sunshine fadeometer, XF-xenon fadeometer]. [Adapted, by permission, from O. Nishimura, H. Kubota, and S. Suzuki, *Kenkyu Hokoku-Kogyo Gijutsuin*, 1981(2)115.]

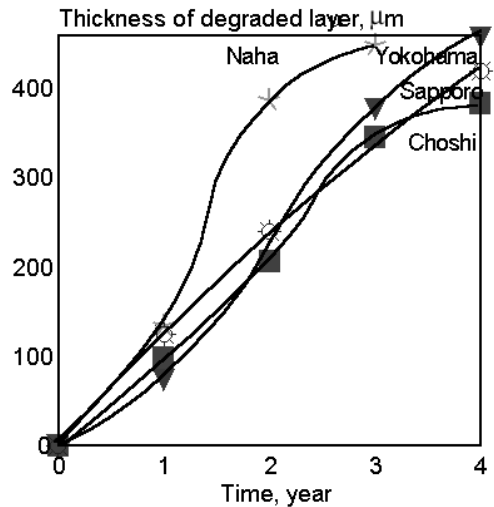
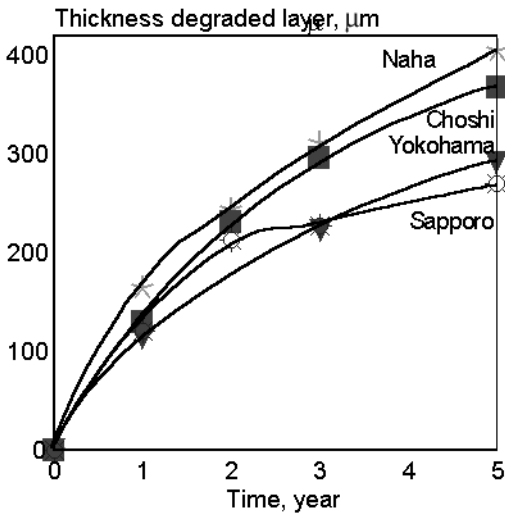
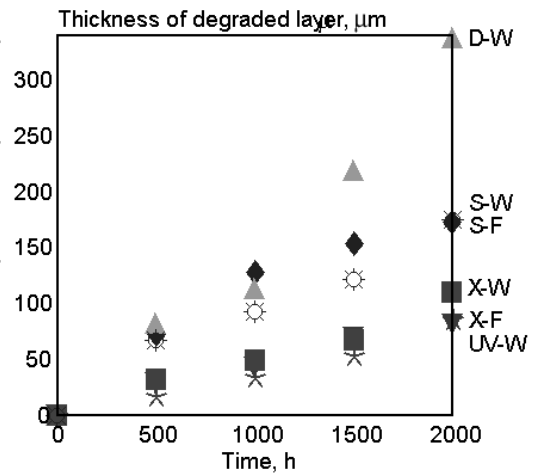
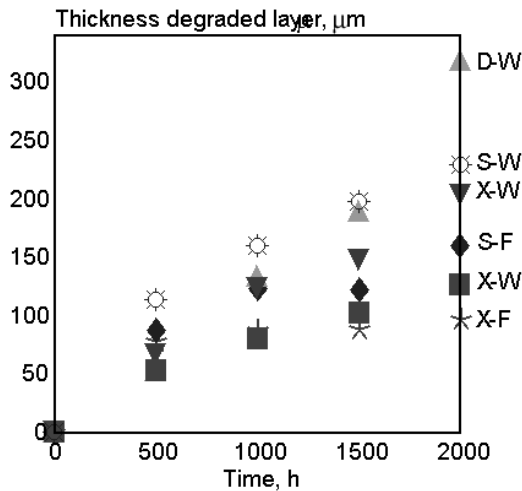


Fig. 10.5. POM. Thickness of degradation layer vs. exposure time. [SW-Sunshine weatherometer, XW-xenon weatherometer, UVW-UV-carbon weatherometer, DW-dewcycle weatherometer, SF-Sunshine fadeometer, XF-xenon fadeometer]. [Adapted, by permission, from O. Nishimura, H. Kubota, and S. Suzuki, *Kenkyu Hokoku-Kogyo Gijutsuin*, 1981(2)115.]

Fig. 10.6. PE. Thickness of degradation layer vs. exposure time. [SW-Sunshine weatherometer, XW-xenon weatherometer, UVW-UV-carbon weatherometer, DW-dewcycle weatherometer, SF-Sunshine fadeometer, XF-xenon fadeometer]. [Adapted, by permission, from O. Nishimura, H. Kubota, and S. Suzuki, *Kenkyu Hokoku-Kogyo Gijutsuin*, 1981(2)115.]

Table 10.1: Thickness ranking

	PS	PVC	PMMA	ABS	POM	PE	Δ score
Sapporo	5	3	1	2	4	6	
Choshi	6	3	1	2	4	5	
Yokohama	5	3	1	2	4	6	
Naha	6	2	1	3	4	5	
Average	5 or 6	3	1	2	4	5 or 6	
S-W	5	3	1	2	6	4	3
X-W	6	3	1	2	5	4	2
UV-W	6	4	1	2	5	3	4
D-W	3	6	1	2	4	5	5
S-F	5	6	1	2	3	4	5
X-F	6	5	1	2	4	3	4

The problems with some weathering equipment become apparent when we start to compare the artificial weathering data on polymers which are competing for the second and third ranked positions with that obtained for these polymers in outdoor exposure. The distinctions made in artificial weathering data are not apparent in the data from samples exposed outdoors which is almost identical for each. Different weathering sites have different accelerating effects on the degradation of various polymers. For example, PS degrades twice as fast in Naha than it does in Sapporo whereas PE has similar degradation rates in both locations. This is most likely due to the fact that Naha has more rain and humidity than Sapporo and that PE is less affected by exposure to water than is PS. Figs. 10.7 to 10.11 show the effect of different weathering conditions on the color change of five polymers. Table 10.2 summarizes this experiment by comparing the ranking of polymers exposed in different sites and equipment. If tables 10.1 and 10.2 are compared it can be seen that the polymers are ranked differently. Not one polymer has the same rank. This might be thought of as surprising but, in fact, a change of color is seldom caused by the same mechanism which leads to a deterioration in mechanical properties. Actually, with some polyurethanes, a color change during exposure indicates that the polymer will retain its mechanical properties. It is not surprising that PE rates highest with respect to color retention because there are practically no mechanisms which can cause a change color during the initial degradation (as determined in this study). The first three weathering devices do a good job of simulating the degradation which causes color changes outdoors. There is just one exception (PVC). It is difficult to explain why PVC consistently performs more poorly than PS in artificial weathering devices when, in natural exposure, it performs much better. Strangely enough, fadeometers, which are supposed to be capable of determining color stability, perform very poorly in this application.

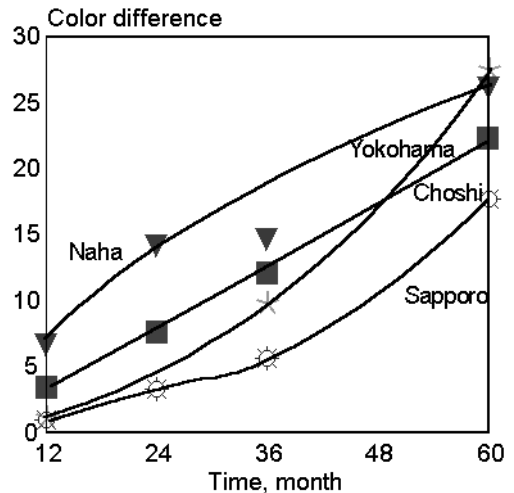
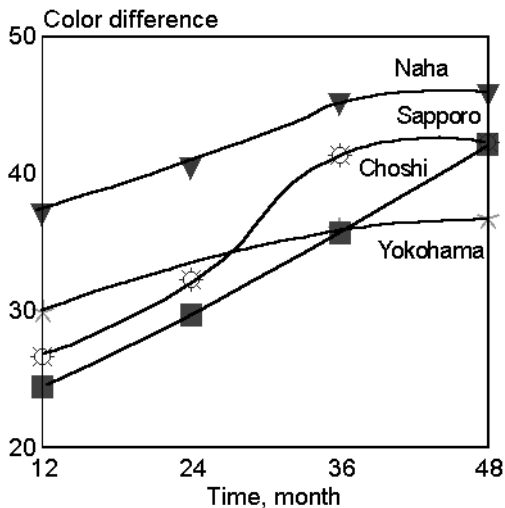
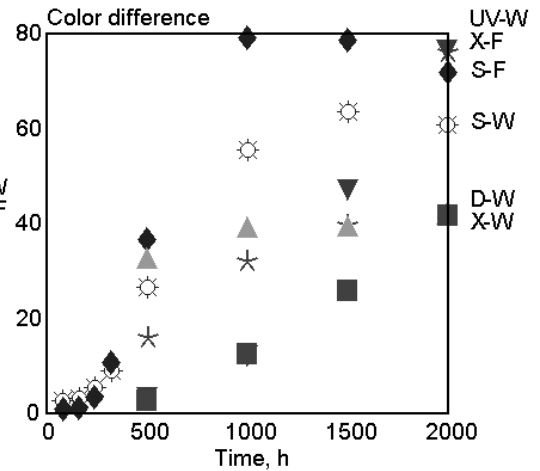
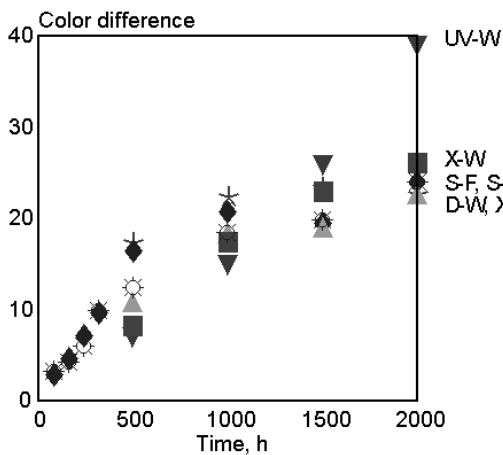


Fig. 10.7. PS. Color difference vs. exposure period in various sites and weathering equipment. [SW-Sunshine weatherometer, XW-xenon weatherometer, UVW-UV-carbon weatherometer, DW-dewcycle weatherometer, SF-Sunshine fadeometer, XF-xenon fadeometer]. [Adapted, by permission, from H. Kubota, S. Suzuki, O. Nishimura, I. Tamura, K. Yoshikawa, and T. Shiota, *Hokkaido Kogyo Kaihatsu Shikensho Hokoku*, 24(1981)96.]

Fig. 10.8. PVC. Color difference vs. exposure period in various sites and weathering equipment. [SW-Sunshine weatherometer, XW-xenon weatherometer, UVW-UV-carbon weatherometer, DW-dewcycle weatherometer, SF-Sunshine fadeometer, XF-xenon fadeometer]. [Adapted, by permission, from H. Kubota, S. Suzuki, O. Nishimura, I. Tamura, K. Yoshikawa, and T. Shiota, *Hokkaido Kogyo Kaihatsu Shikensho Hokoku*, 24(1981)96.]

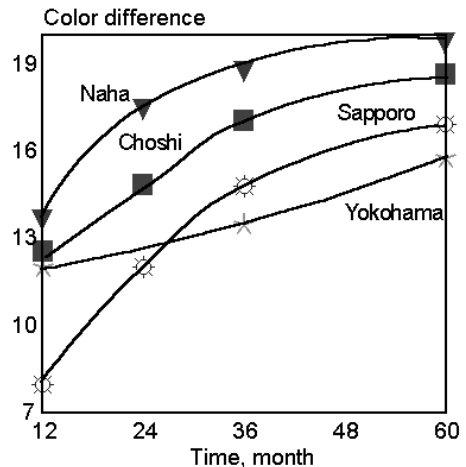
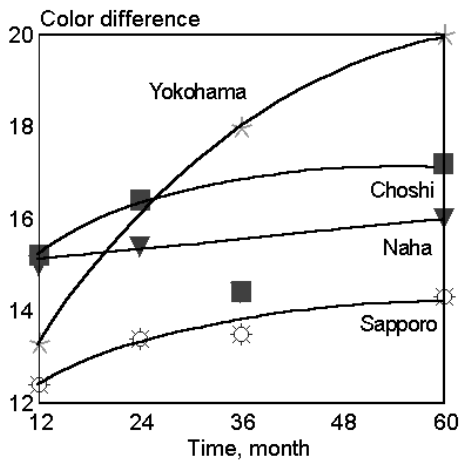
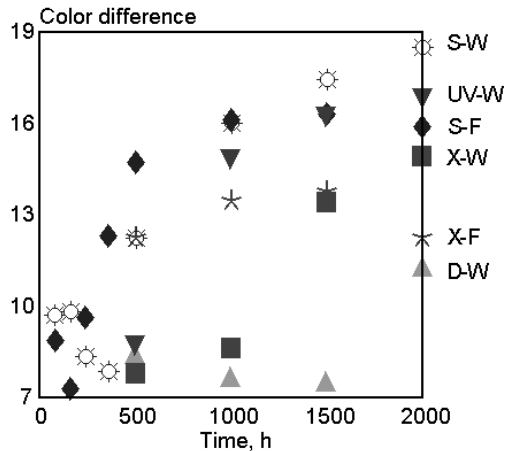
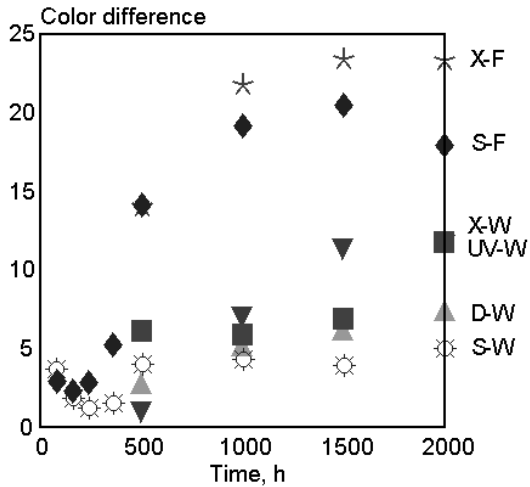


Fig. 10.9. ABS. Color difference vs. exposure period in various sites and weathering equipment. [SW-Sunshine weatherometer, XW-xenon weatherometer, UVW-UV-carbon weatherometer, DW-dewcycle weatherometer, SF-Sunshine fadeometer, XF-xenon fadeometer]. [Adapted, by permission, from H. Kubota, S. Suzuki, O. Nishimura, I. Tamura, K. Yoshikawa, and T. Shirota, *Hokkaido Kogyo Kaihatsu Shikensho Hokoku*, 24(1981)96.]

Fig. 10.10. POM. Color difference vs. exposure period in various sites and weathering equipment. [SW-Sunshine weatherometer, XW-xenon weatherometer, UVW-UV-carbon weatherometer, DW-dewcycle weatherometer, SF-Sunshine fadeometer, XF-xenon fadeometer]. [Adapted, by permission, from H. Kubota, S. Suzuki, O. Nishimura, I. Tamura, K. Yoshikawa, and T. Shirota, *Hokkaido Kogyo Kaihatsu Shikensho Hokoku*, 24(1981)96.]

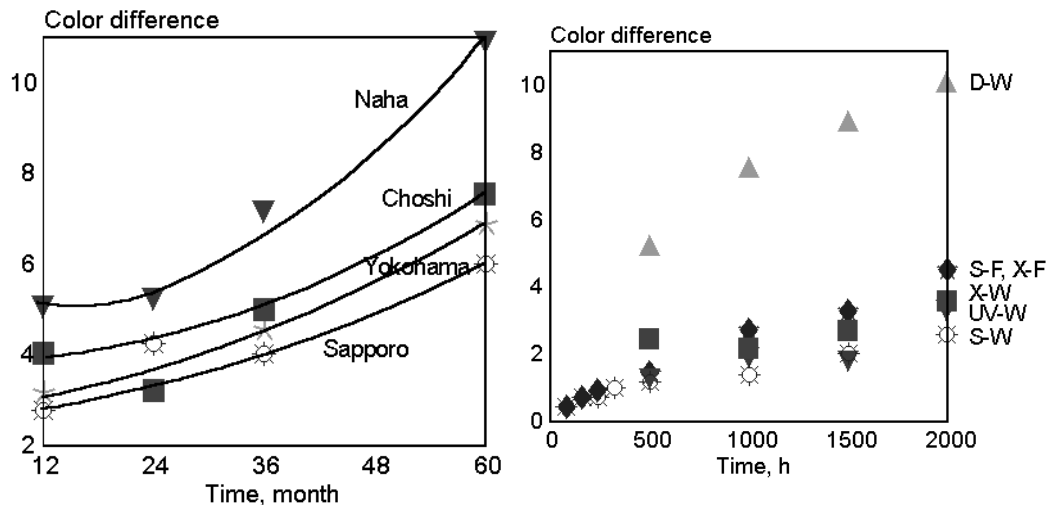


Fig. 10.11. PE. Color difference vs. exposure period in various sites and weathering equipment. [SW-Sunshine weatherometer, XW-xenon weatherometer, UVW-UV-carbon weatherometer, DW-dewcycle weatherometer, SF-Sunshine fadeometer, XF-xenon fadeometer]. [Adapted, by permission, from H. Kubota, S. Suzuki, O. Nishimura, I. Tamura, K. Yoshikawa, and T. Shirota, *Hokkaido Kogyo Kaihatsu Shikensho Hokoku*, 24(1981)96.]

Table 10.2: Color difference ranking

	PS	PVC	ABS	POM	PE	Δ score
Sapporo	5	4	2	3	1	
Choshi	5	4	2	3	1	
Yokohama	5	4	2	3	1	
Naha	5	4	3	2	1	
Average	5	4	2	3	1	
S-W	4	5	2	3	1	2
X-W	4	5	2	3	1	2
UV-W	4	5	2	3	1	2
D-W	4	5	1	3	2	4
S-F	4	5	3	2	1	4
X-F	3	5	4	2	1	6

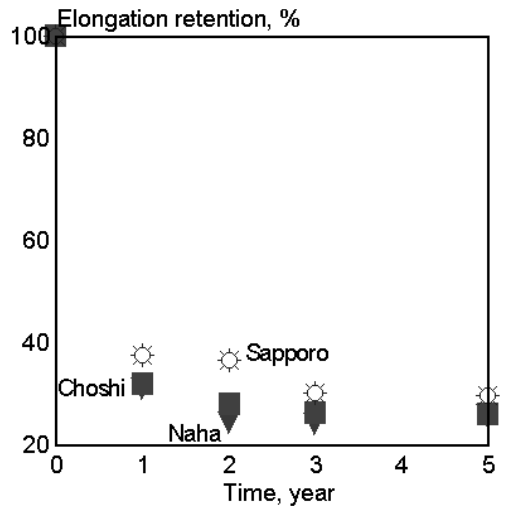
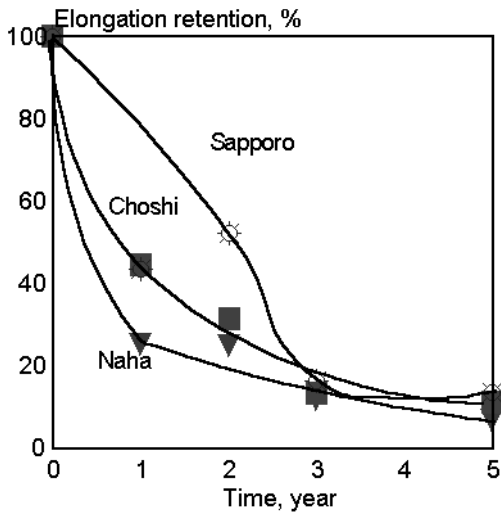
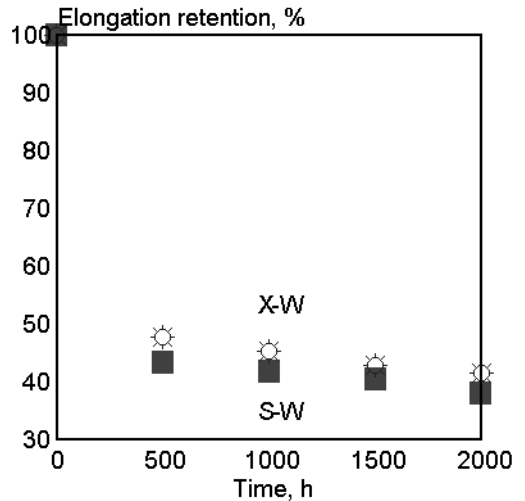
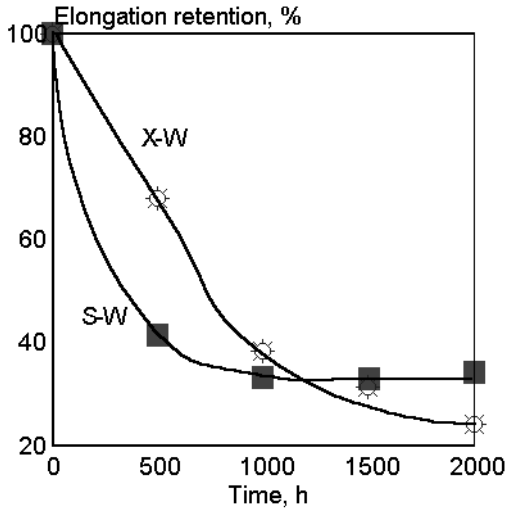


Fig. 10.12. PVC elongation retention vs. exposure period outdoor and in weathering equipment. [XW-xenon weatherometer, SW-Sunshine weatherometer]. [Adapted, by permission, from H. Kubota, S. Suzuki, O. Nishimura, S. Hattari, K. Yoshikawa, and T. Shiota, *Kenkyu Hokoku-Kogyo Gijutsuin*, 1981(2)23.]

Fig. 10.13. ABS elongation retention vs. exposure period outdoor and in weathering equipment. [XW-xenon weatherometer, SW-Sunshine weatherometer]. [Adapted, by permission, from H. Kubota, S. Suzuki, O. Nishimura, S. Hattari, K. Yoshikawa, and T. Shiota, *Kenkyu Hokoku-Kogyo Gijutsuin*, 1981(2)23.]

Table 10.3 Elongation retention, %

	PVC	ABS	ABS/PVC
Sapporo	13.5	29.7	2.2
Choshi	11	25.9	2.35
Naha	6.9	21.8	3.16
S-W	34.2	37.9	1.11
X-W	24.2	41.5	1.71

The general conclusions from the Japanese studies are: both sunshine carbon arc and xenon arc apparatus are useful to predict the service life of materials; the carbon arc lamp accelerates degradation more than other methods. (It is probably for this reason that carbon arc is the most frequently selected method in Japan.) However, from the above analysis, the xenon arc gives a more accurate prediction. The view of the Japanese

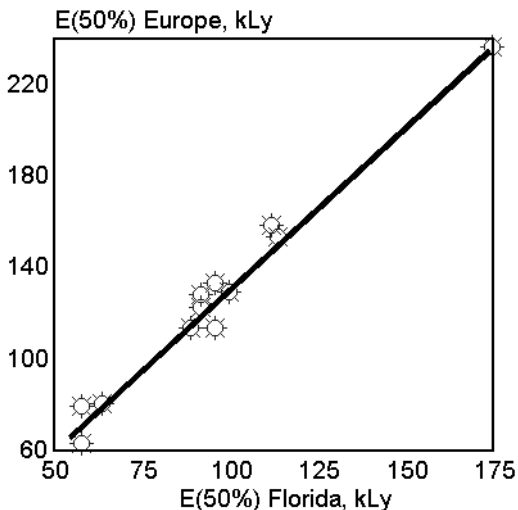


Fig. 10.14. Comparison of exposure in Florida and Central Europe based on energy to 50% retained elongation (E_{50}) for LDPE blown films. [Adapted, by permission, from F. Gugumus, *Dev. Polym. Stab.*, 8(1987)239.]

Figs. 10.12 and 10.13 show elongation retention during natural and artificial weathering of PVC and ABS. Table 10.3 compares the numerical data. A prediction of weathering rate based on changes in elongation agrees with the findings obtained by two other methods (ABS has better performance than PVC). The relative rates of degradation of each polymer in xenon arc are very similar to that which is observed outdoors.

researchers is not shared by all scientists involved in weathering studies. Gugumus⁹ discusses several studies which show correlations between results obtained in natural and accelerated weathering. Very good linear correlation ($r^2=0.99$) was found between weathering studies conducted in outdoor exposure in Central Europe and in Florida (Fig. 10.14)

There was very poor correlation ($r^2=0.45$) between the results from xenon arc and carbon arc Weather-O-Meters (Fig. 10.15). There was no correlation between xenon arc (Xenotest 1200) and QUV. QUV-weathered specimens did not correlate with specimens exposed in Florida (Fig. 10.16). But there is excellent correlation between the data from the Weather-O-Meter and the Xenotest 1200 (Fig. 10.17) and between either of the two xenon arc testers and Florida exposure (Fig. 10.18).

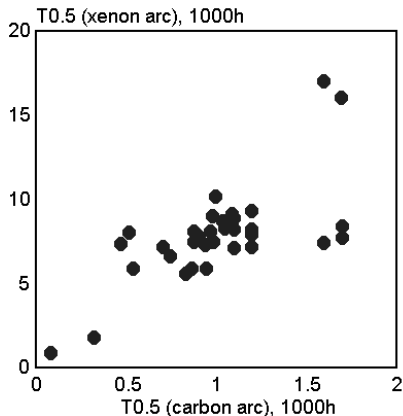


Fig. 10.15. Comparison of xenon-arc and carbon-arc exposure based on time to 0.5 carbonyl absorbance ($T_{0.5}$) for PP films. [Adapted, by permission, from F. Gugumus, *Dev. Polym. Stab.*, 8(1987)239.]

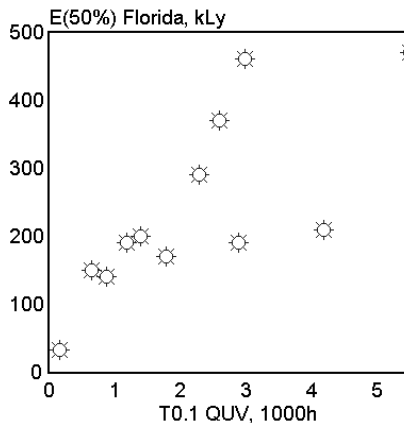


Fig. 10.16. Comparison of QUV and Florida exposure based on time to 0.1 carbonyl absorbance ($T_{0.1}$) and energy to 50% retained elongation (E_{50}) for LDPE blown films. [Adapted, by permission, from F. Gugumus, *Dev. Polym. Stab.*, 8(1987)239.]

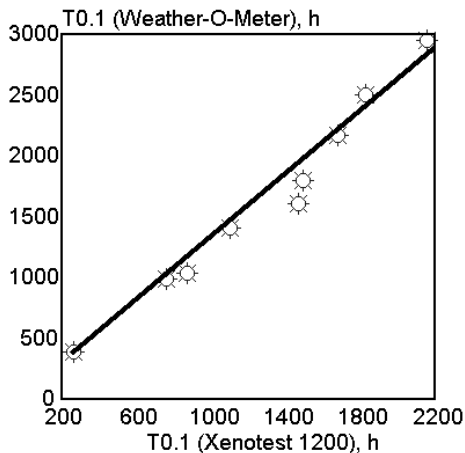


Fig. 10.17. Comparison of Xenotest 1200 and Weather-O-Meter based on time to 0.1 carbonyl absorbance ($T_{0.1}$) for PP film. [Adapted, by permission, from F. Gugumus, *Dev. Polym. Stab.*, 8(1987)239.]

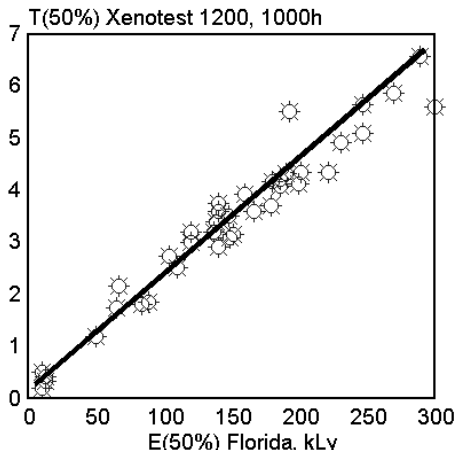


Fig. 10.18. Comparison of Xenotest and Florida exposure based on time to 50% retained tensile strength (T_{50}) and elongation (E_{50}) for PP multifilaments. [Adapted, by permission, from F. Gugumus, *Dev. Polym. Stab.*, 8(1987)239.]

Gugumus⁹ presents other results, all of which are for polyolefins, and makes the clear conclusion that only the xenon arc instrument, when equipped with filters which

give a spectrum similar to that of daylight, is useful for predicting the service life of polymers. Similar conclusions were reached in a review paper¹⁰ where numerous examples of the use of artificial weathering equipment were discussed. The main conclusion from these publications is that the xenon arc source does give the best correlation with daylight exposure.

Several other papers¹¹⁻¹⁴ discuss the various factors which are critical to achieve a correlation with data obtained in a natural environment. Some authors¹⁵⁻¹⁶ underline the deficiencies of QUV weathering in paints, claiming that this method gives acceptable results for some coatings (acrylic-based) but not for others (phthalate-based polyester coatings). Industry has accumulated a great deal of data using three types of weathering equipment (QUV, carbon arc apparatus, and xenon arc apparatus). It is difficult to replace these methods, since a proper assessment of the replacement method requires that the performance of products, which have been available in the market for a long time, be re-tested using the proposed replacement method. Fedor and Brennan used simple tests to evaluate sealants (a visual comparison of cracks, hardness measurement, and hand flexing). These led to the conclusion that QUV correlates better with Florida exposure than does a xenon arc Weather-O-Meter.¹⁷

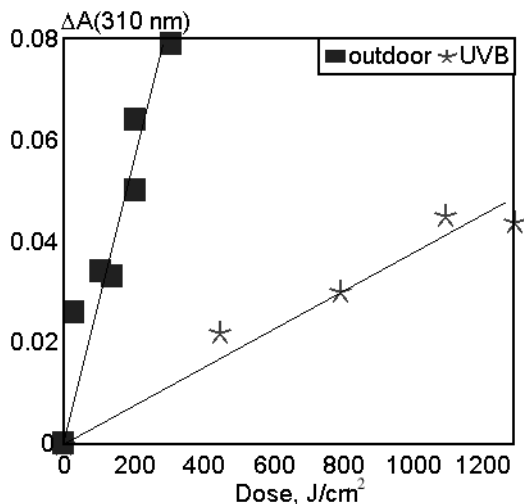


Fig. 10.19. Comparison of PVC dehydrochlorination rate in QUV and outdoor exposure in Brisbane. [Adapted, by permission, from D. J. Hill, F. A. Kroesen, J. H. O'Donnell, and P. J. Pomery, *Mater. Forum*, 14(1990)210.]

The photodegradation of PVC outdoors in Brisbane, Australia was compared to the effect of exposure in QUV equipment with UVB lamps (Fig. 10.19).¹⁸ Note that outdoor weathering was more severe than QUV. The authors of this paper found that the mechanisms of degradation, as determined by the type of degradation product formed, were the same. The difference in degradation rate is attributed to the influence of the higher temperature of outdoor exposure on the dehydrochlorination rate.

It was found¹⁵ that carbon arc exposure causes an unusual oxidation in the tested coatings. The dilemma of which test should be used¹⁹ is worst with paints and coatings since the industries which make them were among the first to initiate weathering studies and this was done at a time when only carbon arc instruments were available. Murase et al.²⁰ used depth profiling analysis to evaluate

the correlation of results between natural exposure and exposure in xenon and carbon arc devices. Different mechanisms degraded the coating in the carbon arc device. Gantcheva²¹ presents results of studies which show the data for PVC sheets during natural and Xenotest 1200 weathering. Factors related to the mechanical and electrical properties of the materials were measured and the results show that a good simulation of degradation in natural conditions can be achieved in a short time using the xenon arc chamber. Rivaton²² presents results of PC testing using different sources of UV radiation and compares them with exposure in natural conditions. Filtered xenon arc radiation correlates with outdoor exposure (see Fig. 5.4). Carbonyl group formation occurred in epoxy resins exposed to four different sources of radiation but the rates and the mechanisms of degradation were affected by changes in the UV wavelength range.²³

Two papers,^{24,25} devoted to the development of methods to compare natural and artificial weathering, stress different factors. Martin²⁵ considers the poor correlation between each method as a result of radiative energy differences. Based on successful studies in biology, Martin proposes that the results of weathering can be improved only if the relevant degradation energy for the material is considered. He attributes the poor correlation to the fact that each material can only absorb and utilize a specific portion of the total available energy whereas, in the artificial sources, the total radiation or, more critically, the UV radiation available, may differ significantly from that available naturally. If these differences are predominantly in the ranges where the material absorbs strongly, there will be poor correlation between the degradative effects.

In another paper,²⁴ the poor correlation is attributed to the assumption that temperature is not an essential factor in degradation. A model was developed in which the conditions of sample exposure at different temperatures and different radiation energy can be compared. Data obtained for PE was used to demonstrate the effectiveness of this approach. Additionally, the authors of this paper recommend that the conditions should be chosen such that there will be no radiation wavelength available which is not present in daylight. This will ensure that there be no degradation mechanisms that would not happen under natural exposure. David *et al.*²⁶ found that the degradation rate of PE was higher in Suntest (Heraus) equipment than in outdoor exposure in Brussels. This was due to a different degradation mechanism caused by the higher temperature in the artificial device.

Bauer²⁷ discusses the use of high energy UV radiation which is used frequently in automotive tests. Experimental results show that such a method can lead to false predictions of coating durability. A small change in polymer composition or the addition of a stabilizer caused a considerable change in the rate of degradation. Several other papers²⁸⁻³⁴ help to explain differences and similarities between sample testing outdoors and sample testing in artificial weathering equipment. These approaches are relevant to the successful studies as discussed in Chapters 5 and 8.

REFERENCES

1. H. Kubota, S. Suzuki, O. Nishimura, S. Hattori, K. Yoshikawa, and T. Shiota, *Kenkyu Hokoku-Kogyo Gijutsuin*, 1981,2,23.
2. Y. Nagatsuka, T. Shiota, K. Yoshikawa, S. Suzuki, H. Kubota, and O. Nishimura, *Kenkyu Hokoku-Kogyo Gijutsuin*, 1981,2,87.
3. H. Kubota, S. Suzuki, O. Nishimura, K. Yoshikawa, and T. Shiota, *Kenkyu Hokoku-Kogyo Gijutsuin*, 1981,2,49.
4. H. Kubota, S. Suzuki, O. Nishimura, I. Tamura, K. Yoshikawa, and T. Shiota, *Hokkaido Kogyo Kaihatsu Shikensho Hokoku*, 24(1981)96.
5. O. Nishimura, H. Kubota, and S. Suzuki, *Hokkaido Kogyo Kaihatsu Shikensho Hokoku*, 24(1981)115.
6. S. Suzuki, H. Kubota, O. Nishimura, and T. Tsurue, *Hokkaido Kogyo Kaihatsu Shikensho Hokoku*, 24(1981)153.
7. E. Takeshima, T. Kawano, H. Takamura, and S. Kato, *Shikizai Kyokaishi*, 56(1983)457.
8. O. Nishimura, S. Suzuki, H. Kubota, K. Yoshikawa, and T. Shiota, *Hokkaido Kogyo Kaihatsu Shikensho Hokoku*, 24(1981)193.
9. F. Gugumus, *Dev. Polym. Stab.*, 8(1987)239.
10. J. N. Patel, *JOCCA*, (1991)105.
11. D. Waksman, W. E. Roberts, and W. E. Byrd, *Durability Building Mater.*, 3(1985)1.
12. S. G. Croll, *Prog. Org. Coat.*, 15(1987)223.
13. G. P. Bierwagen, *Prog. Org. Coat.*, 15(1987)179.
14. P. Eurin, J. C. Marechal, and R. Cope, *NATO ASI Ser.*, 95E(1985)21.
15. D. R. Bauer, J. L. Gerlock, and R. A. Dickie, *Prog. Org. Coat.*, 15(1987)209.
16. R. R. Blakey, *Prog. Org. Coat.*, 13(1985)279.
17. G. Fedor and P. Brennan, *Applicator*, 12(1990)2.
18. D. J. Hill, F. A. Kroesen, J. H. O'Donnell, and P. J. Pomery, *Mater. Forum*, 14(1990)210.
19. J. H. Braun, *Prog. Org. Coat.*, 15(1987)249.
20. A. Murase, Y. Esaki, M. Sugiura, and T. Araga, *Anal. Sci.*, 7(1991)1597.
21. T. Gantcheva, A. Marinova, and P. Genova, *Angew. Makromol. Chem.*, 137(1985)49.
22. G. Zhang, W. G. Pitt, S. R. Goates and N. L. Owen, *J. Appl. Polym. Sci.*, 54(1994)419.
23. A. Rivaton, *Angew. Makromol. Chem.*, 216(1994)147.
24. J. J. C. Cruz-Pinto, M. E. S. Carvalho, and J. F. A. Ferreira, *Angew. Makromol. Chem.*, 216(1994)113.
25. J. W. Martin, *Prog. Org. Coat.*, 23(1993)49.
26. C. David, M. Trojan, A. Daro, and W. Demarteau, *Polym. Deg. Stab.*, 37(1992)233.
27. D. R. Bauer, *Prog. Org. Coat.*, 23(1993)105.
28. A. Tidjani and R. Arnaud, *Polym. Deg. Stab.*, 39(1993)285.
29. M. Sargent, J. L. Koenig, and N. L. Maecker, *Polym. Deg. Stab.*, 39(1993)355.
30. D. R. Bauer, J. L. Gerlock, and D. F. Mielewski, *Polym. Deg. Stab.*, 36(1992)9.
31. A. Wootton, *JSDC*, 108(1992)239.
32. A. J. Watkins, *IEEE Trans. Reliability*, 40(1991)98.
33. F. Gugumus, *Polym. Deg. Stab.*, 34(1991)205.
34. I. Narisawa and T. Kuriyama, *Angew. Makromol. Chem.*, 216(1994)87.

11

IMPORTANT VARIABLES OF WEATHERING

The main focus of studies on material weathering is on elucidation of the mechanisms of the chemical processes occurring during exposure of materials to the UV irradiation that has a major influence on degradative changes. The weathering process in natural conditions is multivariable, and is influenced by stress, temperature, humidity, concentration of reactive pollutants, contact with liquid media, electric stress, etc. The simultaneous effect of these factors creates enormous difficulties in studying the phenomenon and separating the effects of the individual factors. So, it is not surprising that most of the available information concerns UV degradation and the effect of the range of radiation wavelength; only a few studies evaluate the effects of other factors.¹⁻³⁸

Temperature and stress contribute to changes in the material during the course of weathering. Orientation, crystallization, structural stress, molecular mobility, monomolecular degradation, chemical reactivity, radical formation rate, chemical mechanisms, diffusion, sorption, permeability, density, and free volume are all influenced by temperature and stress. In this chapter, an attempt is made to discuss the effects on weathering of all but one of the listed properties and processes. The exception is the effect of material morphology on weathering (orientation, crystallinity, etc.) which is discussed in Chapter 15.

11.1 STRESS

Internal stress may develop in the material for variety of reasons, including condensation, crystallization, solvent evaporation, difference in thermal expansion of components, loads imposed during manufacturing, etc. Stress formed in the material might be relaxed if conditions allow or if it may remain as a material condition. For example, during solvent evaporation from the material, the stress is relaxed for as long as the components of the material are still sufficiently mobile to fill the free volumes created by the solvent removal. Similar conditions occur when material undergoes polymerization (Fig. 11.1). When the molecular weight of a polymer increases sufficiently to restrict

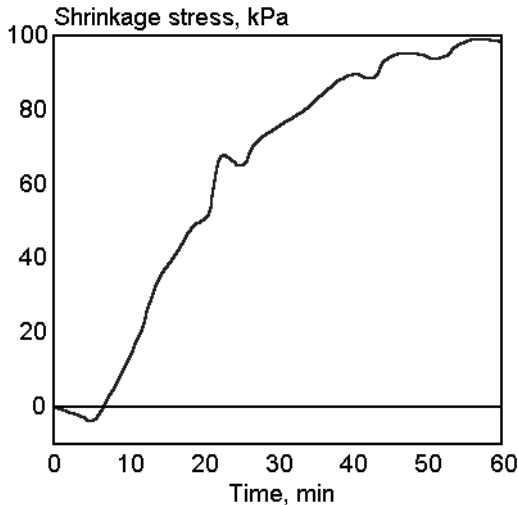


Fig. 11.1. Shrinkage stress vs. curing time of epoxy copolymer. [Adapted, by permission, from C. L. Bauer, R.J. Farris, and R.J. Vratsonos, *Polym. Mat. Eng. Sci.*, 56(1987)560.]

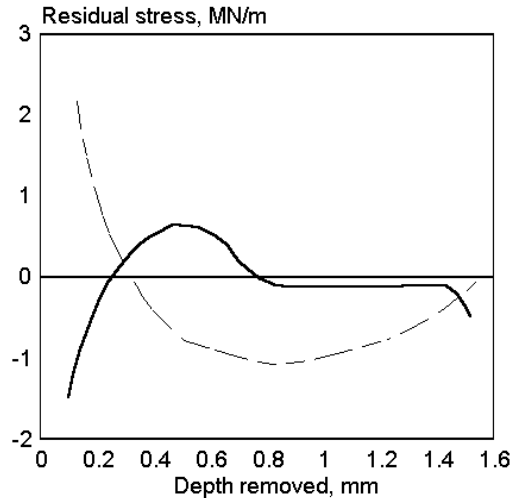


Fig. 11.2. Residual stress distribution computed from unexposed sample (solid line) and sample exposed for 2 years (broken line). [Adapted, by permission, from M. M. Qayyum and J. R. White, *Polym. Deg. Stab.*, 39(1993)199.]

chain mobility, further physical changes in the material, which may alter its volume (temperature, crystallization, evaporation, etc.), create internal stress.

Temperature distribution in the specimen may be another source of stress formation.¹⁷ It is suggested that two mechanisms may account for surface stress formation. De Bruijn¹⁸ concluded that the surface degradation of the polymer releases molecular fragments which change crystallinity, causing densification of the material as well as shrinkage, causing internal stress formation. The other mechanism relates changes in the sample to a temperature gradient caused by the exposed side of the specimen being substantially warmer than the side supported by the backing material. Also, the rate of temperature change on the surface of the sample differs from that on the bottom and this causes stress formation during natural temperature cycling. Fig. 11.2 shows the internal stress distribution which was measured in the samples.¹⁷ The stress distributions of the initial sample differs from that in the exposed sample. The stress near the surface of the sample was compressive and after degradative exposure it was reversed, putting the surface in tension. In coating studies,¹⁹ there were similar findings: temperature related stress affected the T_g of the coating. As long as the sample is in a glassy state, an internal stress is formed in the coating which ultimately leads to crack formation. This should be related to the fact that the T_g of material frequently increases during degradation period. Materials become increasingly more brittle because, at higher temperature gradi-

ents, when still in glassy state, they accumulate stress. Temperature differences are due not only to the insulating properties of materials but also to climatic conditions such as wind.^{20,21} Surface temperature differentials in a 3.5 m long rack reached 10°C.²⁰

Internal stress can also be formed by external forces applied to the material. Polymers are considered viscoelastic materials, which means that they combine the properties of liquids and solids and have plastic and elastic properties. The elastic properties of materials allow for stress relaxation. Consequently, external forces are dissipated with limited changes to the material structure. Plastic deformation leads to stress relaxation as an external force is applied. Stress is eliminated from the material at the expense of structural changes. The elastic properties of materials come into play in crystalline regions, whereas plastic deformation occurs initially in the amorphous region. When the applied force exceeds a specific amount, the crystalline region then becomes affected, resulting in a reorganization of the crystalline structure (finer, oriented crystallites). This brief discussion helps to explain the complex nature of what we simply term “stress”. Not only is it important to know how much force is applied to cause a specific deformation but it is also necessary to understand how these forces relate to material properties and how the applied mechanical energy is distributed and utilized. Thus, it is possible to predict the difference in effects between a low strain, below the elastic modulus, and a high deformation which creates a completely new material structure. Some examples of

the chemical changes in materials, that are caused by stress, are given below (Section 11.5).

Figure 11.3 shows the effect of load on polypropylene weathering.²² The chemical principles of these changes are discussed later in this chapter. A lower load does not seem to affect weathering but after the load is increased above a certain value, the rates of degradation begin to increase. Other data²³ indicate that the effect of stress on the specimen also increases with longer exposure. Fig. 11.4 illustrates this point. Load on the graph proportionally increases up to the point P_p then suddenly drops to P_s , then continues to increase until the specimen breaks. This phenomenon, which has been given the name “pop-in” occurs in conjunction with slow crack growth and depends on the extent of modification of surface layers

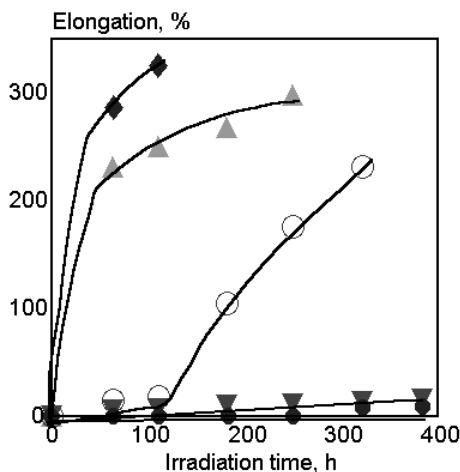


Fig. 11.3. Polypropylene sample deformation under load as a function of irradiation time. ● 0 MPa, ▼ 3.27 MPa, ○ 6.54 MPa, ▲ 8.18 MPa, ◆ 9.81 MPa. [Adapted by permission from R. Baumhardt-Neto and M. -A. De Paoli, *Polym. Deg. Stab.*, 40(1993)53.]

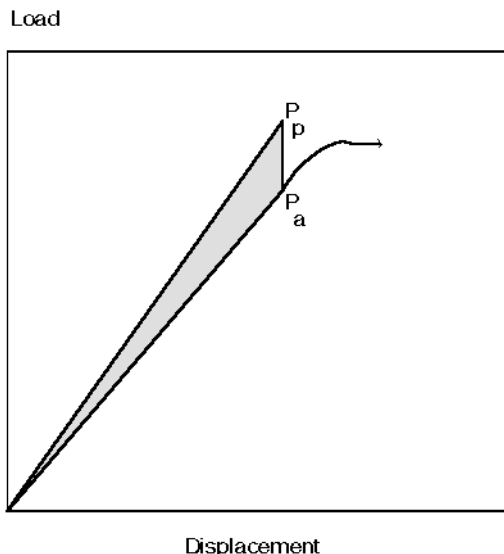


Fig. 11.4. Schematic diagram for evaluating an elastic energy released during the pop-in. [Adapted, by permission, from A. Kim, C. P. Bosnyak, and A. Chudnovsky, *J. Appl. Polym. Sci.*, 51(1994)1841.

in the material and on the way in which the properties change as material is degraded.

When evaluating the effect of stress on the degradation of materials, one should also consider the mechanics of how these forces are applied to the material. In most cases, a load applied to the specimen can be freely distributed within the specimen and the stress distribution depends on the specimen's structure. There are cases in which samples adhere to a substrate (e.g., a coating on concrete²⁴). Movement (extension or compression of the material) is relative to the expansion coefficients and the temperatures of both the material and its substrate. Cracks in the substrate which open and close due to temperature cycling and to absorption and desorption of water may also create a very high, localized stress.

In order to understand the importance of stress on degradation rate and its mechanisms, one needs to evaluate these processes at the molecular level. The material below is organized in such a manner.

11.2 MOLECULAR STRESS

Cycloalkanes were chosen by Popov and Zaikov³⁻⁵ to evaluate the effect of structural stresses on the chemical reactivity of molecules. Table 11.1 gives the values characterizing C₃-C₁₂ cycloalkanes.

Valence angles of cyclopropane and cyclobutane are smaller than in a tetrahedron (109.5°) and they can both be considered as models of molecules under compressive stress. Cyclohexane forms an unstressed ring. Higher cycloalkanes are considered to be models of molecules under tensile strain. Chemical stability may be measured by heat of combustion, dipole moment, or total strain. Depending on its angular deformation, nonvalence interaction, and torsional stress, each molecule has a different stress energy, which can be calculated from the following formula:

Table 11.1: The characteristics of cycloalkanes

	Valency bond angle	Distortion	Combustion heat kJ/CH ₂	Total strain kJ
C3	60	24 44	697	120
C4	90	9 44	685	112
C5	108	0 44	664	35
C6	120	-5 16	659	12
C7	128	-9 33	662	35
C8-11	135-147	-12 to -19	661-665	32-88
C12	150	-20 16	657	

$$E_{\text{exc}} = n(H/n - 157.4)$$

where n number of methylene groups in the ring
 H heat of combustion of the ring
 157.4 heat of cyclohexane combustion per 1 methylene group.

Fig. 11.5 shows the results when excess stress energy is calculated for various cycloalkanes. The small rings of cyclopropane and cyclobutane have a high excess energy of stress because their bond angles are much smaller than the tetrahedral angle, which contributes to a large energy of angular deformation. The high excess energy of stress of a 5-member ring is due to the high energy of nonvalent interaction. In the case of rings larger than cyclohexane, the excess stress energy is due to the large contribution of valence angle deformation.

Figs. 11.6 and 11.7 show the rate constants of reactions between cycloalkanes and O₃ and Br, respectively, relative to cyclohexane. Two general conclusions are obvious: excess stress energy affects the reaction rate constant for cycloalkanes higher than cyclohexane which are in tension. The high excess stress energy of the "compressed" model (cyclobutane) does not translate into increased reactivity. The conclusion drawn is that tensile strain increases the reactivity of molecules.

Popov and Zaikov³⁻⁵ devote a great part of their papers to the kinetic validation of model molecules in relation to the processes occurring in polymers. They conclude that what applies to small molecules can also be applied to polymers. Rappoport¹¹ shows data obtained for polyethylene which suggest that in the course of deformation of oriented PE, the concentration of *trans* conformation increases, as *gauche* conformation decreases (Fig. 11.8).

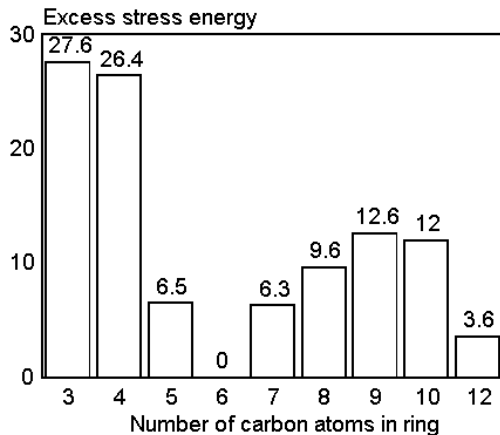


Fig. 11.5. Excess stress energy of cycloalkanes. [Data from A. A. Popov and G. E. Zaikov, *J. Macromol. Sci.-Rev. Macromol. Chem. Phys.*, C27(1987-88)343.]

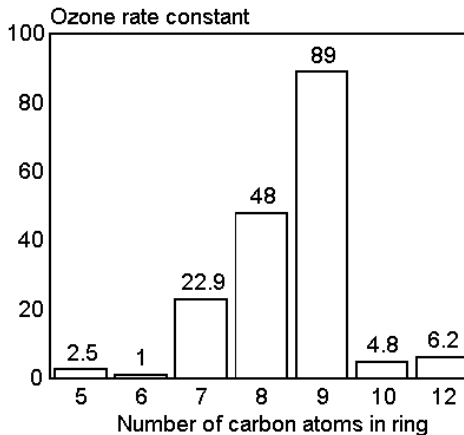


Fig. 11.6. Rate constant (k_{O_3}) of cycloalkanes reaction relative to cyclohexane reaction rate. [Data from A. A. Popov and G. E. Zaikov, *J. Macromol. Sci.-Rev. Macromol. Chem. Phys.*,

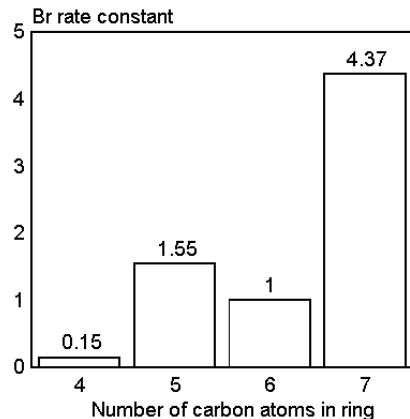


Fig. 11.7. Rate constant (k_{Br}) of cycloalkanes reaction relative to cyclohexane reaction rate. [Data from A. A. Popov and G. E. Zaikov, *J. Macromol. Sci.-Rev. Macromol. Chem. Phys.*, C27(1987-88)343.]

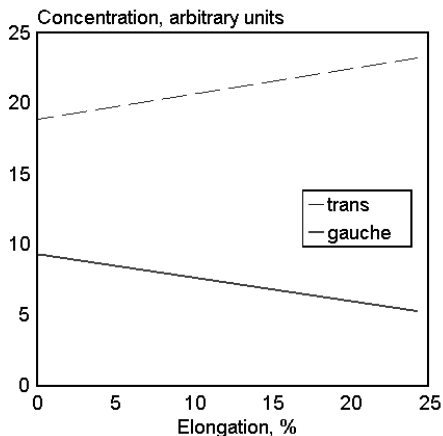


Fig. 11.8. Concentration of *trans* and *gauche* conformations in oriented PE vs. strain. [Data from H. Ya. Rappoport and G. E. Zaikov, *Usp. Khim.*, 52(1983)1586.]

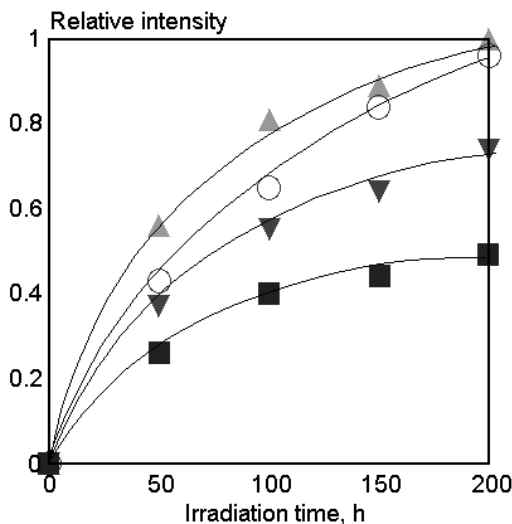


Fig. 11.9. Vinyl formation vs. irradiation time for samples of varying elongation. Elongation: ■ 0%, ▼ 222%, ○ 420%, ▲ 520%. [Adapted, by permission, from R. Gooden, D. D. Davis, M. Y. Hellman, A. J. Lovinger, and F. H. Winslow, *Macromolecules*, 21(1988)1212.]

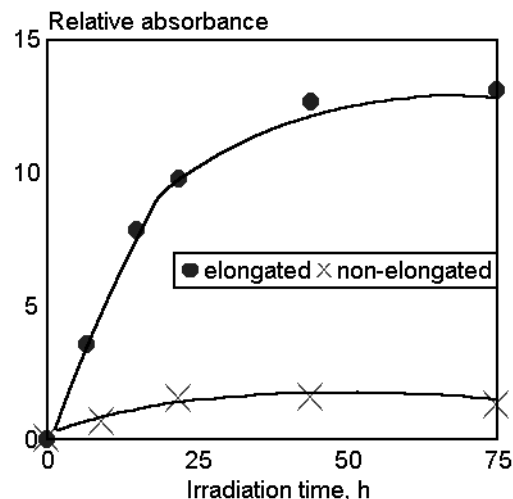


Fig. 11.10. Methyl-end-bond formation in 400% elongated and non-elongated samples vs. irradiation time. [Adapted, by permission, from R. Gooden, D. D. Davis, M. Y. Hellman, A. J. Lovinger, and F. H. Winslow, *Macromolecules*, 21(1988)1212.]

The presence of the *trans* conformation signals an increasing rate of degradation. Gooden¹⁰ presents data on the concentration of vinyl (Fig. 11.9) and methyl (Fig. 11.10) end-groups formed during the process of poly(ethylene-co-(carbon monoxide)) degradation by UV. The polymer may degrade according to Norrish type I and II mechanisms. Norrish type II scission is very dependent on conformation because of the way in which the motion of the polymer chain is restricted. Molecular tension in the chain should favor Norrish type I reactions over type II. Methyl end-groups are formed primarily from Norrish type I scission, whereas vinyl end-groups are formed by both types of scission. In the case of an unelongated sample, 80% of chain scission occurs by type II mechanism. In elongated samples, the Norrish type I scission prevails. This is demonstrated by a rapid increase in the formation of methyl groups and a relatively small increase in vinyl end-group formation. This demonstrates that the orientation of the polymer chain retards its ability to twist into the conformation required for Norrish type II scission. These above data also confirm the earlier assumption that stress on the molecular level affects reactivity.

Rather than demonstrating a relationship between stress and chemical reactivity, these studies show that when conversion occurs, its type and rate are dependent on the

chemical structure of the material rather than on its chemical reactivity. The degree to which the conversion is accelerated or inhibited depends strictly on chemical structure. It is chemical structure, therefore, that must be understood before undertaking weathering studies. Such analysis was done by Miller *et al.*²⁵ for PMMA. Syndio- and iso-tactic polymethylmethacrylates were analyzed during irradiation to detect changes in the main and side chains. From the energetic point of view, the net change of energy due to double bond formation was the same for the main and the side chains (13 kcal/mol). It still does not eliminate the possibility that double bond formation in side chains may be more probable because, in a solid state, a linear conformation of main chain is more stable due to a large increase in steric repulsion between polymer units during main chain double bond formation. The conformational energy change is substantially higher in the syndiotactic form, which contradicts some earlier works, but the total energy of conversion is the same for both conformations in respect to both the side and the main chains if the material can assume bend forms (available in solution).

Several other current papers²⁶⁻²⁹ deal with the effect of stress on degradation of materials. Schoolenberg and Meijer²⁶ found that the degradation process goes through three stages: initial (no change), a rapid change of property (the so-called "crack speed effect"), and finally proportional decrease of degradation rate. If surface layers are only partially degraded, but are generally stronger than the bulk of material, they store more energy and produce deeper cracks on failure. Frequently, the properties of degraded samples seem to recover after additional exposure. Some of these cases may be explained by this phenomenon.

Work done on polyethylene tapes²⁸ indicates that degradation under a tensile load is increased because of increased photooxidation in the amorphous areas of the stressed tapes. As with UV degradation, the rates of γ - and thermal-degradation also increase when sample is stressed.²⁹

11.3 MOLECULAR MOBILITY

Temperature and strain are the major factors affecting molecular mobility. An increase in temperature above the material's T_g increases both segmental and molecular mobility (Fig. 11.11). Evidently, the radiative degradation of polydimethylsiloxane is influenced strongly by temperatures in the range 285-500 K. Temperatures in this range do not, by themselves, cause degradation of silicone polymer. Even at temperatures close to room temperature, the acceleration of photodegradation is clearly visible. Studies of polyoxymethylene⁶ show how the thermal expansion coefficient increases during irradiation (Fig. 11.12) and, using different coordinates (Fig. 11.13), how higher temperatures during irradiation cause greater increases in the thermal expansion coefficient. No matter what the mechanism of these changes is, the coefficient of thermal expansion increases below the material's T_g , as the radiation dose increases, and decreases above its

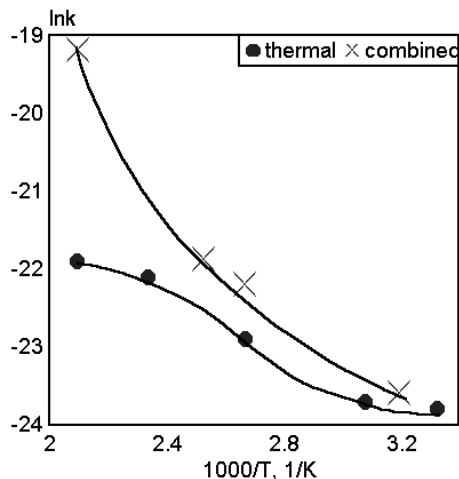


Fig. 11.11. Temperature dependence of the combined thermally and radiation induced chain scission reaction rates in polydimethylsiloxane elastomer subjected to γ -radiation. [Adapted, by permission, from S. W. Addy, D. W. Clegg, A. A. Collyer, G. C. Corfield, and P. Crum, *J. Rheol.*, 31(1987)297.]

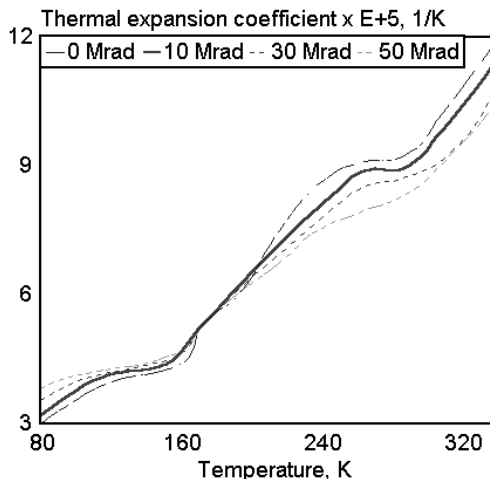


Fig. 11.12. POM thermal expansion coefficient vs. temperature for different doses. [Adapted, by permission, from H. N. Subramanyan and S. V. Subramanyan, *Eur. Polym. J.*, 23(1987)207.]

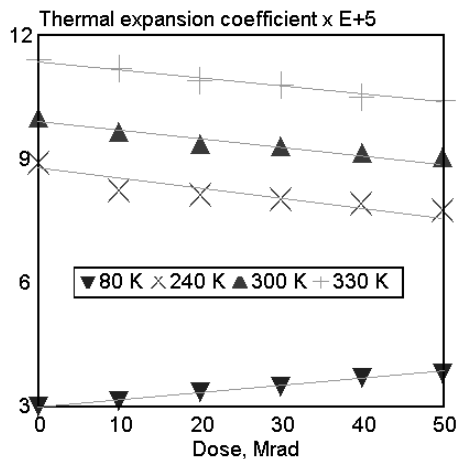


Fig. 11.13. POM thermal expansion coefficient vs. radiation dose at different temperatures. [Adapted, by permission, from H. N. Subramanyan and S. V. Subramanyan, *Eur. Polym. J.*, 23(1987)207.]

T_g (180 K). Also the radical decay rate for UV irradiated polystyrene begins to increase around its secondary transition point (-75°C), which correlates with phenyl ring rotation.⁸

It is very difficult to find similar data to illustrate the effect of strain on molecular mobility because stretching the sample not only decreases mobility but also affects crystallinity, crystalline structure, diffusion, and sorption — factors strongly affecting the photodegradation rate. At the same time, it is known that the NMR spectrum of a strained specimen changes at its T_g temperature. The second component appears above its T_g which is probably due to the presence of a mobile fraction. Solvents, plasticizers, and water that are present in polymers influence the chain mo-

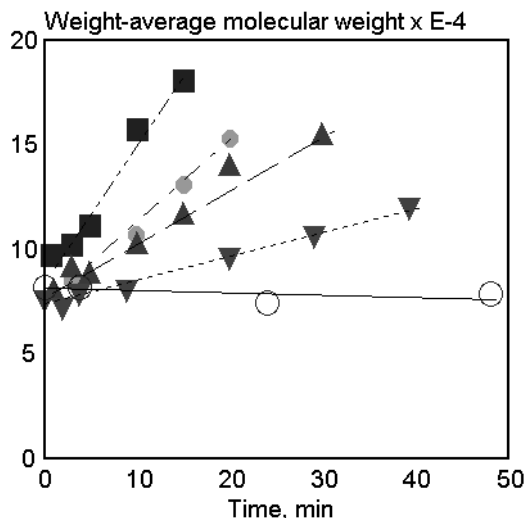


Fig. 11.14. Changes in weight-average molecular weight of polyethersulfone during photodegradation at \circ 25°C, ∇ 170°C, \blacktriangle 200°C, \bullet 225°C, \blacksquare 250°C. [Adapted, by permission, from S. Kuroda, I. Mita, K. Obata, and S. Tanaka, *Polym. Deg. Stab.*, 27(1990)257.]

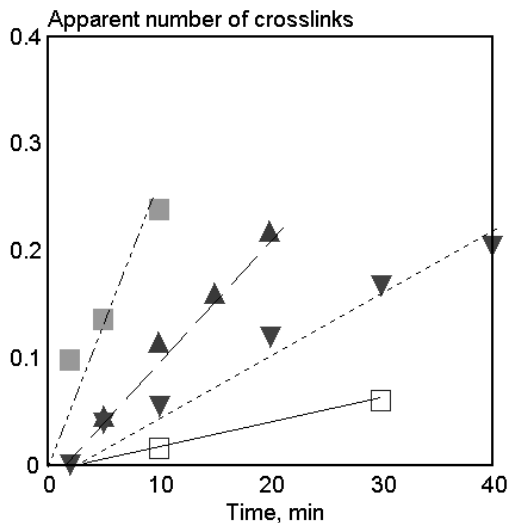


Fig. 11.15. Change in the apparent number of crosslinks per molecular chain, $\zeta_{x,app}$, during the photodegradation of polyethersulfone at \square 130°C, ∇ 170°C, \blacktriangle 200°C, and \blacksquare 250°C. [Adapted, by permission, from S. Kuroda, I. Mita, K. Obata, and S. Tanaka, *Polym. Deg. Stab.*, 27(1990)257.]

bility of these macromolecules. Their presence is likely to increase the photodegradation rate.

Two recent publications confirm these observations.^{30,31} A study of polyether sulfone³⁰ gives information on weight-average molecular weight (Fig. 11.14), on the change of number of crosslinks (Fig. 11.15), and an Arrhenius plot of quantum yields of the processes (Fig. 11.16) occurring during polymer exposure to UV radiation at different temperatures. The T_g of this polymer measured by DSC was found to be 222°C. When reaction rate is controlled by chain mobility, this is a diffusion-controlled process and these factors affect it: the molecular motion of reacting groups, a system's heterogeneity, the status of the matrix structure during the reaction, the energy of migration, etc. Chain mobility and diffusion are increased above T_g . Fig. 11.14 shows that molecular weight increases rapidly when polyether sulfone is exposed to UV at temperatures above 200°C (very close to its T_g). The change in molecular weight depends on the effect of two processes: chain scission and crosslinking. Fig. 11.15 shows that the quantum efficiency of crosslinking increases rapidly when the temperature of the sample approaches its T_g . Fig. 11.16 summarizes degradative processes and shows that the

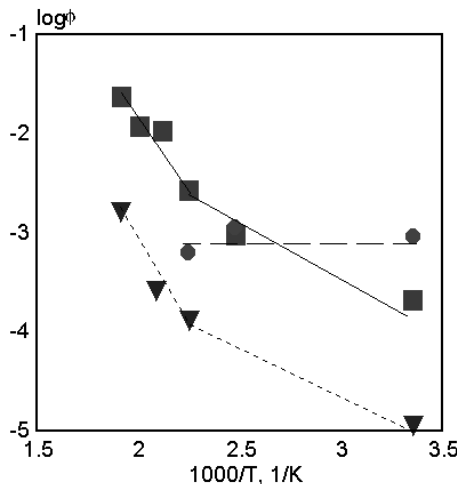


Fig. 11.16. Arrhenius plot of quantum yields for ■ crosslinking, ● chain scission, and ▼ SO₂ formation during photodegradation of polyethersulfone. [Adapted, by permission, from S. Kuroda, I. Mita, K. Obata, and S. Tanaka, *Polym. Deg. Stab.*, 27(1990)257.]

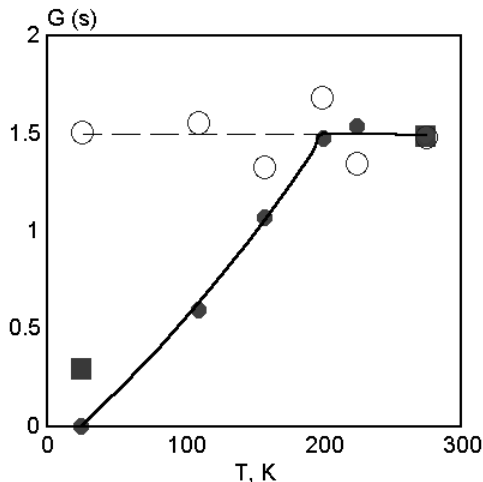


Fig. 11.17. Temperature dependence of G-value of the main-chain scission for ○ purified PMMA, ■ crude PMMA, and ● monomer-doped PMMA. [Adapted, by permission, from T. Ichikawa, K. Oyama, T. Kondoh, and H. Yoshida, *J. Polym. Sci., Polym. Chem.*, 32(1994)2487.]

quantum yield of crosslinking has two different rates (above and below 170°C) whereas chain scission remains unaffected by temperature throughout the range of temperatures used. This is because chain scission is a monomolecular reaction whereas crosslinking requires the participation of at least two molecules (or chain segments). The first reaction depends on delivering a sufficient amount of energy for bond dissociation (substantially higher than that provided by thermal energy) and thus the rate of this reaction is constant (relative to radiation intensity). Crosslinking, on the other hand, is controlled by diffusion and therefore its yield decreases as chain mobility decreases.

A paper by Ichikawa *et al.*³¹ shows us that because of the complexity of polymer systems, many factors come into play. Fig. 11.17 shows that PMMA has a lower chain scission rate when monomer is present in the polymer. This effect is detected up to a specific temperature range. ESR studies indicate that free monomer acts as a radical scavenger preventing main chain scissions. This information is less relevant to our present subject but has been mentioned at this point to indicate that many different influences should be anticipated in complex systems.

11.4 DIFFUSION, FREE-VOLUME, PERMEABILITY, SORPTION, DENSITY

Mass transfer processes occur predominantly in the amorphous phase with the crystalline phase acting as a barrier to diffusion pathways:

$$D = \tau_1 D_a$$

where	D	diffusion coefficient in the polymer
	D_a	diffusion coefficient in the amorphous phase
	τ_1	empirical parameter characterizing the diffusion path extension.

On the other hand, the diffusion coefficient depends also on the size of the diffusing molecule:

$$D = D_0 \exp(-B/f)$$

where	D_0	coefficient characterizing size and shape of the diffusant
	B	coefficient characterizing the minimum hole size required for diffusive displacement
	f	free volume.

Radicals formed in the photolytic process move in space from one cavity to another. The transport of radicals or small molecules in polymer depends on temperature, which should be well above T_g for the polymer to attain chain mobility. Additionally, sufficient free volume is required for the reaction to take place. Either the diffusion coefficient or the free volume may control the reaction rate. Free volume is given by the following equation:

$$V_f = V_{f0} + \varepsilon(1 - 2\mu)/(1 - \kappa)$$

where	V_f	current free volume
	V_{f0}	initial free volume
	ε	strain
	μ	Poisson's ratio
	κ	crystallinity.

This equation shows that sample stretching and crystallinity affect not only free volume, and thus reaction rate, but also that the increase in crystallinity, whether due to strain or to the degradative process, decreases reaction rate. This coincides with the observation that the degradation rate usually decreases as degradation advances.

Fig. 11.18 presents data for polypropylene indicating that the diffusion coefficient depends on a stretching ratio.¹¹

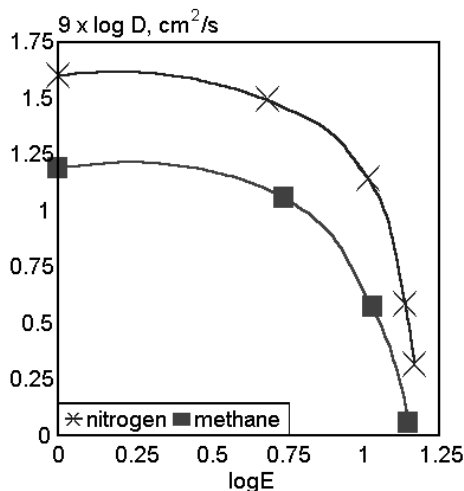


Fig. 11.18. Diffusion coefficient of nitrogen and methane in PP vs. degree of extension (E). [Data from H. Ya. Rappoport and G. E. Zaikov, *Usp. Khim.*, 52(1983)1568.]

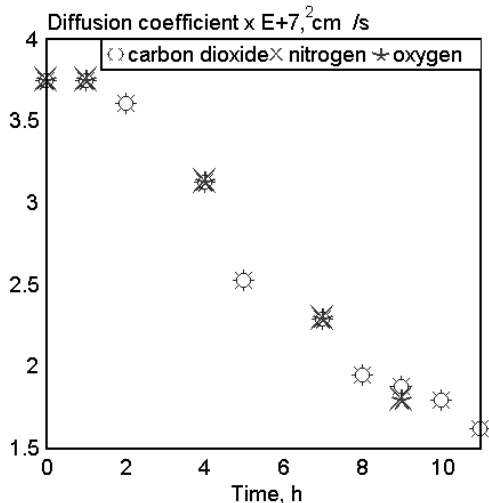


Fig. 11.19. Diffusion coefficient of various gases vs. irradiation time. [Data from J. -L. Philippart and J. -L. Gardette, *Makromol. Chem.*, 187(1986)1639.]

Fig. 11.19 gives information on the change of diffusion rates of some gases during degradation — a phenomenon explained by the increase of crystallinity during the degradation process.⁷ When oxygen diffusion decreases due to degradative changes, the rate of photooxidation must also decrease.

The sorption coefficient is given by the equation:

$$S = S_a(1 - \kappa)$$

where S_a sorption coefficient in amorphous phase
 κ crystallinity.

As with diffusion, sorption occurs mostly in the amorphous phase, with crystallites creating material obstacles on the way. Popov and Zaikov³⁻⁵ discuss their data on permeability of polymer films. They indicate that polyolefin films, which are thinner than 17 μm , and polyamide films, which are thinner than 2 μm , react with oxygen and ozone in a process which is not diffusion-controlled. These findings are in contradiction with the other cited studies and their validity is questionable.

Fig. 11.20 shows the density differences between crystalline and amorphous phases for some common semi-crystalline polymers. A density increase in a crystalline

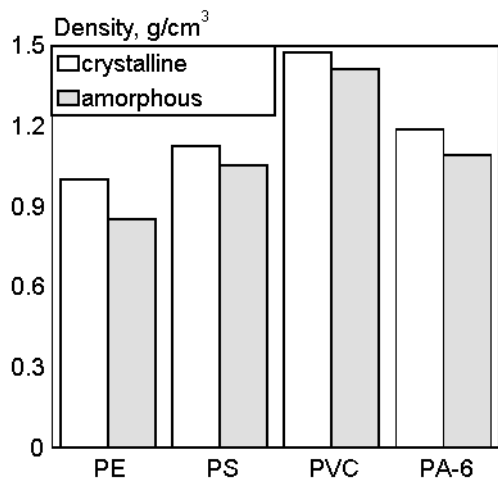


Fig. 11.20. Density of crystalline and amorphous phases.

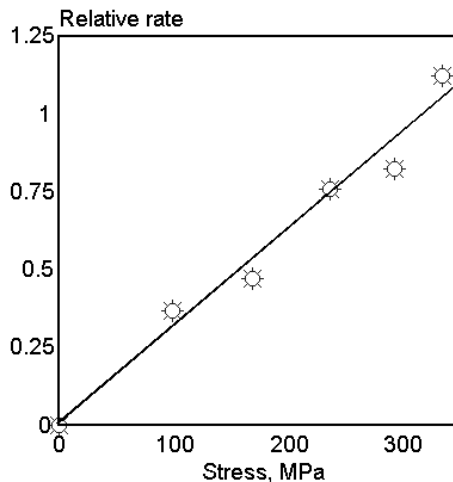


Fig. 11.21. Relative rate of free radical formation in PP during ozonation as a function of stress. [Adapted, by permission, from A. A. Popov and G. E. Zaikov, *J. Macromol. Sci.-Rev. Macromol. Chem. Phys.*, C27(1987-88)379.]

material is caused by compact packing, therefore processes which require free volume, such as chemical reactions, will be slowed.

11.5 CHEMICAL REACTIVITY

The data below outline the character of changes during aging of polymeric materials under various ranges of stress, temperature, and in the presence various pollutant types and concentrations. Stretched polypropylene, exposed to an ozone atmosphere, showed a rate of radical formation which increased proportionally to the stress applied (Fig. 11.21). Note that in this study, the sample to which stress was applied was oriented polypropylene, meaning that its chemical bonds were already stressed.

Studies on polymethylmethacrylate¹ show that the effective activation energy of degradation decreases as stress increases and that a longer duration of UV degradation further increases the degradation rate (Fig. 11.22). The time to failure of irradiated PMMA depends on the stress applied (Fig. 11.23). Also, an increase in photodegradation temperature decreases the time to failure of PMMA. Stress applied to a poly(vinyl alcohol) sample increases the rate of formation of carbonyl groups (Fig. 11.24).

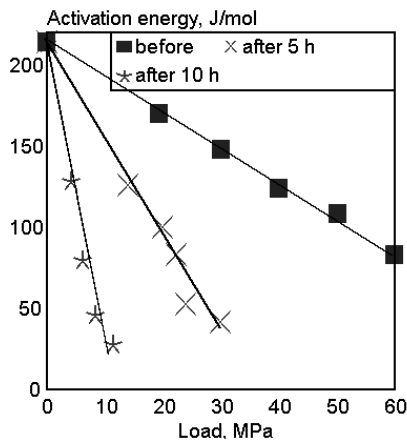


Fig. 11.22. Activation energy of PMMA degradation vs. load applied before and after UV irradiation. [Data from W. P. Yartsev, *Plast. Massy*, 1986(12)16.]

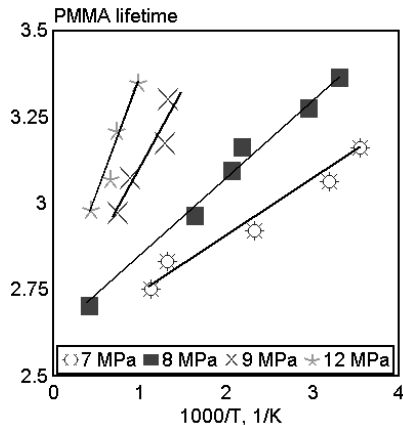


Fig. 11.23. PMMA lifetime after 10 h of irradiation vs. temperature of processing for different loads. [Data from W. P. Yartsev, *Plast. Massy*, 1986(12)16.]

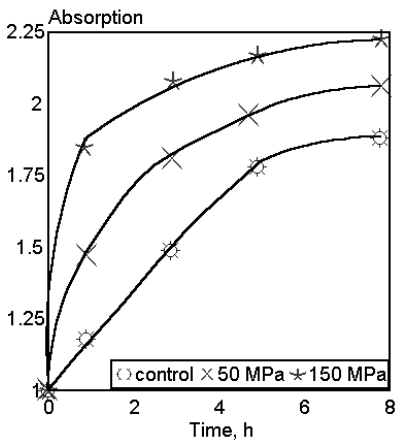


Fig. 11.24. The effect of stress on absorption of PVA films at 1720 cm^{-1} . [Data from E. Baimuratov, B. N. Narzullaev, I. Ya. Kolontarov, and A. W. Zakcharchuk, *Dokl. Akad. Nauk Tadzh. SSR*, 27(1984)204.]

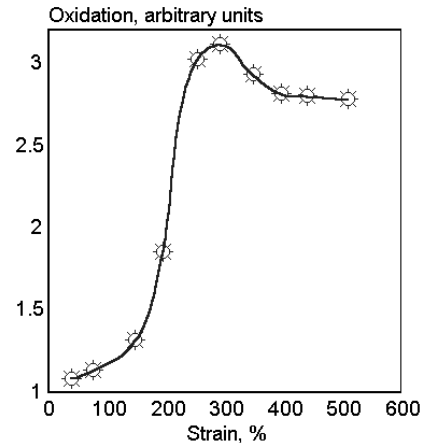


Fig. 11.25. PE oxidation vs. strain (37°C for 5 days). [Adapted, by permission, from R. S. Porter and A. Casale, *Polym. Eng. Sci.*, 25(1985)129.]

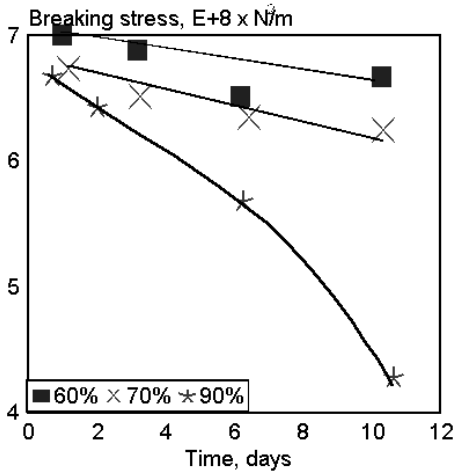


Fig. 11.26. Breaking stress vs. degradation time in air under varying strain/ultimate strain ratio. [Adapted, by permission, from M. Igarashi and K. L. DeVries, *Polymer*, 24(1983)769.]

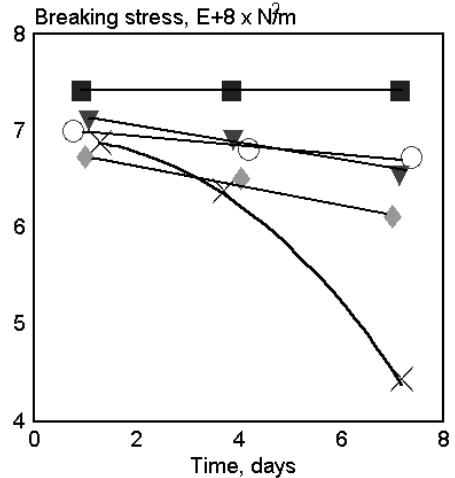


Fig. 11.27. Breaking stress vs. UV degradation time under varying strain/ultimate strain ratio. Strain ratio: ■ 0%, ▼ 60%, ○ 70%, ◆ 80%, × 90%. [Adapted, by permission, from M. Igarashi and K. L. DeVries, *Polymer*, 24(1983)769.]

The carbonyl group formation rate during photodegradation depends on radical formation rate and photooxidation rate. These are also stress related, as Fig 11.24 demonstrates. UV exposure of strained polyethylene samples¹⁶ causes complex oxidative changes (Fig. 11.25).

Three stages can be distinguished:

- slow change - no morphological changes
- fast oxidation - necking which causes drastic morphological changes
- slowdown in oxidation rate - increased crystallinity and fibrillar structure formation.

Stress on a sample during irradiation influences the extent of degradation produced. But the relationship is not simple or linear. Lower stresses, and the strains they produce, are less damaging because they do not induce morphological changes. Higher strains may also cause less change because they induce crystallinity in the material.

Numerous conclusions can be drawn from the data published by Igarashi and DeVries⁹ on polyamides. Samples under load degrade in relation to the load imposed when exposed to air, UV, and exhaust gases (Figs. 11.26-11.28, respectively). Exposure to an exhaust gas is more degrading than the exposure to UV. Loads of up to 70% of the ultimate short-term breaking load did not have a major influence on the degradation rate.

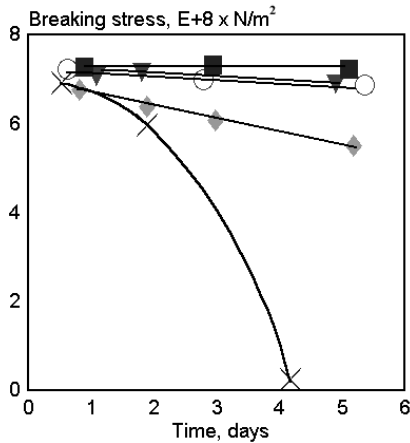


Fig. 11.28. Breaking stress vs. degradation time in exhaust under varying strain/ultimate strain ratio. Strain ratio: ■ 0%, ▼ 60%, ○ 70%, ◆ 80%, × 90%. [Adapted, by permission, from M. Igarashi and K. L. DeVries, *Polymer*, 24(1983)769.]

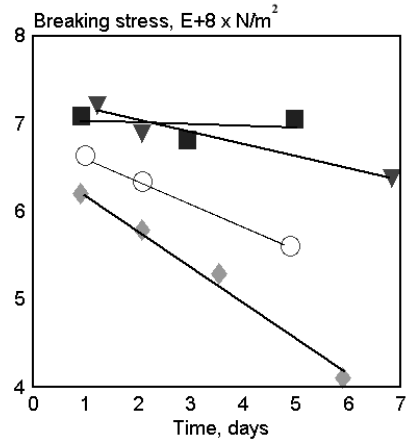


Fig. 11.29. Breaking stress vs. degradation time in ozone under varying strain/ultimate strain ratio. Strain ratio: ■ 60%, ▼ 70%, ○ 80%, ◆ 90% [Adapted, by permission, from M. Igarashi and K. L. DeVries, *Polymer*, 24(1983)769.]

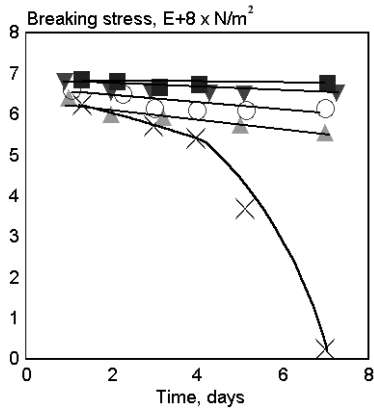


Fig. 11.30. Breaking stress vs. degradation time in SO₂ under varying strain/ultimate strain ratio. Strain ratio: ■ 0%, ▼ 60%, ○ 70%, ▲ 80%, × 90%. [Adapted, by permission, from M. Igarashi and K. L. DeVries, *Polymer*, 24(1983)769.]

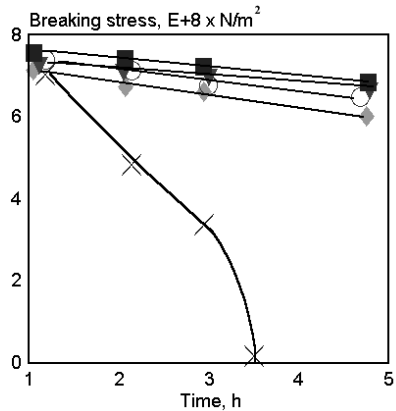


Fig. 11.31. Breaking stress vs. degradation time in NO₂ under varying strain/ultimate strain ratio. Strain ratio: ■ 0%, ▼ 60%, ○ 70%, ▲ 80%, × 90%. [Adapted, by permission, from M. Igarashi and K. L. DeVries, *Polymer*, 24(1983)769.]

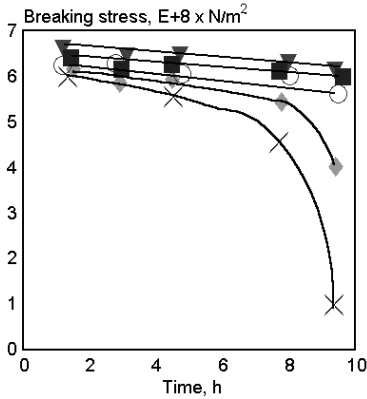


Fig. 11.32. Breaking stress vs. degradation time in NO_x (concentration - 0.86%) under varying strain/ultimate strain ratio. Strain ratio: ■ 0%, ▼ 60%, ○ 70%, ◆ 80%, × 90%. [Adapted, by permission, from M. Igarashi and K. L. DeVries, *Polymer*, 24(1983)769.]

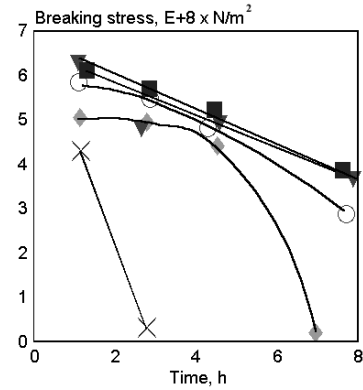


Fig. 11.33. Breaking stress vs. degradation time in NO_x (concentration - 2.58%) under varying strain/ultimate strain ratio. Strain ratio: ■ 0%, ▼ 60%, ○ 70%, ◆ 80%, × 90%. [Adapted, by permission, from M. Igarashi and K. L. DeVries, *Polymer*, 24(1983)769.]

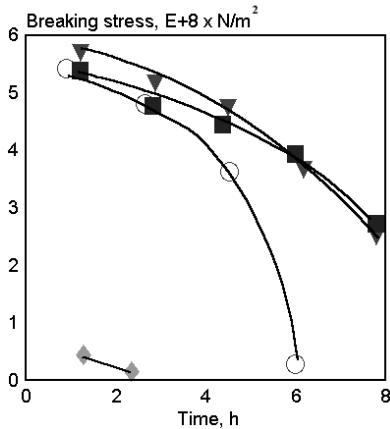


Fig. 11.34. Breaking stress vs. degradation time in NO_x (concentration - 5.16%) under varying strain/ultimate strain ratio. Strain ratio: ■ 0%, ▼ 60%, ○ 70%, ◆ 80%. [Adapted, by permission, from M. Igarashi and K. L. DeVries, *Polymer*, 24(1983)769.]

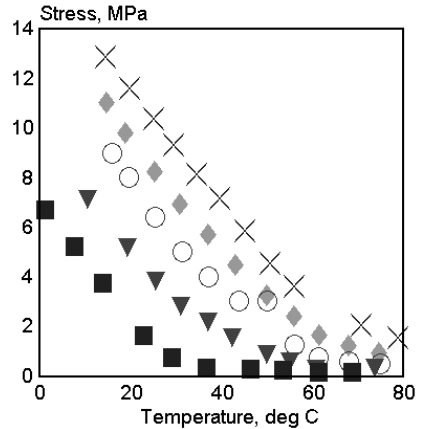


Fig. 11.35. Stress vs. temperature of weathering at 5% relative humidity for various durations of degradation of acrylic/polyurethane coatings. Degradation time (h): ■ 0, ▼ 168, ○ 384, ◆ 672, × 1032. [Adapted, by permission, from D. Y. Perera and M. Oosterbroek, *J. Coat. Technol.*, 66(1994)83.]

Similar changes occurred when samples were exposed to atmospheric pollutants (Figs. 11.29-11.31). The only notable discrepancy was a result of exposing highly loaded samples (at 90% of their ultimate strength), to SO₂ and, more particularly to NO₂, both of which caused drastic increases in the rate of degradation. Figs. 11.32-11.34 show that the concentration of atmospheric pollutants, and perhaps any other reactive chemicals, is an important variable affecting degradation rate.

The NO_x atmosphere was the most degrading. It reduced breaking strength of fibers and decreased the concentration of free radicals (as measured during the final fracture test). Strain, time, temperature, and pollutant concentration influenced the degradative processes and were determining factors in how much damage was done to the fiber.

11.6 OTHER VARIABLES IN PHOTODEGRADATION

Several current papers^{19,32-38} deal with other factors which might affect degradation rate. Most of this work was done to study the effect of humidity or water which is so frequently present in the environments in which degradation occurs. Perera and Oosterbroek¹⁹ studied acrylic/polyurethane coatings exposed to UV under different temperatures and relative humidities. Additionally, they monitored stress in the specimens and the ability of samples to relax this stress. For stress measurement, they used a method based on the assumption that the specimen will deflect in the direction of stress. Measuring this deflection permits an internal stress estimate. These factors encompass all the essential variables of degradation. As shown by Fig. 11.35, stress was measured in samples which were prepared in very low humidity conditions as they were exposed for various lengths of time at different temperatures. Increasing specimen temperature causes a gradual relaxation of stress. At the same time, a longer duration of degradation contributes to an internal stress increase. Increased stress ultimately leads to cracks forming in the coating. Fig. 11.36 shows the effect of weathering time, at constant temperature and variable humidity, on stress formation. Note the direction of stress changes with humidity (stress takes a different direction at low and high humidities). Extreme humidities are detrimental to a coating's performance.

Bauer and Mielewski³³ studied acrylic melamine coatings and some results relative to the effect of humidity are given in Fig. 11.37. Samples were maintained at 25°C but were exposed to both dry conditions (dew point -10°C) and humid conditions (air bubbled through water). The results presented show that hydroperoxide conversion depends on humidity. In wet conditions, more carbonyls are formed and more chain scissions occur, indicating that the durability of the paint and the result of these tests depends on the humidity level.

The effect of wet conditions on the performance of insulated electric cables was also studied.^{32,36} It was discovered that penetration of water into the cable strands reduces cable life by factor of 10. Factors of cable operation, such as electrical stress and fre-

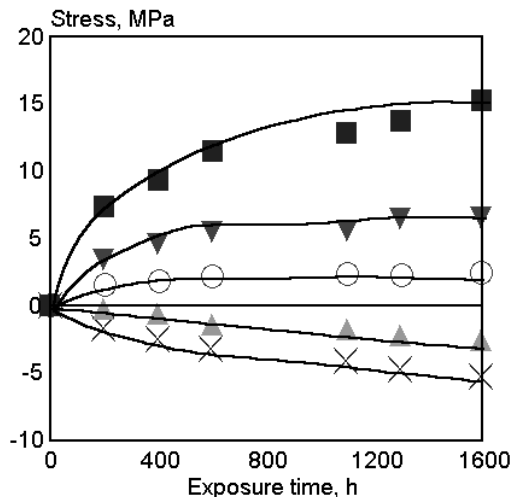


Fig. 11.36. Stress vs. duration of weathering in Weather-O-Meter at 21°C acrylic/polyurethane coatings. Relative humidity (%): ■ 5, ▼ 30, ○ 50, ▲ 75, ×90. [Adapted, by permission, from D. Y. Perera and M. Oosterbroek, *J. Coat. Technol.*, 66(1994)83.]

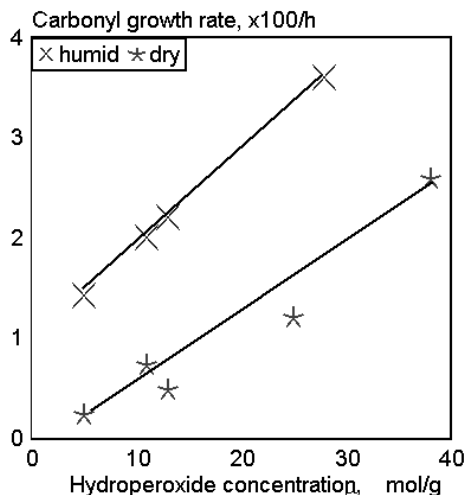


Fig. 11.37. Normalized carbonyl growth rate vs. hydroperoxide concentration for humid and dry exposures of acrylic melamine coating. [Adapted, by permission, from D.R. Bauer and D.F. Mielewski, *Polym. Deg. Stab.*, 40(1993)349.]

quency, are also important. Tests indicated that a higher ion content in water increases the probability of cable breakdown. If some sections of cable are at a high temperature, contact with water is more detrimental because water can more easily penetrate the insulation. When radiation (gamma-neutron), temperature, and humidity,³⁶ are associated with degradation, radiation effect is the most detrimental. Mechanical properties of the insulation are more affected by these factors than is the electrical insulating property.

Plastic films of LDPE and PS, submerged in water, degraded more slowly when exposed to UV than specimens which were not submerged but UV irradiated.³⁴ The difference in behavior is explained by the lower radiation intensity in submerged conditions caused by the water absorbing a substantial amount of energy.

A significant difference was observed in the degradation behavior of polyethylene terephthalate samples which varied in their degree of crystallinity.³⁵ Films of this polymer with high crystallinity were not affected either by temperature or by contact with wet soil during degradation. Under similar conditions, sheets and bottles made from polyethylene terephthalate (low crystallinity) degraded faster when both temperature and humidity were increased. Water diffusion, which is dependent on crystallinity, controls degradation processes involving hydrolysis.

REFERENCES

1. W. P. Yartsev, *Plast. Massy*, 1986,12,16.
2. N. A. Weir, *Dev. Polym. Degrad.*, 7(1987)193.
3. A. A. Popov and G. E. Zaikov, *J. Macromol. Sci.-Rev. Macromol. Chem. Phys.*, C23(1983)1.
4. A. A. Popov and G. E. Zaikov, *J. Macromol. Sci.-Rev. Macromol. Chem. Phys.*, C27(1987-88)343.
5. A. A. Popov and G. E. Zaikov, *J. Macromol. Sci.-Rev. Macromol. Chem. Phys.*, C27(1987-88)379.
6. H. N. Subramanyan and S. V. Subramanyan, *Eur. Polym. J.*, 23(1987)207.
7. J. -L. Philippart and J. -L. Gardette, *Makromol. Chem.*, 187(1986)1639.
8. A. Torikai, A. Takeuchi, and K. Fueki, *Polym. Degrad. Stab.*, 14(1986)367.
9. M. Igarashi and K. L. DeVries, *Polymer*, 24(1983)769.
10. R. Gooden, D. D. Davis, M. Y. Hellman, A. J. Lovinger, and F. H. Winslow, *Macromolecules*, 21(1988)1212.
11. H. Ya. Rappoport and G. E. Zaikov, *Usp. Khim.*, 52(1983)1568.
12. S. W. Addy, D. W. Clegg, A. A. Collyer, G. C. Corfield, and P. Crum, *J. Rheol.*, 31(1987)297.
13. E. Baimuratov, B. N. Narzullaev, I. Ya. Kolontarov, and A. W. Zakchartchuk, *Dokl. Akad. Nauk Tadzh. CCR*, 27(1984)204.
14. C. L. Bauer, R. J. Farris, and M. S. Vratsanos, *Polym. Mat. Eng. Sci.*, 56(1987)560.
15. W. I. Krisyuk, *Dissertation*, 1983.
16. R. S. Porter and A. Casale, *Polym. Eng. Sci.*, 25(1985)129.
17. M. M. Qayyum and J. R. White, *Polym. Deg. Stab.*, 39(1993)199.
18. J. C. M. de Bruijn, *Report K243*, Delft University of Technology, 1991.
19. D. Y. Perera and M. Oosterbroek, *J. Coat. Technol.*, 66(1994)83.
20. K. Tanaka, H. Hashida, T. Kuibira, and M. Koike, *Rep. Res. Lab. Eng. Mater., Tokyo Inst. Technol.*, 15(1990)179.
21. R. M. Fischer, W. P. Murray, and W. D. Ketola, *Prog. Org. Coat.*, 19(1991)151.
22. R. Baumbardt-Neto and M.-A. De Paoli, *Polym. Deg. Stab.*, 40 (1993)53.
23. A. Kim, C. P. Bosnyak, and A. Chudnovsky, *J. Appl. Polym. Sci.*, 51(1994)1841.
24. W. H. Elfring and W. J. Rosano, *Science and Technology of Building Seals, Sealants, Glazing and Waterproofing*, Ed. J. Klosowski, Sec. Vol. ASTM STP 1142.
25. K. J. Miller, J. H. Hellman, and J. A. Moore, *Macromolecules*, 26(1993)4945.
26. G. E. Schoolenberg and H. D. F. Meijer, *Polymer*, 32(1991)438.
27. T. B. Boboev, Kh. Dodomatov, and I. Ya. Kalontarov, *Intern. J. Polym. Mater.*, 19(1993)223.
28. W. K. Busfield and M. J. Monteiro, *Mater. Forum*, 14(1990)218.
29. E. Baimuratov, I. Y. Kalontarov, and D. S. Saidov, *Intern. J. Polym. Mater.*, 19(1993)193.
30. S. Kuroda, I. Mita, K. Obata, and S. Tanaka, *Polym. Deg. Stab.*, 27(1990)257.
31. T. Ichikawa, K. Oyama, T. Kondoh, and H. Yoshida, *J. Polym. Sci., Polym. Chem.*, 32(1994)2487.

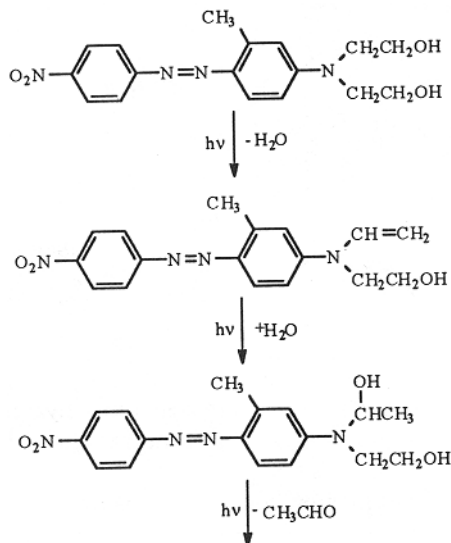
32. R. Bartnikas, R. J. Densley, and R. M. Eichlorn, *IEEE Trans. Power Delivery*, 6(1991)929.
33. D. R. Bauer and D. F. Mielewski, *Polym. Deg. Stab.*, 40(1993)349.
34. K. K. Leonas and R. W. Gorden, *J. Environ. Polym. Deg.*, 1(1993)45.
35. M. Edge, M. Hayes, M. Mohammadian, N. S. Allen, T. S. Jewitt, K. Brems, and K. Jones, *Polym. Deg. Stab.* 32(1991)131.
36. S. P. Cygan and J. R. Laghari, *IEEE Trans. Nucl. Sci.*, 38(1991)906.
37. R. Lehrle, D. Atkinson, S. Cook, P. Gardner, S. Groves, R. Hancox, and G. Lamb, *Polym. Deg. Stab.*, 42(1993)281.
38. R. P. Brown, *Polym. Test.*, 10(1991)3.

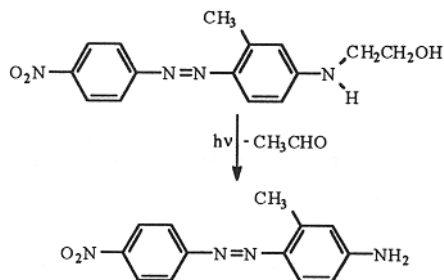
12

COLOR FADING IN TEXTILE MATERIALS

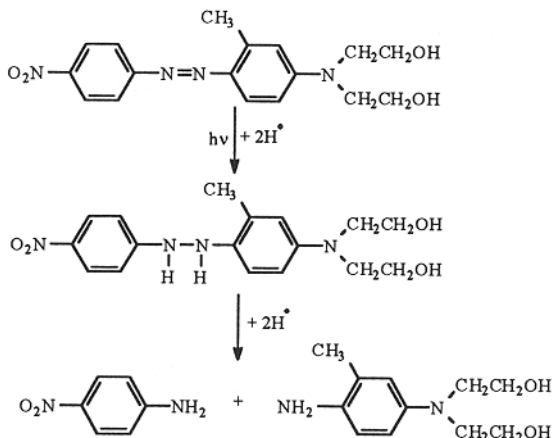
Color fastness depends on dye durability, the substrate properties, dye bonding and distribution in the material, and physical factors such as light intensity, air composition, humidity, and temperature. In relation to these factors a dye may increase the degradation rate of material (phototendering) and may also inhibit photochemical changes in the material. The major findings on these above aspects of color fading are discussed below.¹⁻²⁶

Azo-dyes form a broad group of compounds differing in chemical structure. In spite of differences in chemical structure, some degradation mechanisms are common. Freeman¹⁹ proposes the following mechanism of degradation for red disperse dyes:



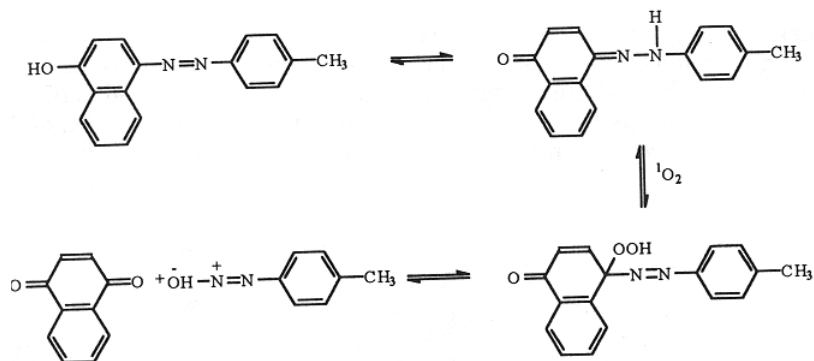


which is complementary to the major photoreductive cleavage of the azo linkage:



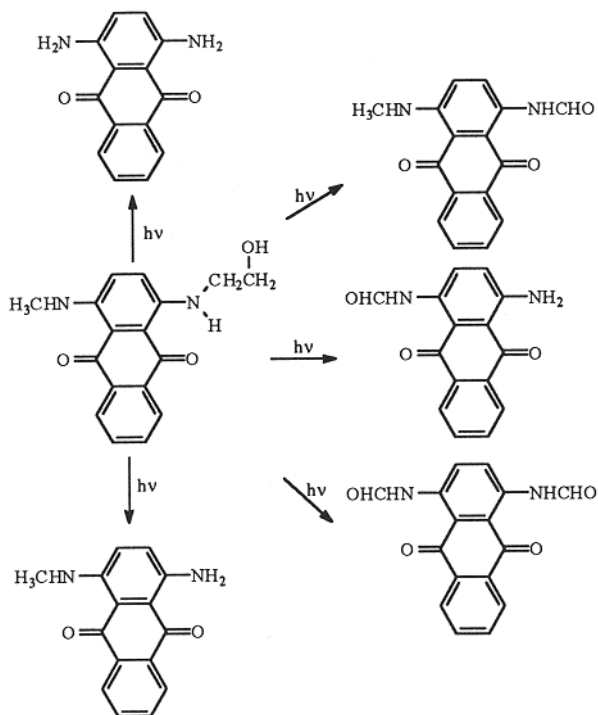
In the first process, the dye loses the pendant hydroxyethyl groups, whereas in the second process the hydrazo-compound is produced and it then cleaves to a substituted aniline.

It is also possible, but not yet proven, that azo-dyes are degraded photooxidatively by singlet oxygen:



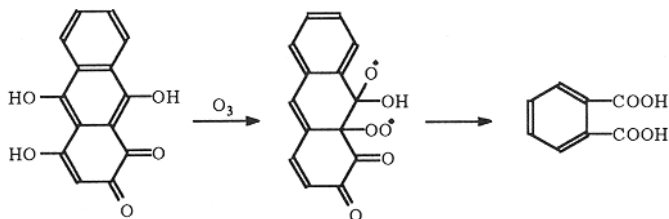
Such a mechanism may affect not only the dye but also the substrate.

Anthraquinone dyes undergo oxidative processes leading to a mixture of degradation products:



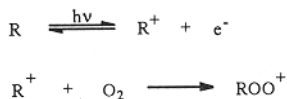
Several reactions occur, including dehydroxyethylation, dealkylation, and oxidation.

Grosjean's⁵ studies on the fading of alizarin pigments showed that ozone is principally responsible for these changes. Alizarin Crimson was studied in this work. It is a calcium-aluminum lake of 1,2-dihydroxy-anthraquinone. The reaction of Alizarin with ozone produces a complex mixture of components suggesting the following mechanism of degradation:

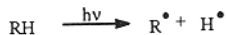


The mechanism shows that ozone may cause a dramatic change in the composition of dyes by reacting with their aromatic components.

Photooxidation of trimethylmethane dyes was also evaluated. This process has several stages which are initiated by electron ejection from a photoexcited dye cation. The radical then reacts with oxygen, forming a hydroperoxide. This reaction is typical of many other dyes and can be written in the following form:



A similar effect is caused by bond scission or hydrogen abstraction:



or



then



An excited dye molecule may participate in an electron transfer to oxygen which generates an anion:



Dyes, like other materials, are mostly affected by radical processes and photooxidative reactions which ultimately lead to the destruction of chromophores. The reactions with substituents also lead to color modification by affecting auxochrome groups.

Dyes which have protective properties usually increase the stability of materials in relation to their concentration. The deeper the shade of the dyed material, the better the protection. Dyes which increase the degradation rate of the matrix usually do so at any concentration.²² Such dyes should not be used in materials that must be light stable. Frequently, TiO₂ is added as a delustrant. Dull fibers contain approximately 2% TiO₂.²² The anatase form of TiO₂ causes degradation but in spite of this, it is frequently added because it is less abrasive to the processing equipment. Morphological studies²² show that the addition of TiO₂ causes the formation of cracks and cavities in materials exposed to UV radiation. Due to these processes, dull and semi-dull fibers are substantially less UV resistant.

The chemical structure of dye cannot alone be responsible for all the color changes observed. Polymer morphology strongly affects azo-dye photofading, as seen from Fig. 12.1 and from the data in Table 12.1. Poly(ethylene terephthalate) films used in the experiment differ in morphology, as explained in Table 12.1.

Table 12.1: Morphology of PET films [Data from P. L. Beltrame, E. Dubini-Paglia, B. Marcandalli, P. Sadocco, and A. Seves, *J. Appl. Polym. Sci.*, 33(1987)2965.]

Sample	Molecular orientation	Trans conformation index	Birefringence
1	0	0.86	0.005
2	4×10^{-1}	2.02	0.140
3	4×10^{-2}	2.88	0.009

Sample 1 was an unoriented film, sample 2 a two-way stretched film, and sample 3 a longitudinally stretched film. Fig. 12.1 shows that the film having the most compact packing or the highest birefringence (sample 2) experienced the lowest dye loss. This demonstrates that light stability is governed primarily by the supermolecular order of the polymer matrix. Several dyes were tested on the same set of substrates and in each case sample 2 had the best dye retention, meaning that the polymer packing was an overriding factor in lightfastness. Two factors are involved: polymer packing and the crystalline structure of the polymer. Better polymer packing slows down the oxygen dif-

fusion rate which, in view of chemical mechanisms discussed above, should decrease the fading rate. The crystalline structure of the polymer affects the aggregation of dyes. Dyes more aggregated in amorphous polymers have higher lightfastness than monodisperse dyes. It is therefore important to consider morphology in a broader context, since all these factors contribute to lightfastness.

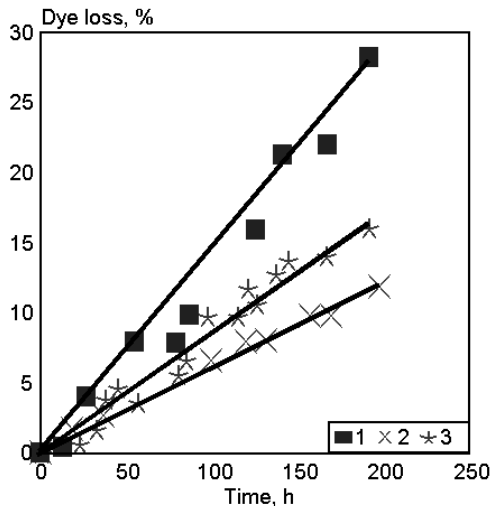


Fig. 12.1. Dye loss vs. exposure time in Xenotest 450 of poly(ethylene terephthalate) films. [Adapted, by permission, from P. L. Beltrame, E. Dubini-Paglia, B. Marcandalli, P. Sadocco, and A. Seves, *J. Appl. Polym. Sci.*, 33(1987)2965.]

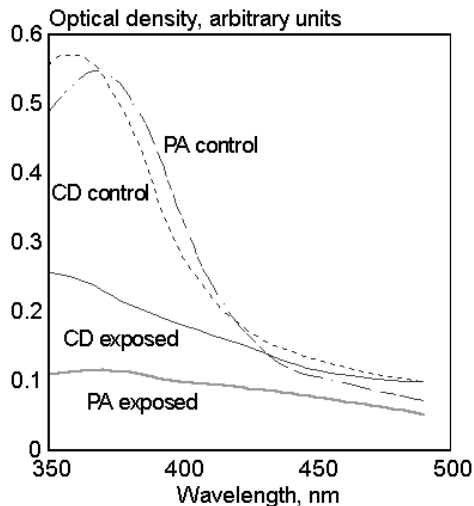


Fig. 12.2. Optical density vs. wavelength for dye on cellulose diacetate (CD) and polyamide (PA) films exposed in lightfastness tester for 140 h. [Adapted, by permission, from F. M. Tera, M. N. Michael, and A. Hebeish, *Polym. Degrad. Stab.*, 16(1986)163.]

No less important than the relationship of the dye distribution to polymer morphology, is the degree of dye bonding with the polymer. Fig. 12.2 shows the dye absorption spectra of an azo-disperse dye in cellulose diacetate and polyamide films.

This comparison shows that the azo-dye fades faster in a polyamide film. The authors of this experiment¹⁷ suggest that the faster fading of the dye in the polyamide film is related to its weaker affinity to the polymer. A similar comparison is made for alizarin dye on cellulose and silica gel substrate (Figs. 12.3 and 12.4). This study⁵ compared the ozone resistance of azo-dyes on two substrates. Alizarin dye on cellulose changed very little, whereas the same dye on silica gel became colorless.

The lightfastness of reactive dyes (Remazol) on cellulose was examined in comparison with their R_f values on thin-layer chromatographic plates. It was established that the lightfastness correlates with the R_f value (Fig. 12.5). The higher the R_f value, the weaker the bonding with the substrate, and consequently the faster the fading. Probably,

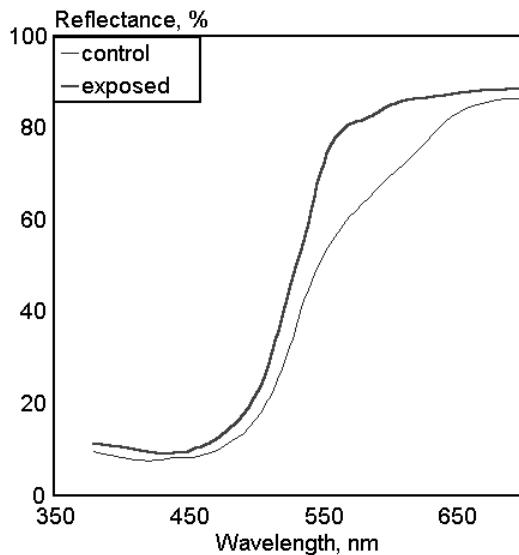


Fig. 12.3. Reflectance spectra of ozone exposed and control samples of Alizarin dye on cellulose. [Adapted, by permission, from D. Grosjean, P. M. Whitmore, C. P. De Moor, G. R. Cass, and J. R. Druzik, *Environ. Sci. Technol.*, 21(1987)635.]

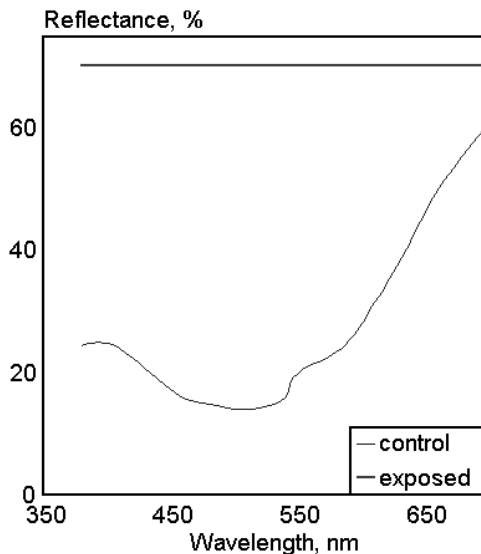


Fig. 12.4. Reflectance spectra of ozone exposed and control samples of Alizarin dye on silica gel. [Adapted, by permission, from D. Grosjean, P. M. Whitmore, C. P. De Moor, G. R. Cass, and J. R. Druzik, *Environ. Sci. Technol.*, 21(1987)635.]

the stronger bond facilitates energy transfer and improves lightfastness. The method, although indirect, offers a means of evaluating bonding strength and can form a base for modelling the lightfastness of various combinations of dyes and substrates. Carpignano¹⁵ proposed that the lightfastness of dyes relative to their chemical structure could be predicted by ¹³C NMR measurement. In this study, the lightfastness of 38 azo dyes correlated with their respective chemical shifts, giving a basis for comparison and prediction. The performance of the dye alone does not warrant that a particular dye is suitable for a specific polymer but rather should be investigated in order to choose the one best suited to a substrate.

Fig. 12.6 explains the effect of dyes on a matrix. The application of disperse dyes to polyesters improves their resistance to phototendering. Polyamide, even when dyed with a photoprotective premetallized dye, is less resistant to weathering than an undyed specimen. The type of dye obviously plays an important role in protecting the matrix (Fig. 12.7). The concentration of dye is also very important (Fig. 12.8). The concentration effect depends on the combination dye-substrate (Fig. 12.9).

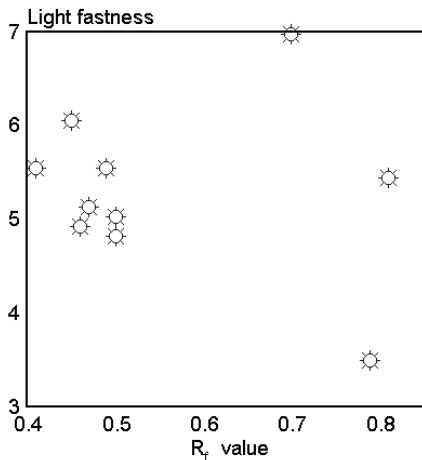


Fig. 12.5. Lightfastness of reactive dyes vs. R_f values. [Adapted, by permission, from W. S. Ha and C. J. Lee, *Melliand Textilber.*, 67(1986)724.]

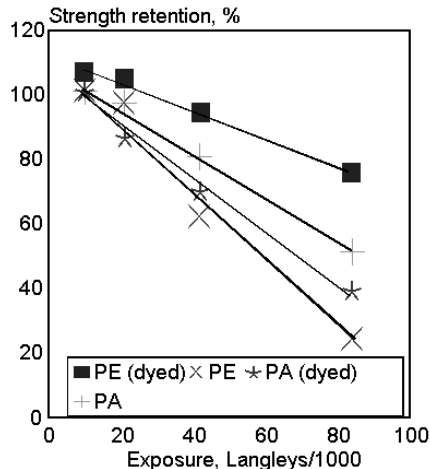


Fig. 12.6. Strength retention of dyed and undyed polyamide-66 and polyester fabrics vs. Florida exposure time. [Data from B. Milligan, *Rev. Prog. Color Relat. Top.*, 16(1986)1.]

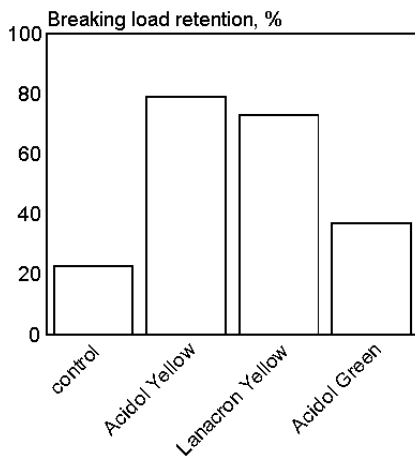


Fig. 12.7. Photoprotective effect on wool fabric of selected premetalized dyes after exposure to 50,000 Langley units. [Data from L. Benisek, C. K. Edmondson, and J. W. A. Mathews, *Text. Res. J.*, 55(1985)256.]

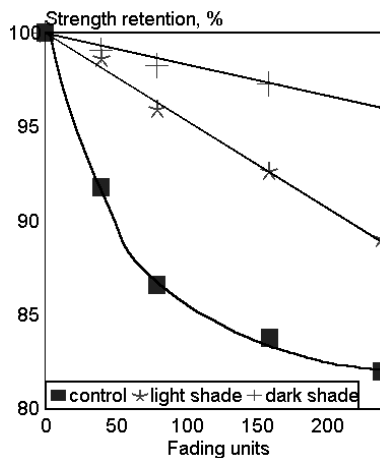


Fig. 12.8. Strength retention vs. exposure time of Reactive Orange II dyed cotton fabric. [Adapted, by permission, from C. M. Ladisch, R. R. Brown, and K. B. Showell, *Text. Chem. Color.*, 15(1983)209.]

The orange dye used in this study offers photoprotection and an increase in its concentration increases the retention of tensile strength in cotton. In contrast, blue dye in-

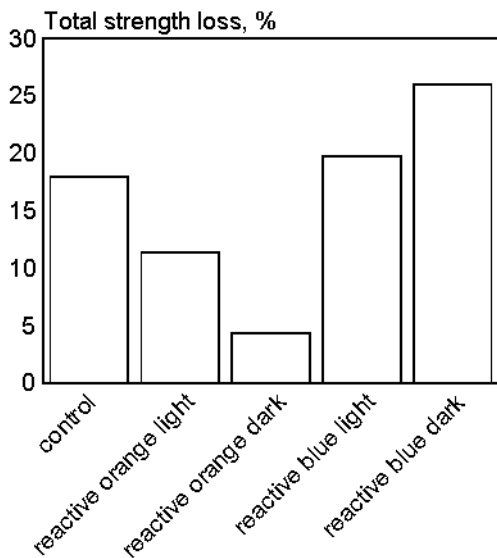


Fig. 12.9. Total strength loss of cotton relative to reactive dye type and its concentration. [Data from C. M. Ladisch, R. R. Brown, and K. B. Showell, *Text. Chem. Color.*, 15(1983)209.]

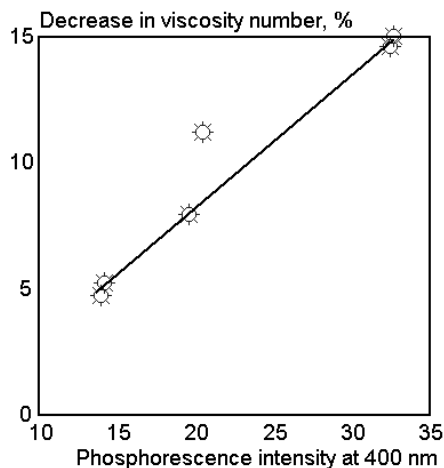


Fig. 12.10. Viscosity number of solution of polyamide-66 film containing variable amount of quenching dye (Acid Yellow 135) after 200 h irradiation vs. phosphorescence intensity at 400 nm. [Adapted, by permission, from N. S. Allen, M. Leward, and G. W. Follows, *Eur. Polym. J.*, 28(1992)23.]

creases the degradation rate when its concentration increases. The performance of a dye depends on its type and color. It has long been accepted that colors such as orange, yellow, and red are the least stable and also most degrading to the matrix material. Although, Fig. 12.9 shows that dye's color is not the only prerequisite for its stability since a blue color should be generally more stable than an orange. Several reasons are quoted in the literature to explain this behavior, such as the participation of the dye in photoreduction of the substrate during the dark cycle (some data puts this reasoning in question), hydrogen abstraction due to $n \rightarrow \pi^*$ transition followed by intersystem crossing and triplet formation, and, most frequently, participation in singlet oxygen generation. Dye types may be classified according to their performance but, when classified by dye process or general dye structure, the guidelines should be used cautiously since some chemical structure differences may influence performance in a way different from other dyes in the group. Generally, dyes which have a strong affinity (chemical, physical) to the material are likely to increase durability.

Fig. 12.10 illustrates one of the possible factors through which a dye enhances system stability. The ability of a dye to quench luminescent impurities correlates with the retention of polyamide-66 properties. The phosphorescence intensity of material increases as polymer molecular weight and thus polymer viscosity increase.

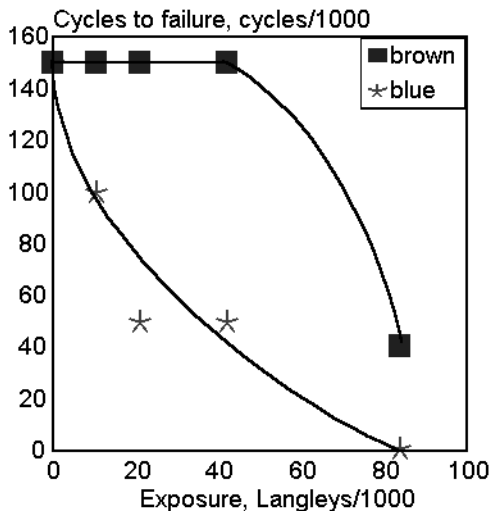


Fig. 12.11. Abrasion resistance of polyamide-66 fabrics relative to the length of exposure and dye color. [Data from G. A. Horsfall, *Text. Res. J.*, 52(1982)197.]

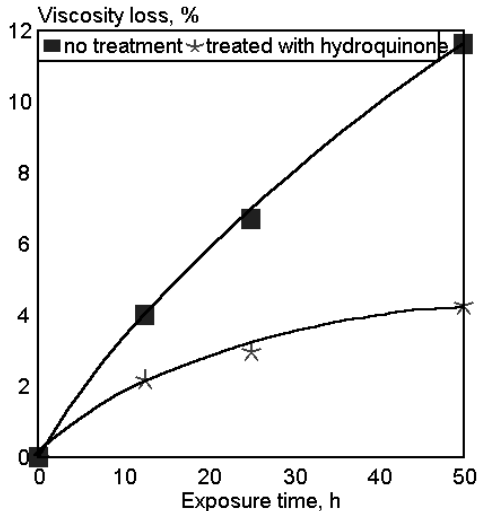


Fig. 12.12. Relative viscosity of polyamide-6 dyed with vat dyes. [Data from C. D. Shah and D. K. Jain, *Text. Res. J.*, 54(1984)844.]

Dyes not only screen the polymer from radiation but also improve abrasion resistance of polyamide-66 fabric (Fig. 12.11). Note also that the type of dye influences the effect in a crucial way. The protective effect of dyeing and aftertreatment can be shown by studying polymer relative viscosity (Fig. 12.12).¹⁰ A reduction in relative viscosity indicates a decrease in molecular weight caused by polymer degradation from bond scission. Hydroquinone reacts with oxygen, forming quinone, which prevents oxidation of polymer, as seen from Fig. 12.12.

Finally, it was demonstrated in several studies that there is a relationship between dyefastness and the protection given to the substrate by the dye. Dyes having high fastness offer better protection to the substrate. The protective effect is increased by the addition of UV absorbers and stabilizers which work well in conjunction with dyes. A typical combination uses a benzophenone type of UV absorber with a copper complex as a stabilizer. Organic copper complexes used in small amounts (less than 50 ppm) decompose peroxides. Since long protection is provided, the mechanism is probably self-regenerating.²²

This proves, once more, that lightfastness of the dye is achieved not only through its composition but also because of the matrix in which dye was incorporated. Interaction produces the final effect. This point is illustrated by a study of metal containing polydyes.² Dyes, which were a part of the backbone of the polymer, have shown to have a

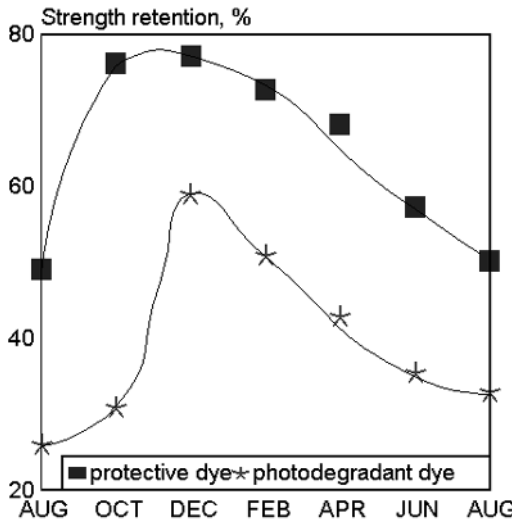


Fig. 12.13. Strength retention vs. month in which exposure of full dull polyamide-6 to 21,000 Langley begins. [Data from G. A. Horsfall, *Text. Res. J.*, 52(1982)197.]

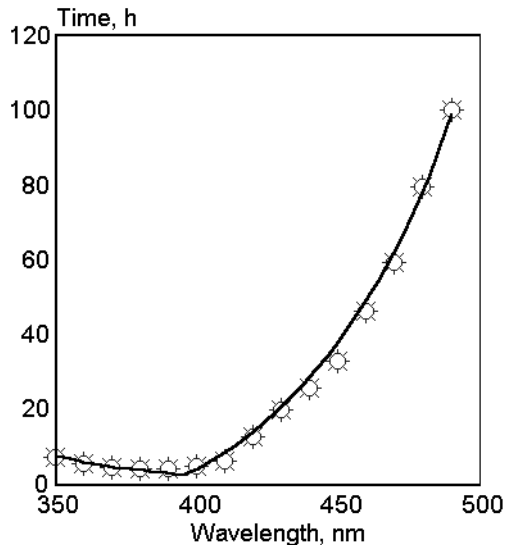


Fig. 12.14. Fading time to 10% fade vs. light wavelength for dye on polyamide film. [Adapted, by permission, from F. M. Tera, M. N. Michael, and A. Hebeish, *Polym. Degrad. Stab.*, 16(1986)163.]

permanent, non-leaching nature. Solutions containing monomeric dyes had a relatively short life.

In addition to the effect that the chemical composition of dye and polymer, dye distribution, and morphology of the polymer has on weathering, external sources, such as irradiation wavelength and intensity, temperature, and humidity also play role. The most important factor in natural weathering is the length of exposure. Fig. 12.13 shows the effect of seasonal variations in the daylight duration on the strength retention by polyamide dyed with photodegradant dye (Nylomine Blue C-G) and protective dye (Acid Brown GL-W). Samples in Florida were exposed to the same amount of radiation energy (21,000 Langley). Summer exposure was twice as damaging as the same amount of energy in winter exposure. All samples behaved in a similar manner. The difference in seasons should account for the differences in temperature and humidity, as well as for differences intensity of radiation. Energy flow rate influences photochemical changes. Energy, depending on the intensity, may be dissipated or utilized for photochemical conversion.

Fig. 12.14 displays the results of weathering studies done with artificial light. This shows the predominant role played by radiation wavelength in the processes which cause dye fading.

The temperature at which degradation occurs has predictable effect on degradation rate. Although the authors of the relevant papers did not control all essential variables of the degradation process, it is obvious that, as in any other chemical reaction, temperature increase also increases the rate of photochemical processes. This concerns both reactions related to chromophore degradation and the degradation rate of the matrix in which the dye is tested. From the studies of polyamide fibers,²² it was found that a temperature increase (during processing and exposure) above 60°C causes formation of degradation products which increases absorption in the UV range. These products cause yellowing but also act as photosensitizers. If the same material is exposed to heat in the absence of oxygen no acceleration of degradation occurs. These observations led researchers to increase the temperature in testing of lightfastness of automotive fabrics. The humidity effect is complex. Water may participate in photochemical reactions, generating very reactive and mobile radicals. The presence of water accelerates hydroperoxide formation and causes hydrolytic processes. Additionally, water swells the polymer matrix and acts as a plasticizer, which increases the mobility of macromolecules and small molecules, thus increasing the probability of effective encounters between excited molecules and other neighboring molecules. Also, the transport of energy and radicals is improved. The swollen structure of the material enhances diffusion and stimulates oxidative processes. These factors work in combination, which complicates the investigation.

REFERENCES

1. P. L. Beltrame, E. Dubini-Paglia, B. Marcandalli, P. Sadocco, and A. Seves, *J. Appl. Polym. Sci.*, 33(1987)2965.
2. C. E. Carraher, V. R. Foster, Q. J. Linville, and D. F. Stevison, *Polym. Mater. Sci. Eng.*, 56(1987)401.
3. G. M'Bon, C. Roucoux, A. Lablache-Combiere, and C. Loucheux, *J. Appl. Polym. Sci.*, 29(1984)651.
4. R. L. Feller, R. M. Johnston-Feller, and C. Bailie, *J. Coat. Technol.*, 59(1987)93.
5. D. Grosjean, P. M. Whitmore, C. P. De Moor, G. R. Cass, and J. R. Druzik, *Environ. Sci. Technol.*, 21(1987)635.
6. P. C. Crews, *Text. Chem. Color*, 19(1987)21.
7. G. A. Horsfall, *Text. Res. J.*, 52(1982)197.
8. B. Milligan, *Rev. Prog. Color Relat. Top.*, 16(1986)1.
9. W. S. Ha and C. J. Lee, *Melliand Textilber.*, 67(1986)724.
10. C. D. Shah and D. K. Jain, *Text. Res. J.*, 54(1984)844.
11. M. A. Herlant, *Am. Dyest Rep.*, 75(1986)38.
12. S. P. Watts and A. Sundaram, *Text. Dyer Printer*, 20(1987)13.
13. A. Wehlow, *Text. Prax. Int.*, 43(1988)277.
14. C. M. Ladisch, R. R. Brown, and K. B. Showell, *Text. Chem. Color*, 15(1983)209.

15. R. Carpignano, P. Savarino, E. Barni, G. Viscardi, S. Clementi, and G. Giulietti, *Anal. Chim. Acta*, 191(1986)445.
16. K. Ogino, H. Uchiyama, and M. Abe, *Colloid Polym. Sci.*, 265(1987)52.
17. F. M. Tera, M. N. Michael, and A. Hebeish, *Polym. Degrad. Stab.*, 16(1986)163.
18. F. M. Tera, M. N. Michael, and A. Hebeish, *Polym. Degrad. Stab.*, 17(1987)13.
19. H. S. Freeman and W.N. Hsu, *Text. Res. J.*, 57(1987)223.
20. N. S. Allen, *Rev. Prog. Color Relat. Top.*, 17(1987)61.
21. P. M. Latzke, *Melliand Textilberichte*, 7(1990)502.
22. G. Reinert, F. Thommen, and J. Isharani, *Text. Chem. Color*, 230(1991)31.
23. G. E. Krichevsky, G. T. Khachaturova, and O. M. Anissimova, *Int. J. Polym. Mater.*, 13(1990)63.
24. N. S. Allen, M. Ledward, and G. W. Follows, *Eur. Polym. J.*, 28(1992)23.
25. W. B. Achwal, *Colourage*, 1(1991)29.
26. P. P. Klemchuk, *Polym. Photochem.*, 3(1983)1.

13

METHODS OF WEATHERED SPECIMEN EVALUATION

The discussion in several preceding chapters focused on the various aspects of weathered material preparation and exposure conditions. This has set up the conditions under which material durability can be repeatably predicted. The choice of the sample testing method is equally important. Sample preparation, weathering method and conditions, and the method of testing have to be well-tuned to obtain reliable data in the shortest possible time. More than fifty techniques are employed to analyze weathered specimens. Since the first edition of this book, the emphasis of weathering studies has clearly shifted to instrumental methods. Infrared spectrophotometry, IR, is a dominating method of sample testing during exposure but other methods including UV spectrophotometry, electron spin resonance, ESR, nuclear magnetic resonance, NMR, and gel permeation chromatography, GPC, are much more frequently used now than before. There are probably several reasons for an increased interest in application of analytical techniques to weathering studies. Here are three:

- analytical equipment has become more commonly accessible
- results can be interpreted by various computerized methods with very little effort
- analytical methods detect degradation in its early stage.

Of these, the last is the most valid. In earlier studies, experiments were conducted to increase the rate of acceleration by changing the parameters of degradation. These experiments did not yield sufficient information about the degradation process because the results only correlated material performance to natural conditions. Now the focus has shifted to a search for a magnifying glass which allows one to see what is hidden to unaided eye. The most relevant findings of this continuing search are reported below.

13.1 VISUAL EVALUATION¹⁻¹⁶

Visual evaluation, usually aided by a standard method such as photographic standards, is still in use in paints, wood finishes, and sealant evaluation. Heading 13.4 reports on methods of color change evaluation in the textile industry which are usually based on visual comparison of a specimen with a standard. Paints are traditionally tested for chalking, adhesion, pitting, white rusting, and flaking. All these assessments are made by subjective methods and the results are usually expressed in a scale from 10 (excellent) to 1 (most severe). Sample evaluation can be performed according to different methods, as exemplified by measurement of chalking. In one method, white cotton is drawn along the panel with constant pressure applied with a finger-tip, then the degree of chalking is rated by comparison with the published photographic standard.¹⁰ A more elaborated technique is reported by Camina,³ who used the DIN 53-159 test method. Exposed and

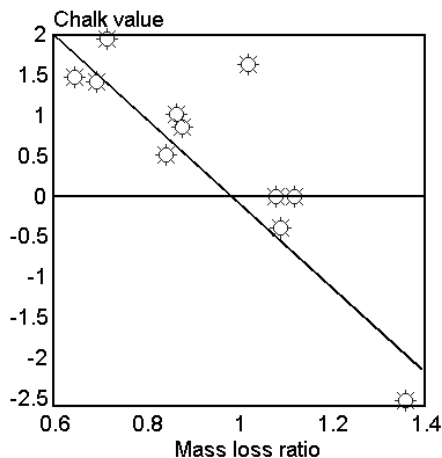


Fig. 13.1. Chalk value vs. mass loss ratio. [Adapted, by permission, from L. A. Simpson, *Austr. OCCA Proc. News*, 20,5(1983)6.]

developed photographic papers are soaked to swell the gelatine, then applied with the use of a rubber stamp (constant force) to the surface of chalking paint which adheres to paper surface. The change in color of the paper is then evaluated against standards. Depending on the experience of the individual involved in testing, such methods might be quite exact, as seen from comparison with the results of mass loss (Fig. 13.1). Still, there is a lot of subjectivity in judgement and sample preparation (e.g., constant pressure of finger-tip). Results of a visual inspection of paint specimens exposed to acid rain were compared with the results of electrical properties measurement¹⁵ and electron spin resonance, ESR, to monitor surface corrosion.¹⁶

In wood studies, visual comparison was used to determine fiber chalking. It has been used to compare transparent finishes and paints for erosion, flaking, and cracking; to evaluate the depth of sample erosion. In the most recent studies,¹¹ the results of morphological studies have been compared with the results of mechanical testing of bond strength in shear and tensile. In sealants, the researcher was looking at the adhesive or cohesive failure of sealant versus weathering time or evaluating the damage to the sealant bead caused by stress applied during various weathering exposure times.

A visual evaluation provides only superficial information. Although, it answers the aesthetic questions which play an essential role in product design, it does not tell what caused the damage. This is what weathering studies must do, hence, we must turn to other methods.

13.2 GLOSS RETENTION AND SURFACE ROUGHNESS^{1,2,17-24}

The weathering mostly affects the material surface, which causes a loss of initial gloss. Therefore, it makes good sense to analyze surface changes, especially since the measurement is simple, and the equipment cheap, relatively accurate, and available. Several standard techniques exist (BS 3900: Part D5; ASTM D523; ISO 2813). The angle of illumination is generally one of three angles: 20, 60, or 85°/the choice depends on the gloss value. Gloss measurement was successfully used in paints to determine: binder durability;

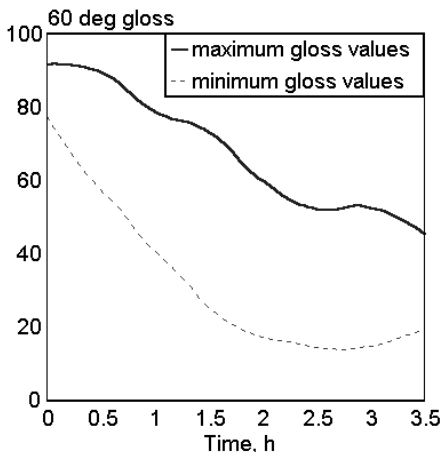


Fig. 13.2. Variation in gloss retention of standard paint exposed in a number of twin carbon arc weathering machines. [Adapted, by permission, from R. R. Blakey, *Prog. Org. Coat.*, 13(1985)279.]

effect of pigment concentration; effect of proportion between the pigment and the extender; effect of pigment type and grade; on the stability of weathered coatings. Braun¹⁸ reports the data from the studies of 150 repeats which illustrate the fact that a discrepancy of 50% has to be accepted. Initial measurements during the first 200 h of exposure were fairly accurate. Bigger discrepancies were observed when specimens were exposed for 300 h and more/the same formulation had 60° gloss readings between 30-80 units. Blakey²⁰ gives graphical illustration of such discrepancies for specimens exposed to natural conditions (Fig. 13.2). This true tendency can only be observed if a substantially large number of specimens is evaluated. Rehfeldt²² proposes Box-Jenkins time series analysis for the evaluation of gloss retention data obtained from weathering studies. Such analysis gives a substantial enhancement to the gloss retention method, providing that the data for sufficient number of repeats, are available.

Ito¹⁷ measured profiles of specimen surface at a depth of 0.1-0.5 mm for initial and naturally weathered specimens of six polymers (Fig. 13.3). The data from surface roughness measurement generally agree with the results of other studies. The degradation depth distribution is very scattered. For example, most of the surface of a weathered

effect of proportion between the pigment and the extender; effect of pigment type and grade; on the stability of weathered coatings. Braun¹⁸ reports the data from the studies of 150 repeats which illustrate the fact that a discrepancy of 50% has to be accepted. Initial measurements during the first 200 h of exposure were fairly accurate. Bigger discrepancies were observed when specimens were exposed for 300 h and more/the same formulation had 60° gloss readings between 30-80 units. Blakey²⁰ gives graphical illustration of such discrepancies for specimens exposed to natural conditions (Fig. 13.2). This true tendency can only be observed if a substantially large number of specimens is evaluated. Rehfeldt²² proposes Box-Jenkins time series analysis for the evaluation of gloss retention data obtained from weathering studies. Such analysis gives a substantial enhancement to the gloss retention method, providing that the data for sufficient number of repeats, are available.

ABS had a roughness in the range of $0.2\ \mu\text{m}$, with some areas more affected (roughness - $8\text{-}10\ \mu\text{m}$). In the more affected areas there are also points of the surface which are elevated above the usual level, suggesting the possibility of chain diffusion, relocation, and reattachment.

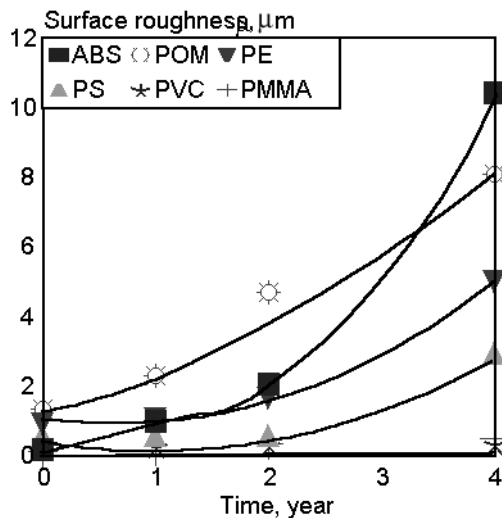


Fig. 13.3. Change of surface roughness during outdoor exposure. [Adapted, by permission, from T. Ito, H. Imai, S. Nagai, and K. Iizuka, *Kenkyu Hokoku-Kogyo Gijutsuin*, 2(1981)159.]

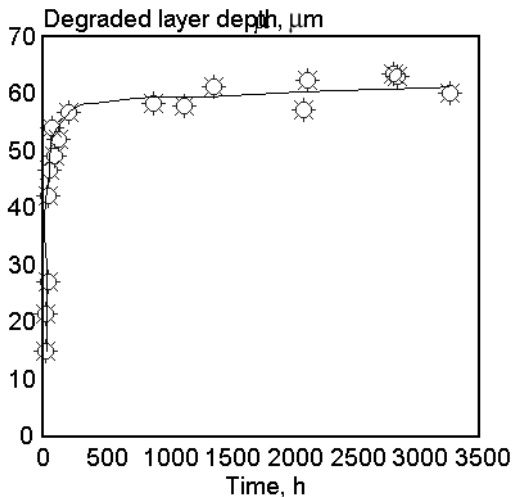


Fig. 13.4. The degraded layer thickness of PP containing 30% talc and 0.2% carbon black vs. degradation time during its exposure to mercury lamp. [Adapted, by permission, from D. Rysavy and H. Tkadleckova, *Polym. Deg. Stab.*, 37(1992)19.]

Thickness measurement of a degraded layer has been used as a sample evaluation method.²³ A weathered specimen of PP was bend through 180° . The depth of the groove formed by material removal was measured (Fig. 13.4). The depth of the eroded groove in PP increases rapidly at the beginning of degradation followed by a plateau, which indicates that the degraded layer protects adjacent layers of material below.

Growing interest in surface etching by laser ablation contributes to knowledge in this area. Fig. 13.5 shows the effect of energy supply on etch rate of polymethylmethacrylate, PMMA.²⁴ Laser ablation is used in practice to selectively remove excess material to obtain a designated shape. The profile and thickness of the polymer layer were measured using a Taylor-Hobson profilometer.

13.3 SURFACE MORPHOLOGY AND IMAGING TECHNIQUES^{7,25-48}

There have been numerous studies of surface morphology. Scanning electron microscopy, SEM, is the major technique used. Morphological studies concentrate either on the

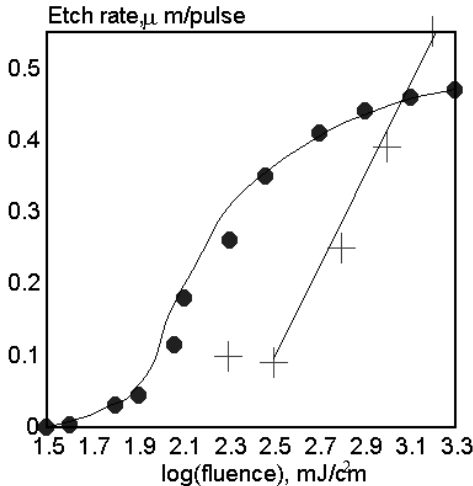


Fig. 13.5. Etch rate of PMMA as a function of log flouence and wavelength radiation. ● 193 nm, + 248 nm. [Adapted, by permission, from M. S. Kitai, V. L. Popkov, and V. A. Semchishen, *Makromol. Chem., Macromol. Symp.*, 37(1990)257.]

exposed surface or on the interface between the coating and substrate or between the fiber and the binder. The SEM study of the interface between aluminum and silicone sealant reveals the growth of aluminum oxide/hydroxide crystals.²⁵ This type of surface modification leads to a weakening of interfacial bonding. SEM micrographs also show formation of large pores in the sealant, suggesting that an increasing porosity in the silicone sealant fails to provide protection to the aluminum surface, which corrodes and thus is unable to continue to maintain a strong bond with silicone sealant.

SEM micrographs of wood show that most exposed transverse surfaces are separated at the middle lamella due to the lignin degradation.²⁶ Also, pits at the radial surface are severely damaged by

light. The same study shows that chromic acid and ferric chloride are capable of protecting wood surfaces against UV radiation.

Acrylic-based plastics are used by the building industry for skylights, domes, glazing, and other light-transmitting applications which require long-term durability.²⁷ SEM photographs show that polymethylmethacrylate, PMMA, experienced very little change during 10 years of exposure, unlike acrylonitrile-butadiene-styrene copolymer, ABS, samples. The same observation was made by Nishimura,³⁴ who studied six polymers including PMMA, ABS, polyoxymethylene, POM, polyethylene, PE, polyvinylchloride, PVC, polystyrene, PS. Surface morphology studies of PMMA and PVC show no change during 5 years of exposure. Surface roughness studies give similar results.¹⁷ PS and ABS are the most affected, showing severe surface cracking.

Bolle and Lazare²⁵ give an excellent example of the application of electron microscopy employed not only as a qualitative technique but to observe submicron periodic structures produced on a polymer surfaces by UV laser. Sample rotational ellipsometry was used to determine ripple spacing smaller than 200 nm which depends on polymer type, wavelength of radiation, and flouence.

A few publications^{28,31,32} show data which relate SEM observations to the mechanical properties and crystalline structure of materials. These data should be treated with caution when SEM observations are interpreted. Materials which exhibit surface cracking are assumed to be non-durable, which is not correct in many cases. It has been con-

firmed conclusively that polyamide, PA, polyurethanes, PU, and LDPE retain better mechanical properties in specimens which surface-crack than in the case of specimens which retain an unaffected surface. All these polymers are semicrystalline materials and cracking is due to internal stress distribution in crystalline and amorphous areas. Since degradation occurs in the amorphous region, the neighboring crystalline areas contribute to stress development around the crack tip, causing orientation. This orientation results in the reinforcement of material below the crack tip, which limits further crack propagation. In completely amorphous specimens such a mechanism of orientation does not exist; therefore, samples degrade uniformly, and although they look all right under the microscope, they do not retain their initial mechanical properties.

Crack formation and its implication on durability of motorcycle helmets were analyzed based on SEM data.⁴¹ In most cases, cracks were initially formed in the areas of internal stress. They run parallel to the flow direction of the injection molding process. Similar behavior was also observed in other materials. Primary cracks formed from stress distribution become wider during the course of degradation. Each pre-existing crack competes for the stored elastic energy received from impact, consequently, each crack receives less energy and does not propagate fast and far.

La Mantia and Curto⁴⁰ used SEM to study the effect of photooxidation on PE. Photooxidation formed graft copolymers which acted as compatibilizers of blend causing consequent improvement in mechanical properties. Polymer composites exposed in space environments⁴⁴ showed severe surface erosion and fully exposed reinforcing fibers. These necked fibers formed preferential sites of crack initiation. SEM and transmission electron microscopy, TEM, are excellent methods for observing defects forming which cause degradation of fibers.⁴⁵ Depending on fiber dimension, cracks can cause extensive damage to mechanical properties.

SEM helped us to recognize the effect of acid rain on polyamide, which was mostly affected by heat and humidity, rather than the acid presence. In the presence of light, acid accelerated degradative changes. The effect of water in Kevlar-epoxy composite weathering was understood because of SEM observations. SEM also helped to explain the mechanisms of plastic pipe or cable weathering. All these examples show that, although SEM alone cannot detect chemical changes, it allows one to consider the chemical mechanisms as well because it gives such a precise picture of damage that many conclusions can be intuitively reached. Further enhancement for this technique comes with the possibility of X-ray emission measurement which allows analysis of the distribution of some elements on observed surfaces. This is discussed below.

Relatively recent developments in image capture and analysis technology allow for further enhancement of surface monitoring.⁴⁶⁻⁴⁸ Although these methods have long been known, an adequate combination of hardware and software either did not exist or was too expensive for the technique to become widely used. Images can be captured and converted to a computer file by various means: scanner; camera; microscope; etc. The re-

sultant image can then be digitized and stored in any format that can be used by the computer program. Having a picture in the computer allows for unlimited manipulations of this image including quantitative analysis which is impossible with conventional microscopy. This method eliminates the main disadvantage of microscopy / its subjectivity when comparing various images. The method addresses the biggest weakness of scientific interpretation / its difficulty in dealing with complex patterns. In the next few years, this method will become the missing link between precise analytical interpretation of changes and what is frequently called "observation from the field". By combining numerical data from sample analysis, using the methods described in this chapter with the real result of degradation, researchers will be able to define reasons for degradation and find remedies.

13.4 COLOR CHANGES^{3,49-62}

The change of material color relates to changes in the chemical composition of the material and in many cases it decreases the material value. Materials are frequently compounded from a mixture of various products. Textiles are dyed with more than one dye. Therefore, the color change, although caused by changes in the dyes and the material blends does not tell what these changes may be. Weathering progress is indicated by color changes in colored products such as artists' pigments, museum textiles, dyed and undyed fabrics, paints and coatings, polymeric materials, building materials, etc. Results from studies of color measurement are typically interpreted in three ways: fading units, color change, and yellowness index. One method commonly used in the textile industry involves comparison of color changes when specimens are exposed to irradiations equivalent to 20, 40, 60, 80 fading units of the reference fabric. A sample might then be evaluated for color change or used for other testing, frequently tensile testing, to estimate the extent of degradation. Results given in the form of color difference, ΔE , are the most common. The color difference, ΔE , is explained by the following equations:

$$\Delta E = [(\Delta L)^2 + (\Delta a)^2 + (\Delta b)^2]^{0.5}$$

$$\Delta L = L - L_s; \quad \Delta a = a - a_s; \quad \Delta b = b - b_s$$

$$L = 16(Y/Y_0)^{1/3} - 16$$

$$a = 500[(X/X_0)^{1/3} - (Y/Y_0)^{1/3}]$$

$$b = 200[(Y/Y_0)^{1/3} - (Z/Z_0)^{1/3}]$$

where X, Y, Z tristimulus values in CIE scale of the sample
 X_0, Y_0, Z_0 tristimulus values for D65 10° observer
 L, a, b values for exposed sample
 L_s, a_s, b_s values for unexposed sample.

Figs. 13.6 and 13.7 show the change of color difference for six polymers.

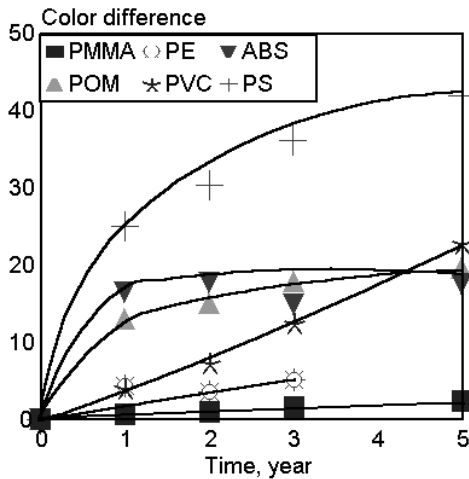


Fig. 13.6. Color difference vs. exposure period in Choshi. [Adapted, by permission, from H. Kubota, S. Suzuki, O. Nishimura, I. Tamura, K. Yoshikawa, and T. Shiota, *Hokkaido Kogyo Kaihatsu Shikensho Hokoku*, 24(1981)96.]

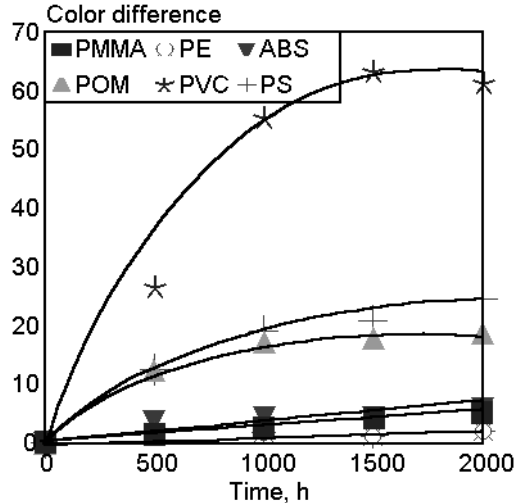


Fig. 13.7. Color difference vs. exposure period in Sunshine Weatherometer. [Adapted, by permission, from H. Kubota, S. Suzuki, O. Nishimura, I. Tamura, K. Yoshikawa, and T. Shiota, *Hokkaido Kogyo Kaihatsu Shikensho Hokoku*, 24(1981)96.]

When one compares ranking of polymers based on Figs. 13.3 and 13.6, it is evident that there is no correlation between surface roughness and color change in these materials. There is also no correlation between natural and artificial weathering (Figs. 13.6 and 13.7).

Yellowness index, ΔYI , is the other method of data presentation. Yellowness index is given by the equation:

$$\Delta YI = 100(1.28\Delta X - 1.06\Delta Z)/\Delta Y$$

where ΔX , ΔY , and ΔZ changes in tristimulus values.

Monitoring of color changes during specimen weathering was used in the following studies:

- evaluation of UV absorbers for museum textiles and wool substrates
- effect of dyes on cotton fabric strength retention
- action of singlet oxygen quenchers in jute fabrics
- effect of antioxidants on dyed polyamides
- effect of the dye carrier on fading of polyamide and polyester substrates
- photodegradation monitoring of PU-acrylic coatings
- color change of various plastics exposed to natural weathering.

From the above list, one can see that this method is mostly used for qualitative purposes. Color measurement can be applied successfully to monitor the effect of various ingredients in the composition but is not useful when comparing different materials (e.g., different polymers).

13.5 SPECTROSCOPIC METHODS

The methods discussed above help to define what changes occur but they don't offer an explanation for the chemical mechanism of these changes. Spectroscopic methods can provide this information.

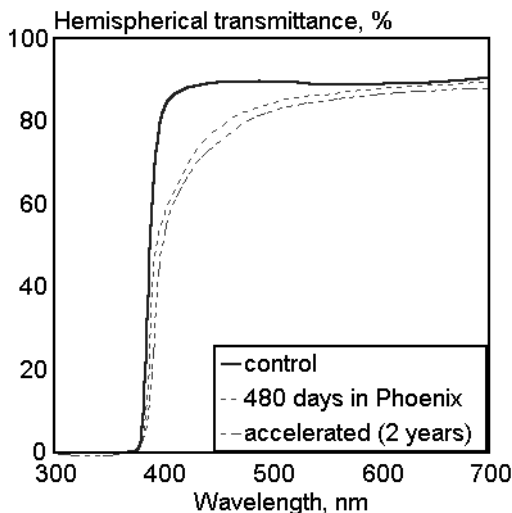


Fig. 13.8. Hemispherical spectral transmittance of cover plates subjected to natural and accelerated weathering. [Data from D. Waksman, W. E. Roberts, and W. E. Byrd, *Durability Building Mater.*, 3(1985)1.]

13.5.1 VISIBLE SPECTROPHOTOMETRY⁶³⁻⁶⁸

Since visible light has little effect on chemical composition, studies done in that range are of little value unless visible light transmission is a primary requirement of the material. Materials which must retain the ability to transmit light for a long time include covers of solar collectors and materials used for glazing applications. These materials are frequently studied by visible spectrophotometry. Waksman⁶⁴ compares spectral transmittance results with frequently-used solar transmittance values. Monitoring the transmittance spectrum gives information about the changes occurring (Fig. 13.8).

Other applications of visible spectrophotometry included:

- outdoor exposure of glass fibre reinforced polyester sheets
- polyurethane films
- development of light dosimeter sensitive to visible region
- study of life-expectation of polycarbonates.

Recent developments in microcomputer-assisted derivative visible spectrophotometry may contribute to renewed interest in this method.⁶³

13.5.2 UV SPECTROPHOTOMETRY^{54,63,66,69-98}

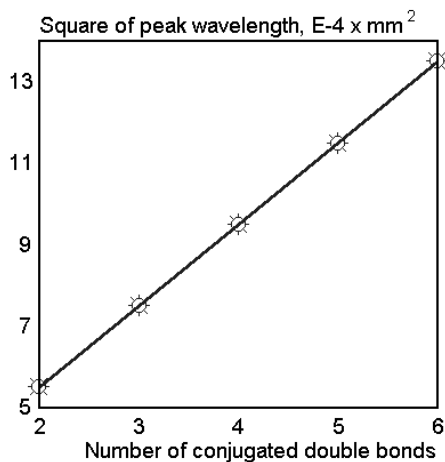


Fig. 13.9. Lewis-Calvin plot of relation between the square of peak wavelength, λ^2 , and the conjugation number, n , of $-(CH=CH)_n-$ for 0 \otimes 1 band. [Adapted, by permission, from K. Maruyama, Y. Kuramoto, M. Yagi, and Y. Tanizaki, *Polymer*, 29(1988)24.]

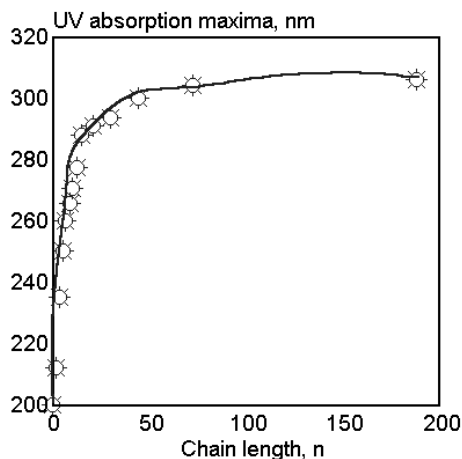


Fig. 13.10. UV absorption maxima vs. chain length of polyalkylsilane. [Adapted, by permission, from P. Trefonas, R. West, R. D. Miller, and D. Hofer, *J. Polym. Sci., Polym. Lett. Ed.*, 21(1983)823.]

The progress of weathering introduces new chromophores in the polymer chain which frequently absorb in the UV region. UV spectrophotometry is very sensitive to these changes and may help to resolve a broad range of technical difficulties related to the monitoring of kinetical changes. The study of the kinetics of polyene formation during the degradation of vinyl polymers (PVA and PVC) is a classical application of UV spectrophotometry (Fig. 13.9). Fig. 13.9 shows that individual polyenes, which vary in conjugation number, can be recognized and thus their formation followed.

The UV absorption maximum depends on the chain length of polyalkylsilane (Fig. 13.10). With the advent of derivative UV spectrophotometry, one becomes able to moni-

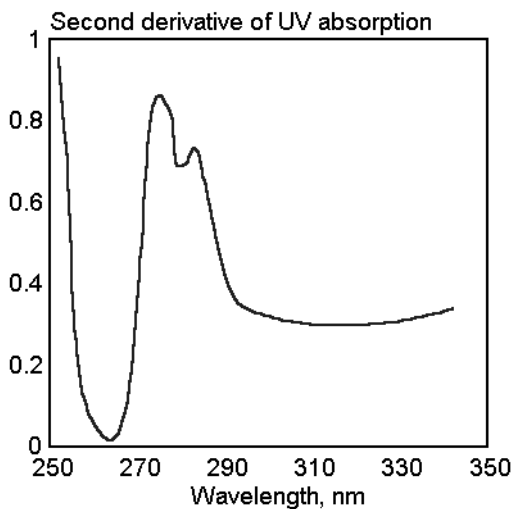


Fig. 13.11. Second derivative of UV spectrum of a mixture of polycarbonate and epoxy resin. [Adapted, by permission, from S. Mori, *J. Appl. Polym. Sci.*, 33(1987)1923.]

tor two polymers in the mixture (Fig. 13.11). All these features create a very powerful method which has been used recently in many applications, including these:

- monitoring the radical scission of silicon-silicon bonds in polyorganosilanes
 - absorption properties of polyorganosilanes varying in chemical composition
 - effect of polystyrene molecular size on optical constants
 - formation kinetics of hydroperoxides in polyacetals
 - absorption spectra of commercial polysulfones
 - absorption spectra of PMMA, PE, PS, PMMA/PS blend, PU, PET, PAR, and PC
 - polyenes formation in PVC
 - quenching studies of polysulfones
- effect of triplet sensitizers on polyurethane degradation
 - UV stabilizers retention and stability of UV absorbers
 - filter effect of UV absorbers
 - dye fading kinetics
 - stability of commercial papers.

The above list shows that UV spectrophotometry is best applied in predicting how materials absorb UV radiation and in determining or monitoring the kinetics of degradation, but it is also useful in studying of the mechanisms of reactions.

13.5.3 INFRARED SPECTROPHOTOMETRY^{62,79,80,84-86,90-93,99-191}

IR spectrophotometry is the leading method used to analyze the changes in weathered specimens. IR has been used for low density polyethylene, LDPE, high density polyethylene, HDPE, polypropylene, PP, acrylic/urethane, polyurethane, PU, polystyrene, PS, polycarbonate, PC, polyesters, polyamide, PA, acrylic resins, epoxy resins, EP copolymer, polyoxymethylene, POM, cotton, coatings of varying chemical composition, and dyed fibers. FTIR is frequently used with photoacoustical, attenuated total reflectance, ATR, and microscopical attachments. It appears from existing information that

photoacoustical FTIR might be the method of choice in the future since its readings are not affected by specimen surface roughness. Weathering damages the surface layers of a specimen, which greatly affects ATR readings but surface damage does not influence photoacoustical measurement. The list of IR applications in monitoring chemical changes during weathering is truly impressive. Carbonyl formation depth in polyethylene was studied by IR.¹⁰⁰ Various conjugated unsaturations formed during PE weathering can be recognized and separately recorded.¹⁰¹ IR was used to determine the concentration of impurity chromophores, such as, dienes, carbonyls, hydroperoxides, and vinyls in several PE samples.¹⁰¹ The effect of stress on PE¹⁰² and the rate of degradation of other olefins¹⁰³ can be observed by monitoring carbonyl absorption. There is a critical strain below which the photostability of polyolefins increases. It then decreases above the value of critical strain.¹⁰³

Carbonyl absorbance readings were used to compare various types of artificial weathering equipment. It is a reliable factor and the degradation rate of polyolefins monitored by carbonyl absorbance correlated well with the degradation rate determined by elongation retention.¹⁰⁴ Urethanes are frequently studied by IR.¹⁰⁵⁻¹¹⁰ The concentration of groups, such as, C-O-C, C=O, CH₂, NH, OH is recorded before, during, and after exposure in order to determine mechanisms of photodegradation, the effects of metals or catalysts on the degradation rate, the inhibiting action of UV stabilizers, etc.

Photodegradation mechanisms of polystyrene¹¹¹⁻¹²² and polycarbonate¹¹⁴⁻¹¹⁶ were also studied by IR. Most frequently, carbonyl and hydroperoxide formation has been monitored. Studies have also been done to evaluate the effect of UV radiation wavelength on the rate of the photolytic process. There have also been studies of C=O, C=C, amide II, OH, NH concentrations in epoxy resins;¹¹⁷ rate of hydroperoxide formation and dissociation¹²¹ and chain scission in epoxy resins; photooxidation of EP copolymers in the presence of various pigments,¹²³ gradient of oxidation photoproducts in PVC determined by micro FTIR;¹²⁵ progress of coating weathering by time-lapse IR; depth of coating degradation;¹²⁹ effect of dyeing on photochemistry of polymeric systems.¹³¹ The data from the most recent studies are included in Table 13.1 which gives application, material type, group monitored, and wavenumbers used. The majority of the work in IR is conducted with bulk samples exposed to a variable length of irradiation. A typical approach consists of monitoring one or more absorption bands in relation to a band which does not change during the irradiation process. Usually, the C-H band (around 2900 cm⁻¹) is taken as reference. The 720, 1390, and 1850 cm⁻¹ bands are also used. Table 13.1 indicates that there is relatively good agreement among the assignments of various absorption maxima. Carbonyl group absorption is the most frequently used indicator of oxidation and this is supported by Table 13.1. Carbonyl absorption is relatively independent of material. However, this absorption maximum shifts slightly during the degradation time.

Table 13.1: IR applications

Material	Group	Wavenumber, cm ⁻¹	Application
ABS	carbonyl (acid)	1718 ¹⁷⁵	
	carbonyl (ester)	1736 ¹⁷⁵	
	carbonyl (main chain)	1725 ¹⁷⁵	
	hydroperoxide	3400-3500 ¹⁷⁵	
	C=C	910-967 ¹⁷⁵	
Cotton	carbonyl (aldehyde/ketone)	1722 ¹⁴⁴	textiles ¹⁴⁴
	carbonyl (carboxylic acid)	1704 ¹⁴⁴	
Cotton	amide I	1658 shifting to 1664 ¹⁴⁴	textiles ¹⁴⁴
urea- treated	amide II	1560-1558 ¹⁴⁴	
EPDM	carbonyl	1710 ¹⁸¹	
	reference	1460 ¹⁸¹	
Epoxy	aromatic ring	1508 ¹⁶¹	adhesive ¹⁶⁰
	carbonyl	1740, ¹⁶⁰ 1721, ¹⁶¹ 1676 ¹⁶¹	
	epoxy ring	914 ¹⁶¹	
	sec aromatic amine	1292 ¹⁶¹	
	C-N	1296, ¹⁶¹ 1233 ¹⁶¹	
	C=N	1696 ¹⁶⁰	
	C≡N	2190 ¹⁶⁰	
	C=C	1486 ¹⁶⁰	
EPR	carbonyl	1730, ¹⁸² 1722 ¹⁸³	
	hydroperoxide	3400 ¹⁸³	
HIPS	carbonyl	1717 shifting to 1725 ¹³⁵	
	hydroxyl	3450 ¹³⁵	
	polybutadiene	966 ¹³⁵	
	polybutadiene (<i>trans</i> 1-2)	911 ¹³⁵	
	polybutadiene (<i>cis</i> 1-4)	727 ¹³⁵	
Model acids in polymer matrix	dimeric acid	1688-1717 ¹³⁸	
	monomeric acid	1717-1758 ¹³⁸	
NBR	carbonyl	1710 & 1770 ¹⁴³	coatings ¹⁴³
	<i>trans</i> C=C	965 ¹⁴³	
PA	carbonyl	1710 ¹⁶⁸	

Material	Group	Wavenumber, cm ⁻¹	Application
PC	aromatic ketone	1690 ¹³⁷	
	tertiary alcohol	3490 ¹³⁷	
PC/PMMA	C=C	164 ¹⁸⁰ (PMMA)	blend ¹⁸⁰
	photo-Fries rearrangement products	1687 ¹⁸⁰ (PC)	
PDMS	alcohol or silanol	3400 ¹⁷²	
	acid	3100, 1703, 1692 ¹⁷²	
	vinyl	1597 ¹⁷²	
PE	aldehyde	1728 ¹⁴⁵	biodegradable
	carbonyl	1715, ^{146,155,158,159,162-4}	film ¹⁶⁴
		1714, ¹⁶⁵ 1716, ¹⁵⁸ 1720 ¹⁶⁶	
	crystallinity	1896 ¹⁶⁶	shopping bags ¹⁵⁹
	ester	1735-40, ¹⁴⁶ 1740 ¹⁴⁵	degradable
	hydroperoxide	3440 ¹⁶⁵	film ^{145,158}
	ketone	1718 ¹⁴⁵	photocrosslinked
	γ-lactone	1782 ¹⁴⁶	film ¹⁶²
	reference	720, ^{155,159} 1465, ¹⁵⁸ 1950, ¹⁶⁵	
	vinyl	908, ¹⁶⁶ 909, ¹⁶⁵ 1640 ^{145,146}	
	C=C	1640 & 940 ¹⁶⁴	
C-O	1020 ¹⁶³		
PET	alcohol	3510 ¹⁷¹	
	benzoic acid/benzaldehyde	1697 ¹⁷¹	
	ester	1716 ¹⁷¹	
	formate	1727 & 1182 ¹⁷¹	
	C=C	1643 ¹⁷¹	
PMMA/PS	carbonyl (PMMA)	1730 ⁹⁰	blend ⁹⁰
	hydroxyl	3450 ⁹⁰	
	C-O-C (PMMA)	1193 ⁹⁰	
Polyimide	carbonyl	1780 ¹⁷⁴	
Polyisoprene	alcohol	3430 ¹⁸⁴	
	carbonyl	1717 ¹⁸⁴	
	hydroperoxide	3400 ¹⁸⁴	
	unsaturations	835 ¹⁸⁴	
POM	carbonyl	1735 & 1760 ¹⁶⁹	

Material	Group	Wavenumber, cm ⁻¹	Application
POM	hydroperoxide	3475 ¹⁶⁹	
PP	aliphatic acid	1710 ¹⁵³	textiles ¹⁴⁴
	anhydride	1775 ¹⁴⁴	stabilizing ^{150,167}
	carbonyl	1705, ¹⁵² 1710, ^{148,149}	nonwoven ¹⁹¹
		1712, ¹⁵⁴ 1715, ^{147,150,191}	
		1720 ¹⁵³	
	ester carbonyl	1735, ¹⁵³ 1738 ¹⁵⁴	
	HALS concentrate	1710 ¹⁶⁷	
	HALS (ester groups in)	1740 ¹⁵⁰	
	hydroperoxide	3430 ¹⁴⁴	
hydroperoxide (hydrogen bonded)	3420 ¹⁵³		
PS	acetophenone	1700 ¹³⁶	film ¹³⁶
	benzophenone (UV stabilizer)	1662 ¹³⁶	
	carbonyl	1730 ¹³⁹	
	ester	1240 ¹³⁹	
	hydroperoxide	3555 ¹³⁶	
PS/PVME	carbonyl	1739 ¹⁹⁰	blend ¹⁹⁰
PU-acrylate	aliphatic CH	2800-3000 ⁹²	clearcoats ⁹²
	aromatic	700 ⁹²	UV-cured
	carbamate	1530 ⁶²	coatings ⁶²
	carbonyl	1730 ^{62,92}	
	ether	1200 ⁶²	
	hydroxyl	3510 ⁶²	
	methylene	2940 ⁶²	
	urethane	1525 & 1250 ⁹²	
PVAI	carbonyl	1720 ⁹⁹	
PVC	carbonyl	1714, ⁸⁴ 1718, ^{141,142} 1720, ¹⁴⁰	
		1730 & 1670 ⁸⁵ shifts to	
		1715 ⁸⁵	
	carbonyl (acid chloride)	1785 ¹⁴²	
	carboxylate stabilizer	1510 ⁸⁵	
	hydroperoxide	3476-3420 ¹⁴²	
hydroxyl	3460 ⁸⁴		
-CH ₂ COOH	1718 ¹³⁴		

Material	Group	Wavenumber, cm^{-1}	Application
PVC	-CHCl-CO-CHCl	1745 ¹³⁴	
	C=C (isolated)	1650 ¹³⁴	
	C=C (conjugated)	1580 ¹³⁴	
	-CH=CH-CO- (isolated)	1695 ¹³⁴	
	-CH=CH-CO- (conjugated)	1605 ¹³⁴	
SIS	ester	1735 ¹⁷⁶	
	hydroperoxide	3325 ¹⁷⁶	
	ketone & acid	1717 ¹⁷⁶	
	C=C	1640, 1665, 885 ¹⁷⁶	
TPU	hydroperoxide	3475 & 3425 ¹³³	
Wood	carbonyl	1727 ¹⁸⁵	

Superscript at wavenumber and application gives a reference number

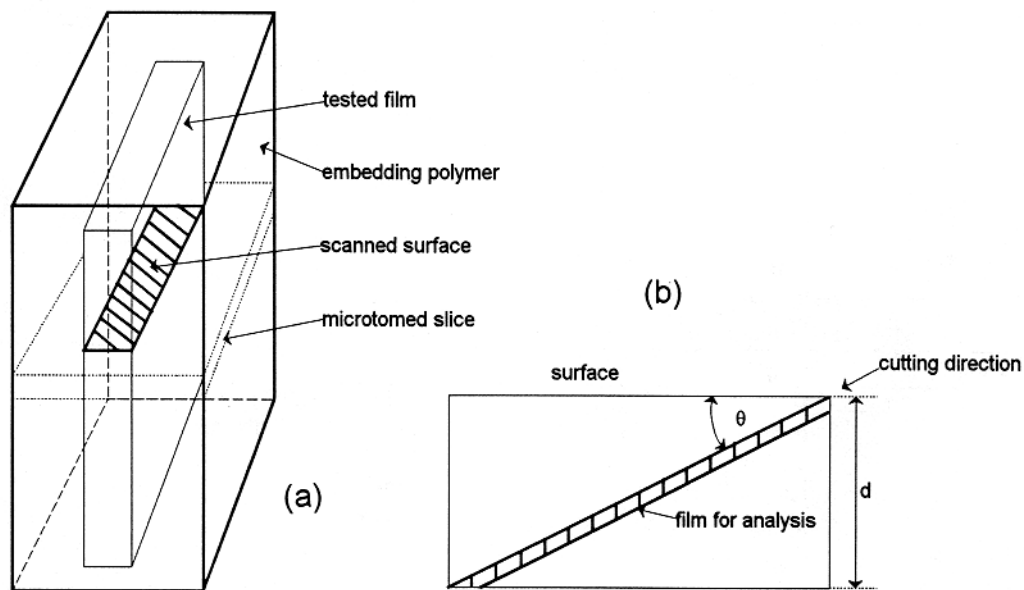


Fig. 13.12. Method of sample preparation for depth profiling. [Based on references 141 (a) and 143 (b).]

Table 13.2: IR data for derivatization method^{134, 146,169,171,172,175}

Polymer	Group	Wavenumber, cm ⁻¹	Reagent	Derivative	Wavenumber of derivative, cm ⁻¹	Ref.
PVC	-CH ₂ -CO-OH	1718	NH ₃	-CO-O ⁻ NH ₄ ⁺	1575	134
			Et ₂ NMe	-CO-O ⁻ Et ₂ N ⁺ NMe	1580	
	-CH ₂ -CO-Cl	1785	NaOH	-CO-O ⁻ Na ⁺	1590	
			H ₂ O	-CO-OH	1718	
			NH ₃	-CO-NH ₂ (amide I)	1685	
			NH ₃	-CO-NH ₂ (amide II)	1629	
			Et ₂ NMe	-CO-NHR	1668	
PE	sec-alcohol	3400	NO	nitrites	1645&776	146
	carbonyl	1715	SF ₄	acid fluorides	1846-48	
	hydroperoxide	3400	NO	nitrites	1276-79,857-9, 1633	
	hydroxyl	3400	SF ₄		1082	
POM	carbonyl	1735&1760	NH ₃		1700-1500	169
		1735	NH ₃	alcohol	3650	
			NH ₃	-CO-O ⁻ NH ₄ ⁺	1792	
			NH ₃	H ₂ N-CO-	3390,3320,1792	
PET	alcohol	3485	CH ₃ COCl	aliphatic ester	1748	171
	benzoic acid	1697	DNPH*		1618&1592	
	carboxylic acid	1696-1717 and	SF ₄	acyl fluorides	1815-1841	
1733-1776		NH ₃	-COO ⁻ NH ₄ ⁺	1543-1595		
PDMS	acid	1692&1703	NH ₃	ammonium salt	1548	172
		1695	SF ₄	acid fluoride	1829	
ABS	carbonyl	1734&1718	NH ₃	carboxylation	1560	175

Degradation depth profiling is the other typical use of IR. Fig. 13.12 shows two methods used for this purpose. In the first method (a), the specimen with a thickness of approximately 300 μm is microtomed to give a thin slice across depth and the specimen is then analyzed using micro IR cell. In the second method (b), a 1-2 μm slice of the specimen is microtomed and specimen surface is analyzed by Micro-ATR scan. The results show a relationship between absorption at any studied wavelength and the sample thickness demonstrating the effect of radiation on the material bulk. Typical results from these studies can be found in Chapter 14 (see Fig. 14.9).

A group of scientists in France developed a system of materials testing to understand mechanisms of degradation using IR.^{134,146,169,171,172,175} Table 13.2 shows some data which illustrate the principles which they used. The assignment of absorption maxima is always uncertain. In order to understand mechanism of degradation, one needs to know which changes in spectrum (increase or decrease of absorption in the course of degradation) are caused by a particular chemical reaction. These scientists verified chemical conversions by derivatization. In their method, spectra are recorded for samples at different stages of degradation followed by subjecting the sample to simple chemical reagents such as NH_3 , H_2O , NO , Et_2NMe , NaOH , SF_4 , CH_3COCl , etc. These reactions change the spectrum of the material and, based on the changes, assignment of a particular band can be confirmed. The method developed is currently the most efficient technique for determining the mechanisms of degradation.

All the above examples show that IR spectrophotometry has a broad range of usefulness in studying weathering characteristics of materials. The most useful area of application is in monitoring the photooxidative changes that occur during exposure.

13.5.4 NUCLEAR MAGNETIC RESONANCE^{72,73,92,102,106,108,109,117,122,131,135,151,154,172,179,184,186,188,192-200}

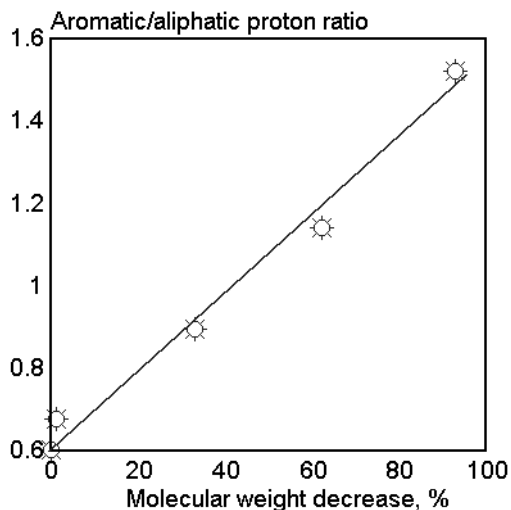


Fig. 13.13. The ^1H NMR aromatic/aliphatic proton ratio vs. decrease in PS molecular weight, $100(1-M_r/M_{no})$ in presence of aluminum chloride at 50°C . [Adapted, by permission, from N. Nanbu, Y. Sakuma, Y. Ishihara, T. Takesue, and T. Ikemura, *Polym. Degrad. Stab.*, 19(1987)61.]

^1H NMR and ^{13}C NMR spectra were used to characterize changes in polysulfones, unsaturated polyester resins, polyurethanes, polyethylene, polyacetal, polystyrene, dyed fibers, and coatings. In polystyrene, it was found that the concentration of phenyl groups in the degraded product was higher than their concentration in the starting material. The aromatic/aliphatic proton ratio, R , correlates with molecular weight decrease during degradation (Fig. 13.13).

^{13}C NMR helped to identify the formation of formate end-group in a polyacetal during the degradation process and played a crucial role in developing an understanding of the degradation mechanism. Application of NMR in polyurethane studies allows one to distinguish between NH in urethane and urea group. Also, comparative IR and NMR measurements show

that the broad carbonyl band includes quinoid, keto, and aldehyde groups. ^{13}C NMR, used to study polyethylene irradiated with UV, showed that much fewer acetyl groups are produced in a stressed, elongated specimen than in a relaxed specimen. This discovery was important in distinguishing between mechanisms of degradation under stress and without stress. Solid state ^{13}C NMR is a unique technique for studying the weathering of compounded polymer because most pigments and fillers do not disturb the measurements.¹²² Also, pulsed NMR, a relatively new technique, is capable of determining morphology of macromolecules and has been proposed for studies of polymer behavior under irradiation.¹⁹³

NMR can distinguish between the different structural forms of polybutadiene in high impact polystyrene, HIPS.¹³⁵ Peak resonances at 27.7 and 32.9 are attributed to CH_2 (*cis* 1-4) and CH_2 (*trans* 1-4). The interpretation of results from IR and NMR confirms mechanism of degradation. NMR was applied to studies of polybutadienes and polyisoprenes.¹⁸⁸ During the degradation of polyisoprene, formation of an epoxy group was confirmed by NMR.¹⁸⁴ Ethylene content and triad sequence distribution were obtained from NMR studies of EP copolymers.¹⁷⁹ Quinone formation during photodegradation of polyacrylophenones was confirmed by IR and NMR analysis.¹⁹⁵

Magic angle NMR is a relatively new method applied to degradation studies. Materials for automotive coatings were studied by magic angle NMR to measure change in the concentration of ketone end-groups in crosslinked coatings as a function of degradation time.¹⁹⁶ Correlation can be established among ketone concentration (using NMR) and hydroperoxide concentration (using titration) and free radical formation (using ESR).

Comparison of NMR spectra for degraded and undegraded polydimethoxy siloxane, PDMS, shows that the methylene group is the main site of silicone oxidation.¹⁷² NMR was also used to study new light stabilizers based on siloxanes combined with hindered amine light stabilizer, HALS, and/or hydroxybenzophenones.^{154,199} Application of NMR shows that stabilizer groups are bound to the siloxane chain mainly (75%) by SiC bonds which are not susceptible to hydrolysis. Also, the composition of HALS-phosphite stabilizers was confirmed by NMR¹⁵¹ and their mechanism of action was studied.¹⁹⁸

These examples show the versatility of the method. It should be noted that NMR is one of the few techniques available for studying crosslinked systems and systems loaded with inorganic materials or other additives all of which may interfere with other spectroscopic measurements. NMR is also a very important method in verifying and confirming results obtained by other methods.

13.5.5 ELECTRON SPIN RESONANCE, ESR^{19,89,112,133,136,150,157,167,180,182,189,201-229}

Since photodegradative processes proceed according to radical mechanisms, ESR is one of the methods of choice in the studies of photodegradation because it is capable of detecting radicals. Since the first edition of this book, several papers have reported the ap-

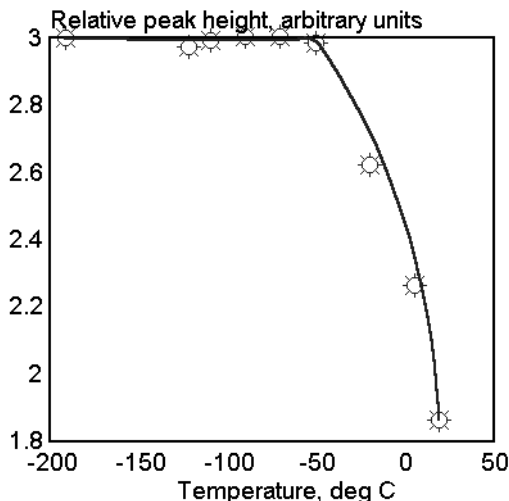


Fig. 13.14. Temperature dependence of the relative ESR peak height due to radicals produced in PS by photoirradiation at -196°C during 3 h irradiation at 250 nm. [Adapted, by permission, from A. Torikai, A. Takeuchi, and K. Fueki, *Polym. Degrad. Stab.*, 14(1986)367.]

ESR, the measurements are made at temperatures close to liquid nitrogen, which stabilizes the radicals (Fig.13.14). Radical decay begins around -75°C ; below -75°C they are stable. Temperature dependency complicates measurement and generates discussions between scientists when they detect different radicals and suggest different mechanisms of degradation.

Gerlock *et al.*²⁰⁴⁻⁶ developed an original approach to this problem. Knowing that a hindered amine light stabilizer, HALS, is able to produce a durable nitroxide radical, he doped polymer coatings with HALS or hindered amine nitroxide, HAN, and measured nitroxide concentration. Nitroxide scavenges the radicals produced by the photolysis of the coating, converting short-lived species to stable radicals. This approach makes possible the quantitative evaluation of radical formation rate. The method called “nitroxide decay assay” seems to offer great sensitivity to changes occurring on irradiation; more importantly, it allows one to drastically reduce the time of coating evaluation (Fig. 13.15). In a matter of minutes of irradiation (and hours of measurement), one may obtain readings of the rate of formation of HAN and correlate it to gloss rate loss. If only gloss retention were studied, it would take months of exposure in order to detect changes (Fig. 13.16). Its sensitivity to changes on irradiation and the speed with which results can be obtained, make this a preferred method for future studies. A study of radicals formed from epoxy resins using this method showed that radicals formed during expo-

lication of ESR to study such materials as polystyrene, polyamide, poly(vinyl alcohol), polypropylene, acrylic/melamine coatings, and for determining the effect of UV stabilizers and iron oxide pigments on weatherability. The full potential of this method has not been realized until recently. During the last five years, the extent of application of ESR has improved and now it is probably the second most frequently used instrumental method in weathering studies next to IR.

ESR allows identification of the radical type. This is critical to the understanding of the mechanism of degradation. Examples of ESR applications include detection and monitoring of polystyryl radicals¹¹² during polystyrene degradation, identification of two types of radicals in polyvinyl chloride,²⁰² etc. The study of such radicals is difficult because their lifetime is short. In order to improve the analytical capabilities of

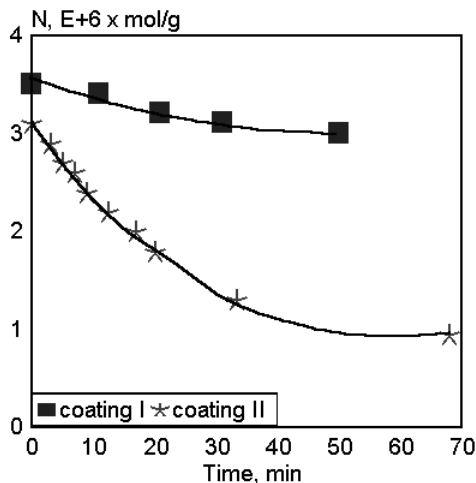


Fig. 13.15. Nitroxide I concentration, N, for two coatings doped with nitroxide I and exposed to UV light at 60°C and dew point 25°C. [Adapted, by permission, from J. L. Gerlock, D. R. Bauer, and L. M. Briggs, *Org. Coat. Sci. Technol.*, 8(1985)365.]

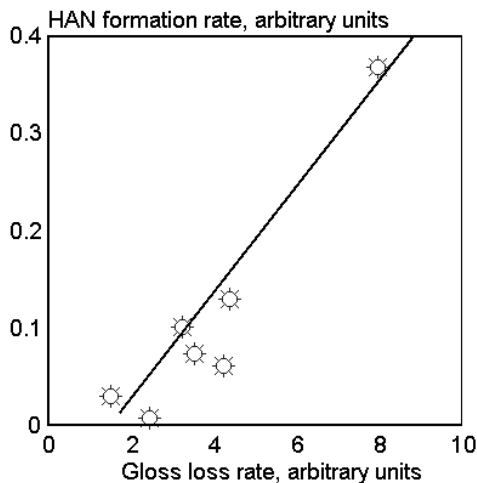


Fig. 13.16. Gloss loss rate vs. initial rate of formation of hindered amine nitroxide, HAN, in HALS doped coatings. [Adapted, by permission, from J. L. Gerlock, D. R. Bauer, and L. M. Briggs, *Org. Coat. Sci. Technol.*, 8(1985)365.]

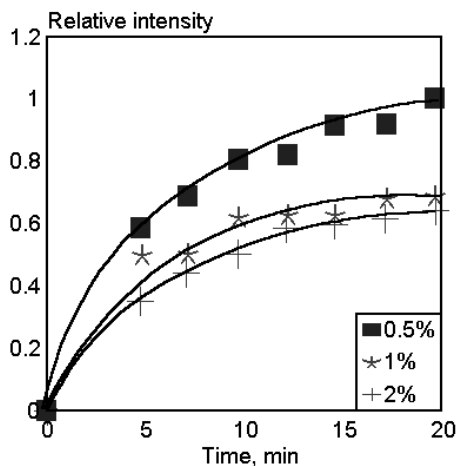


Fig. 13.17. Relative ESR intensity of phenoxyl radical vs. exposure time in QUV of paint containing different amounts of Tinuvin 900. [Adapted, by permission, from S. Okamoto, K. Hikita, H. Ohya-Nishiguchi, *Polym. Paint Colour J.*, 177(1987)683.]

sure are stable and can be studied directly (Fig 13.17). Also, the effect of UV absorber concentration can be assessed. Igarashi²⁰¹ extended the range of applications of this method by using it to demonstrate that samples can be studied under stress.

ESR has been used to analyze the degradation of asphaltic materials.²⁰⁹ Because asphaltic materials have such a broad range of components, ESR offers some advantages because it is molecularly selective and very sensitive. An additional advantage comes from the fact that solid samples can be analyzed, which eliminates the need for solvent dilution which is necessary in many of the other techniques used in weathering studies. Solvents change the material's structure and thus the data for solutions does not always correspond to the changes which occur in materials not in so-

lution. In asphaltic materials studies, the concentration of organic free radicals correlated very well with the viscosity increase of the material during the degradation process.

The versatile nature of this method is further demonstrated by these recently reported applications: Kubota *et al.*⁸⁹ studied the sensitizing influence of benzophenone in model compounds of polyethylene. No formation of radicals was observed in n-hexane. On addition of benzophenone as a sensitizer, radicals formed by the abstraction of hydrogen from methylene groups were found. The concentration of this radical depends on the amount of sensitizer. At low concentrations of sensitizers, formation of this radical is promoted. An increased concentration of sensitizer promotes radical consumption, producing double bonds. Ferrocene compounds form other group of substances which are known to accelerate the photodegradation of polymers. Their effect on polyethylene was studied using ESR.¹⁵⁷ It was confirmed that this process is also concentration-specific. At low concentration of sensitizer, higher quantum yields are detected. The radical formed is a superposition of the alkyl and peroxide radicals. At higher concentrations of sensitizer, the radical formation drops rapidly, meaning that the ferrocenes act as stabilizers. Benzophenone also accelerates the degradation of polystyrene as confirmed by ESR.¹³⁶ Five different radicals were identified in polystyrene during photooxidation.²¹³ It has been predicted that short-lived radicals may be formed but these have not yet been detected.

Studies of ethylene-propylene copolymer identified radicals and showed a different radical composition in oxygen than in the absence of oxygen.¹⁸⁰ The hydroperoxides, which were first formed, decompose during irradiation or under the effect of heat and abstract hydrogen to form more stable peroxy radicals. Ichikawa *et al.*²¹¹ evaluated the effect of temperature and residual monomer on the chemical structures of radicals formed in PMMA. Ranby identified radicals formed during the degradation of wood.²¹⁶ Kubota and Kimura²¹⁸ evaluated the effect of various solvents on PE degradation and radicals formed. In a polypropylene model compound, tertiary hydrogen was shown to be abstracted. Degradation of model compounds depends also on the excitation method.²¹⁰ The crystalline structure of polypropylene restricts the mobility of free radicals formed during photooxidation and this affects the mechanism of polymer degradation.²¹⁹ The effect of dose on the formation of volatiles during γ -irradiation of polyacrylonitrile can be predicted based on the quantum yield of radical formation.²²² Radicals were identified and the effect of dose evaluated for γ -irradiated PTFE.²²⁴ The effect of temperature on UV degradation of cables was determined by ESR.²²⁵ The method was used to understand the mechanism of γ -degradation of styrene-acrylonitrile copolymers.²²⁶ ESR was used to study HALS with urethane functional groups to compare HALS efficiency in polymeric and monomeric forms.^{167,227}

A new approach using ESR to study degradative changes in polymers was developed in Bayer.^{214,215,217} Polymer specimens were directly irradiated in the instrument

and radicals were measured as they were formed. Such an approach allows for a very rapid determination of the degradation rate and the rate can be monitored as a function of time or of the conditions of sample irradiation. In photodegradation studies, the so-called "activation spectrum" is always of interest since it is important to know which wavelength of radiation is the most degrading for a particular composition. Use of this information allows the design of an adequate stabilizing system. The ESR method developed in these studies can measure radicals per photon versus wavelength of radiation giving the "activation spectrum". Specific results obtained by this method can be found in other chapters (see Figs. 5.7, 5.8, 14.43, and 14.82).

The above examples show the versatility of this method. Not only can ESR be used to study photodegradation of pure substances (identification of intermediate products of degradation, understanding mechanism of degradation, determination of activation spectrum of materials, process kinetics, stabilizer efficiency, etc.) but it can also be used to study complex mixtures. In addition, it is a very rapid method.

13.5.6 CHEMILUMINESCENCE, FLUORESCENCE, AND PHOSPHORESCENCE^{102,110,111,230-238}

These three types of emissions can be studied to understand how the energy absorbed by the specimen is dissipated. Emission intensity was studied for a long list of polymers, including polystyrene, polysulfones, polyurethanes, polyolefins, and polyamides. Since data on fluorescence and phosphorescence wavelength are given for individual polymers in Chapter 14, together with the list of absorbing and emitting species, the discussion below is limited to pointing out the major advantages of the method. Emission studies contribute to:

- analysis of irradiation efficiency
- identification of absorbing and emitting species
- following the kinetics of degradation
- identifying species formed during the degradation process
- understanding the stabilization mechanism
- selecting quenchers for specific excited states.

Current literature includes data which can be used to illustrate the capabilities of these methods. Zamotaev et al.²³³ determined absorption and emission bands for over 20 anthraquinone derivatives which may act as photoinitiators of various polymers. All these compounds absorb in the range of 320-340 nm and, depending on temperature, they may emit energy (at low temperatures) or participate in photoreduction (at ambient temperatures). This was studied using polyethylene, PE. The presence of anthraquinone derivatives causes crosslinking reaction which are localized, if the derivatives are insoluble in matrix, or uniformly distributed in the amorphous phase if they are soluble. Heating of polyolefins in the presence of air changes their fluorescent inten-

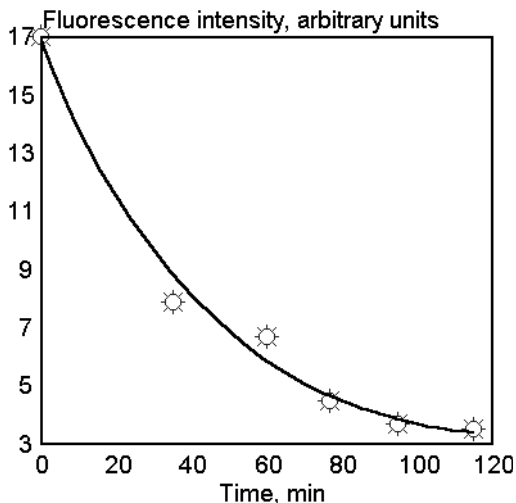


Fig. 13.18. Intensity of fluorescence emission at 345 nm (excitation at 290 nm) by atactic PP vs. time of thermal degradation at 190°C. [Adapted, by permission, from P. L. Jacques and R. C. Poller, *Eur. Polym. J.*, 29(1993)75.]

sity (Fig. 13.18).²³⁴ Carbonyls formed during degradation contribute most to this fluorescence. It is very difficult to obtain repeatable measurements because the intensity of the spectrum is sensitive to the position and orientation of the specimen in the instrument. The authors degraded powdered samples out of the instrument then fed them into the instrument after various exposure intervals.²³⁴ Initially, the degradation of polyolefins generates α,β -unsaturated carbonyl compounds as major products of degradation which accelerate further degradative processes.²³⁵ Lifetimes exceeding 20 μ s were determined for triplets during UV laser degradation of PMMA.²³⁶ These triplets are long lived due to the restricted diffusion of oxygen.

Several effects can be observed in the course of these studies: temperature, sample thickness, and depth of degradation influence the readings and, while it is useful to vary these conditions in degradation studies, error may be introduced. The identification of chromophores and photoinitiators in homopolymers²³⁸ and their blends²³⁷ provide useful insight into the degradation process.

13.5.7 REFLECTANCE SPECTROPHOTOMETRY⁷⁷

Berner⁷⁷ demonstrated the potential of reflectance spectrophotometry for studying the permanence of UV absorbers in coatings. Figs. 18.19 and 18.20 show data recorded using this method. This method is a valuable complementary technique for studying the polymer stabilization with minimum sample preparation.

13.5.8 MASS SPECTROMETRY^{73,114,195,239-241}

A mass spectrometer, when used as the detector in a gas or liquid chromatography, can help to identify components of degraded polymer and thus contribute to the understanding of the degradation mechanism. There is yet another variation of mass spectrometry, called “secondary ion mass spectrometry”, SIMS, which has been used recently to study the photo-degradation of poly(1-butene sulfone),²³⁹ the photooxidation of polystyrene²⁴¹ and acrylic coating containing UV absorber used as a protective coating on polycarbonate.¹¹⁴ Poly(1-butene sulfone) was subjected to high energy radiation under

the high vacuum conditions of MS instruments. The composition of the degradation products was determined by MS. In this study,¹¹⁴ the results from SIMS were compared with a similar type of data offered by “electron spectroscopy for chemical applications”, ESCA.¹⁶³ The goal of the study was to determine if there was interpenetration between a protective 0.2 μm thick coating of polymethylmethacrylate and its polycarbonate substrate. After chemical etching of the coating, SIMS depth profiling was used to determine H, D (coming from acrylate), and C. The results show no interpenetration in either polymer layer. This illustrates how detailed information can be obtained. Time-of-flight mass spectrometry was used to determine velocity distribution of ejected species during the laser ablation of polystyrene doped with anthracene.²⁴⁰ Below the ablation threshold, only anthracene was removed from the surface of the sample. During the etching process anthracene and styrene monomers were recovered. The velocity distribution changed with anthracene concentration, with laser intensity, and with the condition of the surface (a fresh surface had a different velocity distribution than a partially etched surface). An in-line mass spectrometer was used to identify and determine quantitatively the degradation products from model compounds of polyacrylophenone subjected to UV exposure.¹⁹⁵ The degradative changes observed in this work can be related to the mechanism which causes color change in the polymer (yellowing) as well as to the color change of lignins, which contain similar structural elements. The reduction in molecular weight of polystyrene during photooxidation was observed by time-of-flight SIMS.²⁴¹ In addition to the main polymer also trace quantities of impurity (polydimethoxy siloxane) were monitored.

The methods presented here can address several specific questions regarding surface changes and the composition of volatile materials formed in the process of degradation. These methods are very sensitive to admixtures (especially materials deposited on the surface) and this severely limits their application because of the surface contamination caused by exposure.

13.5.9 ATOMIC ABSORPTION SPECTROSCOPY²⁴²

Atomic absorption spectroscopy, AAS, was employed to determine Zn and Ca from runoff samples (rain water which washed sample surface).²⁴² Paints were exposed in two locations under wet and dry conditions to determine the effect of acid rain on the paint surface. ZnO and CaCO₃ are used as pigments/fillers in paints and this study was focused on determining if acid rain can dissolve these pigments. This example gives a simple illustration of the potential use of a cost-effective method for studying inorganic content.

13.6 X-RAY ANALYSIS

13.6.1 WAXS AND SAXS^{102,108,124,219,232,243-246}

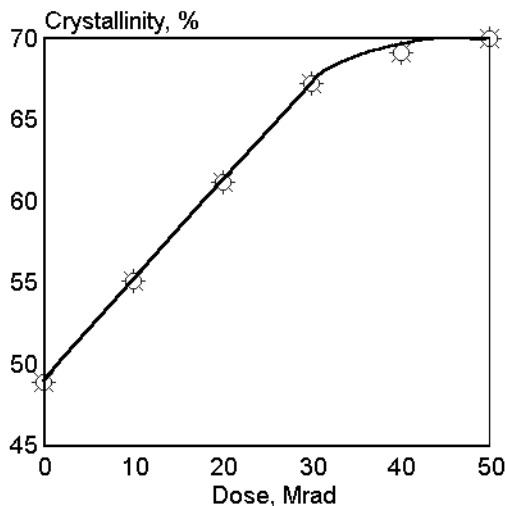


Fig. 13.19. POM crystallinity vs. dose absorbed. [Adapted, by permission, from H. N. Subramanian and S. V. Subramanian, *Eur. Polym. J.*, 23(1987)207.]

Wide angle X-ray scattering, WAXS, and small angle X-ray scattering, SAXS, are two methods that are used occasionally to study changes in the crystalline structure of materials during weathering. The crystallinity of material changes with irradiation dose (Fig. 13.19). At lower doses, the crystallinity increase is more rapid because of the predominant effect of crystallization in the amorphous regions which parallels degradation.

WAXS was employed in PP studies to understand conditions under which grafting can be effectively conducted.²¹⁹ Two PP samples were analyzed (oriented and unoriented). Unoriented samples have a higher content of amorphous regions in which chains are sufficiently mobile to allow radicals formed during irradiation to escape from their surroundings and react or recombine in other areas of the material. Immobilized chains in the crystalline

phase, which is a tightly packed region, cannot move freely and therefore radicals react locally.

WAXS studies²⁴⁴ determined that injection molded articles from PP have a higher degree of orientation at the surface than in the core. On the surface of the material itself, there is a "skin layer" which has low crystallinity. The orientation distribution is high close to the surface and low in the core. The surface is mesomorphic probably because of very fast cooling. The authors used these and other observations to understand biological degradation (by hydrolysis) of various materials such as wood pulp and regenerated cellulose fibers. Based on their success in understanding the process, they consider structural studies a prerequisite to studies on degradation.

SAXS experiments were conducted to compare structure of amorphous and semi-crystalline PET.²⁴⁵ Two amorphous phases exist in PET: the amorphous phase between spherulites and the amorphous phase inside spherulites. Crystallinity restricts molecular mobility.

X-rays were used to monitor cracks formed in materials used in space.²⁴⁶ Cracks were filled with tetrabromoethane which is opaque to X-rays and then a radiograph of the sample was taken and the number of cracks counted.

These studies show that the degradation increases molecular mobility, facilitating the crystallization of molecules in the amorphous phase. This is important because it shows that material frequently changes during weathering into a more crystalline material, which may result in higher UV resistance. It also shows that, if all effort is directed to monitoring chemical changes occurring during photodegradation, the results for various degradation stages are not comparable because the material is actually a continuously changing structure. Polymers are usually semi-crystalline materials and the crystalline structure is responsible for many of their properties. Many studies have neglected structural changes and are thus less helpful in developing an understanding of the weathering process. X-ray analysis provides us with very important information on the proportion of crystalline and amorphous phases, the distribution of crystallites, and it can distinguish between a variety of amorphous states.

13.6.2 X-RAY PHOTOELECTRON SPECTROSCOPY^{16,19,56,74,97,114,129,170,247-257}

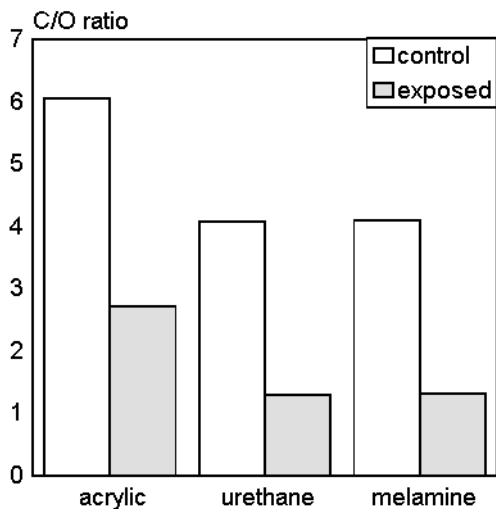


Fig. 13.20. Carbon/oxygen ratio change during 1 year exposure in Naha, Japan, as determined by XPS. [Data from S. Yajima, Y. Togawa, S. Matsushita, T. Suzuki, and T. Okada, *Kinzoku Hyomen Gijutsu*, 37(1986)718.]

X-ray photoelectron spectroscopy, XPS, also called “electron spectroscopy for chemical applications”, ESCA, is a relatively new tool applied to weathering studies. Although new, it has become one of the most frequently used methods. With it, quantitative analysis of oxygen, carbon, and nitrogen, and any heavier element available on the surface is possible. Present research concentrates mostly on evaluation of the degree of surface photooxidation. UV curable acrylics, polyphenylene oxide, polysulfone, polyurethanes, melamine resins, polycarbonate, and polystyrene were all tested by XPS for the degree of surface oxidation. Fig. 13.20 gives some of these data, with other data included in Fig. 17.4. It was discovered¹²⁹ that during UV radiation curing, a substantial photooxidation occurs. The irradiation of polysulfone under nitrogen or vacuum led to surface sulphur decrease and photoreduction of sulfone groups to sulfide.

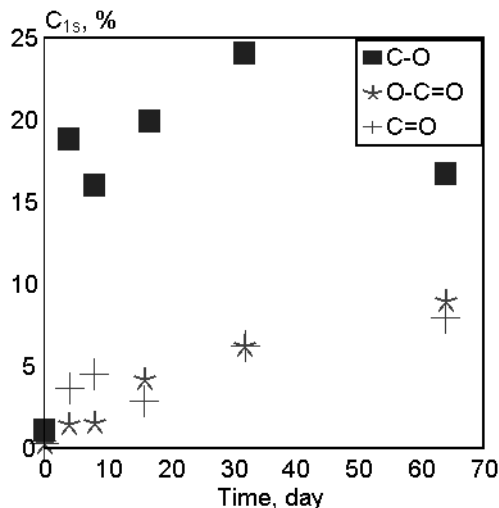


Fig. 13.21. Change in C_{1s} signal (ESCA) for PS vs. weathering time in Dhahran, Saudi Arabia. [Adapted, by permission, from H. S. Munro, D. T. Clark, and J. Peeling, *Polym. Degrad. Stab.*, 9(1984)185.]

Outdoor weathering studies of polystyrene are shown in Fig. 13.21. Photooxidation is predominant in polystyrene weathering. Current studies compare data from XPS with the data from IR and SIMS. Perfect agreement does not yet exist, with discrepancies probably due to differences in the thickness of the surface layer measured by each of these methods. Surface modification of polystyrene by molecular oxygen and nitrous oxide was studied by XPS.^{249,250} More oxidation occurs in the presence of oxygen than in the presence of nitrous oxide even though nitrous oxide is more reactive.²⁴⁹ Also, UV photooxidation is more degrading than plasma oxidation.²⁵⁰ PET exposure to oxygen plasma was also studied.²⁵³

Polyethylene photoinitiated crosslinking was monitored by ESCA.¹⁶³

The O/C ratio was measured to quantify the degree of oxidation. The C/Si ratio was measured to monitor the surface modification of polyacetylene films by silicone-containing compounds.¹⁷⁰ Modified films were then exposed to UV radiation and it was determined that conversion of the silicone-containing modifier occurred by oxidation. Spontaneous oxidation of n-hexane plasma polymers was observed by XPS and IR.²⁵⁵ The results obtained by those two methods were in agreement and allowed the conclusion that only the top few nanometers were oxidized. XPS was used to compare photochemical changes in several high performance fibers²⁵⁶ and cellulose-based fibers.²⁵⁷

XPS was used to determine why some chlorinated rubber coatings failed to prevent the early corrosion of steel.¹⁶ Atomic ratios of Cl/Fe, O/Fe, and Si/Fe were monitored to understand the mechanism of failure. Interfacial rust was found to catalyze the cleavage of C-Cl bonds in the polymer, which formed chloride ions, which in turn corroded the steel and caused deterioration of the paint system.

Materials tested in space gave interesting results.⁹⁷ Several siloxane-containing copolymers were exposed to atomic oxygen. Silicon concentration increased during exposure and silicon to oxygen ratio became almost 1:2, this means that the material that initially contained organic groups was gradually converted to silicate. XPS was used to follow changes in the composition of surface elements. But, XPS can also determine silicon 2p electron binding energy, it also confirmed the chemical character of changes (the

binding energy for organic silicone of 102 eV changed to 103 eV, which is characteristic of inorganic silicone). After this process was completed no more erosion was observed because silica layer was able to protect the polymer bulk from further changes (a layer impermeable to molecular oxygen). A study of PTFE samples exposed to a space environment for 6 years showed that surface molecules reorient themselves in such a way that fluorine atoms were exposed to atomic oxygen.²⁵⁴

Another recent paper evaluates the degrading effect of XPS on polyvinylidene fluoride, PVDF, film.²⁵¹ It is estimated that one hour elapses before any significant degradation occurs. In PMMA studies,²⁵² it was found that even 3 hours exposure did not alter composition. Only chain scission was detected.

The above studies show that XPS has a high applicability to weathering studies, especially since most surface changes are caused by oxidation. XPS monitors the proportions of the several elements of which the material is composed. It is particularly sensitive to an increase in the amount of oxygen during the course of photooxidation. The method is applicable to a quantitative determination of the change particularly when supported by other techniques. As with ESCA, it should be understood that the results are affected by sample surface contamination.

13.7 PHYSICAL PROPERTIES OF MATERIALS

A word of caution should be given to those who would like to follow weathering progress by monitoring the changes in physical properties. Although physical parameters are useful secondary indicators (and necessary to warranty product performance), they do not provide the researcher with an understanding of the reasons for the changes. For example, a mass change may be due to organic binder decomposition but may also be caused by extraction of various materials, filler loss, etc. Similarly, a density increase might be caused by polymer crystallization or the physical loss of low density components. It is therefore suggested that this data should be used only to record changes and not to make fundamental conclusions.

13.7.1 MASS CHANGE^{1,59,60,160258-259}

Measurement of mass change is a relatively simple method of measurement which gives reliable data for the evaluation of changes in weathered materials. Mass loss in paint depends on the amount of pigment (Fig. 16.1) and its flocculation gradient (Fig. 16.7) and correlates with chalk value. Also, correlation of mass loss in PU-acrylate clearcoats with determinations by other methods such as IR, ¹³C-NMR, and GC-MS, indicates that mass loss relates to the presence of secondary hydroxyl groups in the polymer and these groups facilitate degradation. Mass loss accompanies changes in composites (Fig. 17.46). It can also help to monitor interface hydrolytic stability if material absorbs water (Figs. 13.22 and 14.48). Determination of mass change, though it cannot contribute to

the understanding of the mechanisms of change, is useful in judging the effect of weathering given that mass retention is important for product performance.

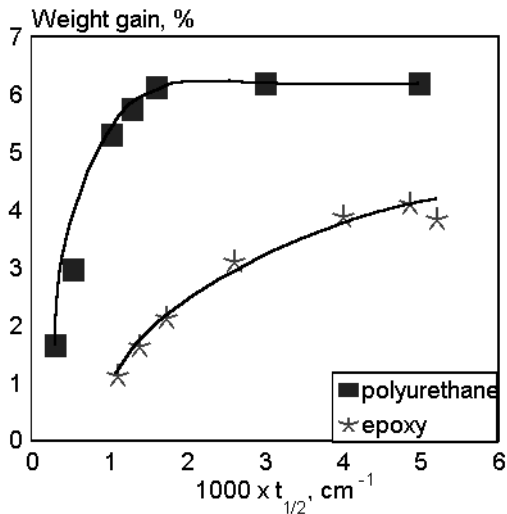


Fig. 13.22. Water uptake by epoxy and polyurethane composites at 100°C. [Adapted, by permission, from A. Apicella, L. Egiziano, L. Nicolais, and V. Tucci, *J. Mater. Sci.*, 23(1988)729.]

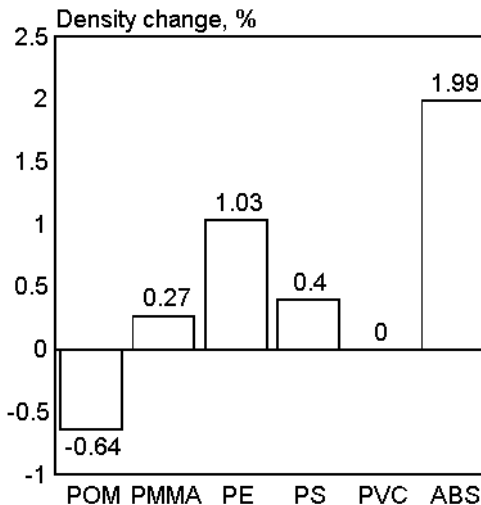


Fig. 13.23. Density change during 5 years of natural exposure. [Data from T. Ito, H. Imai, S. Nagai, and K. Iizuka, *Kenkyu Hokoku-Kogyo Gijutsuin*, 2(1981)159.]

13.7.2 DENSITY^{17,100,260}

Weathered polymers usually undergo a density change. Density usually increases, but the direction it takes depends on the polymer (Fig. 13.23). It is apparent that density change is not an indicator of weatherstability, since PVC would be rated as more stable than PMMA, which is not the case.

The density of a polymer varies with the degradation depth as shown in the evaluation of polyethylene (Fig. 7.15). Wuster²⁶⁰ found that increased density resulted in reduced diffusion, probably as a result of polyethylene crosslinking and crystallinity increasing.

13.7.3 CONTACT ANGLE^{19,261262}

Precise determination of contact angle is possible through the use of a goniometer. From contact angle measurement, the surface energy can be calculated.²⁶¹ Fig. 13.24 shows the change of contact angle during the weathering of two polymers. During the weathering, the properties of polymers change from hydrophobic to hydrophilic, because photooxidation increases the concentrations of hydroxyl, carboxyl, and carbonyl groups, all of which are hydrophilic.

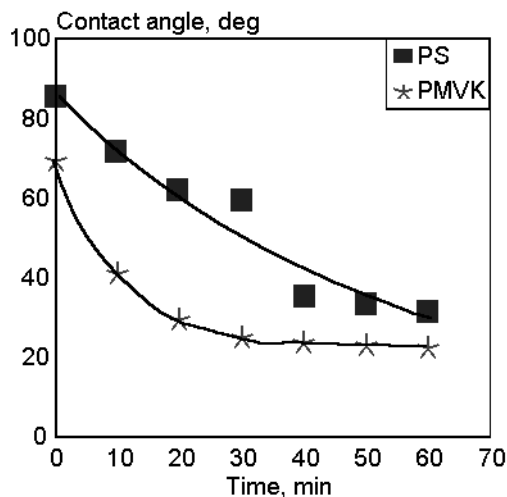


Fig. 13.24. Contact angle vs. irradiation time using unfiltered radiation from low pressure mercury lamp. [Adapted, by permission, from K. Esumi, K. Meguro, A. M. Schwartz, and A.C. Zettlemoyer, *Bull. Chem. Soc. Jpn.*, 55(1982)1649.]

In a recent paper,²⁶² contact angle measurement was used in polystyrene, PS, photolytic studies. Because the degraded layer is only 10 nm thick, other methods would not be effective. It can be assumed that the change of critical surface wetting tension is proportional to the changes in the concentration of oxidation products because oxygen-containing groups will influence the specific free energy of the surface. An initial change of critical surface tension was assumed to be caused by the way in which material was processed. The conclusions drawn about the chemical composition of degradation products and the kinetics of their formation were not supported by evidence from other methods so the proposed presence of these groups is speculative.

Similar studies for paints¹⁹ show that, during weathering, the contact angle for gray polyurethane paint changed more than that for a clear polyurethane, whereas, in all other studies, the gray polyurethane was more resistant. This suggests that, although the information on material surface wetting is important in weathering studies (especially when one considers factors such as acid rain, etc.), contact angle cannot be treated as an indicator of weathering resistance. Especially now, when products have complex composition, their surfaces may differ entirely from the bulk because the surface may be covered by a migrating, incompatible additive which is at a concentration that differs from that in the bulk.

Contact angle measurement does offer important information but the results of these measurements must be related to other data which help to identify the chemical changes that occur on the surface. It is also important to notice that further development of this method will only happen when complex studies are carried out which can form a basis of correlating this data with data from better understood methods of monitoring UV degradation.

13.7.4 DIFFUSION OF GASES AND WATER TRANSPORT IN POLYMERS^{19,260,263,264}

Efforts to relate weathering performance to the difference of gases and movement of water in polymers are reviewed only to show their degree of relevance. They cannot be adequately discussed until extensive studies are completed. Diffusion of gases, such as oxygen and pollutants is obviously of interest because it may affect the degradation rate.

It was observed in poly(ether-block-amide) that the diffusion coefficients of nitrogen and oxygen decrease as irradiation progresses. This may be one of the reasons that the rate of degradation decreases with time.

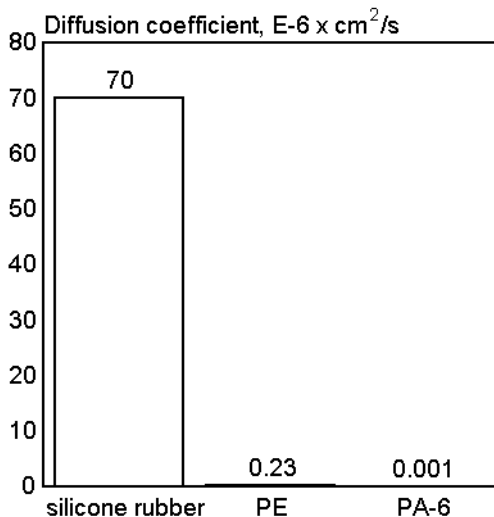


Fig. 13.25. Diffusion coefficients. [Data from C. E. Rogers, *ASC Symp. Ser.*, 220(1983)231.]

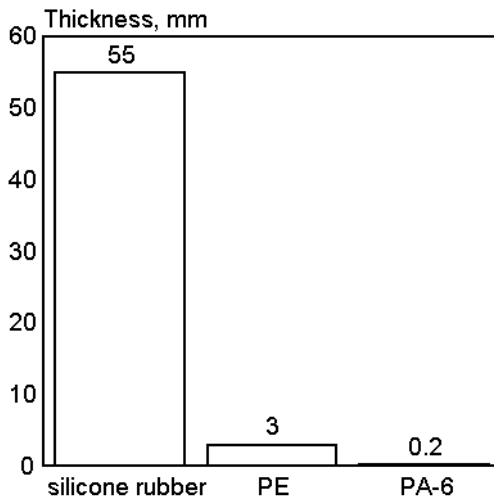


Fig. 13.26. Thickness of protective layer. [Data from C. E. Rogers, *ASC Symp. Ser.*, 220(1983)231.]

Water vapor transmission rate in coatings was shown to be relative to coating durability.¹⁹ Sorption of water decreased as the polyethylene degradation rate increased. Rogers²⁶³ determined the thickness of the layer of polymeric material that was needed to give an interface protection and related it to the water diffusion coefficient. Depending on external conditions and the moisture diffusion coefficient of a material, there is a specific amount of static sorbed moisture at the polymer-substrate interface. Fig. 13.25 gives a comparison of moisture diffusion coefficients for three polymers; Fig. 13.26 gives the values of material thickness needed to achieve a change in the amount of sorbed moisture at the substrate/coating interface. These figures show that silicon rubber would require a much higher thickness in order to prevent presence of static sorbed moisture at the interface. It can be concluded that the above measurements do offer important additional information for the design of durable material although they do not provide an insight into the reasons that a material is, or is not, weather stable.

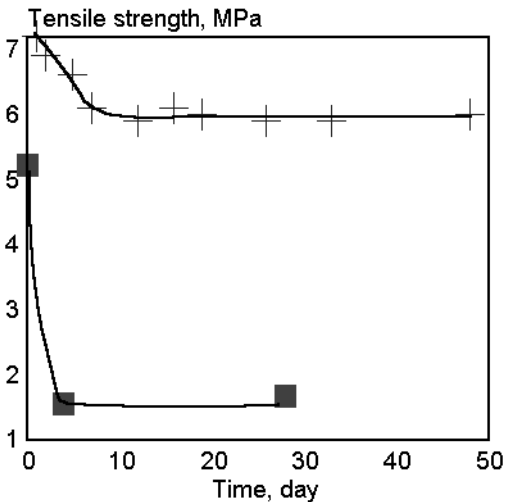
13.7.5 ELECTRICAL PROPERTIES^{15,258,265-269}

Fig. 13.27. Near DC impedance (+) and tensile strength (■) as a function of exposure time to 1 ppm SO₂ and 95% relative humidity. [Adapted, by permission, from T. C. Simpson, H. Hampel, G. D. Davis, C. O. Arah, T. L. Fritz, P. J. Moran, B. A. Shaw, and K. L. Zankel, *Prog. Org. Coat.*, 20(1992)199.]

Electrical properties, such as volume and surface resistivities, permittivities, and dissipation factors, were found to depend on moisture uptake.²⁵⁹ Electrochemical impedance spectroscopy was used to evaluate the damage to painted steel substrates.¹⁵ The method was developed to make continuous measurements of changes when samples were exposed in an atmospheric chamber. Steel coupons had a gold electrode grid deposited on about 10% of their exposed surface. Fig. 13.27 shows that tensile adhesion strength correlates well with impedance and that this data can be used for monitoring the progress of degradation. Impedance change depends on the type of atmosphere in which the sample was exposed. The presence of SO₂ increases the degradation rate of a painted interface. Faradic impedance measurements were conducted to evaluate the protective quality of coatings against corrosion.²⁶⁹

The time to breakdown or voltage breakdown tests were used to test cables exposed to wet conditions.²⁶⁵ Capacitor grade polypropylene films were tested in a nuclear reactor.²⁶⁶ Electrical stress, AC and DC breakdown voltages, and volume resistivity were measured and compared with other characteristics of polymer properties such as tensile strength, elongation, and Young's modulus. The effect of temperature and stress in addition to radiation were evaluated. For PE, the measurement of electric properties was applied to the study of mechanism of degradation.²⁶⁷ Several dielectric properties were used in these studies, including conductivity, isothermal polarization current, dielectric dissipation, and intensity of thermally stipulated polarization current. The kinetics of photodegradation was monitored using these methods.

13.7.6 OTHER PHYSICAL PARAMETERS^{270,271}

Studies of the coefficient of linear thermal expansion of roofing materials did not show great variations.²⁷⁰ Lee and McGarry used a precision glass volume dilatometer to determine and monitor volume changes of polystyrene during quenching and degradation.²⁷¹

13.8 THERMAL METHODS^{15,19,29,32,108,116,145,160,164,174,179,245,258,272-278}

A broad range of methods was developed to study the thermal properties of materials including differential scanning calorimetry, DSC, differential thermal analysis, DTA, differential thermal gravimetry, DTG, dynamic mechanical spectroscopy, DMS, thermogravimetry, TG, thermal mechanical analysis, TMA, and thermogravimetric residual gas analysis, TGRG. All of these methods were used to study some aspects of weathering. Usually, an effort was made to establish the properties of polymer specimens, to compare T_g temperature with the molecular weight trend or with crystallinity data acquired from other methods.

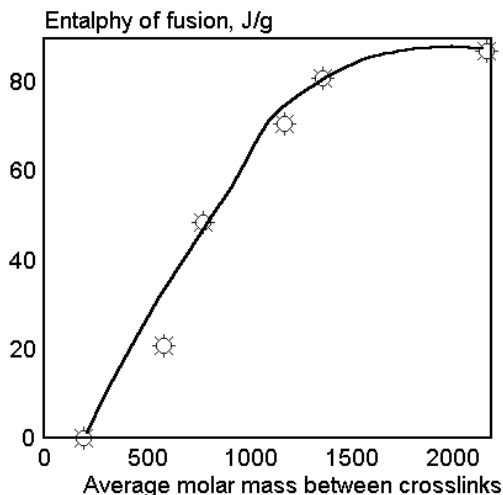


Fig. 13.28. Enthalpies of fusion, ΔH_f , vs. molar mass between crosslinks, M_c , for PEO networks. [Adapted, by permission, from S. J. Clarkson, J. E. Mark, C. -C. Sun, and K. Dodgson, *Eur. Polym. J.*, 28(1992)823.]

FTIR and DSC were used to characterize biodegradation of polyethylene.¹⁶⁴ DSC measurements were performed to study changes in crystallinity during biodegradation and FTIR was used to monitor double bond and carbonyl formation. Biodegradation proceeds in the amorphous regions with an accumulation of oxidation products. Comparison of X-ray results and DSC data was made for an ethylene-propylene copolymer.¹⁷⁹ Increasing the amount of ethylene caused a decrease in crystallinity according to both methods. During degradation, crystallinity initially decreases, then increases later. Analysis of this data was supported by NMR and intrinsic viscosity measurements.

Thermal methods are affected by so many factors that they can never, by themselves, provide quantitative information about the degradation process. One study²⁷²

Gravimetric measurements of sorption and desorption were performed for epoxy resins.¹⁶⁰ Fig. 14.48 shows the data obtained. Chemical (IR) and rheological changes were compared to physical changes. Water plasticizes resins which results in a greater chain mobility and more chain scissions. TGA and DTA were used simultaneously to study PU.²⁷⁴ The results showed that the addition of CaCO_3 to PU gives it fire-resistant properties because CaCO_3 acts as heat sink. In the presence of CaCO_3 , PU degraded in 3 different kinetic steps. The last two steps proceeded as endothermic processes. Fig. 13.28 shows that the enthalpies of fusion of PEO networks increase as molar mass increases between crosslinks.²⁷⁶ Here, bulky junction points which act as defects and retard crystallinity.

discusses thermal properties changes during outdoor exposure of polyethylene. The results obtained by DSC, TMA, TG, DTG did not show relevant changes during 8 months exposure. Some authors have attempted to show that samples have a lower thermal stability due to photooxidation during weathering. However, there are direct methods which can determine the extent of oxidation. Thermal analysis can provide additional information regarding changes in crystallinity and can monitor the concentration of volatile components formed or absorbed by samples.

13.9 RHEOLOGICAL PROPERTIES OF MATERIALS^{33,90,106,109,160,179,201,279-286}

Most studies in this area are limited to a determination of the viscosity of a solution of the initial and the degraded samples. The result is then recalculated to M_v using Mark-Houwink's equation. A creep/recovery test was used to study degradation of bituminous materials (Fig. 13.29). Substantial changes can be observed, as seen from Figs. 17.60 and 17.61. Other studies,²⁸⁰ using the creep-to-failure test, were designed to understand the temperature effect in environmental stress cracking of polyethylene.

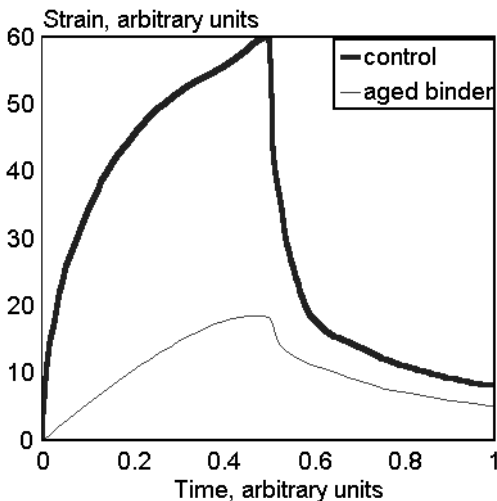


Fig. 13.29. Creep-recovery of SBS binder used in bitumens. [Adapted, by permission, from J. C. Marechal, *Durability Building Mater.*, 1(1982/83)201.]

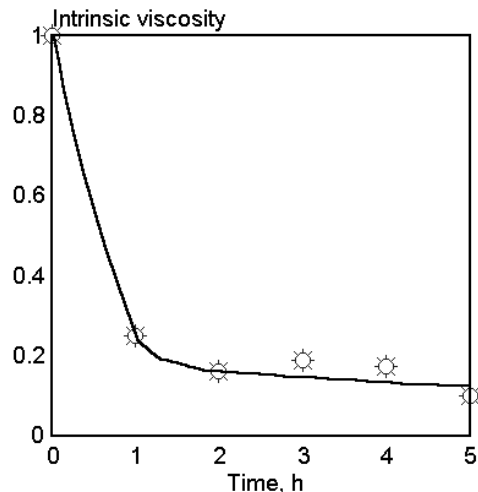


Fig. 13.30. Changes in intrinsic viscosity of PMMA exposed to medium pressure mercury lamp. [Data from A. Torikai, S. Hiraga, and K. Fueki, *Polym. Deg. Stab.*, 37(1992)73.]

The intrinsic viscosity of ethylene-propylene copolymer decreases with time.¹⁷⁹ Since the material became fully soluble, it was concluded that viscosity changes were caused by chain scission. Fig. 13.30 shows changes in intrinsic viscosity of PMMA with exposure time. The degradation mechanism is chain scission or crosslinking when less

material will dissolve. This is indicated by a reduction in intrinsic viscosity. Further calculations are required to make this inference.²⁸⁵ Calculations are based on intrinsic viscosity measurements which give the number average molecular weight. Chain scission can be calculated from the relationship: $CS = (M_o/M_t) - 1$.

Several observations can be made from dynamic mechanical analysis regarding extent of degradation and crosslink density.²⁸⁴ Polyurethane automotive clearcoats were degraded in xenon-arc instrument and in outdoor exposure in Florida. The $\tan\delta$ peak broadens then splits into two peaks in the course of exposure. At the same time, peak height decreases. Crosslink density increases during degradation. This is inferred from $E'(\min)$ measurements. When rheological data was compared with IR data consistent mechanisms were observed. Dynamic mechanical testing was also used to evaluate the effect of absorbed moisture on the mechanical properties of carbon fiber reinforced polyamide-6,6.²⁸⁶

Rheological property measurements are not likely to play an essential role in future studies. They will be useful only in cases where complex chemical material composition makes chemical analysis too complicated.

13.10 MECHANICAL PROPERTIES

Most materials tested for weathering performance must retain their mechanical properties during their expected service-life duration. A specific mechanical property becomes the reference to which most studies relate.

13.10.1 TENSILE STRENGTH^{27,33,36,50,65,101,103,104,152,270,287-314}

Tensile strength retention during weathering was studied for most commonly-used materials. Tensile strength is always an individual characteristics of a material (see Fig. 13.31). Tensile strength may either increase or decrease during weathering. Usually, the changes in tensile strength are quite sensitive to the changes in the molecular weight of the polymer (Fig. 13.32). In most cases, tensile strength decreases during exposure.^{301,306} In some cases, an initial increase of tensile strength is followed by quite rapid deterioration.^{300,306}

Tensile strength can be determined with high precision, as shown by Suzuki²⁹⁰ (Table 13.3).

Tensile strength measurements are more precise when measured on durable specimens and less precise when applied to more severely degraded specimens. However, the precision of the method also depends on the method of specimen preparation and on the morphology of degraded specimen.

Keshavaraj and Tock³⁰³ used the ideal elastomer concept to calculate crosslink density of sealants during weathering. Their calculations were based on tensile test results determined at fixed elongations.

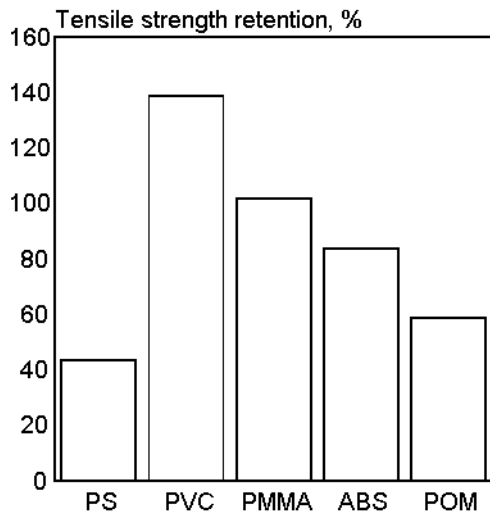


Fig. 13.31. Tensile strength retention during 3 years of natural exposure. [Data from T. Tsurue and S. Suzuki, *Hokkaido Kogyo Kaihatsu Shikesho Hokoku*, 24(1981)136.]

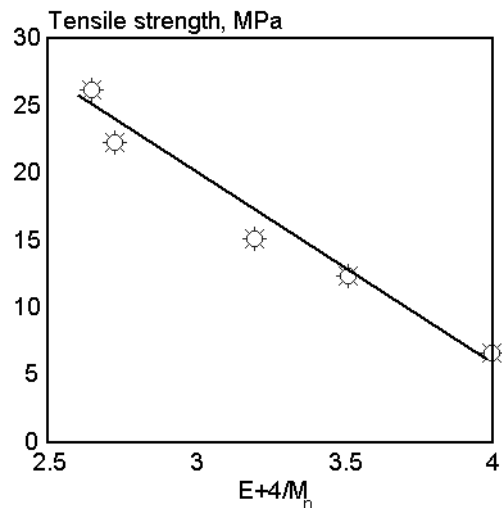


Fig. 13.32. PS tensile strength vs. reciprocal M_n change as an effect of irradiation. [Data from G. Geuskens, G. Delaunois, Q. Lu-Vinh, W. Piret, and C. David, *Eur. Polym. J.*, 18(1982)387.]

Table 13.3: The range of variation coefficients of tensile strength determination for specimens degraded for 0, 500, 1000, 1500, and 2000 h

Polymer	Range of variation coefficient, %
PS	3-6
PVC	0.4-1
PMMA	0.5-2
ABS	2-4
POM	0.5
PE	1

effect” and the subsequent recovery is important to consider when weathering studies seem to give large errors. The joint phenomena cause complex, time-dependent changes in exposed specimens which could be interpreted as errors in determination.

Kim *et al.*³¹¹ discuss what they observed when they exposed PC and tested it. They describe a “pop-in” phenomenon (see Fig.11.4). The phenomenon is related to crack propagation as discussed in Chapter 11. Note that stress distribution in the sample may affect its tensile strength readings. Schoolenberg and Meijer³¹⁴ discuss what they call the “crack speed effect” which causes drastic reduction of strength after a certain level of exposure. After longer exposure, they found that material strength increases. This phenomenon is related to the distribution and the density of surface cracking. The combination of the “crack speed

13.10.2 ELONGATION^{38,65,103,104,110,288,290,293-295,301,306,315-317}

Photodegradation of a material produces a greater effect on its ability to stretch than on its tensile strength. Fig. 7.18 shows that elongation changes also depend on specimen thickness. Elongation retention of a polymer is dependent on its composition and type of polymer (Fig. 13.33).

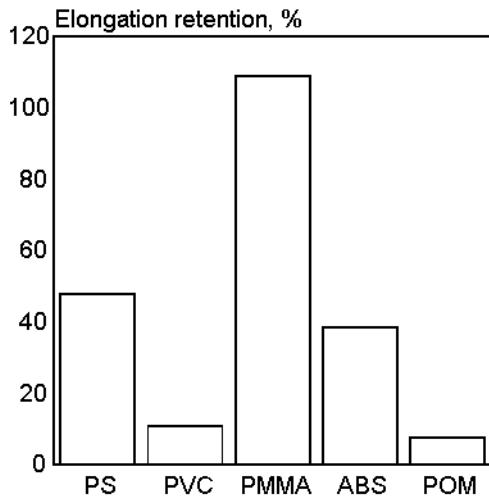


Fig. 13.33. Elongation retention during 3 years of natural exposure. [Data from G. Geuskens, G. Delaunois, Q. Lu-Vinh, W. Piret, and C. David, *Eur. Polym. J.*, 18(1982)387.]

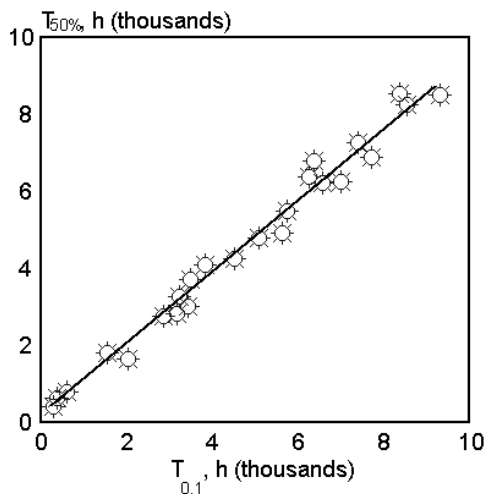


Fig. 13.34. Time to 0.1 carbonyl absorbance ($T_{0.1}$) vs. time to 50% retained elongation for LDPE film exposed in Weather-O-Meter. [Adapted, by permission, from F. Gugumus, *Polym. Dev. Stab.*, 8(1987)239.]

Table 13.4: The range of variation coefficients of elongation determination for specimens degraded for 0, 500, 1000, 1500, and 2000 h

Polymer	Range of variation coefficient, %
PS	6-8
PVC	50-80
PMMA	10-15
ABS	50-60
POM	15-35

The data in Figs. 13.31 and 13.33 shows that there is no correlation between tensile strength and elongation retention. Elongation depends more on changes occurring in the amorphous phase; tensile strength depends more on what happens in crystalline regions. Elongation measurements (Table 13.4) are much less precise than tensile strength measurements (Table 13.3).

Elongation retention correlates very well with chemical change during photooxidation (Fig. 13.34). The 50% elon-

gation retention time has a linear correlation coefficient, $r^2=0.98$ with a time to 0.1 carbonyl absorbance.

13.10.3 FLEXURAL STRENGTH^{270,289,290,295,318-321}

Flexural strength retention is important for many products, especially structural composites used for demanding applications. Flexural strength retention follows the pattern of tensile strength retention (Fig. 13.35).

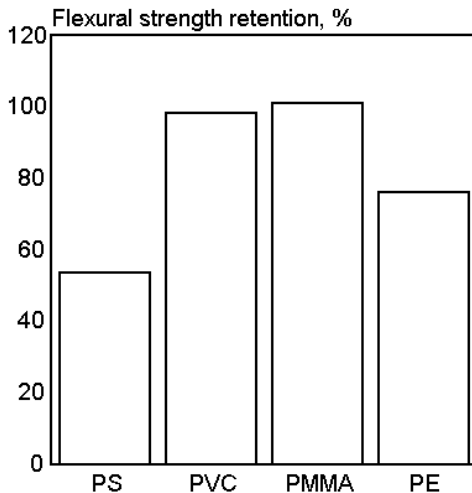


Fig. 13.35. Flexural strength retention during 1 year of natural exposure [Data from S. Suzuki, H. Kubota, O. Nishimura, and T. Tsurue, *Hokkaido Kogyo Kaihatsu Shikensho Hokoku*, 24(1981)153.]

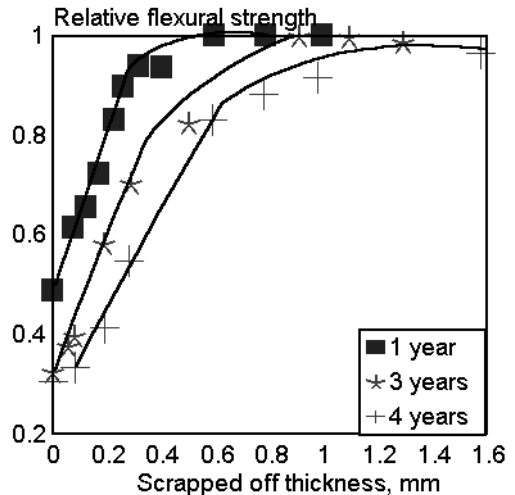


Fig. 13.36. Change of flexural strength after scraping off the surface for exposed PS sheets. [Adapted, by permission, from Y. Watanabe, F. Kitajima, and T. Shiota, *Kenkyu Hokoku-Kogyo Gijutsuin*, 2(1981)155.]

The error of flexural strength determination is similar to that of tensile strength determination (Table 13.5). Watanabe³²¹ measured the flexural strength of exposed specimens of PS and ABS which were surface scrapped after exposure. These measurements were compared to the flexural strength of unexposed material scrapped to the same thickness (Figs. 13.36 and 13.37). Changes of flexural strength are clearly related to material surface deterioration. The cracks in the degraded surface layers act as the notch for fractures and dominate as the failure mode.

13.10.4 OTHER MECHANICAL PROPERTIES

Tear strength retention might be considered as a quality factor in some materials.^{36,51} Photoprotective agents such as antioxidants and UV absorbers were found to improve tear resistance retention (Fig. 13.38). Similarly, the quality of a new reaction injection

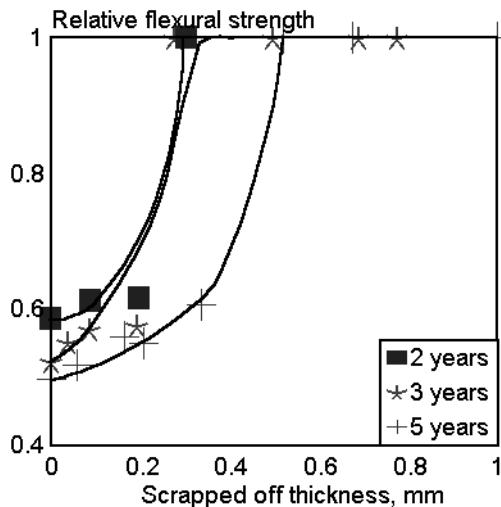


Fig. 13.37. Change of flexural strength after scraping off the surface for exposed ABS sheets. [Adapted, by permission, from Y. Watanabe, F. Kitajima, and T. Shirota, *Kenkyu Hokoku-Kogyo Gijutsuin*, 2(1981)155.]

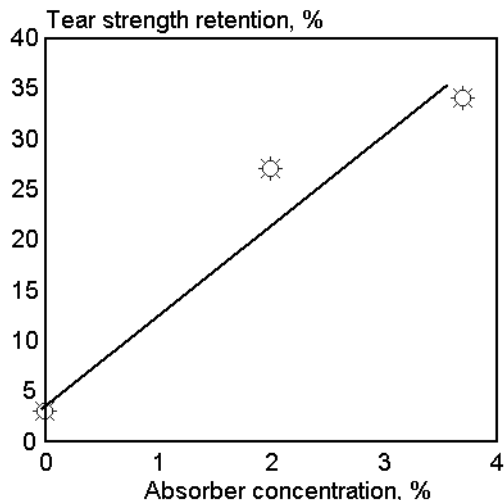


Fig. 13.38. Tear strength retention of wool fabric, exposed to summer light through glass for 22 weeks, depending on concentration of sterically hindered benzotriazolesulfate. [Data from C. M. Carr and I. H. Leaver, *J. Appl. Polym. Sci.*, 33(1987)2087.]

Table 13.5: The range of variation coefficients of flexural strength determination for specimens degraded for 0, 500, 1000, 1500, and 2000 h

Polymer	Range of variation coefficient, %
PS	4.1-5.3
PVC	0.7-5.2
PMMA	0.4-1.1
ABS	0.8-1.0
POM	0.6-1.9
PE	0.7-1.5

molding, RIM, system for automotive window encapsulation was evaluated based on tear strength.³⁶

Shear strength and adhesion are important indicators of quality for products such as sealants,^{25,322,323} adhesives,³²⁴ paints, coatings,⁵⁸ wood coatings,⁵ and composites.³²⁰ Durability of several sealants (Figs. 17.54 to 17.56) was evaluated by measurement of shear strength with a standard deviation of 2-10% for four specimens. Adhesion measurement was effectively used to evaluate the effect of initial erosion of wood on paint performance (Fig. 17.75). The adhesive strength measurement was also

used as an indicator when an artificial weathering system (EMMAQUA) was compared with natural weathering. These studies show that shear strength is a sensitive indicator

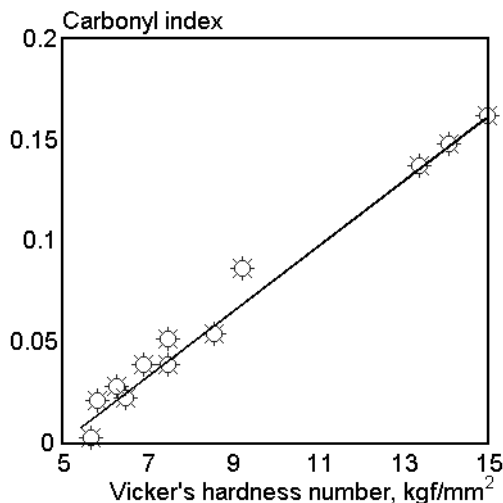


Fig. 13.39. Carbonyl index vs. Vicker's hardness number of weathered polyethylene sheets. [Adapted, by permission, from Y. Watanabe and T. Shiota, *Kenkyu Hokoku-Kogyo Gijutsuin*, 2(1981)141.]

of weathering changes, especially when moisture plays an essential role in weathering behavior.

Hardness^{59,100,325,326} is easy to measure. It inspired Japanese researchers^{100,326} to conduct a thorough examination of hardness measuring methods, including Rockwell, Barcol, and Vicker hardness for several important polymers. The Vicker hardness number correlates very well with the carbonyl index of exposed polyethylene sheets (Fig. 13.39). Barcol and Rockwell hardness correlated very well with one another and with tensile and flexural strength measurements on PS, PVC, PMMA, ABS, POM, PE, which were not exposed to weathering. After weathering, the universal correlation is mostly lost, but Barcol hardness may still be useful for monitoring changes in a single polymer

type. Constant rate penetrometer and Shore hardness measurement were employed in sealant weathering studies.^{59,325} These simple methods can provide some useful information about the degradation process. Sealants, except for polysulfides, consistently increased in hardness during exposure. The microhardness of PMMA/PCTFE blends was measured using the Vicker's diamond pyramid indenter attached to a microscope.³²⁸

Universal fiber tester was used to determine these mechanical properties of fibers under varying conditions of temperature and humidity: tensile strength, creep, dynamic mechanical and fatigue properties.²⁷⁸ The impact strength of ABS and PC was used to monitor the effect of exposure to solar radiation.⁹³ Young's modulus was determined to evaluate the plasticizing effect of water in epoxy resins.¹⁶⁰ Stress relaxation during hydrothermal degradation of coatings was monitored by a tensile testing machine in which the sample was quickly deformed and then the stress required to hold the specimen in the extended position was monitored.¹⁹ A similar method was used for oriented and unoriented samples of PP exposed to UV radiation.¹⁵²

Lightfastness of velour car upholstery was determined by surface abrasion testing. Here, the spacial arrangement of fibers protects the core fabric from degradation but performance of the fabric really depends on how well these surface fibers protect the core and whether or not they have been removed or weakened by abrasion.³⁰² Creep measurement was a method of choice in the evaluation of PE tapes during their exposure to

UV radiation.³²⁶ The effect of exposure under stress was also considered in this study. Lap shear measurements are most frequently used to test the durability of adhesive joints.^{327,330}

The above examples show that many methods exist for mechanical testing and most of them are useful for evaluating degradation. The application of a particular method depends on the requirements of performance of a particular material since the properties of weathered materials are frequently compared with the properties of unexposed materials. Many product specifications require the retention of a particular property after a specified degradation time. It is unusual for a scientific report to give only the result of mechanical analysis without reporting data from other supporting studies designed to understand the nature of changes and what methods can be used to improve stability.

13.11 OTHER METHODS OF ANALYSIS

13.11.1 MOLECULAR WEIGHT

ANALYSIS^{28,38,65,75,79,81,83,84,88,97,102,109,136,139,145,147,154,162,166,173,176,184,192,199,209,211,223,276,281,299,331-345}

Molecular weight is one of the parameters most affected by weathering. However, when molecular weight is used as an indicator of degradation, both crosslinking and chain scission occur simultaneously, and the interpretation of results is complicated by the fact that crosslinking and chain scission occur simultaneously.

Molecular weight distribution is most often determined by gel permeation chromatography, GPC. It is sometimes estimated by measuring polymer solution viscosity using capillary viscometers.⁸¹ When GPC is used, samples of materials are dissolved in a good solvent, filtered to remove insoluble particles, and the solution analyzed by GPC. Changes in molecular weight can be observed from the surface area under the GPC peak and from the change in elution volume as degradation progresses.¹⁸⁴ A calibration curve is obtained, using polystyrene, polyethylene, and n-paraffins as standards but frequently, an absolute viscosity detector (universal calibration procedure) is used. Mark-Houwink constants of standards are used to calibrate a method for each polymer used.¹⁷⁶ The refractive index, IR, or UV detectors are used. In some cases, an internal marker is added to the solvent to monitor the rate of solvent flow which should be constant for the results to be valid.³³⁷ Further details of the method are discussed elsewhere.³³⁷ A method of recalculating results from GPC measurements to determine chain scission can be found in a recent publication.³⁴⁴ In some cases, membrane osmometry is also employed to determine molecular weight change.⁷⁹ This determination might be combined with monitoring low molecular weight substances by MS. Also, steric exclusion chromatography is used.³³⁸

Nagatsuka³³⁵ shows that molecular weight and tensile strength correlate well (Fig. 13.40). The effect of irradiation may cause an increase in molecular weight. This is evi-

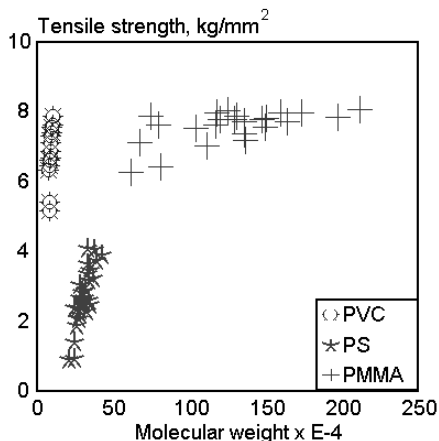


Fig. 13.40. Molecular weight vs. tensile strength of weathered samples. [Adapted, by permission, from Y. Nagatsuka, T. Shiota, K. Yoshikawa, S. Suzuki, H. Kubota, and O. Nishimura, *Kenkyu Hokoku-Kogyo Gijutsuin*, 2(1981)79.]

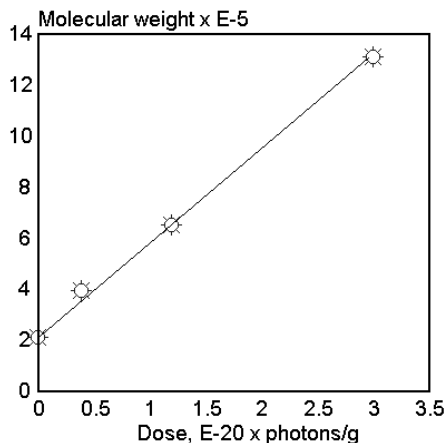


Fig. 13.41. Molecular weight of [(n-dodecyl)(Me)Si]_n vs. absorbed radiation. [Adapted, by permission, from P. Trefonas, R. West, R. D. Miller, and D. Hofer, *J. Polym. Sci., Polym. Lett. Ed.*, 21(1983)823.]

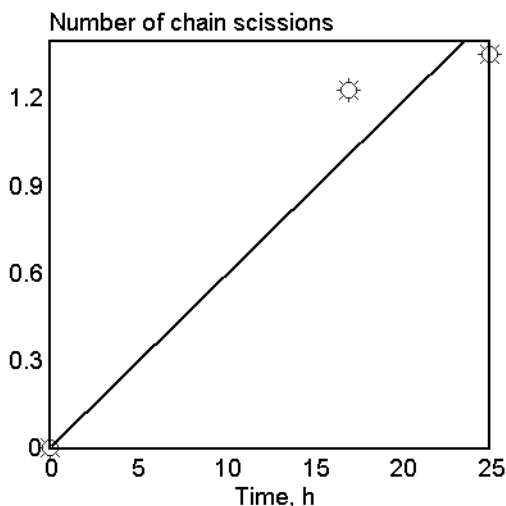


Fig. 13.42. Chain scissions number per PS molecule vs. irradiation time by mercury lamp at 50°C. [Adapted, by permission, from I. Mita, T. Takagi, K. Horrie, and Y. Shindo, *Macromolecules*,

dent in the case of silicones (Fig. 13.41). In most cases, a considerable decrease in molecular weight occurs during the course of degradation (Fig. 13.42).

Much data demonstrates that changes in molecular weight occur on the material surface (Figs. 7.7-7.10). Changes in molecular weight depend on the temperature of irradiation (Fig. 13.43). The curves follow the equation: $1/M_n(D) = 1/M_n(0) + G_s D/9.65$. This suggests that only scissions of the main chain take place without crosslinking.²¹¹ Suppression of scission at lower temperatures is due to impurities (monomer) which are present in the PMMA tested. Purified PMMA behaves differently.

Molecular weight analysis can be used for depth profiling of UV degradation (Fig. 13.44). Molecular weight measurements, although influenced by complexity of degra-

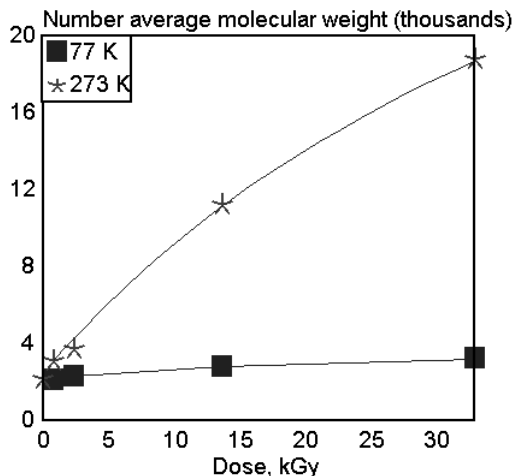


Fig. 13.43. Change in number average molecular weight of PMMA during γ -irradiation at different temperatures. [Adapted, by permission, from T. Ichikawa, K. -I. Oyama, T. Kondoh, and H. Yoshida, *J. Polym. Sci., Polym. Chem.*, 32(1994)2487.]

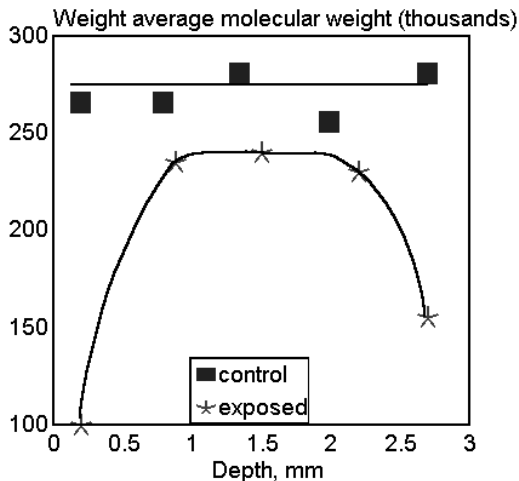


Fig. 13.44. Depth profile of molecular weight of PP as injection molded (control) and exposed for 6 weeks to UV radiation. [Adapted, by permission, from B. O'Donnell, J. R. White, and S. R. Holding, *J. Appl. Polym. Sci.*, 52(1994)1607.]

dation mechanisms, are an important indicator of degradative changes and the number of references indicates that it is certainly the most popular method of degradation monitoring. It cannot be used in the case of crosslinked polymers; crosslinking reactions during degradation may induce considerable error.

13.11.2 GAS AND LIQUID CHROMATOGRAPHY^{154,158,192,199,319,343,345-352}

Several applications of gas chromatography, GC, and liquid chromatography, LC, were used recently in weathering studies. GC and LC are usually interfaced with IR or mass spectroscopy, MS, which are the qualitative detectors. GC-MS or GC-IR are most often used to analyze the volatile components of degradation. Material exposed to weathering was first reduced with LiAlH_4 then analyzed by GC-MS. This gave a detailed analysis of degradation products that has helped to explain the mechanism of degradation.

High pressure liquid chromatography, HPLC, was employed to estimate the purity of monomer used for synthesis of polymeric materials for biological degradation studies.³⁴⁵ In the study of UV stabilizers performance, HPLC was used to identify stabilizers and the reaction products formed by them in the course of degradation.³⁴³ A similar study was conducted for HALS which had been synthesized by hydrosilanization for PP stabilization.^{154,199}

PE was degraded in sealed vials then analyzed by GC to identify and quantify the volatile components produced during degradation.¹⁵⁸ The reaction of HALS in PP was studied using model compounds irradiated in the liquid state and composition of reaction products was followed by GC.³⁵⁰ Similarly, model compounds of polyimides were studied by GC-MS.³⁵² GC is used frequently in γ -irradiation studies. Gas evolution of several aromatic polymers was followed by this method.³⁵¹ This method is suitable for these types of studies because γ -radiation can penetrate most sealed containers (for UV degradation studies, special quartz vials must be used).

It is, in fact, surprising that these methods are not more commonly used in weathering studies; they are precise, economical, and available in most laboratories. Also, many degradative changes result in the formation of gaseous products detectable by GC and GC-MS.

13.11.3 TITRIMETRY^{131,133,189,353,354}

The changes in concentration of piridinyl amine and free base in copolymers were followed by conductometric and potentiometric titrations. Also, in polyurethane studies, the degradation rate was estimated by determining amine and hydroxyl equivalent. Of these methods, hydroperoxide titration is the most suitable considering that hydroperoxides are common by-products of photooxidation.^{133,189,354} A specimen of degraded material is cryogenically ground to a fine powder and a swelling solvent is used to loosen crosslinked particles (if needed) or the material is dissolved in a good solvent. Hydroperoxides are determined by iodometric titration. Titrimetry is an under-utilized method. It has the potential to yield much more information that has been generated by the few recent studies that have been done until now. Titration analysis is selective and accurate and it can often give more precise information than some spectral methods.

13.11.4 DEHYDROCHLORINATION RATE³⁵⁵⁻³⁵⁸

Hydrogen chloride is the major product of PVC degradation. Methods of determining HCl are well developed^{357,358} and have provided researchers in the PVC area with much relevant information. The equipment proposed by Sastre³⁵⁵ may assist in obtaining valuable research data such as given in Fig. 13.45.

It seems that using a similar approach in the study of other polymers that produce a major component during degradation would be helpful in extending the knowledge of degradation mechanisms and the kinetics of these processes.

13.11.5 GEL FRACTION^{40,66,102,112,163,233,305,359-361}

Irradiation of many polymers produces an insoluble gel which cannot be studied by gel permeation chromatography, GPC. The determination of gel fraction circumvents this barrier. Applications of gel fraction analysis for polystyrene, polyurethanes, and polyethylene are reported in the literature.^{66,102,112} Fig. 13.46 gives an interesting compari-

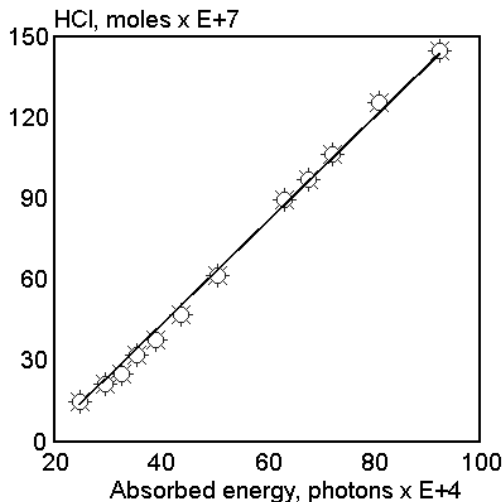


Fig. 13.45. Dehydrochlorination vs. energy absorbed from mercury lamp. [Adapted, by permission, from R. Sastre, F. Castillo, G. Martinez, and J. L. Millan, *Rev. Plast. Mod.*, 54(1987)237.]

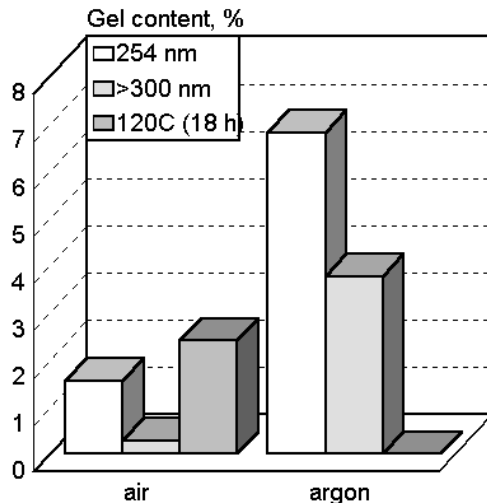


Fig. 13.46. Content of gel after UV irradiation for 18 h and heating at 120°C for 14 h. [Data from P. Jiang-Qing and Z. Jie, *Polym. Deg. Stab.*, 36(1992)65.]

son of gel formation under different conditions of PET sample degradation.³⁰⁵ A substantial difference in mechanism exists between thermal and UV degradation. In UV degradation more crosslinks are formed in the absence of oxygen. Heating the sample in the absence of oxygen does not affect gel content. Oxygen is necessary to form conditions for crosslinking. A mercury lamp without a filter causes type of degradation that differs significantly from that produced in normal conditions of weathering.

When the gel fraction of PE was determined in the presence of a photoinitiator (anthraquinone derivatives of various chemical structure), it was found that gel formation was proportional to the diffusion constant of the photoinitiator.²³³

The amount of gel formed during the photocrosslinking of LDPE was measured to understand the importance of process parameters, such as irradiation time, intensity of radiation, and type of crosslinker.³⁶⁰

13.11.6 OXYGEN UPTAKE^{139,157,168,190,362}

Oxygen uptake can be studied by monitoring oxygen consumption in a closed manometric system,^{139,157,168,190} by analysis of gas phase by GC,³⁶² or from titration of carboxylic groups or IR analysis.^{139,168} In each case, samples must be exposed in a closed system which permits monitoring and control of the surrounding atmosphere. This method permits the direct observation of the kinetics of photooxidation under well controlled condi-

tions. However, the conditions of the experiment are artificial because the composition of gaseous products differs substantially from natural conditions.

REFERENCES

1. L. A. Simpson, *Austral. OCCA Proc. News*, 20(1983)6.
2. L. A. Simpson, *Polym. Paint Colour J.*, 176(1986)408.
3. M. Camina, Evaluation of some artificial weathering cycles, *Report*, PB88-223953(1981).
4. R. S. Whitney, J. I. Fry, and R. J. Cordner, *J. Oil Colour Chem. Assoc.*, 67(1984)63.
5. A. Underhaug, T. J. Lund, and K. Kleive, *J. Oil. Colour Chem. Assoc.*, 66(1983)345.
6. W. C. Feist, *For. Prod. J.*, 37(1987)15.
7. W. C. Feist and J. Sell, *Wood Fiber Sci.*, 19(1987)183.
8. W. R. Sharman, J. I. Fry, and R. S. Whitney, *Durability Building Mater.*, 2(1983)79.
9. K. K. Karpati, *J. Coat. Technol.*, 56,719(1984)57.
10. W. W. Kittelberger and A. C. Elm, *Ind. Eng. Chem.*, 39(1947)876.
11. R. S. Williams and W. C. Feist, *Forest Prod. J.*, 43(1993)8.
12. J. N. Rastogi, B. Singh, K. M. Thomas, and V. K. Verma, *Paint India*, (1991)3, 65.
13. J. W. Hook, P. J. Jakox, and J. W. Spence, *Prog. Org. Coat.*, 24(1994)175.
14. G. Fedor and P. Brennan, *The Applicator*, 12(1990)1.
15. T. C. Simpson, H. Hampel, G. D. Davis, C. O. Arah, T. L. Fritz, P. J. Moran, B. A. Shaw, and K. L. Zankel, *Prog. Org. Coat.*, 20(1992)199.
16. M. Morcillo, J. Simancas, J. L. G. Fierro, S. Feliu, and J. C. Galvan, *Prog. Org. Coat.*, 21(1993)315.
17. T. Ito, H. Imai, S. Nagai, and K. Iizuka, *Kenkyu Hokoku-Kogyo Gijutsuin*, 2(1981)159.
18. J. H. Braun, *Prog. Org. Coat.*, 15(1987)249.
19. S. G. Croll, *Prog. Org. Coat.*, 15(1987)223.
20. R. R. Blakey, *Prog. Org. Coat.*, 13(1985)279.
21. L. A. Simpson, I. Melville, and D. V. Moulton, *Polym. Paint Colour J.*, 177(1987)139.
22. T. K. Rehfeldt, *Prog. Org. Coat.*, 15(1987)261.
23. D. Rysavy and H. Tkadleckova, *Polym. Deg. Stab.*, 37(1992)19.
24. M. S. Kitai, V. L. Popkov, and V. A. Semchishen, *Makromol. Chem., Macromol. Symp.*, 37(1990)257.
25. L. M. Gan, H. W. K. Ong, and T. L. Tan, *Durability Building Mater.*, 4(1986)35.
26. S. -T. Chang, D. N. -S. Hon, and W. C. Feist, *Wood Fiber*, 14(1982)104.
27. A. Blaga and R. S. Yamasaki, *Durability Building Mater.*, 4(1986)21.
28. N. Ogata and K. Yoshida, *Zairyo*, 32(1983)1119.
29. M. J. Cassady, G. C. Derringer, M. M. Epstein, A. Lustiger, R. L. Markham, Outdoor weathering of plastic pipe, *Report*, PB83-162073.
30. M. G. Otey, *Polym. Degrad. Stab.*, 14(1986)285.
31. R. P. Burford and D. R. G. Williams, *J. Mater. Sci. Lett.*, 7(1988)59.
32. Y. Fujiwara, *J. Appl. Polym. Sci.*, 27(1982)2773.
33. K. E. Kyllö and C. M. Ladisch, *ACS Symp. Ser.*, 318(1986)343.
34. O. Nishimura, H. Kubota, and S. Suzuki, *Hokkaido Kogyo Kaihatsu Shikensho Hokoku*, 24(1981)115.

35. R. J. Morgan, F. -M. Kong, and J. K. Lepper, *J. Compos. Mater.*, 22(1988)1026.
36. G. H. Slocum, T. N. Thompson, and C. E. Fluharty, *J. Elastom. Plast.*, 19(1987)50.
37. M. Bolle and S. Lazare, *J. Appl. Phys.*, 73(1993)3516.
38. M. M. Qayyum and J. R. White, *Polym. Deg. Stab.*, 41(1993)163.
39. A. Brandwood, K. R. Noble, K. Schinheim, G. F. Meijs, P. A. Gunatillake, R. C. Chatelier, S. J. McCarthy, and E. Rizzardo, *Biomater.-Tissue Interfaces*, 10(1992)413.
40. F. P. La Mantia and D. Kurto, *Polym. Deg. Stab.*, 36(1992)131.
41. J. Pola, D. Tomanova, P. Schneider, V. Dedek, and J. Tlaskal, *J. Fluorine Chem.*, 50(1990)309.
42. A. Denning and N. J. Mills, *Plast. Rubb. Compos. Process. Appl.*, 18(1992)67.
43. R. S. Robinson and H. H. Yuce, *J. Amer. Ceram. Soc.*, 74(1991)814.
44. B. Z. Jang, J. Bianchi, Y. M. Liu, and C. P. Chang, *NASA Conf. Pub.* 3257, p. 319.
45. M. G. Dobb, R. M. Robson, A. H. Roberts, *J. Mater. Sci.*, 28(1993)785.
46. B. Pourdeyemi and A. Nayernouri, *J. Coat. Technol.*, 66(1994)51.
47. J. Sobus, B. Pourdeyhimi, B. Xu, and Y. Ulcay, *Textile Res. J.*, 62(1992)26.
48. J. Sobus, B. Pourdeyhimi, J. Gerde, and Y. Ulcay, *Textile Res. J.*, 61(1991)557.
49. J. R. Druzik, *Environ. Sci. Technol.*, 21(1987)635.
50. P. C. Crews, *Text. Chem. Color.*, 19,11(1987)21.
51. C. M. Carr and I. H. Leaver, *J. Appl. Polym. Sci.*, 33(1987)2087.
52. C. M. Ladisch, R. R. Brown, and K. B. Showell, *Text. Chem. Color*, 15,11(1983)17.
53. A. B. M. Abdullah and L. W. C. Miles, *Text. Res. J.*, 54(1984)415.
54. C. D. Shah and D. K. Jain, *Text. Res. J.*, 54(1984)844.
55. H. S. Freeman and W. N. Hsu, *Text. Res. J.*, 57(1987)223.
56. S. Yajima, Y. Togawa, S. Matsushita, T. Suzuki, and T. Okada, *Kinzoku Hyomen Gijutsu*, 37(1986)718.
57. H. Kubota, S. Suzuki, O. Nishimura, I. Tamura, K. Yoshikawa and T. Shirota, *Hokkaido Kogyo Kaihatsu Shikensho Hokoku*, 24(1981)96.
58. E. Takeshima, T. Kawano, H. Takamura, and S. Kato, *Shikizai Kyokaishi*, 56(1983)457.
59. J. R. Crowder and M. A. Ali, *Durability Building Mater.*, 3(1985)115.
60. K. G. Martin and R. E. Price, *Durability Building Mater.*, 1(1982)127.
61. M. Baird, C. M. Carr, and L. A. Holt, *Textile Res. J.*, 61(1991)210.
62. C. Decker, K. Moussa, and T. Bendaikha, *J. Polym. Sci., Polym. Chem.*, 29(1991)739.
63. S. Mori, *J. Appl. Polym. Sci.*, 33(1987)1923.
64. D. Waksman, W. E. Roberts, and W. E. Byrd, *Durability Building Mater.*, 3(1985)1.
65. A. Ram, O. Zilber, and S. Kenig, *Polym. Eng. Sci.*, 25(1985)535.
66. Z. Osawa, E. -L. Cheu, and K. Nagashima, *J. Polym. Sci., Polym. Chem.*, 15(1977)445.
67. R. K. Jain, B. K. Saxena, G. D. Bansal, and K. K. Asthana, *Durability Building Mater.*, 2(1983)27.
68. N. S. Allen, E. Pratt, D. M. McCormick, and A. Davis, *Polym. Deg. Stab.*, 42(1993)175.
69. K. Nate, M. Ishikawa, N. Imamura, and Y. Murakami, *J. Polym. Sci., Polym. Chem.*, 24(1986)1551.

70. P. Trefonas, P. J. Djurovich, X. -H. Zhang, R. West, R. D. Miller, and D. Hofer, *J. Polym. Sci., Polym. Lett.*, 21(1983)823.
71. L. H. Garcia-Rubio, *Macromolecules*, 20(1987)3070.
72. N. -L. Yang, V. Patel, T. J. Dolce, and A. Auerbach, *Polym. Mat. Sci. Eng.*, 51(1984)149.
73. F. Abdul-Rasoul, C. L. R. Catherall, J. S. Hargreaves, J. M. Mellor, and D. Phillips, *Eur. Polym. J.*, 13(1977)1019.
74. J. Peeling and D. T. Clark, *J. Appl. Polym. Sci.*, 26(1981)3761.
75. K. Maruyama, Y. Kuramoto, M. Yagi, and Y. Tanizaki, *Polymer*, 29(1988)24.
76. J. Puglisi and P. J. Schirmann, *Polym. Mat. Sci. Eng.*, 47(1982)620.
77. G. Berner and M. Rembold, *Org. Coat. Sci. Technol.*, 6(1983)55.
78. F. M. Tera, M. N. Michael, and A. Hebeish, *Polym. Degrad. Stab.*, 16(1986)163.
79. N. A. Weir, J. Arct, and J. K. Lee, *Eur. Polym. J.*, 29(1993).
80. Y. Fukuda and Z. Osawa, *Polym. Deg. Stab.*, 34(1991)75.
81. A. Torikai, T. Mitsuoka, and K. Fueki, *J. Polym. Sci., Polym. Chem.*, 31(1993)2785.
82. J. Behnisch and H. Zimmermann, *Intern. J. Polym. Mater.*, 16(1992)143.
83. A. G. Andreopoulos, A. Pappa, and N. Tzamtzis, *Polym. Testing*, 13(1994)3.
84. D. J. T. Hill, F. A. Kroesen, J. H. O'Donnell, and P. J. Pomery, *Mater. Forum*, 14(1990)210.
85. P. Genova-Dimitrova and I. Petkov, *Polym. Deg. Stab.*, 33(1991)105.
86. N. S. Allen, M. Edge, S. Conway, D. A. Doyle, E. M. Howells, K. Kikkawa, M. Minagawa, and T. Sekiguichi, *Polym. Deg. Stab.*, 38(1992)85.
87. D. Amos and B. Leake, *J. Hazardous Mater.*, 32(1992)105.
88. F. Severini, R. Gallo, S. Ipsale, and G. Ricca, *Polym. Deg. Stab.*, 41(1993)103.
89. H. Kubota, K. Takahashi, and Y. Ogiwara, *Polym. Deg. Stab.*, 33(1991)115.
90. A. Torikai, S. Hiraga, and K. Fueki, *Polym. Deg. Stab.*, 38(1992)73.
91. L. A. Linden, J. F. Rabek, H. Kaczmarek, A. Kaminska, and M. Scoponi, *Coordination Chem. Rev.*, 125(1993)195.
92. L. G. J. van der Ven and P. J. A. Guerink, *J. Oil Colour Chem. Assoc.*, 11(1991)401.
93. M. Ramasri, S. C. Shit, A. B. Mathur, and K. Rammamurthy, *Pop. Plast. Pack.*, (1992)5,47.
94. I. T. Bustamante and J. Hazai-Horvath, *Acta Chim. Hung.*, 126(1989)567.
95. B. Bell, D. E. Beyer, N. L. Maecker, R. R. Papenfus, and D. B. Priddy, *J. Appl. Polym. Sci.*, 54(1994)1605.
96. J. E. Bonekamp and N. L. Maecker, *J. Appl. Polym. Sci.*, 54(1994)1593.
97. P. R. Young, *NASA Conf. Pub. 3257*, p. 125.
98. J. E. Pickett and J. Moore, *Polym. Deg. Stab.*, 42(1993)231.
100. Y. Watanabe and T. Shirota, *Kenkyu Hokoku-Kogyo Gijutsuin*, 2(1981)141.
101. R. Geetha, A. Torikai, S. Nagaya, and K. Fueki, *Polym. Degrad. Stab.*, 19(1987)279.
102. R. Gooden, D. D. Davis, M. Y. Hellman, A. J. Lovinger, and F. H. Winslow, *Macromolecules*, 21(1988)1212.
103. T. -L. Nguyen and C. E. Rogers, *Polym. Mat. Sci. Eng.*, 53(1985)293.
104. F. Gugumus, *Polym. Dev. Stab.*, 8(1987)239.
105. D. R. Bauer, M. J. Dean, and J. L. Gerlock, *Polym. Mat. Sci. Eng.*, 55(1986)443.

106. V. Rek and M. Bravar, *J. Elastom. Plast.*, 12(1980)245.
106. C. Decker and K. Moussa, *Polym. Mat. Sci. Eng.*, 58(1988)338.
107. J. -L. Gardette and J. Lemaire, *Makromol. Chem.*, 183(1982)2415.
108. R. B. Turner, C. P. Christenson, M. A. Harthcock, D. M. Meadows, W. L. Howard, and M. W. Creswick, *Polym. Mat. Sci. Eng.*, 58(1988)947.
109. V. Rek, H. J. Mencer, and M. Bravar, *Polym. Photochem.*, 7(1986)273.
110. Z. Osawa, *Dev. Polym. Photochem.*, 3(1983)209.
111. Z. Osawa, F. Konoma, and S. Wu, *Polym. Photochem.*, 7(1986)337.
112. A. Torikai, A. Takeuchi, and K. Fueki, *Polym. Degrad. Stab.*, 14(1986)367.
113. G. Geuskens, G. Delaunois, Q. Lu-Vinh, W. Piret, and C. David, *Eur. Polym. J.*, 18(1982)387.
114. S. J. Valenty, J. J. Chera, W. Katz, D. R. Olson, and G. Smith, *Polym. Mat. Sci. Eng.*, 53(1985)288.
115. A. Rivaton, J. -L. Gardette, and J. Lemaire, *Caout. Plast.*, 651(1985)81.
116. J. D. Webb and A. W. Czanderna, *Macromolecules*, 19(1986)2810.
117. N. L. Doss, S. Habib, and M. H. Nosseir, *J. Appl. Polym. Sci.*, 34(1987)1117.
118. E. Fanton, B. Athenor, H. Seiner, R. Arnaud, and J. Lemaire, *Caout. Plast.*, 659(1986)135.
119. P. Gauvin and J. Lemaire, *Makromol. Chem.*, 188(1987)1815.
120. C. Decker and K. Moussa, *Polym. Mat. Sci. Eng.*, 57(1987)900.
121. S. C. Lin, B. J. Bulkin, and E. M. Pearce, *J. Polym. Sci., Polym. Chem.*, 17(1979)3121.
122. A. D. English and H. J. Spinelli, *J. Coat. Technol.*, 56,711(1984)43.
123. J. Lacoste, R. P. Singh, J. Boussand, and R. Arnaud, *J. Polym. Sci., Polym. Chem.*, 25(1987)2799.
124. H. N. Subramanyam and S. V. Subramanyan, *Eur. Polym. J.*, 23(1987)207.
125. X. Jouan and J.-L. Gardette, *Polym. Commun.*, 28(1987)329.
126. C.Q. Yang and W.G. Fateley, *Anal. Chim. Acta*, 194(1987)303.
127. T. Nguyen and E. Byrd, *Polym. Mat. Sci. Eng.*, 53(1985)584.
128. J. H. Hartshorn, *Polym. Mat. Sci. Eng.*, 57(1987)880.
129. B. Ranby and A. Hult, *Org. Coat. Sci. Technol.*, 7(1984)137.
130. M. W. Urban, *J. Coat. Technol.*, 59(1987)29.
131. G. M'Bon, C. Roucoux, A. Lablache-Combiere, and C. Loucheux, *J. Appl. Polym. Sci.*, 29(1984)651.
132. E. Baimuratov, I. Y. Kalontarov, and D. S. Saidov, *Intern. J. Polym. Mater.*, 19(1993)193.
133. J. -L. Gardette and J. Lemaire, *Polym. Deg. Stab.*, 6(1984)135.
134. J. -L. Gardette and J. Lemaire, *Polym. Deg. Stab.*, 34(1991)135.
135. Y. Israeli, J. Lacoste, L. Lemaire, R. P. Singh, and S. Sivaram, *J. Polym. Sci., Polym. Chem.*, 32(1994)485.
136. C. S. Lin, W. L. Liu, Y. S. Chiu, and S. -Y. Ho, *Polym. Deg. Stab.*, 38(1992)125.
137. A. Rivaton, *Angew. Makromol. Chem.*, 216(1994)147.
138. C. Wilhelm and J. -L. Gardette, *J. Appl. Polym. Sci.*, 51(1994)1411.
139. M. Iring, M. Szesztay, A. Stirling, F. Tudos, *J. Macromol. Sci., Pure Appl. Chem.*, A29(1992)865.

140. P. Genova-Dimitrova, *Polym. Deg. Stab.*, 33(1991)355.
141. J. - L. Gardette, *Analisis Mag.*, 21(1993)M17.
142. J. -L. Gardette and J. Lemaire, *Polym. Deg. Stab.*, 33(1991)77
143. A. Murase, Y. Esaki, M. Sugiura, and T. Araga, *Anal. Sci.*, 7(1991)1597.
144. C. Q. Yang, *Ind. Eng. Chem. Res.*, 31(1992)617.
145. A. -C. Albertsson, C. Barenstedt, and S. Karlsson, *Polym. Deg. Stab.*, 37(1992)163.
146. A. Tidjani and R. Arnaud, *Polym. Deg. Stab.*, 39(1993)285.
147. B. A. Gorelik, I. V. Kolganova, L. Matisova-Rychla, G. I. Listvojb, A. M. Drabkina, and A. G. Golnik, *Polym. Deg. Stab.*, 42(1993)263.
148. L. Wenzhong, Q. Juying, H. Xingzhou, and X. Hongmei, *Polym. Deg. Stab.*, 32(1991)39.
149. P. Jiangqing, X. Hongmei, Q. Juying, C. Jinfen, and M. Zhenmin, *Polym. Deg. Stab.*, 33(1991)67.
150. S. Falicki, D. J. Carlsson, J. M. Cooke, and D. J. Gosciniak, *Polym. Deg. Stab.*, 38(1992)265.
151. S. Chmela, W. D. Habicher, U. Hahner, and P. Hrdlovic, *Polym. Deg. Stab.*, 39(1993)367.
152. R. Baumhardt-Neto and M. -A. De Paoli, *Polym. Deg. Stab.*, 40(1993)59.
153. M. Scoponi, F. Pradella, and V. Carassiti, *Coordination Chem. Rev.*, 125(1993)219.
154. H. Friedrich, I. Jansen, and K. Ruhlmann, *Polym. Deg. Stab.*, 42(1993)127.
155. G. M. Ferguson, A. Jefferson, and I. Sihsobhon, *Mater. Forum*, 16(1992)147.
156. O. Osgobe and N. N. Ossai, *Acta Polym.*, 43(1992)173.
157. E. A. Kalennikov, S. I. Kuzina, V. S. Yuran, A. I. Mikhailov, L. V. Popova, A. A. Pendin, and V. N. Babin, *Appl. Organomet. Chem.*, 5(1991)471.
158. A. -C. Albertsson and S. Karlsson, *Polym. Deg. Stab.*, 41(1993)345.
159. G. M. Ferguson, M. Hood, and K. Abbott, *Polym. Intern.*, 28(1992)35.
160. B. De Neve and M. E. R. Shanahan, *Polymer*, 34(1993)5099.
161. G. Zhang, W. G. Pitt, S. R. Goates, and N. L. Owen, *J. Appl. Polym. Sci.*, 54(1994)419.
162. C. David, M. Trojan, A. Daro, and W. Demarteau, *Polym. Deg. Stab.*, 37(1992)233.
163. Y. Qing, X. Wenying, and B. Ranby, *Polym. Eng. Sci.*, 35(1994)447.
164. D. Raghavan and A. E. Torma, *Polym. Eng. Sci.*, 32(1992)439.
165. J. J. C. Cruz-Pinto, M. E. S. Carvalho, and J. F. A. Ferreira, *Angew. Makromol. Chem.*, 216(1994)113.
166. S. A. Jabarin and E. A. Lofgren, *J. Appl. Polym. Sci.*, 53(1994)411.
167. J. Pan, Y. Song, W. W. Y. Lau, and S. H. Goh, *Polym. Deg. Stab.*, 41(1993)275.
168. V. B. Ivanov, I. I. Barashokova, V. V. Selikhov, N. V. Vysotsky, Yu. Yu. Yakovlev, R. A. Sadekova, and N. N. Barashokov, *Polym. Deg. Stab.*, 35(1992)267.
169. J. -L. Gardette, H. -D. Sabel, and J. Lemaire, *Angew. Makromol. Chem.*, 188(1991)113.
170. E. T. Kang, G. K. Neoh, K. L. Tan, and D. J. Liaw, *Polym. Deg. Stab.*, 40(1993)45.
171. A. Rivaton, *Polym. Deg. Stab.*, 41(1993)283.
172. Y. Israeli, J. Lacoste, J. Cavezzan, and J. Lemaire, *Polym. Deg. Stab.*, 42(1993)267.
173. C. E. Hoyle and E. T. Anzures, *Report*, AD-A222 431 (1990).
174. C. E. Hoyle and E. T. Anzures, *J. Polym. Sci., Polym. Chem.*, 30(1992)1233.
175. X. Jouan and J. -L. Gardette, *J. Polym. Sci., Polym. Chem.*, 29(1991).685.
176. M. Getlichermann, M. Trojan, A. Daro, and C. David, *Polym. Deg. Stab.*, 39(1993)55.

177. X Jouan and J. -L. Gardette, *Polym. Deg. Stab.*, 36(1992)91.
178. M. Sargent, J. L. Koenig, and N. L. Maecker, *Polym. Deg. Stab.*, 39(1993)355.
179. R. Mani, R. P. Singh, S. Sivaram, and J. Lacoste, *Polym. J.*, 26(1994)1132.
180. R. P. Singh, R. Mani, S. Sivaram, J. Lacoste, and J. Lemaire, *Polymer*, 35(1994)1382.
181. M. Guzzo and M. -A. De Paoli, *Polym. Deg. Stab.*, 36 (1992)169.
182. S. Baccaro and U. Buontempo, *Radiat. Phys. Chem.*, 40(1992)175.
183. R. P. Singh and A. Singh, *J. Macromol. Sci. - Chem.*, A28(1991)487.
184. C. Adam, J. Lacoste, and J. Lemaire, *Polym. Deg. Stab.*, 32(1991)51.
185. E. L. Anderson, Z. Pawlak, N. L. Owen, and W. C. Feist, *Appl. Spectr.*, 45(1991)641.
186. O. Nuyken, J. Dauth, J. Stebani, *Angew. Makromol. Chem.*, 207(1993)65.
187. Y. Y. Chien, E. M. Pearce, and T. K. Kwei, *Polym. Prep.*, 29(1988)548.
188. J. Lacoste, C. Adam, N. Siampiringue, and J. Lemaire, *Eur. Polym. J.*, 30(1994)433.
189. D. Bauer, *Prog. Org. Coat.*, 23(1993)105.
190. Y. Y. Chien, E. M. Pearce, and T. K. Kwei, *J. Polym. Sci., Polym. Chem.*, 29(1991)849.
191. C. Q. Yang and L. K. Martin, *J. Appl. Polym. Sci.*, 51(1994)389.
192. H. Nanbu, Y. Sakuma, Y. Ishihara, T. Takesue, and T. Ikemura, *Polym. Degrad. Stab.*, 19(1987)61.
193. A. Charlesby, *J. Radioanal. Nucl. Chem.*, 101(1986)401.
194. N. Pourahmady, *US Pat. 5,292,823*, Geon Co., 1994.
195. N. A. Weir, J. Arct, A. Ceccarelli, and A. Siren, *Eur. Polym. J.*, 30(1994)701.
196. K. R. Carduner, D. R. Bauer, J. L. Gerlock, and D. F. Mielewski, *Polym. Deg. Stab.*, 35(1992)219.
197. N. Pourahmady and R. A. Kinsey, *J. Macromol. Sci., - Pure Appl. Chem.*, A29(1992)959.
198. U. Hahner, W. D. Habicher, and S. Chmela, *Polym. Deg. Stab.*, 41(1993)197.
199. H. Friedrich, I. Jansen, and K. Ruhlmann, *Polym. Deg. Stab.*, 42(1993)127.
200. S. G. Bond and J. R. Ebdon, *Polym. Commun.*, 32(1991)290.
201. M. Igarashi and K. L. DeVries, *Polymer*, 24(1983)769.
202. B. S. Rao and M. R. Murthy, *J. Polym. Sci., Polym. Phys.*, 25(1987)1897.
203. K. Kikkawa, Y. Nakahara, and Y. Ohkatsu, *Polym. Degrad. Stab.*, 18(1987)237.
204. D. R. Bauer and L. L. Gerlock, *Polym. Degrad. Stab.*, 14(1986)97.
205. J. L. Gerlock, D. R. Bauer, and L. M. Briggs, *Org. Coat. Sci. Technol.*, 8(1985)365.
206. J. L. Gerlock, D. R. Bauer, L. M. Briggs, and J. K. Hudgens, *Prog. Org. Coat.*, 15(1987)197.
207. S. Okamoto, K. Hikita, and H. Ohya-Nishiguchi, *Polym. Paint Colour J.*, 177(1987)683.
208. M. Koyama, A. Tanaka, M. Ichijima, and Y. Oki, *Kinzoku Hyomen Gijutsu*, 37(1986)25.
209. B. J. Humphrey, Electron Paramagnetic Resonance on Asphaltic Materials, *Report*, ESL-TR-85-72.
210. H. Koizumi, T. Yamaguchi, and H. Yoshida, *Bull. Chem. Soc., Jpn.*, 64(1991)1008.
211. T. Ichikawa, K. -I. Oyama, T. Kondoh, and H. Yoshida, *J. Polym. Sci., Polym. Chem.*, 32(1994)2487.
212. D. R. Bauer and D. F. Mielewski, *Polym. Deg. Stab.*, 40(1993)349.

213. S. I. Kuzina and A. I. Mikhailov, *Eur. Polym. J.*, 29(1993)1589.
214. G. Kampf, K. Sommer, and E. Zirngiebl, *Prog. Org. Coat.*, 19(1991)69.
215. A. Sommer, E. Zirngiebl, L. Kahl, and M. Schonfelder, *Prog. Org. Coat.*, 19(1991)79.
216. B. Ranby, *J. Macromol. Sci. - Pure Appl. Chem.*, A30(1993)583.
217. G. Kampf, K. Sommer, and E. Zirngiebl, *Farbe Lack*, 95(1989)883.
218. H. Kubota and M. Kimura, *Polym. Deg. Stab.*, 38(1992)1.
219. I. L. J. Dogue, N. Mermilliod, and F. Geoud, *J. Polym. Sci., Polym. Chem.*, 32(1994)2193.
220. D. R. Bauer, *J. Coat. Technol.*, 66(1994)57.
221. J. L. Gerlock, D. R. Bauer, L. M. Briggs, and R. A. Dickie, *J. Coat. Technol.*, 57(1985)37.
222. D. J. Hill, A. P. Lang, J. H. O'Donnell, and P. J. Pomery, *Polym. Deg. Stab.*, 38(1992)193.
223. S. A. M. Ali, P. J. Doherty, and D. F. Williams, *J. Appl. Polym. Sci.*, 51(1994)1389.
224. M. D. Chipara and M. I. Chipara, *Polym. Deg. Stab.*, 37(1992)67.
225. A. B. Reynolds and P. A. Wlodkowski, *Radiat. Phys. Chem.*, 38(1991)553.
226. D. J. Hill, A. P. Lang, J. H. O'Donnell, and P. J. Pomery, *Polym. Deg. Stab.*, 38(1992)205.
227. S. Chmela and P. Hrdlovic, *Polym. Deg. Stab.*, 42(1993)55.
228. D. R. Bauer, J. L. Gerlock, and D. F. Mielewski, *Polym. Deg. Stab.*, 36(1992)9.
229. D. F. Mielewski, D. R. Bauer, and J. L. Gerlock, *Polym. Deg. Stab.*, 33(1991)93.
230. N. S. Allen and J. F. McKellar, The Role of Luminescent Species in the Photooxidation of Common Polymers, *Dev. Polym. Degrad.*, 2(1979)129.
231. J. Stumpe and K. Schwetlick, *Polym. Degrad. Stab.*, 17(1987)103.
232. C. E. Hoyle and K. J. Kim, The Effect of Crystallinity and Flexibility on the Photodegradation of Polyurethanes, *Report*, AD-A172-619.
233. P. Zamotaev, O. Mityukhin, and S. Luzgarev, *Polym. Deg. Stab.*, 35(1992)195.
234. P. P. L. Jacques and R. C. Poller, *Eur. Polym. J.*, 29(1993)75.
235. P. P. L. Jacques and R. C. Poller, *Eur. Polym. J.*, 29(1993)83.
236. M. Barra, R. W. Redmond, M. T. Allen, G. S. Calabrese, R. Sinta, and J. C. Scaiano, *Macromolecules*, 24(1991)4972.
237. C. S. Li and R. Kopelman, *J. Phys. Chem.*, 94(1990)2135.
238. N. Fukazawa, K. Yoshioka, H. Fukumura, and H. Masuhara, *J. Phys. Chem.*, 97(1993)6753.
239. J. A. Loo, B. H. Wang, F. C.-Y. Wang, F. W. McLafferty, and P. Klymko, *Macromolecules*, 20(1987)700.
240. H. Fukumura, N. Mibuka, S. Eura, H. Masuhara, and N. Nishi, *J. Phys. Chem.*, 97(1993)1361.
241. L. O'Toole, R. D. Short, F. A. Bottino, A. Pollicino, and A. Recca, *Polym. Deg. Stab.*, 38(1992)147.
242. E. O. Edney, *Report*, EPA/600/3-89/032.
243. H. R. Brown, *Mater. Sci. Rep.*, 2(1987)315.
244. J. Schurz, P. Zipper, and J. Lenz, *J. Macromol. Sci. - Pure Appl. Chem.*, A30(1993)603.
245. G. Vigier and J. Tatibouet, *Polymer*, 34(1993)4257.

246. A. Paillous and C. Pailler, *Composites*, 25(1994)287.
247. H. S. Munro and D. T. Clark, *Polym. Degrad. Stab.*, 17(1987)319.
248. H. S. Munro, D. T. Clark, and J. Peeling, *Polym. Degrad. Stab.*, 9(1984)185.
249. R. K. Wells and J. P. S. Badyal, *J. Polym. Sci., Polym. Chem.*, 30(1992)2677.
250. R. K. Wells, J. P. S. Badyal, I. W. Drummond, K. S. Robinson, and F. J. Street, *Polymer*, 34(1993)3611.
251. I. W. Drummond, K. S. Robinson, A. Carrick, and H. Schmiedel, *Fresenius J. Anal. Chem.*, 346(1993)200.
252. L. P. Buchwalter and G. Czornyj, *J. Vac. Sci. Technol.*, A8(1990)781.
253. J. Friedrich, I. Loeschcke, H. Frommelt, H. -D. Reiner, H. Zimmermann, and P. Lutgen, *Polym. Deg. Stab.*, 31(1991)97.
254. I. Dalins and M. Karimi, *J. Vac. Sci. Technol.*, A10(1992)2921.
255. T. R. Gengenbach, Z. R. Vasic, R. C. Chatelier, and H. J. Griesser, *J. Polym. Sci., Polym. Chem.*, 32(1994)1399.
256. L. E. Hamilton, P. M. A. Sherwood, and B. M. Reagan, *Appl. Spectroscopy*, 47(1993)139.
257. N. M. D. Brown, J. A. Hewitt, and B. J. Meenan, *Surface Interface Anal.*, 18(1992)199.
258. A. Apicella, L. Egiziano, L. Nicolais, and V. Tucci, *J. Mater. Sci.*, 23(1988)729.
259. L. G. van der Ven and P. J. A. Guerink, *JOCCA*, 1991,401
260. T. Wurster, A. Franck, and P. Eyerer, *Angew. Makromol. Chem.*, 137(1985)109.
261. K. Esumi, K. Meguro, A.M. Schwartz, and A. C. Zettlemoyer, *Bull. Chem. Soc. Jpn.*, 55(1982)1649.
262. K. M. Dumayev, N. P. Kuzmina, V. V. Lobko, G. A. Matyushin, V. S. Nechitailo, and A. V. Chadov, *Intern. J. Polym. Mater.*, 17(1992)121.
263. C. E. Rogers, *ACS Symp. Ser.*, 220(1983)231.
264. J. -L. Philippart and J. -L. Gardette, *Makromol. Chem.*, 187(1986)1639.
265. R. Bartnikas, R. J. Densley, R. M. Eichhorn, *IEEE Trans. Power Delivery*, 6(1991)929.
266. S. P. Cygan and J. R. Laghari, *IEEE Trans. Nucl. Sci.*, 38(1991)906.
267. Z. Jelcic, M. Mlinac-Misak, J. Jelenic, and M. Bravar, *Angew. Makromol. Chem.*, 208(1993)25.
268. M. Kendig, R. Addison, J. Lumsden, S. Jeanjaquet, and D. Anderson, *Report*, AD-A222 426, 1990.
269. S. Feliu, Jr., M. Morcillo, and J. M. Bastidas, and S. Feliu, *J. Coat. Technol.*, 65(1993)43.
270. R. G. Mathey and W. J. Rossiter, *Durability Building Mater.*, 2(1983)59.
271. H. H. -D. Lee and F. J. McGarry, *Polymer*, 34(1993)4267.
272. R. Kobayashi and S. Hattori, *Kenkyu Hokoku-Kogyo Gijutsuin*, 2(1981)245.
273. J. H. Flynn, *Polym. Eng. Sci.*, 20(1980)675.
274. S. K. Dolui, *J. Appl. Polym. Sci.*, 53(1994)463.
275. E. J. Goethals and R. R. De Clercq, *J. Macromol. Sci. - Pure Appl. Chem.*, A30(1993)679.
276. S. J. Clarson, J. E. Mark, C. -C. Sun, and K. Dodgson, *Eur. Polym. J.*, 28(1992)823.
277. P. Dave, R. A. Gross, C. Brucato, S. Wong, and S. P. McCarthy, *Polym. Mater. Sci. Eng.*, 62(1990)231.

278. S. K. Mukhopadhyay, D. J. Mwaisengela, and P. W. Foster, *J. Text. Inst.*, 82(1991)427.
279. J. M. Augl, *J. Rheol.*, 31(1987)1.
280. M. E. R. Shanahan, M. Debski, F. Bomo, and J. Schultz, *J. Polym. Sci., Polym. Phys.*, 21(1983)1103.
281. J. Ch. Marechal, *Durability Building Mater.*, 1(1982.83)201.
282. N. S. Allen, M. Leward, and G. W. Follows, *Eur. Polym. J.*, 28(1992)23.
283. R. Flores, J. Perez, P. Cassagnau, A. Michel, and J. Y. Cavaille, *Polymer*, 35(1994)2800.
284. L. W. Hill, H. M. Korzeniowski, M. Ojunga-Andrew, R. C. Wilson, *Prog. Org. Coat.*, 24(1994)147.
285. M. Edge, M. Hayes, M. Mohammadian, N. S. Allen, T. S. Jewitt, K. Brems, and K. Jones, *Polym. Deg. Stab.*, 32(1991)131.
286. Z. A. Mohd Ishak and J. P. Berry, *Polym. Compos.*, 15(1994)223.
287. L. A. Holt and B. Milligan, *Text. Res. J.*, 54(1984)521.
288. H. Kubota, S. Suzuki, O. Nishimura, S. Hattori, K. Yoshikawa, and T. Shirota, *Kenkyu Hokoku-Kogyo Gijutsuin*, 2(1981)23.
289. H. Kubota, S. Suzuki, O. Nishimura, K. Yoshikawa, and T. Shirota, *Kenkyu Hokoku-Kogyo Gijutsuin*, 2(1981)49.
290. S. Suzuki, H. Kubota, O. Nishimura, and T. Tsurue, *Hokkaido Kogyo Kaihatsu Shikensho Hokoku*, 24(1981)153.
291. B. Milligan, *Rev. Prog. Color Relat. Top.*, 16(1986)1.
292. A. G. Strong, *Plast. Rubber Process. Appl.*, 6(1986)235.
293. S. M. Milkovich, C. T. Herakovich, and G. F. Sykes, *J. Compos. Mater.*, 20(1986)579.
294. T. Gantcheva, A. Marinova, and P. Genova, *Angew. Makromol. Chem.*, 137(1985)49.
295. T. Tsurue and S. Suzuki, *Hokkaido Kogyo Kaihatsu Shikensho Hokoku*, 24(1981)136.
296. Y. Nagatsuka, T. Shirota, K. Fukuta, K. Yoshikawa, S. Suzuki, H. Kubota, and O. Nishimura, *Kenkyu Hokoku-Kogyo Gijutsuin*, 2(1981)79.
297. A. G. Horsfall, *Text. Res. J.*, 52(1982)197.
298. J. F. Mandell, *Text. Res. J.*, 57(1987)318.
299. S. A. May, E. C. Fuentes, and N. Sato, *Polym. Deg. Stab.*, 32(1991)357.
300. N. Kharaiishi, A. Al-Robaidi, *Polym. Deg. Stab.*, 32(1991)105.
301. S. Konrad and D. Schuster, *J. Coat. Fabrics*, 22,7(1992)10.
302. P. M. Latzke, *Melliand*, 7(1990)E231.
303. R. Keshavaraj and R. W. Tock, *Polym.-Plast. Technol.*, 33(1994)397.
304. S. Kole, S. K. Srivatava, D. K. Tripathy, and A. K. Bhowmick, *J. Appl. Polym. Sci.*, 51(1994)1329.
305. P. Jiang-Qing and Z. Jie, *Polym. Deg. Stab.*, 36(1992)65.
306. I. Narisawa and T. Kuriyama, *Angew. Makromol. Chem.*, 216(1994)87.
307. M. Raab and V. Hnat, *Arabian J. Sci. Eng.*, 16(1991)37.
308. L. Godjervargov, G. Kustov, and D. Kostoski, *Polym. Deg. Stab.*, 41(1993)173.
309. H. V. Hoppler, *Kunststoffe*, 83(1993)5.
310. M. Henczkowski, *Kunststoffe*, 83(1993)20.
311. A. Kim, C. P. Bosnyak, and A. Chudnovsky, *J. Appl. Polym. Sci.*, 51(1994)1841.
312. K. K. Leonas and R. W. Gorden, *J. Environ. Polym. Deg.*, 1(1993)45.

313. T. B. Boboev, Kh. Dodomatov, and I. Ya. Kalontarov, *Intern. J. Polym. Mater.*, 19(1993)223.
314. G. E. Schoolenberg and H. D. F. Meijer, *Polymer*, 32(1991)438.
315. O. Nishimura, S. Suzuki, H. Kubota, K. Yoshikawa, and T. Shirota, *Hokkaido Kogyo Kaihatsu Shikensho Gijutsuin*, 24(1981)193.
316. M. M. Qayyum and J. R. White, *Polym. Deg. Stab.*, 39(1993)199.
317. Z. A. Kadir, F. Yoshii, K. Makuuchi, and I. Ishigaki, *Angew. Makromol. Chem.*, 174(1990)131.
318. T. Watanabe, *Kobunshi Ronbunshu*, 39(1982)1.
319. C. Giori and T. Yamauchi, *Report*, NASA 3559.
320. T. Okada, S. Nishijima, and H. Yamaoka, *Adv. Cryogenic Eng. Mater.*, 32(1986)145.
321. Y. Watanabe, F. Kitajima, and T. Shirota, *Kenkyu Hokoku-Kogyo Gijutsuin*, 2(1981)155.
322. L. M. Gan, H. W. K. Ong, T. L. Tan, C. H. Chew, and F. N. Lai, *Durability Building Mater.*, 2(1985)379.
323. L. M. Gan, H. W. K. Ong, and T. L. Tan, *Durability Building Mater.*, 3(1986)225.
324. B. H. River, *Adhesive Age*, 27,2(1984)16.
324. M. J. Welch, P. J. C. Counsell, and C. V. Lawton, *J. Oil. Colour Chem. Assoc.*, 63(1980)137.
325. S. Suzuki, H. Kubota, T. Tsurue, and O. Nishimura, *Hokkaido Kogyo Kaihatsu Shikensho Hokoku*, 24(1981)129.
326. W. K. Busfield and Michael Monteiro, *Mater. Forum*, 14(1990)218.
327. B. M. Parker, *Int. J. Adhes. Adhes.*, 13(1993)47.
328. R. Bajpai, P. Agrawal, and S. C. Datt, *Polym. Intern.*, 34(1994)249.
329. A. T. Koshy, B. Kuriakose, and S. Thomas, *Polym. Deg. Stab.*, 36(1992)137.
330. J. P. Bell, R. G. Schmidt, A. Malofsky, and D. Mancini, *J. Adhes. Sci. Technol.*, 5(1991)927.
331. H. N. Neidlinger, M. R. Steffect, and R. Goggin, *Polym. Prep.*, 28,1(1987)205.
332. I. Mita, T. Takagi, K. Horic, and Y. Shindo, *Macromolecules*, 17(1984)2256.
333. Y. Watanabe and T. Shirota, *Kenkyu Hokoku-Kogyo Gijutsuin*, 1(1981)149.
334. S. Matsumoto, H. Ohshima, and Y. Hasuda, *J. Polym. Sci., Polym. Chem.*, 22(1984)869.
335. Y. Nagatsuka, T. Shirota, K. Yoshikawa, S. Suzuki, H. Kubota, and O. Nishimura, *Kenkyu Hokoku-Kogyo Gijutsuin*, 2(1981)87.
336. S. Koda, H. Mori, K. Matsumoto, and H. Nomura, *Polymer*, 35(1994)20.
337. B. O'Donnell, J. R. White, and S. R. Holding, *J. Appl. Polym. Sci.*, 52(1994)1607.
338. F. Thominet, G. Metzger, B. Dalle, and J. Verdu, *Eur. Polym. J.*, 27(1991)55.
339. G. J. Price and P. F. Smith, *Eur. Polym. J.*, 29(1993)419.
340. S. Kuroda, I. Mita, K. Obata, and S. Tanaka, *Polym. Deg. Stab.*, 27(1990)257.
341. N. A. Weir and A. Ceccarelli, *Polym. Deg. Stab.*, 41(1993)37.
342. S. H. Hamid, M. B. Amin, A. G. Maadhan, and A. M. Al-Jarallah, *J. Vinyl Technol.*, 14(1992)182.
343. S. G. Matz, *J. Chromatography*, 587(1991)205.

344. T. Yamashita, H. Tomitaka, T. Kudo, K. Horie, and I. Mita, *Polym. Deg. Stab.*, 39(1993)47.
345. S. T. Oh, B. K. Min, C. S. Ha, and W. J. Cho, *J. Appl. Polym. Sci.*, 52(1994)583.
346. J. D. Webb and A. W. Czanderna, *Sol. Energy Mater.*, 15(1987)1.
347. G. A. Luoma and R. D. Rowland, *J. Chromatog. Sci.*, 24(1986)210.
348. A. Factor, W. V. Ligon, and R. J. May, *Macromolecules*, 20(1987)2461.
349. R. Lehrle, D. Atkinson, S. Cook, P. Gardner, S. Groves, R. Hancox, and G. Lamb, *Polym. Deg. Stab.*, 42(1993)281.
350. C. Neri, V. Malatesta, S. Costanzi, and R. Riva, *Angew. Makromol. Chem.*, 216(1994)101.
351. E. A. Hegazy, T. Sasuga, M. Nishi, and T. Seguchi, *Polymer*, 33(1992)2897.
352. C. E. Hoyle, D. Creed, R. Nagarajan, P. Subramanian, and E. T. Anzures, *Polymer*, 33(1992)3162.
353. K. B. Wischmann, *ACS Symp. Ser.*, 322(1986)341.
354. D. R. Bauer and D. F. Mielewski, *Polym. Deg. Stab.*, 40(1993)349.
355. R. Sastre, F. Castillo, G. Martinez, and J. L. Millan, *Rev. Plast. Mod.*, 54(1987)237.
356. H. J. Bowley, D. L. Gerrard, K. J. P. Williams, and I. S. Biggin, *J. Vinyl. Technol.*, 8(1986)176.
357. J. Wypych, *Poly(vinyl chloride) Degradation*, Elsevier, 1985.
358. J. Wypych, *Poly(vinyl chloride) Stabilization*, Elsevier, 1986.
359. C. Tanielian, R. Mechin, and M. Shakirullah, *J. Photochem. Photobiol., A. Chem.*, 64(1992)191.
360. Y. Qing, X. Wenying, and B. Ranby, *Polym. Eng. Sci.*, 31(1991)1561.
361. B. Ohtani, S. Adzuma, S. Nishimoto, and T. Kagiya, *Polym. Deg. Stab.*, 35(1992)53.
362. P. Gijnsman, J. Hennekens, and D. Tummers, *Angew. Makromol. Chem.*, 216(1994)37.
363. J. H. Khan and H. Hamid, *Polym. Deg. Stab.*, 48(1995)137.
364. J. L. Gerlock, W. Tang, M. A. Dearth, and T. J. Korniski, *Polym. Deg. Stab.*, 48(1995)121.

14

DATA ON SPECIFIC POLYMERS

The information presented below contains subchapters discussing individual polymers. Information on each polymer is divided, for better clarity, into a few sections as follows:

mechanism of degradation:

- **models:** observations obtained from the analysis of model compounds which contribute to the understanding of the mechanism of photodegradation
- **polymer:** results of studies on polymer photodegradation mechanism

Characteristic changes and properties: several graphic representations of the major experimental findings for a particular polymer, illustrating the properties which determine photostability and the changes which occur during photodegradation, accompanied by concise comments and conclusions

Important initiators and accelerators: compounds or functional groups listed in the scientific literature as capable of accelerating photodegradation of a particular polymer

Effect of thermal history: the major influences of thermal treatment prior to photodegradation on the photostability of a particular polymer

Luminescence data: the values given in the literature of the wavelengths of emitted radiation as these depend on the excitation wavelength; spectral sensitivity - the wavelength range in which a particular polymer photodegrades; activation wavelength - the wavelength which caused degradation of a particular polymer

Products of photolysis and photooxidation: tabular comparison of products of photolysis and photooxidation (functional groups, reaction types, chemical compounds, etc.) mentioned in research papers for a particular polymer

Stabilizers: concise guidelines for stabilization based on suggestions in literature

14.1 POLY(VINYL CHLORIDE) (PVC)¹⁻⁶⁷

Poly(vinyl chloride), one of the most commonly used polymers, has been studied for many years. The extent of studies available for this polymer cannot be matched by those

done on any other polymeric material. There continue to be useful discussions on many aspects of the mechanism of PVC degradation because the technical difficulties encountered in sample preparation and development of methods of studies continue to pose problems. These problems are typical of the degradation studies for any polymer. Each method of sample preparation can create difficulties: contaminants in the sample in the form of solvent traces; new groups formed by thermodegradative processes; etc. Also, testing methods cannot always monitor changes related to crosslinking which can cause increasing polymer insolubility.

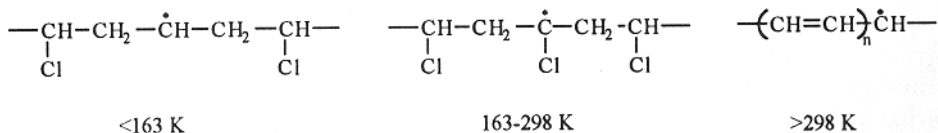
14.1.1 MECHANISM OF DEGRADATION

14.1.1.1 Models

The formation of head-to-tail structures is characteristic of vinyl chloride polymerization. The process is not perfectly regular therefore some head-to-head structures are also formed. The head-to-head structure was long suspected to be one possible initiation center of polymer photodegradation. Mori²⁷ tested this hypothesis, using 2,3-dichlorobutane and 2,4-dichloropentane as models of head-to-head and head-to-tail segments, respectively. His studies indicate that head-to-head structures are not likely to be the vulnerable segments which affect photodegradation initiation rate.

Model compounds were used to evaluate photoinitiation of a sensitized photodehydrochlorination reaction in branched and unbranched chains. The study, which was conducted using secondary and tertiary butylchlorides, showed that both segments may produce dehydrochlorinated structures, in a sensitized reaction.

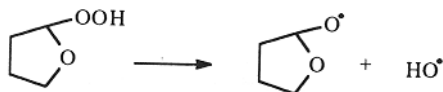
ESR spectroscopic study of model compounds and polymers by Lawton²⁸ and Yang²⁹ helped to identify the types of radicals formed during photodegradation. Radical structure evidently depends on temperature, as demonstrated by the following formulas:



Changes in the radical structure affect the mechanism of most of the essential processes occurring during PVC photodegradation.

14.1.1.2 Polymers

Polymer in a pure form should not be degraded by UV because it contains only C-C, C-H, and C-Cl bonds which do not absorb UV radiation from daylight spectrum. The model studies suggest the possibility of degradation in the presence of some sensitizers. Solvents left in PVC sample may act as sensitizers via the hydroperoxide formation route:

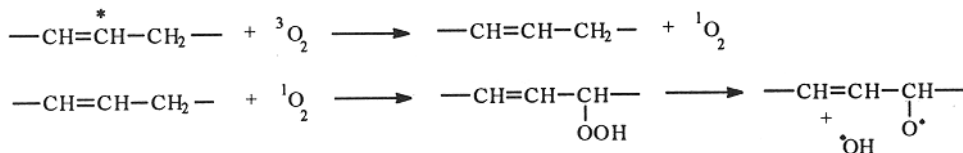


in addition to other compounds, which are listed below. Radicals formed by the reactions may abstract hydrogen, leading to dehydrochlorination of the polymer.

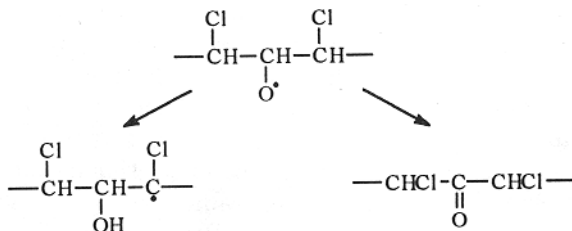
Unsaturation formed during polymerization, processing, or photodegradation participate in the series of photo-conversion reactions proposed by Rabek:³⁰



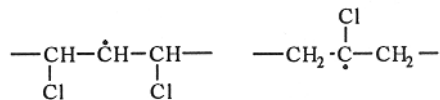
Here, energy absorbed by unsaturated sequences is utilized to form singlet oxygen from ground-state molecular oxygen. Singlet oxygen can, in turn, react with the chain to form a peroxy-radical which, after homolysis of the O-O bond, produces two radicals:



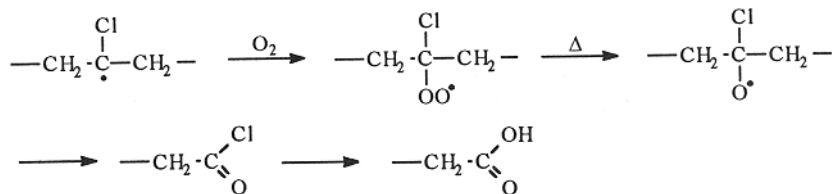
Further conversion of the alkoxy macroradicals may result in one of the two structures below:



Photolysis of the regular chain segment leads to one of two possible radicals:



The hydrogen can be abstracted from either the methylene or the chloromethylene group. In both cases, there can be two sets of conversions. Conversions of the radical formed occurs by the abstraction of hydrogen from the methylene group. Abstraction of hydrogen from the chloromethylene group leads to the following chain of reactions:



It should be noted that the carbonyl group can absorb daylight's UV radiation and initiate further photodegradation:



The above discussion concentrated on the dissociation of the C-H bond. If we now consider the C-Cl bond, we note that research by Gardette and Lemaire⁵³ shows that two principal pathways are possible. The chlorine radical may abstract a neighboring hydrogen and form a conjugated double bond or a chlorine radical may escape from the immediate surroundings and abstract hydrogen from a distant segment (e.g., from another chain). Similarly, the hydroxyl radical can be active within the cage (neighboring segments) or be ejected far from the alkoxy radical and initiate the radical reaction at another site. Then, either long sequences (cage reaction) or short sequences are preferentially formed. Gardette and Lemaire⁵³ conducted studies on PVC degradation using radiation of various wavelengths. Specimens exposed to wavelength of 254 nm

had more numerous, but shorter, polyene sequences and this was attributed to the more pronounced tendency of radicals to be ejected from dissociation sites.

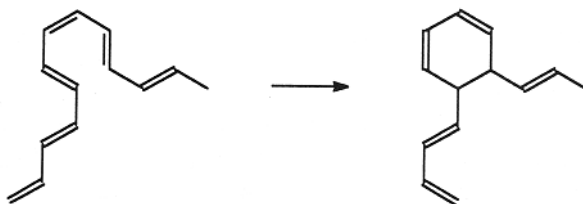
Finally, the formation of radicals increases the probability that they will recombine and crosslink. Crosslinks can be formed by alkoxy radicals and by formation of β -chloroanhydride from β -chloroacetic acid.

From the above discussion, one can see that the variety of radicals formed during the photodegradation of PVC leads to three major processes:

- dehydrochlorination
- chain scission
- crosslinking

The rates of these processes and their mechanisms are highly disputed parts of research on PVC photodegradation and most especially photodegradation in the presence and absence of oxygen. When these processes are allowed to occur freely, the pace of photodegradation is accelerated because of the accumulation of chain segments which are able to absorb UV radiation.

Several additional influences should be mentioned. One is the role of HCl formed during photoinduced dehydrochlorination. Verdu³¹ studied the photo-degradation of PVC films of varying thickness. His results suggest that HCl concentration in a specimen is proportional to the rate of carbonyl group formation. Owen³²⁻³³ suggests that the presence of HCl may also facilitate the formation of longer polyene sequences by promoting the migration of short polyene sequences along the chain. Another mechanism explains PVC photobleaching. Since the color of a PVC specimen depends on the concentration and the number of conjugated double bonds of polyenes, photobleaching could occur by oxidation of double bonds. But color changes do not exactly parallel the carbonyl group formation or hydroperoxide concentration, therefore, an additional mechanism is required to account for loss of double bonds. By analogy to thermal degradation, where benzene formation has been proposed, Owen³²⁻³³ suggests the following photobleaching mechanism:



The formation of cyclohexadiene shortens the length of the polyene sequence because the two double bonds in cyclohexadiene are no longer in conjugation with the double bonds remaining in the chain; moreover, one long sequence is divided into two short ones.

In the beginning of this discussion, some information was included on the irregularities in polymer structure. Broader treatment has been given to this in specialized monographs which discuss thermal and UV degradation of PVC.^{34,35} Imperfections in the chain serve as initiation sites for photodegradation. Also, the crystalline structure of PVC affects initiation and propagation rates. The crystallinity of PVC was found to increase rapidly with its syndiotacticity.⁶⁷ The addition of plasticizers has little effect on polymer crystallinity. It is the original conformation of polymer that is most important. Conformation of the molecule is the primary factor in determining propagation rate. Long syndiotactic sequences form longer polyene structures.⁵⁹ The average polyene sequence length is not controlled by kinetic reasons such as the ratio of initiation and propagation constants but by chain conformation. All trans syndiotactic conformers are, for steric reasons, ideal precursors for all trans polyenes. Also, the direction of the reaction is conformation controlled. Trans-cisoid segments (3% of total in PVC) are precursors of benzene ring formation which decreases color change.

Initiation of photodegradation is also affected by conformation and crystalline structure. Degradation occurs mostly in the amorphous phase and radicals formed in the crystalline domains react through cage reactions. Also, polyenes formed below T_g are unusually long. The abstraction of any atom has higher probability when that atom is readily accessible. Steric hindrance, due to conformation, decreases the probability of participation of segments in photolytic conversions.

Finally, one should consider that most photolytic reactions require readily available oxygen. This has two important implications. One is that the sample thickness should be sufficiently thin that the material is not starved of oxygen due to slow diffusion. The other is that degradation depends on oxygen diffusion which is controlled by product dimensions and by composition. For example, the incorporation of plasticizer increases rate of oxygen diffusion by a factor of 20.⁵³

14.1.2 EFFECT OF THERMAL HISTORY

The dehydrochlorination reaction is a primary route in PVC thermal degradation with unsaturations being its primary result. In the presence of oxygen, hydroperoxides are formed; they are the precursors to carbonyl groups. Conditions during processing (time, temperature) contribute to the formation of groups which photoinitiate degradation. The effect of degradation is limited by incorporation of thermal stabilizers. The type of stabilizer used in protection against thermal degradation also affects PVC stability during outdoor exposure. This is explained in detail in two specialized monographic

sources.³⁴⁻³⁵ Experimental evidence shows⁶⁶ that exposure to visible radiation and oxygen changes the properties of PVC (its ability to absorb UV, molecular weight).

14.1.3 CHARACTERISTIC CHANGES AND PROPERTIES

The temperature of irradiation has a complementary effect on radical formation (Fig. 14.1). More radicals are formed in an oxygen-free atmosphere because, when they are formed in an oxygen-containing atmosphere, they are readily converted to carbonyl groups (Fig. 14.2). The rate of oxygen diffusion and the concentration of HCl in the specimen contribute to formation of carbonyl groups (Fig. 14.3). Higher temperatures and longer thermal oxidation times cause a proportionally greater concentration of hydroperoxides. A higher initial rate of hydroperoxide formation may be caused by HCl autocatalysis (Fig. 14.4). The total amount of oxygen reacted with the polymer depends on the temperature and the duration of thermal degradation (Fig. 14.5). Polyene concentration and polyene segment length are similarly dependent on temperature and degradation time (Fig. 14.6). PVC weathering (natural and induced) causes a molecular weight decrease (Fig. 14.7). An increase in drying temperature causes an increase in absorption of UV light (Fig. 14.8). Oxygen diffusion limits the formation of photooxidation products (Fig. 14.9).

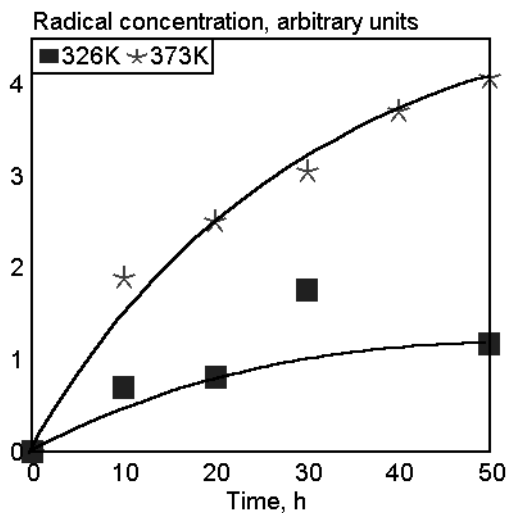


Fig. 14.1. Radical concentration vs. irradiation time at different temperatures. [Data from A. Torikai, H. Tsuruta, and K. Fueki, *Polym. Photochem.*, 2(1982)227.]

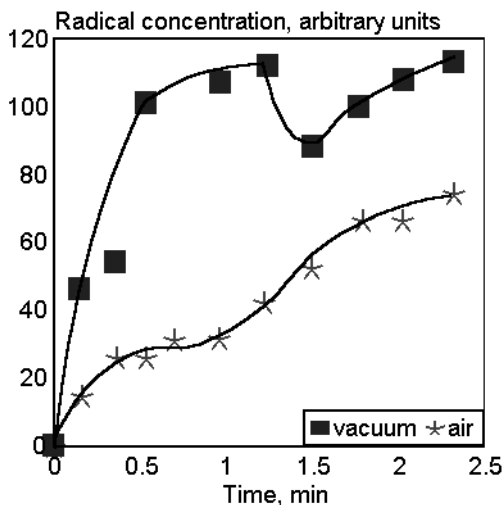


Fig. 14.2. Radical concentration vs. irradiation time in air and in vacuo. [Data from A. Torikai, H. Tsuruta, and K. Fueki, *Polym. Photochem.*, 2(1982)227.]

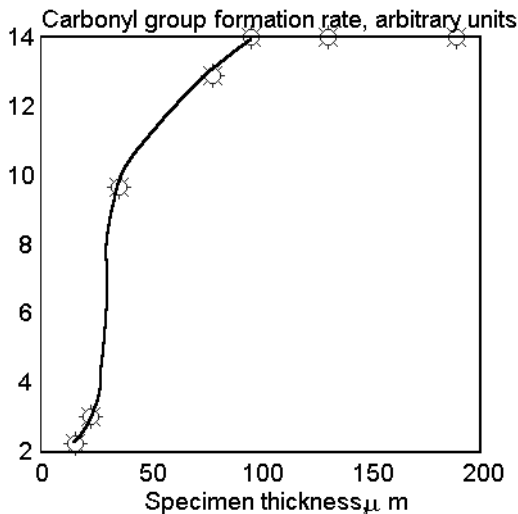


Fig. 14.3. Specimen thickness vs. carbonyl group formation rate. [Data from J. Verdu, *J. Macromol. Sci.-Chem.*, A12(1978)551.]

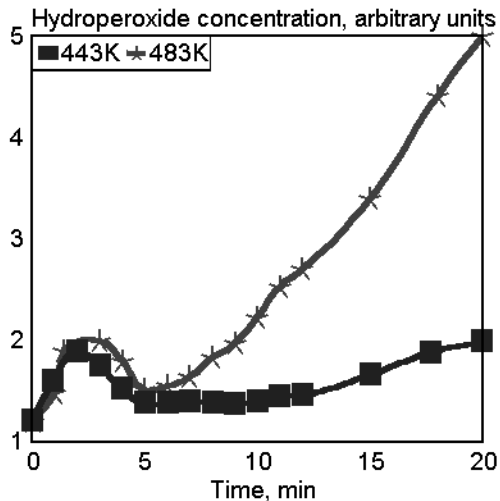


Fig. 14.4. Effect of processing time and temperature on hydroperoxide concentration. [Data from B. B. Cooray and G. Scott, *Polym. Degrad. Stab.*, 3(1980-81)127.]

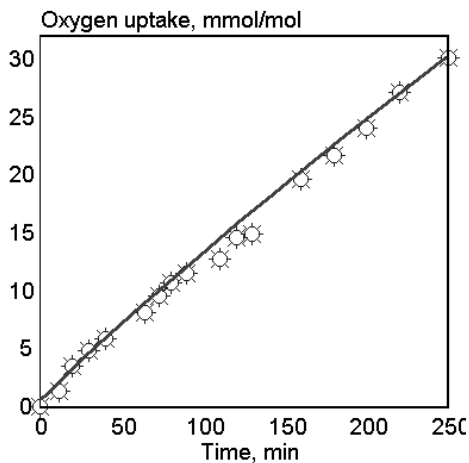


Fig. 14.5. Oxygen uptake vs. degradation time at 453 K. [Data from F. Tudos, T. Kelen, and T. T. Nagy, *Dev. Polym. Degrad.*, Vol. 2, *Applied Science Publishers*, London, 1979.]

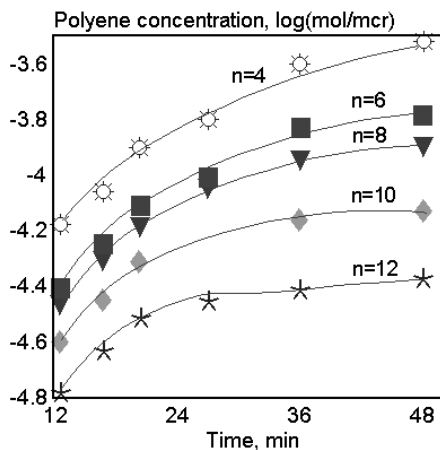


Fig. 14.6. Concentration and distribution of polyenes formed during thermal degradation of PVC in nitrogen at 463 K. [Data from K. B. Abbas, *J. Macromol. Sci.-Chem.*, 12(1978)479.]

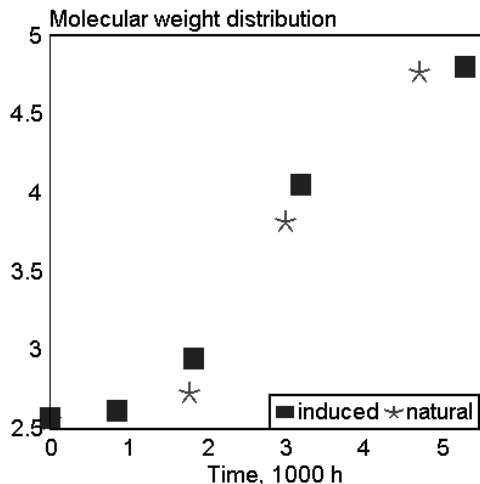


Fig. 14.7. Change in PVC molecular weight distribution during natural and induced weathering (6 months of natural weathering equals 1500 h of induced weathering.) [Data from S. Matsumoto, H. Ohshima, and Y. Hosuda, *J. Polym. Sci., Polym. Chem. Ed.*, 22(1984)869.]

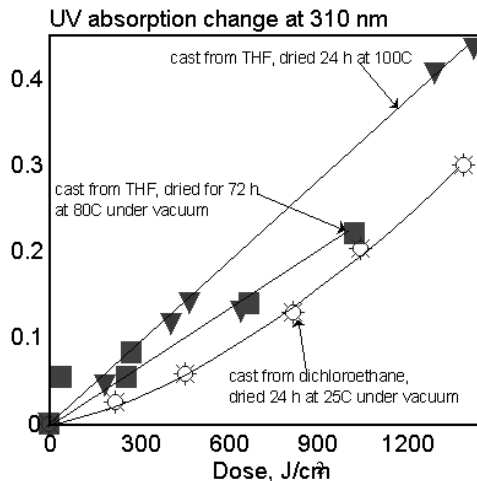


Fig. 14.8. Effect of thermal history of PVC films and solvent traces present on UV absorption change during exposure to UVB. [Adapted, by permission, from D. J. Hill, F. A. Kroesen, J. H. O'Donnell, and P. J. Pomery, *Mater. For.*, 14(1990)210.]

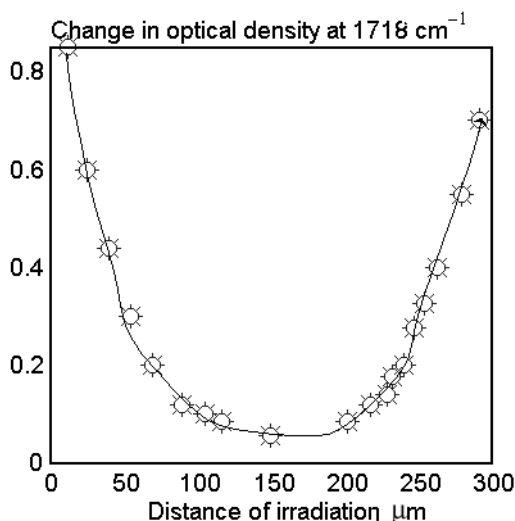


Fig. 14.9. Oxidation profile measured by IR absorption at 1718 cm^{-1} . [Data from J. L. Gardette, *Analisis*, 21,5(1993)M17.]

14.1.4 DATA

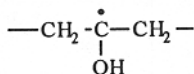
Luminescence data:		
Sample form	Excitation wavelength, nm	Emission wavelength, nm
film	290	350
film	284	440
Spectral sensitivity: 310-370 nm		Activation wavelength: 327, 364 nm
Products of photolysis: free radicals, unsaturations, crosslinks		
Products of photooxidation: free radicals, unsaturations, carbonyl groups, hydroperoxides, chain scissions		
Important initiators and accelerators: carbonyl groups, unsaturations, solvents forming hydroperoxides, sensitizing impurities (e.g., benzophenones), metallo-organics (copper-containing compounds, cadmium acetate, ferrocene, iron salts), metal chlorides produced from thermal stabilizers, products of degradation of some antioxidants, some pigments and fillers (containing cobalt, zinc, manganese, and lead), metal oxides (of titanium, zinc, and aluminum), hydrogen chloride (autocatalytic product of PVC degradation)		
Stabilization: primary thermal stabilizers (Ba-Cd soaps, Ba-Cd-Zn soaps, maleate-based organotins, dibutyltin dilaureate); secondary thermal stabilizers (phosphites, epoxies); UV absorbers (benzotriazole, e.g., Tinuvin P); quenchers (HALS, e.g., Tinuvin 770); pigments (higher loads of TiO ₂ or carbon black)		

14.2 POLY(VINYL ALCOHOL) (PVAI)⁶⁸⁻⁷⁶

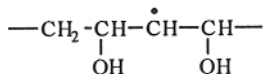
A few available studies on PVAI stability discuss only some important rudiments of the mechanism of its degradation mechanism. Fortunately, its similarity to PVC allows us to draw some analogies and make use of PVC data to explain its degradation mechanisms.

14.2.1 MECHANISM OF DEGRADATION

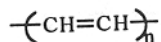
Like PVC, pure PVAI will not degrade when exposed to daylight radiation. The oxygen-carbon bond is more than 2.5 stronger than carbon-chlorine bonding and thus it requires more energy to break than daylight can deliver. Studies done on γ -irradiated material demonstrated the formation of the following radical:



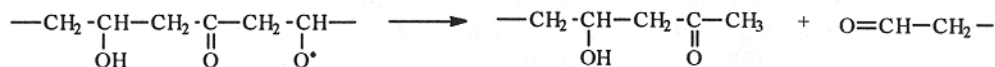
when the study was conducted at elevated temperature. When PVAI was irradiated at liquid-nitrogen, a different radical was found:



These are similar in mechanism to that occurring in PVC degradation and produce polyenes as the final product of photolytic degradation:



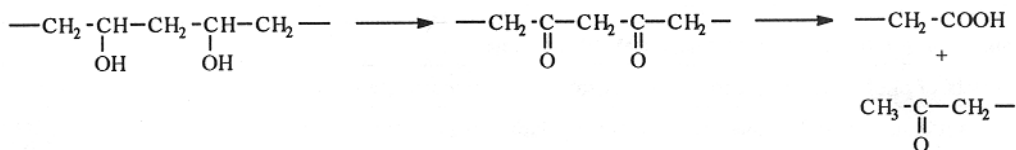
The essential difference between PVC and PVAL is only apparent when the polyenes are exposed to UV radiation. Maruyama⁷³ studied photobleaching of PVAL and determined that polyenes of appropriate chain length could selectively absorb radiation, undergo chemical changes, and form shorter chain polyenes. Other studies show that the photooxidation of PVAL produces carbonyl compounds and aldehydes. Each study sheds light on PVC degradation mechanisms. Rao⁷² explains the latter results by the following reaction:



Aldehydes are formed by the photooxidation of double bonds.

Again, like PVC, PVAL requires free radicals to initiate photodegradation at the site on the molecule which is able to absorb UV radiation. This conversion leads to the formation of polyene structures (color change), chain scission, and/or crosslinking (mechanical property change). The relative rates of these processes depend on the atmosphere in which photo-degradation occurs and other factors which may limit oxygen diffusion (for example - specimen thickness).

PVAL is the only truly biodegradable polymer which has an all C-C backbone. At least 55 microorganism species (bacteria, molds, yeast, and fungi) can degrade PVAL. It is interesting to note is that biodegradation goes through a stage similar to photodegradation:⁷⁶



First ketone (β -diketone) is formed which is then converted to other products as the backbone breaks up. Then hydroxyl radicals can participate in the abstraction of hydrogen

from the hydroxyl group thus converting PVAL to diketone then to acid then to ketone as in the above reaction. Note that partially hydrolyzed PVAL, which is one of the intermediate products in PVAL synthesis, is not biodegradable.⁷⁶

14.2.2 EFFECT OF THERMAL HISTORY

The formation of unsaturations and carbonyl groups is the normal pathway for PVAL degradation and this leads to the formation of key initiators. The kinetics of these processes in PVAL is different from those in PVC in two ways: the hydroxyl group in PVC bonds more strongly to carbon than chlorine does to carbon in PVC; in PVAL water is a by-product of degradation whereas in PVC hydrogen chloride is the by-product. Thus, the stronger hydroxyl-carbon bond requires much higher temperatures before degradation occurs and water lacks the autocatalytic activity possessed by hydrogen chloride. Thus, PVC will degrade under milder conditions than will PVAL.

14.2.3 CHARACTERISTIC CHANGES AND PROPERTIES

All samples absorb UV light at 282 nm, attributable to aldehydes. This means that the products of thermal degradation and photooxidation are the same (Fig. 14.10). Polyenes absorb selectively at 325 nm. Shorter polyenes are formed at the expense of longer ones in a phenomenon called photobleaching (Fig. 14.11). Stress applied on the PVAL sample during UV irradiation contributes to the increase in degradation. Incorporation of dye (C.I. Reactive Yellow 4) decreases the effect of radiation. The rate of decrease depends on the method of dye incorporation. If the dye is chemically bound to PVAL its protective effect increases (Fig. 14.12).

14.2.4 DATA

Luminescence data:		
Sample form	Excitation wavelength, nm	Emission wavelength, nm
film	258, 295, 330	360, 370
film	260-280	436
Spectral sensitivity: <280 nm		
Products of photolysis: free radicals, unsaturations, crosslinks		
Products of photooxidation: free radicals, unsaturations, carbonyl groups, hydroperoxides, chain scissions		
Important initiators and accelerators: carbonyl groups, unsaturations, sensitizers (polynuclear aromatic compounds, benzophenones)		

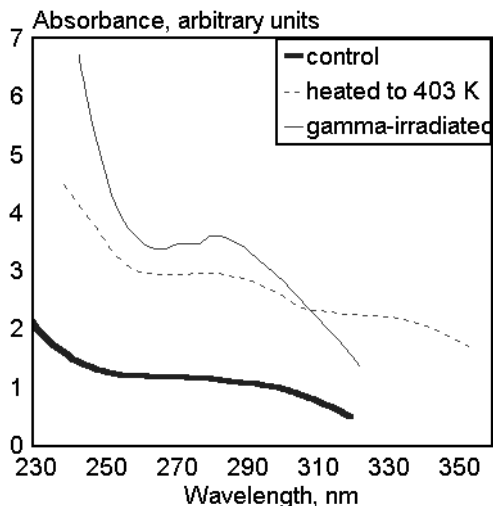


Fig. 14.10. UV absorption spectra of PVAI. [Adapted, by permission, from B. S. Rao and M. R. Murthy, *J. Polym. Sci., Polym. Phys.*, 25(1987)1897.]

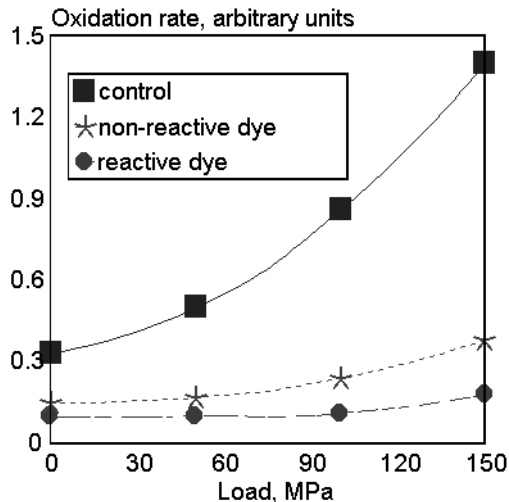


Fig. 14.12. Oxidized groups formation rate vs. mechanical load. [Adapted, by permission, from E. Baimuratov, I. Y. Kalontarov, and D. S. Saidov, *Int. J. Polym. Mater.*, 19(1993)193.]

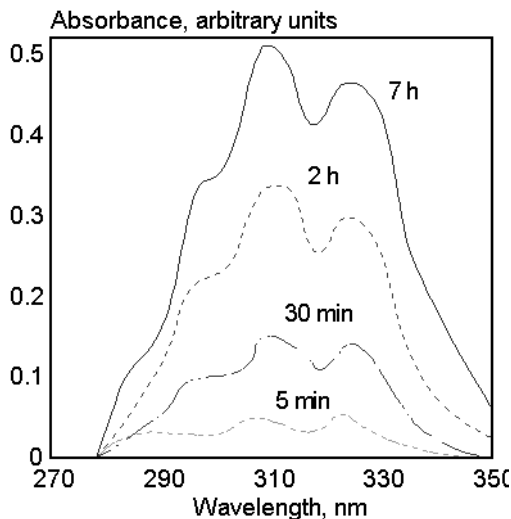
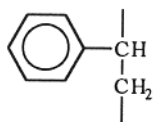


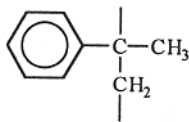
Fig. 14.11. Difference spectra of PVAI irradiated at 325 nm vs. irradiation time. [Adapted, by permission, from K. Muruyama, Y. Kuramoto, M. Yagi, and Y. Tanizaki, *Polymer*, 29(1988)24.]

14.3 POLYSTYRENES (PS)^{3,6-12,14,98-118}

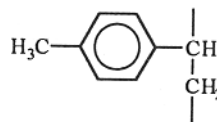
This group includes:



polystyrene



poly(α -methylstyrene)



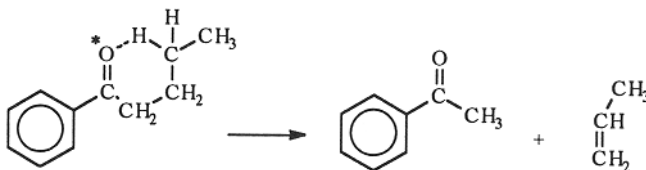
poly(p-methylstyrene)

with polystyrene the most commonly used material.

14.3.1 MECHANISM OF DEGRADATION

14.3.1.1 Models

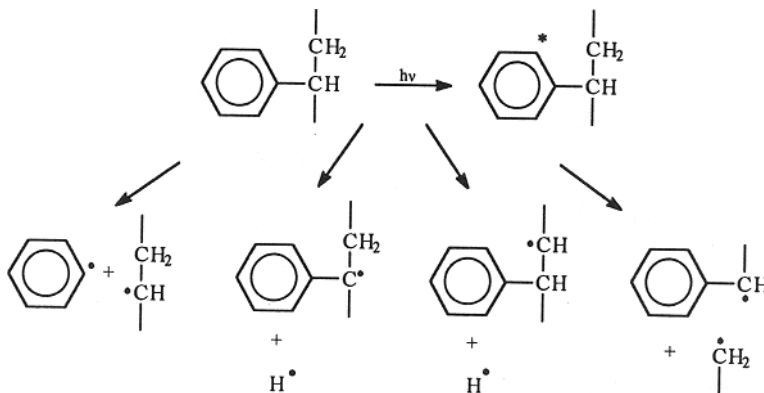
The compound, 1,3,5-triphenylhexane, was used as a model for polystyrene to analyze the effect of aluminum chloride catalyst on degradation. Benzene was found to be the major product of degradation. Valerophenone photolyzed according to a Norrish type II mechanism:



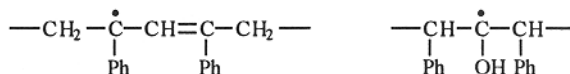
The reactions initiated by hydrogen abstraction result in the components absorbing UV radiation. Various additives of polystyrene were studied to establish their effect on degradation kinetics and to understand the possible effect of impurities (listed below).

14.3.1.2 Polymers

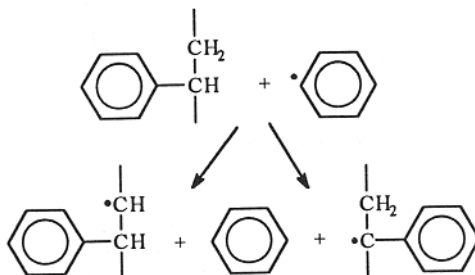
The mechanism of degradation mostly depends on the wavelength of light used for degradation studies and the presence or absence of oxygen. Generally, two sets of studies are available: photolysis at low wavelength (usually 254 nm) and at 300 nm. The first case allows absorption of radiation by the phenyl ring, which leads to radical processes:



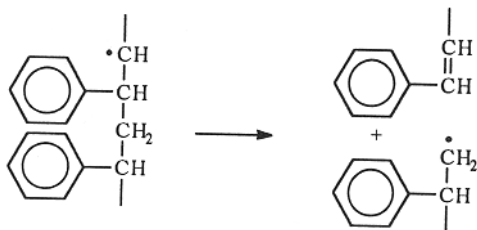
Kuzina and Mikhailov⁹⁹ found two other radicals by ESR in PS exposed to UV radiation above 300 nm:



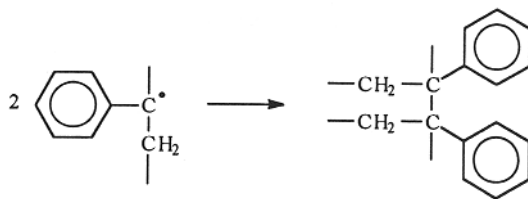
The first radical is present in irradiated samples up to the softening temperature of PS. This occurs because of conjugation of an unpaired electron with the π -electrons of the double bond. The second radical has also high thermal stability and can be preserved in irradiated PS up to 370 K. Radicals formed may participate in hydrogen abstraction from the polymer:



They may disproportionate:

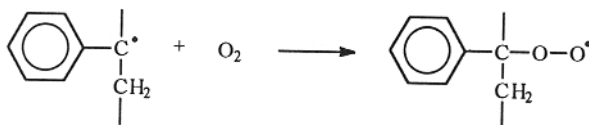


causing chain scission, or, they can recombine:

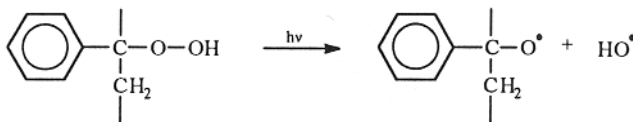


forming crosslinks.

The presence of oxygen complicates the mechanism of degradation. Hydroperoxides are formed:



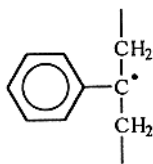
Peroxides are a light-sensitive and absorbing species:



Both radicals formed are active in hydrogen abstraction. The polymer contains small amounts (<0.1% of monomer units) of PS-hydroperoxide which initiates photolytic reactions. The alkoxy radical may also decompose by a β -scission process, forming an acetophenone end-group. It was found recently¹⁰⁰ that the above reaction alone does not explain the observed kinetics of hydroperoxide decomposition. It was proposed¹⁰⁰ that another reaction also takes place:

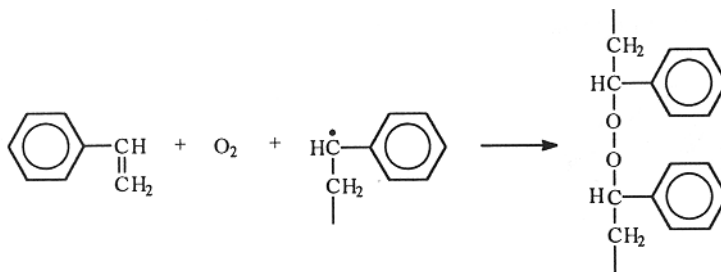


At wavelength of radiation higher than 300 nm, the polymer cannot absorb radiation. Thus above 300 nm excited phenylene rings do not exist and cannot contribute to degradation. But impurities in the PS such as benzophenone, acetophenone, etc., may abstract hydrogen, forming a polystyryl radical:



which seems to dominate initiation, and lead to further changes. Again, in vacuum and in air, radicals may recombine, to form crosslinks. This was confirmed when an increase in gel concentration was detected during degradation. In air, a reaction with oxygen leads to the peroxides dissociating to oxygenated products and causing chain scission.

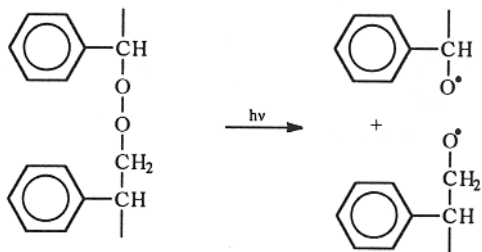
An alternative mechanism of initiation involves peroxy units incorporated into the chain by the random copolymerization of oxygen at synthesis or during processing:



A similar process was also found in the course of photolysis¹⁰⁰ in which peroxyradicals combine to form tetroxide:



This reaction explains the formation of molecular oxygen and absorption at 3550 cm^{-1} . Peroxy unit can easily be activated by daylight:



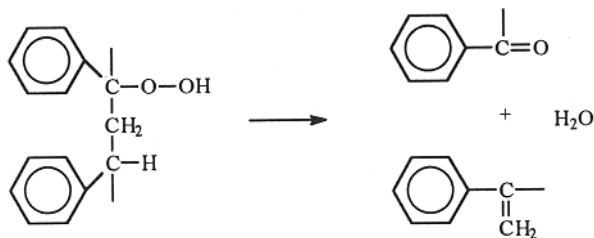
producing chain scissions and, more importantly, producing radicals which can initiate chain reactions.

There is a distinct difference between photolysis and photooxidation in the way in which each forms volatile products and in the mechanisms of yellowing. During photolysis, hydrogen is the only volatile product, whereas water and carbon dioxide are the major products of photooxidation. Weir *et al.*¹⁰⁰ found that water and methane form during the photolysis of PS under vacuum. Formation of hydrogen can be explained by the very high mobility of hydrogen radicals; they can diffuse out of the polymer matrix and then recombine.

Water can be formed by the abstraction of hydrogen by the hydroxyl radical:

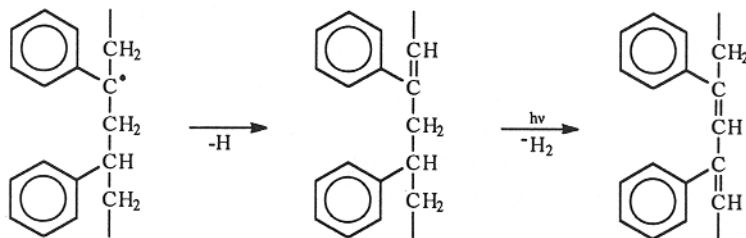


or from hydroperoxide decomposition:¹⁰⁰

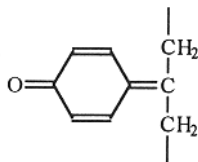


Photodecomposition of PS-hydroperoxides by exposure to radiation above 300 nm under vacuum results in emission of H_2O , CO_2 , CO , O_2 , benzaldehyde, acetophenone, and traces of benzene. The presence of CO , benzene, benzaldehyde, and acetophenone indicates that ketonic species, formed from PS-hydroperoxides, undergo Norrish type I and II decomposition.¹¹⁰

Discoloration of the polymer (yellowing) during photolysis is explained by the formation of conjugated double bonds:



in a process similar to that which occurs in other vinyl polymers. Conjugations of up to four double bonds in the polymer backbone were found. Photoyellowing in the presence of oxygen depends on a long sequence of reactions, beginning with formation of the polystyryl radical and ending with the formation of quinomethane structures:



generated from the oxidation of the phenylene ring and hydroperoxide decomposition.

Wells and Badyal⁹⁸ compared degradation in O₂ and N₂O. Although, N₂O should act in a similar manner to atomic oxygen, its effect on PS degradation was less detrimental than even that of molecular oxygen. The aim of these studies was to compare two surface preparation methods followed by further processing which required surface modification in the areas of optical reflection, adhesion, wettability, permeability, and biocompatibility. Wells *et al.*¹⁰⁵ in another experiment compared plasma oxidation with photooxidation in 240-600 nm region. The more reactive oxygen plasma caused less modification due to the fact that it is an ablative process, therefore the effect of surface degradation was lost with the removed layer of material.

Reprocessing of PS (even several times) does not seem to pose any problems.¹⁰⁶ The mechanical properties of the material are almost completely retained after a series of six reprocessings. The addition of up to 25% of recycled material does not change mechanical properties in any significant way. Elongation and impact resistance are the most vulnerable properties. During processing, bond scission may promote unzipping with monomer yield of 40%.¹¹⁵ Processing temperatures in the range of 180-200°C may be sufficient to promote such changes.

Polystyrene exposed to sunlight darkens due to the absorption of blue light (near 400 nm). Absorption occurs due to the formation of an oxygen complex of excited phenyl groups which then undergoes a ring-opening reaction which forms of mucondialdehyde groups.¹¹⁵

14.3.2 EFFECT OF THERMAL HISTORY

Thermooxidative processes are responsible for introduction of initiation sites namely, in-chain peroxide linkages, hydroperoxides, carbonyl groups, and unsaturations. Peroxide groups are weakly bonded (40-50 kcal/mol)¹¹⁵ and they can be broken by UV or heating.

14.3.3 CHARACTERISTIC CHANGES AND PROPERTIES

Radical decay is accelerated by a temperature increase, especially above the glass transition temperature (Fig. 14.13). Increased temperature favors both formation of carbonyl groups (Fig. 14.14) and gel (Fig. 14.15), which means that both chain scission and crosslinking reactions have higher rates due to radical instability. The simultaneous occurrence of crosslinking and chain scission reactions during photooxidation results in an overall decrease of molecular weight, meaning that scission prevails (Fig. 14.16). Chain scission occurs faster on the sample surface because oxygen is available. Diffusion controls the photooxidative process (Fig. 14.17). Recent data¹⁰⁸ are in agreement with those presented in Figs 14.16 and 14.17. Most damage occurs close to the surface, and only negligible changes were detected during molding. Also, an emission intensity study shows that photodegradation is a surface-related phenomenon (Fig. 14.18). The color of

polystyrene changes to yellow on UV exposure (Fig. 14.19). N_2O is more reactive than O_2 but creates unreactive OH groups, therefore the overall rate of PS oxidation is lower in N_2O than in molecular oxygen (Fig. 14.20). Impact modification of PS increases its degradation rate (Fig. 14.21). Polybutadiene used as impact modifier is the main site of oxidation (HIPS contains from 4 to 26% of polybutadiene); some radicals formed from the photolysis of thermally oxidized polybutadiene can act as initiators of PS oxidation. The effect of a sensitizer (benzophenone) can be seen in Fig. 14.22. PS-hydroperoxide is the major product in a sensitized reaction and polymeric acetophenone is its minor product. Similar studies on anthracene sensitization, using a laser, were conducted by time-of-flight MS.¹⁰⁹ Below the ablation threshold only anthracene was detected. When surface etching was occurring both anthracene and styrene monomer were detected. These results suggest that the energy absorbed by the sample is converted to thermal energy thus, the process can be regarded as thermal decomposition. An introduction of carbonyl groups into a polystyrene backbone chain results in an increased degradation rate (Fig. 14.23).¹¹² This method is used to control PS degradation in photodegradable materials (ECOLYTE copolymer).

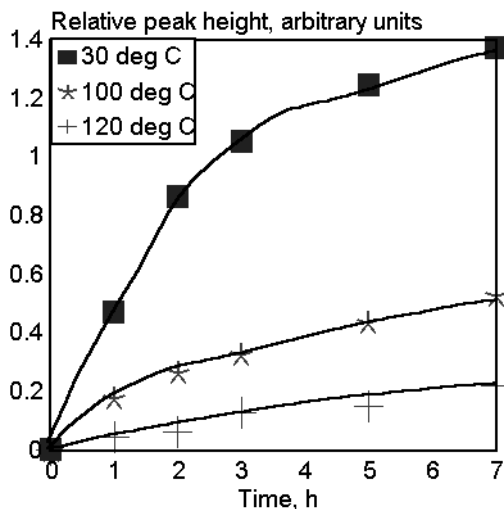


Fig. 14.13. Relative ESR peak heights of radicals formed in vacuum at different temperatures vs. photoinitiation time. [Adapted, by permission, from A. Torikai, A. Takeuchi, and K. Fueki, *Polym. Degrad. Stab.*, 14(1986)367.]

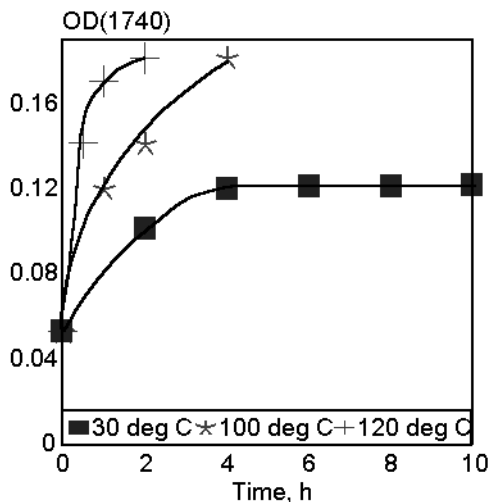


Fig. 14.14. Formation of carbonyl groups in polystyrene irradiated in air at different temperatures. [Adapted, by permission, from A. Torikai, A. Takeuchi, and K. Fueki, *Polym. Degrad. Stab.*, 14(1986)367.]

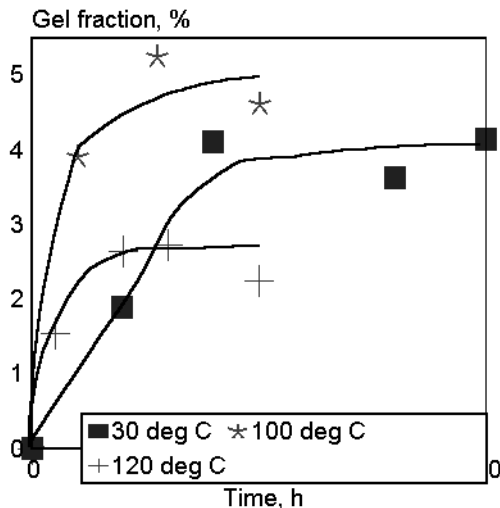


Fig. 14.15. Gel fraction vs. irradiation time in air at different temperatures. [Adapted, by permission, from A. Torikai, A. Takeuchi, and K. Fueki, *Polym. Degrad. Stab.*, 14(1986)367.]

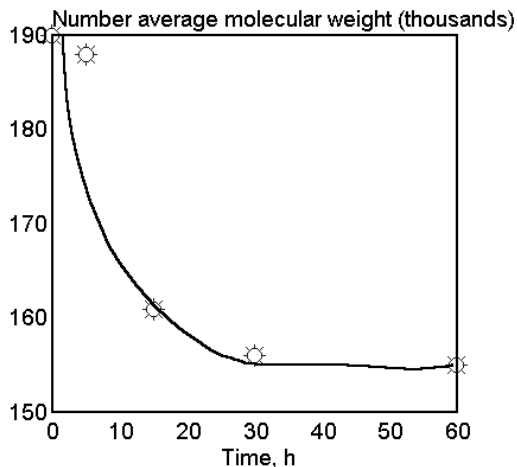


Fig. 14.16. Change in PS molecular weight on irradiation in air. [Data from Z. Osawa, F. Konoma, S. Wu, and J. Cen, *Polym. Photochem.*, 7(1986)337.]

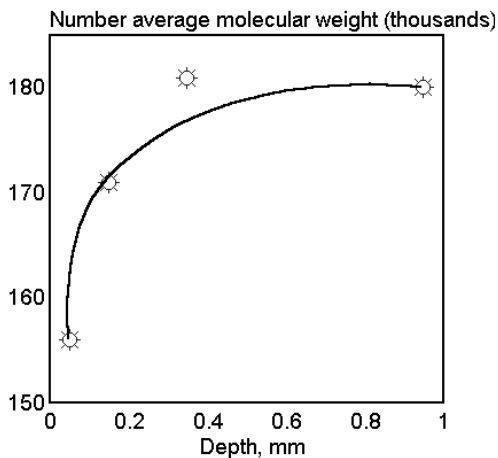


Fig. 14.17. PS molecular weight vs. depth from the surface. [Data from Z. Osawa, F. Konoma, S. Wu, and J. Cen, *Polym. Photochem.*, 7(1986)337.]

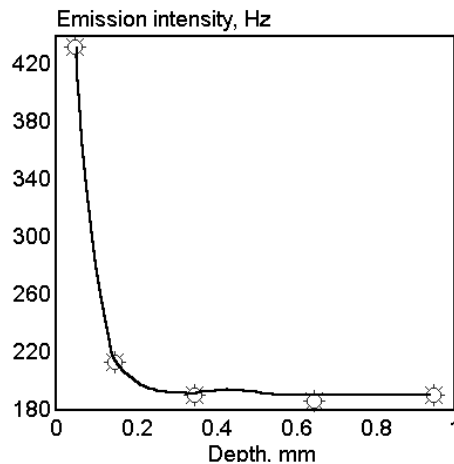


Fig. 14.18. PS emission intensity vs. depth from the surface. [Data from Z. Osawa, F. Konoma, S. Wu, and J. Cen, *Polym. Photochem.*, 7(1986)337.]

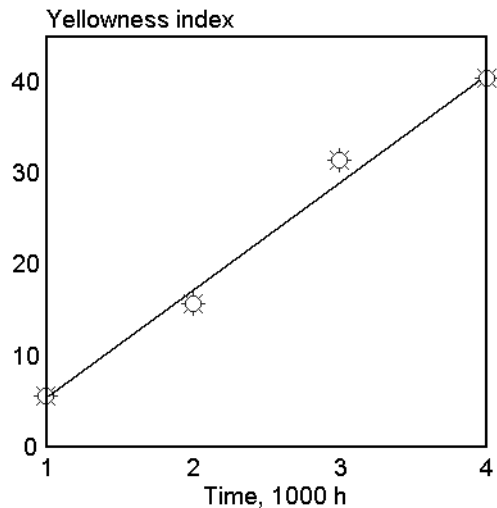


Fig. 14.19. PS yellowness index vs. accelerated exposure time (Xenotest 150). [Data from F. Gugumus, *Dev. Polym. Stab.*, 1(1979)8.]

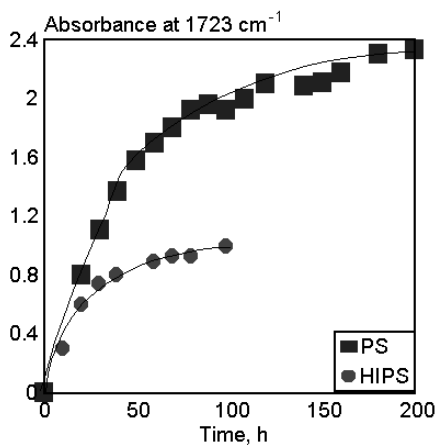


Fig. 14.21. Carbonyl group formation vs. irradiation at $\lambda \geq 300$ nm. [Data from Y. Israeli, J. Lacoste, J. Lemaire, R. P. Singh, and S. Sivaram, *J. Polym. Sci., Polym. Chem.*, 32 (1994)485.]

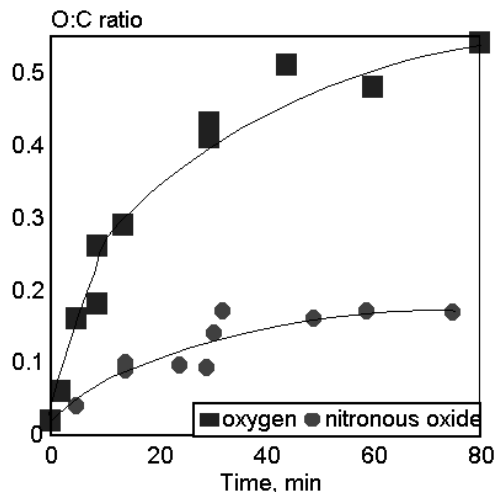


Fig. 14.20. O:C ratio vs. irradiation time in glass reactor by Hg-Xe lamp in the 240-600 region, in presence of 1 - O₂/PS, 2 - N₂O/PS. [Data from R. K. Wells and J. P. S. Badyal, *J. Polym. Sci., Polym. Chem.*, 30(1992)2677.]

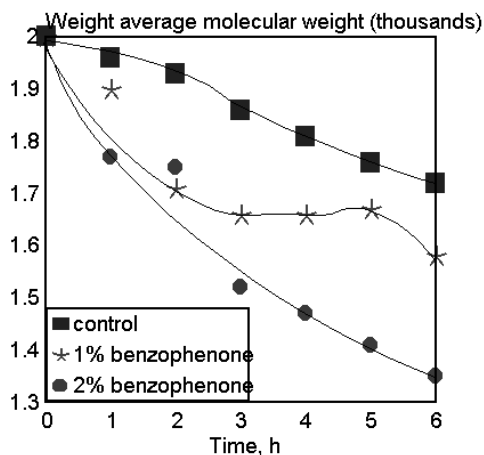


Fig. 14.22. Molecular weight change of PS vs. irradiation time by Hg lamp ($\lambda \geq 300$ nm). [Adapted, by permission, from C. S. Lin, W. L. Liu, Y. S. Chiu, and S.-Y. Ho, *Polym. Deg. Stab.*, 38(1992)125.]

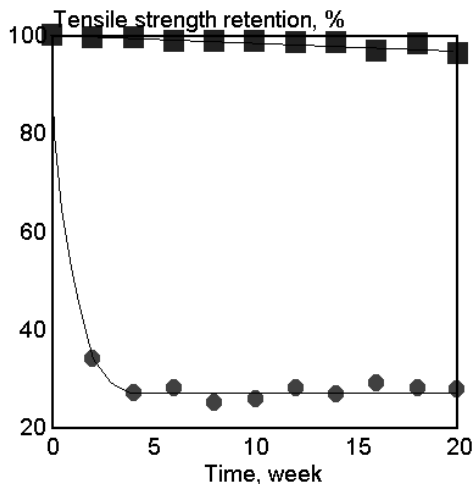


Fig. 14.23. Tensile strength retention during outdoor weathering in Sarnia, Canada. ■ - PS, ● - copolymer containing small amount of carbonyl groups in its backbone (ECOLYTE copolymer). [Data from S.A. May, E.C. Fuentes, and N. Sato, *Polym. Deg. Stab.*, 32(1991)357.]

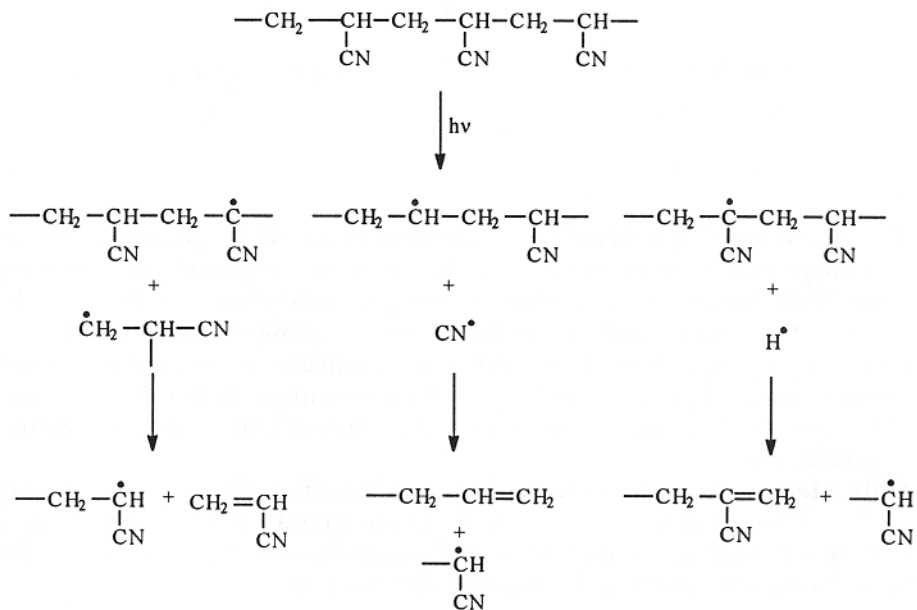
14.3.4. DATA

Luminescence data:		
Sample form	Excitation wavelength, nm	Emission wavelength, nm
film	254	390, 430, 510
chip	318, 330	336, 354, 368
film	290, 300, 336	398, 425, 456, 492
commercial	300	338, 355, 372
commercial	315-335	395, 422, 455, 485
Spectral sensitivity: <340 nm		Activation wavelength: 318 nm
Products of photolysis: hydrogen, crosslinks, benzene, conjugated double bonds, radicals, methane and ethylene (ring substituted polymers only)		
Products of photooxidation: water, carbon dioxide, ketones, unsaturations, hydroperoxides, radicals, chain scissions, quinomethane structures		

14.4 POLYACRYLONITRILE (PAN)

14.4.1 MECHANISM OF DEGRADATION

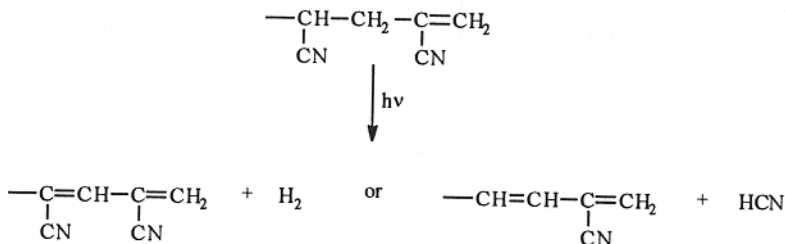
UV irradiation affects the evolution of acrylonitrile, hydrogen, hydrogen cyanide, and methane. The literature cites mechanisms which explain the formation of these compounds:



Hydrogen and cyanide radicals can abstract hydrogen along the polymer chain, forming hydrogen or hydrogen cyanide. At the same time, conjugated double bonds are formed in the chain, leading to an increased UV absorption and colored compounds:



Unsaturation favors the formation of conjugated bonds when irradiated:



The existing findings do not give preference to any of the last two reactions, but it would be surprising if the formation of hydrogen would not prevail, since it is supported by charge distribution in the molecule. The presence of oxygen changes the above mechanisms by contributing to the formation of hydroperoxides, which on further absorption of UV radiation, dissociate to two radicals, causing chain scission and formation of carbonyl group. Knowledge of the mechanism of photodegradation of PAN is still incomplete. It is surprising that it differs so much from the mechanism of PVC photodegradation.

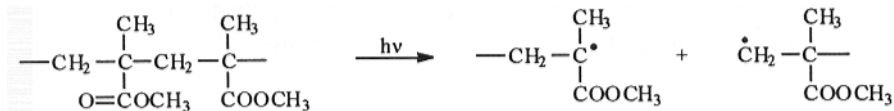
Only a few studies have been conducted on the effect of γ -radiation on PAN. When radical formation is detected by ESR, it shows that PAN photochemistry involves hydrogen abstraction. Radicals were identified and hydrogen was abstracted from both the methylene group and from the tertiary carbon atom.¹¹⁹

14.5 ACRYLIC RESINS¹²⁰⁻¹³⁸

Acrylic polymers are used with confidence in outdoor applications. They have so good weathering characteristics that only limited efforts are being made to study the mechanism of their degradation. Since polymethylmethacrylate was found to be UV-durable, this has resulted in other acrylic polymers, considerably different in chemical structure, being attributed with similar good weatherability.

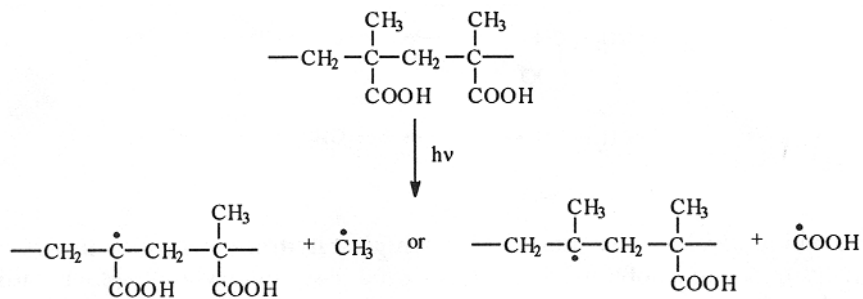
14.5.1 MECHANISM OF DEGRADATION

Acrylic polymers are frequently made from a mixture of monomers. It is therefore important to separate the effect of UV radiation on the backbone from its effect on side groups. UV radiation below 300 nm may cause homolytic chain scission of the polymer backbone:

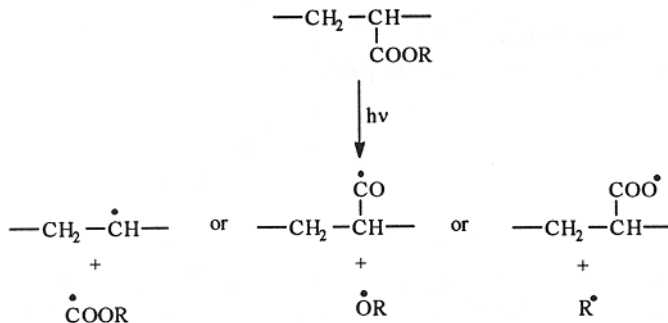


resulting in molecular weight decrease. More frequently, chain scission or crosslinking occurs because of formation of free radicals from radiolysis of bonds in side groups, from atoms in backbone, or from other atoms attached to them. These changes depend on the chemical structure of the functional groups available in the material.

The carboxylic pendant group affects formation of radicals:



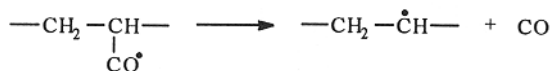
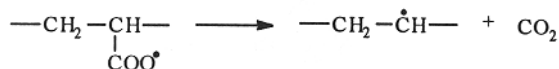
If acrylic acid is a component, the hydrogen radical is formed. When the carboxylic group is replaced by the ester group, three dissociation patterns are possible:



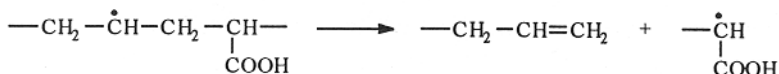
Low-molecular-weight radicals may recombine or undergo further changes (usual case), forming products frequently detected as volatiles:



Macroradicals may also form gaseous products:

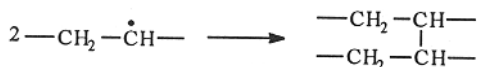


often found in analysis of volatiles. Esters of higher hydrocarbons may produce unsaturated structures (e.g., poly(butyl acrylate) produces isobutylene). Macroradicals undergo further changes; some of them result in chain scission:



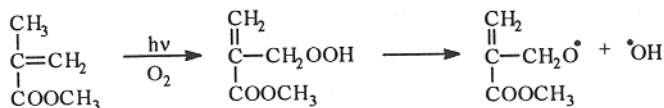
and form radical or unsaturation.

In the absence of oxygen, crosslinking prevails:



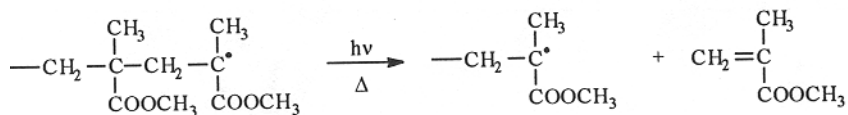
Oxygen presence causes both crosslinking and chain scission. When radicals react with oxygen, they form hydroperoxides which, after decomposition by UV contribute to a carbonyl and hydroxyl accumulation.

Residual monomer increases the degradation rate:



During irradiation, the monomer gradually evaporates and degradation rate decreases.

Temperature has a very pronounced effect on UV degradation rate and products of photolytic reactions. At higher temperatures, there is a greater evolution of monomer:



This is consistent with the mechanism of thermal degradation; UV light is an additional source of energy.

Polyacrylophenones exposed to UV radiation ($\lambda > 300$ nm) undergo degradation at locations where substituent groups are attached to benzene rings. This produces quinone structures which cause yellowing.¹³⁶

Laser exposure of PMMA results in the emission of numerous volatile products, such as, CO, CO₂, C₂H₂, CH₄, CH₃CO, and others. Their concentration depends on the rate of energy transfer. This process is more similar to pyrolysis than to UV degradation.

Buchwalter and Czornyj¹²⁷ found that PMMA degrades during XPS analysis. A main chain scission occurs, resulting in a molecular weight decrease and a solubility change. PMMA is easily degraded by ionizing radiation, and therefore it can be used as positive resist material in X-ray and electron beam lithography.¹³³ Radicals are formed by hydrogen abstraction, followed by the formation of numerous radicals on side groups which may lead ultimately to main chain scission. Direct main chain scission does not occur.

14.5.2 EFFECT OF THERMAL HISTORY

Acrylic resins, when heated, undergo radical depolymerization reaction, which may contribute to unsaturations; radicals formed in this process may simultaneously react with atmospheric oxygen, leading to an accumulation of hydroperoxides, hydroxyl, carbonyl, and aldehyde groups in the polymer.

14.5.3 CHARACTERISTIC CHANGES AND PROPERTIES

Depolymerization occurs during weathering but such changes are mainly restricted to the specimen surface. After 10 years of exposure, the degraded layer is 0.01-0.02" thick

(Fig. 14.24). UV exposure facilitates chain scission (Fig. 14.25). Loss of elongation is the most pronounced but overall changes are not great (Fig. 14.26). Monomer removal from the specimen is a relatively fast process (Fig. 14.27).

14.5.4 DATA

Products of photolysis: crosslinks, formaldehyde, methanol, hydrogen, carbon monoxide, carbon dioxide

Products of photooxidation: crosslinks, hydroperoxides, hydroxyl groups, carbonyl groups, aldehydes

Important initiators and accelerators: phenothiazine, residual initiator, residual monomer

Stabilization: UV absorbers (benzotriazoles preferred); quenchers

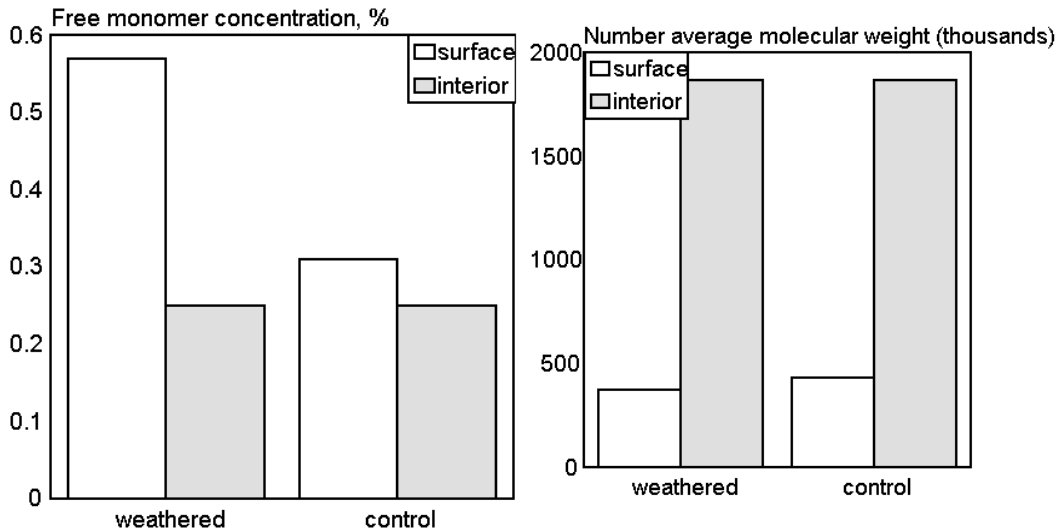


Fig. 14.23. Tensile strength retention during outdoor weathering in Sarnia, Canada. ■ - PS, ● - copolymer containing small amount of carbonyl groups in its backbone (ECOLYTE copolymer). [Data from S. A. May, E. C. Fuentes, and N. Sato, *Polym. Deg. Stab.*, 32(1991)357.]

Fig. 14.24. Free monomer concentration in PMMA (10 years of natural exposure). [Data from J. D. Stachiw and R. B. Dolan, *Trans. ASME*, 104(1982)190.]

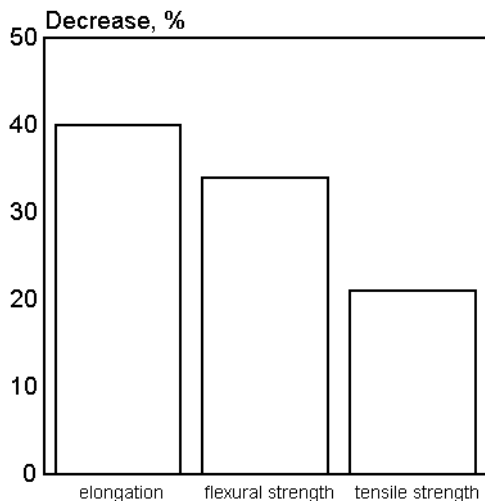


Fig. 14.25. Molecular weight of PMMA (10 years of natural exposure). [Data from J. D. Stachiw and R. B. Dolan, *Trans. ASME*, 104(1982)190.]

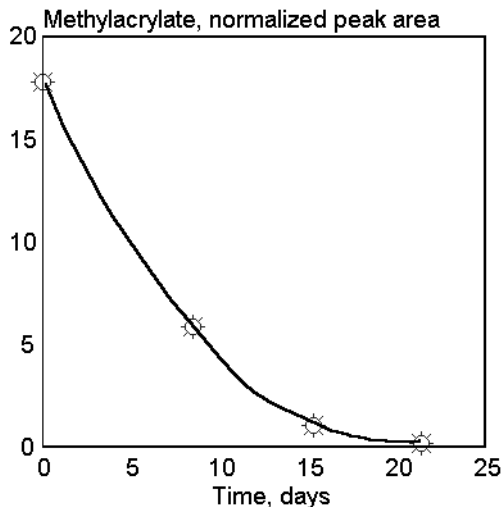


Fig. 14.26. PMMA mechanical properties change (10 years of natural exposure). [Data from J. D. Stachiw and R. B. Dolan, *Trans. ASME*, 104(1982)190.]

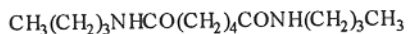
14.6 POLYAMIDES (PA)¹³⁹⁻¹⁶⁶

Both aliphatic and aromatic polyamides were studied, with most emphasis given to aliphatic polyamides. Some findings are relevant for other groups of polymers, especially the studies of degradation under stress, which documented the influence of process conditions - namely, the effect of internal stress relative to drawing conditions.

14.6.1 MECHANISM OF DEGRADATION

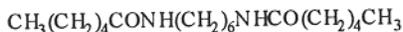
14.6.1.1 Models

Luminescent species were identified using:



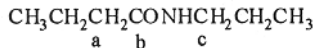
N,N'-di-n-butyladipamide

and



N,N'-dicaproylhexamethylenediamine

as model compounds. The products of their thermal oxidation match excitation and emission spectra of polyamide-6,6. Heating in the absence of oxygen does not produce luminescent species. Sharkey¹⁵⁵ used:



with atoms in positions a, b, c labelled with ¹⁴C. Each group was the precursor of a different volatile product:

CH₂ (a) - caproic acid

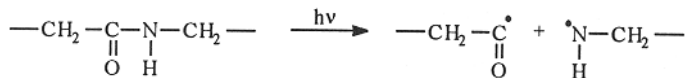
CO (b) - caproic acid and CO₂

CH₂ (c) - N-valeric aldehyde, valeric acid, CO, and CO₂

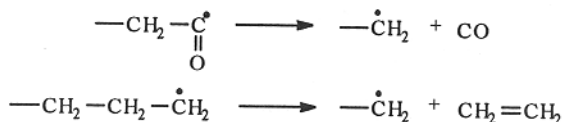
meaning that photooxidation was initiated by abstraction of hydrogen from the α-methylene group. If hydrogen in the α-methylene group is replaced by the methyl group, photooxidation is inhibited.

14.6.1.2 Polymer

Scission of the amide linkage dominates photolytic reactions:



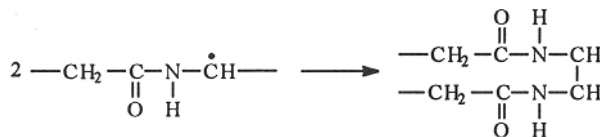
The above reaction is typical for both aliphatic and aromatic polyamides and it is a starting-point of further conversions. The carbonyl radical, after regrouping, forms volatile products:



Both radicals are capable of abstracting hydrogen from other molecules:

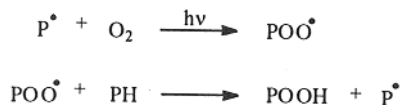


and producing crosslinks:



The above radical is very stable and persists to cause crosslinking. Crystalline structure of polymer affects probability of crosslinking. In amorphous areas, the number of hydrogen bonds is less which allows radicals to migrate freely and cause crosslinking reactions.

The presence of oxygen during photolysis changes the mechanism of degradation, favors individual reactions, and causes an overall increase in the rate of degradation. The initial steps of photooxidation are similar to photolysis. Both carbonyl and amino radicals are formed. The next stage of photooxidation involves the formation of hydroperoxides from existing radicals:

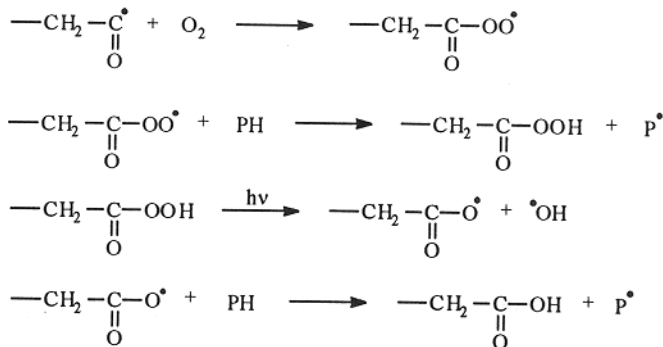


One radical may theoretically produce one molecule of hydroperoxide and a new radical. Hydroperoxide can dissociate further:



with the production of two new free radicals, which autoaccelerate the process. The degree of autoacceleration depends on the energy supplied, and the material composition. Recombination of radicals will decrease the efficiency of photodegradation.

Several typical products are formed during photooxidation. Carboxylic acids are produced as a consequence of carbonyl radical oxidation:



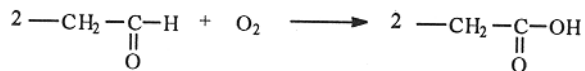
Carboxyl radical may also decompose to form carbon dioxide:



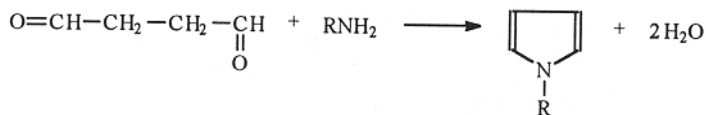
Like carboxylic acids, aldehydes are produced from the carbonyl radical:



and may be further converted to carboxylic acids:

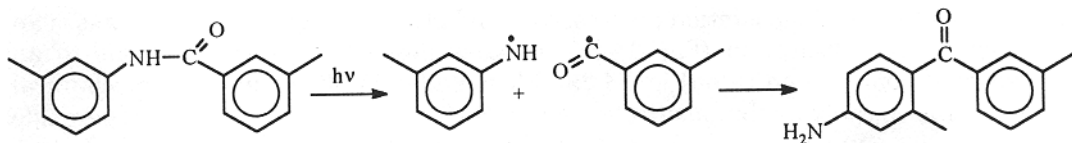


The yellowing of polyamides is explained by the formation of pyrrole-type compounds which are the condensation products of dicarbonyl compounds with primary amines:

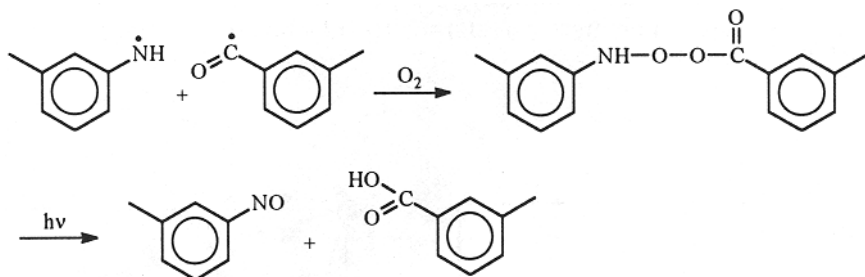


Dicarbonyl compounds and primary amines are formed from oxidation products of methylene groups adjacent to peptides. They are formed in the sequence of reactions, including hydroperoxide formation, hydrolytic breakdown, and subsequent decarboxylation. All these mechanisms, although not proven in detail, explain pyrrole accumulation on aging.

Aromatic polyamides differ from aliphatic polyamides because they can undergo photo-Fries rearrangement:



An alternative mechanism of degradation includes reaction with oxygen:¹⁶⁰



which leads to chains scission and formation of oxygenated compounds. The amount of energy required to degrade aramid fiber at its most sensitive segment (the amide bond) is 222 kJ/mol. It was established that protection of aramid fibers with UV screeners is ineffective because aramid fibers are also affected by visible light.

Studies of textiles shed an interesting light on the degradation process. Depending on the construction of the material, the yarn may be exposed to UV radiation directly (knitted or woven fabric) or exposed at angle smaller than 90° (flocked yarn) or the ends only are exposed to direct radiation (pile, flocked textile). Testing each type of material requires a different method. In the case of the direct exposure of knitted or woven fabric, tensile strength measurement is a reliable method of characterizing changes. With flocked yarn, pile, and flocked textiles, abrasion resistance measurements are the most useful. Polyamide fabric can now be made immensely more durable and suitable for use in outdoor applications through the combined use of color (at high intensity) and UV stabilizer.¹⁵⁹

14.6.2 EFFECT OF THERMAL HISTORY

Thermal degradation of polyamide contributes to increased absorption in the UV region. The absorption is proportional to the accumulation of conjugated structures formed by double bonds and carbonyl groups. Formation of these groups depends on the conditions of thermal degradation and their presence accelerates UV degradation by a few orders of magnitude.

14.6.3 CHARACTERISTIC CHANGES AND PROPERTIES

During the thermal degradation process, carbonyl groups are formed, which causes an increase in UV absorption (Fig. 14.28). Greater absorption of energy leads to an increased decomposition rate (Fig. 14.29). Photooxidation affects not only mechanical properties of the polymer but also its structure. Gas diffusion depends on hydroperoxide concentration. When hydroperoxides are decomposed by treatment with SO_2 , the diffusion coefficient of CO_2 changes (Fig. 14.30). Substantial differences in the stability of various polyamides during natural weathering were recorded (Fig. 14.31). Acid rain increases degradation rate, especially at lower pHs (Fig. 14.32). The changes in mechanical properties of polymers correlate with the changes in their molecular weight (Fig. 14.33).

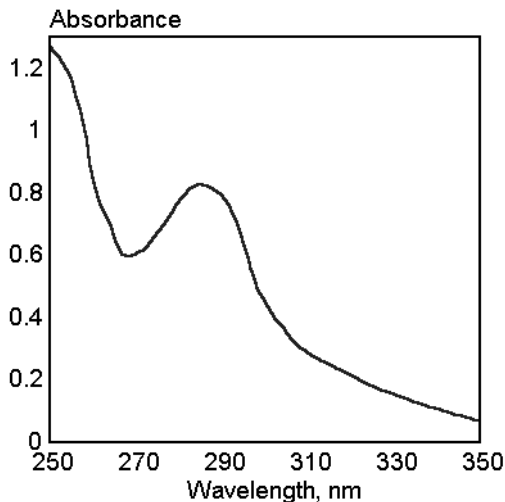


Fig. 14.28. Effect of thermal degradation during 80 h at 100°C on UV absorption by polyamide-6,6 yarn. [Data from A. Anton, *J. Appl. Polym. Sci.*, 9(1965)1631.]

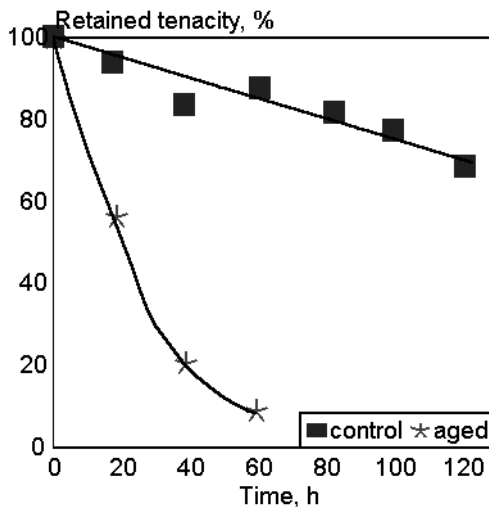


Fig. 14.29. UV degradation of thermally aged polyamide-6,6 (80 h at 100°C). [Data from A. Anton, *J. Appl. Polym. Sci.*, 9(1965)1631.]

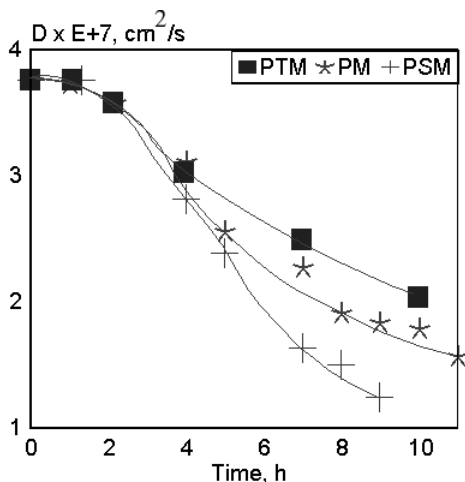


Fig. 14.30. Change of diffusion coefficient during irradiation (PTM - photo- and thermooxidized material; PM - photooxidized material; PSM - photooxidized material treated with SO_2). [Adapted, by permission, from J.-L. Philippart and J.-L. Gardette, *Makromol. Chem.*, 187(1986)1639.]

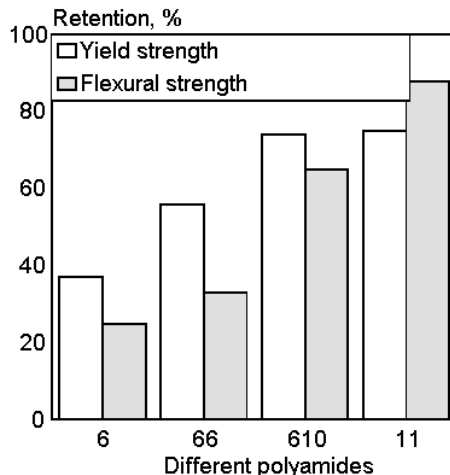


Fig. 14.31. Yield and flexural strength retention after 4 years exposure of various polyamides in hot/wet tropics. [Data from A. Davis and D. Sims, *Weathering of polymers*, *Applied Science Pub-*

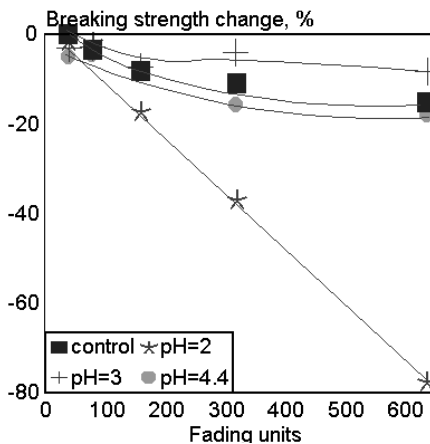


Fig. 14.32. Change in breaking strength vs. light exposure (xenon-arc fadeometer) of polyamide treated with H_2SO_4 at different pH. [Adapted, by permission, from K. E. Kylo and C. M. Ladisch, *ACS Symp. Ser.*, 318(1986)343.]

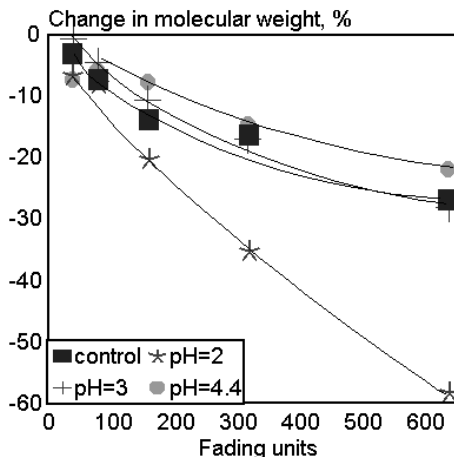


Fig. 14.33. Change in molecular weight vs. light exposure (xenon-arc fadeometer) of polyamide treated with H_2SO_4 at different pH. [Adapted, by permission, from K. E. Kylo and C. M. Ladisch, *ACS Symp. Ser.*, 318(1986)343.]

14.6.4 DATA

Luminescence data:		
Sample form - chip/polymer	Excitation wavelength, nm	Emission wavelength, nm
PA-6	282	380, 420, 455
	300	460
	310	470
PA-6,6	295	410
	310	415, 460
	315	420, 460, 480
PA-11	269, 273	423, 450
	300	460
	310	465
Spectral sensitivity: <450 nm (aromatic polyamides)		
Products of photolysis: amines, carbon monoxide, hydrogen, hydrocarbons, crosslinks		
Products of photooxidation: amines, carbon monoxide, carbon dioxide, acids, ammonia, water, aldehydes, peroxides		
Important initiators and accelerators: conjugated carbonyls-unsaturations, products of photooxidation, titanium dioxide, derivatives of anthraquinone, β -oxyethylsulfonic red and yellow, monochlorotriazine red and yellow, copper compounds		

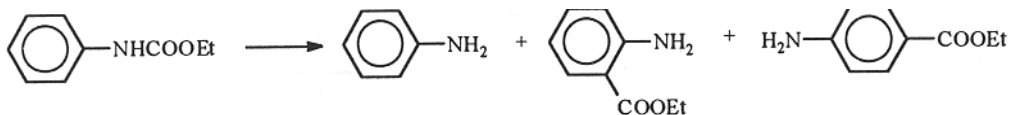
14.7 POLYURETHANES (PU)¹⁶⁷⁻²⁰⁴

This group consists of polymeric materials obtained through a polyaddition reaction from reactants of various chemical composition. The most important materials are polyurethanes, polyureas, and polyisocyanurates. Polyurethanes are formed by reacting hydroxyl bearing polymeric materials (polyols) with isocyanates. Polyureas are the reaction products of amines and isocyanate-containing prepolymers. Polyisocyanurates are formed from polymeric (trimeric) isocyanates. Products also differ in properties because of polyol structure. Two main groups of polyols are used: polyethers and polyesters. Additionally, polymers may include hydroxyl bearing oligomers playing the role of polyols, for example, acrylates or synthetic elastomers, and may also have other functional groups, such as, epoxy, silanol, etc.

14.7.1 MECHANISM OF DEGRADATION

14.7.1.1 Models

Beachell¹⁸³ explained the results of the photolysis of aryl carbamates with the following equation:

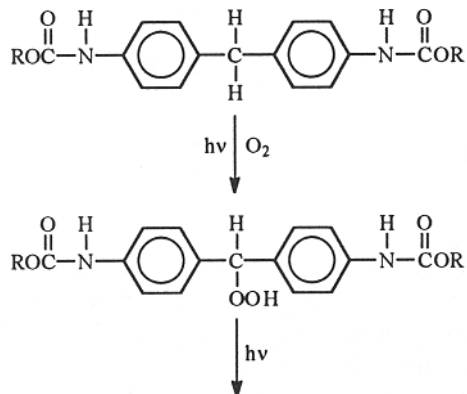


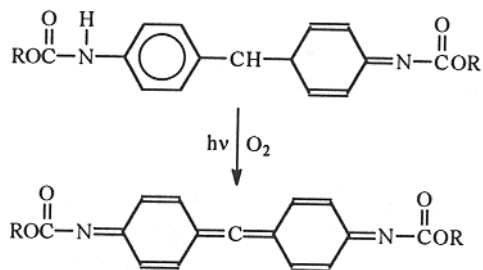
The above changes, called the photo-Fries rearrangement, occur when a material is irradiated at 254 nm. In the presence of oxygen and UV, the material changes to a colored product of the quinoid type.

Chapman's studies on model compounds¹⁹⁵ show that under moderately acidic conditions the urea linkage is less stable to hydrolysis than the urethane linkage. Also, hydrolysis occurs at a slower rate in aliphatic than in aromatic urethanes. Polyether polyols are very stable when exposed to mildly acidic conditions. The half-life of diethyl ether in 1N benzenesulfonic acid at 70°C is 13.8 years, compared with 1.9 years for an aliphatic urethane.

14.7.1.2 Polymers

Schollenberger¹⁷⁴⁻⁵ and Nevskii¹⁸² showed the sequence of changes in polyurethanes based on methylene 4,4-diphenyl diisocyanate, MDI, as follows:





This model explains the frequently-observed discoloration of polyurethanes made from some aromatic isocyanates (MDI) but fails to explain changes in tensile strength and elongation which are also observed during PU degradation. Moreover, color changes of TDI-based polymers cannot be explained by these mechanisms.

The results which Ulrich¹⁷³ published add to the confusion. Model polyurethanes having the following structures:

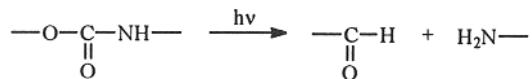
		Irradiation
		4h 12h
1		VLY LY
2		LY Y
3		Y A

V-very; L-light; Y-yellow; A-amber

discolor, regardless of the fact that structures 2 and 3 preclude formation of quinoid species. This shows that there is still uncertainty about the mechanisms of aromatic polyurethane degradation. The most commonly accepted mechanism includes two processes occurring simultaneously:

chromophores). It also shows that, although discoloration is not a problem facing aliphatic polyurethanes, their mechanical properties might be affected in a manner similar to the aromatic polyurethanes.

Another mechanism explains why both aliphatic and aromatic polyurethanes lose their original mechanical properties:

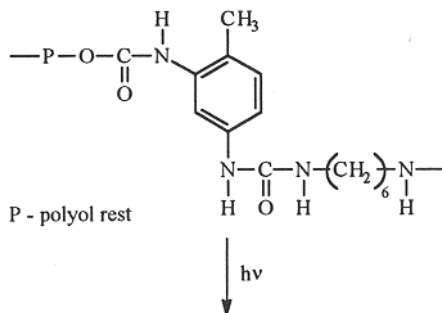


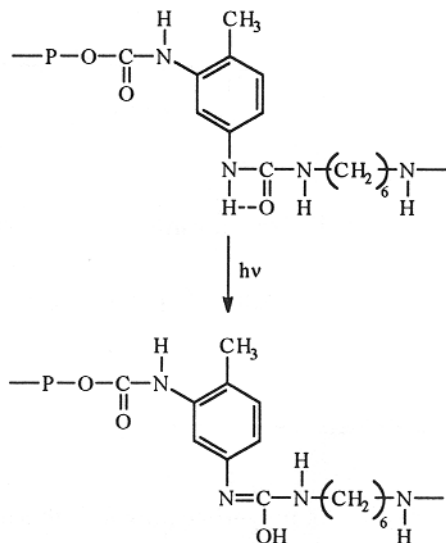
The Norrish type I photocleavage is believed to be more important in the degradation of aliphatic polyurethanes.

Based on extensive studies of aliphatic prepolymers cured with aromatic amines and aromatic prepolymers cured with aliphatic and aromatic amines, it is possible to rationalize these mechanisms and propose one mechanism which explains all the observed changes.²⁰⁴

- if at least one component of polyurea (curative or isocyanate) is aromatic, the resultant material will display color changes on UV exposure but it will have better retention of mechanical properties
- if both components are aliphatic (isocyanate and amine - aliphatic or cycloaliphatic), the resultant material loses mechanical properties on UV exposure but retains most of its initial color.

Let us discuss the reasons for color changes. We use TDI in order to show that the proposed mechanism is consistent for all aromatic isocyanates (also for MDI). The following reaction explains the proposed mechanism of yellowing:



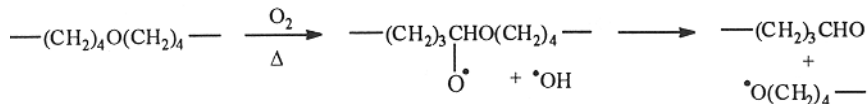


When it absorbs energy, polyurea (or polyurethane) is isomerized to the enol-form which has more than 3 conjugated double bonds and, therefore, is colored. Similar changes in the fully aliphatic system do not result in colored compounds. Here, only part of polyurethane is isomerized because changes occur rapidly on the first exposure to energy, then further color development is inhibited. Before degradation, polyurethanes have only slight fluorescence in UV, as degradation begins, there is a sudden jump to a level 10 times higher than the initial fluorescence. There after, the fluorescence remains at the same level. Fluorescence of aliphatic polyurethanes does not change appreciably throughout the entire degradation process. The difference in fluorescence between each type of polyurethane explains reasons for the differences in their durability related to differences in energy conversion.

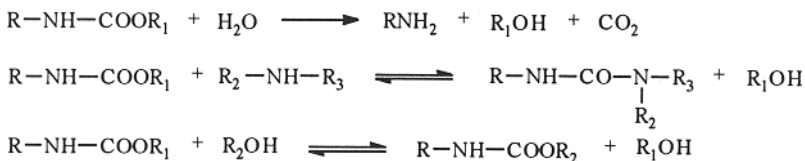
Other properties of aliphatic and aromatic polyurethanes should also be considered to explain their behavior. Aliphatic aldehydes and ketones are known to absorb radiation at 280-290 nm whereas aromatic ketones absorb in a longer wavelength band (see Chapter 2). The lower energy of radiation absorbed by aromatic ketones reduces the probability of their chemical conversion. Aliphatic ketones undergo Norrish type II cleavage from their singlet and triplet states whereas aromatic ketones cleave only from their triplet states which again decreases their probability of conversion.

The polyol segment requires more in-depth study. It can be deduced from existing literature that two mechanisms of degradation might be relevant:

oxidation:



chemical degradation (hydrolysis, transamination, transesterification):



The oxidation mechanism is typical of polyether polyols, whereas polyester polyols are known to be vulnerable to chemical degradation.

Crystallinity in the polymer also plays an important role in the overall picture. Evidence shows that the rate of degradation depends on polymer crystalline structure.¹⁷⁹⁻⁸⁰ The more amorphous (elastic) the polymer, the higher the rate of degradation. The crystalline structure of a polyurethane depends on several important factors, such as the time-temperature regime, the rate of solvent evaporation depending on its solvation activity towards a polymer, the rate of cure, rheological changes in material during curing, the chemical structure of the curative and its effect on microstructure, the type and concentration of additives, etc. These factors in combination form a very complex picture which requires lengthy study and full expertise to optimize conditions for the best performance of the material.

Brandwood *et al.*¹⁹⁶ report on biodegradation of polyurethane medical implants. Oxidative degradation was drastically curtailed by using a polyether polyol with reduced ether linkages. Effect of stress on degradation was also presented. Anderson *et al.*²⁰³ found that surface cracking in medical implants extends 10 μm deep and it is mostly caused by oxidative changes in soft-segments. The degradation products contain carboxyl and hydroxyl groups. The oxidative agents, which attack the polymer, can be effectively deactivated by antioxidants.

14.7.2 EFFECT OF THERMAL HISTORY

Thermal degradation is complex and highly temperature dependent. At 210°C, polyurethanes depolymerize. Products of degradation include: CO, CO₂, HCN, buta-

diene, furans, carbodiimides, and a variety of oxygenated compounds that increase light absorption and yellowness index. The thermal degradation process in polyurethanes is exothermic in air but, when CaCO_3 is added to the polymer, the process becomes endothermic.¹⁹⁹ The reason for the effect is unknown but calcium carbonate seems to act as a fire retardation additive.

14.7.3 CHARACTERISTIC CHANGES AND PROPERTIES

Fig. 14.34 illustrates the advantages of using polyethers to achieve hydrolytic stability in polyurethanes. A polycaprolactone type of polyol gives intermediate resistance between the two groups. The urethane linkage is more stable than the urea linkage. The use of aromatic isocyanate further decreases hydrolytic stability (Fig. 14.35). Aromatic polyurethanes are known to discolor on UV exposure, as opposed to aliphatic polyurethanes. Aromatic polyurethanes also retain mechanical properties better (Fig. 14.36). The length of the hydrocarbon segment of chain extender determines the flexibility of the material. A long chain confers flexibility which increases with chain length increase. A short chain confers rigidity but also increases UV resistance (Fig. 14.37). The more flexible polyurethanes produce more gel on irradiation due to an increased crosslinking rate (Fig. 14.38). The use of 1,4-butanediol (BDO) in the composition increases polymer rigidity and reduces the formation of insoluble gel when the material is irradiated (lower photolytic degradation) (Fig. 14.39). Although higher material flexibility causes a more rapid degradation rate, the overall structure of the material is also a factor. In particular, increased crystallinity also increases degradation rate (Fig. 14.40). Both chemical and crystalline structure influence degradative changes through the photo-Fries rearrangement. Cobalt, copper, tin, and titanium have the strongest effect on the UV degradation rate of polyurethanes (Fig. 14.41). Polyols exposed to UV radiation show accumulation of hydroperoxides in poly(tetramethylene glycol) (Fig. 14.42). The highest radical formation rate in two-component polyurethanes was produced by irradiation at 334 nm. Maximum degradation occurs in a very narrow wavelength range which makes PU easy to stabilize (Fig. 14.43).²⁰¹

14.7.4 DATA

Luminescence data:		
Sample form	Excitation wavelength, nm	Emission wavelength, nm
MDI- based film	372	420
MDI-based film	320	423, 455, 489
Important initiators and accelerators: catalysts used in prepolymer synthesis, catalysts used in the curing process, heavy metals, peroxides in polyol, products of reaction of amine catalysts and polyols, some antioxidants, nitrous oxide, acids, and bases (hydrolysis), traces of solvents of types capable of producing hydroperoxides, products of thermooxidative degradation		

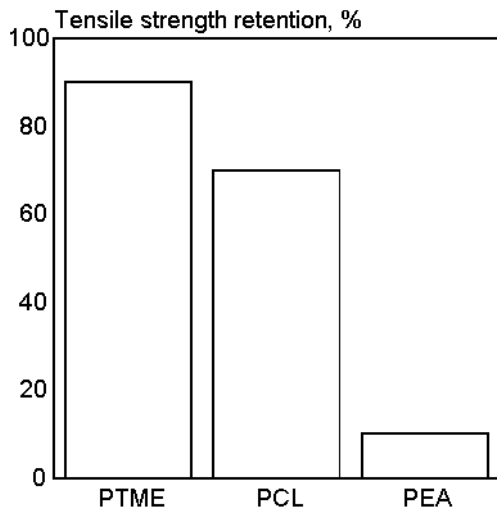


Fig. 14.34. Hydrolytic stability of polyurethanes. [Data from H. Ulrich, *J. Elastomers Plast.*, 18(1986)147.]

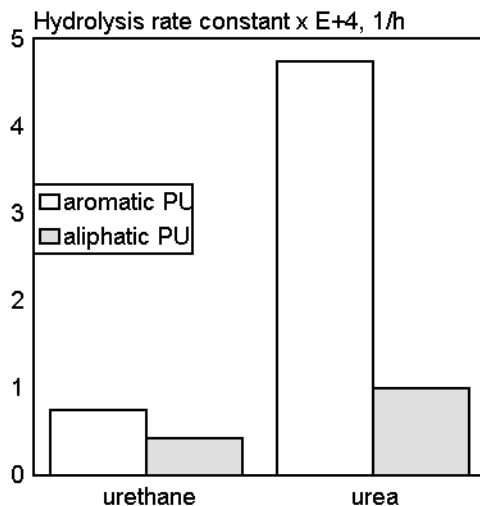


Fig. 14.35. Hydrolysis rate constants of polyurethanes. [Data from T. M. Chapman, *J. Polym. Sci., Polym. Chem.*, 27A(1989)1993.]

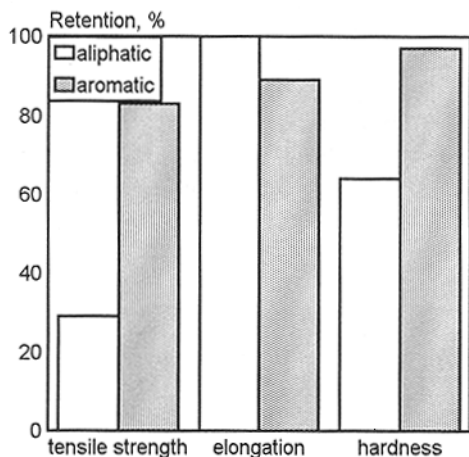


Fig. 14.36. Light stability of polyurethanes.

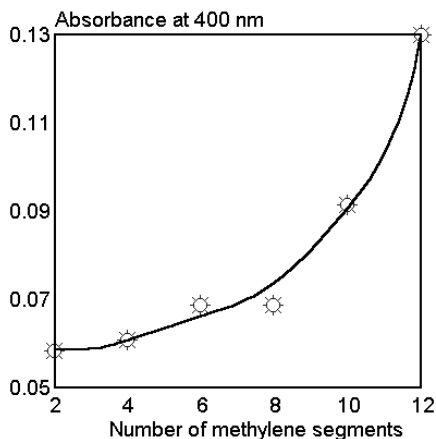


Fig. 14.37. Effect of hydrocarbon segment length of chain extender on the change of film optical properties (2 h irradiation using a 100 W mercury lamp.) [Adapted, by permission, from C. E. Hoyle, K. J. Kim, and Y. G. No, *Report*, ADA 169643.]

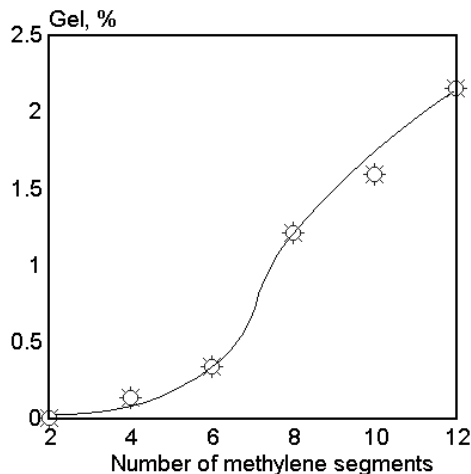


Fig. 14.38. Effect of hydrocarbon segment length of chain extender on the gel formation (2 h irradiation using a 100 W mercury lamp.) [Adapted, by permission, from C. E. Hoyle, K. J. Kim, and Y. G. No, *Report*, ADA 169643.]

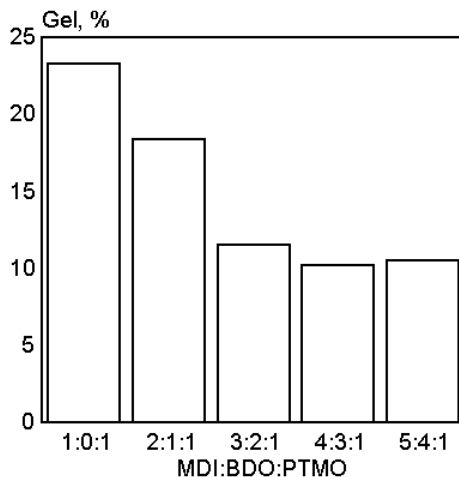


Fig. 14.39. Insoluble gel formation during PU photolysis using a 300 nm source. [Adapted, by permission, from C. E. Hoyle, Y. G. No, K. J. Kim, and G. L. Nelson, *Report*, ADA 169645.]

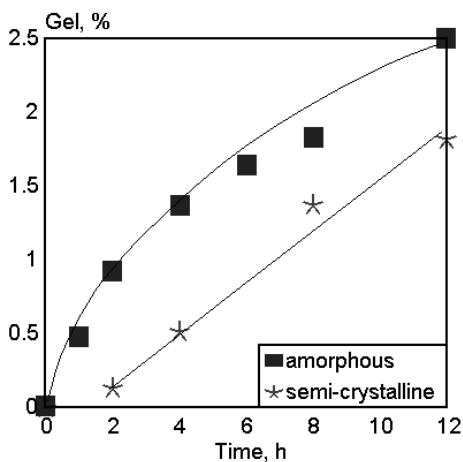


Fig. 14.40. Insoluble gel formation during PU photolysis of MDI polymers, having different crystalline structures, using a 300 nm source. [Adapted, by permission, from C. E. Hoyle, Y. G. No, K. J. Kim, and G. L. Nelson, *Report*, ADA 169645.]

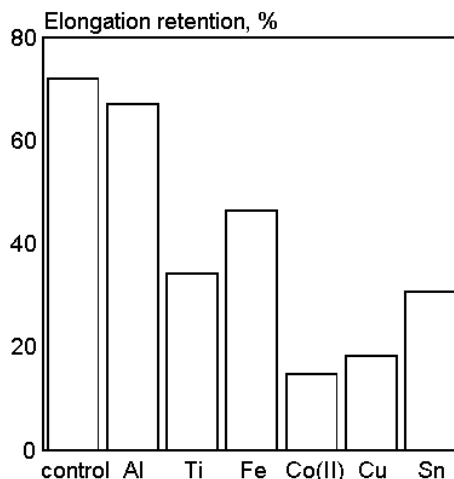


Fig. 14.41. Effect of metals on elongation retention of MDI-based PU irradiated for 50 h. [Data from Z. Osawa, *Dev. Polym. Photochem.*, 3(1981)209.]

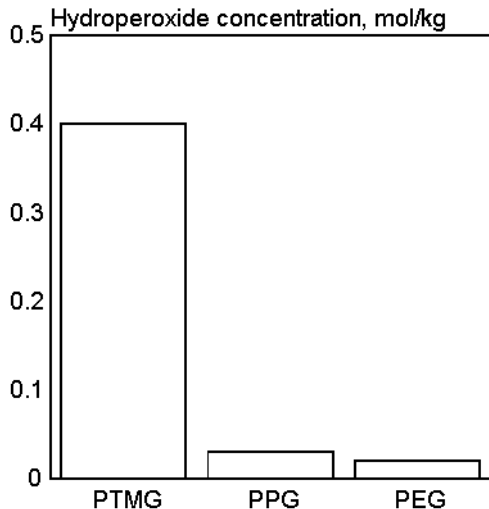


Fig. 14.42. Effect of polyol irradiation on hydroperoxide concentration (96 h at 300 nm). [Data from P. Gauvin and J. Lemaire, *Makromol. Chem.*, 188(1987)1815.]

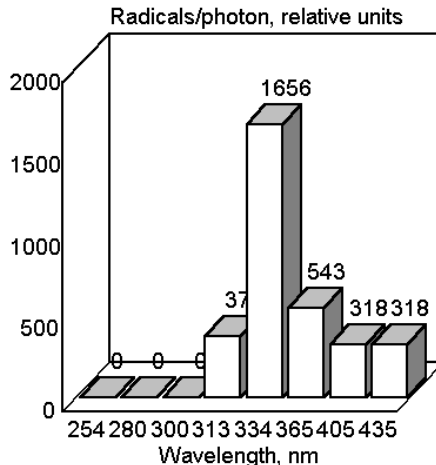


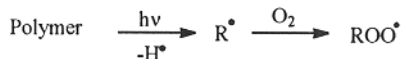
Fig. 14.43. Spectral sensitivity of two-component PU measured by direct ESR determination of radicals formed in specimen exposed to UV radiation in ESR instrument. [Data from A. Sommer, E. Zirngiebl, L. Kahl, and M. Schoenfelder, *Prog. Org. Coat.*, 19(1991)79.]

14.8 EPOXY RESINS (EP)²⁰⁵⁻²²¹

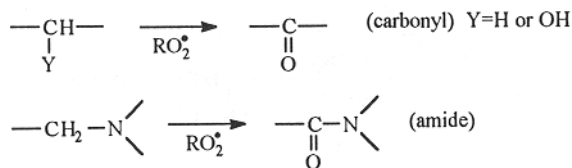
Although, epoxy resins are extensively used, only a few research papers on their weathering are available.

14.8.1 MECHANISM OF DEGRADATION

The photoinitiation of epoxy resins begins, as with other polymers, from radical induced processes:

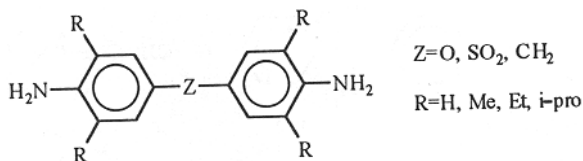


These radicals may then be oxidized which initiates a chain of photooxidative processes. Specific knowledge of the initiation centers helps in the understanding of the degradation mechanism. Bellenger's studies²¹⁸ suggest that, in an amine cured epoxy, it is the epoxy resin segment that is the photoinitiating species. Amines absorb in the near UV region. Photooxidation leads to the formation of carbonyl or amide type moieties, as follows:



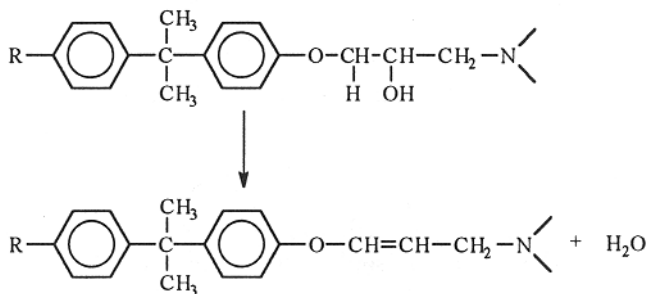
The relative concentration of carbonyl or amide found depends on the amine component (curative). For example, isophorone diamine used as a hardener produces a high concentration of carbonyl groups and a low amide concentration. Aminoethyl piperazine gives the opposite effect, whereas diethyltriamine gives intermediate concentration. This is because diethyl triamine and amino ethyl piperazine do not possess groups capable of being transformed into carbonyl groups (they transform into amides and other structures), whereas the isophorone diamine structure can be converted to a carbonyl. Carbonyl groups are formed not only from the amine moiety but also from the epoxy resin portion.

The effects of the bridge, Z, and alkyl substituent, R, of aromatic amines:

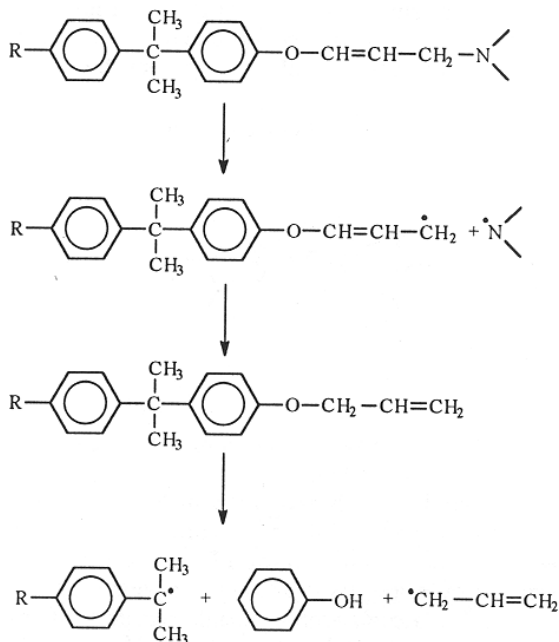


were investigated.²¹⁸ The lowest rates of amine and carbonyl formation occurred with the involvement of the SO₂ bridge.

Wilson,²⁰⁸ studying the effect of ionizing radiation on epoxy resin, found that, initially, chain scission is a prevailing mechanism. After longer exposure, crosslinking reactions prevailed. Lin²¹⁴ found few differences when he compared thermal and thermooxidative degradation. His findings suggest that both thermo- and photooxidative degradations have a comparable initial step and differ mostly in the amount of energy required to induce degradation, as demonstrated by the relative rates of degradation. Nguyen *et al.*²⁰⁹ studied the corrosion-induced degradation in epoxy resins. This is useful information in application of these materials in metal coating and priming. The presence of alkaline products of metal corrosion leads to dehydration of the epoxy resin:

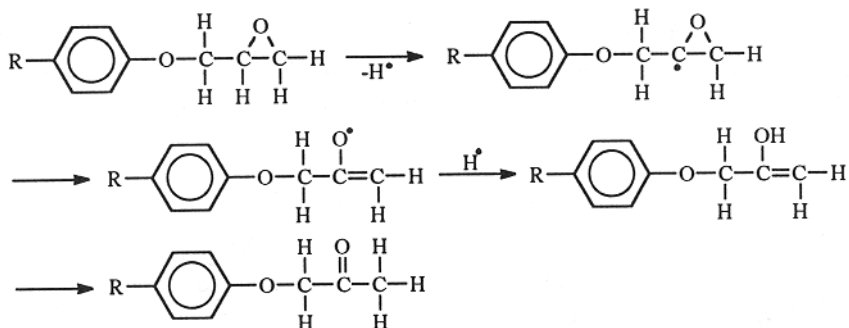


Further chain reactions may influence formation of numerous free radicals and induce chain scission:

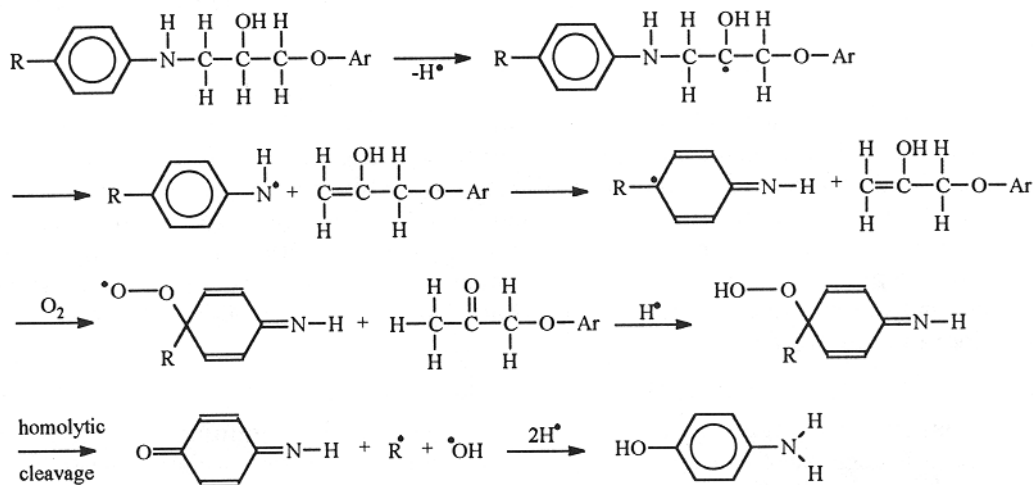


The mechanism outlined by Zhang et al.²²¹ is proposed based on studies of Epolite resins which contain diglycidyl ethers of bisphenol A, glycidyl ethers of aliphatic glycol, 4,4'-methylenedianiline, and polymethylene polyphenyl amine. The following scheme of degradation was proposed:

epoxide rings



cured epoxy

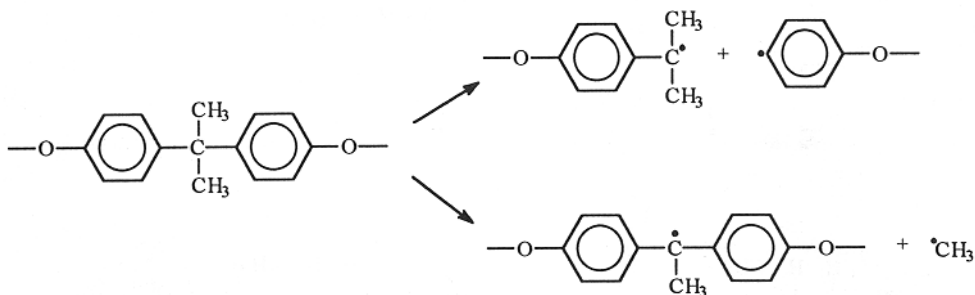


The unreacted epoxy rings are the terminal groups on chains. Hydrogen atoms around the oxirane ring are quite labile. Abstraction of hydrogen atom leads to either alcohol, ketone, or aldehyde. The degradation of the main chain leads to the formation of keto and amine groups, and/or quinone imide. Carbonyl groups formed in the initial stage are decomposed in the course of degradation. The studies were conducted using lamps of various spectral ranges but the products of reaction were essentially the same. Different lamps caused different reaction rates. This study confirmed that carbonyl formation

does not require an external source of oxygen because carbonyls formed in a nitrogen environment (again, reaction rates differed with each lamp).

14.8.2 EFFECT OF THERMAL HISTORY

According to Park and Blount,²¹⁷ thermal degradation of cured epoxy, in the absence of oxygen, results in a decrease in OH groups and an increase in C=O groups. Radicals are probably formed by the following process:



In both cases, there is a possibility that groups form which are able to absorb UV radiation and thus initiate a chain of photolytic reactions. The stability of functional groups found by Lin *et al.*²¹⁴ in order of decreasing stability is as follows: methyl group \approx benzene ring $>$ methylene $>$ p-phenylene $>$ ether linkage $>$ isopropylidene. The difference between the thermal and the thermooxidative reaction is in the degradation rate. In the presence of oxygen, radicals formed are oxidized to form peroxides, which, on dissociation, produce two radicals from each hydroperoxide group which accelerates the degradation process.

14.8.3 CHARACTERISTIC CHANGES AND PROPERTIES

The glass transition temperature, T_g , changes rapidly at the beginning of the degradation process because of widespread chain scission reactions; after longer exposure, more crosslinks are formed (Fig. 14.44). The structure of the bridge, connecting two phenylene rings, determines both the carbonyl (Fig. 14.45) and the amide formation rate (Fig. 14.46) whereas amide growth seems independent of epoxy resin type (amide growth rate is always lower for SO_2 bridge), the increase in concentration of carbonyl groups depends mainly on the type of epoxy resin used. Epoxy resins become opaque during irradiation (Fig. 14.47). Absorption of water leads to a decrease in T_g (absorption of 1% water decreases the T_g by 8°C). Water acts as plasticizer as well as a reactant and, on longer exposure, causes a decrease in molecular weight and Young's modulus because of degradation and plastification (Fig. 14.48).

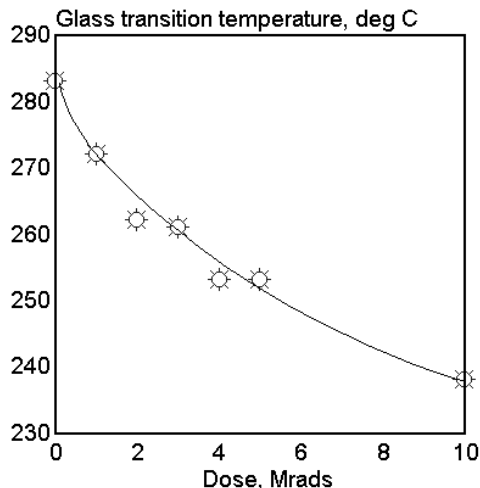


Fig. 14.44. T_g of tetraglycidyl 4,4'-diaminodiphenyl methane (73%) and 4,4'-diaminodiphenyl sulfone (27%) vs. irradiation dose. [Data from T. M. Wilson, R. E. Fornes, R. D. Gilbert, and J. D. Memory, *Polym. Mat. Sci. Eng.*, 56(1987)105.]

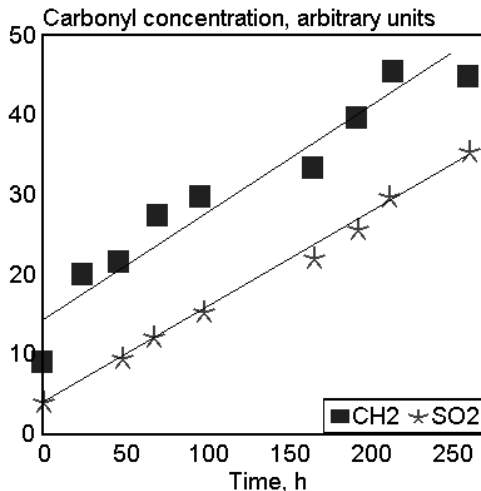


Fig. 14.45. Carbonyl growth on photooxidation of epoxy resins (>300 nm). Curatives based on diphenyl amines having different bridges. [Adapted, by permission, from V. J. Bellenger and J. Verdu, *Polym. Photochem.*, 5(1984)295.]

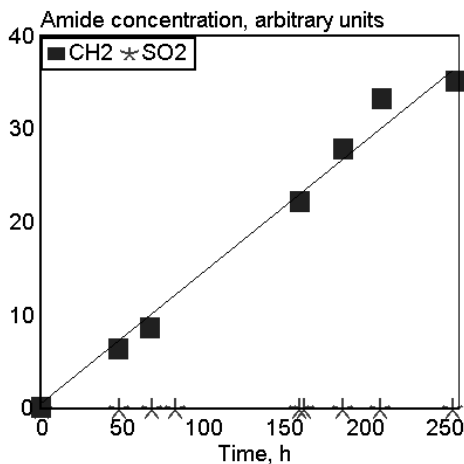


Fig. 14.46. Amide growth on photooxidation of epoxy resins (>300 nm). Curatives based on diphenyl amines having different bridges. [Adapted, by permission, from V. J. Bellenger and J. Verdu, *Polym. Photochem.*, 5(1984)295.]

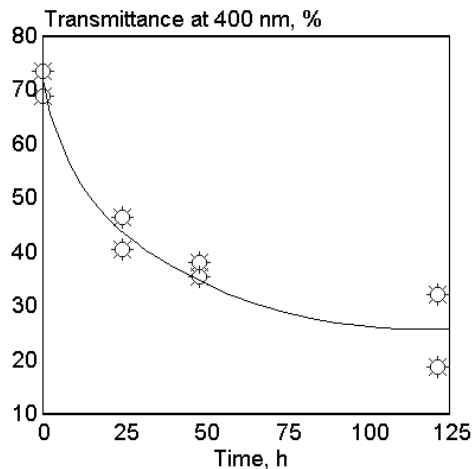


Fig. 14.47. Transmittance of epoxy resin vs. irradiation time (>300 nm). [Adapted, by permission, from V. J. Bellenger and J. Verdu, *Polym. Photochem.*, 5(1984)295.]

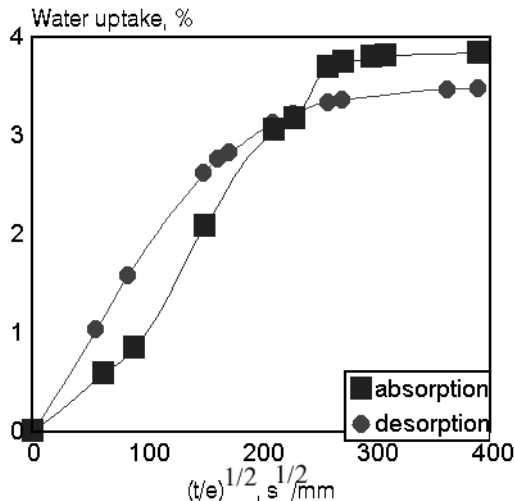


Fig. 14.48. Absorption and desorption of water in epoxy resin at 70°C. [Adapted, by permission, from B. De'Neve and M. E. R. Shanahan, *Polymer*, 34(1993)5099.]

Important initiators and accelerators: aromatic carbonyl groups (thermal oxidation during cure); quinoic structures; impurities (unknown chemical structure); hydroxide ions; double bonds

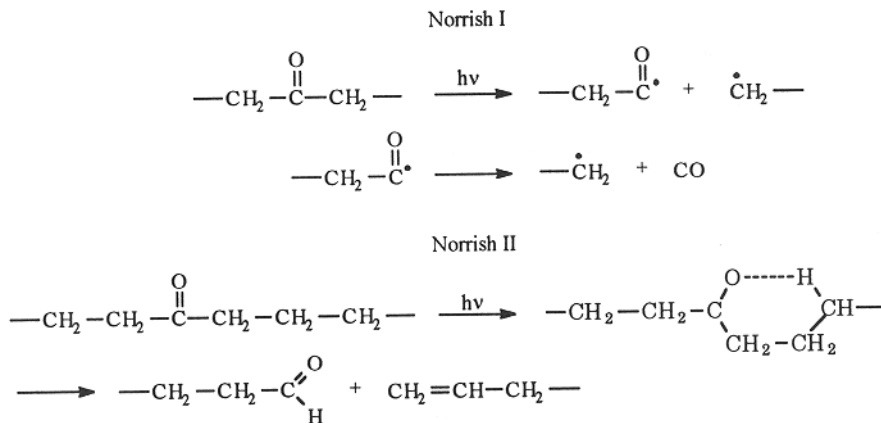
14.9 POLYETHYLENE (PE)^{3-14,221-298}

Polyethylene has a homogeneous chemical composition with the chemical formula: $\text{CH}_3-(\text{CH}_2)_n-\text{CH}_3$. Polyethylenes are divided into low and high density materials by the benchmark density of 0.94 g/cm^3 . Each group is highly diverse because of chain irregularities (branches), unsaturations, molecular weight variations, and components added during the polymerization reaction to influence basic mechanical properties and durability. Thermooxidative processes which occur during polymerization, storage, and processing result in the formation of a crystalline structure which contributes to further diversity. Because of this diversity, it is difficult to apply one general principle to the entire group. General properties depend on a mix of factors which are not easily quantified. Information relevant to polyethylene degradation can also be found in the section on polypropylene.

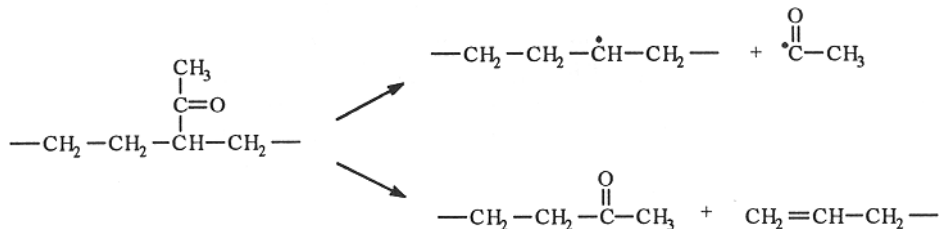
14.9.1 MECHANISM OF DEGRADATION

14.9.1.1 Models

Information on polyethylene degradation is available from model studies done because of the commercial interest in photodegradable polyethylene for applications, such as, garbage bags, agricultural films, etc. Copolymerization of ethylene monomer with small amounts of carbon monoxide forms an ethylene-carbon monoxide copolymer, known to degrade on sunlight exposure by Norrish type I and II reactions:



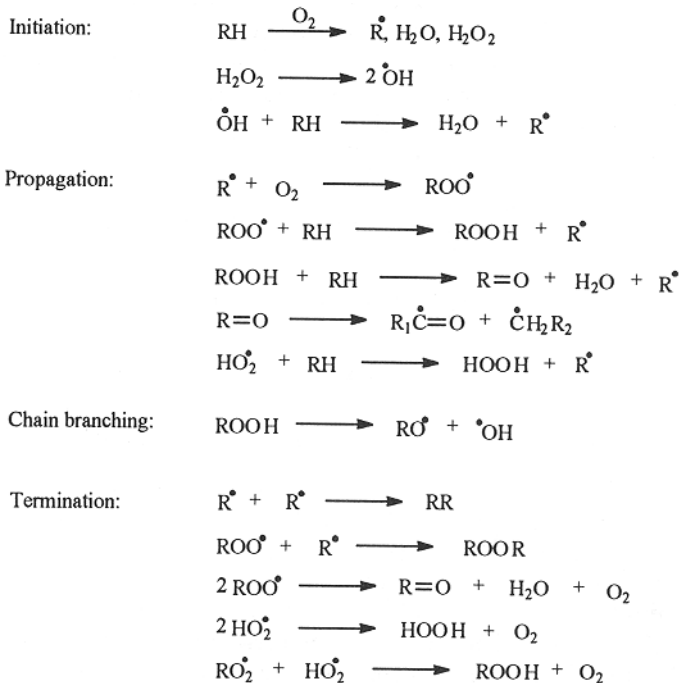
Both cases are equivalently dangerous to the durability of the polymer. If the polymer degrades according to Norrish I mechanism, two free radicals are formed simultaneously. When the Norrish II mechanism controls degradation, two molecules capable of absorbing sunlight are formed. Both cases result in a self-accelerated degradation process. Ethylene-methyl vinyl ketone copolymer is the other model compound studied. It also degrades by two competing reactions:



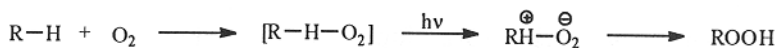
The resultant products of reaction are similar to those discussed above, and the implications of their formation are similar.

14.9.1.2 Polymers

Photooxidation of polyethylene proceeds by a free radical chain mechanism outlined by Bolland,²⁵⁶⁻⁷ Bateman,²⁵⁸ and Gugumus:²⁷²



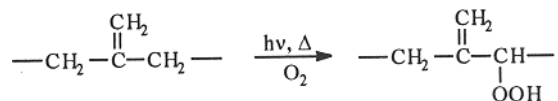
One primary initiation step may produce three free radicals, then secondary processes also give rise to compounds containing hydroxyl, carbonyl, and vinyl groups which also absorb radiation and undergo further degradative processes. The structure of polyethylene determines the probability of further conversion. From studies comparing polyethylene and polypropylene, it is known that the degree of branching, because it controls the amount of more labile hydrogens attached to the tertiary carbon atoms, determines the oxidation rate. Polyethylene forms weakly-absorbing complexes with ground-state molecular oxygen, which, on UV exposure, generate hydroperoxides:



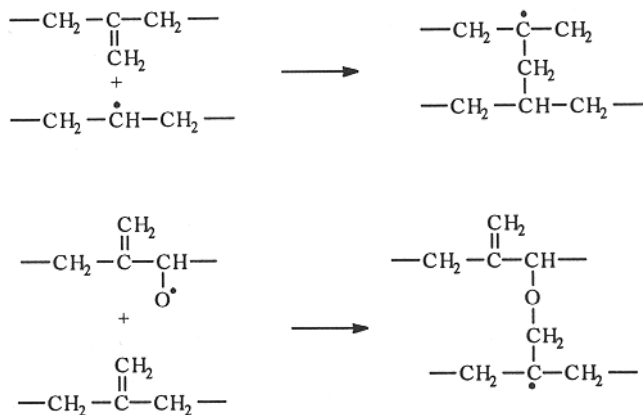
Both high-density PE and low-density PE contain unsaturations, as follows:



The presence of these unsaturations (vinylidene groups) leads to formation of allylic hydroperoxides during the thermooxidative processes, and this becomes the major mechanism of initiation:

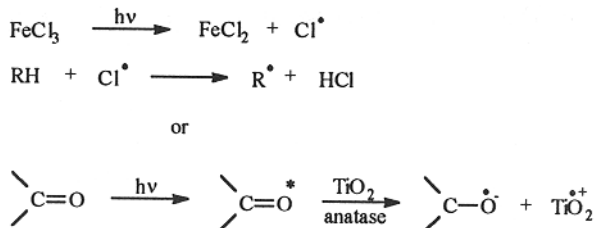


This structure can be further converted by heat, UV, or other radicals to free radicals and/or to structures containing UV-absorbing groups (e.g., carbonyl). Some research²⁶⁹ indicates that peroxide decomposition is limited to local conversion through a cage effect. This would assign a relatively restricted role to hydroperoxide as the initiator of chain reactions because the radicals produced would react to form inert material (water) directly after their formation. Chain scission reactions, as explained above, usually predominate, but crosslink formation also occurs:

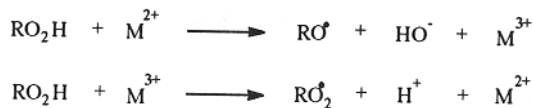


Two oxy-radicals can recombine, forming a crosslinked structures. It was found²⁶⁷⁻⁸ that photoinitiated crosslinking considerably decreases PE durability on exposure to radiation. The decrease of stability can be compensated for by the use of small amounts of HALS (Tinuvin 770). Addition of this stabilizer does not affect photocrosslinking process.

Metals affect polyethylene photostability in several ways. Radicals are able to abstract a hydrogen atom from the polymer:

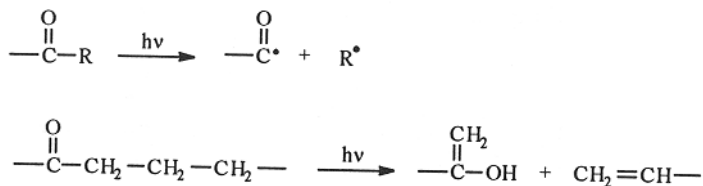


In both cases, the radicals formed are able to attack the polymer. Transition metal ions are known to catalyze hydroperoxide decomposition:



accelerating the photochemical decomposition of the polymer.

Norrish type I and II reactions of the carbonyl group, formed either from hydroperoxide decomposition or processes catalyzed by metals, can be alternative source of free radicals or their precursors:



In summary, three major functional groups are accumulated during degradation: ketones, carboxylic acids, and vinyl groups. Ketones absorb radiation above 300 nm and in the subsequent reaction they are mostly converted to carboxylic acids and vinyl groups. Carboxylic acids accumulate in PE during photooxidation because they apparently do not undergo further reactions. Vinyl groups cannot absorb UV radiation above 300 nm but they can react with the singlet oxygen generated photochemically in PE and then they are susceptible to free radical attack.²⁷² During photolysis, ketones and vinyl groups increase linearly with time of exposure (according to the expression $A + Bt$), whereas carboxylic acids accumulate according to the expression $At + Bt^2$. The proportions of the yields of hydroperoxides : aliphatic ketones : aromatic ketones are: 0.15:0.001:1.8.²⁸⁰

The crystalline structure of the polymer has a very strong influence on its stability (Chapter Fifteen). Crystallinity changes during the course of degradation. In the initial stages of photodegradation, chain scission prevails which reduces molecular weight. Shorter chains are more mobile and are thus able to crystallize more readily. Therefore, embrittlement of PE is controlled by two associated processes: reduction of molecular weight and increased crystallinity.²⁷³ An essential difference in crystalline behavior was observed²⁷⁴ between crosslinked and uncrosslinked samples. During UV photolysis of uncrosslinked samples, tensile stress causes the chain scission of taut tie molecules which weakens the network and assists lamellar unfolding. The lamellar unfolding is restricted in crosslinked samples therefore they exhibit virtually no creep and they take a longer time to break than do uncrosslinked samples.

Samples exposed to UV tend to continue oxidize when stored in darkness. This behavior does not occur in samples not exposed to UV radiation. This behavior finds application in environmentally adaptable polymers.

14.9.3 EFFECT OF THERMAL HISTORY

Depending on the stage of the degradation process, hydroperoxide concentration varies. In the first stage, a rapid increase in hydroperoxide concentration is seen, followed by an equally drastic concentration drop. The reason is that the real concentration of hydroperoxides depends on their rate of formation and dissociation (mostly to carbonyl groups). Concentration of carbonyl groups grows steadily as thermal degradation progresses. Since carbonyl groups are able to absorb sunlight in the UV region, the concentration of the carbonyl group determines polyethylene stability. Similar observations come from recent work by Williams *et al.*²⁶⁴ Just above its melting point, the amount of oxygen increases then decreases as the temperature rises. The change in molecular weight is just the opposite. Initially chain scission is the most prominent but, gradually, crosslinking begins to predominate as the temperature increases further.

14.9.4 CHARACTERISTIC CHANGES AND PROPERTIES

The number of branch points increases as polymer density decreases (Fig. 14.49). The amount of vinylidene unsaturations also increases with decreasing polymer density (Fig. 14.50). Thus, polymer instability increases as its density decreases. Fig. 14.51 shows that the thermal oxidation rates of linear and branched polymer are markedly different below the melting point. These rates are actually proportional to the amorphous fraction (5% for linear PE and 40% for branched PE). When the polymer is melted (140°C), meaning that it is completely disordered, both rates are similar. This suggests that the degradative processes are restricted to the amorphous phase. Further investigation leads to the conclusion that oxygen diffusion into crystalline segments is restricted, which decreases the degradation rate. This principle is again demonstrated in Fig. 14.52 which shows that the photooxidation rate is higher in the more oxygen rich, more gas permeable, amorphous regions. Fig. 14.53 shows the relative importance of various mechanisms in formation of degradation products. A more recent study shows that the relative rates of accumulation of these compounds are similar but that the actual concentrations are slightly different (Fig. 14.54). These sets of values are different from those proportions suggested by Gugumus.²⁷² The mechanical properties of polyethylene are severely affected by UV radiation. Elongation of HDPE especially is reduced to almost zero (Fig. 14.55). Carbonyl formation correlates with chain scissions whether or not degradation accelerators are present (Fig. 14.56).

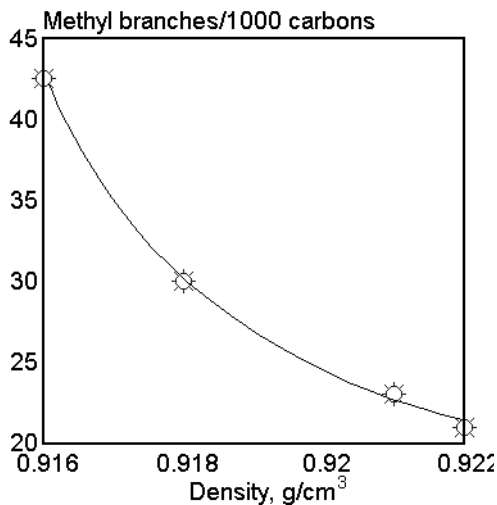


Fig. 14.49. LDPE density vs. branching ratio. [Data from J. Lemaire and R. Arnaud, *Polym. Photochem.*, 5(1984)243.]

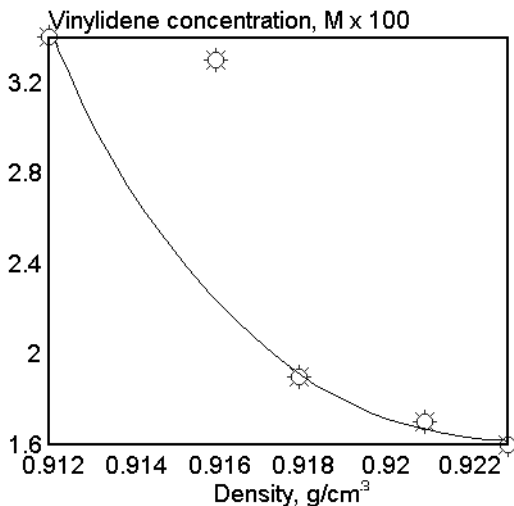


Fig. 14.50. LDPE density vs. vinylidene branches. [Data from J. Lemaire and R. Arnaud, *Polym. Photochem.*, 5(1984)243.]

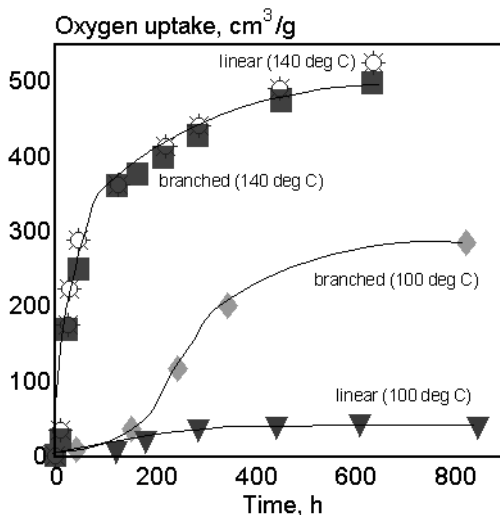


Fig. 14.51. PE oxidation above and below the melting point. [Data from W. L. Hawkins, W. Martreyck, and F. H. Winslow, *J. Polym. Sci.*, 41(1959)1.]

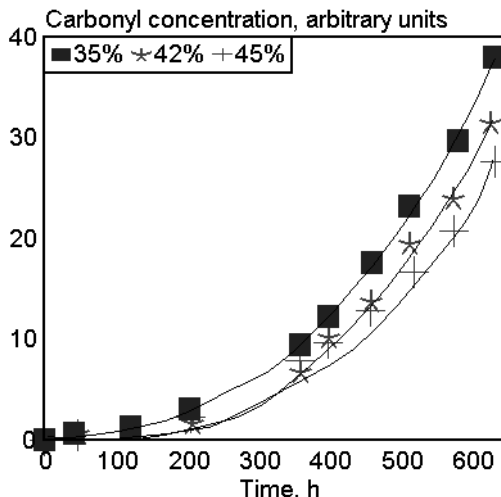


Fig. 14.52. Carbonyl formation during Xenotest irradiation of LDPE samples varying in degree of crystallinity. [Adapted, by permission, from K. Tsuji and H. Nagata, *Rep. Prog. Polym. Phys. Jpn.*,

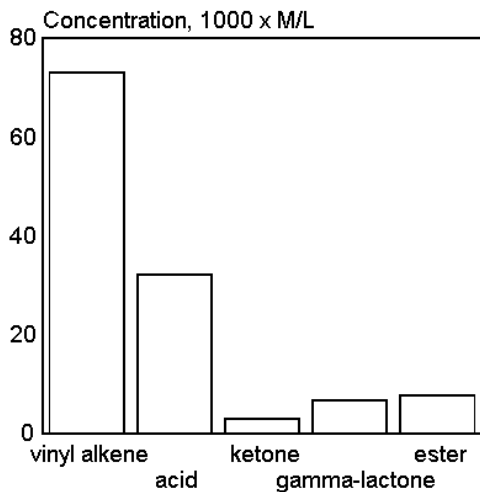


Fig. 14.53. Accumulation of functional groups during PE irradiation at $>290 \text{ nm}$ for 720 h. [Data from J. H. Adams, *J. Polym. Sci.*, 8A(1970)1279.]

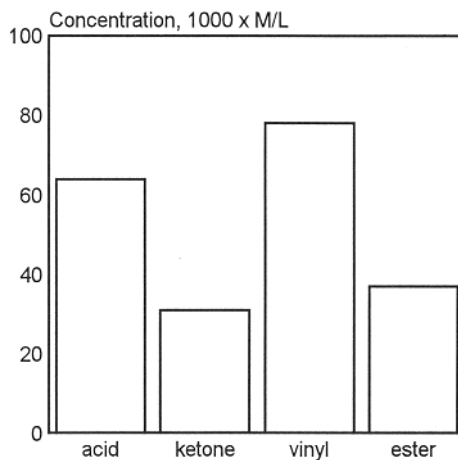


Fig. 14.54. Accumulation of functional groups during PE irradiation at $>300 \text{ nm}$. [Data from A. Tidjani and R. Arnaud, *Polym. Deg. Stab.*, 39(1993)285.]

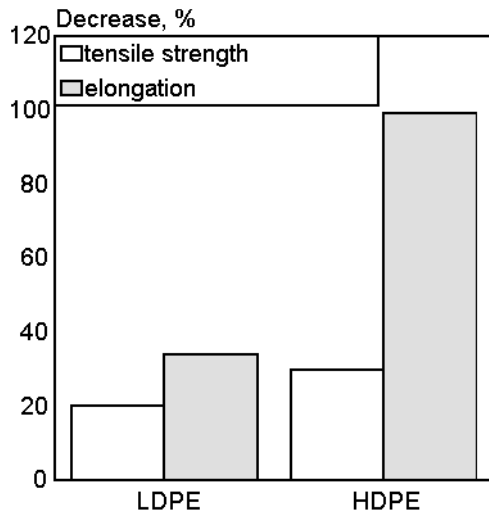


Fig. 14.55. Percentage decrease of PE tensile strength and elongation during natural weathering in Queensland, Australia for 1 year. [Data from P. Dunn and E. J. Hill, *Rep. 421*, Australia, 1971.]

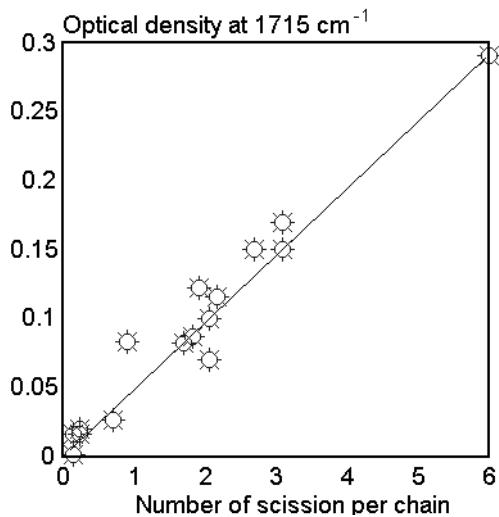


Fig. 14.56. Optical density, OD, at 1715 cm⁻¹ as a function of number of scissions per chain, n. Samples exposed at >300 nm are PE and PE containing various initiators of degradation. [Data from C. David, M. Trojan, A. Daro, and W. Demarteanu, *Polym. Deg. Stab.*, 37(1992)233.]

14.9.5 DATA

Luminescence data:		
Sample form	Excitation wavelength, nm	Emission wavelength, nm
powder	230, 265, 300	335, 350
powder	230, 273	295, 310, 329, 354, 370
film	273, 280	367, 381, 391, 405, 416
LDPE film	278, 280	420
chip	283, 331	370, 435, 455
chip	254	275, 330, 350, 378, 400, 422
chip	300	350, 470
HDPE film	230, 265, 290	295, 312, 330, 344, 358
	275	450
	232	333
	292	340
	249	350-360, 410
Spectral sensitivity: <300 nm		Activation wavelength: 300 nm
Products of photolysis: free radicals, crosslinks		
Products of photooxidation: free radicals, hydroperoxides, carbonyl groups, chain scissions		
<p>Important initiators and accelerators: unsaturations, aromatic carbonyl compounds (deoxyanisoin, dibenzocycloheptadienone, flavone, 4-methoxybenzophenone, 10-thioxanthone), hydrogen bound to tertiary carbon at branching points, aromatic amines, groups formed on oxidation (hydroperoxides, carbonyl, carboxyl, hydroxyl), substituted benzophenones, complexes with ground-state oxygen, quinones (anthraquinone, 2-chloroanthraquinone, 2-tert-butylanthraquinone, 1-methoxyanthraquinone, 2-ethylanthraquinone, 2-methylanthraquinone), transition metal compounds (Ni < Zn < Fe < Co), ferrocene derivatives, titanium dioxide (anatase), ferric stearate, polynuclear aromatic compounds (anthracene, phenanthrene, pyrene, naphthalene)</p>		
<p>Stabilization: carbon black is the best stabilizer for PE (2-4% acts as UV stabilizer and antioxidant). Stabilization is complicated by the fact that a damage of structure during processing cannot be reversed; low compatibility of PE affects stabilizer retention (increase of stabilizer amount does not increase PE durability because equilibrium concentration of stabilizer is low). HALS and other antioxidants are frequently used (UV absorbers are less effective). Butoxy-4-amino-tetramethylpiperidine is a very efficient stabilizer of PE because it acts as chain breaking donor in hydroperoxide decomposition.</p>		

14.10 POLYPROPYLENE (PP)^{240,255,299-334}

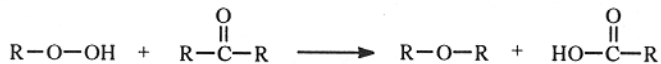
The weather resistance of polypropylene and its degradation mechanism are very similar to polyethylene. In order to avoid repeating the same information, the following survey compares the behavior of polyethylene and polypropylene.

14.10.1 MECHANISM OF DEGRADATION

14.10.1.1 Models

Works by Geuskens³¹⁸ contribute to a fundamental understanding of polyolefin behavior. Ethylene-propylene copolymer was used in these studies as a model compound. It has structural elements of both polymers and, additionally, it helps to avoid experimental difficulties related to the very low solubility of polyolefins and their complex crystalline structure. Ethylene-propylene copolymer, EPM, can be obtained in a completely amorphous form. When EPM is heated in the presence of air, hydroperoxide production goes through a three-phase process. Initially, the concentration of hydroperoxides increases rapidly, then it temporarily remains stable, finally, it decreases almost as rapidly as it increased. The amount of carbonyl groups gradually increases throughout the process. If the oxygen uptake of the specimen is analyzed, the data can be computer-simulated to distinguish between the oxygen used for hydroperoxide conversion and that involved in the formation of carbonyl group from hydroperoxide reaction products. These two reactions are kinetically interdependent.

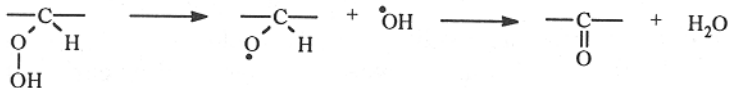
The first stage, when hydroperoxides concentration increases, is accompanied by chain scission, similar to that discussed in the case of polyethylenes. Vacuum photolysis of photooxidized EPM at 365 nm results in hydroperoxide decomposition without production of ketones:



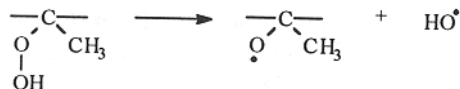
Geuskens³¹⁸ believes that the difference in photooxidation between polyethylene and polypropylene lies in different formation rates of the various end products (alcohols, ketones, and carboxylic acids).

14.10.1.2 Polymers

Hydroperoxides play a more important role in initiation of polypropylene photodegradation than they do in the photodegradation of polyethylene. This is because the tertiary hydroperoxides found in polypropylene are more stable than the secondary ones in polyethylene. On the other hand, polypropylene cannot form macroalkoxy-radical according to the following scheme for polyethylene:

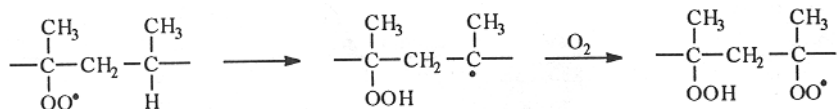


and therefore radical concentration increases:



Although photooxidation of both polymers proceeds according to similar reactions, their initiation, termination, and chain-branching reaction rates are different. For example, the termination reaction rates for polyethylene are 100-1000 times higher than for polypropylene. In the study of PP fabric by FTIR,³²³ alcohols, peroxides, aldehydes, ketones, carboxylic acids, and anhydrides were formed as degradation products. This is a different composition than is typically detected in polyethylene (no vinyl, aldehyde, and anhydride groups). The same products were detected during both thermooxidation and photooxidation.

Additionally, polypropylene contains sequences of hydroperoxides formed because polypropylene has a labile tertiary hydrogen in the β -position:



Further differences between both polymers are discussed in Chapter Fifteen (effect of crystalline structure).

The effect of PP degradation on mechanical behavior makes it possible to distinguish between 3 different stages.³²¹ The first stage is an initiation period in which degradation is not noticeable. In a Xenotest 1200 machine, this stage lasted 150-200 hrs. The next stage is marked by a rapid decrease of mechanical properties and it occurs in a matter of additional 20 to 50 hrs of exposure. In the last stage, the mechanical properties are almost stable, and a specific increase in energy is needed to cause failure. In the second stage, cracks appear on the surface and material becomes brittle. Cracks formation decreases the total energy required for crack propagation. In the last stage, numerous cracks are formed. From this study, it appears that a thin, severely degraded layer allows the sample to retain better mechanical performance than a thick layer of degraded material with a small number of cracks.³²¹

14.10.2 EFFECT OF THERMAL HISTORY

Polypropylene, like polyethylene, oxidizes readily at elevated temperatures and forms hydroperoxides. Hydroperoxides are converted to hydroxyl or carbonyl groups when exposed to UV.

14.10.3 CHARACTERISTIC CHANGES AND PROPERTIES

A higher temperature of oxidation speeds both the formation rate and the decomposition rate of hydroperoxides (Fig. 14.57). When carbonyl concentration is high, the rate of formation of hydroperoxides is dependent on the initial thermooxidative processes (Fig. 14.58). The kinetics and mechanisms of both thermal oxidation and photodegradation are interrelated (Fig. 14.59). A significant difference between the usual photodegradation reaction routes in polypropylene and polyethylene lies in the accumulation of functional groups (compare Figs. 14.53 and 14.60). As a result of photodegradation, more ester groups are formed and an aldehyde group is also generated. Carbonyl groups (Fig. 14.61) and hydroxyl groups (Fig. 14.62) are preferentially formed on the exposed surface, and their concentrations increase almost linearly with time of exposure. Chemical changes coincide with the deterioration of mechanical properties of polypropylene, which is not an UV-durable material even in pigmented form (Fig. 14.63).

14.10.4 DATA

Luminescence data:		
Sample form	Excitation wavelength, nm	Emission wavelength, nm
film	230, 285	309, 320
film	270, 290, 330	420, 445, 480, 510
film (thermally degraded)	330	430, 480, 520
film (thermally degraded)	230	295, 330, 400
film (thermally degraded)	287	320-330, 470
film (thermally degraded)	230, 290	340
film (thermally degraded)	230, 285	340
film (thermally degraded)	232	332
film (thermally degraded)	295	342
atactic PP	232	330
	290	340
Activation wavelength: 310 nm		
Products of photolysis: free radicals, crosslinks		
Products of photooxidation: free radicals, hydroperoxides, carbonyl groups, chain scissions		
Important initiators and accelerators: all listed for PE and additionally titanium catalyst used in polymerization		

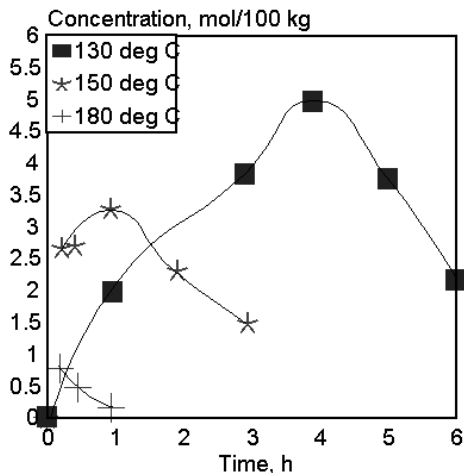


Fig. 14.57. Concentration of hydroperoxides in EPM heated in air at varying temperatures. [Adapted, by permission, from G. Geuskens, F. Debic, M. S. Kabamba, and G. Nedelkos, *Polym. Photochem.*, 5(1984)313.]

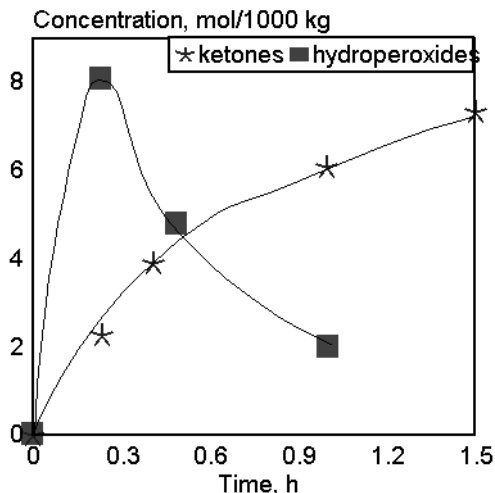


Fig. 14.58. Concentration of ketones and hydroperoxides in EPM heated in air at 180°C. [Adapted, by permission, from G. Geuskens, F. Debic, M. S. Kabamba, and G. Nedelkos, *Polym. Photochem.*, 5(1984)313.]

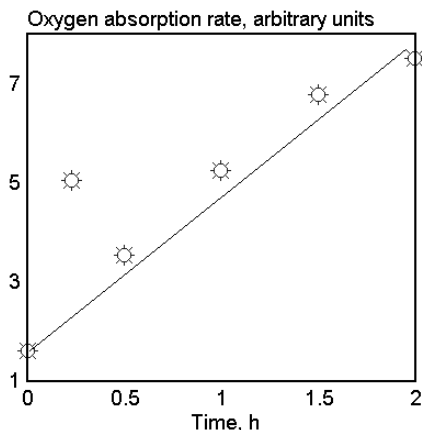


Fig. 14.59. Rate of oxygen absorption in EPM irradiated in air at 310 nm as a function of previous thermal oxidation time at 180°C. [Adapted, by permission, from G. Geuskens, F. Debic, M. S. Kabamba, and G. Nedelkos, *Polym. Photochem.*, 5(1984)313.]

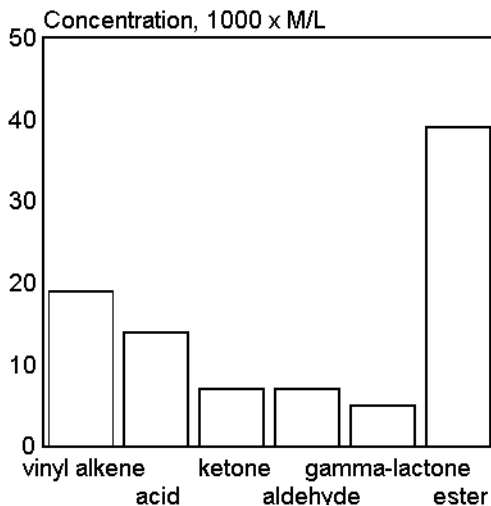


Fig. 14.60. Accumulation of functional groups on polypropylene irradiation at 290 nm for 335 h. [Data from J. A. Adams, *J. Polym. Sci.*, 8A(1970)1279.]

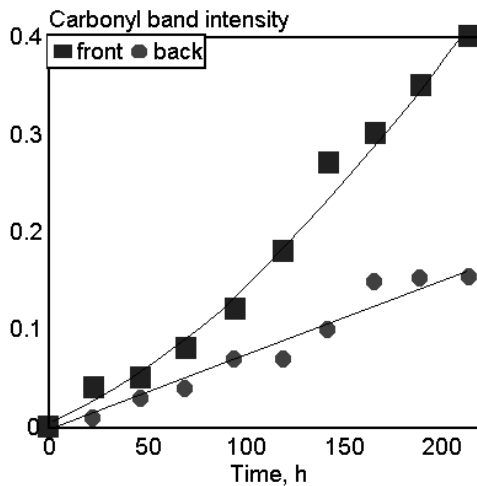


Fig. 14.61. Carbonyl band intensity in PP fabric irradiated at 254 nm vs. irradiation time. 1 - exposed side, 2 - back side. [Data from C. Q. Yang and L. K. Martin, *J. Appl. Polym. Sci.*, 51(1994)389.]

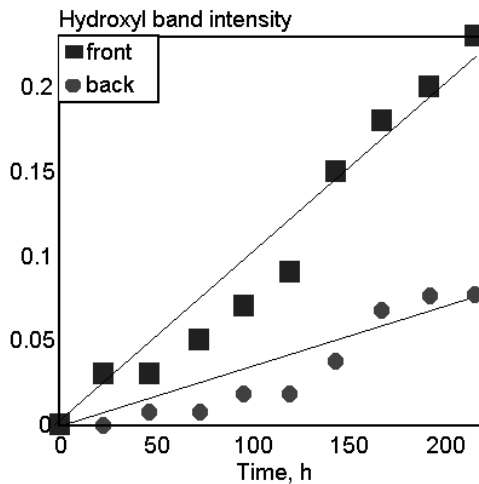


Fig. 14.62. Hydroxyl band intensity in PP fabric irradiated at 254 nm vs. irradiation time. 1 - exposed side, 2 - back side. [Data from C. Q. Yang and L. K. Martin, *J. Appl. Polym. Sci.*, 51(1994)389.]

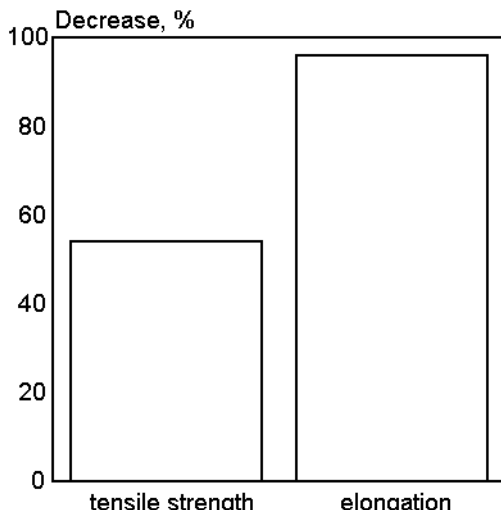


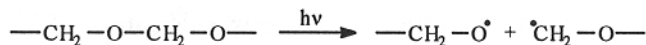
Fig. 14.63. Change of PP properties (% decrease) on natural weathering in Queensland, Australia during 1 year. [Data from P. Dunn and E.J. Hill, Rep. 421, Australia, 1971.]

14.11 POLYOXYMETHYLENE (POM)^{12-14,144,146,335-346}

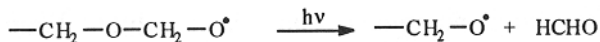
Because of its structure, the polymer does not absorb the UV radiation from the daylight. In spite of this, POM degrades when exposed outdoors, which means that, chromophore-containing impurities are present. The copolymer containing a small amount of oxyethylene was found to be more stable.

14.11.1 MECHANISM OF DEGRADATION

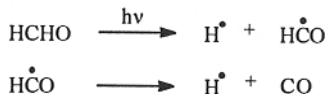
Oxyradicals were identified by ESR spectroscopy in UV irradiated material. This is explained by the following reaction:



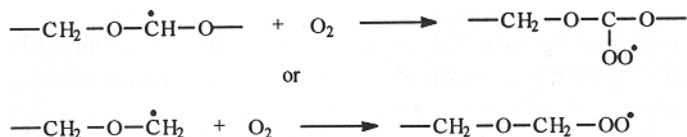
Further photolysis of the radical leads to the formation of formaldehyde:



which can undergo further photolytic processes:



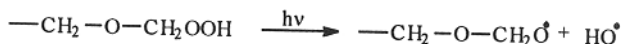
Hydrogen radicals may either recombine with oxyradicals or abstract hydrogen from the polymer molecule, forming macroradicals which can produce formaldehyde as a further step in these chain reactions. Studies of volatiles reveal that, in an oxygen-free atmosphere, hydrogen, carbon oxides, methane, ethane, and formaldehyde are the main products of photolysis. The methylenic hydrogens react readily with free-radicals to form hydroperoxide radicals:



which may then abstract hydrogen from the polymer molecule:



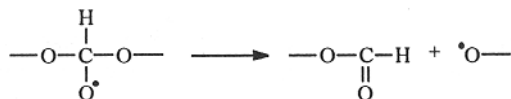
These observations are in agreement with those seen with other polymers of similar composition. The photooxidation of poly(tetramethylene glycol) and poly(ethylene glycol) leads to the formation of hydroperoxide.³⁴³ Poly(propylene glycol) undergoes surprising changes because hydroperoxides are formed at secondary (rather than the expected tertiary) carbon atoms.³⁴³ Studies of copolymers, which included oxymethylene, containing a small fraction of ethylene units and some carbon-carbon crosslinking, showed identical behavior to polyoxymethylene.³⁴³ Radicals participate directly in further chain reactions, whereas hydroperoxides absorb UV then produce:



These radical forming and radical induced processes show that the process, once initiated, is self-accelerated, and contributes to material instability. Examples of further conversions are given below:



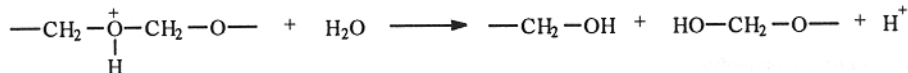
This is a cage reaction, and this:



a reaction leading to the formation of formate and alkoxy macroradicals by β -scission.³⁴³ It should be underlined that the bulk of photooxidative processes involve the formation of hydroperoxides.

In the presence of oxygen, the POM becomes increasingly more capable of absorbing UV radiation as carbonyl group concentration increases. The above reactions show that chain scission has a high probability of occurring, regardless of the irradiation environment.

Thermal oxidation and photooxidation are accelerated in the presence of water. Water can readily cleave the polymer backbone by acid-catalyzed hydrolysis:



Hydroperoxides can oxidize formaldehyde to formic acid, which, in turn, autoaccelerates the degradation process. Stabilizers may slow down these degradative reactions. The best results are achieved by an addition of 1-1.5% of carbon black, but UV absorbers (benzophenones and benzotriazoles) also protect polymer to some extent.

14.11.2 EFFECT OF THERMAL HISTORY

Hydroperoxides accumulate during the oxidative degradation of the POM. This process has a negligible rate in the case of copolymer, but homopolymer shows substantial growth of hydroperoxide concentration on heating.

14.11.3 CHARACTERISTIC CHANGES AND PROPERTIES

Copolymerization increases durability of polyoxymethylene, as does the use of UV absorbers and carbon black (Fig. 14.64). Figs. 14.65 and 14.66 show that polyoxymethylene homopolymer can withstand only a limited weathering period. In particular, elongation decreases during exposure, although initially, there is an increase in elongation accounted for by a molecular weight decrease which causes the elastic material to deteriorate rapidly on longer exposure.

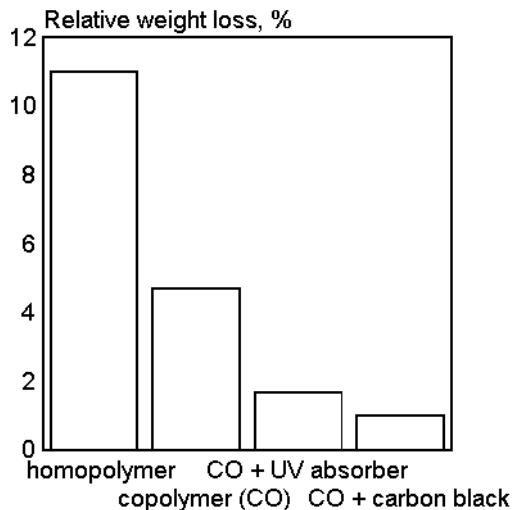


Fig. 14.64. Relative weight loss by polyoxymethylene during 20 months exposure in jungle clearing. [Data from A. Davis, *Polym. Degrad. Stab.*, 3(1981)187.]

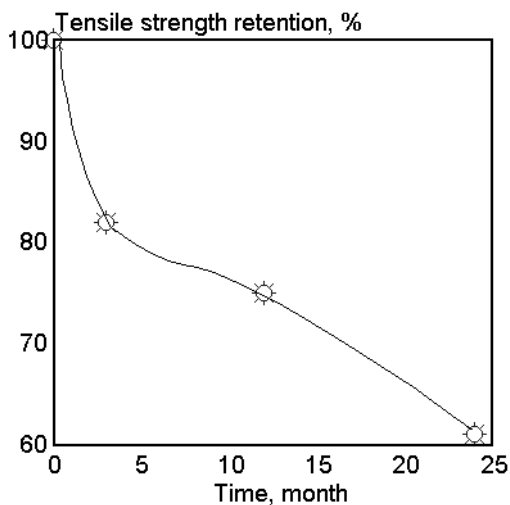


Fig. 14.65. Retention of tensile strength during natural exposure in Southern Slovakia. [Data from R. Vesely and M. Kalenda, *Kunststoffe*, 59(1969)107.]

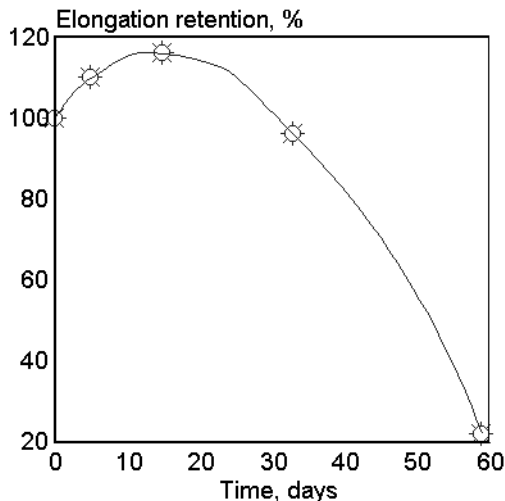


Fig. 14.66. Elongation retention during POM natural exposure in rain tropics. [Data from M. Taylor, *Joint Tropical Trials*, Queensland, Australia.]

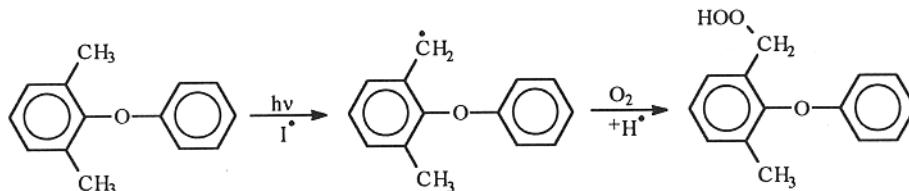
14.12 POLY(PHENYLENE OXIDE) (PPE)²⁴⁷⁻²⁵³

The engineering polymer, poly(phenylene oxide), is in fact poly(2,6-dimethyl-1,4-phenylene oxide). Its photodegradation is interesting, not only because of its application, mostly in alloy form, but also because of its chemical structure, which contains aromatic rings connected by ether linkage.

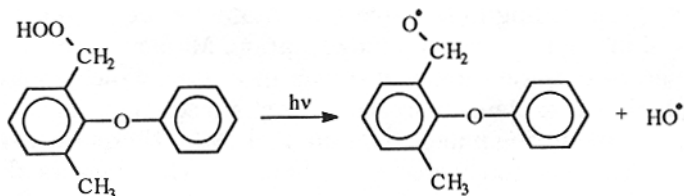
14.12.1 MECHANISM OF DEGRADATION

14.12.1.1 Models

Works by Jerussi³⁴⁷ concentrated on 2,6-dimethyl-1,4-phenylene oxide. Radiolysis of this product leads to side-group oxidation:



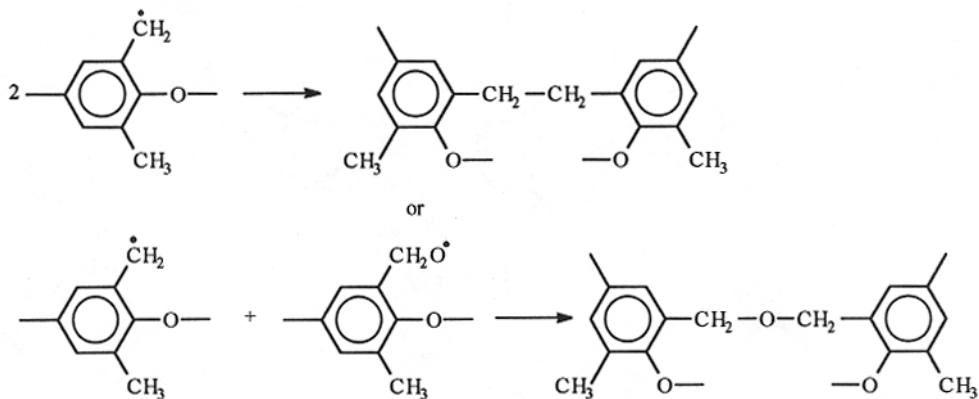
Irradiation of the hydroperoxides produces alkoxy and hydroxy radicals:



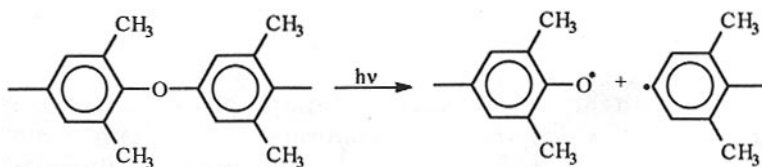
which may disproportionate to aldehyde and alcohol. Further conversions lead also to carboxylic acid, and then to an ester, which forms crosslinks.

14.12.1.2 Polymer

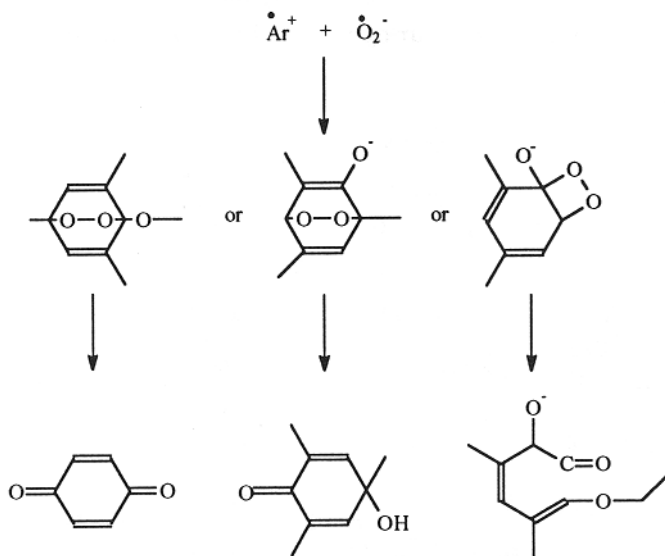
Crosslinking is also believed to occur by a recombination reaction:



A radical mechanism explains chain scission by the following equation:



All these reactions provide a comprehensive explanation for the practical observations of gel formation, yellowing, loss of tensile strength and elongation, if not for Pickett's findings.³⁴⁸ According to him, oxygen uptake by the polymer does not correspond to the loss of methyl groups on photooxidation. Moreover, the molecular weight of polymer exposed to radiation under nitrogen increases, which shows that the last reaction cannot, by itself, explain the reasons for chain scission. A drastic reduction of molecular weight occurs during photooxidation. Pickett,³⁴⁸ therefore, proposed another mechanism called "the electron transfer mechanism". He suggests that the excited polymer unit undergoes electron transfer with another unit and a radical cation and a radical anion are formed. Oxygen reacts rapidly with the radical anion, generating a superoxide which recombines with the radical cation, forming an unstable product that undergoes further reactions, producing a degraded polymer. Pickett gives a few alternatives to the primary processes, as follows:



The only problem with this explanation is that the author was unable to isolate the primary oxidation product, which would have confirmed the mechanism more conclusively than by deducing it by simply saying that other existing mechanisms cannot explain the observed changes.

14.12.2 EFFECT OF THERMAL HISTORY

PPE is stable under vacuum and nitrogen up to 300°C but it degrades when heated in oxygen. Side chain peroxides, which increase the rate of photolysis, are formed by thermal oxidation.

14.12.3 CHARACTERISTIC CHANGES AND PROPERTIES

A decrease in molecular weight follows the uptake of oxygen by PPE (Fig. 14.67). In a nitrogen atmosphere, crosslinking prevails over chain scission. The presence of oxygen considerably decreases the molecular weight of photodegraded PPE (Fig. 14.68). Only a fraction of the methyl groups undergoes oxidation, regardless of the form of the sample (solution, film), showing that there must be an oxidation mechanism which depends on a high oxygen uptake and causes a decrease in molecular weight of the polymer during photooxidation (probably ring oxidation) (Fig. 14.69).

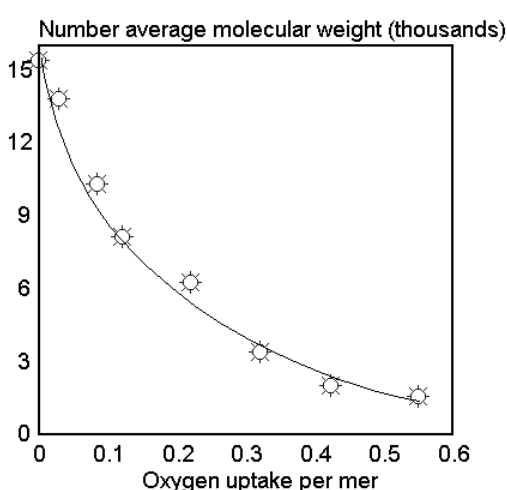


Fig. 14.67. Molecular weight vs. oxygen uptake. [Adapted, by permission, from J. S. Pickett, *ACS Symp. Ser.*, 280(1985)313.]

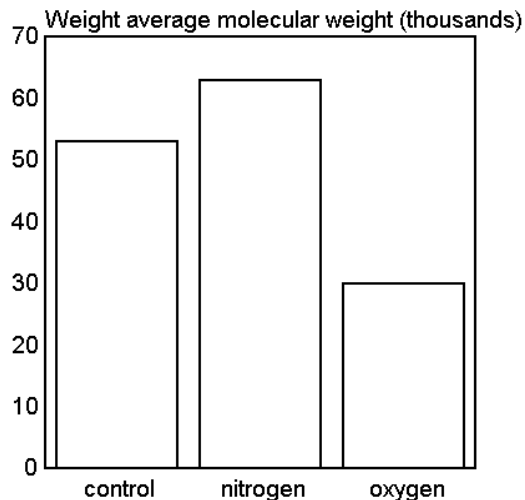


Fig. 14.68. Changes in molecular weight during PPE photodegradation (5 days by Pyrex-filtered mercury lamp). [Adapted, by permission, from J. S. Pickett, *ACS Symp. Ser.*, 280(1985)313.]

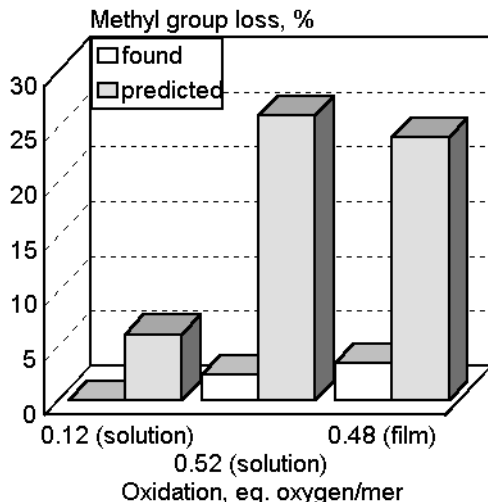


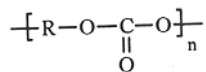
Fig. 14.69. Extend of PPE oxidation (eq. O₂/mer) vs. methyl group loss. [Adapted, by permission, from J. S. Pickett, *ACS Symp. Ser.*, 280(1985)313.]

14.12.4 DATA

Luminescence data:	
Spectral sensitivity: <370 nm	Strong absorption: 290-350 nm
Products of photolysis: crosslinks, radicals, chain scissions	
Products of photooxidation: ester linkages, radicals, hydroperoxides of side groups, additions across the aromatic rings, hydroxyl, aldehyde, and carboxylic groups	
Important initiators and accelerators: 9-cyanoanthracene, 9,10-dicyanoanthracene, methylene blue	
Stabilization: UV absorbers do not protect polymer which has too strong absorption. Trimethoxybenzene, DABCO, and HALS inhibit degradation	

14.13 POLYCARBONATES (PC)^{132,144,145,347-372}

Polycarbonates, expressed by general formula:



can be produced from various difunctional alcohols but most have been based on bisphenol A. The literature on this subject is specific to this particular polymer. Polycarbonate based on bisphenol A has an aromatic group in its chain and can therefore absorb UV radiation from daylight, which makes it prone to photolytic degradation.

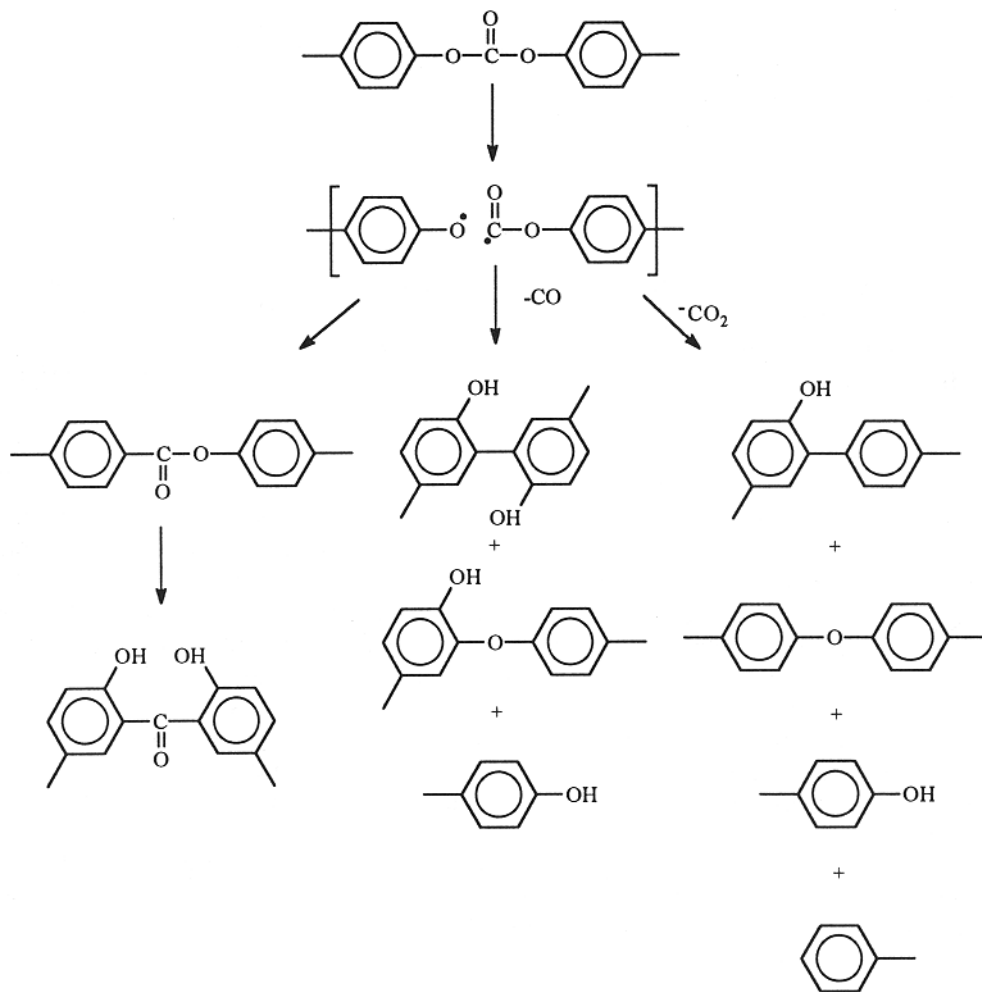
14.13.1 MECHANISM OF DEGRADATION

14.13.1.1 Models

A broad study by Pryde³⁶² is partly devoted to an investigation of the effect of monomeric material and of products which may form on degradation, on the stability of the basic polymer. The polymer is doped with these compounds and the effect studied. Addition of bisphenol A increases the degradation rate which occurs both in nitrogen and in air; polymer yellowing is also more noticeable. Bisphenol A concentration decreases during the course of exposure, which shows that it also undergoes degradation. This is important since bisphenol A is a product of polycarbonate hydrolysis and some is present in the polymer. Observations collected in the study show that hydrolysis influences degradation in the same way as does a bisphenol A addition but to a lesser extent and with a decreased acceleration effect. Pryde³⁶² doped polycarbonate with 4-hydroxystilbene which had been found in products of polymer radiolysis at longer wavelength. The degradation rate was increased. This is not surprising given that the chemical structure of stilbene contains a fairly long sequence of conjugated double bonds which are able to absorb radiation and are accessible to oxidative changes. The 4-hydroxystilbene disappears on irradiation at shorter wavelengths.

14.13.1.2 Polymers

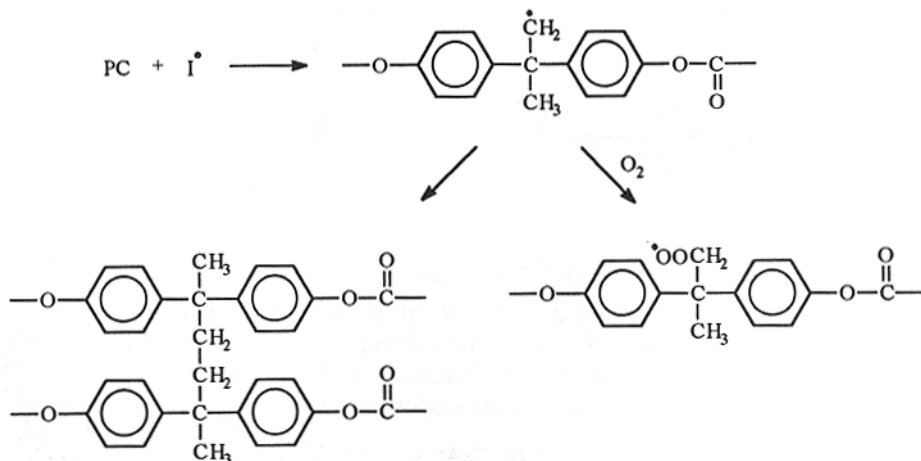
As with other polymers, there are an abundance of proposed degradative mechanisms for polycarbonates. One, which has been mentioned before and has been proposed for polycarbonates, is the photo-Fries rearrangement:



However, no products of the photo-Fries rearrangement were detected in weathered polycarbonate samples. This may simply testify that such a degradation mechanism is not valid or, as demonstrated by Rivaton *et al.*,³⁶¹ that the products of photo-Fries rearrangement are so easily photooxidized that they decompose before they can be analyzed. One important fact decreases the probability of such a mechanism. Hydroxybenzophenone, a common UV stabilizer, is one of the products of these reactions. With it present, we would expect polycarbonates to have good UV resistance or

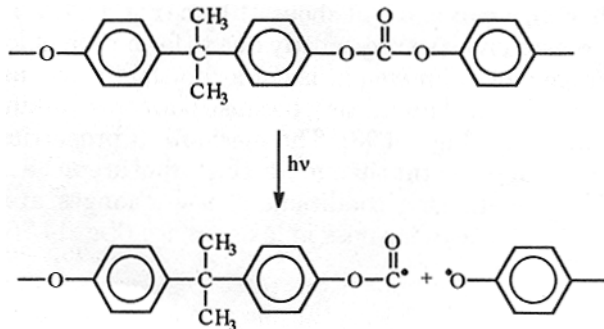
that its degradation would be slowed at the point when a sufficient amount of stabilizer is present, but neither is so.

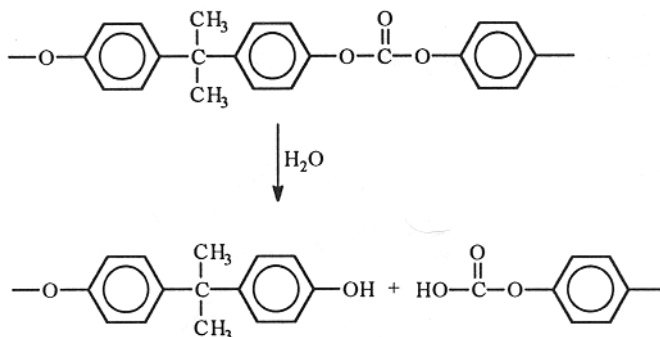
A second proposed mechanism considers methylene groups to be the vulnerable part of the structure:



This mechanism explains most of the observed crosslinking, yellowing, and hydroperoxide formation. The photooxidative pathway is not restricted to these reactions, as other reactions are important also especially since chain scission is commonly observed.

Other reactions which explain how polycarbonates degrade include these:





14.13.2 EFFECT OF THERMAL HISTORY

There is evidence that phenolic end-group concentration increases during storage. This is attributed to a slow oxidation process. Increasing temperature increases oxidation rate. The combined effect of absorbed moisture and elevated temperature initiates further photolytic changes which cause embrittlement.

14.13.3 CHARACTERISTIC CHANGES AND PROPERTIES

Polycarbonates absorb progressively more energy as they are irradiated and this rapid increase in absorption leads to autoaccelerated degradation (Fig. 14.70). However this process does not occur unless the wavelength of irradiation is below 300 nm (Fig. 14.71). It is this, low end of the spectrum that causes the most severe PC degradation. The photo-Fries rearrangement is caused by 260-300 nm radiation.³⁷⁰ Excessive irradiation at 290-320 nm causes the degradation rate to increase beyond that expected.³⁷¹ Shorter wavelength of radiation causes more crosslinking, whereas chain scission prevails at a longer wavelength, with a maximum at about 310 nm (Fig. 14.72). The molecular weight of the polymer decreases on exposure, mostly due to formation of low-molecular-weight products. The average molecular weight is not as much affected, as might be predicted from the change in mechanical properties, because both crosslinking and chain scission take place simultaneously (Fig. 14.73). The mechanical properties of the material do suffer because of molecular weight changes during exposure to natural (Fig. 14.74) and artificial (Fig. 14.75) weathering conditions. These changes are accompanied by a change in color, as seen from yellowness index increase (Fig. 14.76).

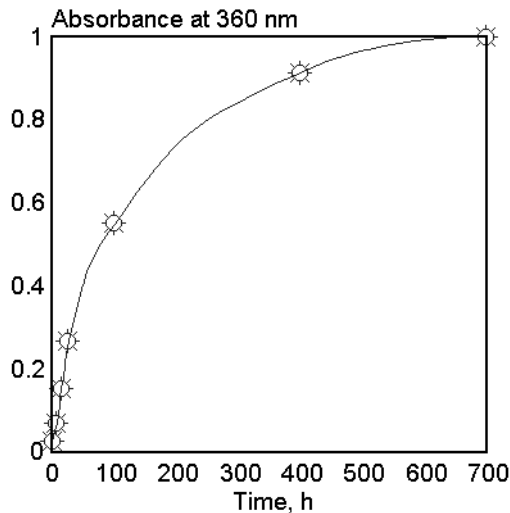


Fig. 14.70. PC photodegradation (>300 nm). [Adapted, by permission, from A. Gupta, A. Rembaum, and J. Maoconin, *Macromolecules*, 11(1978)1285.]

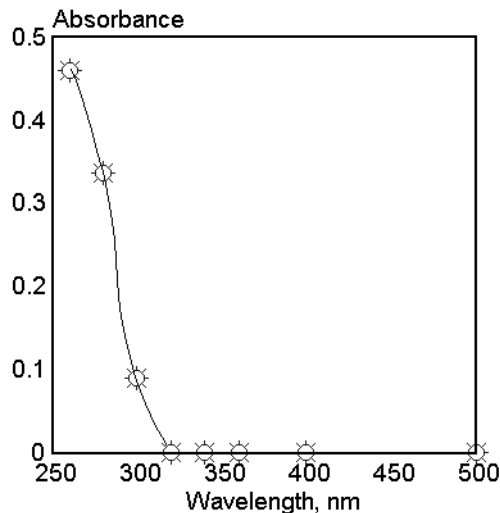


Fig. 14.71. Effect of wavelength on changes of absorbance of PC at 320 nm. Photon intensity 2×10^{19} photons/cm². [Data from Y. Fukuda and

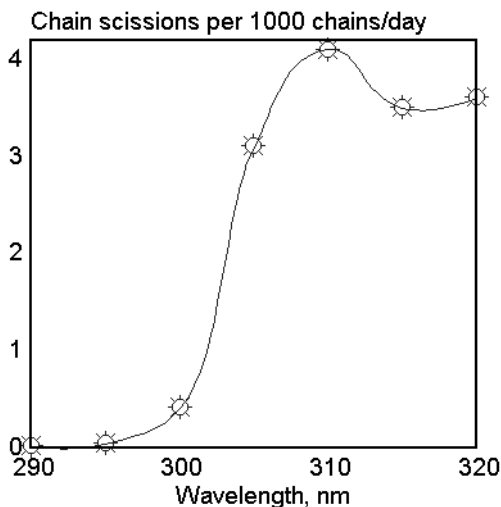


Fig. 14.72. Scission rate vs. irradiation wavelength. [Data from J. D. Webb and A. W. Czanderna, *Sol. Energy Mater.*, 15(1987)1.]

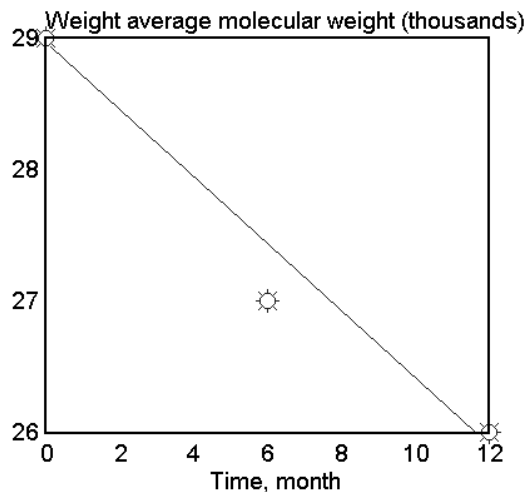


Fig. 14.73. Molecular weight vs. natural exposure time. [Data from A. Ram, O. Zilber, and S. Kenig, *Polym. Eng. Sci.*, 25(1985)535.]

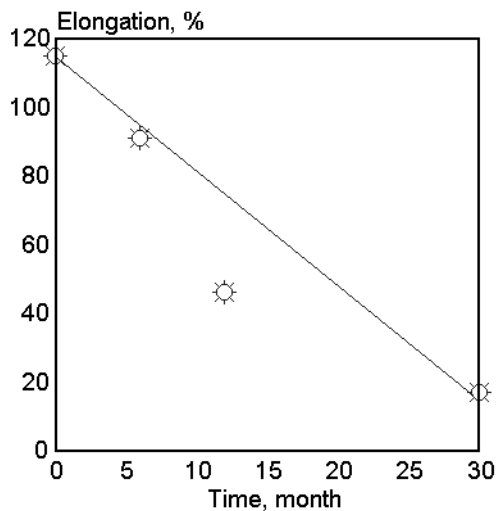


Fig. 14.74. Elongation vs. natural exposure time. [Data from A. Ram, O. Zilber, and S. Kenig, *Polym. Eng. Sci.*, 25(1985)535.]

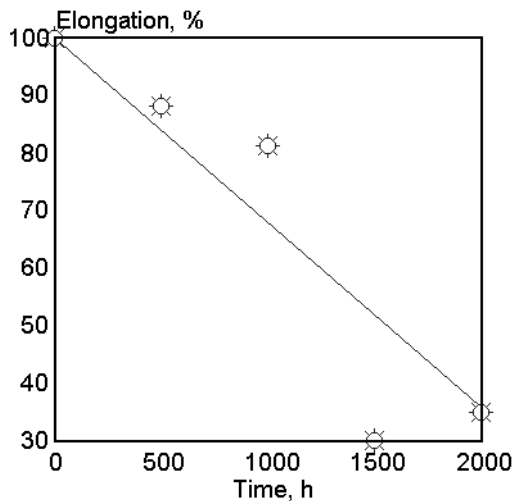


Fig. 14.75. Elongation vs. exposure in Weather-O-Meter. [Data from A. Ram, O. Zilber, and S. Kenig, *Polym. Eng. Sci.*, 25(1985)535.]

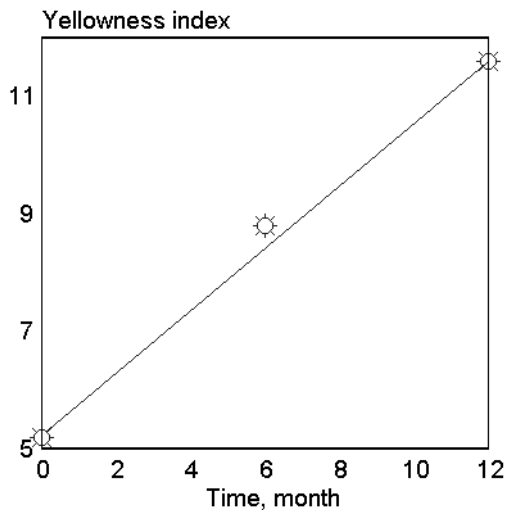
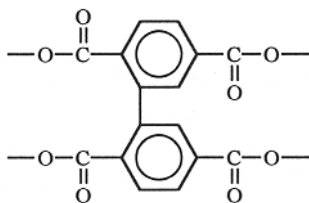


Fig. 14.76. Yellowness index vs. natural exposure time. [Data from A. Ram, O. Zilber, and S. Kenig, *Polym. Eng. Sci.*, 25(1985)535.]

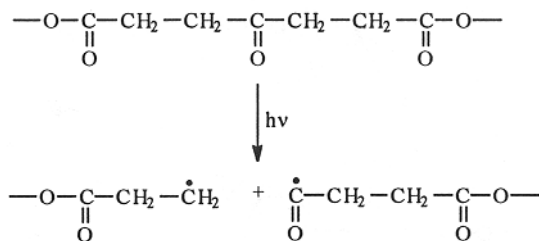
It was established from the studies on PBT³⁷⁹ done in the absence of oxygen that radicals from Norrish type I scissions react with labile hydrogen atoms. The double bonds formed from Norrish type II processes are also photolyzed. Primary radicals may decompose through decarbonylation and decarboxylation.

Free radicals can either recombine or they can abstract hydrogen from polymer molecules. Abstraction of hydrogen leads to mostly chain scission with the subsequent formation of molecules with hydroxyl, carboxyl, and aldehyde end-groups as detected by spectral analysis of the degraded polymers. Hydrogen abstraction may also lead to the formation of radicals which, when they recombine, form crosslinks:

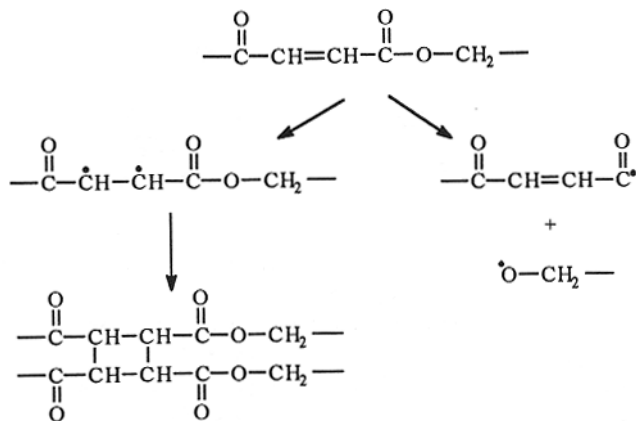


The presence of m-biphenyl systems was confirmed by FTIR analysis of PBT but this did not account for most of the yellowing observed.³⁷⁹

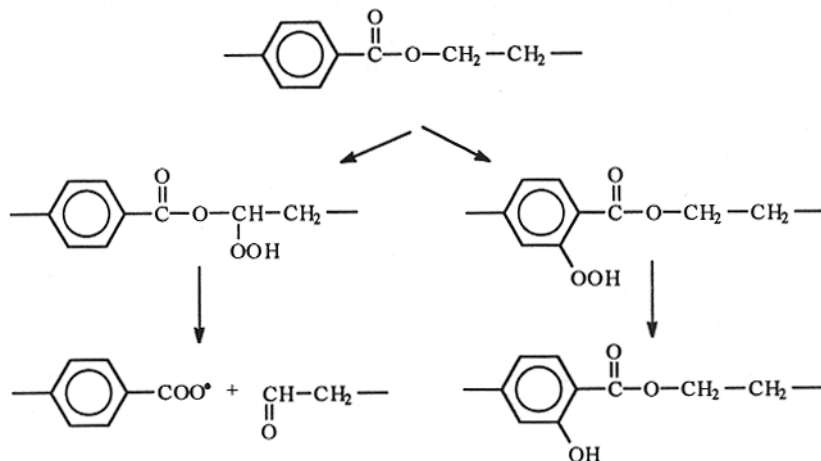
Aliphatic keto-polyesters preferentially form carbonyl radicals:



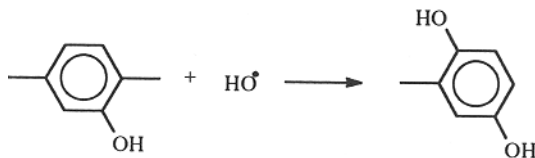
which decompose, producing carbon monoxide. Unsaturated polyesters may undergo either chain scission or crosslinking reactions:



The presence of oxygen contributes to the formation of hydroperoxides:



The formation of hydroperoxides in an aliphatic segment leads simply to chain scission and an increased carbonyl group concentration. Hydroperoxides attached to the aromatic ring lead to the formation of hydroxy-compounds responsible for the photo-yellowing of polyesters. The hydroxyl group can also be directly substituted in a reaction with the hydroxyl radical:



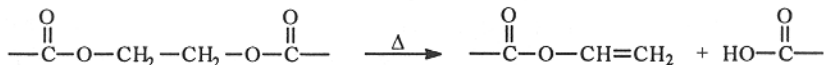
It is suggested³⁷⁹ that, except for the typical photolytical processes discussed above, oxidation of methylene groups occurs as proposed by the above equation. Radicals are preferentially formed by abstraction of hydrogen from the methylene group in the α -position to the ester group. The reaction of these radicals with molecular oxygen produces peroxy radicals which then abstract hydrogen from the macromolecular chain and form hydroperoxides. Hydroperoxides accumulate at fairly low rate which indicates that homolysis of O-O bond occurs simultaneously. The alkoxy radicals thus formed are converted either into anhydrides or, through a cage reaction, into aliphatic aldehydes and carboxyl radicals.

Photolysis is a preferential mode of degradation. The oxidative sites are not very reactive and hydroperoxides appear at a rather low concentration. Chain scission predominates. Photooxidative degradation is mainly governed by UV radiation at around 315 nm but the effect is only apparent in the surface layer. This layer has more carboxylic end-groups and fluorescence intensity decreases exponentially with distance from the surface. The core of the fiber or deeper layers of the material are mostly affected by radiation of longer wavelength (≈ 350 nm). This shows that there are different mechanisms of degradation in the surface than in the bulk. The thickness of the degraded layer was studied by Rivaton.³⁷⁸ About 80% of the observed photochemical changes (absorbance at 3485 cm^{-1} and 330 nm) occurred in the first $15\text{ }\mu\text{m}$ of the surface and 100% changes occurred in the first $45\text{ }\mu\text{m}$ (exposure time was 270 and 500 h, and $\lambda > 300$ nm).

Enzymatic degradation of polyesters³⁷⁴ occurs when the polyester lacks crystallinity and has a low T_g . These two conditions cause the polymer chain to be sufficiently flexible to conform to the transition state of an enzymatic adduct.

14.14.2 EFFECT OF THERMAL HISTORY

The chemical structure of the polyester determines the exact composition of the degradation product but the following equation is representative:



In addition, vinyl and carboxyl end-groups, cyclic ketones, aldehydes, dienes, cyclic ethers, benzoic acid, acetophenone, ketones, etc., were detected.

14.14.3 CHARACTERISTIC CHANGES AND PROPERTIES

The concentration of hydroxyl and carboxyl groups increased rapidly during photooxidation (Fig. 14.77), showing that the chain scission reaction dominates the photooxidative processes. Photolysis and photooxidation each cause changes at comparable rates (Fig. 14.78). Irradiation of polyester-polyether causes more degradation than thermal exposure (Fig. 14.79). As shown by its light absorption profile, PET absorbs in the range from 290 to 350 nm and, as it does, degrades photolytically (Fig. 14.80). Aging of PET is accelerated by high humidity (Fig. 14.81).

14.14.4 DATA

Luminescence data:		
Sample form	Excitation wavelength, nm	Emission wavelength, nm
PBT	340, 383, 395	440-450
PET chip	320, 344, 357	370, 389, 405
chip	280, 318, 351	425, 460
film, fiber	344, 357	370, 389, 405
fiber	284, 310	425, 477
PEN film	375	435
film	375	580
Products of photolysis: radicals, crosslinks		
Products of photooxidation: radicals, crosslinks, hydroperoxides, hydroxyl groups, carboxyl groups		
Important initiators and accelerators: ferrocene, cobalt octoates and naphthenates, compounds containing aromatic keto-ester groups		
Stabilization: UV absorbers (preferably benzotriazoles); HALS		

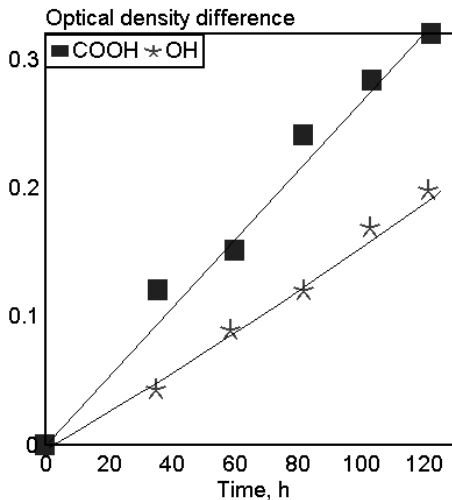


Fig. 14.77. Absorbance in the OH and COOH regions during photooxidation. [Adapted, by permission, from M. H. Tabankia and J. -L. Gardette, *Polym. Degr. Stab.*, 14(1986)351.]

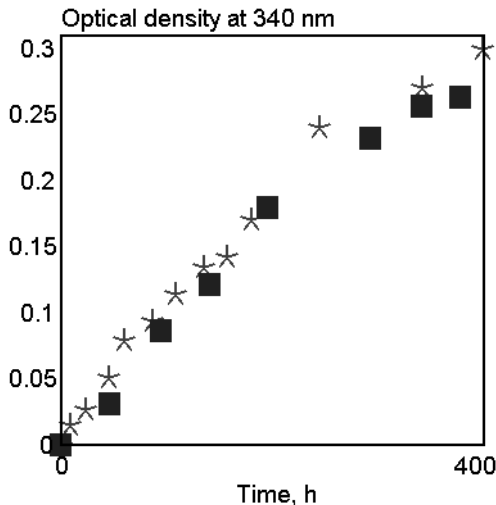


Fig. 14.78. Optical density at 340 nm on irradiation at 300 nm. [Adapted, by permission, from M. H. Tabankia and J. -L. Gardette, *Polym. Degr. Stab.*, 14(1986)351.]

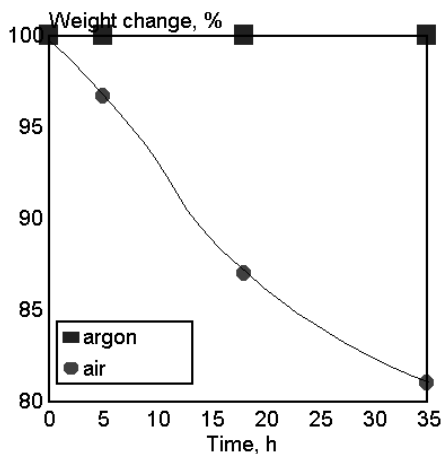


Fig. 14.79. Weight change in polyester polyether during degradation (thermal degradation 120°C, irradiation by a mercury lamp in argon and air). [Adapted, by permission, from J.-Q. Pan and J. Zhang, *Polym. Deg. Stab.*, 36(1992)65.]

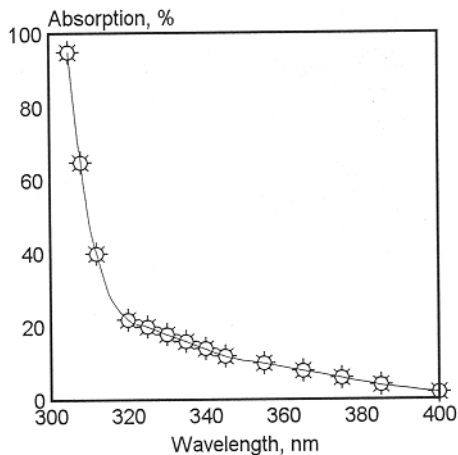


Fig. 14.80. Radiation absorption profile of virgin PBT film (thickness 11 μ m). [Adapted, by permission, from A. Rivaton, *Polym. Deg. Stab.*, 41(1993)283.]

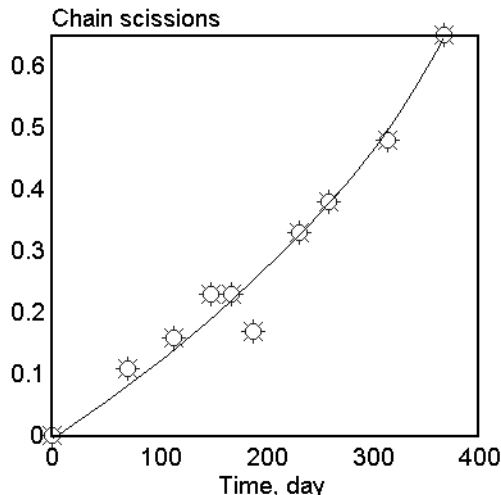


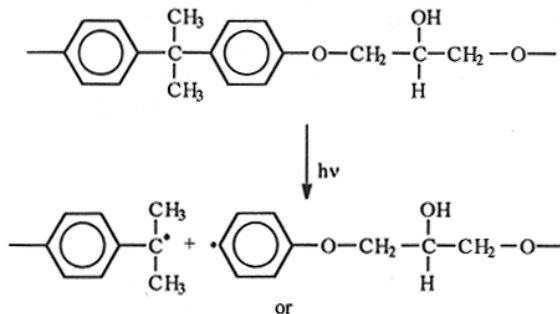
Fig. 14.81. Chain scission at 60°C of amorphous PET sample at 100% relative humidity. [Data from M. Edge, M. Hayes, M. Mohammadian, N. S. Allen, T. S. Jewitt, K. Brems, and K. Jones, *Polym. Deg. Stab.*, 32 (1991)131.]

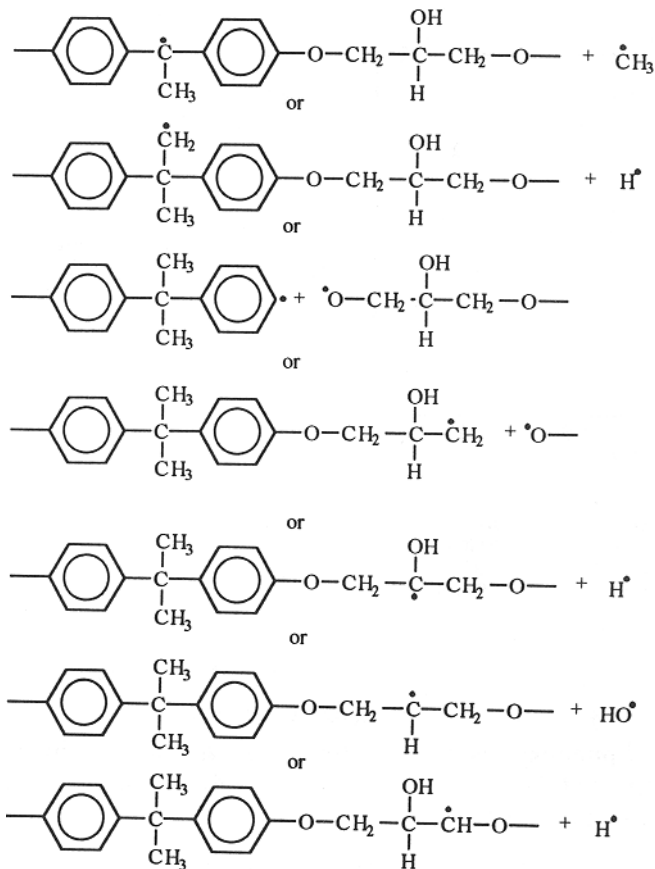
14.15 PHENOXY RESINS

The composition of phenoxy resins, including bisphenol and epichlorohydrin, suggests that their mechanism of degradation is similar to polycarbonates with epichlorohydrin showing some distinct differences.

14.15.1 MECHANISM OF DEGRADATION

UV exposure in the absence of oxygen produces numerous free radicals:

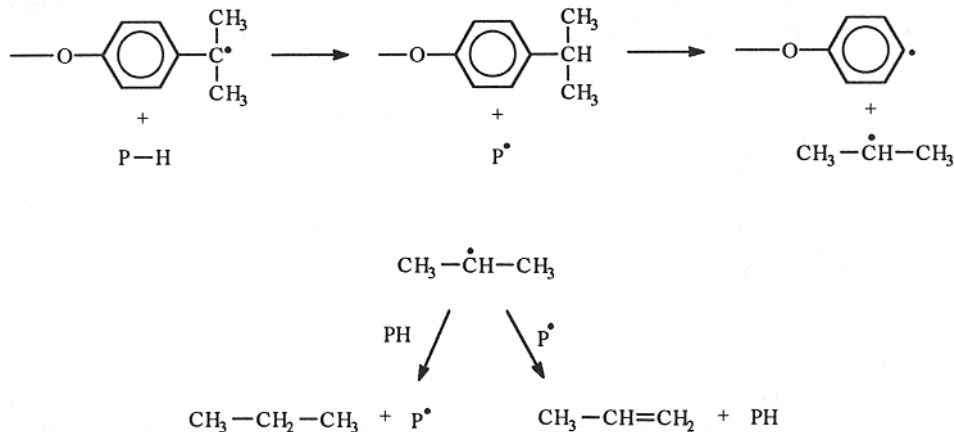




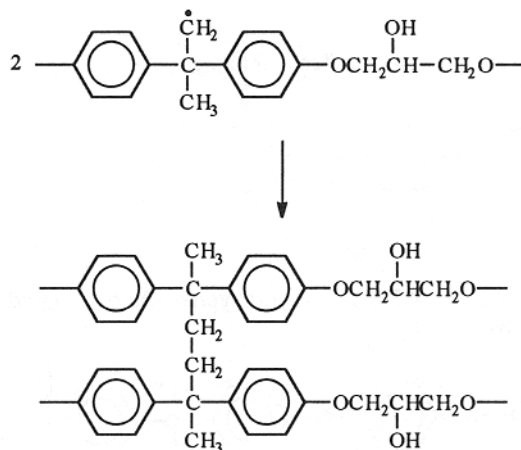
Most bonds are vulnerable and numerous radicals are formed. Analysis of the gaseous products of photolysis shows that hydrogen, water, methane, ethane, propane, and propene are produced. Hydrogen, water, and methane are produced by the simple abstraction of hydrogen from a polymer molecule resulting in gaseous products and a new radical. Ethane is a product either of recombination of two methyl radicals or of abstraction of a methyl group from the polymer:



Propane and propene photosynthesis is described by the following set of reactions:

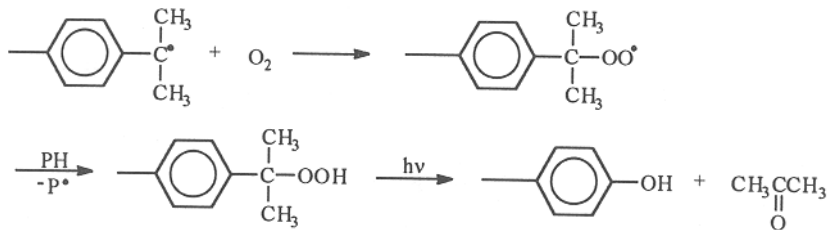


These show that chain scission has several causes. Crosslinking, observed experimentally, occurs as a result of the recombination of previously formed radicals:



There is no explanation given for a quite intensive yellowing which is a visible result of photolysis.

Photooxidative degradation causes less yellowing but more numerous free radicals. Each radical can react with oxygen, producing hydroperoxides which are the precursors of carbonyl and hydroxyl groups. Photooxidative degradation results in more crosslinking (the reasons are mostly unknown) and a volatile product - acetone:

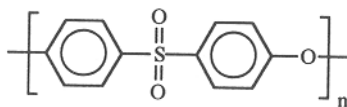


These mechanisms of photodegradation can lead to other products, such as, aldehydes, carboxylic acids, carbon monoxide, and carbon dioxide. The complex changes, which can occur in phenoxy resins, have not been fully researched and much remains to be done.

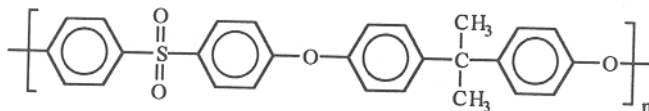
14.16 POLYSULFONES & POLYSULPHIDES (PSF & PPS)^{369,375,384-394}

Polysulfones include materials formed in these ways:

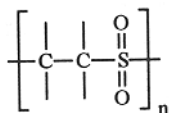
- (i) condensation products of 4,4'-sulfonyl chloride diphenyl and diphenyl ether



- (ii) condensation products of 2,2-bis-4(hydroxyphenyl)propane and 4,4'-dichlorodiphenylsulfone



- (iii) reaction of SO_2 and a double bond containing compound

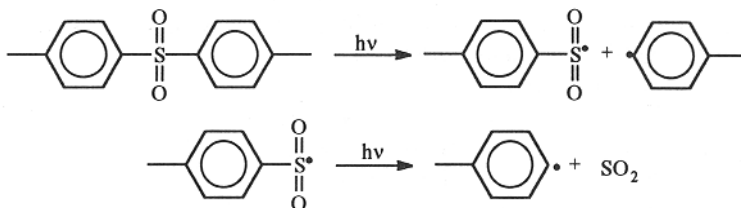


Both aromatic and aliphatic polymers are produced. It is known that these polymers do not weather well but data on their degradation are scarce.

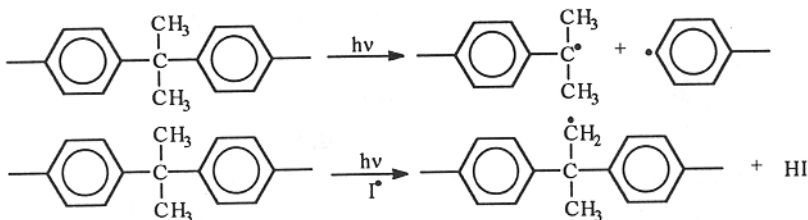
14.16.1 MECHANISM OF DEGRADATION

Practically all the bonds in the macromolecule, except the aromatic carbon-carbon and aromatic carbon-hydrogen, are unstable and are believed to break during exposure to atmospheric conditions.

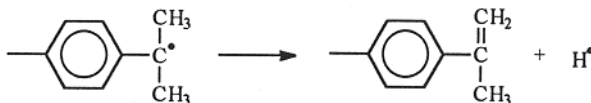
Sulfur dioxide is found in photolytic products of the reaction:



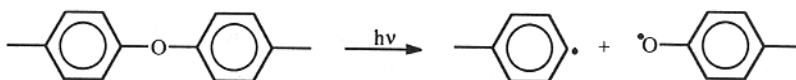
Bisphenol A fragments contribute to free radical formation, according to the reactions:



Unsaturation is formed during radical decomposition by disproportionation:



Bond cleavage at the diphenyl oxygen group is caused by the primary photochemical process:



Photooxidative processes are even more complex, as volatile products such as CO, CO₂, SO₂, CS₂, and COS are emitted during the photooxidation of polysulfones. Munro,³⁸⁸ surprisingly, found evidence for the oxidation of phenyl rings. Hydroperoxides and carbonyl groups are commonly detected, causing radical formation and increase in UV absorption. There are many possible combinations of reactions but what these may be is a matter of speculation based more on analogy with similar polymers than on confirmed facts and mechanisms.

Exposure of PSF samples to UV radiation at room temperature leads to chain scission and crosslinking. At elevated temperature (170°C), only crosslinking is observed.³⁹³ During irradiation at room temperature, it was observed that for one molecule of SO₂ produced (chain scission) twenty crosslinks were formed. In PSF, chains scission is observed even at elevated temperatures due to the existence of the aliphatic group. This donates hydrogen about 20 times more readily than does the aromatic ring.³⁹⁴ There is very little difference between photolysis of either polymer in both oxygen and inert gas.³⁹⁴

14.16.2 EFFECT OF THERMAL HISTORY

Bowden³⁹² suggested that β-elimination might occur during the thermal degradation of poly(1-butene sulfone) with subsequent formation of free radicals and unsaturations.

14.16.3 CHARACTERISTIC CHANGES AND PROPERTIES

The activation spectrum of PPS shows that most of radical formation occurs at 380 nm (Fig. 14.82). Absorption of UV radiation is very strong up to 310 nm then diminishes between 320 and 340 nm but continues throughout the entire UV range. SO₂ emission increases as the temperature of photolysis increases (Fig. 14.83). Molecular weight is less affected by elevated temperatures due to the increased probability of crosslinking reactions (Fig. 14.84). The elongation capability of the polymer changes rapidly during photooxidation and shows that polysulfones are very UV unstable (Fig. 14.85). Elonga-

tion change is a far more sensitive indicator of degradation (Fig. 14.86) than is tensile strength.

14.16.4 DATA

Luminescence data:		
Sample form	Excitation wavelength, nm	Emission wavelength, nm
PSO film	245-255, 270	310, 450
PESO film	320	360, 450
Spectral sensitivity: <320 nm		
Products of photolysis: chain scissions, free radicals, crosslinks, unsaturations, polysulfides		
Products of photooxidation: chain scissions, free radicals, carbonyl groups, hydroperoxides, disulfonic acid, hydroxyl groups		
Important initiators and accelerators: residual monomer, copper stearate		

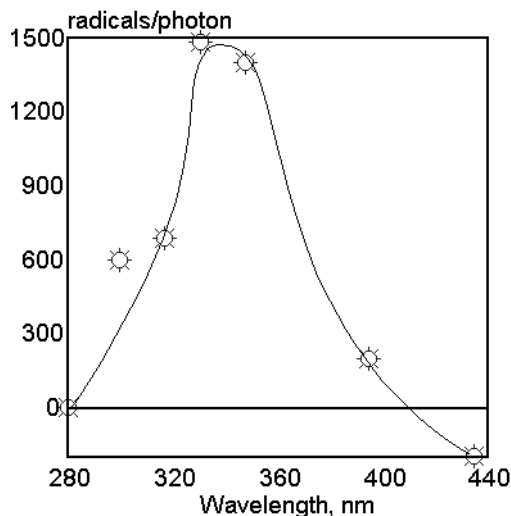


Fig. 14.82. Activation spectrum of PPS. [Data from G. Kämpf, K. Sommer, and E. Zirngiebl, *Prog. Org. Coat.*, 19(1991)69.]

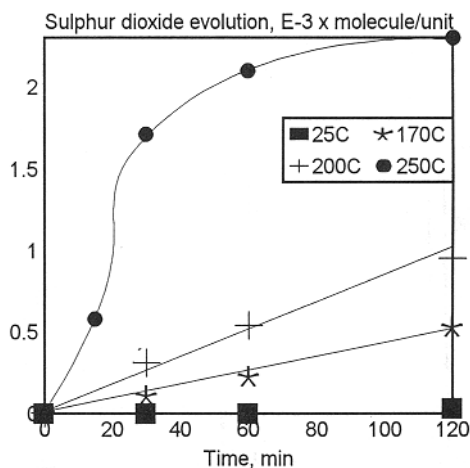


Fig. 14.83. SO₂ evolution during PSF photodegradation at different temperatures. [Adapted, by permission, from S. Kuroda, I. Mita, K. Obata, and S. Tanaka, *Polym. Deg. Stab.*, 27(1990)257.]

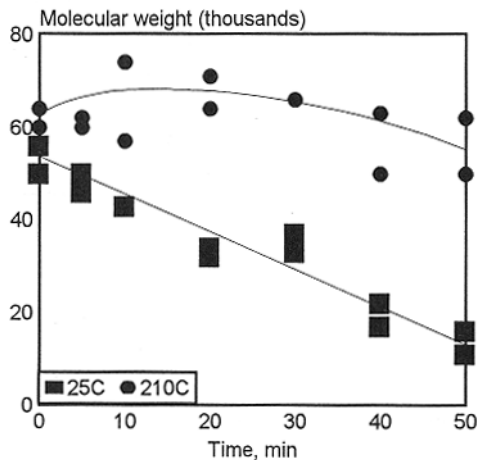


Fig. 14.84. Weight-average molecular weight of PSF change during irradiation at 25 and 210°C. [Data from T. Yamashita, H. Tomitaka, T. Kudo, H. Horie, and I. Mita, *Polym. Deg. Stab.*, 39(1993)47.]

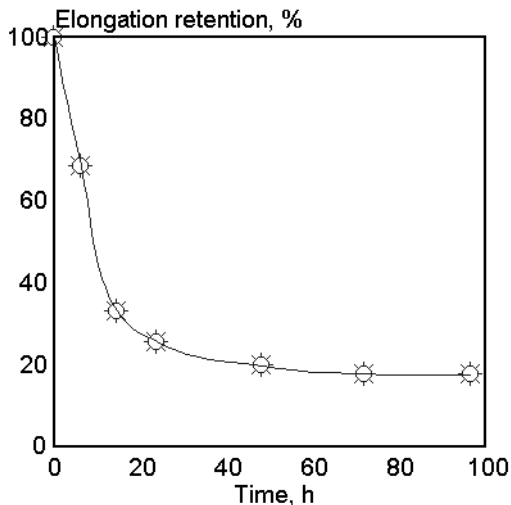


Fig. 14.85. Retention of PSF elongation during photooxidation. [Data from B. D. Gesner and P. G. Kelleher, *J. Appl. Polym. Sci.*, 13(1969)2183.]

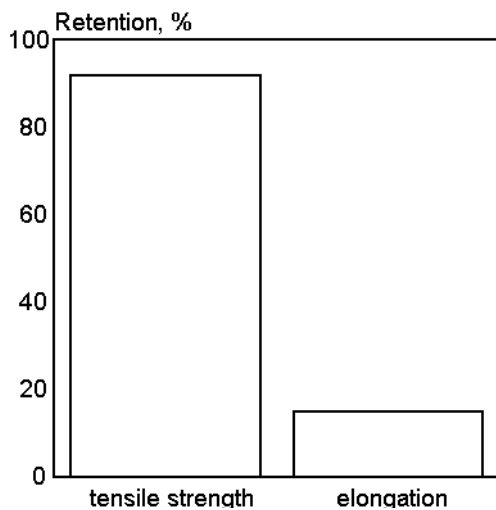


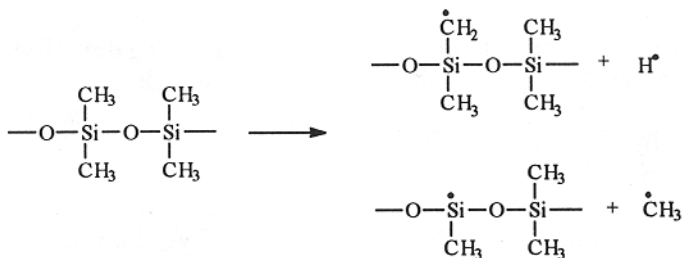
Fig. 14.86. Retention of PSF mechanical properties during 1 week of natural exposure. [Data from B. D. Gesner and P. G. Kelleher, *J. Appl. Polym. Sci.*, 13(1969)2183.]

14.17 SILICONES (SI)³⁹⁵⁻⁴¹⁴

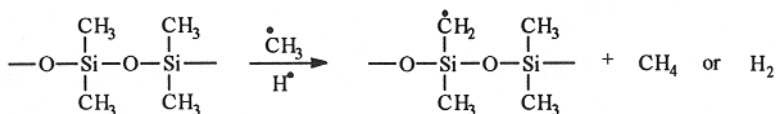
Polysiloxanes should not absorb UV radiation at 300 nm and above, but as is the case with other polymers, they degrade on exposure to daylight. The other commercial member of the silicone family, namely, the organosilane group, is even more vulnerable to UV degradation. Energy of dissociation of some silicon bonds is as follows: Si-H 325-376, Si-C 271-360, Si-Si 280-340, Si-O 443-530 kJ/mol. Except for Si-O bonds, it can be seen that the bonds are weak.

14.17.1 MECHANISM OF DEGRADATION

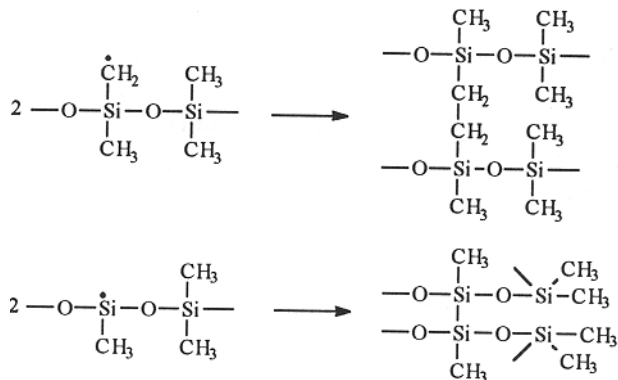
The main gaseous products of photolysis include hydrogen, methane, and ethylene, indicating that degradation involves the methyl group:



Hydrogen and methyl radicals may recombine, forming hydrogen, methane, or ethane, or they may abstract hydrogen from polymer:



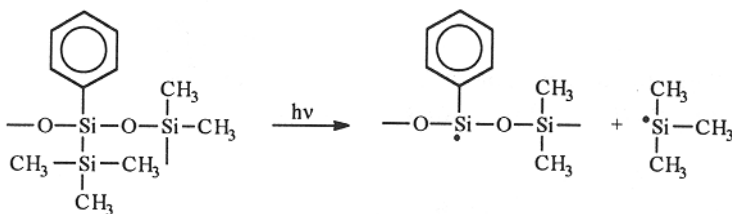
Macroradicals can also recombine:



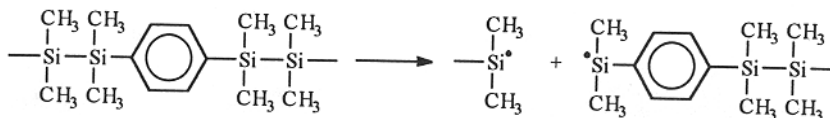
which results in crosslinking.

Studies were done on polydimethylsiloxane containing dimethylene groups.⁴¹⁴ This combination decreases the stability of the polymer. Defects and impurities act as extrinsic chromophores which lead to the formation of radicals. Radicals react readily with the dimethylene group but the methyl group is not affected because of its apparent, very low, reactivity.⁴¹⁴

The above mechanisms have been developed from studies involving UV degradation, thermal degradation, and degradation by γ -rays. Polysiloxanes containing the phenyldisilanyl unit undergo a dissociation of Si-Si bonds:

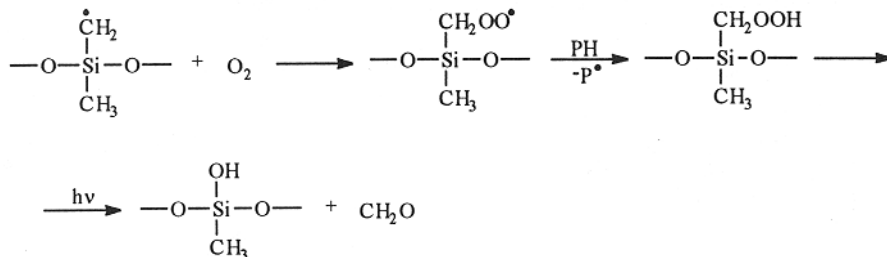


If phenyl is built into the backbone, it also causes Si-Si bond breakage near the phenyl ring:



Phenyl as a pendant group increases UV absorption and accelerates radical formation at the methyl group on the same silicon atom.

Macroradicals can react with oxygen, when present:



which increases the rate of radical formation and that of other groups which tend to make the polymer more hydrophilic.

14.17.2 CHARACTERISTIC CHANGES AND PROPERTIES

Silicone producers tend to evaluate the durability of the polymers more favorably (Fig. 14.88) than does an independent source (Fig. 14.87). Clearly, more studies are required.

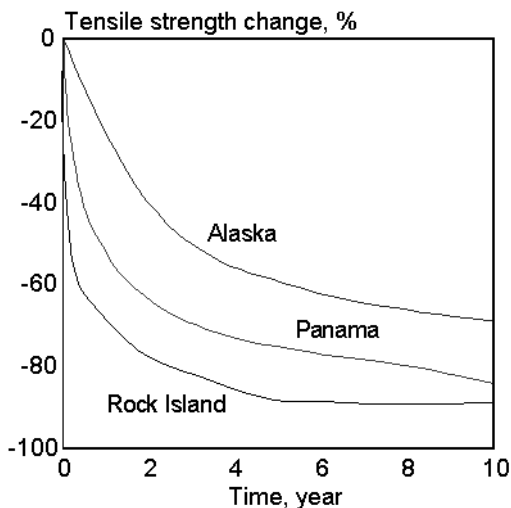


Fig. 14.87. Tensile strength change of white colored silicone rubber during natural exposure in various locations. [Data from E. W. Bengstrom, *Report*, 74-038.]

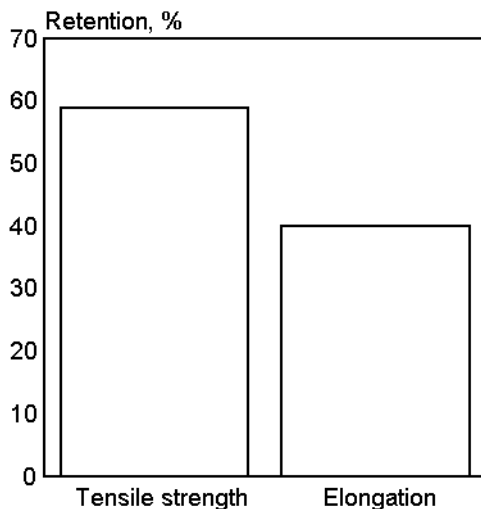
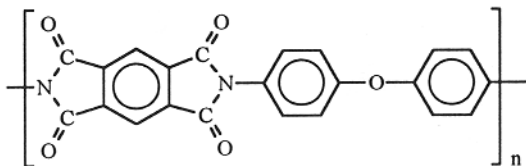


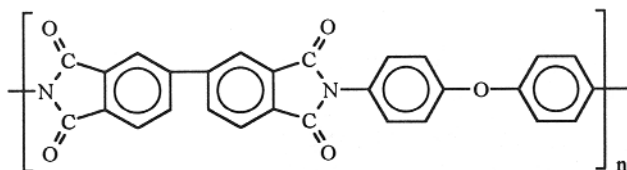
Fig. 14.88. Change in mechanical properties of weathered silicone rubber exposed for 20 years in Florida. [Data from *Dow Corning Bull.*, 1972, 17-158.]

14.18 POLYIMIDES (PI)⁴¹⁵⁻⁴²⁰

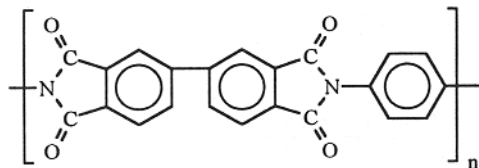
Aromatic polyimides have recently attracted considerable interest due to their excellent mechanical properties, thermal and oxidative stability, and chemical resistance. The most important materials involved have the following formulas:



Kapton™ (DuPont)



Upilex™ (UBE Ind.)



Upilex™ (UBE Ind.)

Interest in these polymers goes beyond UV degradation because they are also considered suitable for applications in a high radiation field (fusion reactors, space vehicles, and satellites) as well as in model compounds for laser ablation studies and for patterning in electronic industry.

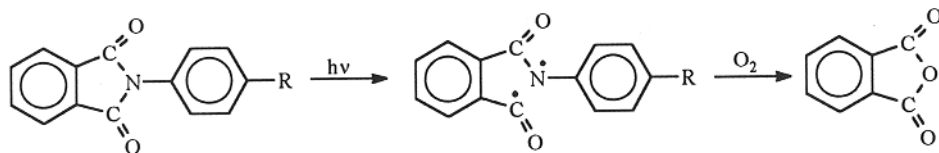
14.18.1 MECHANISM OF DEGRADATION

14.18.1.1 Models

Pyromellitic dianhydride, PDMA, N-phenylphthalimide, PA, and hexafluoroisopropylidene-2,2'-bis(N-phenylphthalimide), 6F, which are components of most polyimide structures, were used in model studies.⁴¹⁷ All of these compounds have similar absorption spectra to their respective polymers. They have strong absorption up to 310 nm and residual absorption up to 360 nm. When excited by 325 nm radiation, 6F has a fluorescence maximum at 520 nm and PA at 560 nm. Major products of photolysis include H₂O, CO₂, CO, and phthalic anhydride.

14.18.1.2 Polymers

Studies on various polymers^{415,416} show that polyimides exposed to UV radiation (including unfiltered mercury lamp radiation) are stable in an inert atmosphere. Oxygen accelerates the degradation process. The mechanism of UV degradation is not yet known. The following scheme has been proposed:⁴¹⁷



Studies using γ -irradiation⁴²⁰ estimated that polyimides in satellite application for 30 years service received a radiation dose equivalent to 10 MGy or 50 MGy when used in a fusion reactor. It was reported that Kapton can withstand 100 MGy of irradiation which makes it a useful candidate material for these applications. The durability of polyimide in these applications is measured by monitoring the amount of evolved gases, such as, CO_2 , CO , N_2 , H_2 , and CH_4 and correlating that with the loss of mechanical performance. The presence of a biphenyl structure (Upilex R) depresses gas evolution at high γ radiation doses, especially the evolution of H_2 and CH_4 . Upilex R evolved more CO and N_2 than did Kapton.

During UV laser ablation,^{418,419} large amount of ultraviolet is absorbed by the material. This energy flux is sufficient to break bonds and thus etch atoms and molecules from the surface. Gaseous products, such as CO_2 , CO , etc., are produced and ablation occurs within the time span of the pulse which is typically several hundred ns ($\lambda=308$). The formation of gaseous degradation products indicates that ablation is a combination of photochemical and photothermal mechanisms. An etch depth of a few micrometers removes material cleanly from the surface.

14.18.2 CHARACTERISTIC CHANGES AND PROPERTIES

Degradation of N-phenylphthalimide leads to the formation of phthalic anhydride as a major product (Fig. 14.89). Minor products include phthalimide and nitrobenzene. Kapton H shows relatively good stability (Fig. 14.90) when compared with other materials produced in the laboratory. Polyimides are durable when exposed to γ -radiation (Fig. 14.91). Upilex R is the most durable among other polyimides, PEEK, PES, and other polymers competing in this area.

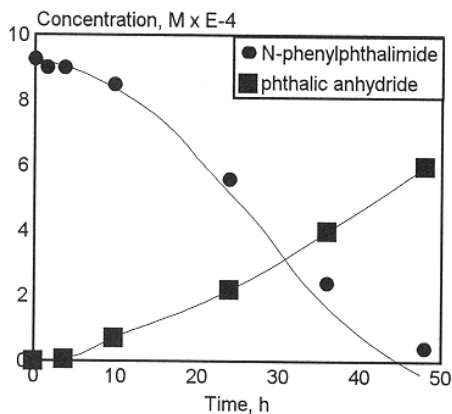


Fig. 14.89. Concentration of substrate (N-phenylphthalimide) and major product (phthalic anhydride) during photodegradation in an air saturated, immersion well apparatus with Pyrex filtered, medium pressure, mercury lamp. [Data from C. E. Hoyle, D. Creed, R. Nagarajan, P. Subramanian, and E. T. Anzures, *Polymer*, 33(1992)3162.]

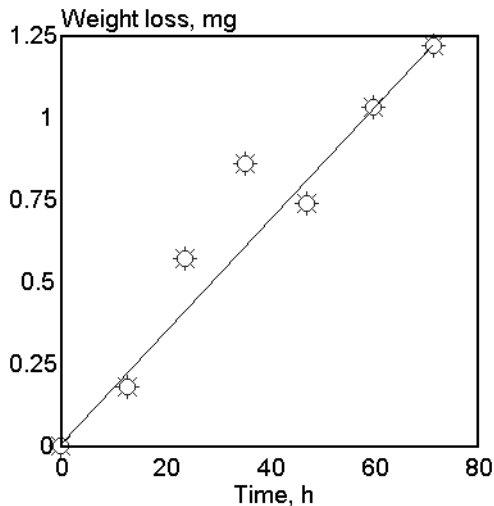


Fig. 14.90. Weight loss of Kapton H exposed to unfiltered medium pressure mercury lamp in air. [Data from C. E. Hoyle and E. T. Anzures, *J. Polym. Sci., Polym. Chem.*, 30(1992)1233.]

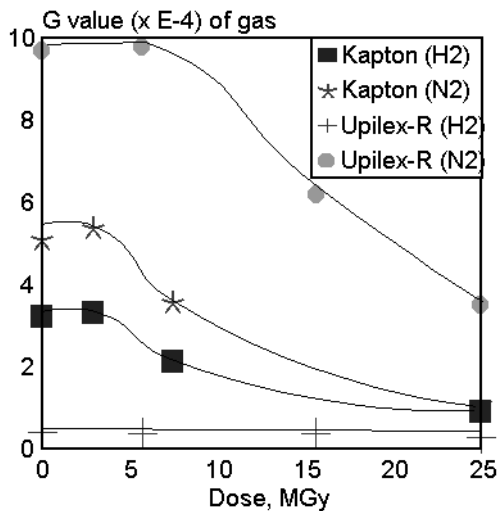


Fig. 14.91. Yield of evolved gases on γ -irradiation of different polyimides. [Data from E.-S. A. Hegazy, T. Sasuga, M. Nishii, and T. Seguchi, *Polymer*, 33(1992)2897.]

14.18.3 DATA

Luminescence data:		
Polymer	Excitation wavelength, nm	Emission wavelength, nm
6F-ODA	380	508
ODPA-ODA	380	505
PMDA-ODA	450	566

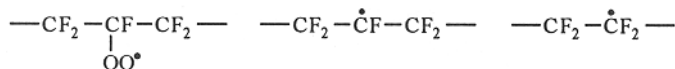
6F - hexafluoroisopropylidene-2,2'-bis(phthalic anhydride), ODA - 4,4'-oxydianiline, ODPA - 4,4'-oxydiphthalic anhydride, PMDA - pyromellitic dianhydride

14.19 POLYTETRAFLUOROETHYLENE (PTFE)⁴²¹⁻⁴²³

PTFE is applicable for many high-end-use applications such as a blanket material on a space craft launched into orbit by the space shuttle or in nuclear plants. These types of applications require knowledge of how it performs in prolonged space exposure. A few data available give some information on its performance.

14.19.1 MECHANISM OF DEGRADATION

Two materials (pure PTFE and carbon black filled PTFE) were exposed in air to radiation from Co⁶⁰ source.⁴²¹ PTFE has an unexpectedly large sensitivity to ionizing radiation. Oxygen increases the degradation rate by factor 40. Carbon black forms a hyperfine structure in the material which reduces oxygen diffusion but without increasing its stability significantly. The following radicals were detected during the degradation process:



The life of the peroxy radical is one order of magnitude longer than the life of the other two radicals. As a result of radical formation, chain scission occurs, which reduces molecular weight, tensile strength, and elongation. As a result of this research, the material was deemed to be unsuitable as a nuclear component or for medical applications because it does not withstand a sterilization.⁴²¹

A sample of PTFE exposed for 6 years in space was studied.⁴²² The surface of sample was severely disrupted due to its reaction with atomic oxygen. Similar surface damage was observed in samples which had undergone plasma treatment. The energy of

particles colliding with the surface of the PTFE depends on spacecraft velocity which is approximately 8000 m/s. For atomic oxygen it translates to be 5 eV. Similar conditions of bombardment by atomic oxygen were simulated in laboratory and its effect compared with sample retrieved from space. The character of surface damage as well as results from ESCA analysis were sufficiently similar to deduce that most degradation occurred in PTFE due to atomic oxygen.

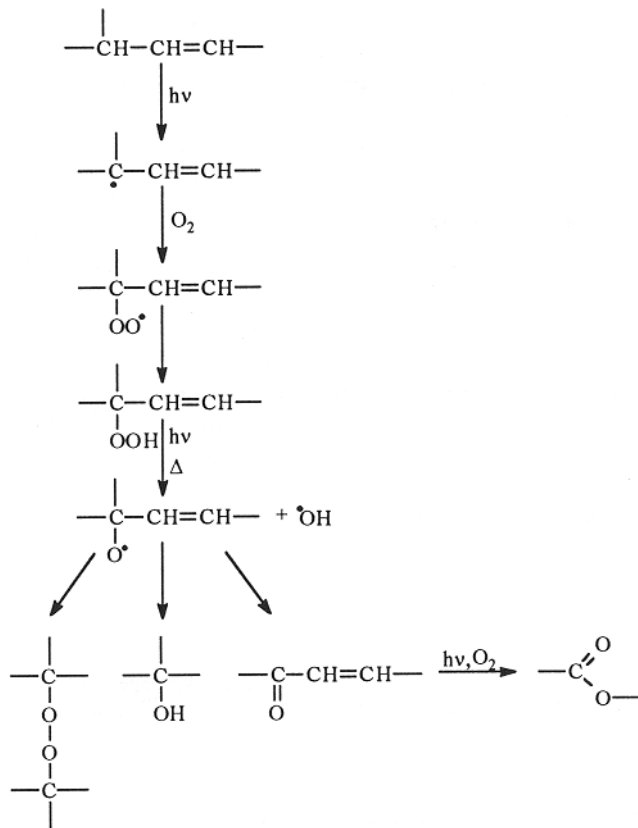
14.20 ACRYLONITRILE COPOLYMERS⁴²⁴⁻⁴²⁸

Acrylonitrile-butadiene-styrene terpolymer (ABS) is known to be unstable when exposed to UV radiation. On the other hand, styrene-acrylonitrile copolymer (SAN) is considered a relatively stable material. These two copolymers are compared below.

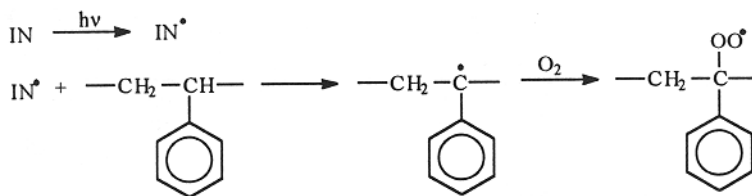
14.20.1 MECHANISM OF DEGRADATION

UV irradiation of ABS at $\lambda > 300$ nm leads to several major changes in its IR spectrum.⁴²⁴ Broad bands appear in the hydroxy (3460 cm^{-1}) and in the carbonyl regions (1718 , 1722 , and 1785 cm^{-1}). An increase of absorbance was observed at C-O stretching vibrations (1450 and 950 cm^{-1}). No change was found in the bands assigned to C=N vibrations (2237 cm^{-1}) and styrene absorption (700 , 765 , 1028 , 1449 , 1456 - 1495 , 1582 - 1601 cm^{-1}). A decrease of absorption was observed in the bands attributed to the C-H deformation vibrations of poly-1,2 butadiene (910 cm^{-1}), poly-*trans*-1,4 butadiene (967 cm^{-1}), and to the band corresponding to C=C stretching vibrations of 1,2 structures (1640 cm^{-1}).⁴²⁴ Although additional effects related to film thickness are covered in the next section, it should be noted here that yellowing decreases gradually towards the sample core. This is attributed to the fact that radiation in the range of 300-400 nm is almost entirely absorbed by the surface layers where the degradation progresses because of the formation of strongly absorbing degradation products.⁴²⁴ It was also discovered that degradation products accumulate when the material is exposed to radiation of wavelength higher than 400 nm (similar to the product accumulated on the back side of sample; detected by measurement of absorption at 1695 cm^{-1}) and disappear when the material is exposed to radiation above 300 nm. Polystyrene, SAN, and polybutadiene do not produce this product when exposed to light above 400 nm. From this, it was concluded that the degradation products of polybutadiene induce oxidation to polystyrene which produce oxidation products which are strong radiation absorbers and are responsible for ABS discoloration.⁴²⁵

The above observations led Jouan and Gardette⁴²⁴ to postulate the following mechanism of ABS degradation:



SAN copolymer in its pure form does not contain any segments which may absorb UV radiation from daylight. Therefore, degradative processes can be initiated only by impurities. The suggested mechanism is as follows:⁴²⁶



Further steps include formation of hydroperoxide then its thermal or UV homolysis, followed by chain scission with formation of carbonyl.

UV degradation studies do not show that acrylonitrile portion of the molecule undergoes any degradative processes. From studies on γ -irradiation,⁴²⁷ it has been suggested that the acrylonitrile segment may stabilize neighboring styrene segments which would explain the relatively high stability of SAN.

14.20.2 CHARACTERISTIC CHANGES AND PROPERTIES

When ABS is exposed to radiation, carbonyl formation increases, double bonds decrease, and the styrene structure remains unaffected (Fig. 14.92). Carbonyl group formation in ABS increases up to sample depth of 71 μm where it reaches plateau (Fig. 14.93). Most carbonyl formation in ABS occurs in the external layers (oxygen diffusion is a contributing factor, but the decrease in radiation also plays a role since absorption is lower on the back side of the sample) (Fig. 14.94). In contrast, double bonds in ABS virtually disappear on the exposed side and are present but in reduced amount on the back side of the sample (Fig. 14.95). The photooxidation of ABS increases drastically its absorption at 410 nm. This change occurs during the first 10 hrs of exposure (Fig. 14.96). PS does not show a similar behavior.

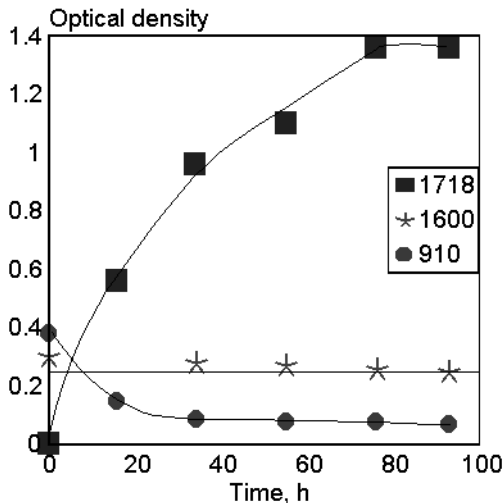


Fig. 14.92. Evolution of absorbance as a function of ABS irradiation time at $\lambda \geq 300$ nm. [Adapted, by permission, from X. Jouan and J.-L. Gardette, *J. Polym. Sci., Polym. Chem.*, 29(1991)685.]

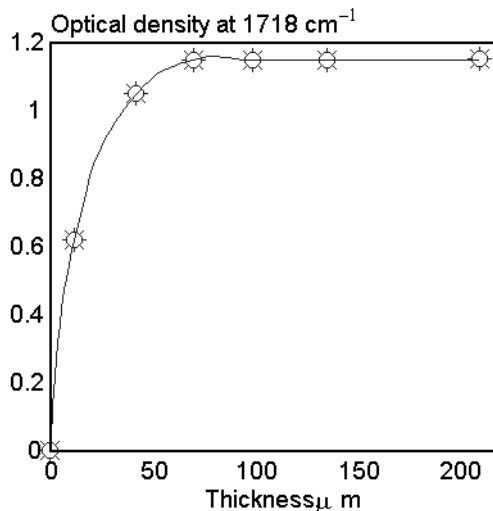


Fig. 14.93. Effect of samples thickness on carbonyl formation in ABS exposed to $\lambda \geq 300$ nm. [Adapted, by permission, from X. Jouan and J.-L. Gardette, *J. Polym. Sci., Polym. Chem.*, 29(1991)685.]

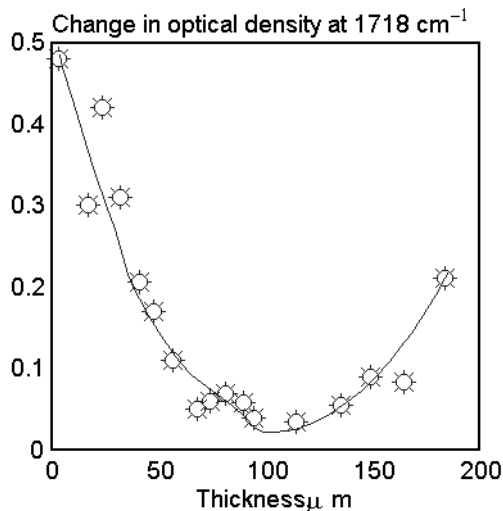


Fig. 14.94. Carbonyl group formation vs. sample thickness in ABS exposed to $\lambda \geq 300$ nm. [Adapted, by permission, from X. Jouan and J. -L. Gardette, *J. Polym. Sci., Polym. Chem.*, 29(1991)685.]

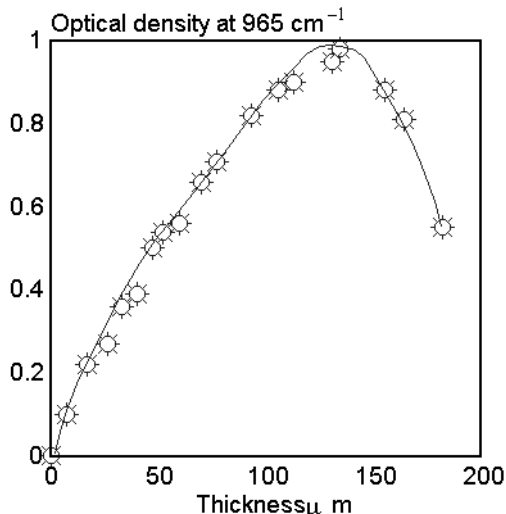


Fig. 14.95. Effect of sample thickness on double bonds in ABS exposed to $\lambda \geq 300$ nm. [Adapted, by permission, from X. Jouan and J. -L. Gardette, *J. Polym. Sci., Polym. Chem.*, 29(1991)685.]

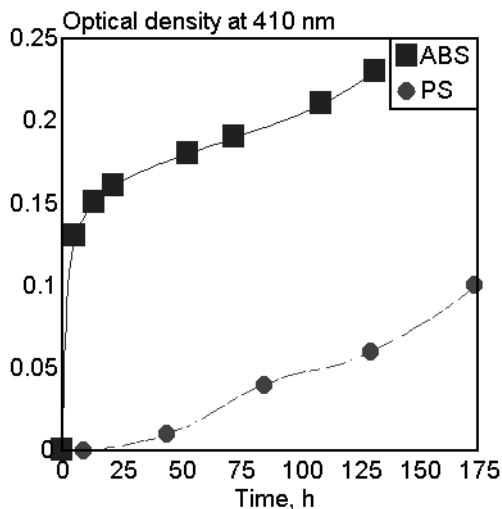


Fig. 14.96. Change of absorbance in ABS and PS exposed to $\lambda \geq 300$ nm versus exposure time. [Adapted, by permission, from X. Jouan and J. -L. Gardette, *Polym. Deg. Stab.*, 36(1992)91.]

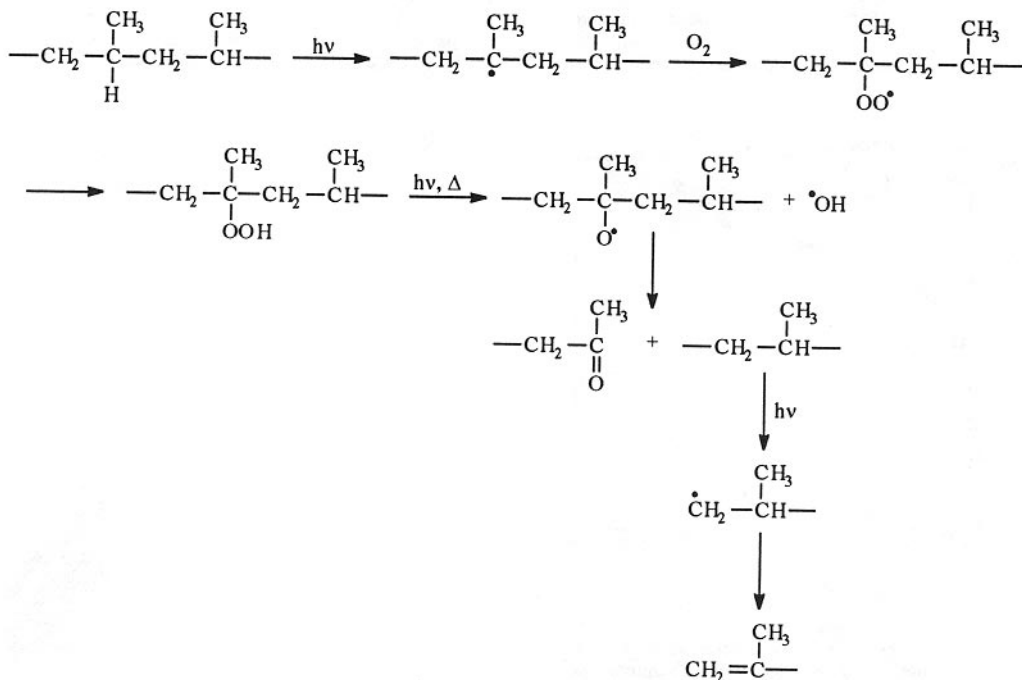
4.21 ETHYLENE-PROPYLENE COPOLYMERS (EPR⁴³⁰⁻⁴³³ & EPDM^{429,434-436})

Ethylene-propylene rubbers, EPR, have been used in many practical applications because their properties range from a thermoplastic to a soft elastomeric.

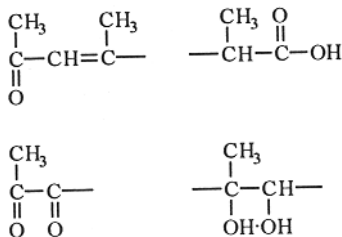
14.21.1 MECHANISM OF DEGRADATION

Numerous studies of homopolymers containing EPR monomers (PE and PP) have been conducted and are discussed above. Several commercial EPR materials have been studied by recording IR spectra directly during UV degradation with radiation above 290 nm.⁴³¹ Major changes are recorded in the carbonyl region (1712, 1738, and 1780 cm⁻¹), vinylidene-type unsaturations (880 and 1640 cm⁻¹), aldehydes (2730 cm⁻¹), and hydroxyls (370-3200 cm⁻¹). The material having the highest melt flow index (lowest molecular weight) had the lowest absorption in the carbonyl region. Throughout degradation process, carbonyl concentration increases rapidly, whereas hydroperoxide concentration remains rather low (in fact, the authors⁴³¹ suggest that only hydrogen bonded hydroperoxides can be detected), suggesting that hydroperoxides decompose. The decomposition of single hydroperoxide group gives the rise to more than one carbonyl.

Based on these results, the following mechanism is proposed:⁴³¹⁻⁴³³



The suggested photooxidation mechanism centers on the propylene segment. Initiation proceeds through hydrogen abstraction at the tertiary carbon atom then hydroperoxides are formed, leading to a variety of degradation products. Other products of photooxidation include:



It should be noted that, if degradation proceeds without the presence of oxygen, peroxy radicals are produced by the photolysis of hydroperoxides which are present in the material.

Studies on EPDM are incomplete. These done suggest that chain scission reactions result from hydrogen abstraction of the tertiary carbon atom whereas crosslinking results from an attack on the secondary carbons.⁴³⁴ Initial absorption of UV radiation is due to aromatic ketone impurities already present in the polymer.

EPDM was found to be very resistant to an accelerated hydrothermal weathering. It was suggested⁴³⁵ that it can be blended into silicone rubber to improve its stability.

14.21.2 CHARACTERISTIC CHANGES AND PROPERTIES

Carbonyl and hydroxyl absorption increase while vinylidyne absorption remains constant during EPR degradation (Fig. 14.97). During γ -irradiation, carbonyl absorption exhibits a linear growth rate (Fig. 14.98). Vulcanized EPDM rubber degrades faster than a non-vulcanized sample. This is explained by the formation of cumoxyl radicals during vulcanization which are able to abstract hydrogen and initiate degradation (Fig. 14.99).

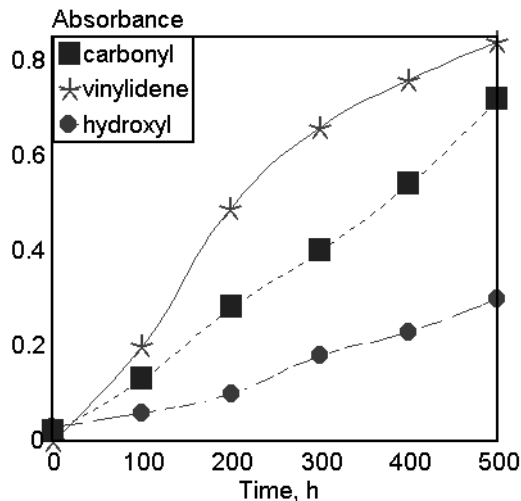


Fig. 14.97. Absorbance at 1722 (carbonyl), 888 (vinylidene), and 3400 cm^{-1} (hydroxyl) by EPR vs. irradiation time by radiation above 290 nm. [Data from R. P. Singh and A. Sing, *J. Makromol. Sci.-Chem.*, A28(1991)487.]

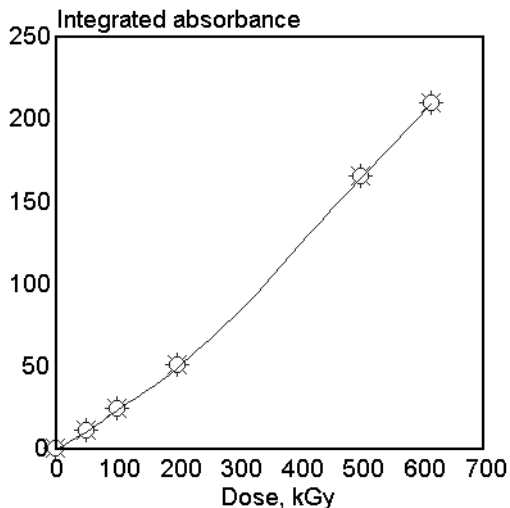


Fig. 14.98. Carbonyl formation in EPR samples exposed to γ -radiation. [Adapted, by permission, from S. Baccaro and U. Buontempo, *Radiat. Phys. Chem.*, 40(1992)175.]

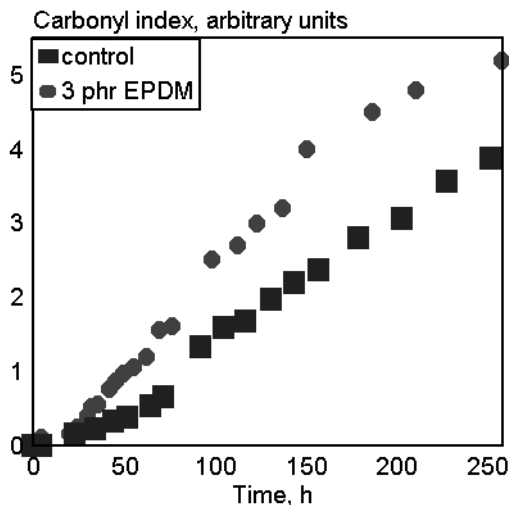


Fig. 14.99. Carbonyl index in EPDM vs. time of exposure to radiation having a maximum at 365 nm. [Data from M. Guzzo and M. -A. De Paoli, *Polym. Deg. Stab.*, 36(1992)169.]

14.22 POLYMER BLENDS⁴³⁷⁻⁴⁷⁸

As polymer blends have developed and their use has become more extensive, a study of their weather stability and the way in which they degrade should include the following:

- An understanding of the dissimilarity between the mechanisms of degradation of component polymers and the blend
- An understanding the fundamentals of the choice of component polymers leading to the blend having enhanced stability (blending should result in amplifying material properties rather than finding the best compromise)
- A knowledge of the interaction between polymers
- The effect of degradative processes on blend morphology
- The evaluation of the stability of important industrial blends and methods of their stabilization
- An analysis of waste polymer utilization by blending.

Literature on the degradation of blends is limited (it consists of about 1-2% of the papers on polymer degradation). No paper is specifically aimed at the mechanism of blend degradation. Rather, blend stability is compared with the stabilities of the original polymers. In some cases, blending of two or more polymers has resulted in a less stable combination.^{447,449,457} Apparently, the more stable polymer was degraded by free radicals which were formed in the less stable polymer. In the majority of blends, the rate of blend degradation was between the degradation rates of each component polymers.^{440,447,448,451,452,454-456,462} Figure 14.100 illustrates such a relationship for a PS/PMMA blend.⁴⁶²

Typically, such relationships are not linear. There are numerous factors involved, not just simple radical transport from one polymer to another. It is likely that more conclusions would have been drawn if more observations on blend morphology were readily available for materials subjected to degradation studies. Most frequently, the observed kinetics of degradation have been explained by the formation of crosslinks between polymers. This suggests that changes in blend morphology occur during degradation. Chemical changes of degraded blends are similar to those which occur in homopolymers. This includes carbonyl index, hydroxyl/hydroperoxide index, optical density of the material in UV, VIS, and IR, gel content, cloud point, and mechanical properties.

Valenza and La Mantia⁴⁵² examined the effect of UV on the stability of photooxidized polypropylene, PP, blended with virgin PP. The results confirm an additive effect of the exposure of homopolymers used for blend preparation and the blend (Figure 14.101). These data validate a method used to determine polymer stability by "radical decay assay" proposed by Gerloch *et al.*⁴⁶⁸ Figure 14.101 shows that degradation kinetics depends on the accumulation of degradation products regardless the stage of polymer processing or exposure.

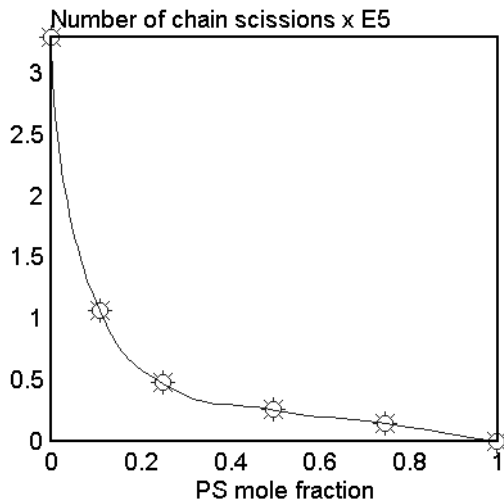


Figure 14.100. Number of chain scissions in photodegraded PS/PMMA blend as function of blend composition. Irradiation for 3 h in vacuum under mercury lamp at 30°C. [Adapted, by permission, from A. Torikai, Y. Sekigawa, and K. Fueki, *Polym. Deg. Stab.*, 21(1988)43.]

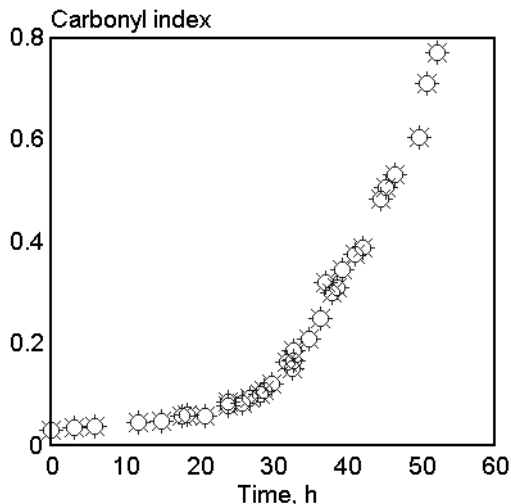


Figure 14.101. Carbonyl index of a blend containing photodegraded and virgin PP vs. cumulative time of exposure to Xenon lamp radiation at 60°C. [Adapted, by permission, from A. Valenza and F. P. La Mantia, *Arabian J. Sci. Eng.*, 13(1988)497.]

It would be useful to establish criteria that would enable chemists to select blend components to obtain a required weather stability of the resultant blend. The paper by Komarov *et al.*⁴⁴⁵ helps to do this. In an EPR/HDPE blend, when EPR is increased above a 30% level, there is a rapid increase in UV stability. A detailed investigation of the reasons for this sudden change shows that, around this concentration (30-40% EPR), the surface lacks HDPE and is entirely EPR. Further increase in EPR above 40% increases the thickness of this EPR skin but the blend stability does not change because it is controlled by EPR chemistry. This use of incompatibility suggests that there is a fundamental alternative to chemical durability. One blend component, present at high concentration or exclusively present on the surface, can protect the less durable component of the blend. This works, because UV light can only penetrate to a limited depth, less than the thickness of the single component, UV resistant, layer (up to 0.15 mm depending on composition, most frequently less than 0.01 mm). Komarov *et al.*⁴⁴⁵ found that, in an automotive application, a rubber modified, high impact polypropylene blend had good UV durability which was attributed to the morphology of the skin.⁴⁴⁸

Papers by Osawa *et al.*^{464,465} include general suggestions for choosing the polymer pair. A PC/PMMA blend was studied under varying radiation wavelength. In the region where both polymers can absorb, PC absorbed more strongly and shielded PMMA from radiation. Even small additions of PC show a stabilizing effect on PMMA. The presence

of PMMA does not have any effect on PC. When the blend is exposed to radiation above 290 nm (PMMA does not absorb this radiation) only PC degrades with a relatively low rate. The inclusion of PMMA in the blend has no bearing on the degradation rate of PC. Two principles are involved in this experiment: one, that, if the polymer does not absorb radiation it cannot decrease the stability of the other polymer (it may only participate in quenching radicals formed by the second polymer in the blend - stabilization); second, if polymers are immiscible and reside in separate phases the only chance for interaction is at their interface. This is substantiated by the results of Hill *et al.*⁴⁵⁸ who studied photodegradation of PVC/SAN and AMS:AN (α -methylstyrene-acrylonitrile-copolymer). The degradation rate of these blends was approximately additive as would be expected in two-phase systems.

Several papers suggest that the interaction between polymers which form blend^{444,447,454,455,459,460,461} leads to the formation of block copolymers. This is caused by radicals which are formed during the photodegradation.⁴⁶⁰ The formation of block copolymers in the blend also affects blend's morphology. The annealing of PPE decreases its fluorescence whereas, when PS is annealed, its fluorescent emission increases. Blend

containing only 8% PPE has a fluorescence emission typical of PPE which indicates that non-radiative energy conversion is favored.

The last study bridges the interaction between polymers and the effect of blend morphology on degradative processes. The process discussed above might be attributed to energy transfer from PS to PPE which quenches PS photodegradation. In fact, Jensen and Kops⁴⁶¹ presented data leading to this conclusion. Nicu *et al.*⁴⁴⁶ explain a sudden change in UV stability of LDPE/ABS blend by a modification of the blend morphology. The broadest evaluation of the effect of degradation on morphological changes in blends can be found in the paper by Chien *et al.*⁴⁵⁹ Figure 14.102 contains data on oxygen absorption during the photodegradation of PS/PVME (polyvinyl methyl ether) blends.

Above a concentration of 30% PVME, there is a sudden increase in oxygen absorption. Also, blends become cloudy (having

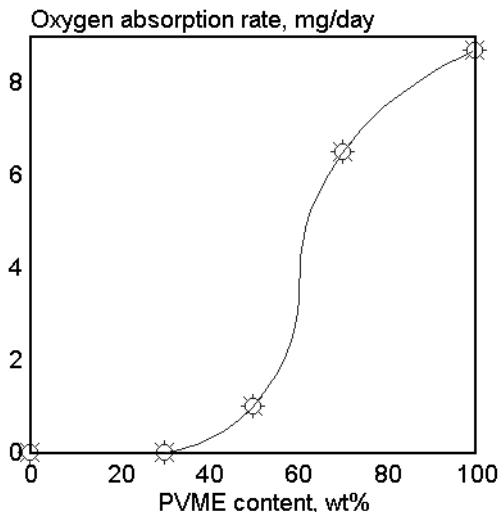


Figure 14.102. Steady-state oxygen absorption during photodegradation of PVME/PS blend depending on the content of PVME in the blend. Source: mercury lamp with pyrex and water filters, temperature 32°C. [Adapted, by permission, from Y. Y. Chien, E. M. Pearce, and T. K. Kwei, *J. Polym. Sci., Polym. Chem.*, 29(1991)849.]

been transparent) just before the end of an induction period. This suggests phase separation. It can be confirmed by DSC that, after an adequate period of degradation (depending on the relative concentrations of both polymers), a blend, which initially had only one T_g , begins to display two T_g s. This implies that phase separation is occurring. Once phase separation does occur, the degradation rate is governed by the PVME content. These observations were confirmed by molecular weight studies of both polymers in blends of varying composition. Li and Kopelman⁴⁶⁶ show that morphological changes might be reversed by annealing so that polymer can assume its former conformation which permits radiative energy conversion as opposed to a degradative processes.

It seems reasonable to expect that the stability of blends can be modified by morphology. Since morphology is one of the areas where studies on blends are focused, these studies might contribute to a better understanding of polymer degradation. Studies³⁴ of polymer degradation have focused primarily on chemical mechanisms, whereas the structure of the polymer plays an important role in the overall stability of the material.

Evaluation of the most important industrial blends shows that no impressive improvements were achieved. High impact PVC is a perfect example. In spite of the substantial progress made in controlling mechanical properties, its UV stability remains a key weakness.⁴⁵⁴⁻⁴⁵⁶ Even small additions of modifiers further decreased generally inadequate UV stability of PVC. Stabilization efforts^{454,455} did not provide viable alternatives.

There is some controversy over the effect of LLDPE on the stability of LDPE in a blend. Some studies^{439,440} show that LLDPE decreases the stability of LDPE in the blends whereas other studies^{441,442} do not confirm this. Daro *et al.*⁴⁴² show good agreement between exposure time (or irradiance) and molecular weight change. Samples of a LLDPE/LDPE blend exposed in various seasons had a rate of chain scission which correlated with the global incident energy of daylight. Natural weathering of blends results mainly in chain scission accompanied by crosslinking.

One may suggest that, due to their commercial application, these materials are studied more extensively that a review of the literature might suggest but it is still an area which requires considerably more emphasis. Some conclusions can be reached from an evaluation of existing commercial blends (Table 14.23.1). Blends listed in this table were rated by their producers as weather resistant materials, and the rationale for the quoted resistance is included in the last column.⁴⁷⁸ It is apparent that most polymers in weather resistant group are A polymers⁴⁷⁷ (polymer non-absorbing; photooxidation depends on normal structure alone). Stable blends are obtained from stable polymers. There are only a few cases where blends are more stable than the component polymers.

Table 14.23.1: Weatherstable commercial blends

Trade name	Producer	Matrix	Minor phase	Producer's comments and observations
Centrex	Monsanto	ASA	AES	excellent weather stability
Chemigum TPE	Goodyear	NBR	CPE	black colored 18 months in Florida with no change
Deflex	D&S	PP	elastomer	withstands 3 years in Florida or 2500 kJ/m ² in xenon arc
Enplex	Kaneka	ABS	PVC, MMA cop.	improved weather stability over flame retarded resins
Formion	Schulman	EAA	PE	most grades are UV stable and suitable for exterior applications
Geloy	GE	ASA	PVC, PC, or PMMA	color and property retention of both light and dark colors after prolonged outdoor exposure
HiFax	Himont	PP	EPDM	4000 h exposure in QUV results in retention of 90% initial properties
Jet-Flex	Multibase	AES	vinyl copolymer	material applicable for outdoor use
Kydex 100	Kleerdex	PVC	acrylics	good weathering properties but material suggested for indoor use
Lupoy	Lucky	PC	ABS	better than ABS worse than PC
Luran S	BASF	SAN	acrylics	one of the most stable impact modified resins mostly due to the type of impact modifier
Mople SP	Himont	PP	TPO	proven good outdoor performance, especially carbon black and UV stabilizer containing
Novalloy-A	Daicel	PA	ABS	better UV stability than component polymers
Novalloy-B	Daicel	PBT	ABS	better UV stability than ABS
Oleflex	Showa Denko	PP	EPR	contrary to the conventional rubber do not have double bonds which makes it more weather stable
Pax-Plus	Paxon	PE	PIB	outstanding weather stability
Polyman	Schulman	SAN	PP	UV stable and suitable for exterior applications
Polystyrol	BASF	PS	PIB	addition of PIB improves weather stability of PS
Rovel	Uniroyal	SAN	EPR	elimination of unsaturated monomer (IB) drastically improves weather stability over ABS
Royaltherm	Uniroyal	EPDM	SI	large improvement over EPDM and almost as weather stable as silicone
Rynite	DuPont	PET	elastomer	addition of elastomer does not lower weather stability of PET
Santoprene	AES	PP	EPDM	very good weather stability
Stapron E	DSM	PBT	PIB	addition of PIB lowers UV stability because of presence of double bonds
Techniace TC	Sumitomo Dow	PC	AES	UV stable composition

Trade name	Producer	Matrix	Minor phase	Producer's comments and observations
Terblend S	BASF	ASA	PC	good color and property retention
Terluran	BASF	ABS	elastomer	substantial improvement over ABS. If PIB used as elastomer, the properties are still improved but loss of mechanical properties is due to the degradation of double bonds
Triax CBE	Monsanto	ABS	PVC	better stability than stabilized ABS or PC
Ultrablend S	BASF	PBT	ASA	full retention of properties on exposure for 2000 h in xenon arc
Ultradur	BASF	PBT	EPDM	3 years exposure with no change of color and mechanical properties
Vinidur	BASF	PVC	acrylics	25 years of performance in window application

Only a few papers are available on the potential of recycling of waste plastics by blending and on the implication of such method on product weathering characteristics.^{450,452} Although, the addition of a polyolefin (functionalized by photodegradation) to a blend may improve the mechanical properties of the blend, the cumulative effect of photodegradation ultimately causes severe deterioration of these mechanical properties. Consequently, such blends, containing recycled materials, are unsuitable for outdoor use. Since photodecomposition of wastes is increasingly criticized, there is a clear need for further studies in this direction. The weight of these studies should be shifted to methods of converting waste plastics to products which do not contain chain reaction initiators prior to their blending with virgin material.

Several papers offer information on blend response to γ -irradiation or other highly degrading environments.⁴⁶⁹⁻⁴⁷⁴ Gorelik *et al.*^{469,470} studied PP/PE blends which for medical applications require radiation sterilization. Contrary to the results reported for UV degradation, these blends were more stable than their component polymers, especially those blends which contained small spherulites of PP.⁴⁷⁰

Punkka *et al.*⁴⁷¹ studied the effect of electron irradiation on the stability of electrically conductive, FeCl₃-doped, blends of poly(3-octylthiophene) and ethylvinylacetate. Crosslinking of the polymer matrix by electron irradiation was monitored but it did not stabilize the conductivity of the blend, because crosslinking causes an increase in size of the conducting islands.

Minkova and Nikolova^{472,473} noted intensive crosslinking in films of LDPE blends with iPP or EVA when these films were irradiated by fast electrons. Crosslinking processes dominated the LDPE and EVA phases whereas chain scission was predominant in iPP. Blends containing EVA exhibited higher crosslinking than those containing LDPE.

Arnold *et al.*⁴⁷⁴ reported on a blend of poly(siloxane imide) segmented copolymers with polybenzimidazole intended for spacecraft application as a coating or as an adhe-

sive. Poly(siloxane imide), due to its low surface energy, was expected to dominate the surface. But polybenzimidazole is not resistant to atomic oxygen which is a requirement in this application. It was intended that the copolymer found on the surface would decompose to silicate to form a protective layer. An XPS study and an atomic oxygen stability test confirmed that this, indeed, was the mechanism of action in this blend.

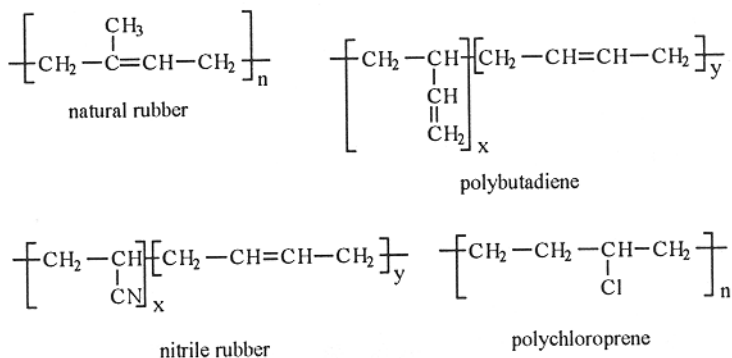
14.23 RUBBERS⁴⁷⁹⁻⁴⁸⁸

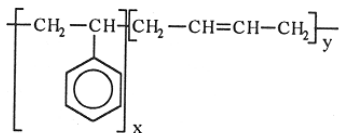
This group includes materials which possess elastomeric properties, regardless of their chemical structure and the historical meaning of the word "rubber". Many materials included in this group have mechanisms of degradation similar to some of the polymers previously discussed. The unique structural feature is in the number of unsaturated segments in rubber molecules.

14.23.1 MECHANISM OF DEGRADATION

Several polymers, such as butyl rubbers, olefinic termoelastomers, ethylene-propylene copolymers, and terpolymers are classified as saturated rubbers. Their chemical structure and properties are similar to other saturated polymers, such as polyethylene and polypropylene. The exact mechanism of degradation has not been well defined in the literature. The discussion which follows is based more on an adaptation of the data from studies on polyethylene and polypropylene than on a fragmentary data from studies on products which may not typify rubbers. From more recent data,⁴⁸⁸ one may conclude that butyl rubber retains its initial electrical properties (permittivity and dielectric loss) when stored at room conditions for 17 years. The addition of fillers such talc kaolin, barytes, calcium carbonate, and silica contribute to changes in electric properties during use.

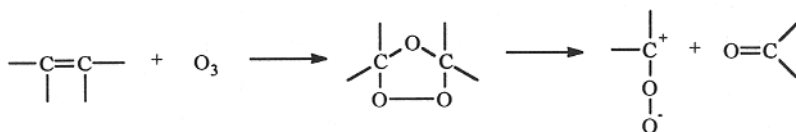
Unsaturated rubbers include:





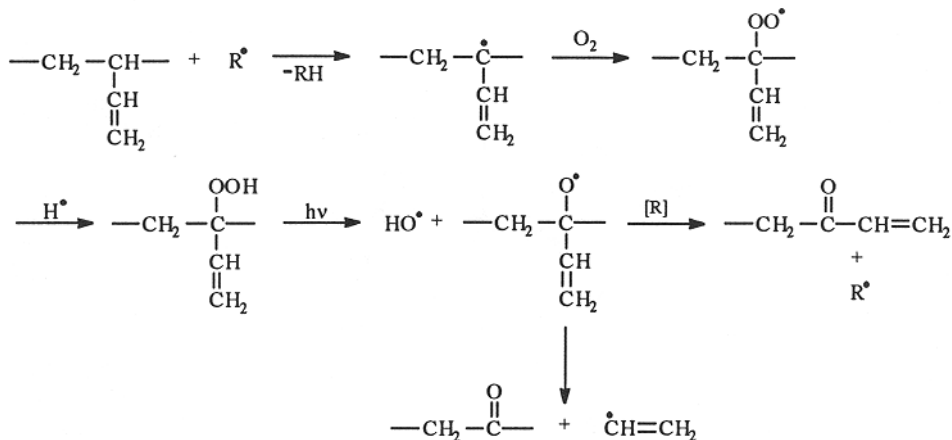
styrene-butadiene rubber

All have double bonds in the polymer backbone. Their properties vary due to the presence of various side groups. Ozonolysis is the single most important reaction which determines degradation rate. A double-bond containing polymer exposed to ozone forms ozonides which can undergo further changes:



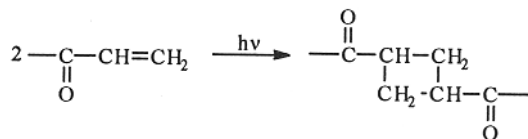
One product, may be a ketone or an aldehyde, the other, called zwitterion, may finally form a hydroperoxide, which follows the normal photolytic route. The next step is chain-scission, then radical formation, followed by an increased absorption of radiation.

The presence of radicals triggers photooxidative processes around the double bond. By themselves, pure unsaturated rubbers, such as polyisoprene and polybutadiene, cannot absorb light:



formed along the backbone but changes do occur in pendant groups.⁴⁸⁵ A typical hydroperoxide route is postulated with hydroperoxide homolysis and formation of hydroxyl and ketone groups in the side groups. Similar changes were observed in the photooxidation of polybutadiene. Polyisoprene behaves differently from polybutadiene and other similar polymers. The methylene group in polyisoprene causes it to degrade through the formation of tertiary hydroperoxides and subsequent chain scission. In polybutadiene, hydroperoxides have a lower concentration due to their lower stability, and they are rapidly decomposed to hydroxyl and carbonyl groups attached to the chain. These changes do not lead to a marked decrease in molecular weight.⁴⁸⁵

Crosslinking reactions are explained by photolytic process involving allylic structures:



It is apparent that crosslinking occurs more in polybutadiene than in polyisoprene, although, it should be stressed that the crosslinking reaction in polyisoprene competes with the chain scission reaction. As degradation starts (when double bond concentration rapidly decreases - see Figure 14.106 below), chain scission reactions prevail. Later on, in the more advanced stages of the reaction, the crosslinking rate is substantially increased.⁴⁸⁵

The different type of degradation may occur due to sensitized photooxidation. It was demonstrated⁴⁸⁶ that methylene blue promotes chain scission in polybutadiene which rapidly decreases its molecular weight.

Yellowing occurs, due to the formation of polyene structures, as shown by the fact that polyenyl radicals were detected by ESR.

14.23.2 EFFECT OF THERMAL HISTORY

The double bonds in most rubbers are especially vulnerable to thermooxidative degradation, which involves chain scission and the formation of hydroperoxides and related products.

14.23.3 CHARACTERISTIC CHANGES AND PROPERTIES

Double bonds lead to degradation by ozone. Substitution of chlorine, as in polychloroprene, increases the resistance of the rubber (Fig. 14.103). Elongation change is again the most sensitive means of monitoring degradative changes. Introduction of

styrene helps to retain tensile strength but has a negligible effect on elongation (Fig. 14.104). Double bonds in rubber are vulnerable to oxygen attack. This causes the rubber to change properties on storage (Fig. 14.105). A typical course of degradation (based here on polyisoprene) includes the formation of carbonyl groups followed by hydroxyl groups at the expense of double bonds (Fig. 14.106).

14.23.4 DATA

Luminescence data:		
Sample form	Excitation wavelength, nm	Emission wavelength, nm
photooxidized polybutadiene	310	475
thermally oxidized polybutadiene	340	520

Spectral sensitivity: <380 nm (polybutadiene, ABS)

Important initiators and accelerators: allylic structures, hydroperoxides, cymene, metal acetyloacetones, anthraquinone, ferrocene, aluminum chloride, hydroxyrene, methylene blue

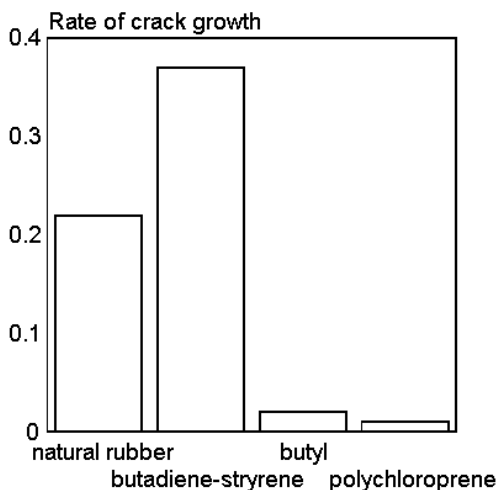


Fig. 14.103. Rate of crack growth in ozone cabinet. [Data from E. H. Andrews, D. Barnard, M. Braden, and A. N. Gent, *Chemistry and physics of rubber-like substances*, McLaren, London, 1963.]

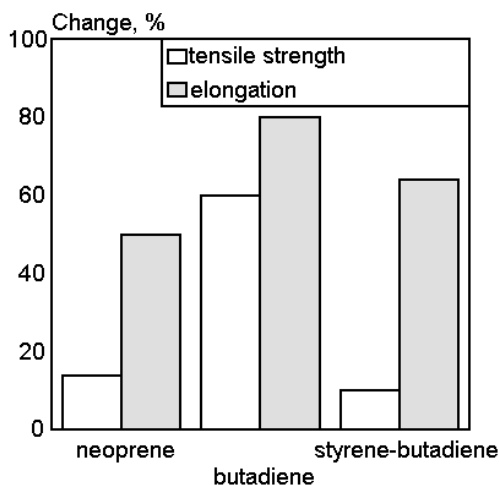


Fig. 14.104. Decrease in rubber properties during natural weathering for 5 years in Panama. [Data from E. W. Bergstrom, *Technical Report 74-038* and D. W. Cumberland, *DuPont Report SD226*.]

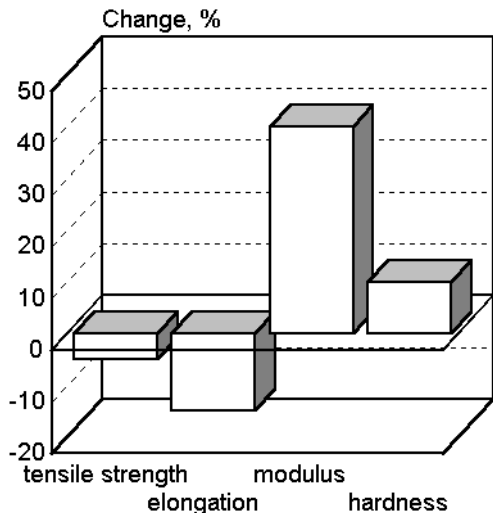


Fig. 14.105. Natural rubber properties change during storage for 15 years in tropics. [Data from R. C. Moakes, *Rapra J.*, 1975(6)57.]

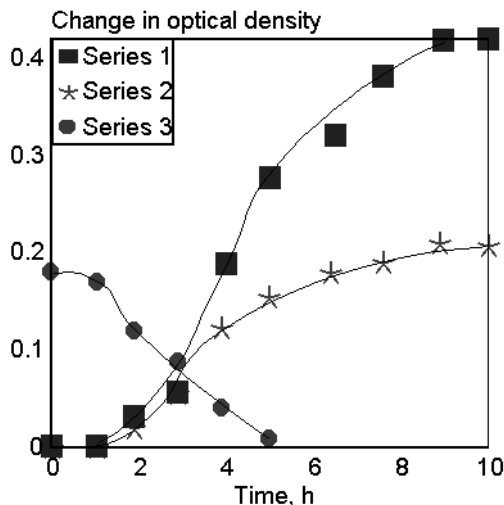


Fig. 14.106. Photodegradation products of 1-4-cis polyisoprene degradation at $\lambda \geq 300$ nm. [Adapted, by permission, from C. Adam, J. Lacoste, and J. Lemaire, *Polym. Deg. Stab.*, 32(1991)51.]

REFERENCES

1. A. A. Chadina, A. S. Chantseva, E. N. Cherkashin, and Y. V. Ovchinnikov, *Plast. Massy*, 1982,1,52.
2. H. Kubota, S. Suzuki, O. Nishimura, S. Hattori, K. Yoshikawa, and T. Shiota, *Kenkyu Hokoku-Kogyo Gijutsuin*, 1981,2,23.
3. Y. Nagatsuka, T. Shiota, K. Yoshikawa, S. Suzuki, H. Kubota, and O. Nishimura, *Kenkyu Hokoku-Kogyo Gijutsuin*, 1981,2,87.
4. T. Ito, H. Imai, S. Nagai, and K. Iizuka, *Kenkyu Hokoku-Kogyo Gijutsuin*, 1981,2,159.
5. H. Kubota, O. Nishimura, S. Suzuki, K. Yoshikawa, and T. Shiota, *Kenkyu Hokoku-Kogyo Gijutsuin*, 1981,2,225.
6. H. Kubota, S. Suzuki, O. Nishimura, I. Tamura, K. Yoshikawa, and T. Shiota, *Hokkaido Kogyo Kaihatsu Shikensho Hokoku*, 1981,24,96.
7. O. Nishimura, H. Kubota, and S. Suzuki, *Hokkaido Kogyo Kaihatsu Shikensho Hokoku*, 1981,24,115.
8. S. Suzuki, H. Kubota, T. Tsurue, and O. Nishimura, *Hokkaido Kogyo Kaihatsu Shikensho Hokoku*, 1981,24,129.
9. T. Tsurue and S. Suzuki, *Hokkaido Kogyo Kaihatsu Shikensho Hokoku*, 1981,24,136.
10. O. Nishimura, H. Kubota, and S. Suzuki, *Hokkaido Kogyo Kaihatsu Shikensho Hokoku*, 1981,24,145.

11. S. Suzuki, H. Kubota, O. Nishimura, and T. Tsurue, *Hokkaido Kogyo Kaihatsu Shikensho Hokoku*, 1981,24,153.
12. S. Suzuki, H. Kubota, T. Tsurue, and O. Nishimura, *Hokkaido Kogyo Kaihatsu Shikensho Hokoku*, 1981,24,167.
13. O. Nishimura, S. Suzuki, H. Kubota, K. Yoshikawa, and T. Shiota, *Hokkaido Kogyo Kaihatsu Shikensho Hokoku*, 1981,24,193.
14. H. Kubota, S. Suzuki, O. Nishimura, I. Tamura, K. Yoshikawa, and T. Shiota, *Kenkyu Hokoku-Kogyo Gijutsuin*, 1981,2,107.
15. Z. Osawa and M. Aiba, *Polym. Photochem.*, 2(1982)339.
16. T. A. Skowronski, J. F. Rabek, and B. Ranby, *Polymer*, 24(1983)1189.
17. S. Matsumoto, H. Ohshima, and Y. Hasuda, *J. Polym. Sci., Polym. Chem. Ed.*, 22(1984)869.
18. R. P. Braginskii, *Dokl. Akad. Nauk CCCR*, 272(1983)889.
19. C. Decker and M. Balandier, *Polym. Photochem.*, 5(1984)267.
20. L. Jirackova-Audouin, V. Bellenger, and J. Verdu, *Polym. Photochem.*, 5(1984)283.
21. E. D. Owen and S. R. Brooks, *Polym. Photochem.*, 6(1985)21.
22. T. A. Skowronski, J. F. Rabek, and B. Ranby, *Polym. Degrad. Stab.*, 12(1985)229.
23. F. Castillo, G. Martinez, R. Sastre, and J. L. Millan, *Makromol. Chem., Rapid Commun.*, 7(1986)319.
24. M. A. Zhuravlev, A. A. Molchanov, and V. B. Ivanov, *Plast. Massy*, 1986,10,12.
25. J. B. Adeniyi, S. Al-Malaika, and G. Scott, *J. Appl. Polym. Sci.*, 32(1986)6063.
26. J.-L. Gardette and J. Lemaire, *Polym. Degrad. Stab.*, 16(1986)147.
27. F. Mori, M. Koyama, and Y. Oki, *Angew. Makromol.Chem.*, 68(1978)137.
28. E. J. Lawton and J. S. Balwit, *J. Phys. Chem.*, 65(1961)815.
29. N.-L. Yang, J. Liutkus, and H. Haubenstein, *ACS Symp. Ser.*, 142(1980)35.
30. J. F. Rabek, B. Ranby, B. Oestensson, and P. Flodin, *J. Appl. Polym. Sci.*, 24(1979)2407.
31. J. Verdu, *J. Macromol. Sci.-Chem.*, A12(1978)551.
32. E. D. Owen, I. Pasha, and F. Moayyedi, *J. Appl. Polym. Sci.*, 25(1980)2331.
33. E. D. Owen and R. L. Read, *J. Polym. Sci., Polym. Chem. Ed.*, 17(1979)2719.
34. J. Wypych, *Poly(vinyl chloride) Stabilization*, Elsevier, 1986.
35. J. Wypych, *Poly(vinyl chloride) Degradation*, Elsevier, 1985.
36. F. Castillo, G. Martinez, R. Sastre, and J. Millan, *Rev. Plast. Mod.*, 53(1987)86.
37. A. Kaminska and H. Kaczmarek, *Angew. Makromol. Chem.*, 148(1987)93.
38. S. Gaumet, J.-L. Gardette, and J. Lemaire, *Polym. Degrad. Stab.*, 18(1987)135.
39. A. Saxena, V. Kalliyana-Krishnan, and S. N. Pal., *J. Appl. Polym. Sci.*, 34(1987)1727.
40. J. Boenisch, M. A. Zhuravlev, and V. B. Ivanov, *Vysokomol. Soed.*, 29B(1987)787.
41. J.-L. Gardette and J. Lemaire, *Rev. Gen. Caoutch. Plast.*, 672(1987)133.
42. D. W. Allen, J. S. Brooks, J. Unwin, and J. D. McGuinness, *Appl. Organomet. Chem.*, 1(1987)311.
43. J. B. Adeniyi and G. Scott, *J. Polym. Mater.*, 4(1987)207.
44. M. G. Otey, *Polym. Degrad. Stab.*, 14(1986)285.
45. A. Torikai, H. Tsuruta, and K. Fueki, *Polym. Photochem.*, 2(1982)227.
46. B. B. Cooray and G. Scott, *Polym. Degrad. Stab.*, 3(1980-81)127.

47. F. Tudos, T. Kelen, and T.T. Nagy, *Dev. Polym. Degrad.*, 2(1979).
48. K. B. Abbas, *J. Macromol. Sci.-Chem.*, 12A(1978)479.
49. P. Genova-Dimitrova, *Polym. Degrad. Stab.*, 33(1991)355.
50. P. Genova-Dimitrova and I. Petkov, *Polym. Degrad. Stab.*, 33(1991)105.
51. P. Simon, *Polym. Degrad. Stab.*, 35(1992)45.
52. P. Simon, *Polym. Degrad. Stab.*, 36(1992)85.
53. J. -L. Gardette and J. Lemaire, *Polym. Degrad. Stab.*, 34(1991)135.
54. J. -L. Gardette and J. Lemaire, *Polym. Degrad. Stab.*, 33(1991)77.
55. H. V. Hoppler, *Kunststoffe*, 83(1993)389.
56. S. H. Hamid, M. B. Amin, A. G. Maadhah, and A. M. Al-Jarallah, *J. Vinyl Technol.*, 14(1992)182.
57. D. J. T. Hill, F. A. Kroesen, J. H. O'Donnell, and P. J. Pomery, *Mater. For.*, 14(1990)210.
58. M. P. Ebdon, *Corrosion Austral.*, 17,10(1992)10.
59. J. Behnisch and H. Zimmermann, *Int. J. Polym. Mater.*, 16(1992)143.
60. F. Thominet, G. Metzger, B. Dalle, and J. Versu, *Eur. Polym. J.*, 27(1991)55.
61. J. -L. Gardette, *Analisis*, 21,5(1993)M17.
62. J. Imhof, P. Stern, and A. Egger, *Angew. Makromol. Chem.*, 176/177(1990)185.
63. N. Pourahmady and P. I. Bak, *J. Macromol. Sci.*, A31(1994)185.
64. *US Patent* 5,292,823.
65. H. Kashiwabara and T. Seguchi, *Radiation Processing in Progress of Polymer Processing*, Ed. L. A. Utracki, *Karl Hanser Verlag*, Munich, 1992.
66. A. G. Andreopoulos, A. Pappa and N. Tzamtzis, *Polym. Testing*, 13(1994)3.
67. R. Flores, J. Perez, P. Cassagnau, A. Michel, and J. Y. Cavaille, *Polymer*, 35(1994)2800.
68. V. Rek and M. Bravar, *Glas. Hem. Drus. Beograd*, 47(1982)331.
69. N. Ya. Andryanova, S. S. Muatsakanov, and L. F. Korsunskii, *Lakokras. Mater. Ikh Primen.*, 1985,2,35.
70. K. Cheng, C. Yang, and M. Wang, *Fushe Yanjiu Yu Fushe Gongyi Xuebao*, 4(1986)34.
71. Y. Feng, S. Li, L. Zhang Y. Zhang, Z. Zheng, X. Cheng, and J. Yen, *Fushe Yanjiu Yu Fushe Gongyi Xuebao*, 4(1986)26.
72. B. S. Rao and M. R. Murthy, *J. Polym. Sci., Polym. Phys.*, 25(1987)1897.
73. K. Moruyama, Y. Kuramoto, M. Yagi, and Y. Tanizaki, *Polymer*, 29(1988)24.
74. E. Baimuratov B. N. Narzullayev, I. R. Kalontapov, and A. W. Zakharchuk, *Dokl. Akad. Nauk. Tadzh. CCR*, 27(1984)204.
75. E. Baimuratov, I. Y. Kalontarov, and D. S. Saidov, *Int. J. Polym. Mater.*, 19(1993)193.
76. R. W. Lenz, *Adv. Polym. Sci.*, Vol. 107, *Springer Verlag*, Berlin 1993.
77. R. Sastre and F. Gonzales, *Polym. Photochem.*, 1(1981)153.
78. J. P. T. Jensen and J. Kops, *J. Polym. Sci., Polym. Chem.*, 19(1981)2765.
79. Y. Watanabe and T. Shirota, *Kenkyu Hokoku-Kogyo Gijutsuin*, 1981,2,87.
80. T. Ho, H. Imai, S. Nagai, and K. Iizuka, *Kenkyu Hokoku-Kogyo Gijutsuin*, 1981,2,159.
81. Y. Watanabe, F. Kitajima, and T. Shirota, *Kenkyu Hokoku-Kogyo Gijutsuin*, 1981,2,155.

82. S. Suzuki, H. Kubota, O. Nishimura, S. Hattori, K. Yoshikawa, and T. Shirota, *Hokkaido Kogyo Kaihatsu Shikensho Hokoku*, 24(1981)17.
83. K. Esumi, K. Meguro, A. M. Schwartz, and A. C. Zettlemoyer, *Bull. Chem. Soc. Jpn.*, 55(1982)1649.
84. G. Geuskens, G. Delaunois, Q. Lu-Vinh, W. Piret, and C. David, *Eur. Polym. J.*, 18(1982)387.
85. S. I. Kuzina and A. I. Mikhailov, *Teor. Eksp. Khim.*, 20(1984)372.
86. I. Mita, T. Tagaki, K. Horie, and Y. Shindo, *Macromolecules*, 17(1984)2256.
87. H. S. Munro, D. T. Clark, and J. Peeling, *Polym. Degrad. Stab.*, 9(1984)185.
88. S. I. Kuzina and A. I. Mikhailov, *Vysokomol. Soed.*, 26B(1984)788.
89. V. Kovacevic, M. Bravar, L. Lorvic, N. Segudovic, and D. Hace, *Polym. Photochem.*, 4(1984)459.
90. N. A. Weir, *New Trends Photochem. Polym.*, 1985,169.
91. A. Torikai, A. Takeuchi, and K. Fueki, *Polym. Degrad. Stab.*, 14(1986)367.
92. O. Puglisi, A. Licciardello, L. Calcagno, and G. Foti, *Nucl. Instrum. Methods Phys. Res.*, B19-20(1987)865.
93. A. Stoyanov and G. Nenkov, *Plaste Kautsch.*, 34(1987)7.
94. H. Nanbu, Y. Sakuma, Y. Ishihara, T. Takesue, and T. Ikemura, *Polym. Degrad. Stab.*, 19(1987)61.
95. Z. Osawa, F. Konoma, S. Wu, and J. Cen, *Polym. Photochem.*, 7(1986)337.
96. P. E. Cassidy and T. M. Aminabhavi, *J. Macromol. Sci.-Rev. Macromol. Chem.*, C21(1981)89.
97. F. Gugumus, *Dev. Polym. Stab.*, 1(1979)8.
98. R. K. Wells and J. P. S. Badyal, *J. Polym. Sci.*, *Polym. Chem.*, 30(1992)2677
99. S. I. Kuzina and A. I. Mikhailov, *Eur. Polym. J.*, 29(1993)1589.
100. N. A. Weir, J. Arct, and J. K. Lee, *Eur. Polym. J.*, 29(1993)731.
101. G. J. Price and P. F. Smith, *Eur. Polym. J.*, 29(1993)419.
102. Y. Israeli, J. Lacoste, J. Lemaire, R. P. Singh, and S. Sivaram, *J. Polym. Sci., Polym. Chem.*, 32(1994)485.
103. L. O'Toole, R. D. Short, F. A. Bottino, A. Pollicino, and A. Recca, *Polym. Deg. Stab.*, 38(1992)147.
104. C. S. Lin, W. L. Liu, Y. S. Chiu, and S.-Y. Ho, *Polym. Deg. Stab.*, 38(1992)125.
105. R. K. Wells, J. P. S. Badyal, I. W. Drummond, K. S. Robinson, and F. J. Street, *Polymer*, 34(1993)3611.
106. M. Henczkowski, *Kunststoffe*, 83(1993)473.
107. C. Wilhelm and J.-L. Gardette, *J. Appl. Polym. Sci.*, 51(1994)1411.
108. B. O'Donnell, J. R. White, and S. R. Holding, *J. Appl. Polym. Sci.*, 52(1994)1607.
109. H. Fukumura, N. Mibuka, S. Eura, H. Masuhara, and N. Nishi, *J. Phys. Chem.*, 97(1993)13761.
110. N. A. Weir and A. Ceccarelli, *Polym. Deg. Stab.*, 41(1993)37.
111. K. M. Dyumayev, N. P. Kuzmina, V. V. Lobko, G. A. Matyushin, V. S. Nechitailo, and A. V. Chadov, *Int. J. Polym. Mater.*, 17(1992)121.
112. S. A. May, E. C. Fuentes, and N. Sato, *Polym. Deg. Stab.*, 32(1991)357.
113. M. Bolle and S. Lazare, *J. Appl. Phys.*, 73(1993)3516.

114. M. Iring, M. Szesztay, A. Stirling, and F. Tüdös, *J. Macromol. Sci., Pure Appl. Chem.*, A29(1992)865.
115. B. Rånby, *J. Macromol. Sci., Pure Appl. Chem.*, A30(1993)583.
116. S. V. Maistrovi and Yu. I. Reutov, *Plast. Massy*, 1993,5,27.
117. J. Verdu, *Plast. Kautch.*, 1992,3-4,37.
118. H. H.-D. Lee and F. J. McGarry, *Polymer*, 34(1993)4267.
119. D. J. T. Hill, A. P. Lang, J. H. O'Donnell, and P. J. Pomery, *Polym. Deg. Stab.*, 38(1992)193.
120. G. A. Luoma and R. D. Rowland, *J. Chromat. Sci.*, 24(1986)210.
121. J. D. Stachiw and R. B. Dolan, *Trans. ASME*, 104(1982)190.
122. N. P. Novikov, *Fiz.-Khim. Mekh. Mater.*, 19(1983)115.
123. C. Decker and K. Moussa, *Polym. Mat. Sci. Eng.*, 57(1987) 900.
124. H. N. Neidlinger, M. R. Steffek, and R. Goggin, *Polym. Prep.*, 28(1987)205.
125. R. Bajpai, P. Agrawal, and S. C. Datt, *Polym. Int.*, 34(1994)249.
126. M. Barra, R. W. Redmond, M. T. Allen, G. S. Calabrese, R. Sinta, and J. C. Scaiano, *Macromolecules*, 24(1991)4972.
127. L. P. Buchwalter and G. Czornyj, *J. Vac. Sci. Technol.*, A8(1990)781.
128. C. S. Li and R. Kopelman, *J. Phys. Chem.*, 94(1990)2135.
129. M. S. Kitai, V. L. Popkov, and V. A. Semchishen, *Makromol. Chem., Makromol. Symp.*, 37(1990)257.
130. N. Ueno, M. Komada, Y. Morimoto, M. C. K. Tinone, M. Kushida, K. Sugita, K. Honma, and K. Tanaka, *Jpn. J. Appl. Phys.*, 32(1993)229.
131. A. Torikai, S. Hiraga, and K. Fueki, *Polym. Deg. Stab.*, 37(1992)73.
132. Y. Fukuda and Z. Osawa, *Polym. Deg. Stab.*, 34(1991)75.
133. T. Ichikawa, K.-I. Oyama, T. Kondoh, and H. Yoshida, *J. Polym. Sci., Polym. Chem.*, 32(1994)2487.
134. K. J. Miller, J. H. Hellman, and J. A. Moore, *Macromolecules*, 26(1993)4945.
135. C. Decker, K. Moussa, and T. Bendaikha, *J. Polym. Sci., Polym. Chem.*, 29(1991)739.
136. N. A. Weir, J. Arct, A. Ceccarelli, and A. Siren, *Eur. Polym. J.*, 30(1994)701.
137. K. R. Carduner, D. R. Bauer, J. L. Gerlock, and D. F. Mielewski, *Polym. Deg. Stab.*, 35(1992)219.
138. L. A. Linden, J. F. Rabek, H. Kaczmarek, A. Kaminska, and M. Scoponi, *Coordination Chem. Rev.*, 125(1993)195.
139. D. R. Bauer, M. J. Dean, and J. L. Gerlock, *Polym. Mat. Sci. Eng.*, 55(1986)443.
140. M. P. Nosov, N. K. Tarasenko, T. S. Nazarenko, R. V. Cheishvili, R. Ziemelis, and M. M. Kabaev, *Khim. Volokna*, 1982,5,31.
141. M. Igarashi and K. L. DeVries, *Polymer*, 24(1983)769.
142. T. B. Boboev and Kh. D. Dadomatov, *Fiz. Tverd. Tela (Leningrad)*, 28(1986)1202.
143. J. L. Philippart and J. T. Gardette, *Makromol. Chem.*, 187(1986)1639.
144. E. Imai, *Gyomu Nenpo-Tochigi-ken Ken'nan Kogyo Shidosho*, 1986,31.
145. T. Hirade, *Gyomu Nenpo-Tochigi-ken Ken'nan Kogyo Shidosho*, 1986,35.
146. J. R. Morgan and C. O. Pruneda, *Polymer*, 28(1987)340.
147. K. Sugiura, A. Yamaguchi, K. Fujita, and K. Hara, *Kenkyu Shiryo-Mikawa Sen'i*, 36(1986)2.

148. P. Gauvin, J. Lemaire, and D. Sallet, *Makromol. Chem.*, 188(1987)1815.
149. N. S. Allen, M. J. Harrison, G. W. Follows, and V. Matthews, *Polym. Degrad. Stab.*, 19(1987)77.
150. C. H. Do, E. M. Pearce, B. J. Bulkin, and H. K. Reimschuessel, *J. Polym. Sci., Polym. Chem.*, 25(1987)2301.
151. M. S. Toy and R. S. Stringham, *ACS Symp. Ser.*, 364(1988)326.
152. G. Reinert, *Melliand Textilber.*, 69(1988)58.
153. Y. Fujiwara and S. H. Zeronian, *J. Appl. Polym. Sci.*, 27(1982)2773.
154. R. P. Burford and D. R. G. Williams, *J. Mater. Sci. Lett.*, 7(1988)59.
155. W. H. Sharkey and W. E. Mochel, *J. Am. Chem. Soc.*, 81(1959)3000.
156. K. E. Kyllö and C. M. Ladisch, *ACS Symp. Ser.*, 318(1986)343.
157. A. Anton, *J. Appl. Polym. Sci.*, 9(1965)1631.
158. A. Davis and D. Sims, *Weathering of Polymers*, Applied Science Publishers, 1983.
159. W. B. Achwal, *Colourage*, 1991,1,29.
160. S. Konrad and D. Schuster, *J. Coated Fabrics*, 22,2(1992)10.
161. I. Narisawa and T. Kuriyama, *Angew. Makromol. Chem.*, 216(1994)87.
162. F. P. La Mantia and D. Curto, *Polym. Deg. Stab.*, 36(1992)131.
163. V. B. Ivanov, I. I. Barashkova, V. V. Selikov, V. N. Vysotsky, Yu. Yu. Yakovlev, R. A. Sadekova, and N. N. Barashkov, *Polym. Deg. Stab.*, 35(1992)267.
164. N. S. Allen, M. Ledward, and G. W. Follows, *Eur. Polym. J.*, 28(1992)23.
165. Z. A. Mohd Ishak and J. P. Berry, *Polym. Compos.*, 15(1994)223.
166. M. Raab and V. Hnat, *The Arabian J. Sci. Eng.*, 16(1991)37.
167. J. Mead, S. Singh, D. Roylance, and J. Patt, *Polym. Eng. Sci.*, 27(1987)131.
168. J.-L. Gardette and J. Lemaire, *Makromol. Chem.*, 183(1982)2415.
169. C. Decker and K. Moussa, *Polym. Mat. Sci. Eng.*, 58(1988)338.
170. J. Stumpe and K. Schwetlick, *Polym. Degrad. Stab.*, 17(1987)103.
171. C. E. Hoyle, K. J. Kim, and Y. G. No, *Water-Borne Higher-Solids Coatings Symp., New Orleans*, 1986.
172. C. E. Hoyle, Y. G. No, K. J. Kim., and G. L. Nelson, Report, AD-A169 645, 1986.
173. H. Ulrich, *J. Elastom. Plast.*, 18(1986)147.
174. C. S. Schollenberger and F. D. Stewart, *J. Elastoplastics*, 3(1971)28.
175. C. S. Schollenberger and F. D. Stewart, *J. Elastoplastics*, 4(1972)294.
176. G. Capocci, *Plast. Comp.*, 10(1987)13.
177. N. A. Tschernykh, L. A. Suchareva, Yu. B. Kipnis, and A. I. Zemcov, *Kozh.-Obuv. Prom.-st*, 1986,5,43.
178. R. B. Turner, C. P. Christenson, M. A. Harthcock, M. D. Meadows, W. L. Howard, and M. W. Creswick, *Polym. Mat. Sci. Eng.*, 58(1988)947.
179. C. E. Hoyle and K. J. Kim, Report, AD-A172 619, 1986.
180. C. E. Hoyle and K. J. Kim, *Polym. Prep.*, 28(1987)415.
181. Z. Osawa and K. Nagashima, *Polym. Degrad. Stab.*, 10(1980)311.
182. L. V. Nevskii, O. G. Tarakanov, and V. Belyakov, *J. Polym. Sci., Polym. Lett. Ed.*, 23(1968)193.
183. H. C. Beachell and L. C. Chang, *J. Polym. Sci., Polym. Chem. Ed.*, 10(1972)503.
184. J.-L. Gardette and J. Lemaire, *Polym. Degrad. Stab.*, 14(1984)135.

185. J. M. Widmaier, J. P. Balmer, and G. C. Meyer, *Polym. Mat. Sci. Eng.*, 58(1988)96.
186. Z. Osawa, *Dev. Polym. Photochem.*, 3(1983)209.
187. E. L. Cheu and Z. Osawa, *J. Appl. Polym. Sci.*, 19(1975)2947.
188. R. Noack and K. Schwetlick, *Tetrahedron*, 30(1974)3799.
189. C. S. Schollenberger and F. D. Stewart, *J. Elastom. Plast.*, 8(1976)11.
190. H. Djomo, A. Morin, M. Damyanidu, and G. Meyer, *Polymer*, 24(1983)65.
191. J. H. Flynn, *Polym. Eng. Sci.*, 20(1980)675.
192. K. Wongkamolsesh and J. E. Kresta, *Polym. Mat. Sci. Eng.*, 49(1983)465.
193. S. Yajima, Y. Togawa, S. Matsushita, T. Suzuki, and T. Okada, *Kinzoku Hyomen Gijutsu*, 37(1986)718.
194. Z. Roslaniec and H. Wojcikiewicz, *Polimery (Warsaw)*, 31(1986)204.
195. T. M. Chapman, *J. Polym. Sci., Polym. Chem.*, 27A(1989)1993.
196. A. Brandwood, K. R. Noble, K. Schindhelm, G. F. Meijs, P. A. Gunatillake, R. C. Chatelier, S. J. McCarthy, and E. Rizzardo, *Biomaterial Tissue Interface*, 10(1992)413.
197. J. Pan, Y. Song, W. W. Y. Lau, and S. H. Goh, *Polym. Deg. Stab.*, 41(1993)275.
198. A. T. Chen, T. R. McClellan, R. L. Ray, and C. K. Groseth, *Elastomerics*, 1991,9,9.
199. S. K. Dolui, *J. Appl. Polym. Sci.*, 53(1994)463.
200. D. R. Bauer, *J. Coat. Technol.*, 66,835(1994)57.
201. A. Sommer, E. Zirngiebl, L. Kahl, and M. Schönfelder, *Prog. Org. Coat.*, 19(1991)79.
202. B. P. Thapliyal and R. Chandra, *Prog. Polym. Sci.*, 15(1990)735.
203. J. M. Anderson, A. Hiltner, Q. H. Zhao, Y. Wu., M. Renier, M. Schubert, M. Brunstedt, G. A. Lodoen, and C. R. Payet, *Conf. Biodegradable Polym. Plast.*
204. G. Wypych, *unpublished information*.
205. H. Schoenbacher, B. Schreiber, and R. Stierli, *Kunststoffe*, 76(1986)759.
206. L. Egiziano, G. Lupo, V. Tucci, and L. Centurioni, *Conf. Rec. IEEE Int. Symp. Electr. Insul.*, 6(1986)196.
207. J. M. Augl, *J. Rheol.*, 31(1987)1.
208. T. W. Wilson, R. E. Fornes, R. D. Gilbert, and J. D. Memory, *Polym. Mat. Sci. Eng.*, 56(1987)105.
209. T. Nguyen and E. Byrd, *Polym. Mat. Sci. Eng.*, 56(1987)584.
210. J. Bartova, K. Bily, and P. Marek, *Crosslinked Epoxies Conf.*, 9(1986)557.
211. D. J. Won, Y. K. Park, and C.S. Jhoun, *Nonmunjip-Sanop Kwahak Kisul Yonguso*, 15(1987)171.
212. A. Yu. Filipovich and S. I. Skiba, *Plast. Massy*, 1986,7,16.
213. W. A. Lipskaya, G. T. Yevtushenko, D. N. Lobacheva, O. B. Goncharova, H. A. Tkachuk, and G. A. Voloskov, *Plast. Massy*, 1985,8,20.
214. S. C. Lin, B. J. Bulkin, and E. M. Pearce, *J. Polym. Sci., Polym. Chem.*, 17(1979)3121.
215. G. A. George, R. E. Sacher, and J. F. Sprouse, *Appl. Polym. Sci.*, 8(1977)2241.
216. N. S. Allen, J. P. Binkley, B. J. Parsons, G. O. Phillips, and N. H. Tennent, *Polym. Photochem.*, 2(1982)97.
217. W. R. R. Park and J. Blount, *Ind. Eng. Chem.*, 49(1957)1879.
218. V. Bellenger and J. Verdu, *Polym. Photochem.*, 5(1984)295.

219. N. Rose, M. Le Bras, R. Delobel, B. Costes, and Y. Henry, *Polym. Deg. Stab.*, 42(1993)307.
220. B. De'Neve and M. E. R. Shanahan, *Polymer*, 34(1993)5099.
221. G. Zhang, W. G. Pitt, S. R. Goates, and N. L. Owen, *J. Appl. Polym. Sci.*, 54(1994)419.
222. R. S. Porter and A. Casale, *Polym. Eng. Sci.*, 25(1985)129.
223. N. Ogata and K. Yoshida, *Zairyo*, 32(1983)1119.
224. P. Komitov, G. Kostov, and B. Michnev, *Kunstst. Fortschrittsber.*, 7(1980)57.
225. Z. Nikolova, S. Karaenev, and I. Mladenov, *Kunstst. Fortschrittsber.*, 7(1981)69.
226. Y. Watanabe and T. Shiota, *Kenkyu Hokoku-Kogyo Gijutsuin*, 1981,2,141.
227. R. Kobayashi and S. Hattori, *Kenkyu Hokoku-Kogyo Gijutsuin*, 1981,2,245.
228. O. Nishimura, H. Kubota, S. Suzuki, J. Iyoda, K. Yoshikawa, and T. Shiota, *Hokkaido Kogyo Kaihatsu Shikensho Hokoku*, 24(1981)80.
229. Yu. I. Vasilenok, V. N. Lagunova, N. P. Solov'eva, O. D. Lesnykh, E. I. Ermakov, I. N. Kotovich, V. A. Emel'yanova, and V. N. Rudnistkii, *Plast. Massy*, 1982,6,7.
230. N. I. Kondrashkina, T. N. Zelenkova, M. Z. Borodulina, and B. I. Sazhin, *Zh. Prikl. Khim. (Leningrad)*, 55(1982)1196.
231. J. Y. Moisan and R. Lever, *Eur. Polym. J.*, 18(1982)407.
232. K. Arakawa, T. Seguchi, Y. Watanabe, and N. Hayakawa, *J. Polym. Sci., Polym. Chem.*, 20(1982)2681.
233. R. J. Gonzales, V. L. Martin, and M. S. Santolino, *Rev. Plast. Mod.*, 44(1982)385.
234. Z. Osawa, K. Kobayashi, and E. Kayano, *Polym. Degrad. Stab.*, 11(1985)63.
235. L. N. Sal'vitskaya, D. G. Pereyaslova, and M. Ya. Zabara, *Plast. Massy*, 1985,6,29.
236. K. Wolny, *Kunststoffe*, 76(1986)145.
237. Z. Osawa and H. Kuroda, *Nippon Kagaku Kaishi*, 1986,6,811.
238. K. Sijarto, E. Lovas, B. Kolozsvari, and J. Nyitrai, *Muanyag Gumi*, 23(1986)196.
239. A. Torikai, R. Geetha, S. Nagaya, and K. Fueki, *Polym. Degrad. Stab.*, 16(1986)199.
240. C. Andrei, *Rev. Chim. (Bucharest)*, 37(1986)677.
241. S. S. Bamji, A. T. Bulinski, and R. J. Densley, *J. Appl. Phys.*, 61(1987)694.
242. G. Papet, L. Jirackova-Audouin, and J. Verdu, *Radiat. Phys. Chem.*, 29(1987)65.
243. M. Schulz and K. Seiffarth, *Mitteilungsbl.-Chem. Ges. DDR*, 34(1987)3.
244. U. Kubo and Y. Matsuura, *Kinki Daigaku Rikogakubu Kenkyu Hokoku*, 22(1986)217.
245. D. Mlynek and G. Lewin, *Wiss. Z. Tech. Hochsch. Magdeburg*, 30(1986)19.
246. D. Liu, L. Zhang, Y. Wang, and W. Chen, *Radiat. Phys. Chem.*, 29(1987)175.
247. E. G. El'darov and J. Muras, *Plast. Kauc.*, 23(1986)358.
248. Y. Uemichi and H. Kanoh, *Kenkyu Hokoku-Asahi Garasu Kogyo Gijutsu Shoreikai*, 49(1986)225.
249. F. Severini, R. Gallo, S. Ipsale, and N. Del Fanti, *Polym. Degrad. Stab.*, 17(1987)57.
250. P. J. A. Chirinos, Z. Rubintzain, and M. A. Colmenares, *Eur. Polym. J.*, 23(1987)729.
251. M. Raab, V. Hnat, P. Schmidt, L. Kotulak, L. Taimr, and J. Pospisil, *Polym. Degrad. Stab.*, 18(1987)123.
252. A. J. Chirinos-Padron, P. H. Hernandez, E. Chavez, N. S. Allen, C. Vasilion, and M. DePoortere, *Eur. Polym. J.*, 23(1987)935.
253. R. Geetha, A. Torikai, S. Nagaya, and K. Fueki, *Polym. Degrad. Stab.*, 19(1987)279.
254. F. K. Meyer and E. Pedrazzetti, *Plast. Rubber Process. Appl.*, 8(1987)29.

255. S. Al-Malaika, *Polym.-Plast. Technol. Eng.*, 27(1988)261.
256. J. L. Bolland, *Trans. Faraday Soc.*, 44(1948)669.
257. J. L. Bolland, *Quart. Rev.*, 3(1949)1
258. L. Bateman, *Quart. Rev.*, 8(1954)147.
259. J. Lemaire and A. Arnaud, *Polym. Photochem.*, 5(1984)243.
260. W. L. Hawkins, W. Martreyek, and F. H. Winslow, *J. Polym. Sci.*, 41(1959)1.
261. K. Tsuji and H. Nagata, *Rep. Progress Polym. Phys. Japan*, 18(1975)517.
262. J. H. Adams, *J. Polym. Sci.*, 8A(1970)1279.
263. P. Dunn and E. J. Hill, *Report 421*, Australia, 1971
264. G. Williams, M. R. Kamal, and D. G. Cooper, *Polym. Deg. Stab.*, 42(1993)61.
265. N. S. Allen, M. Edge, J. He, W. Chen, K. Kikkawa, and M. Minagawa, *Polym. Deg. Stab.*, 42(1993)293.
266. N. Kharaiishi and A. Al-Robaidi, *Polym. Deg. Stab.*, 32(1991)105.
267. Y. Qing, X. Wenying, and B. Ranby, *Polym. Eng. Sci.*, 34(1994)446.
268. Y. Qing, X. Wenying, and B. Ranby, *Polym. Eng. Sci.*, 31(1991)1561.
269. M. E. S. Carvalho and J. J. C. Cruz-Pinto, *Polym. Eng. Sci.*, 32(1992)567.
270. D. Raghavan and A. E. Torma, *Polym. Eng. Sci.*, 32(1992)439.
271. J. J. C. Cruz-Pinto, M. E. S. Carvalho, and J. F. A. Ferreira, *Angew. Makromol. Chem.*, 216(1994)113.
272. F. Gugumus, *Angew. Makromol. Chem.*, 182(1990)111.
273. S. A. Jabarin and E. A. Lofgren, *J. Appl. Polym. Sci.*, 53(1994)411.
274. W. K. Busfield and M. J. Monteiro, *Mater. For.*, 14(1990)218.
275. G. M. Ferguson, A. Jefferson, and I. Sihsobhon, *Mater. For.*, 16(1992)147.
276. O. Ogbode and N. N. Ossai, *Acta Polym.*, 43(1993)173.
277. E.A. Kalennikov, S. I. Kuzina, V. S. Yuran, A. I. Mikhailov, L. V. Popova, A. A. Pendin, and V. N. Babin, *Appl. Organometal. Chem.*, 5(1991)471.
278. A.-C. Albertsson and S. Karlsson, *Polym. Deg. Stab.*, 41(1993)345.
279. F. Severini, R. Gallo, S. Ipsale, and G. Ricca, *Polym. Deg. Stab.*, 41(1993)103.
280. G. Gueskens, *Int. J. Polym. Mater.*, 16(1992)31.
281. S. G. Matz, *J. Chromatog.*, 587(1991)205.
282. K. K. Leonas and R. W. Gorden, *J. Environ. Polym. Deg.*, 1(1993)45.
283. Z. Jelcic, M. Mlinac-Misak, J. Jelencic, and M. Bravar, *Angew. Makromol. Chem.*, 208(1993)25.
284. G. M. Fergusson, M. Hood, and K. Abbott, *Polym. Int.*, 28(1992)35.
285. S. Bualek, K. Suchiva, S. Boonariya, and B. Ratana-Arakul, *J. Sci. Soc. Thailand*, 17(1991)103.
286. M. P. Ebdon, *Corros. Astral.*, 17,3(1992)10.
287. P. P. L. Jacques and R. C. Poller, *Eur. Polym. J.*, 29(1993)75.
288. P. P. L. Jacques and R. C. Poller, *Eur. Polym. J.*, 29(1993)83.
289. H. Kubota, K. Takahashi, and Y. Ogiwara, *Polym. Deg. Stab.*, 33(1991)115.
290. F. Gugumus, *Polym. Deg. Stab.*, 34(1991)205.
291. P. Zamotaeov, O. Mityukhin, and S. Luzgarev, *Polym. Deg. Stab.*, 35(1992) 195.
292. A.-C. Albertsson, C. Barenstedt, and S. Karlsson, *Polym. Deg. Stab.*, 37(1992)163.
293. H. Kubota and M. Kimura, *Polym. Deg. Stab.*, 38(1992)1.

294. N. S. Allen, M. Edge, S. Conway, D. A. Doyle, E. M. Howells, K. Kikkawa, M. Minagawa, and T. Sekiguichi, *Polym. Deg. Stab.*, 38(1992)85.
295. C. David, M. Trojan, A. Daro, and W. Demarteau, *Polym. Deg. Stab.*, 37(1992)233.
296. M. M. Qayyum and J. R. White, *Polym. Deg. Stab.*, 39(1993)199.
297. A. Tidjani and R. Anaud, *Polym. Deg. Stab.*, 39(1993)285.
298. L. Gordjevargov, G. Kostov, and D. Kostoski, *Polym. Deg. Stab.*, 41(1993)173.
299. O. N. Karpukhin, E. M. Mostovaya, B. V. Novozhilov, and E. M. Slobodetskaya, *Plast. Massy*, 1981,11,24.
300. C. S. Wang and G. S. Y. Yeh, *Polym. J.*, 13(1981)741.
301. G. Penot, R. Arnaud, and J. Lemaire, *Makromol. Chem.*, 183(1982)2731.
302. N. C. Billingham, P. D. Calvert, and J. B. Knight, *Proc. IUPAC Macromol. Symp. 28th*, 1982,291.
303. A. Torikai, K. Suzuki, and K. Fueki, *Polym. Photochem.*, 3(1983)379.
304. W. S. Subowo, M. Barmawi, and O. B. Liang, *J. Polym. Sci., Polym. Chem.*, 24(1986)1351.
305. E. T. Denisov, A. I. Vol'pert, and V. P. Filipenko, *Vysokomol. Soed.*, 28A(1986)2083.
306. K. B. Chakraborty and G. Scott, *Polym. Degrad. Stab.*, 16(1986)1.
307. A. Faucitano, A. Buttafava, F. Martinotti, V. Comincioli, and F. Gratani, *Polym. Photochem.*, 7(1986)483.
308. A. Faucitano, A. Buttafava, F. Martinotti, V. Comincioli, and P. Bortolus, *Polym. Photochem.*, 7(1986)491.
309. I. S. Polikarpov, N. N. Simkovich, and I. V. Kuz'mina, *Tekst. Prom-st. (Moskow)*, 1986,12,35.
310. D. J. Carlsson, Z. Can, and D. M. Wiles, *J. Appl. Polym. Sci.*, 33(1987)875.
311. Z. Zamorsky and J. Muras, *Verarb. Anwendungstech. Probl. Org. Hochpolym. Tagungsskr., TECHNOMER '85*, 1(1986)102.
312. E. A. Sporyagin, P. I. Bashtannik, Yu. V. Brazhnik, V. G. Ovcharenko, V. D. Zinukhov, M. M. Kremlev, and N. P. Bezverkhii, *Verarb. Anwendungstech. Probl. Org. Hochpolym. Tagungsskr., TECHNOMER '85*, 2(1986)404.
313. S. Al-Malaika, E. O. Omikoreda, and G. Scott, *J. Appl. Polym. Sci.*, 33(1987)703.
314. V. Choudhary, S. Varshney, and I. K. Varma, *Angew. Makromol. Chem.*, 150(1987)137.
315. S. Al-Malaika, A. Marogi, and G. Scott, *Polym. Degrad. Stab.*, 18(1987)89.
316. A. A. Popov, A. V. Rusak, E. S. Popova, N. N. Komova, and G. E. Zaikov, *Vysokomol. Soed.*, 30A(1988)159.
317. O. Durcova, I. Diacic, M. Mitterpachova, and P. Stefanik, *Vysokomol. Soed.*, 29A(1987)2143.
318. G. Geuskens, F. Debie, M. S. Kabamba, and G. Nedelkos, *Polym. Photochem.*, 5(1984)313.
319. B. A. Gorelik, I. V. Kolganova, L. Matisova-Rychla, G. I. Listvojb, A. M. Drabkina, and A. G. Golnik, *Polym. Deg. Stab.*, 42(1993)263.
320. L. Wenzhong, Q. Juying, H. Xingzhou, and X. Hongmei, *Polym. Deg. Stab.*, 32(1991)39.
321. G. E. Schoonenberg and H. D. F. Meijer, *Polymer*, 32(1991)438.
322. C. Neri, V. Malatesta, S. Constanzi, and R. Riva, *Angew. Makromol. Chem.*, 216(1994)101.

323. C. Q. Yang and L. K. Martin, *J. Appl. Polym. Sci.*, 51(1994)389.
324. I. L. J. Dogue, N. Mermilliod, and F. Genoud, *J. Polym. Sci., Polym. Chem.*, 32(1994)2193.
325. Z. A. Kadir, F. Yoshii, K. Makuuchi, and I. Ishigaki, *Angew. Makromol. Chem.*, 174(1990)131.
326. S. P. Cygan and J. R. Laghari, *IEEE Trans. Nucl. Sci.*, 38(1991)906.
327. J. Schurz, P. Zipper, and J. Lenz, *J. Macromol. Sci., Pure Appl. Chem.*, A30(1993)603.
328. P. Jiangqing, X. Hongmei, Q. Juying, C. Jinfen, and M. Zhenmin, *Polym. Deg. Stab.*, 33(1991)67.
329. D. Rysavy and H. Tkadleckova, *Polym. Deg. Stab.*, 37(1992)19.
330. S. Falicki, D. J. Carlsson, J. M. Cooke, and D. J. Gosciniak, *Polym. Deg. Stab.*, 38(1992)265.
331. S. Chmela, W. D. Habicher, U. Hähner, and P. Hrdlovic, *Polym. Deg. Stab.*, 39(1993)367.
332. R. Baumhardt-Neto and M.-A. De Paoli, *Polym. Deg. Stab.*, 40(1993)59.
333. R. Baumhardt-Neto and M.-A. De Paoli, *Polym. Deg. Stab.*, 40(1993)53.
334. M. M. Qayyum and J. R. White, *Polym. Deg. Stab.*, 41(1993)163.
335. O. Nishimura, S. Suzuki, H. Kubota, K. Yoshikawa, and T. Shirota, *Hokkaido Kogyo Kaihatsu Shikensho Hokoku*, 24(1981)69.
336. H. N. Subramanyam and S. V. Subramanyam, *Eur. Polym. J.*, 23(1987)207.
337. R. P. Kusy and D. T. Turner, *Macromolecules*, 8(1975)235.
338. N. L. Yang, V. Patel, T. J. Dolce, and A. Auerbach, *Polym. Mat. Sci. Eng.*, 51(1984)149.
339. F. M. Berardinelli, T. J. Dolce, and C. Walling, *J. Appl. Polym. Sci.*, 9(1965)1419.
340. A. Davis, *Polym. Degrad. Stab.*, 3(1981)187.
341. R. Vesely and M. Kalenda, *Kunststoffe*, 59(1969)107.
342. M. Taylor, *Joint Tropical Trials*, Queensland, Australia.
343. J.-L. Gardette, H.-D. Sabel, and J. Lamaire, *Angew. Makromol. Chem.*, 188(1991)113.
344. E. J. Goethals, R. R. De Clercq, and S. R. Walraedt, *J. Macromol. Sci., Pure Appl. Chem.*, A30(1993)679.
345. S. J. Clarson, J. E. Mark, C.-C. Sun, and K. Dodgson, *Eur. Polym. J.*, 28(1992)823.
346. E. T. Kang, K. G. Neoh, K. L. Tan, and D. J. Liaw, *Polym. Deg. Stab.*, 40(1993)45.
347. R. A. Jerussi, *J. Polym. Sci., Polym. Chem.*, 9(1971)2009.
348. J. S. Pickett, *Polym. Stab. Degrad.*, 280(1985)313.
349. P. G. Kelleher, J. B. Jassic, and B. D. Gesner, *J. Appl. Polym. Sci.*, 11(1967)137.
350. J. Petruj and Z. Slama, *Makromol. Chem.*, 181(1980)2461.
351. A. Dilks and D. T. Clark, *J. Polym. Sci., Polym. Chem.*, 19(1981)2847.
352. B. Dolezel and L. Admirova, *Plast. Kauc.*, 20(1983)18.
353. R. Chandra, S. Mishra, P. Kumar, and L. Rajabi, *Angew. Makromol. Chem.*, 214(1994)1.
354. J. B. Webb and A. W. Czanderna, *Sol. Energy Mater.*, 15(1987)1.
355. K. Moriawaki, *Asahi Garasu Kenkyu Hokoku*, 36(1986)167.
356. I. V. Krylova and I. A. Rodina, *Zh. Fiz. Khim.*, 61(1987)1688.
357. A. Factor, W. V. Ligon, and R. J. May, *Macromolecules*, 20(1987)2461.

358. A. Factor, J. C. Lynch, and F. H. Greenberg, *J. Polym. Sci., Polym. Chem.*, 25(1987)3413.
359. P. A. Mullen and N. Z. Searle, *J. Appl. Polym. Sci.*, 14(1970)765.
360. A. Gupta, A. Rembaum, and J. Moacanin, *Macromolecules*, 11(1978)1285.
361. A. Rivaton, D. Sallet, and J. Lemaire, *Polym. Photochem.*, 3(1983)463.
362. C. A. Pryde, *ACS Symp. Ser.*, 280(1985)329.
363. J. D. Webb and A. W. Czanderna, *Macromolecules*, 19(1986)2810.
364. J. D. Cooney, *Polym. Eng. Sci.*, 22(1982)492.
365. A. Rivaton, J. L. Gardette, and J. Lemaire, *Rev. Gen. Caoutch. Plast.*, 651(1985)81.
366. A. Ram, O. Zilber, and S. Kenig, *Polym. Eng. Sci.*, 25(1985)535.
367. I. N. Cerskij and T. A. Starzeneckaya, *Plast. Kauc.*, 34(1987)142.
368. J. D. Webb and A. W. Czanderna, *J. Mater. Sci., Polym. Prep.*, 28(1987)29.
369. G. Kämpf, K. Sommer, and E. Zirngiebl, *Prog. Org. Coat.*, 19(1991)69.
370. A. Torikai, T. Mitsouka, and K. Fueki, *J. Polym. Sci., Polym. Chem.*, 31(1993)2785.
371. A. Rivaton, *Angew. Makromol. Chem.*, 216(1994)147.
372. A. Kim, C. P. Bosnyak, and A. Chudnovsky, *J. Appl. Polym. Sci.*, 51(1994)1841.
373. M. H. Tabankia and J.-L. Gardette, *Polym. Degrad. Stab.*, 14(1986)351.
374. C. G. Pitt, *Conf. Biodegradable Polym. Plast.*
375. M. Ramasri, S. C. Shit, A. B. Mathur, and K. Ramamurthy, *Pop. Plast. Packaging*, 1992,5,47.
376. G. Vigier and J. Tatibouet, *Polymer*, 34(1993)4257.
377. J.-Q. Pan and J. Zhang, *Polym. Deg. Stab.*, 36(1992)65.
378. A. Rivaton, *Polym. Deg. Stab.*, 41(1993)283.
379. A. Rivaton, *Polym. Deg. Stab.*, 41(1993)297.
380. M. Edge, M. Hayes, M. Mohammadian, N. S. Allen, T. S. Jewitt, K. Brems, and K. Jones, *Polym. Deg. Stab.*, 32(1991)131.
381. J. Friedrich, I. Loeschke, H. Frommelt, H.-D. Reiner, H. Zimmermann, and P. Lutgen, *Polym. Deg. Stab.*, 31(1991)97.
382. N. Fukazawa, K. Yoshioka, H. Fukumura, and H. Masuhara, *J. Phys. Chem.*, 97(1993)6753.
383. S. K. Mukhopadhyay, D. J. Mwaisengela, and P. W. Foster, *J. Text. Inst.*, 82(1991)427.
384. B. Santos and G. F. Sykes, *Natl. SAMPE Tech. Conf.*, 13(1981)256.
385. E. Ya. Beider, L. I. Kantsevich, L. V. Shalaeva, L. I. Reitburd, A. E. Semenkova, and L.M. Bolotina, *Plast. Massy*, 1984,9,16.
386. A. K. Verma, *Prog. Polym. Sci.*, 12(1986)219.
387. J. A. Loo, B. H. Wang, F. C. Y. Wang, and F. W. McLafferty, *Macromolecules*, 20(1987)698.
388. H. S. Munro and D. T. Clark, *Polym. Degrad. Stab.*, 17(1987)319.
389. T. Sasuga and M. Hagiwara, *Polymer*, 28(1987)1915.
390. F. Abdul-Rasoul, C. L. R. Catherall, J. S. Hargreaves, J. M. Mellor, and D. Phillips, *Eur. Polym. J.*, 13(1977)1019.
391. J. Peeling and D. T. Clark, *J. Appl. Polym. Sci.*, 26(1981)3761.
392. M. J. Bowden, L. F. Thompson, W. Robinson, and M. Biolsi, *Macromolecules*, 15(1982)1417.

393. S. Kuroda, I. Mita, K. Obata, and S. Tanaka, *Polym. Deg. Stab.*, 27(1990)257.
394. T. Yamashita, H. Tomitaka, T. Kudo, K. Horie, and I. Mita, *Polym. Deg. Stab.*, 39(1993)47.
395. L. N. Pankratova, T. I. Sunekants, N. V. Oleinik, V. V. Severnyi, and M. V. Zheleznikova, *Plast. Massy*, 1986,10,40.
396. S. P. Sawan, Y. G. Tsai, and H. Y. Huang, *Polym. Prepr.*, 28(1987)260.
397. M. Ishikawa, *Polym. Prepr.*, 28(1987)426.
398. J. Stein and L. C. Prutzman, *Polym. Prepr.*, 28(1987)377.
399. W. F. Manders and J. M. Bellama, *J. Polym. Sci., Polym. Chem.*, 23(1985)351.
400. J. M. Klosowski and M. J. Owen, *Polym. Mat. Sci. Eng.*, 56(1987)469.
401. K. Nate, M. Ishikawa, N. Imamura, and Y. Murakami, *J. Polym. Sci., Polym. Chem.*, 24(1986)1551.
402. L. C. Ewanowski, Report, NUREGCR 4543(1986).
403. N. A. Shtserbakova, G. A. Podgrebenkova, Yu. D. Zyuzina, T. G. Puzyreva, N. B. Varlamova, E. A. Rogal, N. A. Aleksandrova, and O. N. Karaseva, *Lakokras. Mater. Ikh Primen.*, 1983,4,46.
404. N. A. Weir, *Dev. Polym. Degrad.*, 7(1987)193.
405. K.-H. Schimmel, *Acta Polym.*, 38(1987)495.
406. K.-H. Schimmel and J. Schultz, *Acta Polym.*, 38(1987)536.
407. Yu. I. Dorofeev and W. E. Skurat, *Dokl. Akad. Nauk CCCR*, 292(1987)654.
408. S. W. Addy, D. W. Clegg, A. A. Collyer, G. C. Corfield, and P. Crum, *J. Rheol.*, 31(1987)297.
409. L. N. Pankratova, *Vestn. Mosk. Univ., Ser. 2, Khim.*, 28(1987)608.
410. W. K. Matveev, N. A. Smirnova, and W. K. Milintchuk, *Vysokomol. Soed.*, 29B(1987)214.
411. E. W. Bengstrom, *Report*, 74-038.
412. *Dow Corning Bull.*, 1972, 17-158.
413. V. Jancovicova, D. Marianiova, D. Bakos, and L. Lapcik, *Chem. listy*, 85(1991)337.
414. Y. Israëli, J. Lacoste, J. Cavezzan, and J. Lemaire, *Polym. Deg. Stab.*, 42(1993)267.
415. C. E. Hoyle and E. T. Anzures, *Report*, AD-A222 431.
416. C. E. Hoyle and E. T. Anzures, *J. Polym. Sci., Polym. Chem.*, 30(1992)1233
417. C. E. Hoyle, D. Creed, R. Nagarajan, P. Subramanian, and E. T. Anzures, *Polymer*, 33(1992)3162.
418. J. R. Sobehart, *J. Appl. Phys.*, 74(1993)2630.
419. S. R. Cain, *J. Phys. Chem.*, 97(1993)7572.
420. E.-S. A. Hegazy, T. Sasuga, M. Nishii, and T. Seguchi, *Polymer*, 33(1992)2897.
421. M. D. Chipara and M. I. Chipara, *Polym. Deg. Stab.*, 37(1992)67.
422. I. Dalis and M. Karimi, *J. Vac. Sci., Technol.*, A10(1992)2921.
423. J. Pola, D. Tomanova, P. Schneider, V. Denek, and J. Tlaskal, *J. Fluorine Chem.*, 50(1990)309.
424. X. Jouan and J.-L. Gardette, *J. Polym. Sci., Polym. Chem.*, 29(1991)685.
425. X. Jouan and J. L. Gardette, *Polym. Deg. Stab.*, 36(1992)91.
426. M. Sargent, J. L. Koenig, and N. L. Maecker, *Polym. Deg. Stab.*, 39(1993)355.

427. D. J. Hill, A. P. Lang, J. H. O'Donnell, and P. J. Pomery, *Polym. Deg. Stab.*, 38(1992)205.
428. M. Getlichermann, M. Trojan, A. Daro, and C. David, *Polym. Deg. Stab.*, 39(1993)55.
429. A. B. Reynolds and P. A. Wlodkowski, *Radiat. Phys. Chem.*, 38C(1991)553.
430. S. Baccaro and U. Buontempo, *Radiat. Phys. Chem.*, 40C(1992)175.
431. R. P. Singh and A. Singh, *J. Makromol. Sci., -Chem.*, A28(1991)487.
432. R. P. Singh, R. Mani, S. Sivaram, J. Lacoste, and J. Lemaire, *Polymer*, 35(1994)1382.
433. R. Mani, R. P. Singh, S. Sivaram, and J. Lacoste, *Polym. J.*, 26(1994)1132.
434. M. Guzzo and M.-A. De Paoli, *Polym. Deg. Stab.*, 36(1992)169.
435. S. Kole, S. K. Srivastava, D. K. Tripathy, and A. K. Bhowmick, *J. Appl. Polym. Sci.*, 54(1994)1329.
436. N. Pourahmady, P. I. Bak, and R. A. Kinsey, *J. Macromol. Sci., Pure Appl. Chem.*, A29(1992)959.
437. L. A. Utracki, *Polym. Networks Blends*, 1(1991)1.
438. L. A. Utracki, *Polymer Alloys and Blends*, Hanser Publishers, Munich, 1989, and Japanese edition by Tokyo Kagaku Dozin Comp. Ltd., Tokyo, 1991.
439. M. Trojan, A. Daro, R. Jacobs, and C. David, *Polym. Degrad. Stab.*, 28(1990)28.
440. P. F. La Mantia, *Polym. Degrad. Stab.*, 13(1985)297.
441. F. Henninger and E. Pedrazzetti, *Arabian J. Sci. Eng.*, 13(1988)473.
442. A. Daro, M. Trojan, R. Jacobs, and C. David, *Eur. Polym. J.*, 26(1990)47.
443. S. H. Hamid and J. H. Khan, *Eur. Regional Meeting, PPS*, Palermo, 1991.
444. C. David, F. Zabeau, and R. A. Jacobs, *Polym. Eng. Sci.*, 22(1982)912.
445. S. A. Komarov, E. E. Piskunova, V. N. Kuleznev, V. V. Korovkin, A. A. Kolesnikov and I. K. Prik, *Kolloidn. Zh.*, 48(1986)152.
446. M. Nicu, V. Nicu, and N. Asandei, *Bulgarian Acad. Sci., Commun. Dept. Chem.*, 20(1987)493.
447. C. Sadrmoaghegh, G. Scott, and E. Setoudeh, *Polym. Degrad. Stab.*, 3(1980-81)469.
448. F. Kloos, H. Strouk, R. Uebe, and G. Heufer, *Angew. Makromol. Chem.*, 185-186(1991)97.
449. M. A. Nocilla and F. P. La Mantia, *Polym. Degrad. Stab.*, 29(1990)331.
450. D. Curto, A. Valenza, and F. P. La Mantia, *J. Appl. Polym. Sci.*, 39(1990)865.
451. S. Al-Malaika and E. J. Amir, *Polym. Degrad. Stab.*, 26(1989)31.
452. A. Valenza and F. P. La Mantia, *Arabian J. Sci. Eng.*, 13(1988)497.
453. M. A. Nocilla and P. F. La Mantia, *Eur. Regional Meeting, PPS*, Palermo, 1991.
454. D. Lala, J. F. Rabek, and B. Ranby, *Polym. Degrad. Stab.*, 3(1980-81)307.
455. T. Skowronski, J. F. Rabek, and B. Ranby, *Polym. Eng. Sci.*, 24(1984)278.
456. A. Kaminska and H. Kaczmarek, *Angew. Makromol. Chem.*, 144(1986)139.
457. A. Kaminska, S. Sanyal, and H. Kaczmarek, *J. Therm. Anal.*, 35(1989)2135.
458. D. T. J. Hill, F. A. Kroesen, J. H. O'Donnell, and P. J. Pomery, *Polym. Degrad. Stab.*, 34(1991)125.
459. Y. Y. Chien, E. M. Pearce, and T. K. Kwei, *J. Polym. Sci., Polym. Chem.*, 29(1991)849.
460. M. Kryszewski, B. Wandelt, D. J. S. Birch, R. E. Imhof, A. M. North and R. A. Pethrick, *Polym. Commun.*, 24(1983)73.
461. J. P. T. Jensen and J. Kops, *J. Polym. Sci., Polym. Chem.*, 19(1981)2765.

462. A. Torikai, Y. Sekigawa, and K. Feuki, *Polym. Degrad. Stab.*, 21(1988)43.
463. A. Kaminska, H. Kaczmarek, and S. Sanyal, *Polym. Networks Blends*, 1(1991)165.
464. Z. Osawa and Y. Fukuda, *Polym. Degrad. Stab.*, 32(1991)285.
465. Y. Fukuda and Z. Osawa, *Polym. Degrad. Stab.*, 34(1991)75.
466. C. S. Li and R. Kopelman, *J. Phys. Chem.*, 94(1990)2135.
467. E. G. Kolawole, *Eur. Polym. J.*, 20(1984)629.
468. J. L. Gerloch, D. F. Mielewski, and D. R. Bauer, *Polym. Degrad. Stab.*, 26(1989)241.
469. B. A. Gorelik, L. A. Sokolova, A. G. Grigoriev, S. D. Koshelev, E. I. Semenenko, and G. A. Matiushin, *Makromol. Chem., Macromol. Symp.*, 28(1989)249.
470. B. A. Gorelik, G. A. Matjushin, V. S. Nechitailo, and L. A. Sokolova, *Radiat. Phys. Chem.*, 35, 218 (1990)218.
471. E. Punkka, J. Laakso, H. Stubb, and P. Kuivalainen, *Synthetic Metals*, 41-43(1991)983.
472. L. Minkova and M. Nikolova, *Polym. Degrad. Stab.*, 23(1989)217.
473. L. Minkova and M. Nikolova, *Polym. Degrad. Stab.*, 25(1989)49.
474. C. A. Arnold, D. H. Chen, Y. P. Chen, R. O. Waldbauer, M. E. Rogers, and J. E. McGrath, *High Perform. Polym.*, 2(1990)83.
475. J. Wypych, *Polym. Networks Blends*, 2(1992)53.
476. G. Wypych, *Recycling of PVC and Mixed Plastic Waste*, ChemTec Publishing, in press.
477. J. Lemaire, *Report*, PB90-2002482 NTIS, 1989.
478. *Encyclopaedic Dictionary of Commercial Polymer Blends*, Ed. L. A. Utracki, ChemTec Publishing, Toronto, 1994.
479. W. H. Buckalew, *Report*, NUREG/CR-4543.
480. M. E. Abu-Zeid, *J. Appl. Polym. Sci.*, 32(1986)2875.
481. R. Chandra, *Prog. Polym. Sci.*, 11(1985)1.
482. R. P. Singh, *Prog. Polym. Sci.*, 11(1985)201.
483. E. H. Andrews, D. Barnard, M. Braden, and A. N. Gent, *Chemistry and Physics of Rubber-like Substances*, McLaren, London, 1963.
484. R. C. Moakes, *RAPRA J.*, 1975,6,57.
485. C. Adam, J. Lacoste, and J. Lemaire, *Polym. Deg. Stab.*, 32(1991)51.
486. C. Tanielian, R. Mechin, and M. Shakirullah, *J. Photochem., Photobiol. A: Chem.*, 64(1992)191.
487. A. T. Koshy, B. Kuriakose, and S. Thomas, *Polym. Deg. Stab.*, 36(1992).
488. A. L. G. Saad and A. W. Aziz, *Polym. Deg. Stab.*, 41(1993)31.

15

**EFFECT OF POLYMER MORPHOLOGY
ON PHOTODEGRADATION KINETICS**

Chapters 2 and 14 outline the mechanisms of photochemical and photooxidative degradation which involve various polymeric materials. It may be concluded from the discussion in these two chapters that the complex nature of degradation mechanisms is not fully understood. On the other hand, it should be noted that the sequences of reactions, given in these two chapters, are presented without considering the morphology of polymer chains or their segments. Only the chemistry of the degradation process is considered. The organic chemistry of small molecules recognizes the fact that the configuration of the molecule and steric hindrance are essential factors in the reaction mechanisms, similar in importance to the particular chemical bonds that are required for chemical conversion. It is, therefore, obvious that any change in structure or hindering of the active centers by the organization of molecules affects chemical (meaning photochemical and photooxidative) processes to the extent that a complete change of mechanism is possible.

The fringed-micelle model of polymeric texture (Fig. 15.1) was developed as a concept before modern electron microscopes were available. Crystallite sizes estimated from the width of X-ray diffraction rings were in the range of a few tens of nanometers - a size which, at that time, could not be seen under existing microscopes. It is now confirmed that such structures exist. The fragments of polymer chains which form a crystalline entity are very close to each other, and they are held together by the forces of the bonds between them (e.g., hydrogen bonding), which limit their freedom of movement. If bonds hold chains or their segments together, one may safely assume that distances between the chains in the fringed-micelle are very small; therefore, the access of other compounds to this molecular fragment is very difficult. For example, radicals or stabilizers cannot move easily in such an environment.

Parts of the chain, which are not structurally aligned, participate in the formation of an amorphous region which differs from that of the crystalline regions. One difference

between these regions is the freedom of chain movements - restricted in the crystalline area and more free in the amorphous area. Another difference involves the concentration of chain ends: The amorphous part of the polymer has a higher concentration of chain ends (chain ends frequently contain groups which are not typical of the rest of the chain). There is also a difference between the packing densities. These are considerably higher in the crystalline area. Differences between crystalline and amorphous areas result in different reactions in each area.

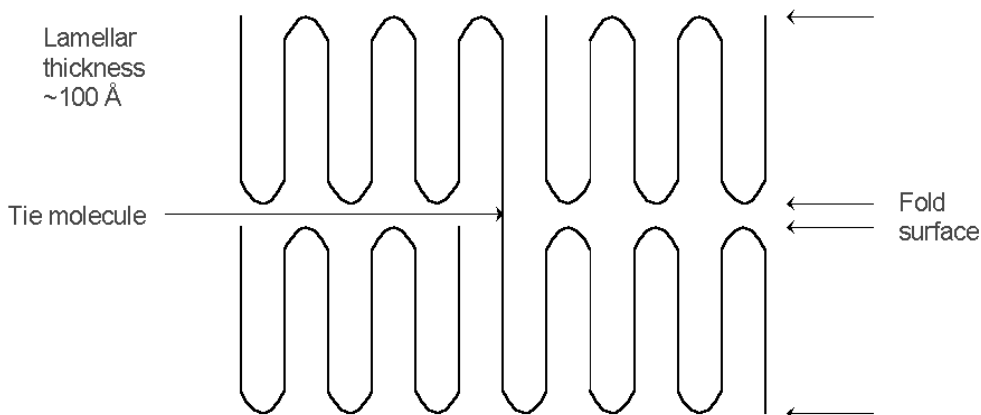
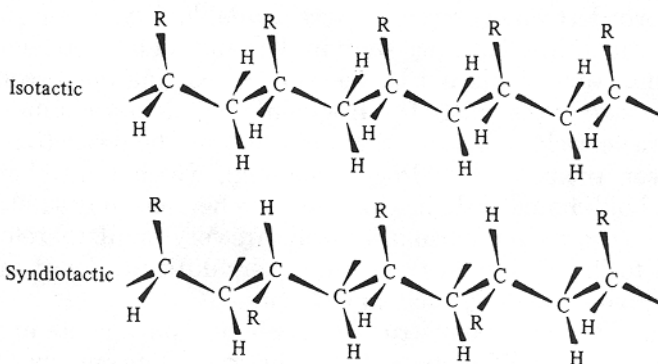
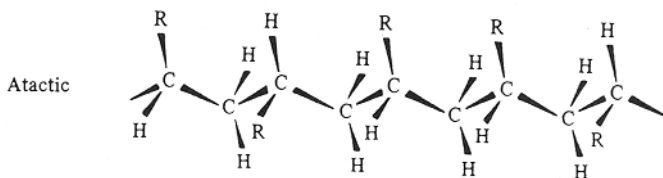


Fig. 15.1. Chainfolded conformation. [Adapted, by permission, from D. C. Bassett. *Principles of polymer morphology*. Cambridge University Press, Cambridge, 1981.]

The formation of a crystalline structure requires that we know more about the structure of the polymer chain. Depending on its internal order, the polymer chain can exist in the following configurations:





The atactic configuration is definitely a disordered form, and it cannot crystallize, as confirmed for polystyrene, polypropylene, and many other polymers. The ability of molecule to crystallize begins with a properly organized, regular configuration of polymer chains. But the chain configuration may either expose or hinder some structural elements of the chain, which may then become more or less reactive.

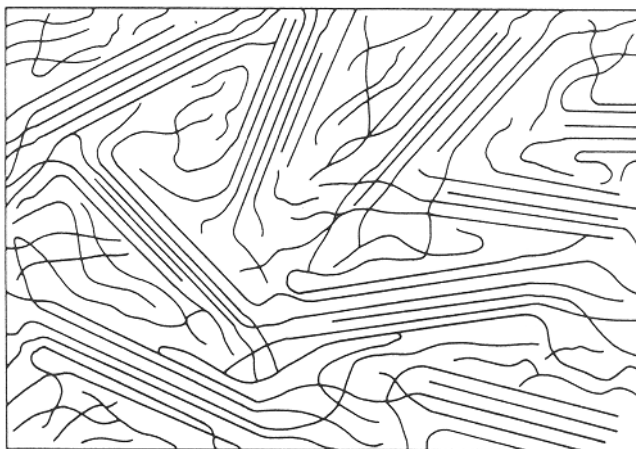


Fig. 15.2. The fringe-micelle model of polymeric texture. [Adapted, by permission, from D. C. Bassett. *Principles of polymer morphology*. Cambridge University Press, Cambridge, 1981.]

Earlier studies prompted Keller¹ to propose lamellae as an element of polymeric texture (Fig. 15.2). Polymers in a lamellae texture are in a chain-folded conformation. A few typical elements of such a structure are: lamellar thickness (usually $\cong 20$ nm), lamellar width ($\cong 5$ μ m), folds, and fold surfaces. The lamellar thickness, the number of folds, and the fold surface area, depend on crystallization temperature. If a polymer property, such as photostability, depends on these texture characteristics, that property will become dependent on the processing parameters which determine polymer texture.

Similarly, the concentration of crystallizing polymer has an effect on the thickness of the crystal. Very dilute solutions give monolayered crystallites; when concentration increases, multilayered crystallites are formed. This may also influence the chemical properties of the material. The other important implication of lamellar structure is that the parallel sections of chain, which form lamellae, have a more restricted motion and less access to other molecules than does the fold surface, which may again cause different behavior. Additionally, chain segments in the fold surfaces have a different configurations which may influence segmental reactivity.

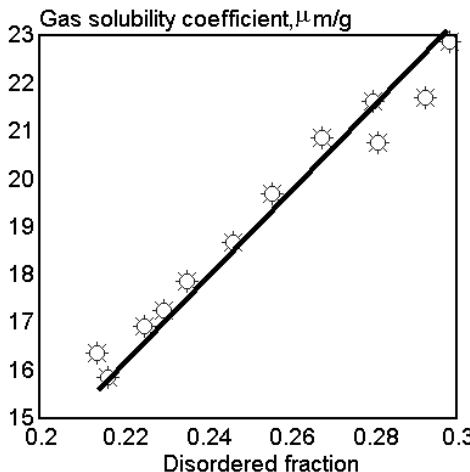


Fig. 15.3. Gas solubility coefficient in melt-crystallized polyethylene vs. disordered fraction. [Data from N. G. McCrum and P. N. Lowell, *J. Polym. Sci., Polym. Phys. Ed.*, 5(1967)1145.]

A few simple chemical experiments provide evidence of the different reactions in the amorphous and crystalline regions. Polyethylene treated with fuming nitric acid yields lamellar fragment. Nitric acid apparently penetrates and removes fold surfaces and interlamellar regions before it attacks the crystalline structure. The rate of material digestion and the selectiveness of the process depends on acid concentration. The experiment confirms that the amorphous region is more penetrable than the crystalline region. Similarly, the solubility of gas depends on the amount of amorphous fraction in the polyethylene (Fig. 15.3). This shows that if gases, liquids, radicals, stabilizers, etc. are expected to react in a particular system, they will react at sites which they are able to penetrate, namely fold surfaces or

amorphous regions. Indeed, the chlorination of poly(4-methyl-pentene-1) or the bromination of polyethylene occur preferentially in the fold surface region.

An experiment involving the diffusion of ozone into a polyethylene matrix shows that most terminal double bonds in polyethylene chains can be found in the interlamellar spaces. This is not unexpected, since chains protrude from the fold surfaces or form fringes in the micellar structures.

There is another important aspect of these studies. Treatment with fuming nitric acid rapidly converts polyethylene to a brittle powder. This shows that material removed, which is not brittle (the amorphous fraction), is responsible for connecting these brittle fragments and thus for the material's elastomeric properties. This mechanism explains environmental stress cracking, which causes the failure of some materials when exposed to organic chemicals. Morphological studies revealed that polymer,

heated over its melting point then cooled, forms a crystalline structure in the same locations where it was crystalline before melting which means that the seeds of crystallization are not lost when the polymer is melted. Only prolonged heating removes this memory. New crystallization centers are created due to the polymer degradation which can occur during extended heating. The memory of crystallite distribution can also be removed if the melted polymer is dispersed in the form of small droplets, which may cause the seeds of crystallization to lose their relative location. This shows that the structure of the material imposes certain restrictions on its crystallization behavior.

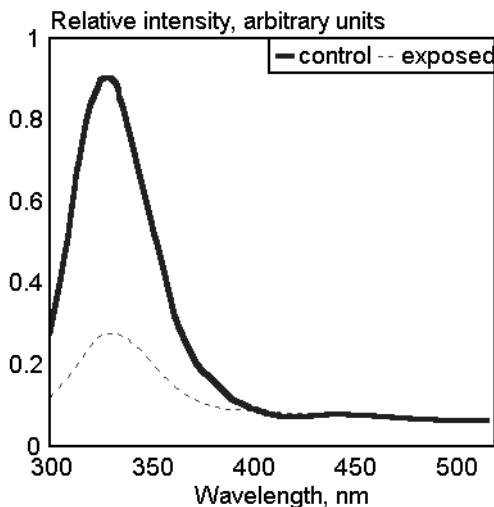


Fig. 15.4. Fluorescence spectra of annealed 1,12-dodecanediol PU before and after photolysis at 300 nm for 25 min. [Adapted, by permission, from C. H. Hoyle and K. J. Kim, *The effect of crystallinity and flexibility on the photodegradation of polyurethanes, Report, ADA 172619.*]

Electron microscopy, has, over the years, provided enough data to suggest that the degradation of polymers exposed to radiation is morphology specific. Thus, it is important to consider the polymer morphology when interpreting the results of degradation. The only question is, how far we are able, with existing knowledge, to include polymer morphology in the overall picture of degradative changes. Fig. 14.40 shows that the rate of gel formation in amorphous polyurethane is higher than in a semicrystalline (annealed) sample. X-ray analysis of these samples revealed that the annealed sample has a sharp-ring diffraction pattern, whereas the quenched specimen (amorphous) has a diffuse pattern. Similarly, their DSC patterns indicate that the annealed specimen has a crystalline structure. Fig. 15.4 shows emission spectra of the annealed specimen (semicrystalline) which should be compared with Fig. 15.5 for the quenched (amorphous) specimen.

Semicrystalline material has only one emission maximum at around 350 nm, whereas the amorphous sample also has a 350 nm emission maximum before irradiation and a second emission maximum at about 420 nm after irradiation. The fluorescence decay analysis of the photolyzed film indicates the presence of two major components with lifetimes 10.8 ns and 2.8 ns. Hoyle and Kim³ assign these components to the emission from a product of an ortho photo-Fries rearrangement (10.8 ns) and an unsubstituted arylamine cleavage (2.8 ns). The studies of fluorescence decay of model compounds confirm that this assignment is correct. From these results, it can be postulated that the

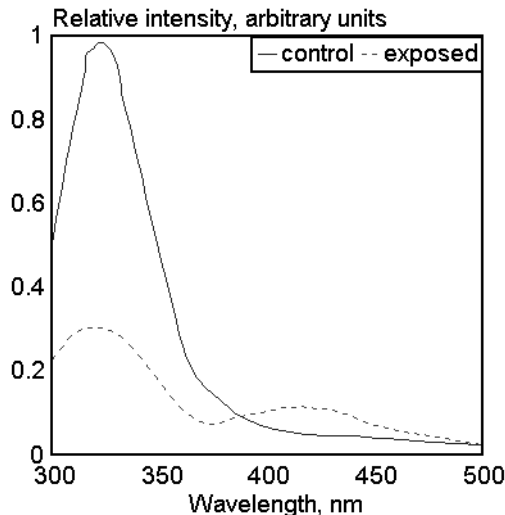


Fig. 15.5. Fluorescence spectra of quenched 1,12-dodecanediol PU before and after photolysis at 300 nm for 20 min. [Adapted, by permission, from C. H. Hoyle and K. J. Kim, The effect of crystallinity and flexibility on the photodegradation of polyurethanes, *Report*, ADA 172619.]

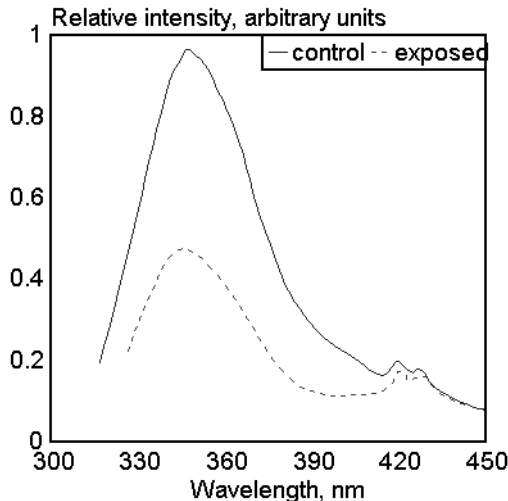


Fig. 15.6. Fluorescence spectra of stiff polyurethane before and after photolysis at 300 nm for 40 min. [Adapted, by permission, from C. H. Hoyle and K. J. Kim, The effect of crystallinity and flexibility on the photodegradation of polyurethanes, *Report*, ADA 172619.]

photo-Fries rearrangement is typical of amorphous material. Further studies by the same authors, concern the effect of chain flexibility on photolysis of MDI-based polyurethanes. It is well-known that polyurethanes consist of hard and soft blocks. The soft blocks in the study have a polyether backbone of a varying number of repeated units.

Fig. 15.6 shows the emission spectrum of the polyurethane film with a short soft block. Compare this to Fig. 15.7, which presents similar data for the polyurethane film having a longer soft block. Both spectra have similar characteristics to those included in Figs. 15.4 and 15.5, respectively, meaning that the polyurethane sample which has the longer soft block (more flexible chain) has a strong emission at about 420 nm. This indicates that increased chain flexibility promotes the photo-Fries rearrangement. Fujiwara and Zeronian⁴ studied the formation of cracks on photodegraded polyamide-6 filaments (amorphous), drawn filaments (semicrystalline), and drawn filaments extracted with methanol (extraction removes low molecular weight oligomer). The conditions of degradation included UV irradiation from a source having a wavelength longer than 250 nm both in the presence of moisture and in a dry environment. Fig. 15.8 shows that, while all drawn samples exhibit shrinkage, the undrawn sample expands when exposed to heating. Additionally, Fig. 15.8 shows that hot methanol extraction also relaxes

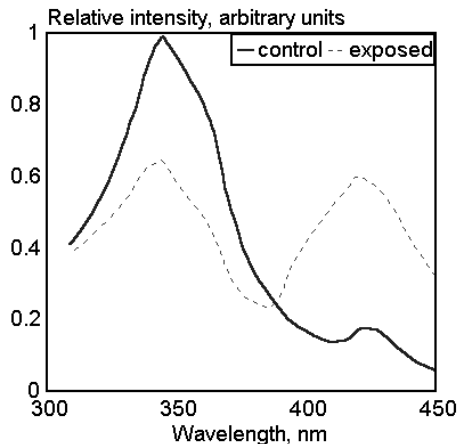


Fig. 15.7. Fluorescence spectra of flexible polyurethane before and after photolysis at 300 nm for 40 min. [Adapted, by permission, from C. H. Hoyle and K. J. Kim, The effect of crystallinity and flexibility on the photodegradation of polyurethanes, *Report*, ADA 172619.]

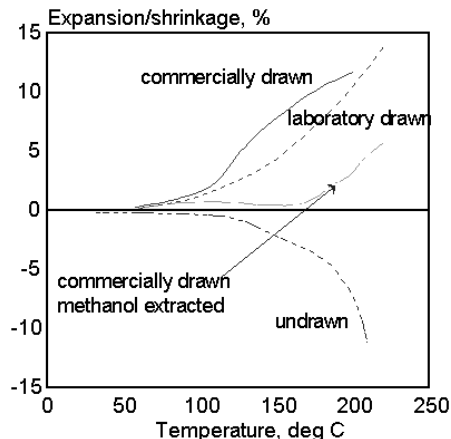


Fig. 15.8. Effect of drawing on TMA curve of polyamide-6 filaments. [Adapted, by permission, from Y. Fujiwara and S. H. Zeronian, *J. Appl. Polym. Sci.*, 27(1982)2773.]

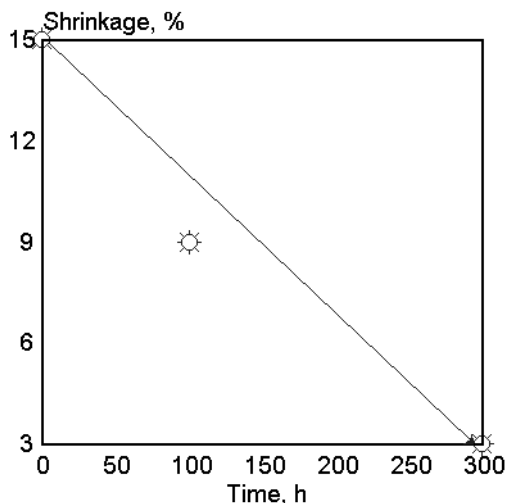


Fig. 15.9. Effect of UV degradation time on TMA shrinkage. [Data from Y. Fujiwara and S. H. Zeronian, *J. Appl. Polym. Sci.*, 27(1982)2773.]

the material in filaments because the extent of shrinkage decreases. After 300 h of exposure, extracted drawn filaments did not have any surface cracking, while drawn filaments were severely cracked. Only after 600 h of exposure did extracted drawn filaments reach the extend of cracking of non-extracted drawn filaments. The undrawn specimen did not crack at all during exposure (600 h).

There was a substantial difference in mechanical properties of these specimens - the undrawn specimen was highly degraded and easily broken when touched. The drawn specimens were cracked but retained at least part of their initial mechanical properties. The authors suggested that cracking is mostly a surface-related phenomenon which occurs in the amorphous regions. Photodegradation leads to chain scission,

probably occurring in tie molecules (chains which connect neighbouring lamellae), which permits the movement of polymer chains and allows retraction to occur after a sufficient amount of chain scission has occurred. Filament shrinkage changes as degradation progresses (Fig. 15.9). This shows that shrinkage is reduced by the relaxation of stress in the filament through scission of tie molecules and formation of cracks. When water is present in the polymer, it may act as a plasticizer to increase chain mobility which would explain the increased crack vulnerability of wetted polymers.

Gooden⁵ studied the photochemistry of poly[ethylene-co-(carbon monoxide)] and the effect of radiation exposure on elongation and crystallinity. He too, found that specimen irradiation resulted in an increase in crystallinity (Fig. 15.10). The degradation of a specimen prior to its exposure to UV leads to the formation of a monoclinic form and a reduction in crystallite size (Fig. 15.11). Morphological changes affect the diffusivity and solubility of smaller molecules in the polymer as well as other physical properties.

As a result of morphological changes in the material, chemical mechanisms are also changed. Degradation of unelongated samples occurs mainly by the Norrish type II mechanism rather than the Norrish type I in elongated samples. These differences are due to the fact that the orientation inhibits the ability of polymer chains to twist into the conformation necessary for the type II scission. Norrish type I processes occur 3 times

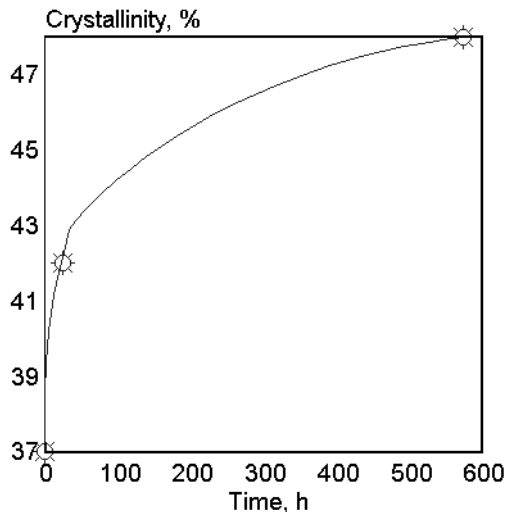


Fig. 15.10. The effect of UV radiation on the crystallinity of poly[ethylene-co-(carbon monoxide)]. [Data from R. Gooden, D. D. Davis, M. Y. Hellman, A. J. Lovinger, and F. H. Winslow, *Macromolecules*, 21(1988)1212.]

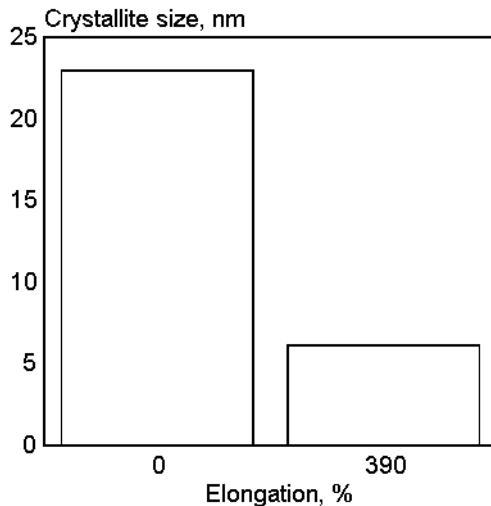


Fig. 15.11. The effect of UV radiation on crystallite size of poly[ethylene-co-(carbon monoxide)]. [Data from R. Gooden, D. D. Davis, M. Y. Hellman, A. J. Lovinger, and F. H. Winslow, *Macromolecules*, 21(1988)1212.]

faster in drawn film and Norrish type II processes are 8 times slower than in undrawn film. This detailed study shows that conclusions about the effect of polymer morphology on photochemical mechanisms and on the rate of the photochemical process should be drawn with caution since total crystallinity is not the only parameter which should be considered when interpreting the data. Crystallite size, the type of crystalline structures, and their effect on conformation also need to be known.

Polyolefins get a lot of research attention because they are photolytically unstable. Their properties also depend to a great extent on their crystallinity. It has long been known that branched polyethylene oxidizes faster than linear polyethylene, and it has been discovered that its oxidation rate is roughly proportional to the amount of amorphous fraction present. This suggests that the oxidation of semicrystalline polyethylene is restricted to its amorphous region. It was subsequently discovered that the crystalline region absorbs practically no gas which implies that oxygen is simply not available in the crystalline region. The crystallinity of polyethylene depends on the configuration and the conformation of the polymer chain and relates to the conditions of polymerization and to the rate of cooling from the molten state. Also, as reported above for other polymers, the crystallinity of polyethylene increases during the photodegradation process.

Polyethylene of low crystallinity has a high rate of carbonyl formation and a low concentration of radicals. The carbonyl formation rate increases as crystallinity decreases because it is an oxidative process which must occur almost exclusively in the amorphous regions. In material of low crystallinity, the chains have increased segmental mobility and radicals can react with oxygen faster. In highly crystalline materials, radicals participate more readily in recombination reactions.

Busfield and Monteiro⁶ explain creep results based on PE tapes morphology. PE tapes under tensile stress degrade faster than those with no stress imposed. PE tape consist of crystalline regions and amorphous regions. The role of the crystalline region is to supply integrity and strength. The amorphous region confers flexibility. During creep experiments the amorphous component uncoils and the taut tie molecules become increasingly stretched until they yield to the extensive force. Material then loses the integrity of both its components. This explanation is relevant for all materials under stress.

Ohtani *et al.*⁷ introduced extra-fine particles of TiO₂ into PE. This film, after exposure to UV radiation, was studied by X-ray diffraction and TEM. TiO₂ particles were distributed in amorphous region, the extent of which gradually decreased during exposure. At the same time, large voids (about 1000 nm) appeared in the amorphous region. This experiment shows that fillers catalyze the degradation of the amorphous phase.

The influence of its morphology on polyethylene degradation is generally representative of its effect on most other polymers. Polypropylene, which can be considered as a very densely branched polyethylene, seems not always to confirm previous findings. For example, polypropylene of higher density (higher crystallinity) degrades faster on UV

exposure than that of lower density. Also, polymers of low atactic content (higher crystallinity) degrade faster than those having more atactic segments. Similarly, more carbonyl groups are formed in isotactic than atactic polypropylene. All the above differ from the case of polyethylene. The explanation of this behavior is related to its spherulitic structure. Polypropylene has at least two crystalline modifications: stable monoclinic units and less stable hexagonal units. Overall stability depends on the proportion of each crystalline form. Polyethylene is composed of a well-ordered crystalline phase dispersed in a less rigid amorphous phase. An increase in the crystalline phase leads to increased stability. The contrast in behavior between polyethylene and polypropylene is not surprising; similar observations were also reported for poly[ethylene-co-(carbon monoxide)].

In ethylene-propylene copolymers, crystallinity changed during irradiation. First crystallinity decreased then increased. These results can be explained by the formation of short chain oligomers which are sufficiently mobile to move into the amorphous phase and crystallize.⁸

Vigier and Tatibouet⁹ compared the behaviors of amorphous and semi-crystalline PET. In semi-crystalline PET, the amorphous zone between the crystalline lamellae was very thin (estimated 3.5 nm). It is probable that most chains in the amorphous zone originate in the adjacent crystalline lamellae. It was noted that the mobility of these chains was drastically reduced compared with the mobility of similar chains in the bulk of fully amorphous PET. Thus, in modelling degradation patterns, the information gathered from studies of amorphous PET could not be applied to model amorphous regions in semi-crystalline PET.

Behnisch and Zimmermann¹⁰ summarize existing literature on the effect of conformation on PVC degradation. For more than 20 years, there has been agreement that PVC chain conformation affects its stability.^{11,12}

A review of the paper by Schurz et al.¹³ titled "Structural studies on polymers as prerequisites for degradation" serves as the conclusion to this chapter. These authors were interested in explaining differences between biodegradation of natural and regenerated cellulose. Because these materials are morphologically more complex than any synthetic polymers, polypropylene was chosen as a model for evaluation of the effect of morphology on the material performance. Figs. 15.12 and 15.13, respectively, show wide-angle x-ray scattering profiles and background scattering of an injection molded sample of polypropylene. Fig. 15.12 shows the distribution of crystalline structures in the specimen. Starting at the front (the scattering axis side), there is a thin layer which has very low crystallinity, followed by a highly crystalline layer, then rather amorphous center. The other side (the back) of the sample presents a mirror image. The amorphous area on the surface is formed by the mold which provides a rapid heat exchange (a high cooling rate). The next layer (highly crystalline) is cooled by the first layer which, because it is a thermal insulator, allows for slow crystalline growth. Thus, this layer con-

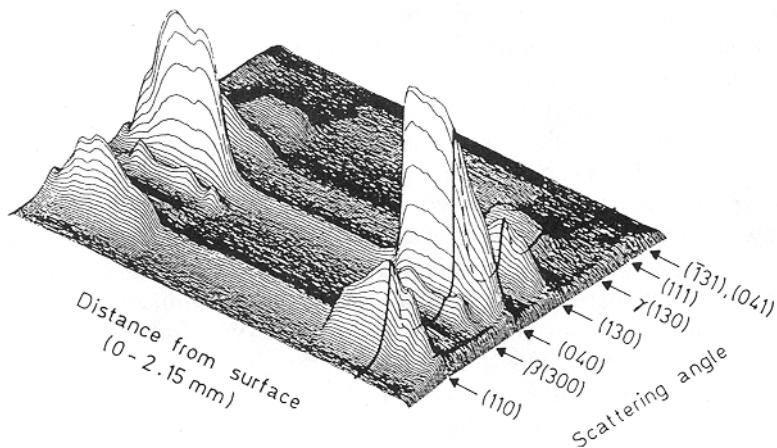


Fig. 15.12. Cross-section of PP specimen (2 mm thick) wide-angle x-ray scattering plotted vs. the scattering angle. [Adapted, by permission, from J. Schurz, P. Zipper, and J. Lenz, *J. Macromol. Sci., Pure Appl. Chem.*, A30(1993)603.]

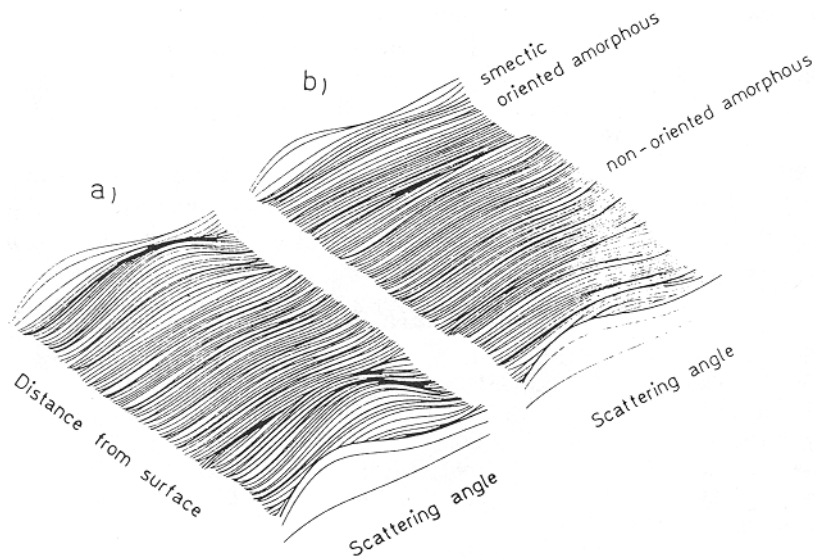


Fig. 15.13. Cross-section of PP specimen (2 mm thick) wide-angle x-ray background scattering plotted vs. the scattering angle. [Adapted, by permission, from J. Schurz, P. Zipper, and J. Lenz, *J. Macromol. Sci., Pure Appl. Chem.*, A30(1993)603.]

tains large crystallites. The reference to Fig. 15.13 helps to explain what happens in the core of the specimen. This figure shows that the layers adjacent to mold walls have a high orientation compared with the non-oriented core of the specimen. This orientation is due to other processes occurring when the mold is filled with melted PP. During filling, material is under high shear close to the walls of the mold and at very low shear in the center. High shear produces a high degree of orientation. This lack of orientation in the core hinders crystallization and therefore material in the core has the amorphous structure shown in Fig. 15.12. These data help in understanding of the various phenomena observed during degradation. In this particular specimen, the surface is composed of amorphous material which will degrade faster (this condition is relevant to this particular method of sample preparation and material type and should not be extrapolated to all specimens used in weathering). The specimen also has an inhomogeneous distribution of crystallites under its skin which results in non-homogeneous internal stress distribution which, in turn, should result in cracking. The morphology of the specimen is determined by the method of sample preparation selected. So the sample preparation method strongly influences the degradative process and, as these authors emphasize, knowledge of polymer structure is a prerequisite to carrying out degradation studies. Polymer morphology may, in some cases, be a greater influence on degradation than its chemical structure or composition. This paper shows, in fact, that morphology influences the degradation rate of all polymeric materials. Experiences from one material can be used to understand another (as authors did to evaluate effect of morphology on cellulose and wood cell wall) providing that the fundamental physical meaning is extracted from the experimental information.

Although the available data are not extensive they offer consistent explanation for degradation phenomena. The reader interested in this subject should also consult Chapter 11, which contains information on the effect of stress on material photolytic stability.

REFERENCES

1. A. Keller, *J. Polym. Sci.*, 39(1959)151.
2. N. G. McCrum and P. N. Lowell, *J. Polym. Sci., Polym. Phys.*, 5(1967)1145.
3. C. H. Hoyle and K. J. Kim, The Effect of Crystallinity and Flexibility on Photodegradation of Polyurethanes, *Report*, ADA 172169.
4. Y. Fujiwara and S. H. Zeronian, *J. Appl. Polym. Sci.*, 27(1982)2773.
5. R. Gooden, D. D. Davis, M. Y. Hellman, A. J. Lovinger, and F. H. Winslow, *Macromolecules*, 21(1988)1212.
6. W. K. Busfield and M. J. Monteiro, *Mater. Forum*, 14(1990)218.
7. B. Ohtani, S. Adzuma, S. Nishimoto, and T. Kagiya, *Polym. Deg. Stab.*, 35(1992)53.
8. R. Mani, R. P. Singh, S. Sivaram, and J. Lacoste, *Polym. J.*, 26(1994)1132.
9. G. Vigier and J. Tatibouet, *Polymer*, 34(1993)4257.
10. J. Behnisch and H. Zimmermann, *Intern. J. Polym. Mater.*, 16(1992)143.
11. J. Wypych, *PVC Degradation*, Elsevier, 1985.

-
12. J. Wypych, *PVC Stabilization*, Elsevier, 1986.
 13. J. Schurz, P. Zipper, and J. Lenz, *J. Macromol. Sci., Pure Appl. Chem.*, A30(1993)603.

16

EFFECT OF ADDITIVES ON WEATHERING

Additives are commonly used with processed polymers, often constituting more than 50% of the total composition. Although their effect on weathering resistance has either been demonstrated in service or predicted based on theoretical assumptions, the number of weathering studies related to additives effect is rather small.¹⁻³⁷ This is most probably because of the more pressing need to study polymers, which are the components most responsible for the essential physical properties and material durability. The discussion below therefore includes only the limited scope of additives used by industry for which references can be found in literature.

Titanium dioxide, the white pigment used in many products, is probably the best studied additive. When titanium dioxide is irradiated with radiation wavelength less than 405 nm, the absorbed energy is sufficient to promote electrons from the valence band to the conduction band. Positive holes are formed in the valence band with both holes and electrons able to move within the crystal lattice. During such movement, some holes and electrons will recombine, but these available on the crystal surface can initiate chemical reactions. Electrons may combine with oxygen forming radicals, whereas positive holes combine with hydroxyl groups, forming hydroxyl radicals. These radicals may then react with organic matter or water, initiating a radical reaction chain. In order to limit possibility of such a reaction, producers of titanium dioxide pigments developed methods to promote recombination reactions. This is done either by using admixtures of transition metals (zinc or aluminum) or by coating TiO₂ particles with alumina or silica. The presence of transition metals acts as a recombination center for both electrons and holes. Coating helps to destroy the hydroxyl radicals by facilitating their recombination to water and oxygen. Such measures improve the quality of titanium dioxide but they are not able to completely eliminate radical formation.

The stabilizing effect of pigments added to polymers is discussed in Chapter 18. Considering the fact that titanium dioxide plays the dual role of stabilizer and sensitizer, one may anticipate that its effect depends not only on the type and quality of

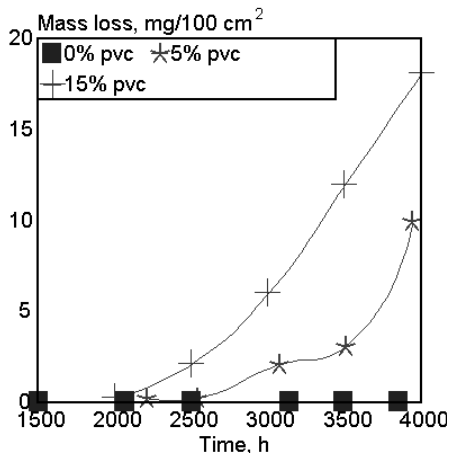


Fig. 16.1. Mass loss in the case of durable binder vs. exposure time relative to pigment load. [Adapted, by permission, from L. A. Simpson, *Austral. OCCA Proc. News*, 20(1983)6.]

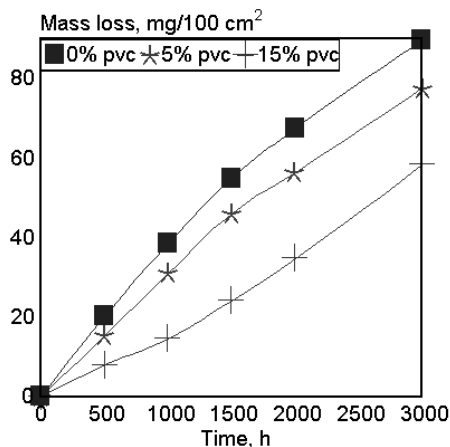


Fig. 16.2. Mass loss in the case of non-durable binder vs. exposure time relative to pigment load. [Adapted, by permission, from L. A. Simpson, *Austral. OCCA Proc. News*, 20(1983)6.]

titanium dioxide but also on the properties of the binder (polymer). Figs. 16.1 and 16.2 show the effect of titanium dioxide on mass loss during the weathering of a durable and a non-durable binder. The durable binder is sufficiently stable to withstand weathering without the need for UV stabilization. The addition of titanium dioxide causes formation of free radicals in the vicinity of its crystals in the binder, which triggers rapidly accelerating degradative changes leading to the decreased weather stability of the material. A non-durable binder (Fig. 16.2) is also the subject of radical formation in the vicinity of titanium dioxide particles but the protective effect of the pigment is sufficient to offset the negative effect of radical process, resulting in a net improvement in weather stability of the material. Since most of the changes in the material occur around titanium dioxide particles, eventually the binder is sufficiently eroded to cause pigment and binder separation or chalking (Fig. 16.3).

Different grades of titanium dioxide produce different effects. The mechanism of chalking described by Fig. 16.3 results in changes in material gloss, as can be seen in Figs. 16.4 and 16.5. Both durable and non-durable binder respond to an increasing concentration of titanium dioxide in similar ways.

Other parameters affect how titanium dioxide participates in degradative processes. In the non-durable binder, titanium dioxide acts to screen the binder from UV radiation. The efficiency of screening depends on the degree to which TiO₂ is dispersed. Flocculated pigment has a lower screening power, as seen from Figs. 16.6 and 16.7. Less flocculated pigments inhibit both gloss deterioration and mass loss of the material.

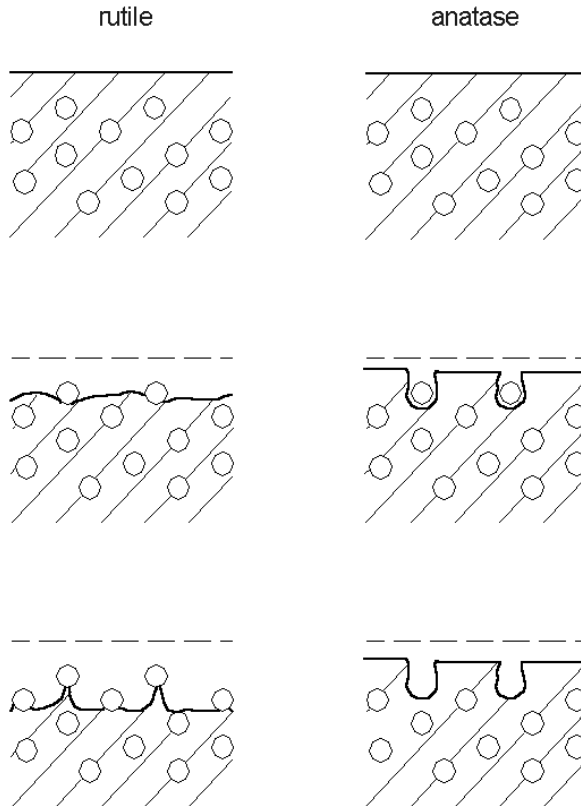


Fig. 16.3. Model of binder degradation. [After J. H. Braun, *Prog. Org. Coat.*, 15(1987)249.]

The temperature at which degradation occurs is also an important factor (Fig. 16.8). Gloss is better retained when samples are irradiated at lower temperatures. This suggests that the rate of formation of free radicals is controlled by two processes: photon absorption; reaction of the excited species followed by radical formation. The quantum efficiency of radical formation is reduced when radicals recombine. Because radicals are formed within rigid matrix, it is difficult for them to escape (the cage escape efficiency reduced). At low temperatures, the matrix is more rigid than at high temperatures and recombination is the more probable outcome. Around T_g , cage escape efficiency is rapidly reduced.

The effect of pigment properties on photochemical activity is shown in Fig. 16.9. Surface passivated titanium dioxide (RL90) and CdS both decrease the amount of car-

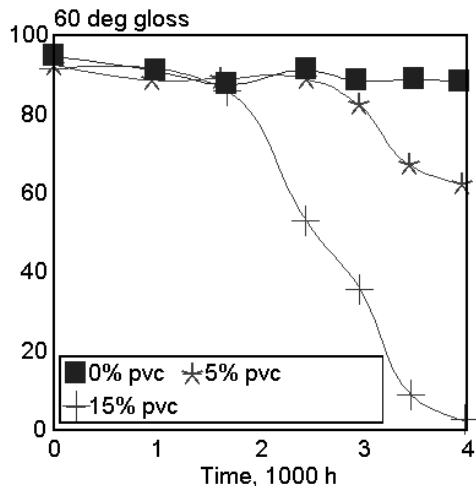


Fig. 16.4. Gloss change in the case of durable binder vs. exposure time relative to pigment load. [Adapted, by permission, from L. A. Simpson, *Austral. OCCA Proc. News*, 20(1983)6.]

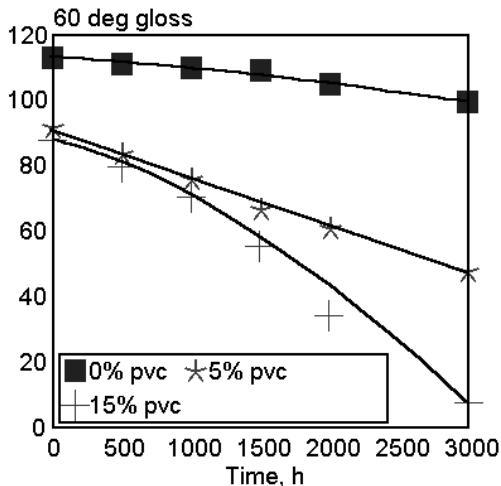


Fig. 16.5. Gloss change in the case of non-durable binder vs. exposure time relative to pigment load. [Adapted, by permission, from L. A. Simpson, *Austral. OCCA Proc. News*, 20(1983)6.]

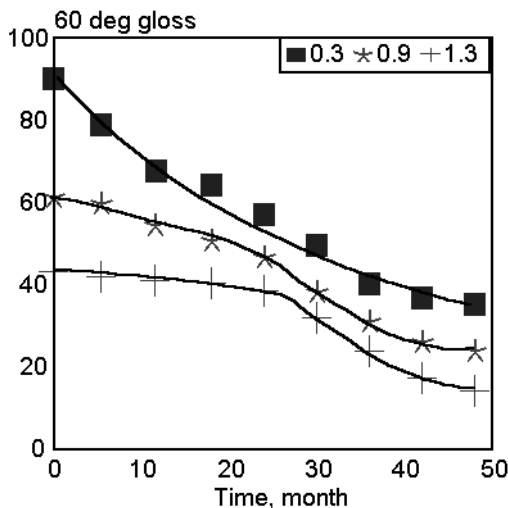


Fig. 16.6. Gloss change vs. exposure time relative to flocculation gradient. [Adapted, by permission, from L. A. Simpson, *Austral. OCCA Proc. News*, 20(1983)6.]

bonyl group formation as the concentration of pigment increases. ZnO and untreated titanium dioxide also contribute to a decrease in carbonyl group formation but only at low concentrations. Above a certain level each cause a rapid increase in the formation of carbonyl groups. Treated TiO₂ and CdS have poor photocatalytic activity and they participate in photodegradative processes by actively screening radiation. In the first part of the curve (Fig. 16.9), there is a very low quantum yield of photocatalysis due to electron-hole recombination and ZnO and untreated TiO₂ provide screening at low concentrations. At higher concentrations, their photocatalytic effect becomes predominant and carbonyl concentration increases. On the other hand, ZnO has long been known to stabilize some polymers (Fig.

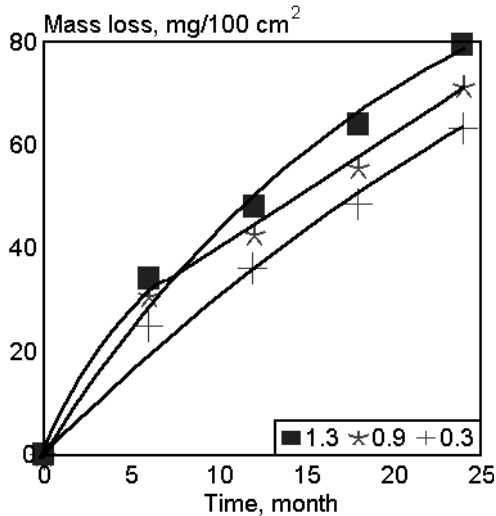


Fig. 16.7. Mass loss vs. exposure time relative to flocculation gradient. [Adapted, by permission, from L. A. Simpson, *Austral. OCCA Proc. News*, 20(1983)6.]

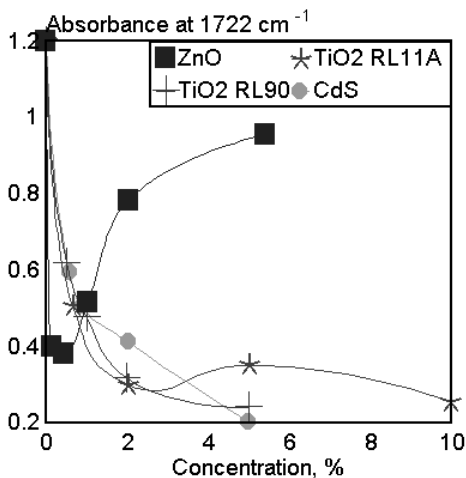


Fig. 16.9. Carbonyl content in photooxidized EP copolymer film vs. pigment concentration (irradiation 260 h, 300 nm). [Adapted, by permission, from J. Lacoste, R. P. Singh, J. Boussand, and R. Arnaud, *J. Polym. Sci., Polym. Chem.*, 25(1987)2799.]

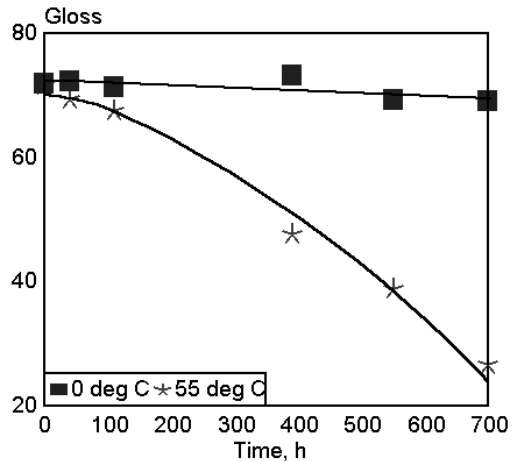


Fig. 16.8. Gloss of TiO₂ pigmented coating vs. exposure time in a modified QUV-like weathering chamber at different temperatures. [Adapted, by permission, from J. L. Gerlock, D. R. Bauer, L. M. Briggs, and J. K. Hudgens, *Prog. Org. Coat.*, 15(1987)197.]

16.10). No photo-catalytic influence of TiO₂ and ZnO was detected by UV and IR spectra during PVC degradation.²⁹ The tensile strength of the material and other mechanical properties were better preserved when pigment, regardless of the color, was added. Studies of fourteen iron oxide pigments in a PVC matrix showed that pigments, which have a large inherent ESR spectrum strength, have poor weatherability.⁵ PVC plates with an ESR spectrum strength lower than 1 exhibited very good weatherability, equivalent to five years of outdoor exposure. The type of pigment used in PC greatly influenced the UV stability of the polymer (Fig. 16.11). Gerlock *et al.*¹ studied the effect of initiator concentration, used in an acrylic copolymer synthesis, on the UV stability of products. Nitroxide decay assay

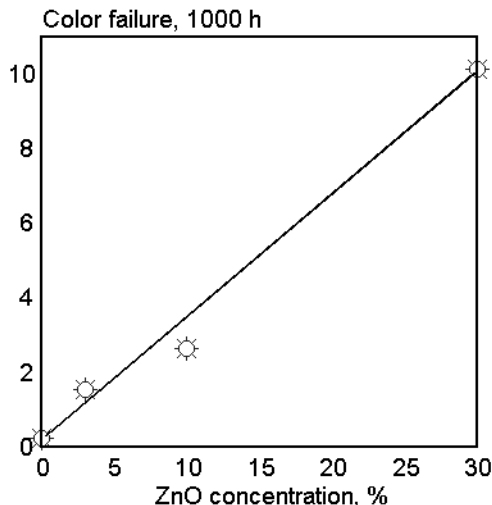


Fig. 16.10. Effect of ZnO on UV stability of plasticized PVC. [Data from B. D. Gupta and J. Verdu, *J. Polym. Eng.*, 8(1988)81.]

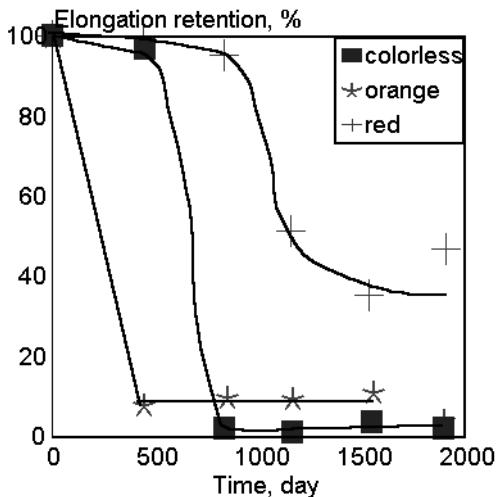


Fig. 16.11. Elongation retention vs. time of natural exposure of colored PC. [Adapted, by permission, from B. Dolezel and L. Adamirova, *Plast. Kauc.*, 20(1983)18.]

was the method used (Fig. 16.12). Photoinitiation rate increases with the concentration of initiator. In experiments, two initiators (cumene hydroperoxide and *t*-butylperbenzoate) were used, showing that the type of initiator was not as critical as its concentration.

Klemchuk¹⁸ conducted broad studies on the effect of pigments and TiO₂ on the degradation and stabilization properties of polymer matrices. These properties are important: dispersibility, light absorbing characteristics, semi-conductor properties, metal content, influence on polymer matrix, surface properties, composition of products of degradation. This list could be expanded to include: pigment surface area, absorption of components of matrix (e.g., stabilizers), wavelength of emitted radiation by pigment on energy absorption, generation of singlet oxygen, hydrogen abstraction, effect on polymer morphology (some pigments interfere in crystallization), interaction with polymer, etc. The way in which a pigment interacts with the polymer network is known to have an effect on the UV stability of the material but this effect can vary widely. For example, the stability of a composition to radiation at 375 nm can be increased by increasing pigment concentration. But there are also exceptions. Ultramarine blue increases durability of PP by 75% but does not absorb UV. TiO₂ has an absorption of UV similar to channel black but only a fraction of its stabilizing activity. Some types of dyes, such as, for exam-

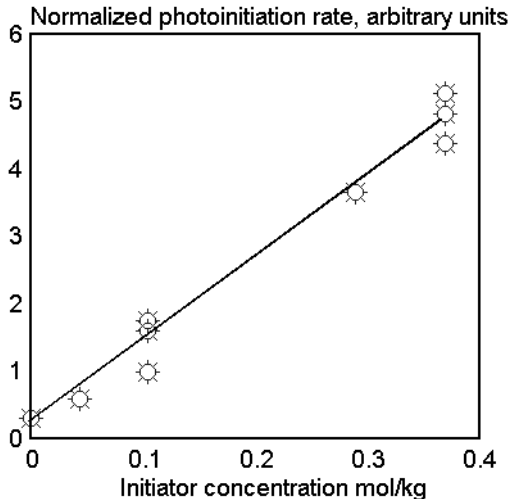


Fig. 16.12. Normalized photoinitiation rate vs. initiator concentration in coatings. [Adapted, by permission, from J. L. Gerlock, D. R. Bauer, L. M. Briggs, and J. K. Hudgens, *Prog. Org. Coat.*, 15(1987)197.]

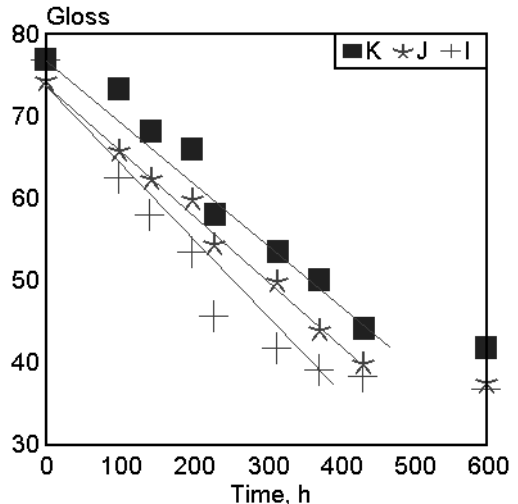


Fig. 16.13. Gloss of coatings vs. exposure time in QUV. [Adapted, by permission, from J. L. Gerlock, D. R. Bauer, L. M. Briggs, and J. K. Hudgens, *Prog. Org. Coat.*, 15(1987)197.]

ple, azo condensation yellow, red and orange are known to decrease the stability of some polymers (e.g., PP fiber). In some polymers (e.g. PVC) most pigments (especially inorganic and carbon black) considerably increase durability. Phthalocyanine blue is a relatively good stabilizer of PP fiber but a rather poor pigment for PVC. Some dyes behave quite differently in low relative humidity than in moisture close to saturation. These examples show that there is a substantial amount of work to be done to explore the very wide range of pigment, dye, and polymer combinations.

The addition of CaCO_3 to PP causes a slight reduction in carbonyl formation.¹⁶ The efficiency of some antioxidants, such as Irganox 1010, was found to be reduced by the presence of CaCO_3 . In another study,²⁶ PP stability was increased by the addition of CaCO_3 especially in combination with small addition of TiO_2 (0.5%) or HALS. In polyurethanes, it was discovered that CaCO_3 acts as a heat sink.³³

The typical concentrations of silica do not affect radical decay, during the degradation of PMMA by UV, nor is radical composition affected.²⁰ Large additions (above 50%) of silica modify the material structure due to matrix absorption on the silica surface which also increases radical decay rate.

Fig. 16.13 shows the gloss retention of coatings. Samples J and K (in xylene) differ from sample I (in 2-heptanone). This figure shows that UV stability is a multidimen-

sional property which depends on a great number of interrelated parameters. An initiator, in radical form, can abstract hydrogen from either solvent. The radical thus formed is likely to be incorporated as an end-group in the copolymer. An ketonic end-group is a more photoactive source of free radicals than a benzyl end-group. Additionally, cumene hydroperoxide may decompose to acetophenone and a methyl radical, either of which will affect the photodegradation rate. The effect of solvent on the degradation rate goes beyond factors involving its chemical composition or its ability to form radicals or UV absorbing groups. It can also increase chain mobility, which increases the probability of a reaction occurring. These effects are discussed in more detail in Chapter 15.

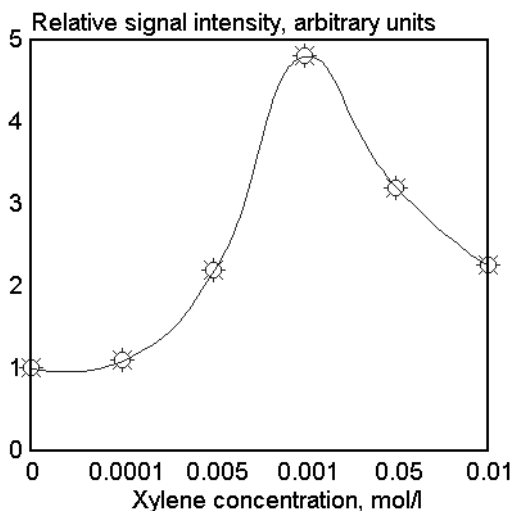


Fig. 16.14. Spectral intensity of n-octane radical formed during irradiation of PE at -196°C for 30 min vs. concentration of p-xylene. [Adapted, by permission, from H. Kubota and M. Kimura, *Polym. Deg. Stab.*, 38(1992)1.]

Fig. 16.14 shows the effect of p-xylene on ESR signal. This is as a result of n-octane radical formation during the degradation of PE.²² The effect of p-xylene is larger than that of phenanthrene sensitizer. The p-xylene radicals contribute to abstraction of hydrogen in the α -position to double bonds which results in the formation of allyl radicals. Thus, p-xylene is a photoinitiator of PE degradation. Solvent type and concentration affect the rate of ultrasonic degradation of PS.²⁸ The degradation rate constant increases as the polymer-solvent interaction parameter decreases. PVC films were prepared from solutions in tetrahydrofuran and dichloroethane and subsequently removed by thermal treatment.³⁶ Thermal treatment caused PVC degradation which was monitored by double bond formation. Exposure of these samples showed that a higher degradation rate was caused by the prior thermal degradation.

Capocci¹² describes the effect of peroxide concentration in the polyol on the yellowness index of a polyurethane made from it (Fig. 16.15). A high yellowness index indicates a high concentration of chromophores. This, in turn, means that, if these chromophores are present before exposure, the polyurethane, when exposed to radiation, will degrade more rapidly because of the inherently higher absorptivity. The initial color depends not only on peroxide concentration but also on the type and the amount of amine catalyst

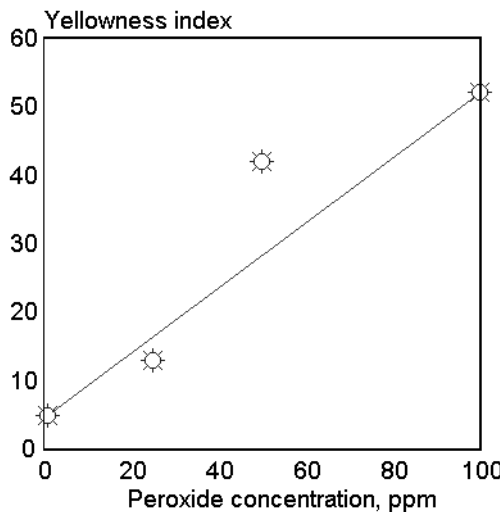


Fig. 16.15. Effect of peroxide concentration in polyether polyol on the initial color of polyurethane. [Data from G. Capocci, *Plast. Compd.*, 10(1987)13.]

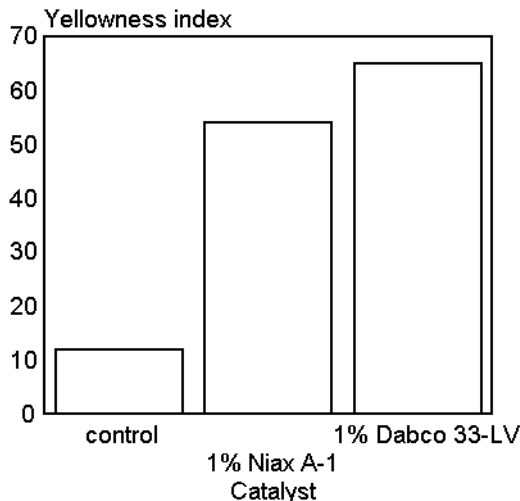


Fig. 16.16. Effect of amine catalyst on initial color of polyurethane foam produced from polyol containing 207 ppm of peroxide. [Data from J. Lacoste, R. P. Singh, J. Boussand, and R. Arnaud, *J. Polym. Sci., Polym. Chem.*, 25(1987)2799.]

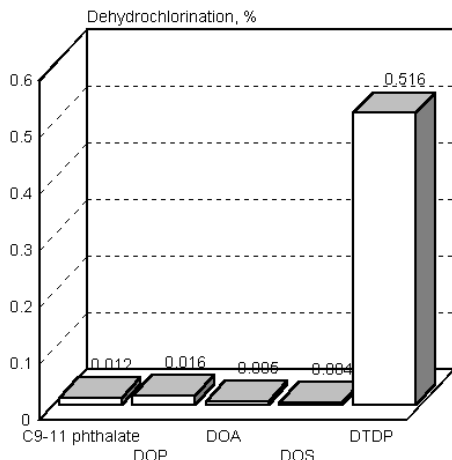


Fig. 16.17. Dehydrochlorination of PVC plasticized with 60 parts of various plasticizers. [Data from H. J. Bowley, D. L. Gerrard, K. J. P. Williams, and I. S. Biggin, *J. Vinyl Technol.*, 8(1986)176.]

used in foam processing (Fig. 16.16). When the polyol does not contain peroxides, the effect of the catalyst is negligible. It is also known from these and other polyurethane studies that commonly-used tin catalysts affect the UV stability of polymers. The effect of the catalyst is associated with the presence of a heavy metal and this also infers that other heavy metals present in polymers may affect their stability. The degradation rate of pure PMMA was unaffected by temperature but the degradation rate of monomer-doped PMMA increased with increasing temperature (see Fig. 11.17).²⁴

Plasticizers are common additives which can influence UV stability, as data for PVC show (Fig. 16.17). Evidently, the

degree of branching of the plasticizer affects the dehydrochlorination rate of plasticized PVC exposed to UV. Other plasticizers seem to affect the degradation rate in a manner which parallels their efficiency as plasticizers. In radiochemical PVC degradation, the amount of plasticizer influenced the mechanism of degradation. As the plasticizer amount was increased (from 15 to 30%), less crosslinking and more chains scission was observed.²⁷

The effect of many other additives on polymer's UV stability is known but not quantified, and frequently the reasons for their action are unknown. This includes many organic and inorganic compounds containing metals, such as copper, cobalt, iron, cadmium, etc. A broad range of admixtures is listed in Chapter 14, but clearly the effect of additives common in polymer processing requires more extensive studies.

REFERENCES

1. J. L. Gerlock, D. R. Bauer, L. M. Briggs, and J. K. Hudgens, *Prog. Org. Coat.*, 15(1987)197.
2. J. H. Braun, *Prog. Org. Coat.*, 15(1987)249.
3. S. Skledar, *Mater. Plast.*, 21(1984)29.
4. L. A. Simpson, *Austral. OCCA Proc. News*, 20(1983)6.
5. M. Koyama, A. Tanaka, M. Ichijima, and Y. Oki, *Kinzoku Hyomen Gijyutsu*, 37(1986)25.
6. L. D. Strelkova, G. F. Fedoseeva, S. N. Potepalova, L. I. Batueva, and W.P. Lebedev, *Plast. Massy*, 1986,5,46.
7. B. Dolezel and L. Adamirova, *Plasty Kauc.*, 20(1983)18.
8. A. Charlesby, *J. Radioanal. Nucl. Chem.*, 101(1986)401.
9. H. J. Bowley, D. L. Gerrard, K. J. P. Williams, and I. S. Biggin, *J. Vinyl Technol.*, 8(1986)176.
10. A. L. Andraday and A. R. Shultz, *J. Appl. Polym. Sci.*, 33(1987)1389.
11. J. E. Pickett, *J. Appl. Polym. Sci.*, 33(1987)525.
12. G. Capocci, *Plast. Compd.*, 10(1987)13.
13. J. Lacoste, R. P. Singh, J. Boussand, and R. Arnaud, *J. Polym. Sci., Polym. Chem.*, 25(1987)2799.
14. S. Skledar, *Angew. Makromol. Chem.*, 137(1985)149.
15. B. D. Gupta and J. Verdu, *J. Polym. Eng.*, 8(1988)81.
16. J. Pan, H. Xu, J. Qi, J. Ce, and Z. Ma, *Polym. Deg. Stab.*, 33(1991)67.
17. P. Genova-Dimitrova, *Polym. Deg. Stab.*, 33(1991)355.
18. P. P. Klemchuk, *Polym. Photochem.*, 3(1983)1.
19. A. L. G. Saad and A. W. Aziz, *Polym. Deg. Stab.*, 41(1993)31.
20. E. Ya. Davydov, V. P. Pustoschniy, A. P. Vorotnikov, and G. B. Pariyskiy, *Intern. J. Polym. Mater.*, 16(1992)295.
21. J. Imhof, P. Stern, and A. Egger, *Angew. Makromol. Chem.*, 176/177(1990)185.
22. H. Kubota and M. Kimura, *Polym. Deg. Stab.*, 38(1992)1.
23. T. B. Boboev, Kh. Dodomatov, and I. Ya. Kalontarov, *Intern. J. Polym. Mater.*, 19(1993)223.

24. T. Ichikawa, K. -I. Oyama, T. Kondoh, and H. Yoshida, *J. Polym. Sci., Polym. Chem.*, 32(1994)2487.
25. E. Baimuratov, I. Y. Kalontarov, and D. S. Saidov, *Intern. J. Polym. Mater.*, 19(1993)193.
26. D. Rysavy and H. Tkadleckova, *Polym. Deg. Stab.*, 37(1992)19.
27. F. ThomINETTE, G. Metzger, B. Dalle, and J. Verdu, *Eur. Polym. J.*, 27(1991)55.
28. G. J. Price and P. F. Smith, *Eur. Polym. J.*, 29(1993)419.
29. J. -L. Gardette and J. Lemaire, *Polym. Deg. Stab.*, 33(1991)77.
30. J. -L. Gardette and J. Lemaire, *Polym. Deg. Stab.*, 34(1991)135.
31. Z. A. M. Ishak and J. P. Berry, *Polym. Compos.*, 15(1994)223.
32. N. S. Allen, M. Ledward, and G. Follows, *Eur. Polym. J.*, 28(1992)23.
33. S. K. Dolui, *J. Appl. Polym. Sci.*, 53(1994)463.
34. P. Dave, R. A. Gross, C. Brucato, S. Wong, and S. P. McCarthy, *Polym. Mater. Sci. Eng.*, 62(1990)231.
35. C. David, M. Trojan, A. Daro, and W. Demarteau, *Polym. Deg. Stab.*, 37(1992)233.
36. D. J. T. Hill, F. A. Kroesen, J. H. O'Donnell, and P. J. Pomery, *Mater. Forum.*, 14(1990)210.
37. B. Ohtani, S. Adzuma, S. Nishimoto, and T. Kagiya, *Polym. Deg. Stab.*, 35(1992)53.

17

WEATHERING OF COMPOUNDED PRODUCTS

Our discussion below includes results of studies of finished products. The intent is to review existing information on material durability, identify reasons for conducting weathering studies in selected groups of materials, and list areas which require more extensive studies in the future.

17.1 COATINGS¹⁻²⁹

Coatings perform two primary functions - protection and decoration. Durability can be severely affected by coating degradation during exposure, which creates the need for weathering studies. Several factors contribute to coating degradation (Fig. 17.1).

Solar radiation	Photocatalytic admixtures
Water and moisture	Chemical degradation
Molecular and singlet oxygen	Temperature
Ozone	Abrasion
Internal and external stress	Pigment fading
Swelling and permeability	Biodegradation

Fig. 17.1. Causes of coating degradation.

Color	Blistering and crater formation
Gloss	Permeability
Loss of weight	Tensile and elongation
Optical properties	Radical concentration
Electric conductivity	Chemical composition
Peeling	Crystalline structure
Cracking and crazing	Thermal properties
Substrate corrosion	

Fig. 17.2. Durability measures.

Similarly, there are several ways to measure coating durability which can be used to follow the degradation process (Fig. 17.2). The sequence of events during degradation is well-known and is characterized in Fig. 17.3.

These changes finally lead to a deterioration of coating properties. The time-scale of these changes and the type of degradative effect depends mostly on the type of polymer used as a binder. The data below characterize the types of changes observed, as well as the effect of the degradative environment.

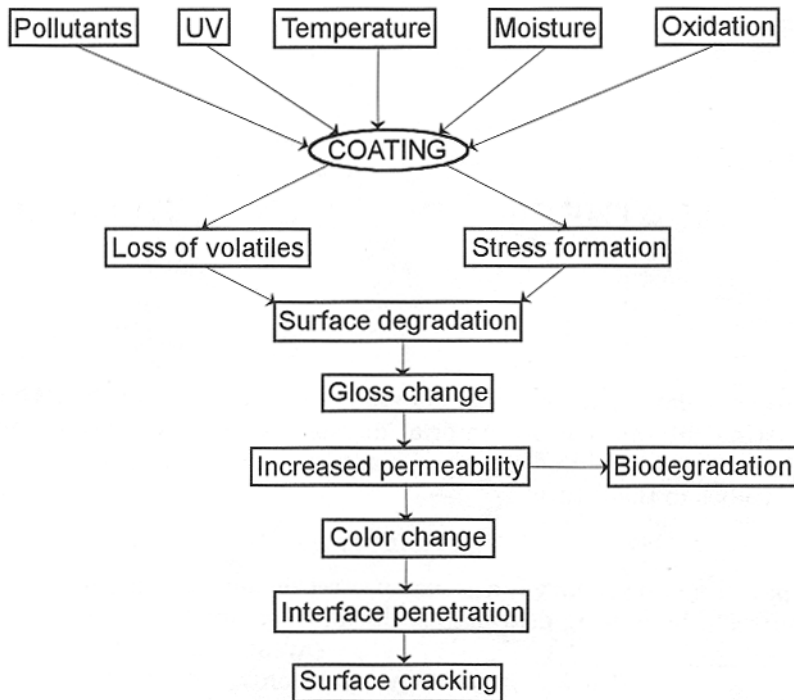


Fig. 17.3. Sequence of events during coating degradation.

Ranby² studied photooxidation of UV-cured epoxy-acrylate coatings. Fig. 17.4 shows the progress of the photooxidative process. Changes in the coating surface are quite rapid at the beginning but, after about 48 hrs, they approach a limiting value. The degradation intensity ratio between the top and the bottom of the sample shows that UV degradation also occurs during the UV-curing process. Fig. 17.5 shows the degradation depth profile. Only the surface shows a high concentration of OH groups, which indicates that the oxidation process mostly affects surface, at least in the initial stages of the photooxidation.

UV is usually necessary to induce oxidative changes but, in some cases, the prevailing mode of binder degradation is hydrolysis (Fig. 17.6). An automotive acrylic enamel apparently degrades by hydrolysis. Additional studies show that, when the enamel is exposed to UV without moisture present, no detectable spectral changes are observed. Fig. 17.7 shows that, in samples of a coatings exposed in Florida, monitored by measuring the concentration of ether crosslinks and C-N stretching in the IR spectra, methoxy

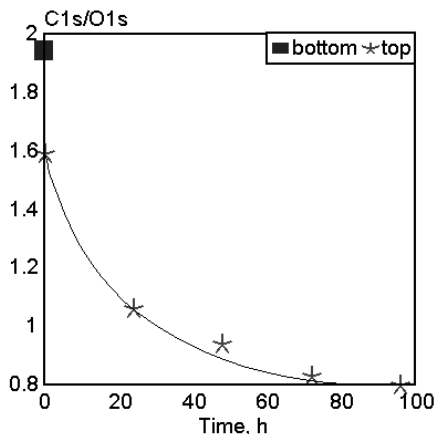


Fig. 17.4. Intensity ratio of C_{1s} and O_{1s} bands in ESCA spectrum of UV cured epoxy-acrylate resin coating vs. exposure time in UVCON. [Adapted, by permission, from B. Ranby and A. Hult, *Org. Coat. Sci. Technol.*, 7(1984)145.]

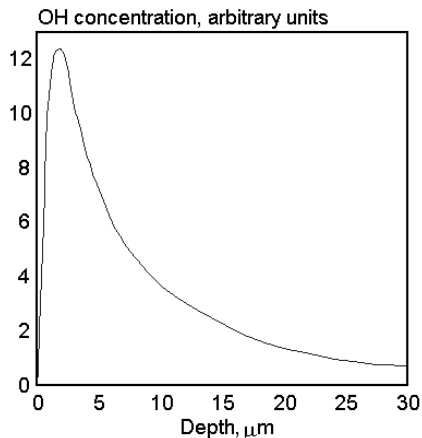


Fig. 17.5. The OH concentration vs. depth from the surface of UV-cured epoxy-acrylate coating after irradiation in UVCON. [Adapted, by permission, from B. Ranby and A. Hult, *Org. Coat. Sci. Technol.*, 7(1984)145.]

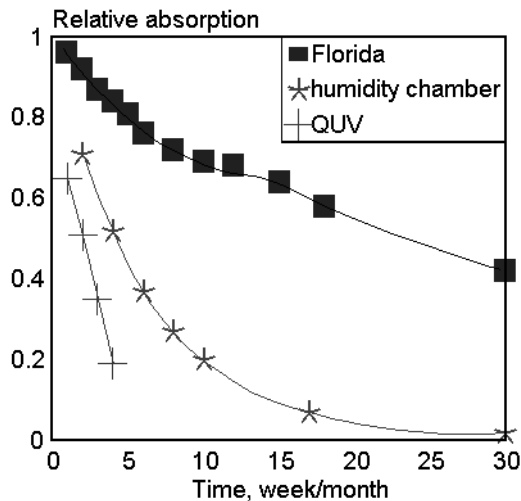


Fig. 17.6. Acrylic-melamine enamel exposure in QUV (weeks), humidity chamber (weeks) and Florida (months). [Adapted, by permission, from J. H. Hartshorn, *Polym. Mat. Sci. Eng.*, 56(1987)881.]

groups are most affected which indicates that changes are indeed caused by hydrolysis. Observations made on this enamel show that the type of exposure climate has an important impact on the deterioration rate.

Acrylic/urethane coatings are not affected by moisture, as seen from Figs. 17.8 and 17.9. A very small difference is observed in the rate of carbonyl group formation and in the disappearance of amide IV when humidity increases. The increase in intensity of the carbonyl is caused by photooxidation. Amide IV loss is due to the rupture of urethane crosslinks, which leads to a loss of mechanical properties in the material. Urethane content loss does not depend only on the structure and composition of the polyurethane (Fig. 17.10). Pigmented material is substantially less resistant than a clearcoat. It is known from ESR studies that

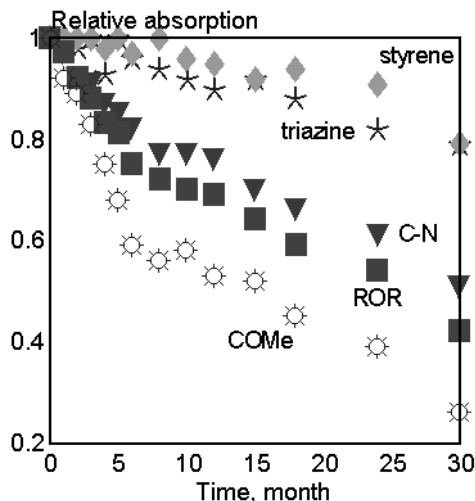


Fig. 17.7. Relative absorption of various functional groups in acrylic-melamine enamel vs. exposure time Florida black box. [Adapted, by permission, from J. H. Hartshorn, *Polym. Mat. Sci. Eng.*, 56(1987)881.]

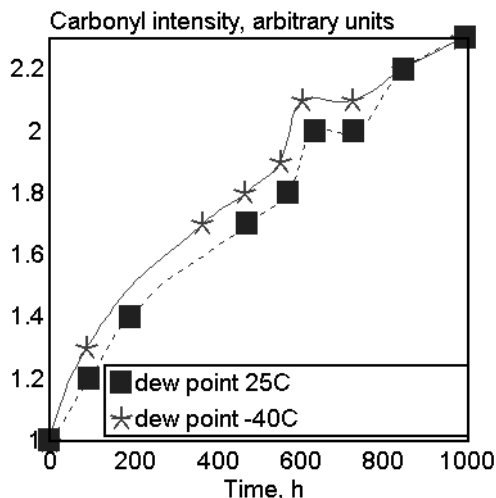


Fig. 17.8. Carbonyl intensity vs. exposure time in Atlas UV2 at different dew points (unstabilized PU). [Adapted, by permission, from D. R. Bauer, M. J. Dean, and J. L. Gerlock, *Polym. Mat. Sci. Eng.*, 56(1987)443.]

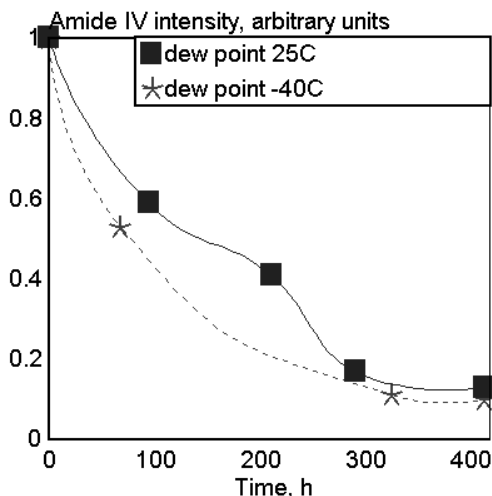


Fig. 17.9. Amide IV intensity vs. exposure time in Atlas UV2 at different dew points (unstabilized acrylic-urethane). [Adapted, by permission, from D. R. Bauer, M. J. Dean, and J. L. Gerlock, *Polym. Mat. Sci. Eng.*, 56(1987)443.]

the rate of photoinitiation is rapidly reduced after the initial period of exposure.¹⁸

Gloss is the most sensitive measure of deterioration because the degradative process affects the surface first. The surface does not have protection against oxygen diffusion and UV absorption (most of degradative processes are diffusion-controlled). A study of acrylic/melamine coatings shows the effect of photoinitiation rate on coating gloss (Fig. 17.11). The rate of gloss deterioration is linear to the square root of photoinitiation rate, which means that the initial concentration of photoinitiation centers controls the durability of material. Temperature and time of exposure are additional factors in determining the extent of damage to the coating. Moisture may play an essential role

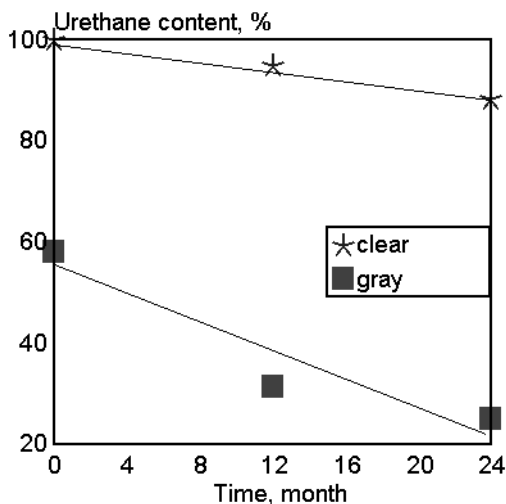


Fig. 17.10. Urethane content in Florida exposed clear and pigmented coating. [Adapted, by permission, from S. G. Croll, *Prog. Org. Coat.*, 15(1987)223.]

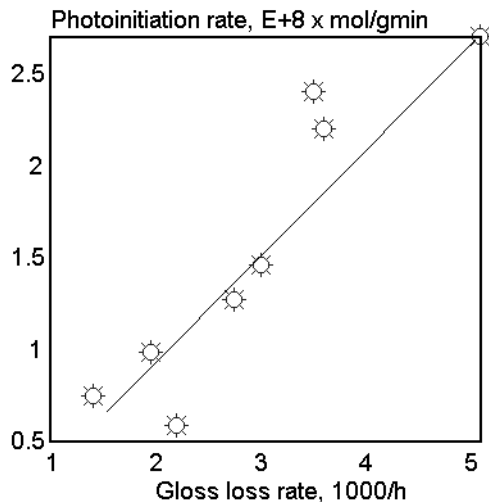


Fig. 17.11. Gloss loss rate vs. the square root of the photoinitiation rate. [Adapted, by permission, from J. L. Gerlock, D. R. Bauer, and L. M. Briggs, *Org. Coat. Sci. Technol.*, 8(1985)365.]

in some types of coatings, which emphasizes the importance of the exposure site on the rate of degradative processes (Fig. 17.12). Of all the exposure sites, Asahikawa and Tokyo have the lowest amount of radiation (difference between the sites is in the range of 10% of average value). Asahikawa has the lowest mean temperature and humidity, whereas Naha has the highest values of temperature, humidity, and radiation. All three factors influence degradation rate.

Binder durability can be increased by the use of stabilizers which also improve gloss retention. The addition of UV absorber alone does not give adequate protection (Fig. 17.13). Depending on the thickness of a clear top coat layer, 79 or 95% of UV radiation is absorbed by the top coat containing a reasonable concentration of absorber. An increase in absorber concentration beyond this level does not contribute to solving the problem. The best gloss retention can be achieved by use of a combination of a UV absorber and hindered amine light stabilizers, HALS (Fig. 17.14). Unlike a UV absorber, HALS is able to protect a surface since it acts both as an antioxidant and as a radical scavenger. It is very important to protect the surface of the coating because, when the surface is penetrated by degradative processes, changes occur more quickly and are more detrimental (Fig. 17.15). For most of the exposure period changes occur slowly then there is a dramatic change in properties within a short period of time. Increased porosity allows moisture penetration to the substrate and interface, which causes visible failure of the coating.

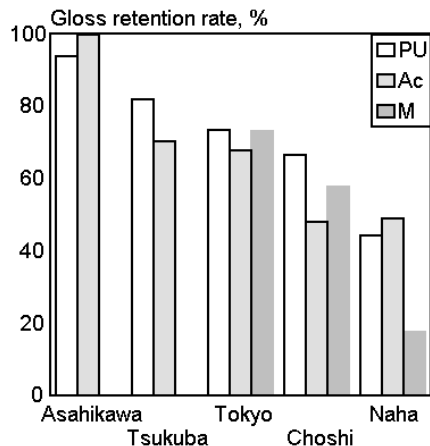


Fig. 17.12. Gloss retention at various exposure sites for coatings containing different resins. [Data from S. Yajima, Y. Togawa, S. Matsushita, T. Suzuki, and T. Okada, *Kinzoku Hyomen Gijutsu*, 37(1986)718.]

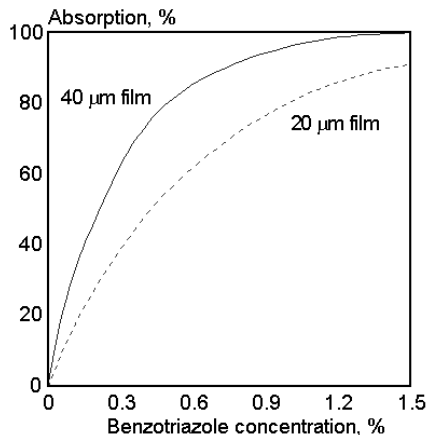


Fig. 17.13. External filter effect of benzotriazole at 350 nm as a function of thickness and concentration. [Adapted, by permission, from G. Berner and M. Rembold, *Org. Coat. Sci. Technol.*, 6(1983)55.]

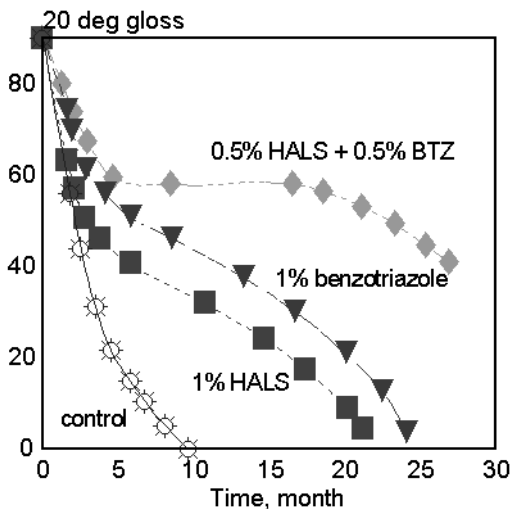


Fig. 17.14. Gloss of high solid coating vs. time of Florida exposure depending on stabilizer. [Adapted, by permission, from G. Berner and M. Rembold, *Org. Coat. Sci. Technol.*, 6(1983)55.]

Traditional automotive coatings consisted of a pigmented layer which, when exposed to environmental condition, gradually eroded resulting in a reduction in gloss. Introduction of a more complex system in the 1980s, composed of clearcoat, basecoat, and primer, changed the mode of degradation. This system may deteriorate severely with damage such as cracks and delamination which could only be repaired by repainting. This system depends for its protection on the photostability of the clearcoat layer which must withstand not only the typical factors of exposure (UV, temperature, moisture) but also the effect of acid rain. Industry demanded better performance and approval procedures. Typically, at least 5 years of exposure in both Florida and Arizona is required to gain coating approval. A 5 years evaluation period does not allow for sufficiently fast changes in formu-

lation therefore laboratory methods of testing are a high priority studies conducted by the automotive industry. It is well established¹⁸ that accelerating degradation by changing the conditions of irradiation does not yield results which correlate with long-term observations in natural conditions. Therefore, processes of degradation are studied by sophisticated analytical methods.¹⁹ Humidity also plays a very important role (see Fig. 11.37).²¹ Carbonyl concentration by IR, hydroperoxide concentration by titration, and measurement of nitroxide concentration by ESR are the most frequently used indicators to predict durability and monitor the degradation rate of automotive clearcoats.^{19,20}

Martin²² presents a different point of view regarding the conditions under which studies on coating degradation should be interpreted. Based on results of successful studies in medical, biological, and agricultural fields, he argues that a lack of correlation is frequently caused by the method of estimating the effective dose of exposure. He says, it should be based on the spectral absorption of material and its spectral quantum yield. In other words, effective exposure should not be based on the energy supplied to the sample but rather on the energy which can be used by a particular material for photoconversions.

Edney²³ introduces still another approach to coating testing. His studies were designed to determine the effect of pollutants on weathering of coatings due to their wet and dry deposition. A special rack was build which was automatically moved under a shelter whenever natural precipitation was detected. Also, samples were exposed in wet conditions and the water run off from the sample surface was collected. Elemental analysis (AAS) of the run off was used to determine if the elements of fillers used in coating were present. This permitted conclusions to be drawn about the influence of acid rain on material erosion.

Perera and Oosterbroek²⁵ consider internal stress as one of the major factors affecting coating durability. They provide evidence to support this conclusion and describe a method measuring residual stress in the coating. They propose that hydrothermal stress formation in clearcoats causes their cracking.

New methods are available to study coatings and their degradation. Application of these methods will give us testing proto-

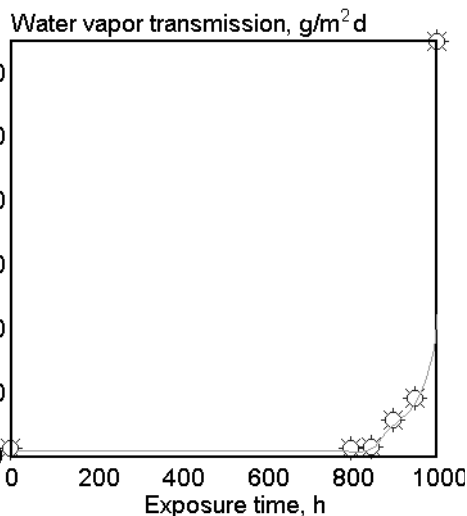


Fig. 17.15. Water vapor transmission rate of QUV exposed PU coating. [Data from S. G. Croll, *Prog. Org. Coat.*, 15(1987)223.]

cols which will yield an improved quality of data and better methods of interpretation. More verification of results obtained to date is required to make confident service life predictions.

17.2 PAINTS³⁰⁻⁴³

Most of these explanations of coating degradation mechanisms apply to paints. This distinction was made to underline subjective differences between coatings and paints. Coating should be designed to protect a material whereas paint is designed to decorate it. Thus, a coating should be durable to protect substrate while paint should be durable to protect itself. There is very little difference between the mechanisms responsible for the durability of each kind, except for the fact that TiO_2 plays a more dominant role in paints since most paint colors contain it.

Durability of paints mainly depends on their resistance to photochemical and photocatalytic degradation. A schematic explanation of these mechanisms is given in Fig. 16.3. If pigments were inert, the binder would be the sole factor responsible for paint durability. During exposure, degradation would continue to erode increasingly thicker layers of material, causing significant loss of mass of both binder and fillers. In reality, some fillers (pigments), including TiO_2 , are photoactive species which cause binder degradation to concentrate around the pigment particles with the pigment playing a role of a photocatalyst intensifying the degradation rate.

Most paints contain at least two fillers - one usually referred to as a pigment, the other as an extender. Pigment (e.g., TiO_2) gives the paint more opacity at lower concentration than does the extender. Pigment also has a very small particle size which provides more efficient screening. The disadvantage of titanium dioxide is related to its photocatalytic activity, which causes various effects detrimental to paint durability, as shown in Figs. 16.1, 16.2, and 16.4-9. Extender offers less pronounced opacity and screens less UV radiation, but usually does not exhibit these negative features of pigment which contribute to the catalysis of the photodegradation of the binder.

Thus, the observed durability of paint is determined by a combination of two factors: the degree to which UV radiation is screened and the increase in binder photodegradation rate by a photocatalytic effect. UV resistant binder is affected by the photocatalytic activity of pigment to an extent which may offset the screening effect (Fig. 16.1). A binder which is not very durable degrades at a slower rate when pigment is present because screening usually gives more protection than that which is lost by the photocatalytic activity of pigment.

By the same reasoning, an extender might be helpful in retaining the initial properties of paints. Increased additions will contribute to a lowering of the photocatalytic activity of fillers which is dependent on the concentration of the photoactive pigment. At the same time, opacity is more difficult to achieve and some screening effect is lost. A combination of binder, pigment, and extender in the correct proportions contributes to

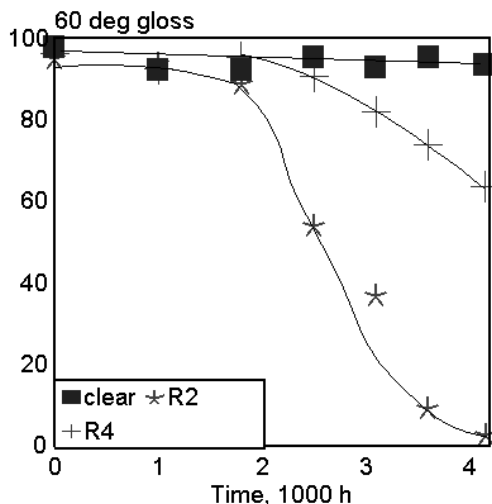


Fig. 17.16. Gloss change of polyester/isocyanate paints vs. exposure time (clear and pigmented). [Adapted, by permission, from L. A. Simpson, I. Melville, and D. V. Moulton, *Polym. Paint Colour J.*, 177(1987)139.]

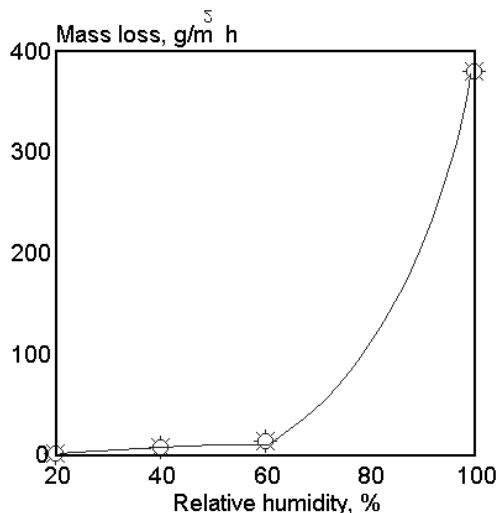


Fig. 17.17. The effect of relative humidity on the mass loss by paint exposed to xenon lamp irradiation. [Data from E. Hoffman, *J. Oil Colour Chem. Assoc.*, 54(1971)450.]

an optimization of the required properties. The discussion in Chapter 18 also helps us to understand the screening effect of particulate materials. Fig. 17.16 shows how improvement in pigments may result in better gloss retention. Two coated grades of titanium dioxide were introduced to a paint based on a polyester/isocyanate resin which was considered to be a resistant binder. Evidently, the addition of any pigment reduces resistance, but the pigment R₄, which has a lower photocatalytic activity, due to an appropriate coating, affects binder durability to a lesser extent (it is note worthy that a clear paint has the best durability).

The discussion in Chapter 16 refers to the reasons for photocatalytic activity of pigments in relation to formation of holes, free electrons, hydroxy and peroxy radicals. These radicals are formed only when water is present, thus moisture plays a key role in the whole process of paint degradation (Fig. 17.17). A relative humidity of over 60% contributes to fast deterioration of paint quality. Temperature increase also accelerates the degradation process by increasing chemical reactivity.

The chemical composition of paint, the humidity, and temperature of the environment and the radiation wavelength are the most important factors affecting deterioration rate. Several other factors should also be considered: type of substrate, preparation of substrate, substrate movement (stress), and biological effects.

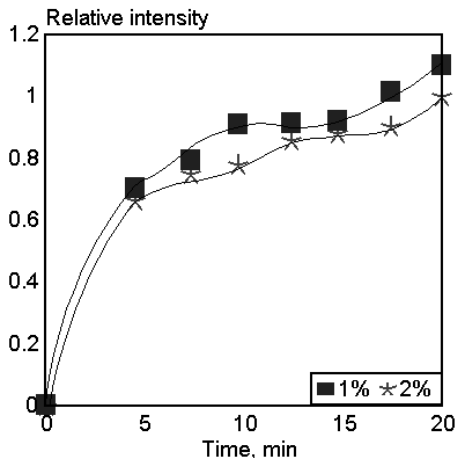


Fig. 17.18. Relative ESR intensity of phenoxyl radical vs. irradiation time in QUV (paint contains different concentrations of Tinuvin 327). [Adapted, by permission, from S. Okamoto, K. Hikita, and H. Ohya-Nishiguchi, *Polym. Paint Colour J.*, 177(1987)683.]

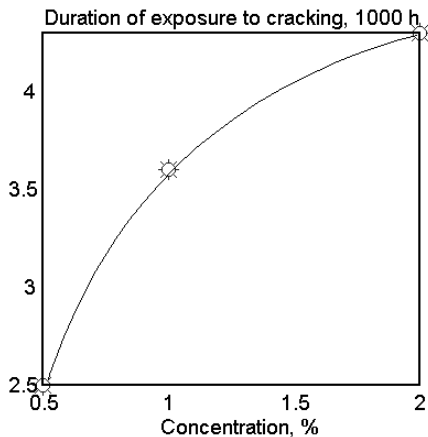
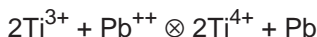


Fig. 17.19. The effect of Tinuvin 327 concentration in acrylic paint on exposure time required to cause paint cracking. [Data from S. Okamoto, K. Hikita, and H. Ohya-Nishiguchi, *Polym. Paint Colour J.*, 177(1987)683.]

Paint weathering properties can be improved by the use of UV absorbers (Figs. 17.18 and 17.19). Phenoxy radicals are formed in acrylic paints from epoxy resins added as radical trapping agents. The relative ESR intensity of this radical acts as a measure of the paint's photoconversion. The data from ESR measurement correlate with paint cracking. Data also show that the absorber concentration above 1% becomes less effective.

New proposals for the testing of the involvement of TiO_2 in paint degradation have been made by Braun.³⁹ Since the degradation chemistry of paints is dominated by TiO_2 , Braun³⁹ based his methods on the validity of the following equations:



These reactions can be described as follows: Titanium in the presence of water (hydroxyl anion) is photoreduced. In the presence of lead salt, titanium is oxidized back to its initial form with the lead cation being reduced to form the metal. If this reaction is conducted without oxygen (oxygen may oxidize formed lead metal), each act of quantum

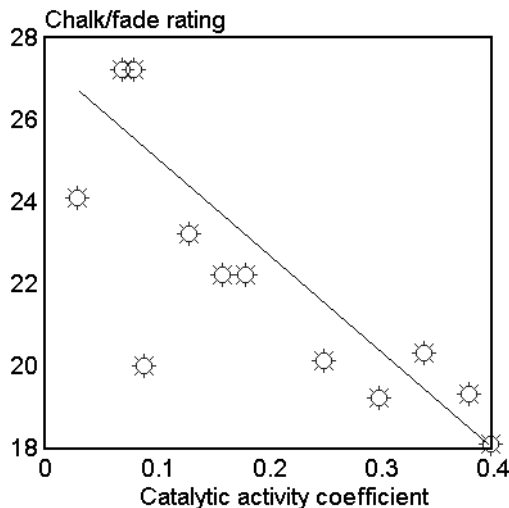


Fig. 17.20. Chalk/fade rating vs. catalytic activity coefficient of TiO_2 . [Adapted, by permission, from J. H. Braun, *J. Coat. Technol.*, 62,785(1990)37.]

absorption produces a molecule of metal (black). The accumulation of metal can be measured by optical methods and rate of sample blackening used as a measure of TiO_2 catalytic activity. The relationship between the catalytic activity coefficient (as determined by proposed method) and the chalk/fade rating of commercially available TiO_2 is given (17.20). Standard deviations of both methods of determination indicate that some scatter is caused by chalk/fade ratings. The paper³⁹ gives full details of method and equipment used. Some details of the experiment are not clear but the concept seems very interesting. Metallic lead acts as an internal dosimeter which gauges catalytic activity of a particular grade of TiO_2 .

Pourdeyhimi and Nayernouri⁴² proposed a quantitative approach to defect ob-

servation based on image analysis technology. Results from image analysis are compared with existing visual appearance standards. This technology, still under development, is very important for future quantification of results of work on degradation since numerical data should always be related to the defects formed in materials during their exposure.

Two current publications discuss properties and mechanisms of degradation of zinc-rich⁴⁰ and chlorinated rubber⁴¹ paints. The later paper gives an interesting interpretation of the interdependence of substrate corrosion, cleavage of C-Cl bonds in the binder and the effect of chloride ions on substrate corrosion. Both components of the system (substrate and paint) can interact to cause catastrophic failure.

This literature review shows that progress in the study of both coatings and paints has been made. The major obstacle to durable paint - the failure to use stable pigments - is addressed in depth both from the point of view of pigment technology and the methods of studying the effects involved. Further studies should concentrate on the interaction of pigments and binder and the effect of pigments on the crystalline structure of composition.

17.3 TEXTILE MATERIALS⁴⁴⁻⁵⁹

Cellulose does not absorb UV radiation. Other absorbing species must be present to initiate the radical processes which trigger chain reactions. Singlet oxygen involvement in

cellulose degradation is a matter of controversy. Dye-sensitized oxidative processes may involve either hydrogen abstraction or singlet oxygen sensitizing. Almost every efficient singlet oxygen sensitizer is able to abstract hydrogen; therefore, it is difficult to prove either mechanism. Hydrogen abstraction is the more likely because there is no evidence to support the attack of singlet oxygen on the polysaccharide backbone. Anthraquinoid vat dyes are commonly known as sensitizers which lead to cellulose degradation. They act through hydrogen abstraction mechanism as do azo, reactive, disperse, and some other dyes. The general rule is that, the more stable the dye, the less effect it has on phototendering of cellulose-containing material.

Wool exposed to weathering shows a decrease in tear strength, tensile strength, and abrasion resistance as well as an increase in its yellowness index.⁵² The complex structure of wool keratin allows for many possible degradative changes. Most chemical changes are attributed to the presence of tryptophan, histidine, and cystine. Tyrosine, phenylalanine, methionine, glycine, and alanine are also believed to be photoactive. Energy at 310 nm causes the formation of thyl radical ($R-CH_2-S^{\cdot}$) from the homolytic fission of the disulfide bond of cystine or by the rearrangement of a cystinyl radical ion. The breakdown of the disulfide bond is the main reason for wool phototendering. Irradiated tryptophan forms the 3-indolyl radical by N-H bond fission. The energy absorbed by tyrosine is transferred to tryptophan.

The yellowing of wool occurs when keratin is exposed to radiation in the 290-380 nm range and it is most probably caused by the oxidation of tryptophan by singlet oxygen. It is also known that radiation in the 420-450 nm range causes wool to photobleach. The more yellow the wool, the faster the photobleaching. Both processes (yellowing and photobleaching) occur simultaneously with different kinetics. The reason for absorption at 420-450 nm is not known, nor is the mechanism of the photobleaching process. Wool turns green when exposed to UV radiation in the absence of oxygen but returns to yellow when exposed to oxygen afterwards.

Temperature is an important factor in the degradative process (Figs. 17.21 and 17.22). High temperatures contribute to fast yellowing of wool. Also tensile strength decreases faster at elevated temperature. Treatment with UV absorbers and antioxidants prevents both tensile strength decrease and yellowing (Figs. 17.23 and 17.24). A benzotriazole type of UV absorber is more effective in preventing of yellowing than benzophenone. The addition of antioxidant further inhibits degradative changes. This is in agreement with studies which show that both yellowing and a decrease in tensile strength are related to oxidative processes. The stability of jute, which is very poor, can be improved by the use of DABCO and β -carotene both of which quench singlet oxygen.

A nonwoven polypropylene fabric was exposed to UV radiation at 254 and 350 nm.⁵³ At 254 nm, alcohol, peroxide, ketone, aldehyde, carboxylic acid, and anhydride were detected by FTIR. The exposed surface was substantially more affected than the back surface of the fabric. No photooxidation was observed in fabric exposed to wavelength of 350

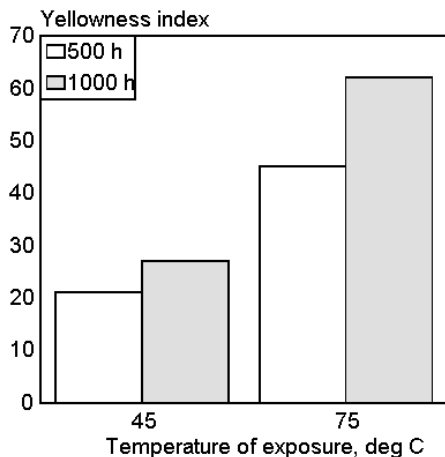


Fig. 17.21. Yellowness index of wool exposed to irradiation at different temperatures and times. [Data from L. A. Holt and B. Milligan, *Text. Res. J.*, 54(1984)521.]

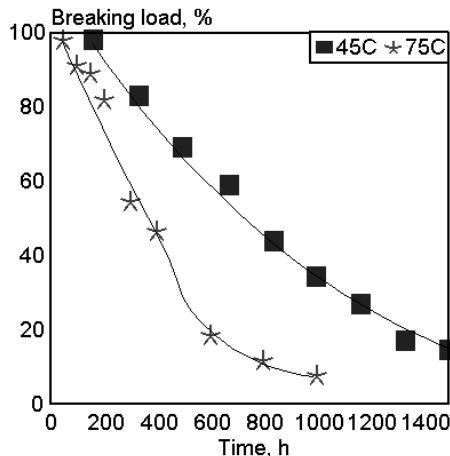


Fig. 17.22. Relative ultimate load of wool fabric vs. irradiation time (mercury vapor tungsten phosphor lamp B) at different temperatures. [Adapted, by permission, from L. A. Holt and B. Milligan, *Text. Res. J.*, 54(1984)521.]

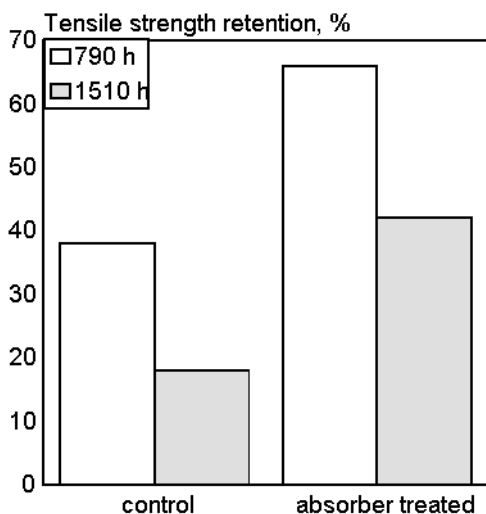


Fig. 17.23. Effect of wool treatment by benzophenone absorber on tensile strength retention depending on irradiation time. [Data from L. A. Holt and B. Milligan, *Text. Res. J.*, 54(1984)521.]

nm. The following typical frequencies of IR bands can be used for analysis: alcohol and peroxide hydroxyl - 3430, ketone and aldehyde carbonyl - 1711-1719, carboxyl carbonyl - 1713-1731, and anhydride carbonyl - 1775-1778 cm^{-1} .

During work done on the protection of aramide yarns and fabrics against degradation, it was discovered that both UV and visible light can cause degradation. Three methods of protection were investigated: covering of yarns with optically tight sheaths of cotton or polyester/cotton, Cu and Al sputtering of fabric, and application of an anti-slip finish to the fabric. The last method was the most promising. Application of UV absorbers is limited because of the effect of visible light. The effect of load and pollutants on single fibers from Kevlar 49 and polyamide-6 was studied. If loads of 80-90% of ultimate tensile are used, they

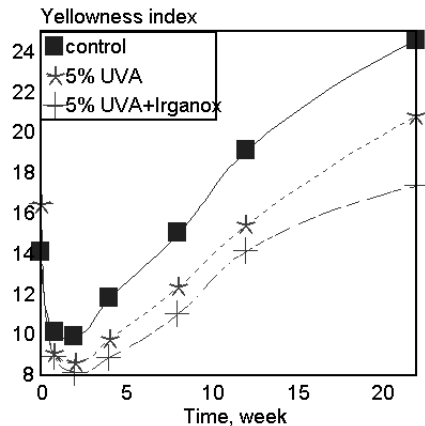


Fig. 17.24. Yellowness index of wool treated with stabilizers vs. sunlight exposure time through glass (UVA=2-hydroxyphenyl-s-triazine). [Adapted, by permission, from C. M. Carr and I. H. Leaver, *J. Appl. Polym. Sci.*, 33(1987)2087.]

dominate degradation kinetics. Lower loads in the range of 40-80% incrementally increase degradation rate in NO_x .⁵⁶ Large (wedge-shaped) cracks were discovered by TEM in Kevlar 149 fibers exposed to UV radiation at 3100-8000 nm.⁵⁷ The formation of these cracks exposes the fiber to radiation which penetrates layers deeply inside the fibers and causes substantial damage to the original mechanical properties. The extent of photooxidation of Nomex aramid fibers, measured by XPS, corresponds to the loss of mechanical performance.⁵⁸

Several fabrics (PP, cotton, fire retardant cotton, and silk) were used to study the applicability of FTIR-PAS (photoacoustic spectroscopy) for determining the distribution of degradation products in weathered fabrics.⁵⁵ The bulk of the fabric can easily be

distinguished from the surface layers, indicating that this method is precise, especially since there is no band distortion. Hundred of hours of exposure of cotton fabric to natural conditions was sufficient to produce substantial changes at 1743, 1722, and 1704 cm^{-1} . This method was enhanced by spectral subtraction technique.

Studies of textile materials are complex due to use of variety of materials (the type of fiber and the method of finishing). Both affect the result. Naturally obtained products have very broad range of chemical compositions which makes comparative studies difficult. The positive factor in these studies is the application of instrumental techniques which will eventually lead to an understanding degradation mechanisms. We need to understand the mechanisms of wool degradation and photobleaching (a practical knowledge of protection exists but it is not supported by chemical mechanism) and the interaction between dyes and fibrous materials.

17.4 UPHOLSTERY FABRICS⁶⁰⁻⁶⁵

Upholstery fabrics used by the automotive industry are discussed separately because their degradation conditions differ. Upholstery fabrics are usually exposed to less intensive radiation because of the filtering effect of glass but at the same time they are subjected to extremely high temperatures which, in a closed car, can reach up to 100°C. The combined effect of radiation and temperature affects fiber properties in application where fabric is also subjected to high stresses and abrasion.

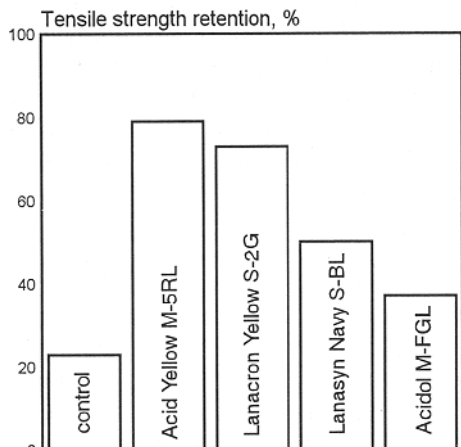


Fig. 17.25. Effect of some dyes on tensile strength retention of wool fabric exposed to 50,000 Langley units through glass. [Data from L. Benisek, G. K. Edmondson, and J. W. A. Matthews, *Text. Res. J.*, 55(1985)256.]

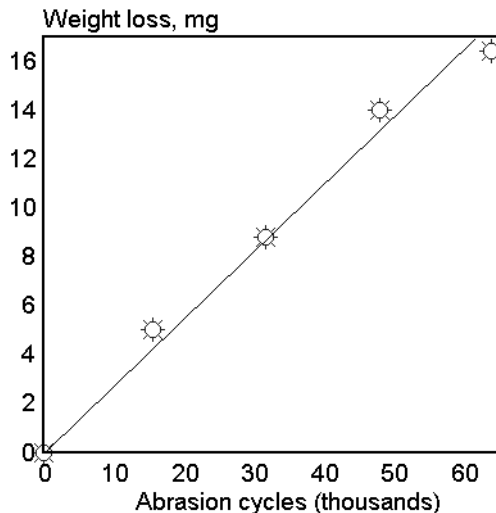


Fig. 17.26. Weight loss vs. number of abrasion cycles for polyester velour upholstery fabric. [Adapted, by permission, from P. M. Latzke, *Meliand Textilberichte*, 7(1990)502.]

The weathering conditions of automotive upholstery fabrics strongly depend on the type of glass used in the car. Most windscreens use laminated glass which has an intermediate layer of poly(vinyl butyral) containing a UV absorber which absorbs light below 380 nm. Some manufacturers use UV-absorbing films which give similar protection. Tinted automotive glass is able to absorb UV radiation below 340 nm. A temperature increase from 60°C to 90°C doubles the degradation rate of wool exposed to the same level of radiation. Temperatures above 70°C cause a rapid photoyellowing process.

Polyamide, polyester, wool and, recently, polypropylene fibers, are used in automotive upholstery manufacture. The available means of protection used in fiber manufacture (stabilizers) do not provide the required durability. The other possibility is to protect the material with a proper choice of dyes. It is known that some dyes may even sensitize degradation of polymers - a process depending both on dye and polymer (see Fig. 12.6). Benisek⁶⁰ gives data characterizing a protective value for some premetallized dyes (Fig. 17.25). Two yellow dyes give the best protection and both of them contain some amounts of cobalt. The other two dyes contain chromium.

Polyamides, frequently used for the manufacture of automotive upholstery in the past, are losing their market share to PET fabrics due to their lack of lightfastness.⁶⁴ SEM and TEM studies show that TiO₂ is one of the main causes of degradation. Surface of fibers is heavily eroded around the pigment particles. Also, dyes and delustrants de-

crease the lightfastness and the mechanical properties of polyamide fibers. The process of degradation is initiated by sensitizers formed during fiber manufacture and storage, mostly due to thermal treatment. It is suggested that the durability of automotive fabrics is best tested by determining abrasion resistance after exposure. This suggestion recognizes that the fabric structural elements, which are responsible for tensile properties, are protected by flock fibers.^{64,65} Fig. 17.26 shows that the loss of weight of automotive fabric is proportional to abrasion cycles.

17.5 MUSEUM TEXTILES⁶⁶

Museum curators made attempts to evaluate lighting levels, types of light, and light filters in order to reduce the exposure of museum textiles to radiative energy. Despite these measures, textile materials still undergo undesirable color change while on display. Up till now, there is no known level of lighting or light source which does not cause some degree of color change. A recent study evaluates the possibility of using UV absorbers for the protection of museum textiles. Several fabrics, including cotton, linen, silk, and wool, were studied in conjunction with natural dyes, such as cochineal, madder, fus-

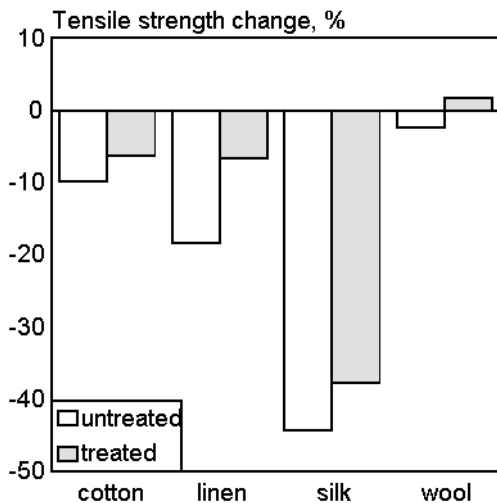


Fig. 17.27. Tensile strength change of various untreated fabrics and the same fabrics treated with 2-hydroxy-4-octyloxybenzophenone before xenon-fadeometer exposure to 80 AFU. [Data from P. C. Crews and B. M. Reagan, *Text. Chem. Color.*, 19(1987)21.]

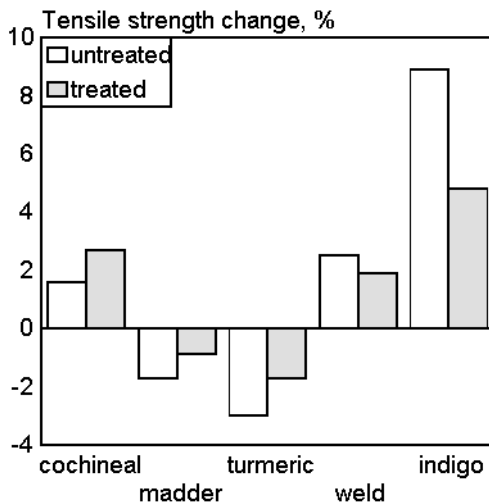


Fig. 17.28. Tensile strength change of wool specimens dyed with various dyes; untreated and treated with 2-hydroxy-4-octyloxybenzophenone (exposure in xenon-fadeometer to 80 AFU). [Data from P. C. Crews and B. M. Reagan, *Text. Chem. Color.*, 19(1987)21.]

tic, weld, turmeric, and indigo. Dyed and undyed samples of fabrics were included in the study; in each case fabrics were scoured in a soap solution at 90°C prior to UV absorber treatment to remove impurities.

Several UV absorber properties are important: commercial availability, lack of color, and ease of application. Four benzophenone-type stabilizers were tested. UV absorbers were applied on textile material in a manner closely resembling customary cleaning procedures. Use of this approach would be a practical means to apply them to museum textiles when they are scheduled for cleaning. One water soluble UV absorber was applied from a water solution and the remaining three from a solution in perchloroethylene. Dye fastness was not dramatically improved by any tested UV stabilizer. Only dyes of low lightfastness became more resistant when treated with UV absorber but changes in lightfastness were still minor. Two reasons might be cited to explain this phenomenon: light stabilizer cannot protect surface layers of material; dye fading is also caused by visible light which is not absorbed by UV stabilizer. The tensile properties of fabrics were improved by UV absorber treatment (Figs. 17.27 and 17.28). Improvement of tensile strength retention clearly shows that the chosen direction of the study may eventually offer a solution, but more data is needed and a broader study of stabilizers should be carried out to find a solution.

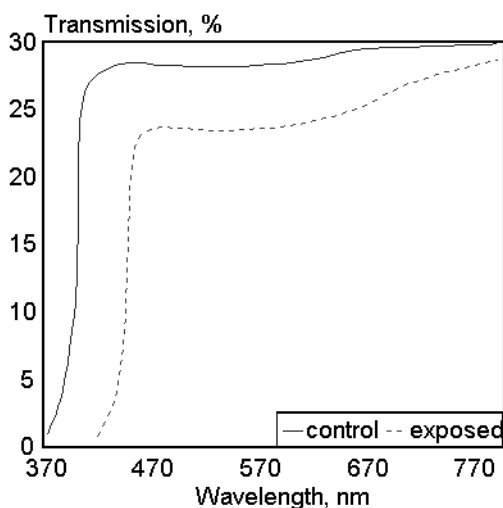


Fig. 17.29. Effect of natural exposure, for 6 years, of PVC coated material on light transmission. [Adapted, by permission, from R. Frey, *Bautenschutz Bausamierung*, 9(1986)87.]

17.6 COATED FABRICS^{67,68}

Most coated fabrics are used outdoors, some in very demanding conditions, exposed to intensive radiation, winds, and stress. However, there are only a few weathering studies available, most probably because individual polymers used for coating are studied separately, not in combination with textile materials. Frey⁶⁷ reports that PVC coated material changes its optical properties during natural exposure (Fig. 17.29).

The stress-strain characteristic of this material also changes with time (Fig. 17.30). The material loses its flexibility and elastic properties. The initial changes are small because the coating retains its protective properties and the textile material responsible for the mechanical properties is less affected by the corrosive environment.

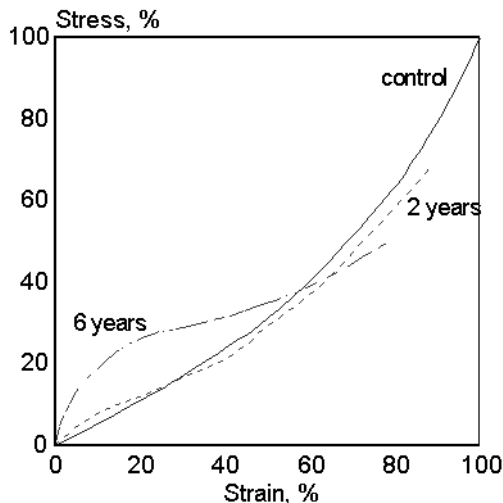


Fig. 17.30. Stress-strain of coated fabric exposed to natural weathering. [Adapted, by permission, from R. Frey, *Bautenschutz Bausamierung*, 9(1986)87.]

Lonza⁶⁸ presents results of weathering studies of plasticized PVC used for textile coating. Several variable components, are considered including thermal stabilizers, UV absorbers, PVC and plasticizer type, adhesion promoters, and costabilizers. The formulation of top and ground coating, and the adhesion between the coating and textile material play an essential role in the weatherstability of material. The fabric component retains more of its initial properties than does the coating.

17.7 GEOSYNTHETICS⁶⁹⁻⁷³

Geosynthetics include three groups of materials: geotextiles, geogrids, and geomembranes. From the point of view of weathering they form two groups of materials: geotextiles and geogrids have exposed fibrous material whereas geomembranes are made from films or have coating exposed. Such a division means that two different groups of polymers are exposed to

primary degradation. There is also another important consideration: many of these materials are not exposed to radiation at all because they are buried in the soil or covered with soil or water on the surface; therefore, in these cases their durability will be limited by biological processes or hydrolysis, rather than photolytical or photooxidative processes. Whichever is the case, there is sufficient reason for broader studies since the existing data are very limited and some common materials were not studied at all or, if studied, data were not published.

Polypropylene and polyester geotextiles were subjected to weathering tests in natural and in artificial weathering conditions. Fig. 17.31 shows tensile strength retention of textiles exposed to artificial weathering in Australia. Tests conducted using a xenon lamp also showed that polypropylene better retains tensile strength on exposure to UV light.

Tisinger⁷⁰ tested five samples of polypropylene geotextiles which were exposed for a short period of time to UV radiation during installation and then buried for 11 years. Some decrease in original crystallinity was observed (on average, about 10%). The oxidative induction period was also measured (Fig. 17.32). Each textile lost stability during the exposure period. The author has assumed that the observed stability decrease could

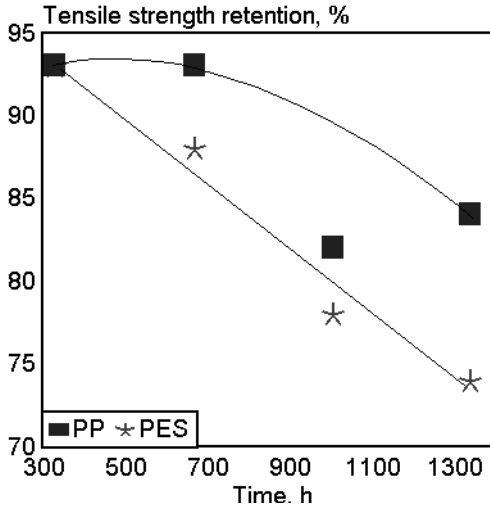


Fig. 17.31. Tensile strength retention of nonwoven geotextiles (mercury-tungsten-phosphor light source). [Data from J. R. Montalvo, *Geosynthetics '89*, February, 1989, San Diego, California, Conf. Proc., Vol. 2, p. 501]

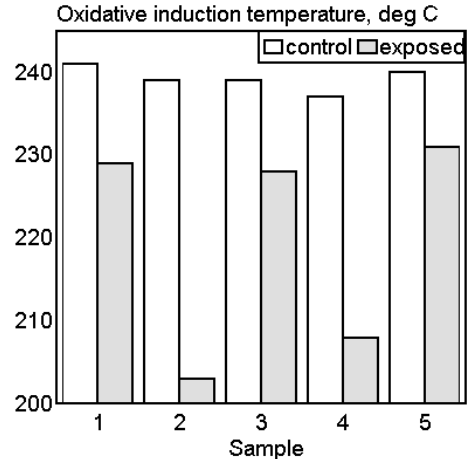


Fig. 17.32. Oxidative induction temperature for polypropylene geotextiles buried for 11 years. [Data from L. G. Tisinger, *Geosynthetics '89*, February, 1989, San Diego, California, Conf. Proc., Vol. 2, p. 513.]

be accounted for by the short UV exposure during installation but there is no data supporting such a conclusion; on the other hand, damage from biological or hydrolytic causes is of low probability with a material such as polypropylene. The author's conclusion may be valid or the cause may be related to changes caused by oxidation.

Fourteen geotextiles were studied in Hong Kong.⁷³ Geotextiles were made mostly from stabilized and unstabilized polypropylene and polyester (only one was made from the combination of polyester and polyamide). Materials were exposed in natural conditions where the annual average level of SO_2 is $27 \mu\text{g}/\text{m}^3$, NO_2 $65 \mu\text{g}/\text{m}^3$ and O_3 $21 \mu\text{g}/\text{m}^3$. Polyester geotextiles generally performed better than polypropylene but stabilized polypropylene was more durable than unstabilized polyester. Textile structure was the essential factor in mechanical property retention. Needle-punched geotextiles were suggested for this application. Assuming that even relatively short exposure causes damage, textile should be exposed for the shortest time. When stored outside they should be in rolled form. Textiles should be covered immediately after installation.

Geomembranes are most frequently covered with a layer of soil which protects them from direct irradiation but, in some constructions, the geomembranes are exposed to direct sunlight. South African studies of EPDM and butyl/EPDM provide information on the effect of weathering on mechanical properties and the influence of pigments and temperature on the weathering rate. Fig. 17.33 shows that weathering conditions cause only slow deterioration of a butyl lining.

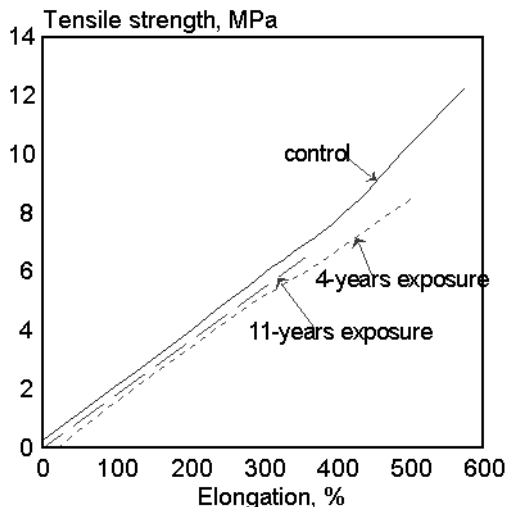


Fig. 17.33. Tensile strength of butyl lining vs. elongation relative to exposure time. [Adapted, by permission, from A. G. Strong, *Plast. Rubber Process. Applic.*, 6(1986)235.]

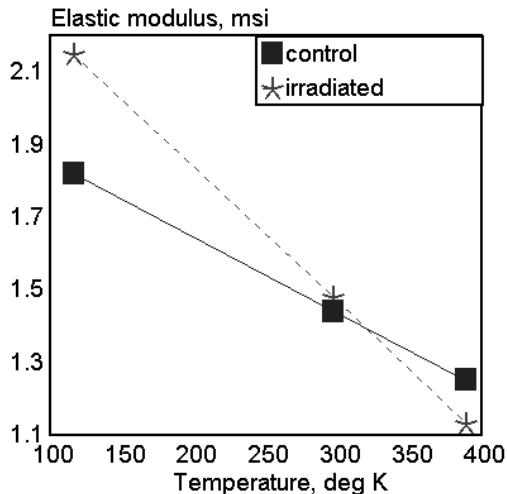


Fig. 17.34. Elastic modulus of graphite-epoxy composite vs. temperature for control and irradiated specimens (10^{10} rads). [Adapted, by permission, from S. M. Milkovich, C. T. Herakovich, and G. F. Sykes, *J. Compos. Mater.*, 20(1986)579.]

As might be expected, a white-colored membrane degraded faster than a black-colored one. Black membrane deterioration should be accounted for by temperature effect rather than radiation since the natural weathering of the black membrane occurred in a temperature range of 80-90°C.

17.8 COMPOSITES^{56,74-81}

The useful life of a composite depends on the stability of the fiber, the matrix resin, and the adhesion between them. The degradative changes occur mostly on the material surface and it is assumed that the degradation depth is sufficiently shallow to cause little real damage, therefore, there has been no strong incentive to carry out studies on composite stability and not many have been done.

When epoxy-graphite composites were irradiated by an electron beam, the mechanical properties were affected by temperature changes (Figs. 17.34 to 17.36). The lower modulus of irradiated material at elevated temperatures is consistent with the increase in plasticity associated with a lower glass transition temperature. The products of degradation fill the free volume, embrittle, and stiffen the epoxy matrix.

Tensile strength is more affected in the transverse than in the axial direction. SEM analysis of the fracture surface of electron-beam-irradiated graphite/epoxy composite did not show evidence of matrix-fiber interface failure but the fracture surface was rougher than a non-irradiated specimen, indicating that the matrix was degraded. The

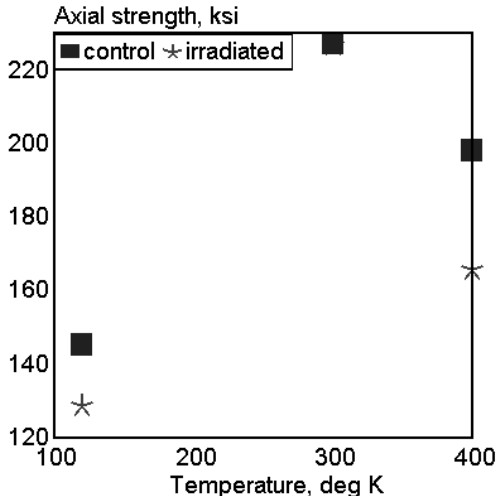


Fig. 17.35. Axial strength of graphite-epoxy composite vs. temperature for control and irradiated specimens (10^{10} rads). [Adapted, by permission, from S. M. Milkovich, C. T. Herakovich, and G. F. Sykes, *J. Compos. Mater.*, 20(1986)579.]

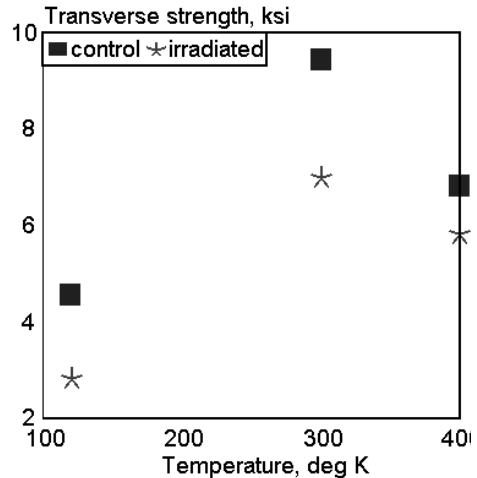


Fig. 17.36. Transverse strength of graphite-epoxy composite vs. temperature for control and irradiated specimens (10^{10} rads). [Adapted, by permission, from S. M. Milkovich, C. T. Herakovich, and G. F. Sykes, *J. Compos. Mater.*, 20(1986)579.]

effect of irradiation was visible from the T_g data; the T_g was 50°C lower for the irradiated sample than for the control. The interlaminar shear strength of γ -irradiated glass fiber/epoxy laminates decreased as the dose increased (Fig. 17.37). Similarly, its tensile and flexural strengths were reduced but there was an induction period during which the mechanical properties were constant followed by a rapid decrease in both tensile and flexural strength.

A surprisingly fast degradation of tensile strength was observed for aramid/epoxy composites weathered in natural conditions in California.⁷⁹ Specimens lost 24% of their initial strength after exposure for 77 days. A similar effect was achieved during a 5-year-long irradiation using fluorescent light. The same composite was studied to determine how laser irradiation temperature and humidity affected it (Fig. 17.38). A decrease in fiber strength as temperature is increased can initiate a catastrophic failure in stressed composites. The composite failure is rapid because, upon fracture of the exterior fibers, the remaining load-bearing fibers carry a higher load and are more susceptible to failure at lower temperatures and stresses.

Moisture in the composite deforms and ultimately ruptures the matrix as it escapes when heated. Pressure also develops at the fiber-matrix interfacial region.

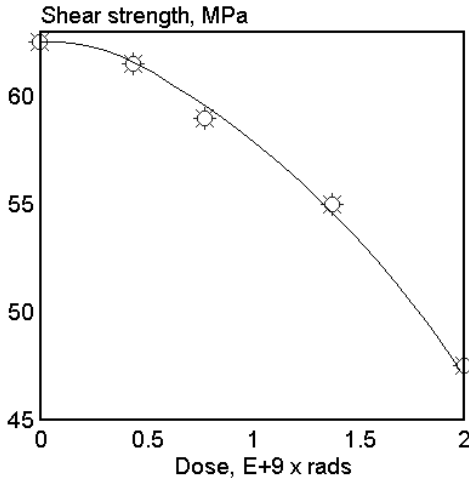


Fig. 17.37. Degradation of interlaminar shear strength induced by gamma irradiation. [Adapted, by permission, from T. Okada, S. Nishijima, and H. Yamaoka, *Adv. Cryogenic Eng. Mater.*, 32(1986)145.]

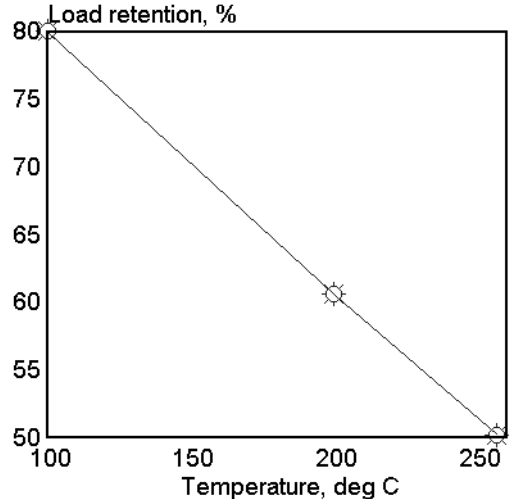


Fig. 17.38. Ultimate load retention (relative value at 23°C) vs. temperature for Kevlar 49 yarn. [Adapted, by permission, from R. J. Morgan, F.-M. Kong, and J. K. Lepper, *J. Compos. Mater.*, 22(1988)1026.]

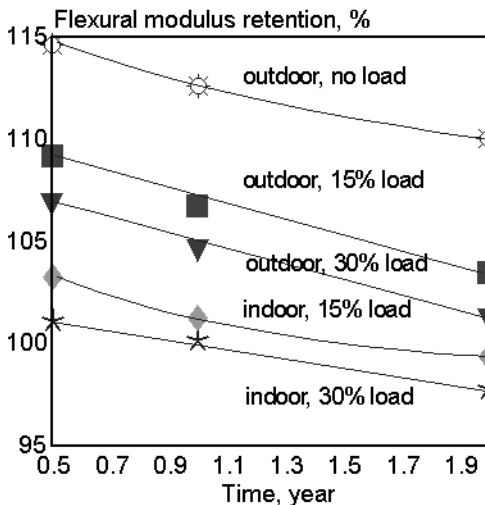


Fig. 17.39. Flexural modulus retention vs. exposure time of fiberglass reinforced composite. [Data from T. Watanabe, *Kobunshi Ronbunshu*, 39(1982)1.]

Ehrenstein⁸⁰ discusses the effect of chemical and physical parameters on aging and corrosion of composites due to the loss of the protective functions of the polymeric material.

Watanabe⁸¹ shows the rates of composite weathering at different loads (Fig. 17.39). Fiberglass-reinforced plastic, during the first half year of weathering, has undergone a crosslinking process which contributed to an increase in flexural modulus. However, as the load force applied was increased, the flexural modulus decreased.

Perry *et al.*⁵⁶ present data on the combined effect of stress and pollutants (NO_x) on bare fibers and fibers embedded in resins. Combination of stress (especially at higher levels — 70% and above of

ultimate strength) with NO_x present (even at low concentrations, 0.1% — close to that found in nature) has an accelerating effect on the deterioration of both bare fibers and composites.

17.9 SPACE APPLICATIONS^{74,82-91}

Space programs find applications for high performance composites which are able to withstand these harsh conditions:

UV radiation	> 230 μm
temperature range	-52-+85°C
proton and electron radiation	4.5×10 ⁴ rad/year
cosmic radiation	<2 rad/year
micrometeoroid and debris impact	6000/year/station
atomic oxygen fluence	6.6×10 ¹³ - 4.3×10 ¹⁸ atoms/cm ²
vacuum	10 ⁻⁶ -10 ⁻⁷ torr

Since the materials must endure these conditions for 25-30 years, there is an obvious interest in studies which can help to predict problems or confirm the stability of the material over this period of time (see Table 17.1 to evaluate interrelation between environment, its effect, and design factors).

Table 17.1: Environments, effects, and design factors for organic matrix composites for space applications [Information from P. E. George and H. W. Dursch, NASA Conf. Publ. 3257 (1994)]

Environments	Effects	Design factors
Atomic oxygen	Erosion	Dimensional stability
Ultraviolet radiation	Bulk chemical changes	Stiffness
Thermal	Surface chemical changes	Strength
Particle radiation	Microcracking	Outgassing
Contamination	Outgassing	Optical properties
Microvacuum	Physical damage	Damage resistance
Meteoroid and debris impact	Discoloration	Weight

Extensive studies have been done for NASA⁷⁴ on composites of graphite fiber and polysulfones and graphite fibers and epoxy resins. The effect of a mercury-arc lamp radiation was compared to radiation from an electron linear accelerator. The major gaseous products of irradiation for both resins included: H₂, CH₄, CO, CO₂, C₂H₆, C₃H₈, benzene, acetone, toluene, ethylbenzene, styrene, and isopropylbenzene. The mechanism of for-

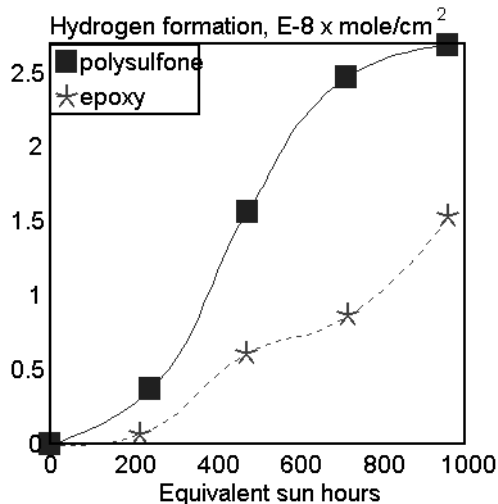


Fig. 17.40. Hydrogen formation during UV irradiation exposure. [Adapted, by permission, from C. Giori and T. Yamauchi, *NASA Contractor Rep.*, 3559.]

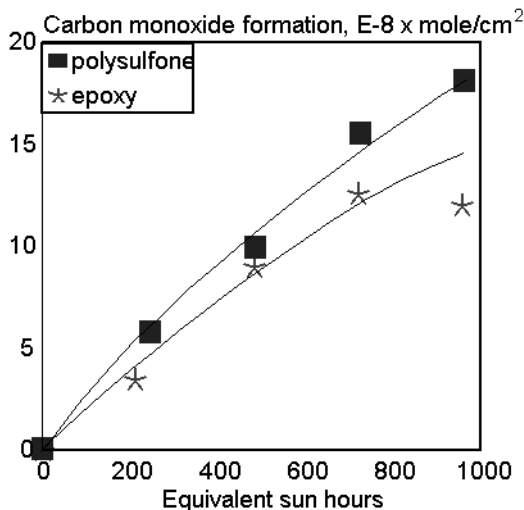


Fig. 17.41. Carbon monoxide formation during UV exposure. [Adapted, by permission, from C. Giori and T. Yamauchi, *NASA Contractor Rep.*, 3559.]

mation of these components was discussed and it is the same as the explanations of the mechanisms of degradation for these two polymers given in Chapter 14. Carbon monoxide and hydrogen are the main products of photolysis, and it is interesting to compare their evolution both for polymers and for the sources of radiation (Figs. 17.40 to 17.43). The epoxy resin composite is more resistant than the polysulfone composite. The epoxy resin was cured with an amine, and it is interesting to note that no nitrogen-containing compound was found in the products of degradation. The amine cure contributes to the higher stability of epoxy resins. Degradation by electron beam produced more volatiles. The measurement of compressive and flexural strength did not give a distinctive difference because the radiation doses were not sufficient to cause change.

Samples of numerous polymers (PTFE, Kynar, PSF, PIM, PS, PVT, PMMA, PA, PET, PU, SI), their laminates on metal foils, and composites were exposed in space for 5.8 years.⁸² None of the films survived this exposure. Samples exposed for 10 months were exposed to different conditions in which they were exposed to less atomic oxygen because they were tested at a lower orbit and sealed in a vacuum canister. The 10 months samples exhibited both crosslinking and chain scission as determined by GPC studies. It was found that organic silicone is oxidized to silicate which retards further erosion of samples by atomic oxygen. The degradation of samples is retarded by their surface contamination which is called "nicotine stain". Often, this stain contains silicon. Paints, which were tested in this and preceding programs suffered a loss in gloss which

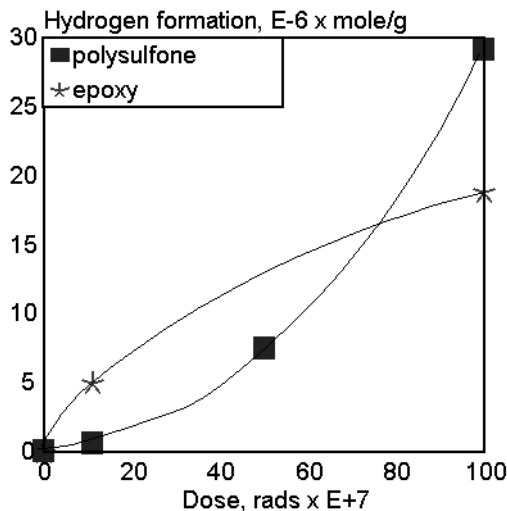


Fig. 17.42. Hydrogen formation during electron radiation exposure. [Adapted, by permission, from C. Giori and T. Yamauchi, *NASA Contractor Rep.*, 3559.]

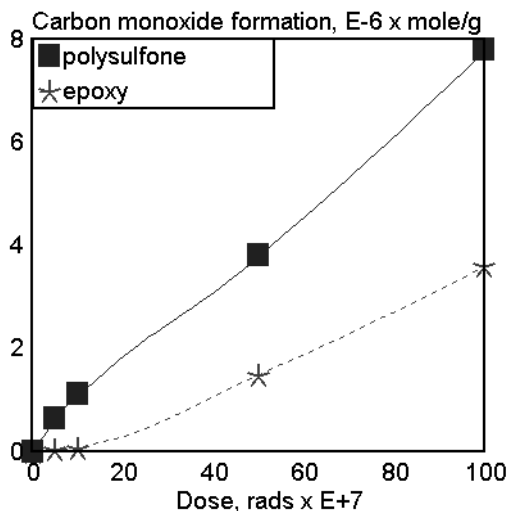


Fig. 17.43. Carbon monoxide formation during electron radiation exposure. [Adapted, by permission, from C. Giori and T. Yamauchi, *NASA Contractor Rep.*, 3559.]

was regained after conditioning in the laboratory. A French study⁸⁵ shows that paint recovered its original reflectance after 5 days of conditioning in laboratory conditions after over 2000 days of space exposure (in American studies, paint samples were tested after several months delay. The recovery process had occurred before samples were tested). Black-colored paints are bleached due to the simultaneous action of UV and molecular oxygen.⁸⁵

Metal film laminates were inspected for defects in the protective metal layers.⁸³ It was found that defects in the film allow molecular oxygen to directly interact with the polymer and cause a much faster erosion. This takes the form of deep but narrow cavities which increase in size during exposure. The process could be simulated by computer modelling.

Several epoxy composites were studied in this project, including glass, carbon, and Kevlar fibers.⁸⁴ Fig. 17.44 shows that these composites lost mass in the simulated environment. Carbon fiber suffered the greatest mass loss. Glass fiber was more resistant to atomic oxygen. Atomic oxygen degradation is a two-step reaction: first, the matrix between the fibers is eroded then fibers themselves. Partially damaged fibers are the sites of crack initiation. Samples of composites exposed in space showed very little change in mechanical properties in all conditions other than when atomic oxygen is present.⁸⁶ In the absence of atomic oxygen, carbon fiber reinforced composite performed best. It did not undergo the heavy discoloration typical of a glass fiber reinforced composite. Expo-

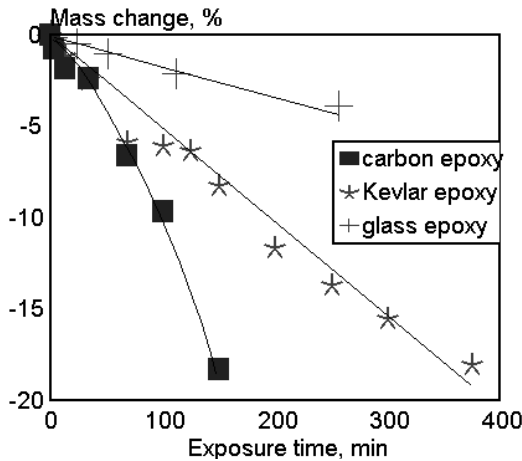


Fig. 17.44. Mass loss per surface area of composite exposed to atomic oxygen. [Adapted, by permission, from B. Z. Jang, J. Bianchi, Y. M. Liu, and C. P. *Change in LDEF Materials Results for Spacecraft Applications*, Eds. A. F. Whitaker and J. Gregory, *NASA Conf. Publ.*, 3257, 1994.]

sure to the full conditions (including atomic oxygen) changed the picture. The glass fiber reinforced material had only surface erosion. Exposed glass fibers shielded the composite from further damage. The carbon fiber composite lost fiber down to 0.12 mm below the surface. In spite of this, this composite did not have a substantial loss of mechanical properties.

Knowing the severe effect of atomic oxygen on samples and the difficulty in simulating space conditions in the laboratory, a space shuttle missions was partially devoted to determining the exact exposure to atomic oxygen and its effect on polymer degradation.⁸⁷ Using mass spectrometer data, it was established that samples were exposed in this experiment to a fluence of 2.07×10^{20} atoms of atomic oxygen. Also, the composition of atmosphere in space was estimated. Water and carbon dioxide are absent in space. Atomic oxygen has approximately 1000 times higher concentration

than molecular oxygen and about 10 times higher concentration than molecular nitrogen. The efficiency of sample oxidation was determined by measuring the volume of sample removed per one atomic oxygen atom. Data from this study are given in Table 17.2.

These studies could have been executed in a more effective manner if the researchers had made better use of data collected previously in earth-bound experiments. Example of this is the disappearance of samples during exposure. Also, materials used in the studies were different from those normally used on earth and this choice was made because of the expected severity of the conditions. Cost cutting measures in this very expensive program resulted in no funds being available to test the samples immediately on their return from space (e.g., samples of paint were exposed in space and not tested in time because of the lack of funds). Such studies should not be undertaken unless there is a well developed program in place to evaluate all of the possible effects. The other area which requires improvement is related to the method of exposure. Based on the data available in the current literature, there is a lack of definition of the exposure conditions. In order to obtain comparative values from the different programs conducted throughout the world, the amount of energy and its type must be monitored.

Table 17.2: Reaction efficiencies of different polymers in space [Information from L. J. Leger, S. L. Koontz, J. T. Visentine, and D. Hunton, NASA Conf. Publ. 3257 (1994)]

Polymer	Producer	Reaction efficiency $\times 10^{24}$ cm ³ /atom
Aclar (33C)	Allied	1.1
Halar	Allied	2.2
High density polyethylene (EMH6606)	Phillips	4.3
Kynar	Penwalt	1.4
Liquid crystalline (LCP 4100)	DuPont	3.7
Liquid crystalline (Xydar)	Amoco Chemical	3.3
Mylar A	DuPont	4.4
Polycarbonate (C-39)		7.0
Polychlorotrifluoroethylene		1.0
Polyetheretherketone (Victrex)	ICI	3.9
Polyimide (Eymyd F)	Ethyle Corp.	3.0
Polymethylpentene		6.1
Polyphosphazene (X-221)	Ethyl Corp.	$<5 \times 10^{-2}$
Polytetrafluoroethylene		6.5×10^{-2}
Tedlar	DuPont	4.3
Tefzel blue (WP-4)	Raychem	1.3
Tefzel white (WP-4)	Raychem	1.0

17.10 BUILDING MATERIALS⁹²⁻¹⁰¹

Building materials form a very diverse group from the point of view of material origin, chemical composition, and function. Since buildings are in service for very long time, there is a great deal of experience available, but there is also a surprising lack of systematic studies. Until quite recently most building materials have been natural materials with good durability. There was no pressing need to study durability. This has changed with the introduction of polymeric materials. They lack the benefit of longstanding observations and they are not as durable as traditionally-used products. The situation is complicated by the fact that frequent changes and improvements in these materials do not offer an opportunity for their broader understanding because studies take a long time and the life of a commercial product in the market is relatively short. Yet buildings are expected to last at least 60 years; bridges are designed to last 120 years. Some misconceptions which exist in countries with a hot climate (the Middle East) have resulted in the complete degradation of buildings in 5-10 years, and it is also not unusual for damage to occur in 15-20 years in European buildings which are traditionally believed to last for centuries. Major problems which occur throughout the world are:

- fading and hardening of plastics
- rotting of timber window frames
- fading, flaking, and deterioration of paints
- debonding of jointing materials
- cracking of roofing materials
- softening and expansion of brickwork
- debonding of tiles
- condensation in insulating materials
- corrosion of metal components.

A complete list of all the problems would be much longer. Many new studies are required to be done in a systematic way to investigate these issues.

UV radiation, temperature, and humidity are not the only important factors in determining degradation as seen from the list in Table 17.3. It can be concluded from Table 17.3 that the factors are numerous and they usually act jointly, complicating the formulation of testing conditions.

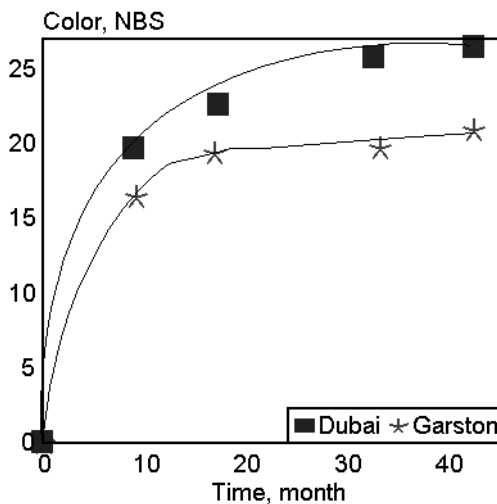


Fig. 17.45. Color change in NBS units of glass-reinforced polyesters vs. exposure time in two locations. [Adapted, by permission, from J. R. Crowder and M. A. Ali, *Durability Building Mater.*, 3(1985)115.]

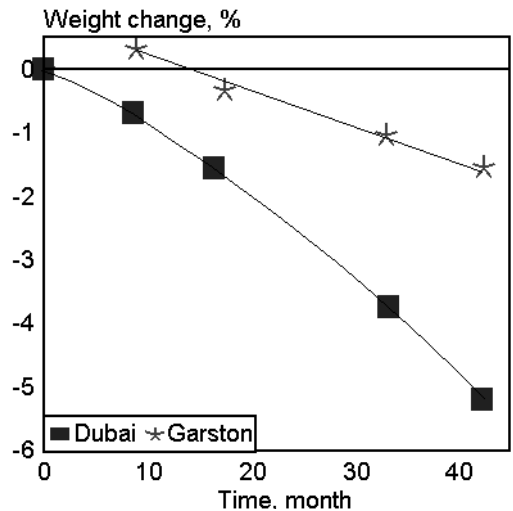


Fig. 17.46. Weight change of glass-reinforced polyesters vs. exposure time in two locations. [Adapted, by permission, from J. R. Crowder and M. A. Ali, *Durability Building Mater.*, 3(1985)115.]

Table 17.3: Factors affecting the degradation of building components

Weathering:	
Radiation:	solar, cosmic, nuclear, thermal
Temperature:	mean, extreme, cycles
Water:	vapor, condensation, rain, ice, snow
Air components:	oxygen, ozone, carbon dioxide
Pollutants:	gases, mists, particulates
Freeze/thaw	
Wind	
Biological:	
Fungi	
Bacteria	
Stress:	
Sustained	
Periodic	
Random:	action of water, snow, hail, wind, settlement, vibrations
Incompatibility:	
Chemical	
Physical	
Use:	
Abuse	
Design	
Installation	
Maintenance	
Wear and tear	

Based on practical observations, the British Building Agency estimated the life expectancy of external wall materials (Table 17.4). Life expectancy of various components varies between 20 to 100 years. This means that certain building elements require frequent maintenance and repair which is what is found in Britain where expenditures are: 40% for maintenance and 60% for new construction.

Some well organized weathering studies have begun to appear in the literature. Glass fiber reinforced polyester sheet has become a commonly-used building material. One study compared the rate of degradation in the Middle East and in England (Figs. 17.45 and 17.46).

Most degradative changes in glass fiber reinforced polyesters involves discoloration, erosion of the resin, fiber prominence, crazing, and pitting. Changes in mechani-

Table 17.4: Life expectancy of building components

	Expected life, years
Brickwork	95
Concrete blocks	65
Reinforced concrete	100
Cellular concrete	50
Timber framing	50
Cedar shingles	45
Asbestos sheeting	40
Aluminum panels	50
Stone masonry	95
Vinyl siding	30
Asphalt waterproofing	24
Mortar waterproofing	19
Exterior wall tiles	30
Steel exterior fixtures	30
Wood interior fixtures	30

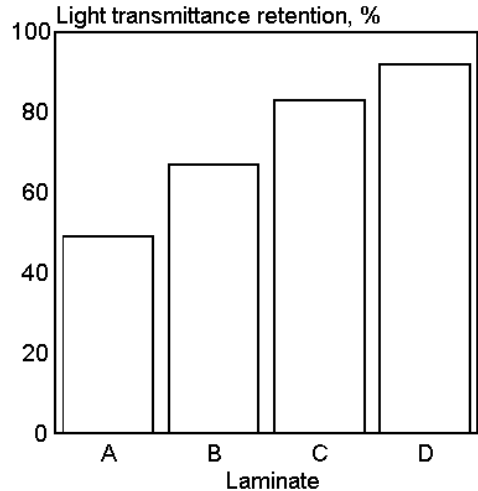


Fig. 17.47. Light transmittance retention by various laminates exposed for 1 year in Mandapam (A-A type glass fibre, B-E type glass fibre, C-surface mat, D-gel mat). [Adapted, by permission, from R. K. Jain, B. K. Saxena, G. D. Bansal, and K. K. Asthana, *Durability Building Mater.*, 2(1983)27.]

cal properties are mostly related to occurrences at the interface between fiber and binder. One Indian study⁹⁶ concentrates on the effect of weathering conditions and the effect of technology on degradation rate. Fig. 17.47 shows the change in light transmittance of various specimens, manufactured in different ways, when exposed to severe weather conditions in Mandapan. The exposure sites with the lower temperature, humidity, and UV radiation had about a 5 times lower degradation rate. Long-term weathering caused changes in flexural strength and weight, as illustrated by Figs. 17.48 and 17.49. Weight loss recorded in India is comparable with the data for England. Data for transparent PVC exposed in Dubai and England⁹⁵ are given by Figs. 17.50 and 17.51.

Relatively small changes and differences between the sites were recorded for light transmission. Color change, mostly related to the intensity and the amount of radiation, is understandably more pronounced in Dubai. Three years of exposure of PVC window frames caused very small changes in color but gloss was drastically reduced.

Blaga and Yamasaki⁹⁷ studied, during 10 years of outdoor exposure, the changes which occurred in two commercial materials made from poly(methyl methacrylate) and used for skylights, enclosures, etc. (Figs. 17.52 and 17.53). High impact poly(methyl methacrylate) is clearly inferior, due to the presence of the impact modifier, which is not weather stable.

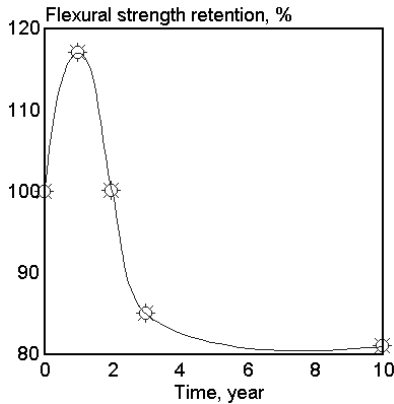


Fig. 17.48. Flexural strength retention of glass fiber reinforced polyester sheet (natural exposure in Roorkee, India - mild climate). [Adapted, by permission, from R. K. Jain, B. K. Saxena, G. D. Bansal, and K. K. Asthana, *Durability Building Mater.*, 2(1983)27.]

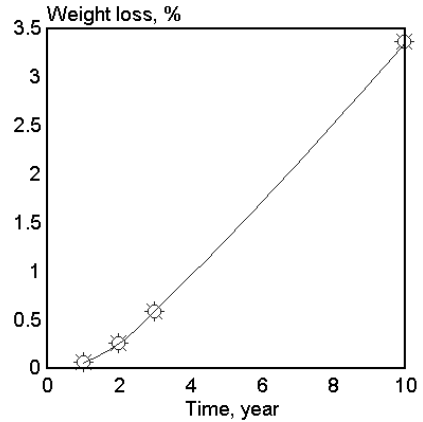


Fig. 17.49. Weight loss of glass fiber reinforced polyester sheet (natural exposure in Roorkee, India - mild climate). [Adapted, by permission, from R. K. Jain, B. K. Saxena, G. D. Bansal, and K. K. Asthana, *Durability Building Mater.*, 2(1983)27.]

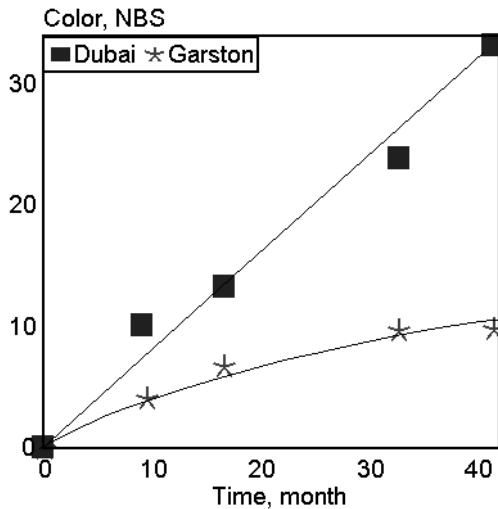


Fig. 17.50. PVC color change in NBS units vs. exposure time in two locations. [Adapted, by permission, from J. R. Crowder and M. A. Ali, *Durability Building Mater.*, 3(1985)115.]

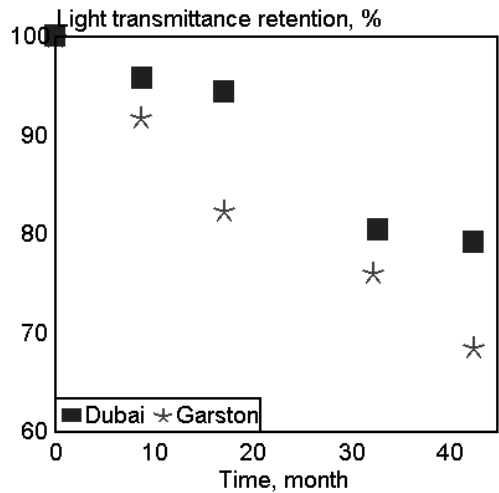


Fig. 17.51. PVC light transmission retention vs. exposure time in two locations. [Adapted, by permission, from J. R. Crowder and M. A. Ali, *Durability Building Mater.*, 3(1985)115.]

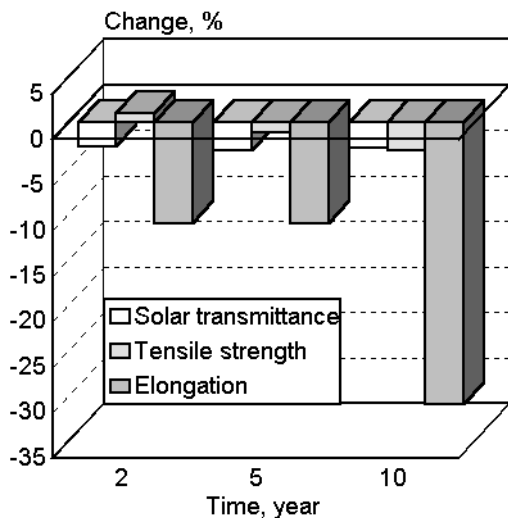


Fig. 17.52. Changes in PMMA sheets (natural exposure). [Data from A. Blaga and R. S. Yamasaki, *Durability Building Mater.*, 4(1986)21.]

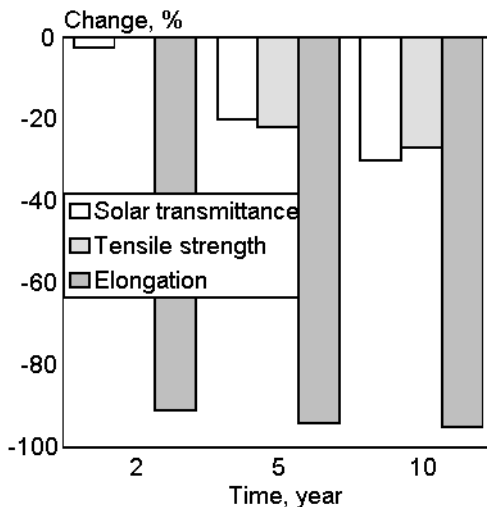


Fig. 17.53. Changes in high-impact PMMA sheets (natural exposure). [Data from A. Blaga and R. S. Yamasaki, *Durability Building Mater.*, 4(1986)21.]

17.11 SEALANTS¹⁰²⁻¹²⁰

Sealant is a material creating a barrier between two environments. The roles sealants play include: joining two dissimilar materials, absorbing the thermal movement of these materials, forming air, water, and sound barrier. A great variety of sealants perform these functions while being exposed to the environment. Thus, they are affected by the daylight radiation, temperature, moisture, pollutants, and stress. Sealants contribute only a small fraction of the building cost but they are responsible for much of the building's performance. The cost of failure and replacement is usually high, prompting a growing interest in the long-term performance of sealants. Several groups of polymeric materials, including acrylics, bitumen, oil-based, rubbers, polyurethanes, polysulfides, and silicones are used in sealant manufacture.

Welch¹⁰² studied polysulfide, bitumen, oil-based, and silicone sealants for seven years in several locations in Queensland, Australia. Constant rate penetrometer readings, changes in surface appearance, adhesion, shrinkage, bleeding, and staining were used as quality indicators. The hardness of all, except polysulfide sealants, increased with aging. Adhesion loss was observed in the case of silicone and oil-based sealants. Surface cracking and chalking were very severe in bitumen and oil-based sealants. Silicone sealants had a tendency to support microbiological growth and accumulate dirt, which resulted in a masking of their initial color.

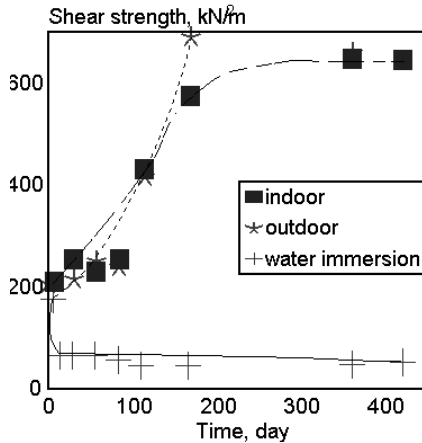


Fig. 17.54. Bond durability of aluminum/acrylic lap joint in different environments. [Adapted, by permission, from L. M. Gan, H. W. K. Ong, and T. L. Tan, *Durability Building Mater.*, 3(1986)225.]

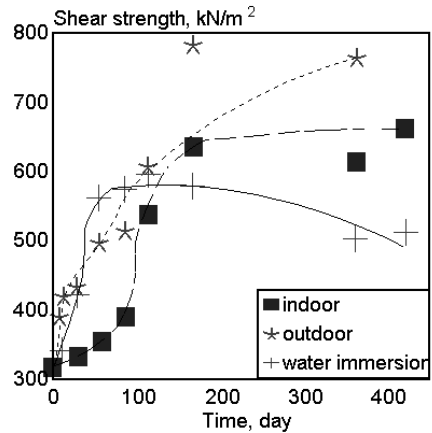


Fig. 17.55. Bond durability of aluminum/polysulfide lap joint in different environments. [Adapted, by permission, from L. M. Gan, H. W. K. Ong, and T. L. Tan, *Durability Building Mater.*, 3(1986)225.]

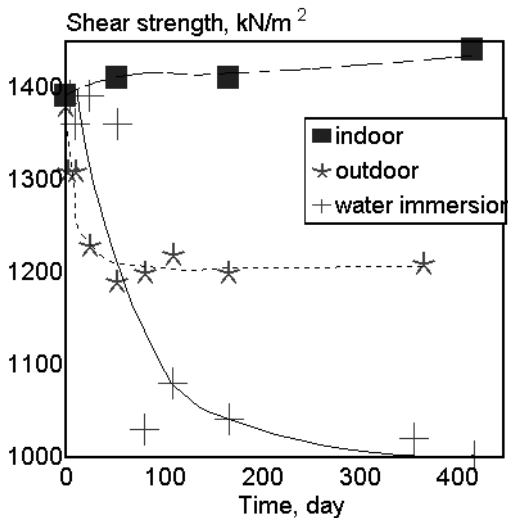


Fig. 17.56. Bond durability of aluminum/silicone lap joint in different environments. [Adapted, by permission, from L. M. Gan, H. W. K. Ong, and T. L. Tan, *Durability Building Mater.*, 3(1986)225.]

Gan¹⁰³⁻⁵ reported a detailed study of the mechanical properties of acrylic, polysulfide, epoxy, and silicone sealants during natural exposure. Figs. 17.54 to 17.56 show the adhesion of acrylic, polysulfide, and silicone sealants exposed to natural weathering and water immersion.

Epoxy adhesive performance depends on the surface treatment of the aluminum and the stress developed in a sealant joint.¹¹² The higher the stress the faster the adhesion joint failure. Relative humidity and moisture diffusion correlated with adhesive strength retention in the joint. Formation of an oxidized layer on the surface of aluminum gradually decreases adhesion and leads to eventual failure.

Water-based acrylic and silicone sealants lose their shear strength when exposed

to water immersion. Additionally, silicone sealants have lower shear strength after outdoor exposure. Studies conducted in New Zealand by Sharman¹⁰⁶ show a similar trend for water-based acrylics (solvent-based acrylics have a better performance). Silicone sealants are the best-performing sealants in this study, which also included polysulfides and polyurethanes, although out of 7 silicone sealants tested, 4 failed adhesively in butt joints during 2-5 years of exposure. Adhesive failure seems to be a major mode of failure of silicone sealants. Thornton,¹⁰⁹ studying the performance of silicones in highway joints, suggests that the main reason for silicone sealant adhesive failure is the mechanism of their cure, which requires water. The moisture from wet joints causes a fast skinning process which severely retards its adhesion to wet substrates.

Three commercial silicone sealants (DC-983, DC-995, and DC-790) were studied to determine the effect of ozone and moisture.¹¹³ The low modulus formulation (DC-790) showed the lowest resistance. A synergism in action of ozone, moisture and acid rain caused substantial surface damage. The medium modulus sealant had the best resistance to weathering. The molecular weight between crosslinks increased for this sealant (DC-995) during exposure but no substantial change in tensile properties was observed. External loading had the most pronounced effect on the high modulus sealant due to the creation of stress centers. Shore C hardness development was studied for about 20 sealants exposed in Florida and Arizona.¹¹⁴ Exposure in Florida increases hardness more than does exposure in Arizona. 30 months exposure did not produce decrease in hardness for any of the studied sealants which indicates that degradation does not affect their mechanical performance.

Bridgewater and Carbarby¹¹⁷ suggest that sealant testing should be expanded to include QUV and elevated temperature testing which, according to their data, should identify sealants which will not perform in the field. Beech and Beasley¹¹⁸ noted that sealants change their hardness during their service life which might be related, in their opinion, to the weather resistance of these sealants (work on weatherstability is still in progress). Minkarah *et al.*¹¹⁹ performed studies on sealants using existing standard methods and determined that these methods do not predict the long time behavior of sealants (sealants were exposed for 608 h).

Karpati¹¹¹ studied the effect of cyclic movement on the performance of polysulfide sealants. Sealants exposed to natural weathering conditions were subjected to cyclic movement in the range of 0 to 30% in a compression/extension cycle. The results of mechanical properties testing (stress-strain curves) do not show that cycling has any effect on mechanical properties but photographs of the beads demonstrated that movement above 21% resulted in material failure. Sealants exposed to both natural and accelerated weathering were tested in a variety of ways to evaluate these different methods.¹¹⁶ With most sealants, 2000 hours of exposure to accelerated weathering corresponded to 2 years of Florida exposure based on the formation of cracks of similar shape and density.

The conclusions of these works on sealants have been included in this review to show that studies on sealants have very little consistency and sense of direction. Compared with any other group of products tested, the methods used in sealant testing are the least advanced (they practically do not go beyond a visual observation of cracks). It is evident from the above review that there is no mention of chemical mechanisms of degradation (it has not been omitted - such data simply does not exist) and only such a treatment would allow us to understand material performance and how to improve its performance. The level of understanding of sealant material performance is no different from that reported in the earlier edition of this book, 5 years ago. This can be explained in part by the fact that, although some of this work has been done, the results have never been published.

17.12 PLASTIC PIPES¹²¹⁻¹²³

Plastic pipes are used in many common applications. Underground fuel gas distribution pipes are one of most demanding applications because of the high risk involved, due to the nature of the piped product. Such pipes are usually covered and are therefore not prone to weathering after they are installed. Prior to installation, however, pipes are not

always stored in controlled conditions. Polyethylene and polybutylene are the common materials used for fuel gas transportation piping, which aggravates the storage problem, since both polymers are not weather stable.

A study using the compressed-ring environmental stress cracking resistance test¹²¹ shows that polyethylene pipe can be degraded in a short exposure time (Fig. 17.57). Polybutylene pipe showed significant evidence of deterioration after 3 months of exposure (similar to presented by Fig. 17.57 for polyethylene pipe). Tests on a second lot of polyethylene pipe showed that it was more durable, since changes in it occurred between the 9th and 15th month of exposure. No explanation was given for the difference in behavior. Microscopic evaluation of the exposed samples shows severe, regular, surface crazing and cracking, which is made worse by the stress applied to the material during weathering.

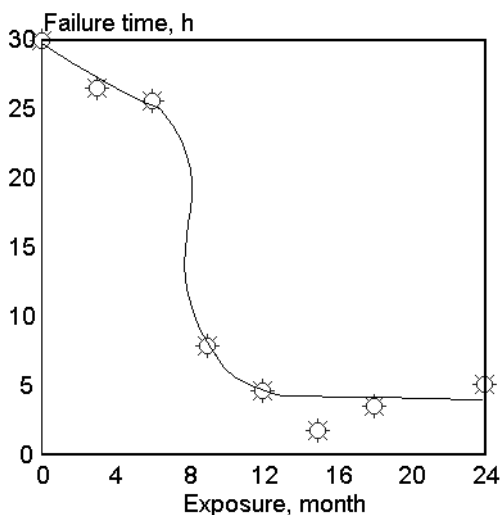


Fig. 17.57. Compressed-ring test of failure time vs. pipe exposure to natural conditions. [Adapted, by permission, from M. J. Cassady, M. M. Epstein, A. Lustiger, and R. L. Markham, *Report (NITS)*, PB83-162073.]

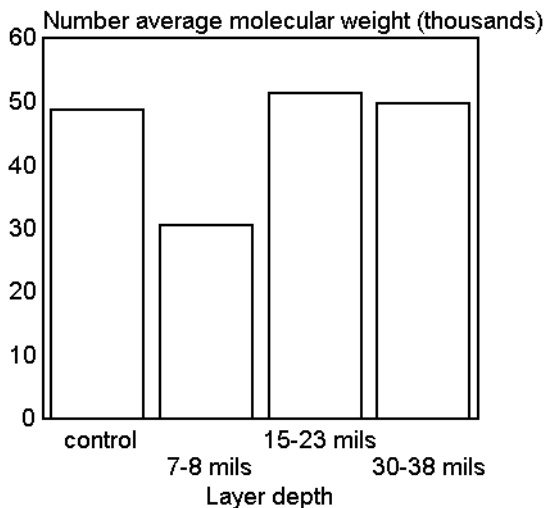


Fig. 17.58. Molecular weight of polybutene vs. layer depth (36 months of natural exposure in Florida). [Data from M. J. Cassady, M. M. Epstein, A. Lustiger, and R. L. Markham, *Report (NITS)*, PB83-162073.]

Since cracking is mostly a surface phenomenon, it was interesting to evaluate the depth of deterioration. Fig. 17.58 shows the average molecular weight of material samples obtained from different layers. Only the surface layer appears to be affected by degradation process. Deeper layers have molecular weights similar to the unweathered sample. These data are also confirmed by differential scanning calorimetry, which shows that the induction period of degradation is changed only in the surface layer. Because it constitutes only a fraction of pipe thickness (7-8 mils), the authors¹²¹ were satisfied with the pipe's performance but proposed improvements be made in the method of pipe storage. Since a pipe cracks on its external surface and its performance depends on how it can withstand internal pressure, surface cracking

is potentially dangerous. Impact resistance is always substantially less on the unexposed side.

Hamid *et al.*¹²² present results of PVC pipe exposure in various parts of Saudi Arabia. The molecular weight of the polymer changes quite rapidly (after one year of exposure the molecular weight is less than 50% of the original). Carbonyl group formation increases with time of exposure. Chemical changes correspond to a lowering of mechanical performance. There is a detectable difference between the various exposure sites. Exposure duration is the dominant factor affecting degradation.

17.13 BITUMINOUS PRODUCTS¹²⁴⁻¹²⁸

Bituminous products are in widespread use in the roofing industry, in pavements, and in membranes. Their complex chemical nature, which is related to the chemical composition of asphalt, is difficult to study. Additionally, various polymeric materials are frequently added to modify the properties of asphalt and these, usually small, additions play a very essential role in the final properties of the product.

Asphalt contains various components which give it good weathering properties. Most degradation occurs, not due so much to irradiation, but due to the high temperatures generated in asphalt-containing materials because of their high absorption of energy related to their black color. This degradation mechanism (thermooxidation)

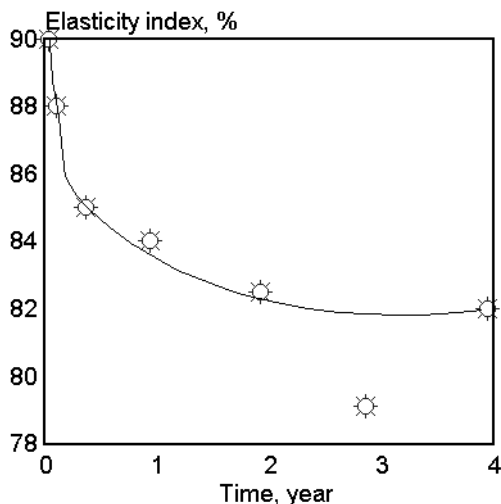


Fig. 17.59. Elasticity index of roofing membrane vs. time of outdoor exposure. [Adapted, by permission, from J. C. Marechal, *Durability Building Mater.*, 1(1982/83)201.]

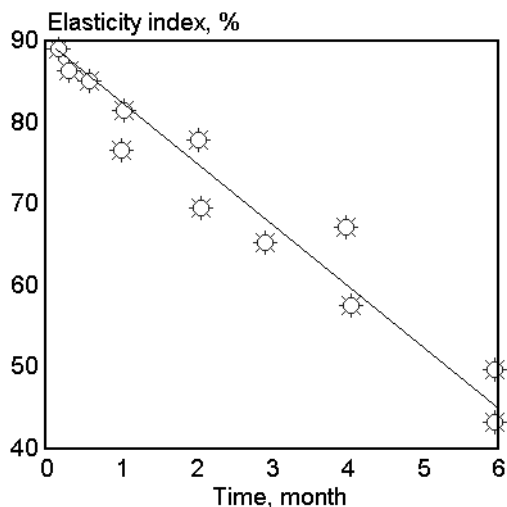


Fig. 17.60. Elasticity index of roofing membrane vs. time in 70°C oven. [Adapted, by permission, from J. C. Marechal, *Durability Building Mater.*, 1(1982/83)201.]

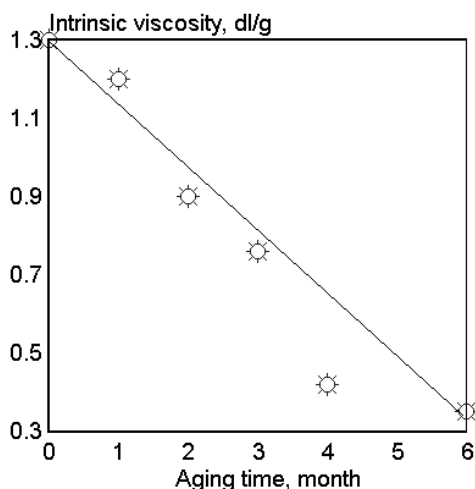


Fig. 17.61. Thermal degradation of SBS binder at 70°C. [Data from J. C. Marechal, *Durability Building Mater.*, 1(1982/83)201.]

suggests to many authors that natural conditions can be best simulated by aging materials at elevated temperature, rather than by exposing them to UV radiation.

Marechal¹²⁴ studied the aging of SBS modified bitumens, protected against UV by a covering of a fine layer of mineral granules. Here, the aging effects were caused by thermooxidation. These studies did show that natural aging can be simulated by thermal degradation (Figs. 17.59 and 17.60). Oven tests accelerate changes in elasticity beyond those caused by natural conditions. Studies using GPC show that both naturally aged and oven aged samples lose elasticity because butadiene double bonds are oxidized. Also, an increase in the asphaltene content increases the elasticity of bituminous materials. The intrinsic viscosity of polymeric material extracted from

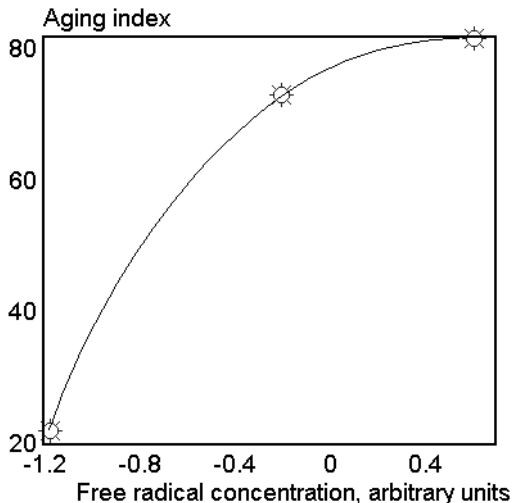


Fig. 17.62. Aging index of various types of asphalt vs. change in free radical concentration between aged and unaged specimens. [Adapted, by permission, from B. J. Humphrey, *Report*, ADA 178471.]

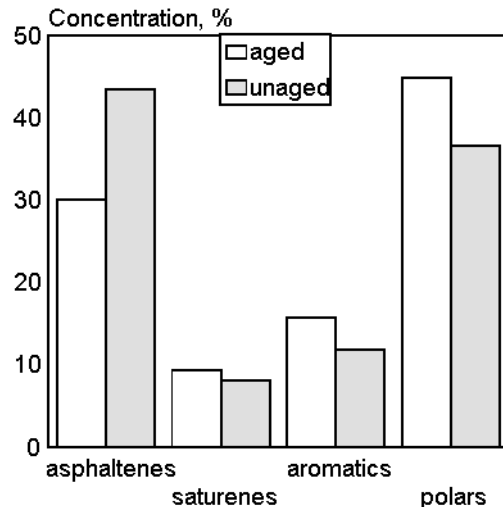


Fig. 17.63. Compositional analysis of Huntway asphalt. [Data from B. J. Humphrey, *Report*, ADA 178471.]

compound was correlated with durability (Fig. 17.61). The rheological properties of the material change during aging from elastic behavior to plastic behavior.

Humphrey¹²⁵ used ESR to analyze a large number of bitumen-related material including some which were oven-aged. The change in free radical concentration, R , between aged and unaged samples correlates with an aging index (Fig. 17.62). The increase of free radical concentration can be explained by oxidative changes which occurred with aging. A chemical composition study also determined that there was an increase in asphaltenes and a decrease in all other components (Fig. 17.63). This change in composition can be explained by the oxidative changes which occur in the material.

Studies of aged roofing membranes, which have been rejuvenated by treatment with resaturants, showed that the tensile strength of a material decreases as its modulus increases when the membranes are exposed to long-term natural weathering. Increased temperature and greater moisture penetration cause faster degradation of roofing materials. Resaturant treatment was found to be ineffective in the membranes studied. The methods of measuring the effectiveness of the treatment were also not appropriate.

Tanaka *et al.*¹²⁸ developed a method to estimate the thermal degradation load which is calculated according to the equation:

$$\frac{1}{n+1} \left(\frac{1}{y^{n+1}} - \frac{1}{y_0^{n+1}} \right) = A \sum \exp(-B/T)t$$

where	n	apparent reaction order
	A,B	material constant related to thermal degradation
	y	value of a physical property of the material
	y ₀	initial value of y
	T	material temperature in K
	t	time in h.

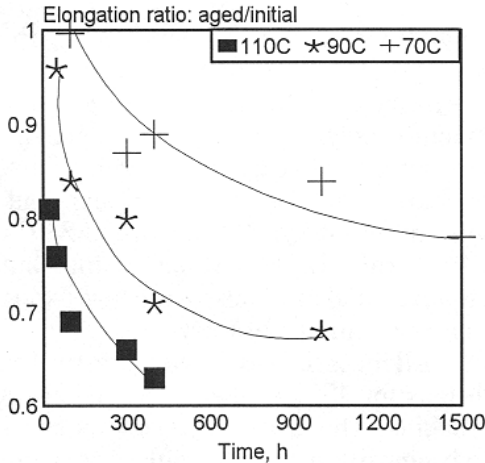


Fig. 17.64. Comparison between heat aging test results and calculated values (lines). [Adapted, by permission, from K. Tanaka, H. Hashida, T. Kuibira, and M. Koike, *Rep. Res. Lab. Eng. Mater., Tokyo Inst. Technol.*, 15(1990)179.]

ture.

17.14 COVER PLATES FOR SOLAR COLLECTORS¹²⁹⁻¹³¹

The selection of material for cover plates of solar collectors should take into consideration several of these factors listed in Fig. 17.65. Most of these indicators of material suitability relate to a long-term stability. Materials used for solar collectors are usually

The right side of the equation determines the degree of roofing material degradation and it is here referred to as the thermal degradation load. Fig. 17.64 shows the result of using this model to predict roofing membrane degradation. Lines are calculated from equation and points determined in the test of materials. Agreement between the experiment and the prediction is very good. The results from laboratory were then compared with observations in field and, again, very good correlation was obtained. The model was then used to develop a load map of Japan. After some experience with this method, the authors believe that this method gives very good prediction of material performance in the field, although one should be aware that the predicted degradation is always slightly less than actual because the material also degrades due to UV and mois-

Transmittance of solar radiation

Mechanical properties

Durability

Cost of materials and labor

Cost of maintenance

Dust deposition

Fig. 17.65. Selection rationale of the material.

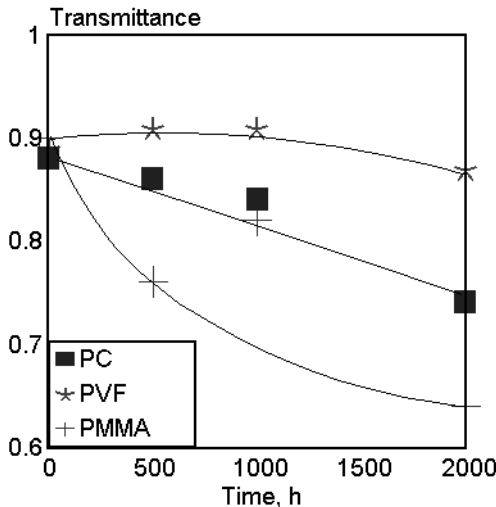


Fig. 17.66. Effect of specimen exposure to 95% RH at 95°C. [Data from D. Waksman, W. E. Roberts, and W. E. Byrd, *Durability Building Mater.*, 3(1985)1.]

selected from readily available materials regardless of the fact that the conditions in this application differ from the conditions to which typical polymeric products are exposed. Materials for cover plates are continuously exposed to radiation at elevated temperatures. The temperature of a solar collector can be as high as 150°C. A broad range of working temperatures induces stress which is high relative to the thermal expansion coefficient. Additional stress can be produced by the exposure of the collector to wind. Finally, the composition of air at the exposure site (humidity, particulate materials, pollutants) contributes to the rate of material degradation.

Several materials, including poly(ethylene terephthalate), polycarbonate, poly(vinyl fluoride), poly(methyl methacrylate), fluorinated ethylene-propylene copolymer, and glass fiber composites, were studied by the National Bureau of Standards. Materials were exposed in four different sites (Phoenix, AZ; Cape Canaveral, FL; Palo Alto, CA; and Gaithersburg, MD) and these were also exposed in a xenon arc laboratory tester.

All materials exposed to natural conditions for 480 days, experienced surface cracking. The crack pattern was specific to composition and exposure site. Generally, greater changes were observed in sites with high humidity (Palo Alto and Cape Canaveral). Microcracks did not form during artificial weathering studies

regardless of the temperature. Most materials retained their initial visible light transmission properties. From all the studies conducted, exposure to high temperature (90°C) and high relative humidity (95%) had the most detrimental effect on light transmission retention (Fig. 17.66). Poly(methyl methacrylate) is most affected by the combined effect of temperature and humidity. All materials retained their transmittance when exposed to outdoor weathering for 480 days or accelerated weathering.

17.15 AUTOMOTIVE MATERIALS¹³²⁻¹³⁵

Materials for automotive applications are probably the most extensively studied. The relatively small number of references in this section is due to the fact that most compounds used in the automotive industry were discussed earlier in Chapter 14 under individual polymers. Also, some other sections in this chapter contain some automotive materials (coatings, upholstery). Below, some of the less usual materials are discussed.

Engineering plastics form a group of materials widely used by automotive industry. They are seldom composed of one polymer. They are blends or alloys of several polymers (see Blends in Chapter 14) or compounds containing several additives used to modify the properties of the polymer. The main polymers in this group are PC, PEST, PSF, PET, PAR, PPO, and PA. Most of them contain aromatic groups which can absorb UV radiation.

Motorcycle helmets are frequently formed from PC and ABS and are representative of automotive products. Both polymers are degraded by exposure to UV. After 18 months of exposure, cracks can be observed in an ABS helmet at low magnification (35x).¹³³ The cracks run parallel to the flow direction of injection molding indicating that they develop through an enlargement of initial imperfections in the material. Impact at low temperature (-20°C) increases the probability of cracking. Cracks are also formed along weld lines in the front of helmet. The rear of the helmet, which is exposed to more radiation from daylight, and degrades more extensively, has numerous cracks and is extensively yellowed. The other affected areas degrade due to design weaknesses and stress concentration in the shell. Their structural properties may be sufficiently decreased after 2 years of use that the helmet may not be able to absorb impact without failing. Polycarbonate helmets are more durable, although blue pigmented products are known to degrade after two years of exposure. Black shells are significantly more durable than blue or red ones.

Amos and Leake¹³⁴ evaluated desorption of residual chemicals deposited on the surface of automotive paint. Chemicals are absorbed less readily by polyurethane paints than by alkyd paints and are removed more easily. There is a large difference between removal of residual contamination in summer and winter. In summer, a 3% residual contamination can be removed within 2-4 hours. In winter, removal of residual chemicals is 8 times less effective.

Wootton¹³⁵ discussed methods used in testing products used by the automotive industry. He pointed out that, due to the worldwide cooperation among automotive companies and their joint ventures, the use of the same methods is becoming more common.

17.16 VINYL SIDING¹³⁶

A large portion of the world's production of PVC is used to make vinyl siding. The product is expected to perform in various climatic zones for extended period of time (20 years or more). Weathering studies are therefore critical to product development. The major aim of the extensive studies conducted by the Vinyl Siding Institute has been to develop methods of comparison, to evaluate effect of exposure on various colors (and to qualify new colors), and compare degradation in full spectrum of climatic conditions where siding

must perform. Four sites were selected for comparative studies: Florida, New Jersey, Ohio, and Arizona. Both Florida and Arizona are well equipped sites which offer accelerated degradation and the other locations represent environments close to industrial centers where the presence of various pollutants adds extra stress factors. Hunter "L", "a", and "b" color components were used throughout this ten years program as a means of applying numeric quantification to the observed changes.

Stoloff¹³⁶ discusses the results obtained which are shown in Fig. 17.67. The first striking observation from this data is the relatively low degradation of specimens in Arizona. TiO₂ acts, in the presence of water, to accelerate degradation and, in the dry Arizona climate, this factor does not come into play (for further explanations see Chapters 13 and 16). It should be pointed out that the results obtained in Arizona do not deny the influence of radiation which is a major degrading force and acts in combination

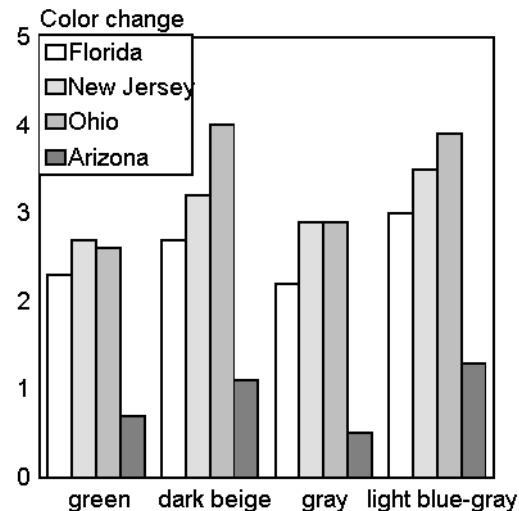


Fig. 17.67. Weathering of vinyl siding for a period of 18 months in different locations (exposure 45° South). [Data from A. Stoloff, *J. Vinyl Technol.*, 15(1993)208.]

with other factors. The high humidity of the Florida climate accelerates degradation by a factor from 2 to 4. The greater acceleration, observed close to the industrial sites, is due to industrial emissions.

Fig. 17.67 shows only the initial (the most rapid) stages of degradation. The data in the paper shows that color becomes relatively stable after 3-4 years of exposure (in fact, in most cases some of the initial color changes were gradually reversed).

17.17 FILMS,¹³⁷⁻¹⁴⁷ CABLES,¹⁴⁸⁻¹⁴⁹ AND TAPES¹⁵⁰

Films find numerous applications in consumer products. Polyethylene is often used as a greenhouse film and, since it is not the most stable polymer, specific grades with good stabilization must be selected based on weathering studies. Matz¹³⁸ developed a method based on HPLC which permits the monitoring of the UV stabilizer in greenhouse film during its processing and exposure. Fig. 17.68 shows the results obtained with stabilized greenhouse film used in Jordan.¹³⁹ It was discovered that incorporation of stabilizers interferes with the crystallization in polyethylene film which then becomes more amorphous. At a sufficiently high level of stabilizer, the amorphous regions become well enough protected to use the film for at least a year without much loss in its original properties. Similar studies were conducted in Thailand.¹⁴¹ It was found that the addition of 0.2% UV stabilizer can extend the life of greenhouse film 4-5 times. It was also found that film degrades 7-9 times faster in accelerated conditions than in a natural environment. The degradation of a film without stabilizer was much faster in this study than in others.

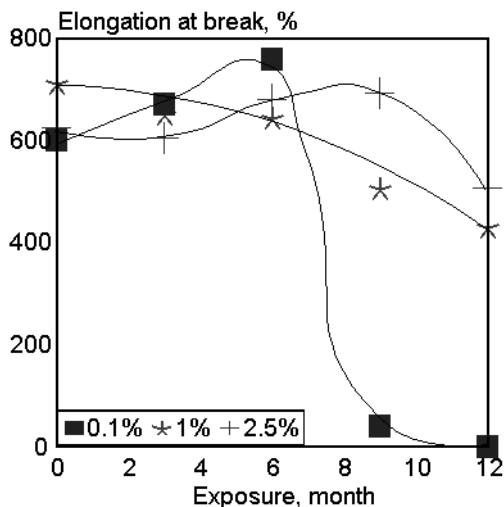


Fig. 17.68. Elongation of LDPE films vs. weathering time for different levels of Chimassorb 705. [Adapted, by permission, from N. Khraishi and A. Al-Robaidi, *Polym. Deg. Stab.*, 32(1991)105.]

application. Some of these studies were used to determine degradation of shopping bags.¹⁴² According to these results, the bags degrade 2-4 times faster than normal bags and they can be completely degraded and reabsorbed in the environment. A similar development is reported for bottle cups which contain 10% degradable polymer.¹⁴³ Degradable polyethylene films were studied in detail under UV^{144,145} and in a simulated aquatic environment.¹⁴⁶ A review paper summarizes the current achievements in this area.¹⁴⁷

Multistress aging studies (radiation, temperature, and electrical) were conducted on capacitor-grade polypropylene.¹⁴⁸ Also, an accelerated aging test was developed for polymer insulated cables designed for use in wet conditions.¹⁴⁹ Polyethylene tapes which were crosslinked before UV exposure did not show an increase in creep rate.¹⁵⁰

There is a growing body of literature which discusses developments in photodegradable (environmentally friendly) materials.^{137,142-146} Fergusson *et al.*¹³⁷ discussed a broad group of sensitizers which can be used in this ap-

plication. There is a growing body of literature which discusses developments in photodegradable (environmentally friendly) materials.^{137,142-146} Fergusson *et al.*¹³⁷ discussed a broad group of sensitizers which can be used in this ap-

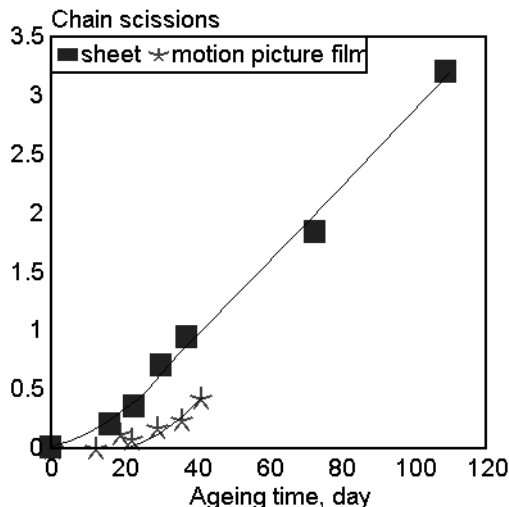


Fig. 17.69. Chain scission of PET used for motion picture and amorphous sheets vs. aging time at 90°C and 100% relative humidity. [Adapted, by permission, from M. Edge, M. Hayes, M. Mohammadian, N. S. Allen, T. S. Jewitt, K. Brems, and K. Jones, *Polym. Deg. Stab.*, 32(1991)131.

Fig. 17.69 shows that PET, used to make motion picture film, has different aging kinetics from PET used for bottles and sheets. The greater crystallinity of motion picture film accounts for the difference. The presence of iron (from storage containers) accelerates degradation to some extent.¹⁴⁰

17.18 WOOD^{34,151-158}

Solar energy, moisture, temperature, ozone, oxygen, pollutants, and microorganisms (mostly fungi), are responsible for the degradation of wood. However, UV radiation is the single most important factor. Solar degradation can penetrate wood only up to a depth of 75 μm . Thus, degradation is a surface phenomenon. Century-old wood is degraded 6-7 mm below its original surface and the changes are faster at the beginning of the degradation process resulting in damage down to 3 mm within one year exposure.

Wood is an excellent UV absorber, since almost all components (cellulose, hemicelluloses, lignin, and extractives) are sensitive to UV light. Electron spin resonance studies revealed that phenoxy radicals, derived from lignin photooxidation, are the principal radicals formed during photodegradation. Lignin in wood plays the role of a binder whose function is to hold together the fibers of cellulose and hemicelluloses. When lignin degrades, it loses its adhesive power which results in a loosening of the fibrous material and causes surface roughness. The chromophores in lignin are able to absorb UV. Cellulose and hemicelluloses do not absorb incident radiation and thus are less vulnerable to radiation damage.

Several softwoods were exposed to artificial weathering and the effect monitored by IR.^{155,156} Initially, different types of wood could be distinguished based on their IR spectra. As degradation progressed, the individual features of each wood were gradually lost and after 2400 hrs exposure, the surface features of all specimens became almost identical and closely resembled oxidized cellulose. Water alone did not produce changes. Exposure to visible light alone produced changes which were somewhat similar to those produced by exposure to the full spectrum of daylight. Lignins and other polyphenolic compounds were the primary absorbing chromophores. Radiation wavelength at around

348 nm causes most of the degradation. Quinone methide is thought to be the active photochemical species which abstracts hydrogen from cellulose and lignins. These changes also cause yellowing and the proposed mechanism of degradation is outlined.¹⁵⁵ The regions in the IR spectrum, which give the greatest response, are: 1730 (carbonyl); 1650 cm^{-1} (quinones and quinone methides). Hardwoods differ from softwoods in their behavior.¹⁵⁶ Lignin removal from the surface and the general degradation mechanism are the same as in softwoods but the rate of the process is different. Since the lower density hardwoods degraded in a manner more similar to softwoods as a whole, it was deduced that the wood's density, and thus the penetrability of liquids is the major factor rather than the chemical composition.

Numerous preparations are offered in the market and are claimed by their producers to prevent deterioration. The chemical composition and physical properties of these products along with the condition of the wood, at the time of application, are the factors which have the greatest influence on the durability of the treated wood. Wood exposed to a natural outdoor environment without treatment rapidly deteriorates on the surface (Fig. 17.70)

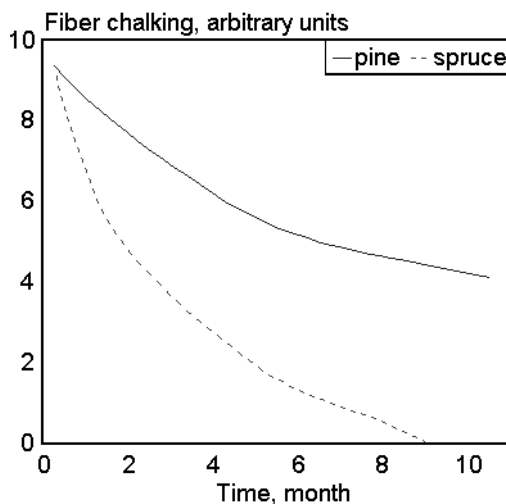


Fig. 17.70. Fibre chalking vs. exposure time in Norway. [Adapted, by permission, from A. Underhaug, T. J. Lund, and K. Kleive, *J. Oil Colour Chem. Assoc.*, 66(1983)345.]

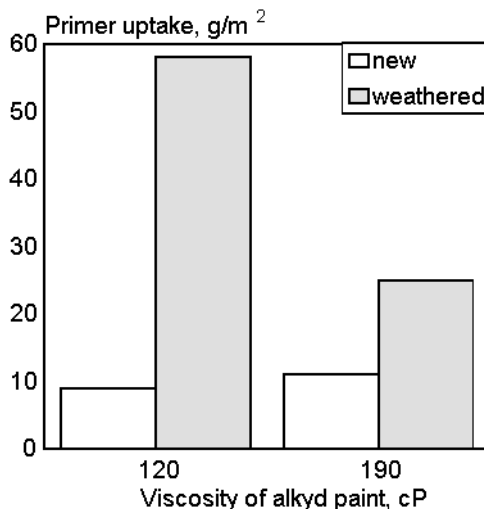


Fig. 17.71. Primer penetration in a new and 1 year old weathered spruce. [Data from A. Underhaug, T. J. Lund, and K. Kleive, *J. Oil Colour Chem. Assoc.*, 66(1983)345.]

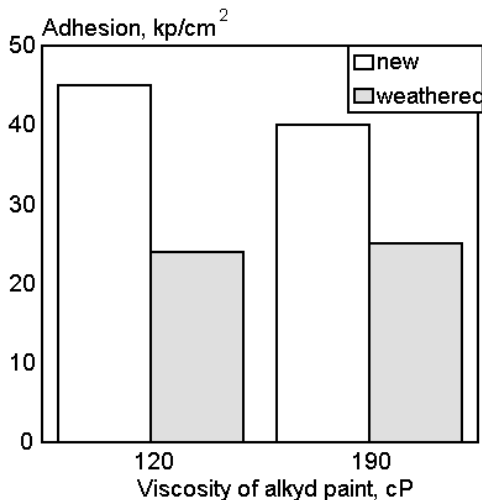


Fig. 17.72. Primer adhesion in a new and 1 year old weathered spruce. [Data from A. Underhaug, T. J. Lund, and K. Kleive, *J. Oil Colour Chem. Assoc.*, 66(1983)345.]

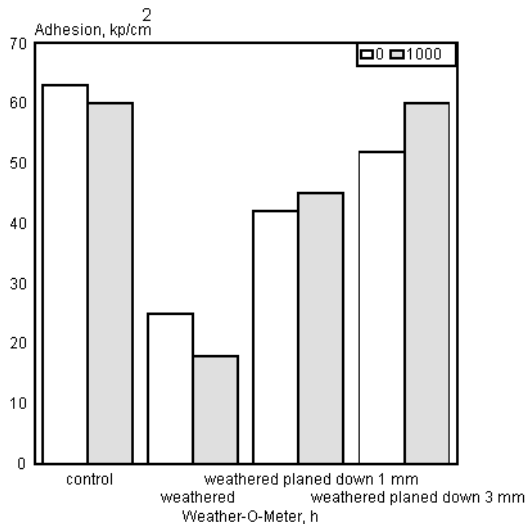


Fig. 17.73. The adhesion of primer to wood exposed for 1 year prepared in different regimes. [Data from A. Underhaug, T. J. Lund, and K. Kleive, *J. Oil Colour Chem. Assoc.*, 66(1983)345.]

A weathered wood surface contains loosely connected wood fibers which can be easily removed by abrasive action. Figs. 17.71 and 17.72 compare properties of new and one-year-aged wood and analyze primer uptake and adhesion. Evidently, new wood requires less primer and primer uptake is not strongly related to its viscosity (dilution). More primer penetrates the weathered wood. Its much higher uptake does not compensate for the damage done by weathering because primer adhesion is lower on weathered wood than on new wood. A SEM study shows that, in new spruce, the primer forms a film on the surface because new spruce is not permeable to primer. In weathered wood, the cells near the surface are all filled with primer, which apparently does not give better adhesion. Another set of experiments shows the depth of damage to wood exposed to weathering without protection (Figs. 17.73 and 17.74).

Degradative changes were 3 mm deep, and only removal of this layer could return the wood to new condition and make further treatment successful. Since primer adhesion is a good indicator of its performance in weathered wood, it may be used to study the rate of degradative processes (Fig. 17.75). After one to two months of exposure, the wood surface is sufficiently damaged to prevent any chemical treatment from being successful.

Feist¹⁵³ discussed the effect of heat treatment of wood on its UV stability. Such treatment is used in order to improve the dimensional stability of wood. Fig. 17.76 shows how thermal treatment affects the rate of erosion of a wood which was chemically pro-

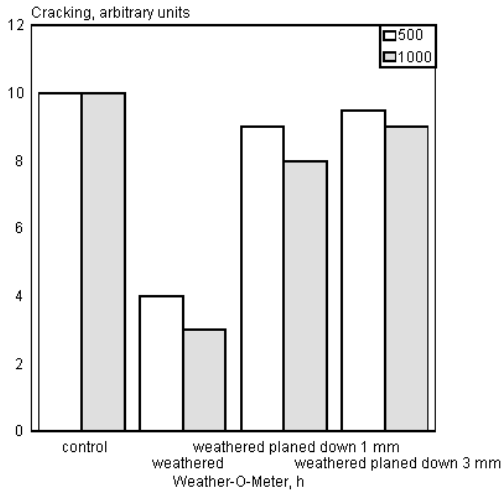


Fig. 17.74. Spruce cracking during Weather-O-Meter exposure after being protected by various regimes following 1 year exposure. [Data from A. Underhaug, T. J. Lund, and K. Kleive, *J. Oil Colour Chem. Assoc.*, 66(1983)345.]

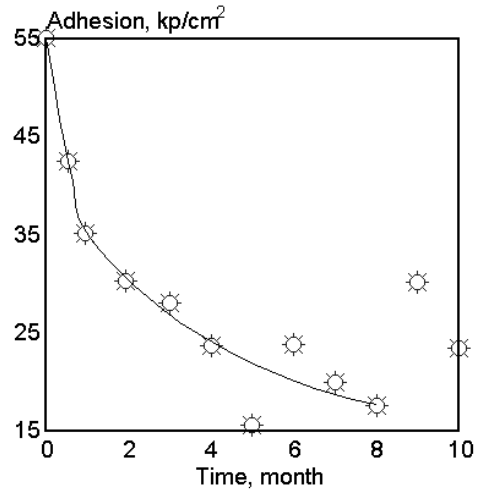


Fig. 17.75. Paint adhesion to wood previously weathered. [Data from A. Underhaug, T. J. Lund, and K. Kleive, *J. Oil Colour Chem. Assoc.*, 66(1983)345.]

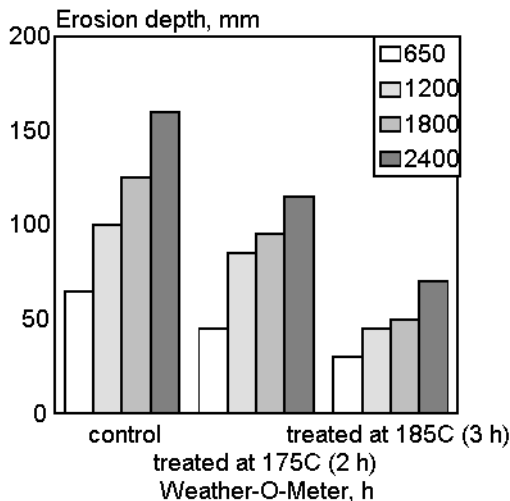


Fig. 17.76. Erosion of heat treated beech wood after exposure to artificial weathering. [Data from W. C. Feist and J. Sell, *Wood Fiber Sci.*, 19(1987)183.]

tected prior to its exposure in a Weather-O-Meter. Heat treatment of beech wood reduces its erosion rate. Similar data for spruce, although not as consistent, show an improvement in weather stability. This improvement is explained by the fact that heat treatment causes the degradation of wood hemicelluloses. Another approach includes chemical treatment of weathered wood by water repellent preservatives such as an acrylic latex primer applied prior to painting.¹⁵⁷ Paint adhesion testing shows that such treatment seems to increase the durability of finishes.

The effect of acid rain on coated wood was recently examined.¹⁵⁸ In this study wet and dry depositions were studied using rack developed specially for this purpose. Fig. 17.77 shows that wet deposition causes sili-

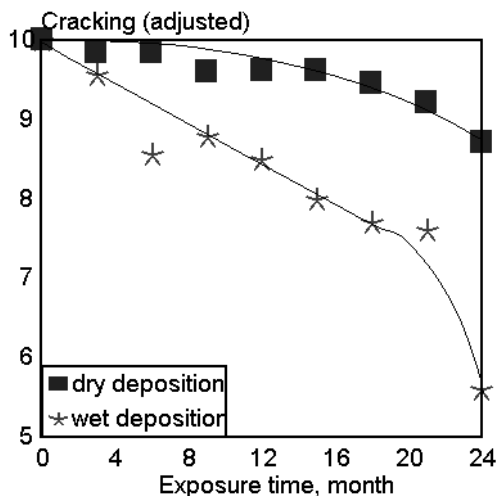


Fig. 17.77. Cracking of carbonate paint vs. time of exposure. [Data from J. W. Hook, P. J. Jacox, and J. W. Spence, *Prog. Org. Coat.*, 24(1994)175.

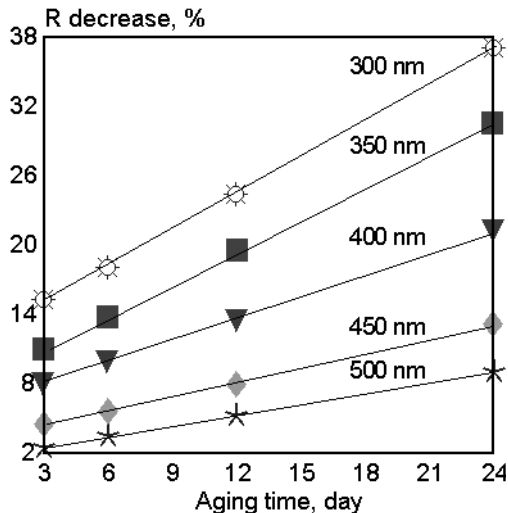


Fig. 17.78. Remission vs. aging time. [Adapted, by permission, from I. T. Bustamante and J. Hazai-Horvath, *Acta Chim. Hungarica*, 126(1989)567.]

cate paint to degrade badly. Dry deposition with occasional wet sprays produces effects which vary between paint types.

It is evident from this literature review that a relatively small group of researchers have made systematic progress in the studies of these complex materials and they are using increasingly more precise methods of testing.

17.19 PAPER^{159,160}

Fig. 17.78 shows the increase in absorption of paper versus exposure time. More pronounced changes occur in the UV than in the visible range.¹⁵⁹ The application of sizing in a neutral medium in the presence of calcium carbonate increases paper stability. Calcium carbonate acts as buffer and neutralizes the acid formed during the aging process. Carbonyl group formation causes changes in paper brightness.

Fig. 17.79 shows data on the degradation of various paper-containing packaging materials exposed outdoors and in a Weather-O-Meter. Parameter b is taken from the following equation: $\text{tensile} = a + 10^{-b}$. The larger the value of b the faster the degradation.

17.20 DATA FROM MEDICAL APPLICATIONS¹⁶¹⁻¹⁶⁷

Here, the human body is linked to manufactured goods. Such a discussion might be surprising, yet nobody would object to a discussion of photochemical changes in wool which

contains keratin composed of the similar aminoacids as are found in the human body; thus whatever changes occur in wool might be relevant to solar erythema, keratitis solaris, or skin cancer. We should, therefore, have no hesitation in using results to improve our knowledge and apply it to synthetic materials. The discussion below is not so much directed to explain medical phenomena as to channel the information collected for medical purposes to those active in polymer studies in order to show the benefits of interdisciplinary treatment.

Exposure to UV radiation may cause keratitis solaris. These reactions are frequently observed among skiers who are exposed to radiation for several hours and also among those who work in areas where intensive UV radiation is available, e.g., welding. In both cases, special protective glasses may eliminate the danger. It was established that keratitis photoelectrica is caused by a short-term exposure to artificial sources of UV radiation with a threshold radiant exposure evaluated set at 40 J/m^2 level. A group of Austrian scientists, involved in a project to measure radiant doses in the Jungfrauoch in the Alps, was interested in finding if the dose determined to cause keratitis photoelectrica can be used to estimate the threshold radiant exposure which causes keratitis solaris. This Alpine station is very well equipped with radiant energy measure-

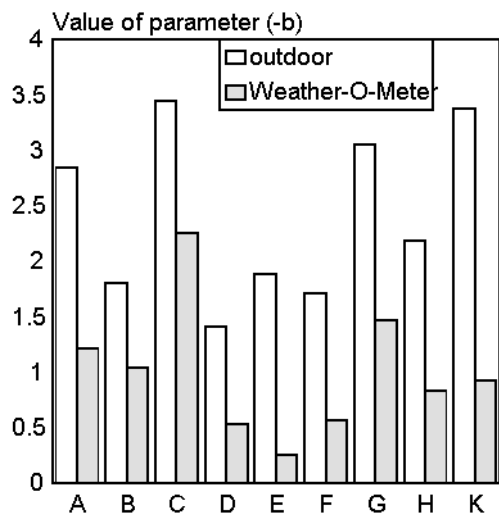


Fig. 17.79. Values of parameter -b for different packaging materials. [Data from A. L. Andrad, V. R. Parthasarathy, and Y. Song, *Tappi J.*, (1991)185.]

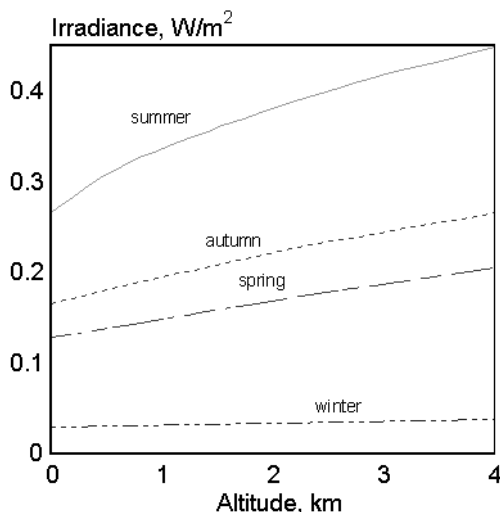


Fig. 17.80. Keratitis-effective irradiance at noon vs. altitude (latitude= 47°N). [Adapted, by permission, from M. Blumthaler, W. Ambach, and F. Daxecker, *Invest. Ophthal. Visual Sci.*, 28(1987)1713.]

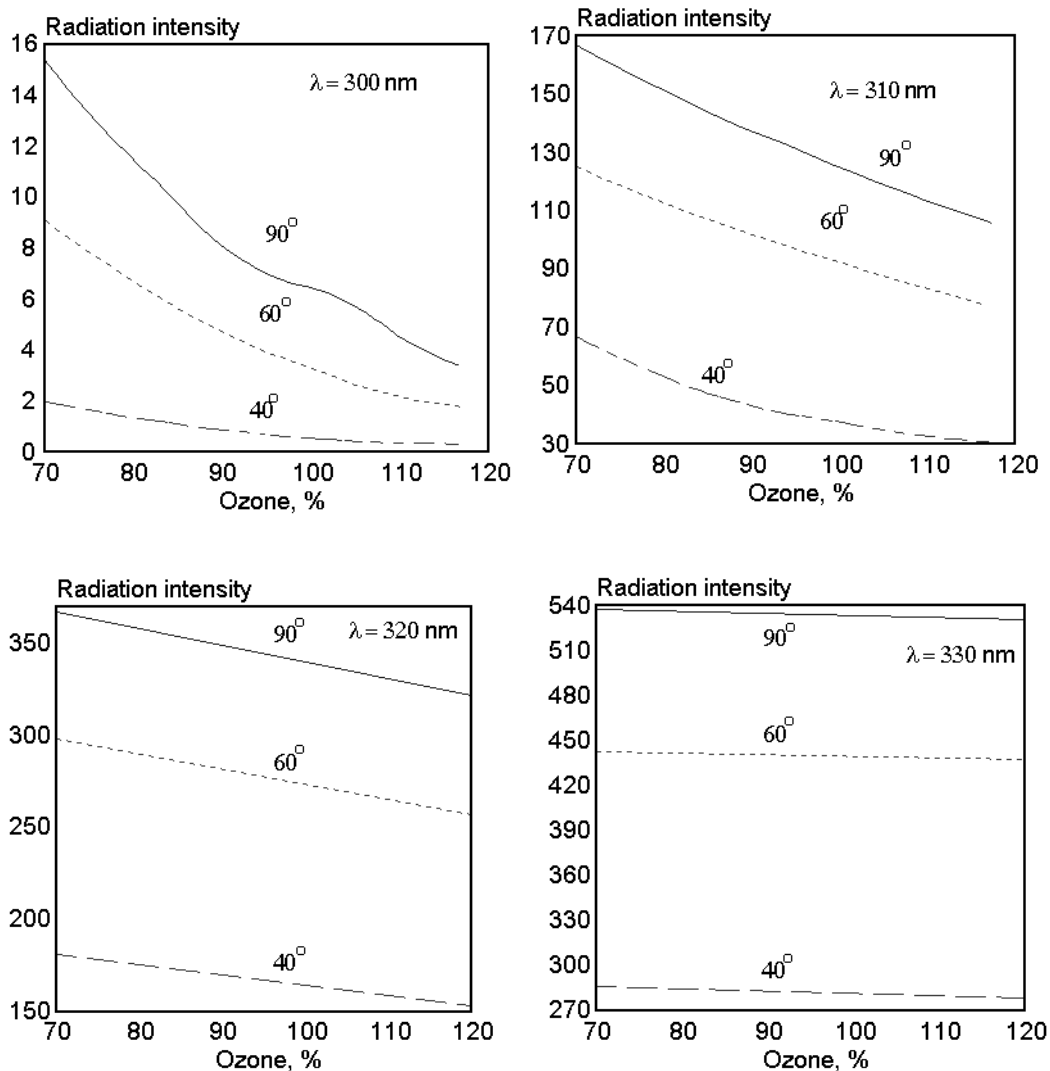


Fig. 17.81. Radiation intensity of different bands vs. ozone concentration and the angle of solar radiation. [Adapted, by permission, from H. G. Lasch, P. Matis, and F. Knuechel, *Medizinische Welt*, 34(1983)204.]

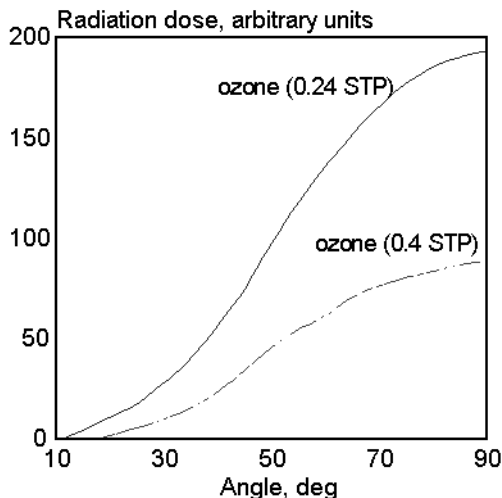


Fig. 17.82. Erythema dose (amount of radiation) vs. angle of solar elevation for two ozone concentrations. [Adapted, by permission, from H. G. Lasch, P. Matis, and F. Knuechel, *Medizinische Welt*, 34(1983)204.]

sun's elevation, which is the same in spring and autumn. The observed difference is due to the higher spring concentration of ozone which absorbs part of the UV radiation.

Ozone concentration and solar elevation are the variables which determine spectral intensity. Their influence on particular wavelengths, however, are not the same (Fig. 17.81). The increased amount of ozone acts mostly in the 300-310 nm range (most important for polymer degradation). It would not affect radiation at 330 nm. When one combines these two variables (ozone concentration and angle of solar elevation) their joint effect on radiation intensity is greater than expected (Fig. 17.82). These factors determine, to large extent, the radiation which a specimen receives over a short time period. Daily 30 to 46% of radiation is delivered (depending on season) between 11 a.m. and 1 p.m., and it is this interval of exposure which is most damaging.

Similar studies were conducted for an erythema dose, which is also caused by radiative energy between 300 and 320 nm. The authors found that global radiation increases only 9% per 1000 m of altitude, whereas the erythema causing dose (300-320 nm) increases by 23.7%. Altitude should, therefore, be considered as a very important variable in weathering studies. Also, a 25% decrease of ozone concentration causes a 40% increase in erythema dose. This means that in a polluted environment, the degradation of specimens might be accelerated more than they would be in the full sun of Florida or Arizona.

ment equipment. For this study, an instrument was used which measures radiation in the range of 295-322 nm which is a portion of the keratitis causing wavelengths. By comparing the exposure time of patients of a neighboring hospital with the measured quantity of effective radiation, a threshold radiant exposure of 300-600 J/m² was estimated, which was quite different in value from that assumed for keratitis photoelectrica. At the same time, many universally important observations were made, as reported below.

It was established that the radiation which causes keratitis (300-320 nm) varies substantially with the season and the altitude (Fig. 17.80). An interesting difference was observed between spring and autumn. Solar radiation differences were not the reason since they depend on the

A recent paper by Martin²³ shows how important it is to crossexamine developments in different fields. Based on the results obtained in skin cancer studies which are similar to those presented above, Martin proposes that only a dose which may cause chemical changes in the material (rather than the total energy of incident radiation) should be used as a base to compare results in coatings degradation.

Currently, a new field of degradation studies is rapidly developing, that of degradation of biomedical polymers. To achieve biocompatibility of biomedical polymers, they must be checked in the physiological environment of human body. In laboratory studies, it was found that hydroxyl radicals might be the main cause of degradation of implantable devices.¹⁶⁶ *In vivo* studies of various polyurethanes were conducted by implanting dumbbells of films in sheep.

17.21 WEATHERING STUDIES OF OTHER MATERIALS¹⁶⁸⁻¹⁸⁷

Potthoff¹⁶⁸ studied the aging behavior and service life of bottle crates (Fig. 17.83). The benefit of UV stabilization is clearly visible from a comparison of the service life of samples a and b. Regrind from exposed crates should be used with caution, since severely degraded material, even when stabilized, does not produce durable crates.

Selected material may be reused, providing that UV stabilization is properly implemented. Mukhopadhyay¹⁶⁹ reports on weathering studies on polyethylene film used for greenhouses. Film thickness and UV stabilization limit durability of this film. Films of 100 μm made from UV-stabilized LDPE can withstand 1 year of service. The thickness of the film should be doubled if a service life of 2 years is expected.

Stachiw and Dolan¹⁷⁰ contributed a detailed study on the structural performance of acrylic plastics. Ten years of natural weathering caused the following changes in PMMA:

Molecular weight	80% decrease
Free monomer concentration	130% increase
Elongation	40% decrease
Flexural strength	34% decrease
Tensile strength	21% decrease
Shear strength	9% decrease
Depth of weathered layer	0.5 mm

UV radiation followed by pollutants and internal stress were the most degrading factors. Exposure to pollutants had, in fact, a rate of degradation similar to natural weathering. The expected life of a PMMA structure is now estimated at 20 years, versus the 10 years warranty which is offered at present.

Slocum¹⁷¹ developed a weather resistant RIM system for automotive window encapsulation based on an aromatic isocyanate-containing polyurethane. Six months of direct exposure in Florida did not cause any detectable changes in the mechanical

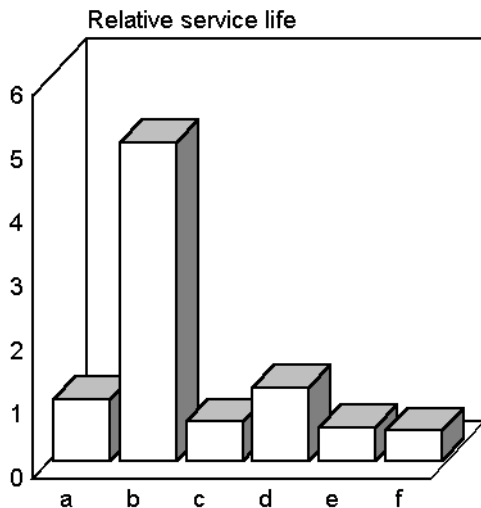


Fig. 17.83. Relative service life of HDPE bottle crates made from materials of different histories and formulations (a-virgin HDPE; b-HDPE+UVS; c-HDPE regrind from crates 12-15 years old; HDPE regrind, without much degradation, UVS; e-HDPE regrind, severely degraded; f-HDPE regrind, severely degraded, UVS). [Data from P. Potthoff, *Kunststoffe*, 75(1985)481.]

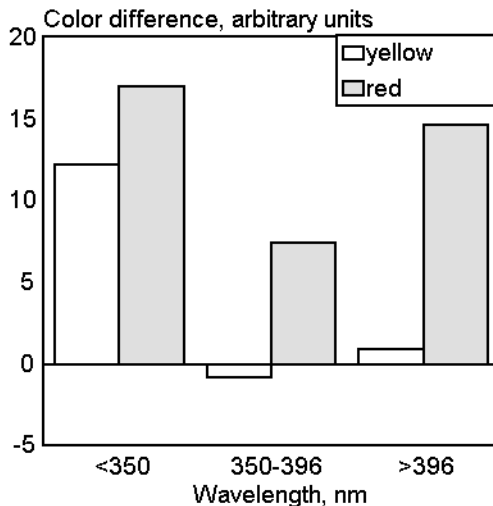


Fig. 17.84 Wavelength sensitivity of printing inks. [Data from N.D. Searle, *Atlas Sun Spots* 17(1987)38.]

properties of the material which even retained its initial gloss. Structural epoxy adhesives were studied by Wilson¹⁷² for use in space environments where materials are exposed to vacuum, ionizing radiation, and extremely high temperatures. At low radiation doses (below 5000 Mrads), epoxides degraded by chain scission; at higher radiation doses, the crosslinking process was predominant.

The paper industry shows an interest in the effects of UV radiation. Reinhardt¹⁷⁴ evaluated the possible application of UV radiation for paper-bleaching purposes. Skledar¹⁷⁵ studied the effect of filler on the rheological behavior of filled polymers which were exposed to UV rays in the presence of moisture. Searle¹⁷⁶ evaluated the sensitivity of printing inks to UV irradiation wavelength (Fig. 17.84). UV radiation wavelength less than 350 nm is the most destructive to printing inks. No correlation was found between xenon arc and carbon arc radiation.

Carpet dye fading problems were discussed in detail by Schulze,^{177,178} one of the early researchers working on this subject. The major weathering factor was the pres-

ence of pollutants, such as NO₂ and SO₂. Herlant¹⁷⁹ offers suggestions on how to inhibit the fading of acid dyes used in polyamide carpets by ozone. Alizarin and related artists' pigments fade on exposure to UV radiation and to atmospheric ozone.¹⁸¹ Apicella¹⁸² evaluated the environmental degradation of the electrical properties of insulating materials containing epoxy resins and polyurethanes. The change of properties is attributed to water uptake which causes microstructural damage and plastification.

Multiple processing of styrene-containing polymers and copolymers confers good properties to the materials.¹⁸³ The effect on weathering differs depending on the chemical structure of the copolymer. ABS and PS have substantially reduced weather stability whereas SAN is only slightly affected. Thermal stabilizers for an extruded PVC window profile were evaluated to determine their effect on the weatherstability of the profile.¹⁸⁴ A heavy metal-free stabilizer was found useful for the purpose. The conditions under which optical fibers were aged were studied by measurement of surface roughness.¹⁸⁵ The effect of environmental exposure on charcoal filter performance was studied.^{186,187}

REFERENCES

1. G. Berner and M. Rembold, *Org. Coat. Sci. Technol.*, 6(1983)55.
2. B. Ranby and A. Hult, *Org. Coat. Sci. Technol.*, 7(1984)137.
3. J. L. Gerlock, D. R. Bauer, and L. M. Briggs, *Org. Coat. Sci. Technol.*, 8(1985)365.
4. J. L. Gerlock, D. R. Bauer, L. M. Briggs, and J. K. Hudgens, *Prog. Org. Coat.*, 15(1987)197.
5. J. Puglisi and P. J. Schirmann, *Polym. Mat. Sci. Eng.*, 57(1987)620.
6. A. D. English and H. J. Spinelli, *J. Coat. Technol.*, 56(1984)43.
7. J. H. Hartshorn, *Polym. Mat. Sci. Eng.*, 57(1987)880.
8. T. Nguyen and E. Byrd, *Polym. Mat. Sci. Eng.*, 56(1987)584.
9. D. R. Bauer, M. J. Dean, and J. L. Gerlock, *Polym. Mat. Sci. Eng.*, 56(1987)443.
10. S. G. Croll, *Prog. Org. Coat.*, 15(1987)223.
11. S. Yajima, Y. Togawa, S. Matsushita, T. Suzuki, and T. Okada, *Kinzoku Hyomen Gijutsu*, 37(1986)718.
12. T. K. Rehfeldt, *Prog. Org. Coat.*, 15(1987)261.
13. P. J. Schirman, *Polym. Mat. Sci. Eng.*, 57(1987)870.
14. G. P. Bierwagen, *Prog. Org. Coat.*, 15(1987)179.
15. R. S. Whitney, J. I. Fry, and R. J. Cordner, *J. Oil Colour Chem. Assoc.*, 67(1984)63.
16. J. L. Gerlock, D. R. Bauer, L. M. Briggs, and R. A. Dicke, *J. Coat. Technol.*, 57(1985)37.
17. D. F. Mielewski, D. R. Bauer, and J. L. Gerlock, *Polym. Deg. Stab.*, 33(1991)93.
18. D. R. Bauer, J. L. Gerlock, and D. F. Mielewski, *Polym. Deg. Stab.*, 36(1992)9.
19. D. R. Bauer, *J. Coat. Technol.*, 66(1994)57.
20. D. R. Bauer, *Prog. Org. Coat.*, 23(1993)105.
21. D. R. Bauer and D. F. Mielewski, *Polym. Deg. Stab.*, 40(1993)349.
22. J. W. Martin, *Prog. Org. Coat.*, 23(1993)49.
23. E. O. Edney, *Report*, EPA/600/3-89/032.

24. L. G. J. van der Ven and P. J. A. Guerink, *JOCCA*, (1991)11,401.
25. D. Y. Perera and M. Oosterbroek, *J. Coat. Technol.*, 66(1994)83.
26. L. W. Hill, H. M. Korzeniowski, M. Ojunga-Andrew, and R. C. Wilson, *Prog. Org. Coat.*, 24(1994)147.
27. T. C. Simpson, H. Hampel, G. D. Davis, C. O. Arah, T. L. Fritz, P. J. Moran, B. A. Shaw, and K. L. Zankel, *Prog. Org. Coat.*, 20(1992)199.
28. M. Kendig, R. Addison, J. Lumsden, P. Stocker, S. Jeanjaquet, and D. Anderson, *Report*, AD-A222 426.
29. A. T. Chen, T. R. McClellan, R. L. Ray, and C. K. Groseth, *Elastomerics*, (1991)11,9.
30. L. A. Simpson, *Polym. Paint. Colour J.*, 176(1986)408.
31. L. A. Simpson, *Austral. OCCA Proc. News*, 20(1983)6.
32. L. A. Simpson, I. Melville, and D. V. Moulton, *Polym. Paint Colour J.*, 177(1987)139.
33. K. G. Martin and R. E. Price, *Durability Building Mater.*, 1(1982)127.
34. R. R. Blakey, *Prog. Org. Coat.*, 13(1985)279.
35. J. H. Braun, *Prog. Org. Coat.*, 15(1987)249.
36. E. Hoffman, *J. Oil Colour Chem. Assoc.*, 54(1971)450.
37. S. Okamoto, K. Hikita, and H. Ohya-Nishiguchi, *Polym. Paint. Colour J.*, 177(1987)683.
38. J. N. Patel, *JOCCA*, (1991)3,104.
39. J. H. Braun, *J. Coat. Technol.*, 62,785(1990)37.
40. S. Feliu Jr., M. Morcillo, J. M. Bastidas, and S. Feliu, *J. Coat. Technol.*, 65,826(1993)43.
41. M. Morcillo, J. Simancas, J. L. G. Fierro, S. Feliu Jr., and J. C. Galvan, *Prog. Org. Coat.*, 21(1993)315.
42. B. Pourdeyhimi and A. Nayernouri, *J. Coat. Technol.*, 66,834(1994)51.
43. J. N. Rastogi, B. Singh, K. M. Thomas, and V. K. Verma, *Paint India*, (1991)3,65.
44. L. A. Holt and B. Milligan, *Text. Res. J.*, 54(1984)521.
45. C. M. Carr and I. H. Leaver, *J. Appl. Polym. Sci.*, 33(1987)2087.
46. I. H. Leaver, *J. Appl. Polym. Sci.*, 33(1987)2795.
47. A. B. M. Abdullah and L. W. C. Miles, *Text. Res. J.*, 54(1984)415.
48. C. M. Ladisch, R. C. Brown, and K. B. Showell, *Text. Chem. Color.*, 15(1983)209.
49. C. H. Nicholls, *Dev. Polym. Photochem.*, 1(1980)125.
50. P. J. Baugh, *Dev. Polym. Photochem.*, 2(1981)165.
51. G. E. Krichevsky, G. T. Khachaturova, and O. M. Anissimova, *Intern. J. Polym. Mater.*, 13(1990)63.
52. M. Baird, C. M. Carr, and L. A. Holt, *Textile Res. J.*, 61(1991)210.
53. C. Q. Yang and L. K. Martin, *J. Appl. Polym. Sci.*, 51(1994)389.
54. S. Konrad and D. Schuster, *J. Coated Fabrics*, 22(1992)10.
55. C. Q. Yang, *Ind. Eng. Chem. Res.*, 31(1992)617.
56. M. C. Perry, M. A. Vail, and K. L. DeVries, *Polym. Eng. Sci.*, 35(1995)411.
57. M. G. Dobb, R. M. Robson, and A. H. Roberts, *J. Mater. Sci.*, 28(1993)785.
58. L. E. Hamilton, P. M. A. Sherwood, and B. M. Reagan, *Appl. Spectros.*, 47(1993)139.
59. S. K. Mukhopadhyay, D. J. Mwaisengela, and P. W. Foster, *J. Text. Inst.*, 82(1991)427.
60. L. Benisek, G. K. Edmondson, and J. W. A. Matthews, *Text. Res. J.*, 55(1985)256.

61. A. Anton and J. C. Browne, *Text. Chem. Color*, 16(1984)185.
62. R. D. Wagner, R. C. Leslie, and F. Schlaeppl, *Text. Chem. Color.*, 17(1985)20.
63. B. Milligan, *Rev. Prog. Color Relat. Top.*, 16(1986)1.
64. G. Reinert and F. Thommen, *Text. Chem. Color*, 230(1991)31.
65. P. M. Latzke, *Melliand Textileberichte*, (1990)502.
66. P. C. Crews and B. M. Reagan, *Text. Chem. Color.*, 19(1987)21.
67. R. Frey, *Bautenschutz Bausamierung*, 9(1986)87.
68. *Lonza*. PVC-beschichtete Verbundwerkstoffe auf Synthetiks substraten.
69. J. R. Montalvo, *Geosynthetics '89, February 1989, San Diego, Conf. Proc.*, Vol. 2, p. 501.
70. L. G. Tisinger, *Geosynthetics '89, February 1989, San Diego, Conf. Proc.*, Vol. 2, p. 513.
71. A. G. Strong, *Plast. Rubber Process. Applic.*, 6(1986)235.
72. G. W. Kamykowski, *Polym.-Plast. Technol. Eng.*, 33(1994)281.
73. E. W. Brand and P. L. R. Pang, *J. Geotech. Eng.*, 117(1991)979.
74. C. Giori and T. Yamauchi, Investigation of Degradation Mechanism in Composite Matrices, *NASA Contractor Rep.*, 3559.
75. S. M. Milkovich, C. T. Herakovich, and G. F. Sykes, *J. Compos. Mater.*, 20(1986)579.
76. J. G. Funk and G. F. Sykes, *J. Compos. Technol. Res.*, 8(1986)92.
77. T. Okada, S. Nishijima, and H. Yamaoka, *Adv. Cryogenic Eng. Mater.*, 32(1986)145.
78. T. T. Chiao, R. L. Moore, and H. T. Hahn, *Compos. Technol. Rev.*, 5(1983)98.
79. R. J. Morgan, F. -M. Kong, and J. K. Lepper, *J. Compos. Mater.*, 22(1988)1026.
80. G. W. Ehrenstein and A. Schmiemann, *VDI-Ber.*, 600.2(1986)173.
81. T. Watanabe, *Kobunshi Ronbushu*, 39(1982)1.
82. P. R. Young, W. S. Slemp, and B. A. Stein in *LDEF Materials Results for Specacraft Applications*, Eds. A. F. Whitaker and J. Gregory, *NASA Conf. Publ.*, 3257, 1994.
83. B. A. Banks, K. K. de Groh, B. M. Auer, L. Gebauer, and C. LaMoreaux in *LDEF Materials Results for Specacraft Applications*, Eds. A. F. Whitaker and J. Gregory, *NASA Conf. Publ.*, 3257, 1994.
84. B. Z. Jang, J. Bianchi, Y. M. Liu, and C. P. Chang in *LDEF Materials Results for Specacraft Applications*, Eds. A. F. Whitaker and J. Gregory, *NASA Conf. Publ.*, 3257, 1994.
85. J. -C. Guillaumon and A. Paillous in *LDEF Materials Results for Specacraft Applications*, Eds. A. F. Whitaker and J. Gregory, *NASA Conf. Publ.*, 3257, 1994.
86. P. E. George and H. W. Dursch in *LDEF Materials Results for Specacraft Applications*, Eds. A. F. Whitaker and J. Gregory, *NASA Conf. Publ.*, 3257, 1994.
87. L. J. Leger, S. L. Koontz, and J. T. Visentine in *LDEF Materials Results for Specacraft Applications*, Eds. A. F. Whitaker and J. Gregory, *NASA Conf. Publ.*, 3257, 1994.
88. J. B. Pallix, K. A. Lincoln, C. J. Miglionico, R. E. Roybal, C. Stein, and J. H. Shively in *LDEF Materials Results for Specacraft Applications*, Eds. A. F. Whitaker and J. Gregory, *NASA Conf. Publ.*, 3257, 1994.
89. Y. Haruvy, *Radiat. Phys. Chem.*, 35(1990)204.
90. A. Paillous and C. Pailler, *Composites*, 25(1994)287.
91. I. Dalins and M. Karimi, *J. Vac. Sci. Technol.*, A10(1992)2921.
92. R. Browne, *Chem. Ind.*, (1986)837.

93. R. Beard, *Chem. Ind.*, (1986)849.
94. Y. Ishizuka, *Durability Building Mater.*, 1(1983)345.
95. J. R. Crowder and M. A. Ali, *Durability Building Mater.*, 3(1985)115.
96. R. K. Jain, B. K. Saxena, G. D. Bansal, and K. K. Asthana, *Durability Building Mater.*, 2(1983)27.
97. A. Blaga and R. S. Yamasaki, *Durability Building Mater.*, 4(1986)21.
98. J. Morgan, *Chem. Ind.*, (1986)845.
99. R. Bonafont, *Chem. Ind.*, (1986)854.
100. A. J. Newman, *Chem. Ind.*, (1987)583.
101. E. Keeble, *Chem. Ind.*, (1987)593.
102. M. J. Welch, P. J. C. Counsell, and C. V. Lawton, *J. Oil Colour Chem. Assoc.*, 63(1980)137.
103. L. M. Gan, H.W.K. Ong, and T. L. Tan, *Durability Building Mater.*, 3(1986)225.
104. L. M. Gan, H.W.K. Ong, and T. L. Tan, *Durability Building Mater.*, 4(1986)35.
105. L. M. Gan, H. W. K. Ong, T. L. Tan, C. H. Chew, and F. N. Lai, *Durability Building Mater.*, 2(1985)379.
106. W. R. Sharman, J. I. Fry, and R. S. Whitney, *Durability Building Mater.*, 2(1983)79.
107. J. R. Crowder and M. A. Ali, *Durability Building Mater.*, 3(1985)115.
108. B. H. River, *Adhesive Age*, 27,2(1984)16.
109. J. B. Thornton, *Adhesive Age*, 26,9(1983)24.
110. J. M. Klosowski and M. J. Owen, *Polym. Mat. Sci. Eng.*, 56(1987)469.
111. K. K. Karpati, *J. Coat. Technol.*, 56(1984)57.
112. B. M. Parker, *Int. J. Adhes. Adhes.*, 13(1993).
113. R. Keshavaraj and R. W. Tock, *Polym.-Plast. Technol. Eng.*, 33(1994)397.
114. L. Gomez and M. R. Colella in *Building Sealants, ASTM STP 1069*, Ed. T. F. O'Connor, ASTM, Philadelphia, 1990.
115. T. F. O'Connor and J. R. Panek in *Science and Technology of Building Seals, Sealants, and Waterproofing. ASTM STP 1200*, Ed. J. M. Klosowski, ASTM, Philadelphia, 1992.
116. G. R. Fedor in *Science and Technology of Building Seals, Sealants, and Waterproofing. ASTM STP 1200*, Ed. J. M. Klosowski, ASTM, Philadelphia, 1992.
117. T. J. Bridgewater and L. D. Carbary in *Science and Technology of Building Seals, Sealants, and Waterproofing. ASTM STP 1200*, Ed. J. M. Klosowski, ASTM, Philadelphia, 1992.
118. J. Beech and J. Beasley in *Science and Technology of Building Seals, Sealants, and Waterproofing. ASTM STP 1200*, Ed. J. M. Klosowski, ASTM, Philadelphia, 1992.
119. I. Minkarah, J. P. Cook, and A. S. Rajagopal in *Science and Technology of Building Seals, Sealants, and Waterproofing. ASTM STP 1200*, Ed. J. M. Klosowski, ASTM, Philadelphia, 1992.
120. G Fedor and P. Brennan, *Applicator*, 12,1(1990)1.
121. M. J. Cassady, G. C. Derringer, M. M. Epstein, A. Lustiger, and R. L. Markham, *Outdoor Weathering of Plastic Pipe, Report*, (NTIS) PB83-162073.
122. S. H. Hamid, M. B. Amin, A. G. Maadhan, and A. M. Al-Jarallah, *J. Vinyl Technol.*, 14(1992)182.
123. M. P. Ebdon, *Corrosion Australasia*, 17,3(1992)10.

124. J. C. Marechal, *Durability Building Mater.*, 1(1982/83)201.
125. B. J. Humphrey, Electron Paramagnetic Resonance on Asphaltic Materials, *Report*, ADA 178-471.
126. H. W. Busching, W. J. Rossiter, and R. G. Mathey, *Durability Building Mater.*, 3(1987)323.
127. R. G. Mathey and W. J. Rossiter, *Durability Building Mater.*, 2(1983)59.
128. K. Tanaka, H. Hashida, T. Kuibira, and M. Koike, *Rep. Res. Lab. Eng. Mater., Tokyo Inst. Technol.*, 15(1990)179.
129. D. Waksman, W. E. Roberts, and W. E. Byrd, *Durability Building Mater.*, 3(1985)1.
130. R. S. Yamasaki and A. Blaga, *Durability Building Mater.*, 1(1980)874.
131. J. E. Gilligan, *Sun Spots*, 10(1980)1.
132. M. Ramasri, S. C. Shit, A. B. Mathur, and K. Ramamurthy, *Pop. Plast. Packaging*, (1992)5,47.
133. A. Denning and N. J. Mills, *Plast. Rubb. Compos. Proces. Appl.*, 18(1992)67.
134. D. Amos and B. Leake, *J. Hazardous Mater.*, 32(1992)105.
135. A. Wootton, *JSDC*, 108(1992)239.
136. A. Stoloff, *J. Vinyl Technol.*, 15(1993)208.
137. G. M. Ferguson, A. Jefferson, and I. Sihsobhon, *Mater. Forum*, 16(1992)147.
138. S. G. Matz, *J. Chromatog.*, 587(1991)205.
139. N. Khraishi and A. Al-Robaidi, *Polym. Deg. Stab.*, 32(1991)105.
140. M. Edge, M. Hayes, M. Mohammadian, N. S. Allen, T. S. Jewitt, K. Brems, and K. Jones, *Polym. Deg. Stab.*, 32(1991)131.
141. S. Bualek, K. Suchiva, S. Boonariya, and B. Ratana-Arakul, *J. Sci. Soc. Thailand*, 17(1991)103.
142. G. M. Ferguson, M. Hood, and K. Abbott, *Polym. Intern.*, 28(1992)35.
143. K. S. Chon, J. H. Idrovo, D. S. Remer, K. Pawlek, and K. Janati, *SAMPE Qrtly.*, 1990,10,37.
144. A. -C. Albertsson and S. Karlsson, *Polym. Deg. Stab.*, 41(1993)345.
145. A. -C. Albertsson, C. Barenstedt, and S. Karlsson, *Polym. Deg. Stab.*, 37(1992)163.
146. K. L. Leonas and R. W. Gorden, *J. Environ. Polym. Deg.*, 1(1993)45.
147. P. J. Hocking, *J. Macromol. Sci.-Rev. Macromol. Chem. Phys.*, C32(1992)35.
148. S. P. Cygan and J. R. Laghari, *IEEE Trans. Nucl. Sci.*, 38(1991).906.
149. R. Bartnikas, R. J. Densley, and R. M. Eichhorn, *IEEE Trans. Power Delivery*, 6(1991)929.
150. W. K. Busfield and M. J. Monteiro, *Mater. Forum*, 14(1990)218.
151. A. Underhaug, T. J. Lund, and K. Kleive, *J. Oil Colour Chem. Assoc.*, 66(1983)345.
152. W. C. Feist and J. Sell, *Wood. Fiber. Sci.*, 19(1987)183.
153. W. C. Feist, *For. Prod. J.*, 37(1987)15.
154. S. -T. Chang, D. N. -S. Hon, and W. C. Feist, *Wood Fiber*, 14(1982)104.
155. E. L. Anderson, Z. Pawlak, N. L. Owen, and W. C. Feist, *Appl. Spectros.*, 45(1991)641.
156. E. L. Anderson, Z. Pawlak, N. L. Owen, and W. C. Feist, *Appl. Spectros.*, 45(1991)648.
157. R. S. Williams and W. C. Feist, *Forest Prod. J.*, 43(1993)8.
158. J. W. Hook, P. J. Jacox, and J. W. Spence, *Prog. Org. Coat.*, 24(1994)175.
159. I. T. Bustamante and J. Hazai-Horvath, *Acta Chim. Hungarica*, 126(1989)567.

160. A. L. Andrady, V. R. Parthasarathy, and Y. Song, *Tappi J.*, (1991)185.
161. M. Blumthaler, W. Ambach, and F. Daxecker, *Invest. Ophthal. Visual Sci.*, 28(1987)1713.
162. H. G. Lasch, P. Matis, and F. Knuechel, *Medizinische Welt*, 34(1983)204.
163. M. Blumthaler, W. Rehwald, and W. Ambach, *Arch. Met. Geogh. Biocl.*, 35B(1985)389.
164. M. Blumthaler and W. Ambach, *Human Exposure to Ultraviolet Radiation*, Elsevier, Amsterdam, 1987.
165. V. Ambach and W. Rehwald, *Radiat. Environ. Biophys.*, 21(1983)295.
166. S. A. M. Ali, P. J. Doherty, and D. F. Williams, *J. Appl. Polym. Sci.*, 51(1994)1389.
167. A. Brandwood, K. R. Noble, K. Schindhelm, G. F. Meijs, P. A. Gunatillake, R. C. Chatelier, S. J. McCarthy, and E. Rizzardo, *Biomater.-Tissue Interfaces*, 10(1992)413.
168. M. Potthoff, *Kunststoffe*, 75(1985)481.
169. G. Mukhopadhyay and M. K. Banerjee, *Pop. Plast.*, 1987,7,15.
170. J. D. Stachiw and R. B. Dolan, *Trans. ASME*, 104(1982)190.
171. G. H. Slocum, T. N. Thompson, and C. E. Fluharty, *J. Elastom. Plast.*, 19(1987)50.
172. T. W. Wilson, R. E. Fornes, R. D. Gilbert, and J. D. Memory, *Polym. Mat. Sci. Eng.*, 56(1987)105.
173. G. A. Luoma and R. D. Rowland, *J. Chromatogr. Sci.*, 24(1986)210.
174. B. Reinhardt and U. Arneberg, *Wochenbl. Papierfabr.*, 115(1987)223.
175. S. Skledar, *Mater. Plast.*, 21(1984)29.
176. N. D. Searle, *Sun Spots*, 17(1987)38.
177. F. Schulze, *Sun Spots*, 12(1981/82)26.
178. F. Schulze, *Sun Spots*, 12(1982)27.
179. M. A. Herlant, *Am. Dyestuff Rep.*, 75,7(1986)38.
180. R. L. Feller, R. M. Johnston-Feller, and C. Bailie, *J. Coat. Technol.*, 59(1987)93.
181. D. Grosjean, P. M. Whitmore, C. P. De Moor, G. R. Cass, and J. R. Druzik, *Environ. Sci. Technol.*, 21(1987)635.
182. A. Apicella, L. Egiziano, L. Nicolais, and V. Tucci, *J. Mater. Sci.*, 23(1988)729.
183. M Honeczkowski, *Kunststoffe*, 83(1993)30.
184. J. Imhof, P. Stern, and A. Egger, *Angew. Makromol. Chem.*, 176/177(1990)185.
185. R. S. Robinson and H. H. Yuce, *J. Am. Ceram. Soc.*, 74(1991)814.
186. J. C. Wren and C. J. Moore, *Nucl. Technol.*, 94(1991)242
187. J. C. Wren and C. J. Moore, *Nucl. Technol.*, 94(1991)252

18

STABILIZATION AND STABILIZERS

Stabilizers are designed to either inhibit or delay degradative changes rather than to stabilize properties. Chapters 1 and 2 outline the possible effects of radiation on commonly-used materials, which gives the framework for the protective measures which can be applied. The best approach in stabilization would be to not allow radiation to be absorbed by vulnerable groups. Such preventive techniques utilize screening or absorption. If the energy does reach vulnerable sites in the material, free radicals can be formed which could then initiate chain processes which would result in severe damage to the material. This situation can be dealt with through the elimination of radicals or the deactivation of photoexcited chromophores. This is performed by additives known as excited state quenchers. Photolytic degradation of materials, in combination with photooxidative mechanisms, leads to the formation of hydroperoxides, free radicals, and chromophores which accelerate degradative changes by increasing the amount of energy absorbed. To counter this, it would help to decrease the rate of these photooxidative reactions. This can be accomplished by using antioxidants, singlet oxygen quenchers, and substances which react with hydroperoxides. If these measures fail to prevent degradation of the material, it may be possible that the vulnerable locations that are formed during photolytic degradation can be eliminated by incorporating specific additives designed to react with and stabilize them. These are rare situations and only a few examples of such solutions are known. Some are discussed below.

We can briefly summarize the components of a stabilization mechanism in the form presented in Table 18.1.

Table 18.1: Components of stabilizing action

Action	Means
UV screening	Surface coating; pigments; metal powders
UV absorption	UV absorbers
Deactivation of photoexcited states	Excited-state quenchers
Elimination of free radicals	Free radical quenchers
Elimination of singlet oxygen	Singlet oxygen quenchers
Limiting of oxidative changes	Antioxidants
Peroxide decomposition	Hindered amines
Removal of defects	Specific compounds

18.1 LIMITING THE INCOMING RADIATION

The Beer-Lambert Law, commonly used for the quantitative evaluation of radiant energy absorption, shows that:

$$\ln I_t/I_0 = -Ecl$$

where:

I_t	intensity of transmitted light
I_0	intensity of incident light
E	molar absorption coefficient
c	concentration of chromophores
l	material thickness.

This implies that a material's optical properties depend on the concentration of groups which may absorb radiation. This statement would have been valid if the basic assumptions of Beer-Lambert Law were fulfilled, namely:

- incident radiation is monochromatic
- the light intensity decrease depends on absorption alone
- absorption occurs in a volume of limited cross-section
- each absorbing center is independent of all others.

In reality, none of these assumptions are met, so there are substantial deviations from the Beer-Lambert Law. Garcia-Rubio¹ adapted the Mie's theory of interpreting the absorption spectra of macromolecules, and by doing so, he was able to analyze the effect of the molecular size of macromolecules in solution on radiation absorption (Fig. 18.1).

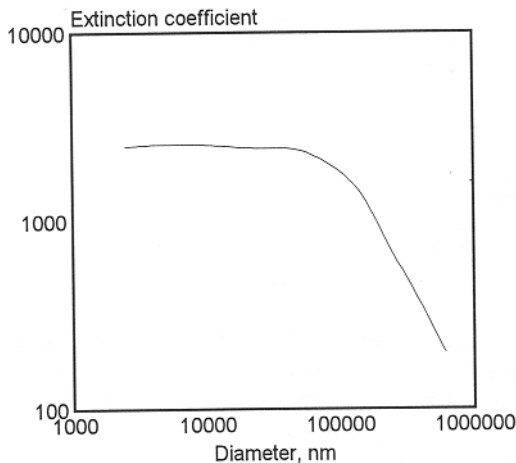


Fig. 18.1. Calculated effect of molecular size on the extinction coefficient for an isorefractive system. [Adapted, by permission, from L. Garcia-Rubio, *Macromolecules*, 20(1987)3070.]

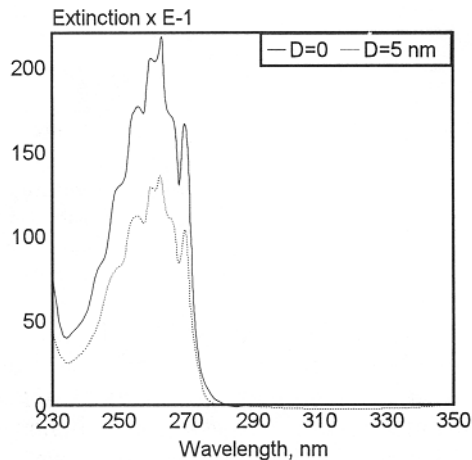


Fig. 18.2. Calculated effect of 50 Å particles on the extinction spectra of polystyrene in tetrahydrofuran. [Adapted, by permission, from L. Garcia-Rubio, *Macromolecules*, 20(1987)3070.]

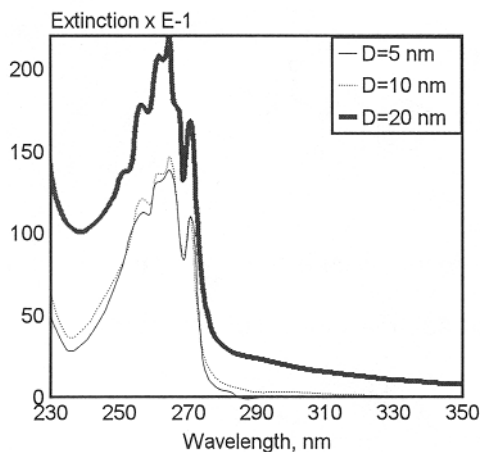


Fig. 18.3. Calculated effect of the molecular size on the extinction spectra of polystyrene in tetrahydrofuran. [Adapted, by permission, from L. Garcia-Rubio, *Macromolecules*, 20(1987)3070.]

The absorption coefficient and molecular size affect the extinction coefficient. With small molecular sizes (below 100 Å) the extinction coefficient is smaller than the absorption coefficient ($\epsilon(\lambda)$ is estimated when $D \rightarrow 0$) (Fig. 18.2.). The extinction coefficient increases as molecular size increases (Fig. 18.3). Experimental data confirm these calculations¹ which show that the Beer-Lambert Law is fulfilled only for small molecules (below 100 Å).

This expression can be used to determine how much of the total energy absorbed by the UV absorber containing system is absorbed by the polymer:

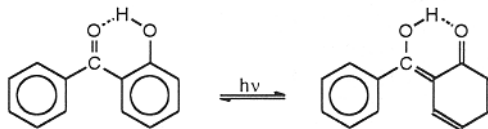
$$I_L = I_0(1+3V/2)^{L/2r} \exp[-(k_p+k_a)L]$$

where:	I_L	light intensity at depth L
	I_0	light intensity
	V	pigment volume fraction
	r	area-average particle radius
	k_p	linear absorption decrement of the polymer
	k_a	linear absorption decrement of the UV absorbing additive.

The relative values of each decrement (k_p and k_a) determine the amount of energy absorbed by the polymer and consequently the protective effect of the UV absorber.

Fig. 18.4 gives the chemical structures of the most common UV absorbers. These stabilizers were selected for inclusion in Fig. 18.4 to emphasize their chemical composition rather than to show the variety of commercial products. Each category contains a variety of commercial compounds which are distinguished from one another by having different substituent groups.

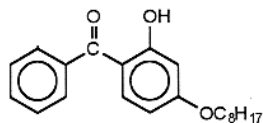
Regardless of the chemical composition of UV absorber, its mechanism of energy dissipation is essentially similar to all others. This involves tautomeric forms which exist in excited or ground states. 2-hydroxybenzophenones normally exist in the keto-form which then changes to the enol-form as they absorb energy:



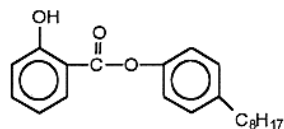
Dissipation of energy returns the UV absorber to its initial keto-form without a change in the chemical composition of the stabilizer.

Hydroxyphenylbenzotriazole absorbs light and reacts in a similar manner:

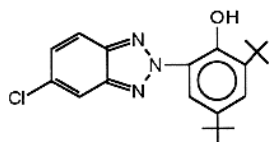




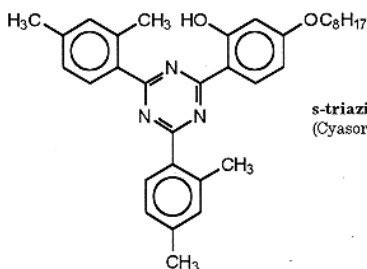
2-hydroxybenzophenone
(Chimassorb 81, Ciba-Geigy
Cyasorb UV 531, American Cyanamid
Hostavin VP AR08, Hoechst
Mark 1413, Asahi Denka Kogyo
Sumisorb 130, Sumitomo)



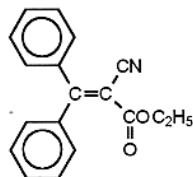
arylsalicylate (Inhibitor OPS, Eastman)



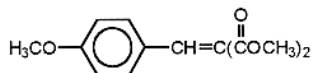
benzotriazole
(Tinuvin 327, Ciba-Geigy
Mark LA-34, Asahi Denka Kogyo
Sumisorb 320, Sumitomo)



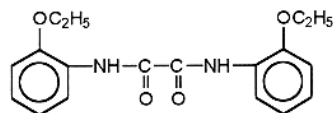
s-triazine
(Cyasorb UV 1164, American Cyanamide)



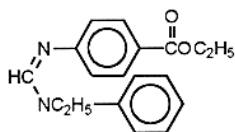
diphenyl cyanoacrylate
(Uvinul N-35, BASF)



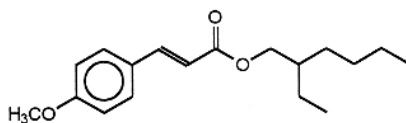
benzylidenemalonate
(Cyasorb UV 1988, American Cyanamide)



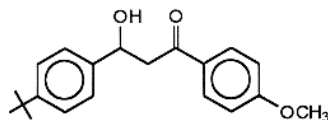
oxanilide
(Tinuvin 315, Ciba-Geigy
Sandovur E PU, Sandoz)



phenylformamidine
(Givisorb UV-2, Givaudan)



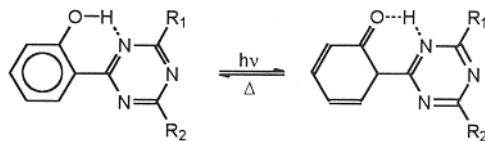
methoxycinnamate
(Parsol MCX, Givaudan)



methoxydibenzoyl methane
(Parsol 1789, Givaudan)

Fig. 18.4. Chemical structures of UV absorbers. [Data from J. Pospisil, *Chem. Listy*, 85(1991)904 and other sources.]

as does 2-hydroxyphenyl-S-triazine:



the common feature of these conversions is a rapid internal hydrogen transfer. The reverse reaction is exothermic. Heat produced is dissipated in the matrix. It should be noted that this energy dissipation can only occur if internal hydrogen bonding is possible. If there is hydrogen bonding between the UV absorber and the matrix, energy transfer becomes disrupted which may cause stabilizer degradation.

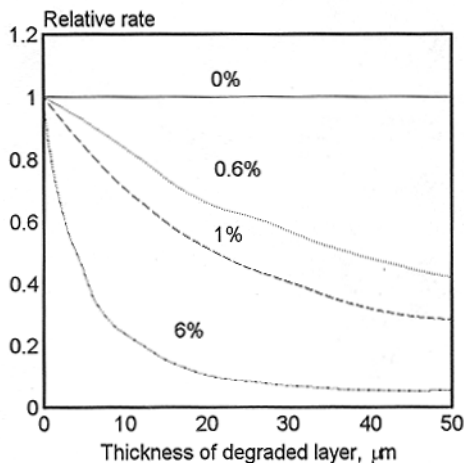


Fig. 18.5. Calculated rate reductions due to several loadings of UV screener in a highly absorbing polymer vs. thickness of degraded layer. [Adapted, by permission, from J. E. Pickett, *J. Appl. Polym. Sci.*, 33(1987)525.]

The absorptivity of a polymer is practically independent of UV absorber concentration. Fig. 18.5 contains data calculated for a highly-absorbing polymer. It also characterizes the effect of UV absorber concentration for a relatively non-absorbing polymer.² It is evident that, even of very high levels of UV absorber (6%) which are not realistic in industrial practice, the surface layers of the highly absorbing polymer cannot be protected.

As the level of TiO₂ in pigmented films increases, the UV absorber becomes less efficient. This is because a reduction in polymer degradation rate is caused mostly by pigment screening (Fig. 18.6). Fig. 18.7 demonstrates the effect of UV absorber, and an inorganic UV screening compound on light intensity at various depths.³ Each type of component (polymer, UV absorber, screening compound) absorbs energy but each responds differently to the energy absorbed. Radiative energy absorbed by the polymer may lead to photochemical degradation. UV absorbers are usually able to survive excitation and can

absorbs energy but each responds differently to the energy absorbed. Radiative energy absorbed by the polymer may lead to photochemical degradation. UV absorbers are usually able to survive excitation and can

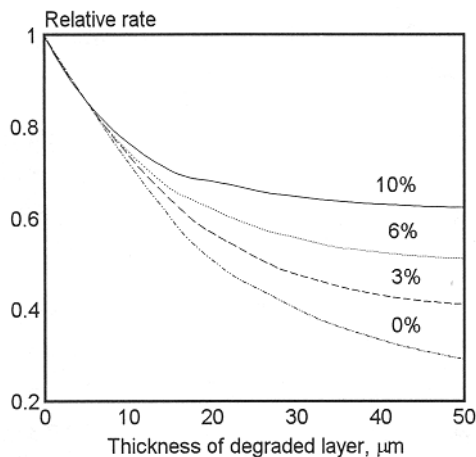


Fig. 18.6. Calculated rate reduction due to 1% UV screener and several loadings of TiO_2 vs. thickness of degraded layer. [Adapted, by permission, from J. E. Pickett, *J. Appl. Polym. Sci.*, 33(1987)525.]

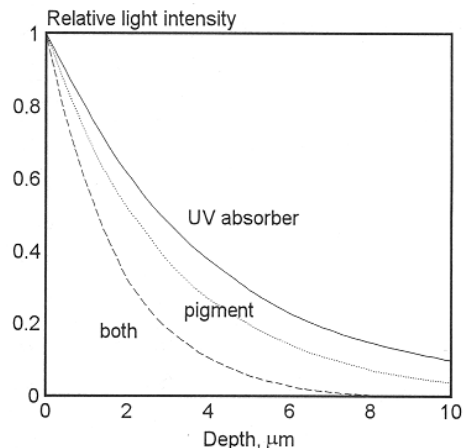


Fig. 18.7. Light intensity vs. depth from material surface depending on UV absorber and pigment loading. [Adapted, by permission, from A. L. Andrady and A. R. Shultz, *J. Appl. Polym. Sci.*, 33(1987)1389.]

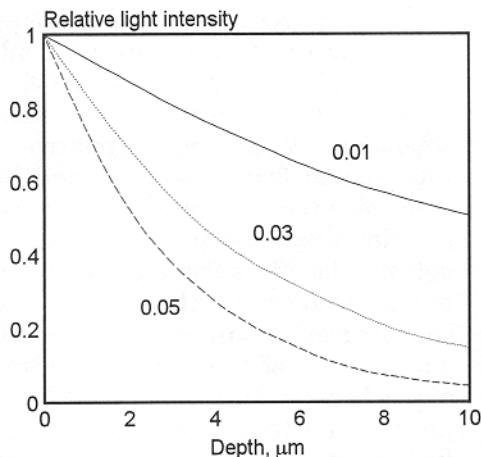


Fig. 18.8. Light intensity vs. depth from material surface depending on pigment volume fraction. [Adapted, by permission, from A. L. Andrady and A. R. Shultz, *J. Appl. Polym. Sci.*, 33(1987)1389.]

dissipate energy in a manner which is harmless to the polymer. Pigments acting as screening compounds reflect part of the radiation causing the radiation to travel through the matrix layer more than once. A screening compound protects the interior of the material but the radiant energy reflected back to the surface layers increases the deterioration rate.

UV absorbers are chosen because of their molar absorptivity, the absorption maxima of the polymer and the UV absorber (the absorption characteristics of each should match in order to protect the polymer), compatibility, and UV absorber stability in the particular matrix during weathering and polymer processing. Spectral data for individual polymers are given in Chapter 14. Table 18.2 shows the relevant data for some important UV absorbers.⁴

Table 18.2: Properties of selected UV absorbers

UVA	MW	MP	WMA	SE	MEC	TE	Dose
1	228	334	286	64	14.6	23.8	0.1-1.5
2	274	403	339	48	13.2		0.1-1
3	277	368	303	46	12.8		0.1-3
4	361	263	303	34	12.3		0.1-5
5	224	402	341	70	15.6	22.0	0.1-0.3
6	322	426	345	46	14.8		0.2-0.5
7	316	413	352	50	15.9		0.3-0.5
8	358	430	351	50	18.0		0.2-0.3
9	214	316	310	33	7.0	22.7	0.5-3

MW-molecular weight, MP-melting point, WMA-wavelength of maximal absorption [nm], SE-specific extinction coefficient [l/gcm], MEC-molar extinction coefficient [1000 l/molcm], TE-triplet energy [1000 cm⁻¹], Dose-usual amount [phr].

1=2-hydroxy-4-methoxybenzophenone (Uvinol M-40, Cyanosorb UV-9, AM-300);

2=2,2'-dihydroxy-4,4'-dimethoxybenzophenone (Uvinol N-53); 3=ethyl-2-cyano-3,3'-diphenylacrylate (Uvinol N-35);

4=2-ethylhexyl-2-cyano-3,3'-diphenylacrylate (Uvinol-529); 5=2-(2'-hydroxy-5'-methylphenyl)benzotriazole (Tinuvin P);

6=2-(3',5'-dialkyl-2'-hydroxyphenyl)benzotriazole (Tinuvin 320);

7=2-(3'-tert-butyl-2'-hydroxy-5'-methylphenyl)-5-chlorobenzotriazole (Tinuvin 326);

8=2-(3',5'-di-tert-butyl-2'-hydroxyphenyl)-5-chlorobenzotriazole (Tinuvin 327); 9=phenyl salicylate (Salol).

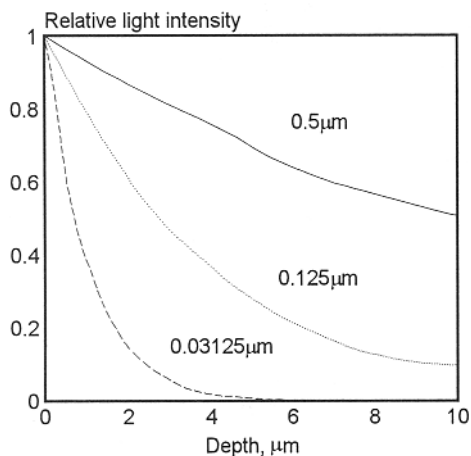


Fig. 18.9. Light intensity vs. depth from material surface depending on particle radii. [Adapted, by permission, from A. L. Andradý and A. R. Shultz, *J. Appl. Polym. Sci.*, 33(1987)1389.]

The protective action of pigments depends on their extinction coefficient, concentration, and particle size distribution. Fig. 18.8 shows the light shielding effect of pigments relative to their volume fraction. As expected, by increasing the amount of pigment one also increases the protection of the polymer, but the surface layer cannot be effectively shielded by pigment. The shielding effect also depends on the particle size of the pigment, as explained by Fig. 18.9. Filler particles, 1 μm in diameter and over, offer very little protection to the polymer. Heavy filler loadings therefore are not an effective method of providing polymer protection.

White pigment reflects most wavelengths of incoming radiation, whereas colored pigments absorb selectively wavelength bands, which affects the surface layers of the material. Carbon black is the best UV screening compound, and provides long-term protection. Carbon black not only screens out UV but also inhibits photooxidation through a complex autooxidative mechanisms. For these reasons, not only is the particle size of carbon black important (the best performance is in the range of 15-25 nm), but also the chemical composition of its surface. It was proven experimentally that the best results were obtained when so-called Channel Black was used. Channel Black is no longer manufactured by the channel process but by modern techniques which are able to simulate the channel process and produce a surface composition similar to the original. Inorganic pigments should be used cautiously. They do provide a screening effect but, at the same time, they may contain components which can catalyze polymer degradation. If so, this could offset the gains obtained by screening. This calls for careful testing of potential candidates in the actual formulation.

The evaluation of UV absorbers and screening compounds can be performed using one of the mathematical equations given below:

$$PE = 0.43(1-10^{-D}/D)$$

where: PE the protective efficiency of the UV absorber
D the optical density of the UV absorber.

$$R_k = a_k c_k [1 - 10 \exp(-x \sum a_i c_i)] / a_i c_i [1 - 10 \exp(-x \sum a_k c_k)]$$

where: R_k the residual absorption of the k^{th} species
 a_k the absorptivity of the k^{th} species
 c_k the concentration of the k^{th} species
 a_i the absorptivity of the i^{th} species
 c_i the concentration the i^{th} species
x the sample thickness.

Both equations estimate the protective value of UV absorbers and screening compounds. If the calculated protective value is higher than the value obtained from experiment, it means that the UV absorber or screening compound was degraded in the production process, or its effect was lost due to incompatibility, or, either by participating in the photochemical process or by emitting harmful radiation, it caused polymer degradation. If the UV absorber or screening compounds performs better than predicted by the equation, it means that they take part in the other processes discussed below, such as quenching, antioxidation, etc., or they facilitate intersystem crossing. The stability of UV absorbers is discussed in Section 18.5.

18.2 DEACTIVATION OF EXCITED STATES AND FREE-RADICALS

Absorption of radiant energy promotes molecules to higher energy states called excited states. If the surplus energy is not taken from the molecule by the means of secondary radiation, by a radiationless process, or by energy transfer to another molecule, the excited molecule may undergo chemical changes when the excess energy is higher than the energy of the weakest bond in the promoted atom. Energy from the excited molecule can be transferred by collision which requires close contact between the donor and acceptor. The distance for effective transfer of energy between two molecules is estimated to be between 1 and 1.5 nm. The distance between the molecules which are transferring the energy can be estimated from the Stern-Volmer equation:

$$R_0 = 0.735Q^{1/3}$$

where: R_0 the distance between the donor and acceptor
 Q the half value concentration of the acceptor.

or from the Perrin equation:

$$\psi_{D0}/\psi_D = \exp(VN[Q])$$

where: ψ_{D0} the quantum yield of donor fluorescence at a quencher concentration $[Q]=0$
 ψ_D the quantum yield of donor fluorescence at a quencher concentration equal to $[Q]$
 V the volume of the quenching sphere around an excited molecule or its segment
 N Avogadro constant
 $[Q]$ the concentration of the quencher.

When the result of the calculation is less than 1.5 nm (as may be confirmed by either equation), then it is assumed that the energy transfer is due to the collisions. If the result is higher than 1.5 nm (usually assumed distance is less than 10 nm), the process of energy transfer is called a long-range or Foerster transfer process. This long-range transfer may only occur if there is an overlap between the emission spectrum of the donor and the absorption spectrum of the quencher, and if the energy level of the acceptor (the triplet energy) is below that of the donor (see Table 18.2 for the triplet energy values of popular UV absorbers).

Some UV stabilizers may act partially through these mechanisms. A study by Stumpe⁵ discusses the energy transfer from the excited states in polyurethanes to salicylic acid derivatives. Fig. 18.10 shows that quenching of polyurethane fluorescence is

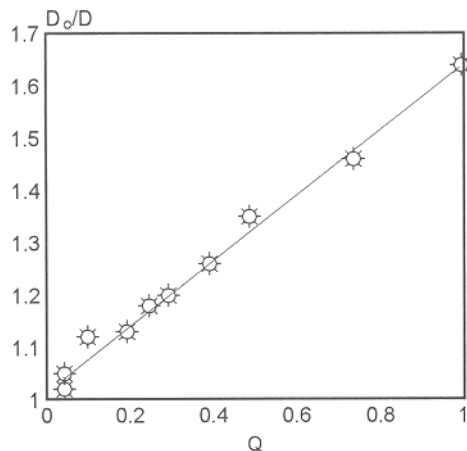


Fig. 18.10. Stern-Volmer relationship of fluorescence quenching of polyurethane by 1,6-hexamethylene disalicylate. [Adapted, by permission, from J. Stumpe and K. Schwetlick, *Polym. Degrad. Stab.*, 17(1987)103.]

Table 18.3: pK_B values of some HALS

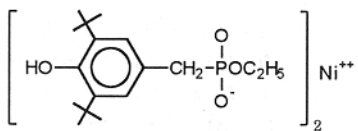
basic structure	pK _B	commercial name
	4-6	Tinuvin 770
	5-7	Tinuvin 292
	9-10	Tinuvin 123
	>12	Tinuvin 440

lizer) and include numerous commercial and patented compounds. Their representative structures are given in Fig. 18.12 and these include common monomeric HALS, their combinations with antioxidants, and polymeric hindered amines in the molecular back-

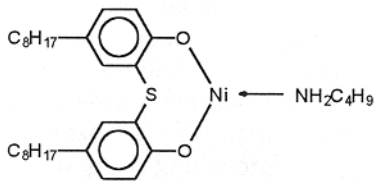
proportional to the concentration of the quencher. The process of quenching occurs by long-range transfer (Foerster transfer process).

Several other compounds used as UV stabilizers may act according to this mechanism, including Ni(II) chelates of varying chemical composition, hydroxybenzophenones, and hydroxybenzotriazoles. Nickel chelates are an exceptional example as they were used to prove the mechanism of stabilization by excited state quenching. It is well established that nickel chelates, having a relatively low absorption of radiation, are more effective in polypropylene stabilization than the better known UV absorbers such as hydroxybenzophenones or hydroxybenzotriazoles. Other polymers successfully stabilized by excited state quenchers include polystyrene, polyamides, etc. Fig. 18.11 shows some common metal complexes used as excited-state quenchers and hydroperoxide deactivators. Some of these compounds are multifunctional. For example, Cyasorb UV 1084 is considered a UV absorber, a thermal stabilizer, a quencher, and an antioxidant for PE.

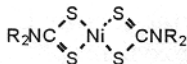
Concerted, multidisciplinary efforts resulted in the development of a series of new stabilizers based on hindered amines. They are usually called HALS (for hindered amine light stabi-



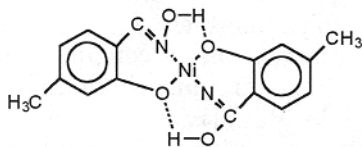
organophosphate nickel salt
(Irgastab 2002, Ciba-Geigy)



thiooctylphenolato nickel
(Cyasorb UV 1084, American Cyanamide
Chemissorb N-705, Ciba-Geigy)



dithiocarbamid
(Robac PD, Robinson)

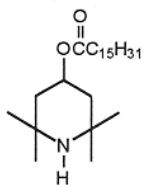


nickel chelate
(Negopex, ICI)

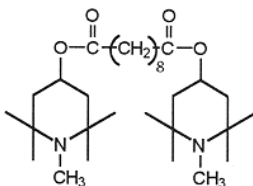
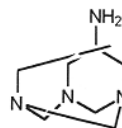
Fig. 18.11. Metal complexes.

bone or in the form of pendant groups. Other combinations include products of reactions with phosphites,^{7,8} siloxanes,⁹ and hydroxybenzophenones.¹⁰

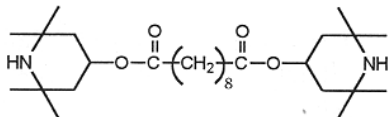
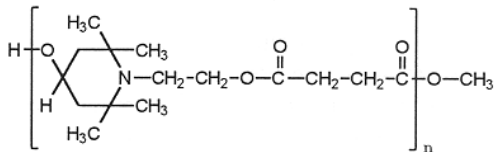
The mechanism of action of HALS differs from UV absorbers in that they are unable to absorb UV radiation. Instead, they protect materials by their ability to terminate the radicals formed. The selection of specific HALS is determined by properties of the system in which it must perform. Table 18.3 shows pK_B of various Tinuvin produced by Ciba-Geigy. Depending on the group attached to the nitrogen atom they vary in basicity. Their basicity should be synchronized with the basicity of the material to be protected. Basic HALS should be used for basic material and *vice versa*. Acid components in the material will react with basic HALS to hinder its performance. It is also essential to determine if the selected HALS is compatible with the matrix. A variety of HALS with varying solubility in different materials are available.



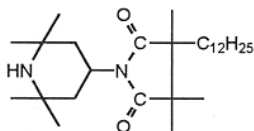
Dastib 845, Chemco

Tinuvin 765, Ciba-Geigy
Sanol LS 765, Sankyo

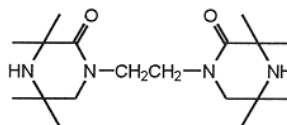
Goodrite UV 3034, BFGoodrich

Tinuvin 770, Ciba-Geigy
Mark LA-77, Asahi Denka Kogyo
Sanol LS-770, Sankyo

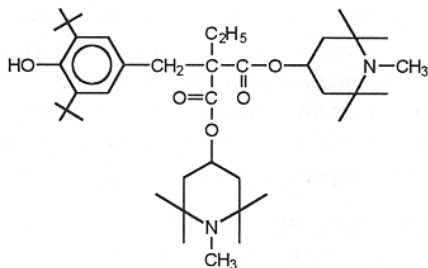
Tinuvin 622LD, Ciba-Geigy



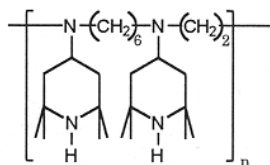
Cyasorb UV 3581, American Cyanamide



Goodrite 3034, BFGoodrich



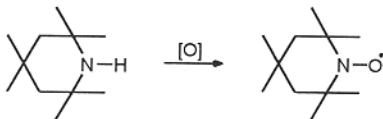
Tinuvin 144, Ciba-Geigy



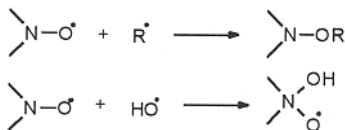
Spinuvex A-36

Fig. 18.12. Hindered amine light stabilizers.

The single most important feature of HALS is their ability to form stable radicals always available in the material to participate in reactions which lead to increased stability. Stable radicals are formed during the oxidation process and are called nitroxyl radicals:



They are very stable and, under some conditions, they behave as free radicals. Their stability is very important because it means that they will not abstract hydrogen from polymer molecules - a reaction which can lead to chain processes. At the same time, they are reactive towards free-radicals as the following reactions show:

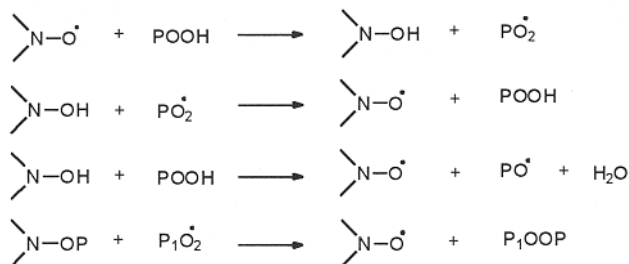


These reactions deactivate free-radicals and contribute to the increased stability of polymers because they break the chain reaction process. ESR studies¹² show the possibility of free electron exchange between two nitroxyl groups placed in one molecule but this process does not seem to result in an increased ability to quench excited states. Mono-, bi-, and poly-nitroxyl compounds react with radicals at similar rates.

Several other groups of compounds are known to scavenge radicals.¹³ The most common are phenolic antioxidants and secondary aromatic and cycloaliphatic amines and diamines. Their use is less common due to the high popularity of HALS.

18.3 ELIMINATION OF SINGLET OXYGEN, PEROXIDE DECOMPOSITION, AND LIMITING OXIDATIVE CHANGES

The major strength of HALS is their participation in peroxide decomposition. The reaction which forms nitroxyl radical leads to the elimination of singlet oxygen. Both nitroxyl radicals and hydroxylamines formed from them may participate in reactions with peroxides:



The last reaction is especially important because it allows the nitroxyl radical to regenerate when peroxides are eliminated from the polymer. The use of HALS is extremely efficient in most polymers; moreover, it improves the stability of polymers such as polyolefins, which were previously very difficult to stabilize (Figs. 18.13-18.16). Polymeric HALS are better retained by the material. The combination of a UV absorber and a quencher is almost universally more efficient than an application of one of these stabilizers alone.

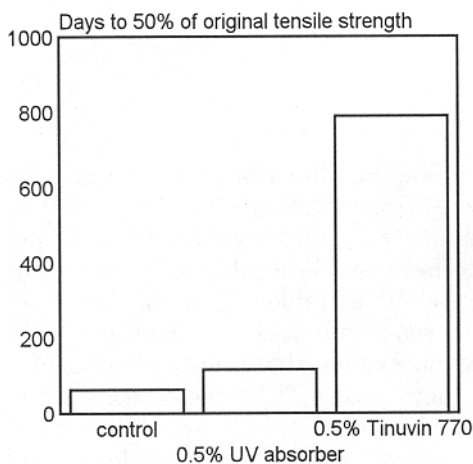


Fig. 18.13. Outdoor weathering of PP tape. [Data from H. K. Mueller, *ASC Symp. Ser.*, 280(1985)55.]

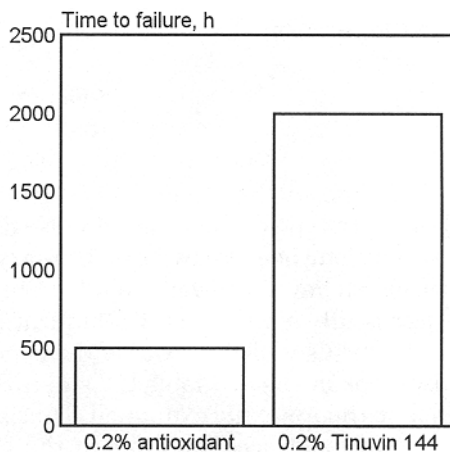


Fig. 18.14. PP fiber light stability in Xenotest 1200 until failure. [Data from H. K. Mueller, *ASC Symp. Ser.*, 280(1985)55.]

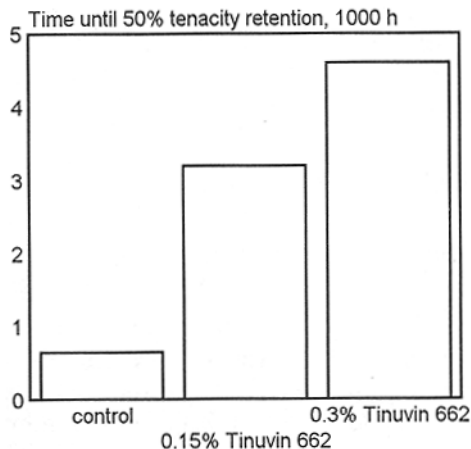


Fig. 18.15. Light stability of PP multifilaments weathered in Xenotest 1200 until 50% retention of tenacity. [Data from H. K. Mueller, *ASC Symp. Ser.*, 280(1985)55.]

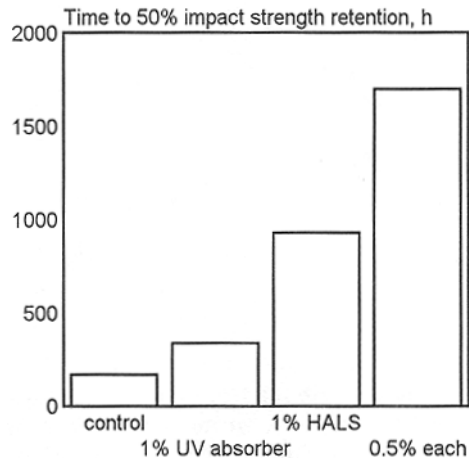


Fig. 18.16. Light stability of ABS exposed in Xenotest 450 until 50% retention of initial impact strength. [Data from H. K. Mueller, *ASC Symp. Ser.*, 280(1985)55.]

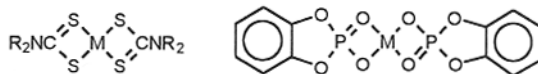
Phosphites are also known to participate in the decomposition of peroxides, according to the reaction:



It is known that some PVC stabilizers, including sulphur-containing organotins and maleate type organotins, can also decompose hydroperoxides.

It has long been known that primary antioxidants of the amine and hindered phenol types, which have been very popular in preventing thermooxidative degradation, cannot be successfully applied to UV stabilization. They are UV unstable and can be converted to free radicals which is exactly the opposite of the requirement of stabilization.^{14,15} In a closer look at the available UV stabilizers, it became evident that their high efficiency cannot be theoretically explained. This is because they participate in mechanisms which were simply not accounted for in the theoretical considerations. These stabilizers in question include commonly-used benzophenones, benzotriazoles, metal chelates, and hindered amines. The participation of these stabilizers in the antioxidation mechanisms is believed to explain their high efficiency, and they are looked on as UV stable antioxidants.

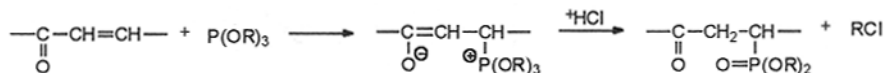
Some newer candidates are also used, including:



The metal is either nickel or zinc, and the compounds effectively decompose hydroperoxides. Kikkawa¹⁶ gives some details on the possible inhibiting effect of sulphur-containing compounds on the stabilizing effect of hindered amine light stabilizers.

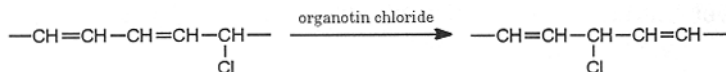
18.4 DEFECT REMOVAL

The principle of such a mechanism would be to eliminate the defects induced during the photodegradation process. By induced defects, we mean a change in the molecular weight of the polymer or an introduction of groups which absorb radiation, change the color of the polymer, or are vulnerable to photooxidative changes. Some mechanisms of this type are known but are used infrequently. One such effect can be achieved by balancing the chain scission and crosslinking reactions, which produces a retention of constant molecular weight. Such cases were reported for PVC formulations, where studies showed that there was no change in the molecular weight of polymer during the process of photodegradation.⁴ The molecular weight of other formulations decreased during irradiation.⁴ The difference in result is either a question of experimental error or simply because the formulations can be adjusted to balance the rates of scission and crosslinking. Double bonds, which can absorb radiation, undergo photooxidative processes and change polymer color, are produced during PVC processing technology. Phosphites can substitute at the double bonds according to the equation:



This reaction not only eliminates the double bond but does so at a very vulnerable location - the ketoallyl formation. Some PVC stabilizers also seem to be capable of eliminating ketoallylic chlorine. By doing, so they can break the chain reaction which causes formation of the sequence of conjugated double bonds that change polymer color.

Organotin chloride is believed to cause double bond migration (or isomerization), which breaks the sequence of conjugated double bonds and preserves color:



These are not numerous examples but they may generate more interest in the search for more which would increase the chances of preserving the original properties of polymers.

18.5 STABILITY OF UV STABILIZERS

The growing demand for high performance materials which are able to withstand long exposures, creates the need for efficient stabilization. It also requires that stabilizer be highly permanent. A set of papers^{9,12,13,17-27} contributes to our understanding of stabilizer durability. The sources of stabilizer loss from the material include:

- their limited light stability
- extraction
- volatility/incompatibility.

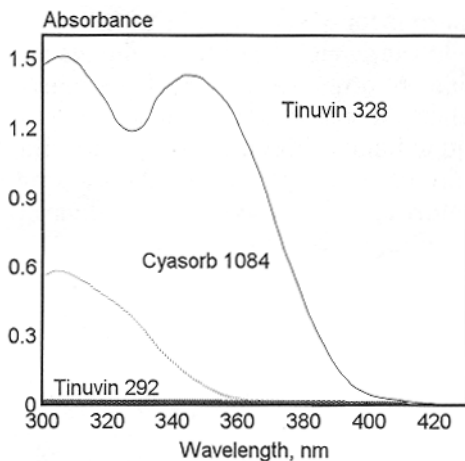


Fig. 18.17. UV-visible spectra of UV stabilizers (10^{-4} M in chloroform). [Adapted, by permission, from B. Ranby and A. Hult, *Org. Coat. Sci. Technol.*, 7(1984)137.]

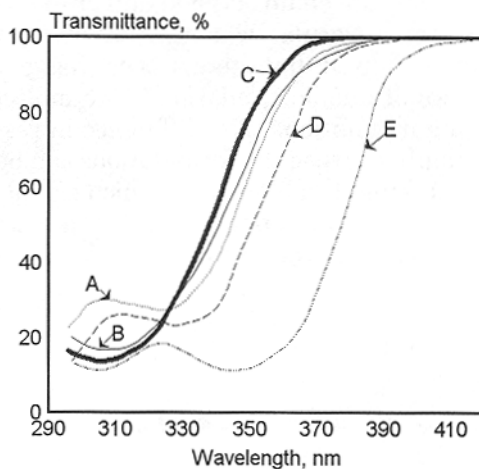


Fig. 18.18. Absorption spectra of UV absorbers (6×10^{-5} M/l in chloroform). (A-2,4-dihydroxy-benzophenone; B-cyanoacrylate, C-oxalic anilide, D-2-hydroxy-4-dodecyloxybenzophenone, E-benzotriazole I). [Adapted, by permission, from G. Berner and M. Rembold, *Org. Coat. Sci. Technol.*, 6(1983)55.]

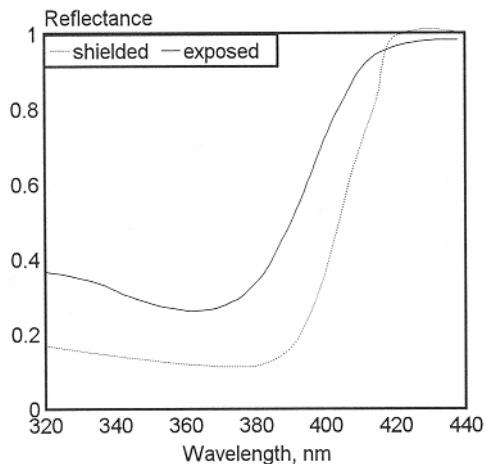


Fig. 18.19. Reflectance spectra of a two-coat top-coating (1% benzotriazole). [Adapted, by permission, from G. Berner and M. Rembold, *Org. Coat. Sci. Technol.*, 6(1983)55.]

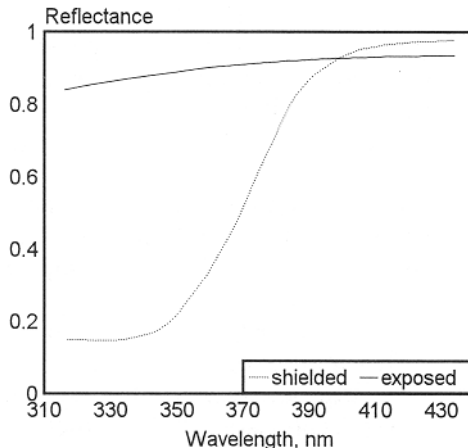


Fig. 18.20. Reflectance spectra of a two-coat top-coating (3% oxalic anilide). [Adapted, by permission, from G. Berner and M. Rembold, *Org. Coat. Sci. Technol.*, 6(1983)55.]

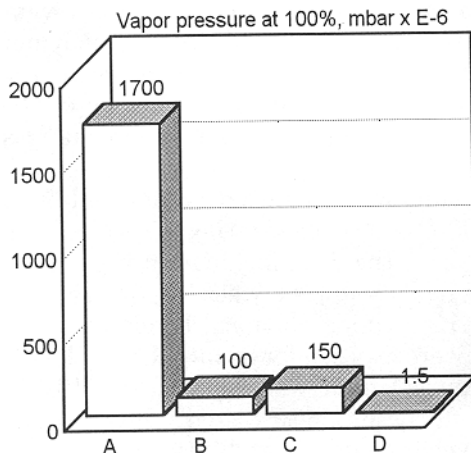


Fig. 18.21. Vapor pressure of various stabilizers. (A=2,4-dihydroxybenzophenone, B=2-hydroxy-4-dodecyloxybenzophenone, C=oxalic anilide, D=benzotriazole I). [Adapted, by permission, from G. Berner and M. Rembold, *Org. Coat. Sci. Technol.*, 6(1983)55.]

UV absorption is a required function of most UV stabilizers (Figs. 18.17 and 18.18). All UV absorbers (Fig. 18.18) have strong and comparable absorption in the UV range. HALS (Fig. 18.17) does not absorb UV radiation at all, while Ni-chelate absorption is only minimal. Absorbing of radiation in the UV range does not necessary mean that the stabilizer has to undergo chemical changes (Fig. 18.19). It is quite well established that benzophenones and benzotriazoles have inherent light stability attributable to their ability to rapidly deactivate excited states via proton transfer. Some other compounds used as UV absorbers may not necessarily have the same properties (Fig. 18.20). Oxalic anilide is known to have poor light stability. Losses due to volatility are often predicted from the vapor pressure of the stabilizer at elevated tem-

perature (Fig. 18.21). Friedrich *et al.*⁹ show that HALS reacted with siloxanes remains in the material after extraction. Tinuvin 770 and siloxane-containing stabilizers were compared in this study. If samples of polypropylene film were exposed to UV radiation without previous extraction, then Tinuvin 770 was the most efficient stabilizer followed by synthesized products of different molecular weights. The higher the molecular weight of the stabilizer the lower its efficiency as a UV stabilizer which makes sense when one considers that the molecular mobility of the stabilizer is a key to its performance. After films were extracted with methylene chloride, sample containing Tinuvin 770 behaved in a similar manner to the control (no stabilizer) when exposed to UV. Whereas HALS, which had been reacted with siloxane, were not extracted by the solvent and performed well. The optimal performance was obtained when their molecular weight was between 2000 and 4000. This molecular weight gave a proper balance between molecular mobility and retention after extraction. This experiment illustrates, vividly, the importance of the physical characteristics of stabilizers. Matz²⁶ gives an interesting account of his findings regarding the durability of Cyasorb UV 1084 (nickel chelate) in polyethylene film. The durability of the stabilizer was monitored by atomic absorption spectroscopy (nickel) and by HPLC (entire molecule). Nickel was well retained by the samples throughout processing and exposure but the original molecular structure was not retained due to degradation during processing (after processing, the material retained only a small fraction of the original stabilizer). Studies of extraction by various solvents indicated that the extraction of stabilizer is most efficient if the stabilizer is soluble in the solvent and if the solvent swells the matrix. This information shows that changes in polymer matrix (either due to solvents or degradation) affect stabilizer permanence in the system. In many studies, observations are made that initially the efficiency of the stabilizer is higher. After the material surface becomes degraded, more rapid changes occur.

Benzotriazole should be the most resistant stabilizer because it is thermally and photochemically stable. Ten days exposure at 100°C of a thermosetting acrylic coating containing 3% of each stabilizer (Fig 18.22) confirms the data included in Fig. 18.21. 2,4-dihydroxybenzophenone does not follow the relationship between vapor pressure and stabilizer retention, which is explained by its forming chemical bonds with the coating during crosslinking. The acrylic coatings were exposed for 28 months in Florida and the concentration of stabilizers in the exposed area was tested (Fig. 18.23). Benzotriazole stabilizer is the most durable of all the products tested. The chemical bonding of 2,4-dihydroxybenzophenone seems to change its UV stability, as shown by the high losses detected. Six benzotriazole UV stabilizers and one s-triazine were studied in rubber modified acrylic film by non-destructive UV/visible spectrophotometry developed to monitor their retention.²⁷ After 3000 h exposure in Atlas Ci65, 35% to 53% of the initial stabilizer was retained. The most durable were s-triazine (Cyasorb UV 1164)

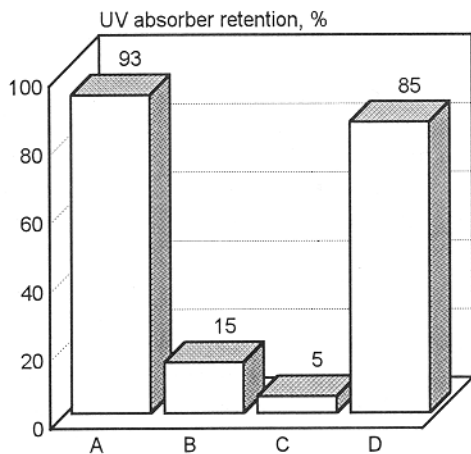


Fig. 18.22. Loss of UV absorbers from thermosetting acrylic coating exposed for 10 days to 100°C. (A=2,4-dihydroxybenzophenone, B=2-hydroxy-4-dodecyloxybenzophenone, C=oxalic anilide, D=benzotriazole I). [Adapted, by permission, from G. Berner and M. Rembold, *Org. Coat. Sci. Technol.*, 6(1983)55.]

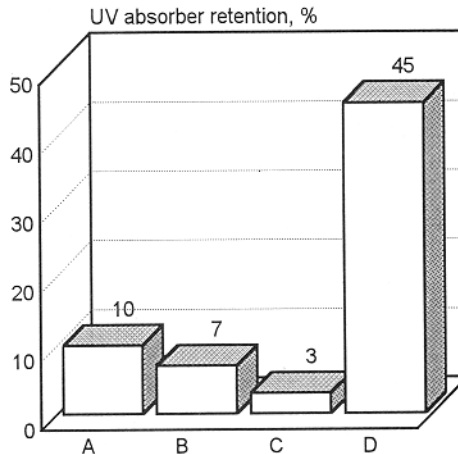


Fig. 18.23. UV stabilizer retention in the thermosetting acrylic coating after 28 months of Florida exposure. (A=2,4-dihydroxybenzophenone, B=2-hydroxy-4-dodecyloxybenzophenone, C=oxalic anilide, D=benzotriazole I). [Adapted, by permission, from G. Berner and M. Rembold, *Org. Coat. Sci. Technol.*, 6(1983)55.]

and a benzotriazole having a tertiary octyl substituted to its benzene ring. The rate of retention suggests first-order kinetics.

A recent study by Pickett and Moore²³ included several important UV screening compounds such as benzophenone (Cyasorb UV 531), benzotriazole (Cyasorb 1164), diphenyl cyanoacrylate (Uvinul N-35), oxanilide (Sanduvor VSU), and s-triazine (Cyasorb UV 1164). Also two HALS (Tinuvin 770 and Goodrite 3034) were included. Several polymers (PMMA, PS, PC, UV-cured acrylics) were studied. This broad study, which was part of a long term effort in the field, provides a considerable number of useful observations. The study includes an experimental part in which the results are compared with models to verify the correctness of the model and to better understand the data. A monochromatic model developed for the study simulates data precisely. The depletion of UV screening compounds begins at the surface and, as exposure continues, extends more deeply. The kinetics of the loss of UV screening compounds is best described by a zero-order kinetics when stabilizer concentration is high, followed by first-order kinetics for lower concentrations. The degradation of the screening compounds is caused by light with a wavelength lower than 350 nm. The suggested mechanism for benzophenone sta-

bilization includes formation of benzoic acid (which is energetically possible if the radiation has wavelength of 318 nm or less based on calculations of bond dissociation energy). The study indicates that the type of matrix in which the stabilizer is dispersed has a prevailing effect on its durability. Comparison between PMMA (a more durable matrix) and a UV-cured acrylic polymer, shows that rapid degradation of the matrix affects the durability of screening compound. Comparison of the performance of UV screening compounds in PMMA (hydrogen bonding between hydroxyl group of UV screening compound and the carbonyl group in the polymer) and PS indicates that the matrix can engage the hydroxyl groups required by the UV screening compound to perform its function and thus reduce its efficiency. The concentration of the UV absorber does not much influence its degradation rate. The wavelength of exposure has a more complex effect. In terms of stabilizer durability, the use of a broader band, than is available in daylight, does not seem to have any effect. But, considering the fact that matrix has also effect on the retention of the UV screening compound, the radiation wavelength has an essential influence. This point was well demonstrated by conducting experiments with PC (it absorbs the UV radiation of QUV) in QUV and xenon lamp. More UV screening compound was retained during short exposure to QUV because the polymer was shielding the UV screening compound. Fig. 18.24 shows the retention of benzotriazole (Cyasorb 5411) and benzophenone (Cyasorb 541) UV screening compounds in Florida. Comparison of artificial weathering with Florida exposure gives very good agreement in a model prediction and 1 year in Florida exposure equals 1100 h in xenon arc Weather-O-Meter. Such good agreement was not obtained for benzophenone which degrades faster in Florida exposure. The reasons cannot be explained by experimental data. From this and other experiments, it can be predicted that a UV screening compound is depleted from a polar matrix within 3-5 years of exposure in Florida or several thousand hours in xenon arc which indicates the limit of durability of such stabilized materials.

Unfortunately, similar data do not exist for HALS. It is known from studies on crosslinked polyurethane elastomers that the presence of HALS in polyurethane helps to retain the UV stabilizer (Fig. 18.25). The authors explain this result by proposing that HALS helps to preserve the original structure of polyurethane, which in turn allows the UV absorber to remain longer in the polymer matrix. Pickett and Moore²³ conducted similar experiments for UV-cured acrylics. Their findings are essentially similar, indicating that the addition of HALS helps to retain the UV screening compound. When similar samples were exposed behind quartz, the retention of the UV screening compound remained better when the specimen contained HALS. This experiment seems to contradict the explanation proposed by Decker and Moussa¹⁸ that HALS protects the UV screening compound against its physical loss from a faster degrading matrix. Clearly, more data are needed to understand the durability of HALS in systems as well as their effect on UV screening compound retention.

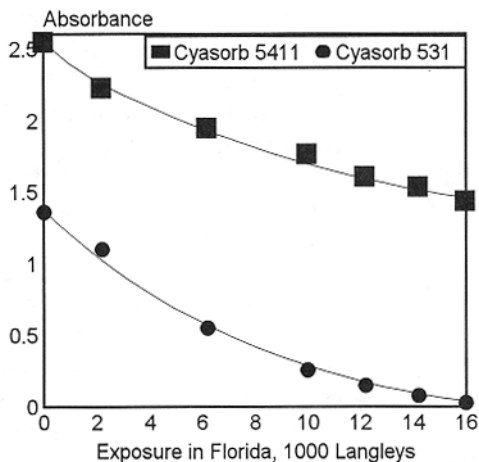


Fig. 18.24. Concentration of UV screeners vs. exposure of PMMA containing 1% UV screener in Florida. (6000 Langley equals 1 year in Florida). [Adapted, by permission, from J. E. Pickett and J. E. Moore, *Polym. Deg. Stab.*, 42(1993)231.]

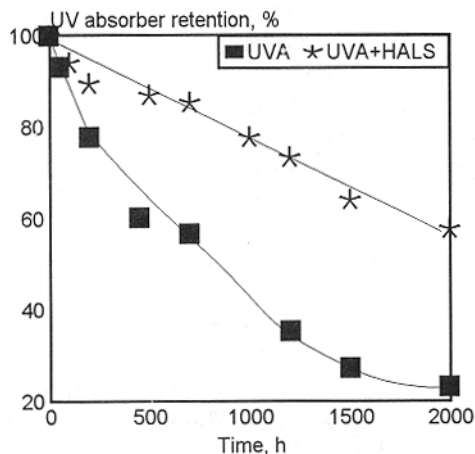


Fig. 18.25. Loss of UV absorber during photoaging of an aliphatic polyurethane acrylate (HALS=0.5% Tinuvin 292, UVA=0.5% Tinuvin 900). [Adapted, by permission, from C. Decker and K. Moussa, *Polym. Mat. Sci. Eng.*, 57(1987)338.]

18.6 EFFECT OF STABILIZATION

Recent publications⁹⁻⁵² contain information which can be used in the design of a durable stabilizing system. The combination of UV screening compounds and HALS with siloxane oligomers allows the development of more durable stabilizers.⁹ To optimize durability, it is essential to generate an adduct which has a molecular weight which not only gives the required degree of physical stability to the new stabilizer formation but also allows it to remain mobile and efficient in the matrix. Balancing both results in an improved performance. Chemical synthesis of UV screening compounds which contain an antioxidant segment results in materials which give better performance than UV screening compounds alone.²⁵ Although, based on the available data, it is difficult to assess if this improvement is due to the fact that two stabilizers were added in the place of one (no data on control available) or if there is some advantage in having this combination in one molecule. Some combinations of UV screening compounds with HALS and phenolic antioxidants have proven inefficient. HALS-phosphite combinations were proposed for polypropylene stabilization and showed some improvements.^{7,8} Keto-enol tautomerism of β -dicarbonyls containing the CF_3 groups has been proposed as a new avenue for stabilization.³⁹ These products have been applied in the protection of cosmetics against photodegradation. HALS with a regulated molecular mass were synthesized in

order to achieve equilibrium between the physical loss of the stabilizer and its photochemical efficiency.⁴² Urethane functional HALS were synthesized resulting in reduced stabilizing efficiency but increased stability to solvent extraction.³³

Addition of Cyasorb UV 1084 to LDPE increased its lifetime to 12 months in Florida exposure, compared with 2.5 months without stabilizer. Similar films for greenhouse applications were produced in Jordan.²⁹ Stabilization with nickel chelate stabilizer extended their useful life to 1 year. Hydrolysis of ester and amide linkages, and oxidation and halogenation of stabilizers were observed when plastics containing stabilizers were exposed to UV in the presence of chemicals used in spas. The useful life of a stabilizer was rapidly reduced by the presence of chemicals. The effect of the addition of HALS to PE was studied by oxygen uptake and the detection of low molecular weight compounds. In the presence of HALS, only 20% of the oxygen was converted to CO or CO₂. The remaining oxygen was converted to water. The presence of HALS changes the mechanism of degradation. The mechanism and kinetics of polyolefin photostabilization was discussed based on extensive experimental data. Denisov⁵⁰ brings a new data to highlight the role of various components of the photooxidative processes in chain-termination in the presence of HALS. It is reported that HALS can be inhibited in PP by the addition of CaCO₃. A brittle surface layer, produced in the presence or absence of UV stabilizers, did not greatly affect the mechanical performance if the bulk of the material was not degraded.⁴⁸ The internal stress of a material was preserved in stabilized compositions. HALS used in PP exposed to γ -radiation was rapidly degraded.³⁴ A twenty-fold increase in stabilizing efficiency was observed when a combination of HALS and UV absorber was used in UV-cured coatings based on PU-acrylate networks. Aromatic PUs were more difficult to stabilize because they compete with the absorber. Selection of UV stabilizers for screening cosmetics from UV is discussed in detail in the technical literature.⁵¹⁻⁵²

REFERENCES

1. L. H. Garcia-Rubio, *Macromolecules*, 20(1987)3070.
2. J. E. Pickett, *J. Appl. Polym. Sci.*, 33(1987)525.
3. A. L. Andradý and A.R. Schultz, *J. Appl. Polym. Sci.*, 33(1987)1389.
4. J. Wypych, *Poly(vinyl chloride) Stabilization*, Elsevier, Amsterdam, 1986.
5. J. Stumpe and K. Schwetlick, *Polym. Degrad. Stab.*, 17(1987)103.
6. H. K. Mueller, *ACS Symp. Ser.*, 280(1985)55.
7. U. Hähner, W. D. Habicher, and S. Chmela, *Polym. Deg. Stab.*, 41(1993)197.
8. S. Chmela, W. D. Habicher, U. Hähner, and P. Hrdlovic, *Polym. Deg. Stab.*, 39(1993)367.
9. H. Friedrich, I. Jansen, and K. Rühlmann, *Polym. Deg. Stab.*, 42(1993)127.
10. N. S. Allen, M. Edge, J. He, W. Chen, K. Kikkawa, and M. Minagawa, *Polym. Deg. Stab.*, 42(1993)293.
11. M. S. Holt, *Light and heat stabilization of coatings*, ASNAW 1995.

12. C. Neri, V. Malatesta, S. Constanzi, and R. Riva, *Angew. Makromol. Chem.*, 216(1994)101.
13. J. Pospisil, *Angew. Makromol. Chem.*, 216(1994)135.
14. J. Lucki, J. F. Rabek, and B. Ranby, *Polym. Photochem.*, 5(1984)351.
15. G. Scott, *New Trends in the Photochemistry of Polymers*, Elsevier, London, 1985.
16. K. Kikkawa, Y. Nakahara, and Y. Ohkatsu, *Polym. Degrad. Stab.*, 18(1987)237.
17. H. E. A. Kramer, *Farbe Lack*, 92,10(1986)919.
18. C. Decker and K. Moussa, *Polym. Mat. Sci. Eng.*, 57(1987)338.
19. A. Sustic, A. C. Albertsson, and O. Vogl, *Polym. Mat. Sci. Eng.*, 57(1987)231.
20. W. B. Hardy, *Dev. Polym. Photochem.*, 3(1987)287.
21. B. Ranby and A. Hult, *Org. Coat. Sci. Technol.*, 7(1984)137.
22. G. Berner and M. Rembold, *Org. Coat. Sci. Technol.*, 6(1983)55.
23. J. E. Pickett and J. E. Moore, *Polym. Deg. Stab.*, 42(1993)231.
24. B. Bell, D. E. Beyer, N. L. Maecker, R. R. Papenfus, and D. B. Priddy, *J. Appl. Polym. Sci.*, 54(1994)1605.
25. N. S. Allen, M. Edge, S. Conway, D. A. Doyle, E. M. Howells, K. Kikkawa, M. Minagawa, and T. Sekiguichi, *Polym. Deg. Stab.*, 38(1992)85.
26. S. G. Matz, *J. Chromatog.*, 587(1991)205.
27. J. E. Bonekamp and N. L. Maecker, *J. Appl. Polym. Sci.*, 54(1994)1593.
28. M. M. Qayyum and J. R. White, *Polym. Deg. Stab.*, 39(1993)199.
29. N. Khraishi and A. Al-Robaidi, *Polym. Deg. Stab.*, 32(1991)105.
30. W. B. Achwal, *Colourage*, (1991)1, 29.
31. J. Pospisil, *Chem. Listy*, 85(1991)904.
32. G. E. Krichevsky, G. T. Khachaturova, and O. M. Anissimova, *Intern. J. Polym. Mater.*, 13(1990)63.
33. J. Pan, Y. Song, W. W. Y. Lau, and S. H. Goh, *Polym. Deg. Stab.*, 41(1993)275.
34. S. Falicki, D. J. Carlsson, J. M. Cooke, and D. J. Gosciniak, *Polym. Deg. Stab.*, 38(1992)265.
35. L. Wenzhong, Q. Juying, H. Xingzhou, and X. Hongmei, *Polym. Deg. Stab.*, 32(1991)39.
36. J. Pan, H. Xu, J. Qi, J. Cen, and Z. Ma, *Polym. Deg. Stab.*, 33(1991)67.
37. C. Decker, K. Moussa, and T. Bendaikha, *J. Polym. Sci., Polym. Chem.*, 29(1991)739.
38. H. E. A. Kramer, *Angew. Makromol. Chem.*, 183(1990)67.
39. B. K. Wu, Y. F. Chang, Y. Mou, and J. F. Rabek, *Polym. Bull.*, 26(1991)423.
40. F. Gugumus, *Polym. Deg. Stab.*, 34(1991)205.
41. B. P. Thapliyal and R. Chandra, *Prog. Polym. Sci.*, 15(1990)735.
42. S. Chmela and P. Hrdlovic, *Polym. Deg. Stab.*, 42(1993)55.
43. A. B. Reynolds and P. A. Wlodkowski, *Radiat. Phys. Chem.*, 38(1991)553.
44. I. Narisawa and T. Kuriyama, *Angew. Makromol. Chem.*, 216(1994)87.
45. J. - Q. Pan and J. Zhang, *Polym. Deg. Stab.*, 36(1992)65.
46. P. Gijsman, J. Hennekens, and D. Tummers, *Angew. Makromol. Chem.*, 216(1994)37.
47. Y. Qing, X. Wenyang, and B. Ranby, *Polym. Eng. Sci.*, 34(1994)446.
48. M. M. Qayyum and J. R. White, *Polym. Deg. Stab.*, 41(1993)163.
49. A. G. Andreopoulos, A. Pappa, and N. Tzamtzis, *Polym. Test.*, 13(1994)3.
50. E. T. Denisov, *Polym. Deg. Stab.*, 34(1991)325.

51. *Parsol 1789. The safe and effective UV-A filter. Givaudan 1988.*
52. *Parsol MCX. The effective non-paba UV-B filter. Givaudan 1988.*

19

BIODEGRADATION

Two groups of scientists are involved in researching this subject: those who are interested in extending the service life of materials and those who focus on the development of materials which can be reabsorbed by the environment after performing their functions. In both cases, the main goal is the same. That is, to assure that energy is utilized to good purpose rather than for creating waste. The information in this chapter will be useful to both groups because the methods and the materials studied are the same. Our main concern is extending the life of materials. This chapter has been included in this edition to review essential principles of biodegradation since biodegradation and UV degradation occur simultaneously and are self-supportive.

19.1 BIODEGRADATION ENVIRONMENT

Four biodegradation environments for polymers and final products are dealt with:¹

- soil
- aquatic
- landfill
- compost

Each environment contains different microorganisms and has different conditions of degradation. We will deal mainly with soil and the aquatic environment.

Three classes of microorganisms are responsible for the biodegradation of organic matter: fungi, bacteria, and actinomycetes. They have the following concentrations in soil: $5-900 \times 10^3$, $3-500 \times 10^6$, and $1-20 \times 10^6$ counts/g soil, respectively.¹ In soil, fungi are mostly responsible for the degradation of organic matter including polymers. Materials which are above soil level are degraded by similar microorganisms but their number is limited. Anaerobic bacteria do not play a role at the soil surface.

The aquatic environment differs from soil because fungi do not play a role and this environment is dominated by bacteria which are present at 10^6 counts/ml. There are two

major concentrations of bacteria in an aquatic environment: on the surface and in the sediment (the sediment is the most concentrated source of microorganisms). Bacterial concentration decreases in water with depth increasing. In landfill environments, most degradative processes occur without oxygen (anaerobic) whereas compost is aerated to increase the biodegradation rate.

Microorganisms are the most adaptable living species on earth. They are also the most vulnerable to external conditions which is the reason that they can be easily transformed to new species through the mutagenic processes. The number of microorganisms which participate in the degradative processes is so large that even specialized sources² can only list the major groups. Microorganisms biodegrade organic materials by the use of their enzymatic apparatus. Enzymatic reactions are discussed below.

19.2. ENZYMATIC REACTIONS

Enzymes are complex proteins (molecular weight 10,000 to 1,000,000) which are able to catalyze specific reaction (each enzyme catalyzes one specific chemical reaction). About 2000 enzymes are known which can be assigned to one of these categories:³

- hydrolase - hydrolysis (esters, amides, acetals, etc.)
- esterase or amidase - esterification or amidation
- isomerase or transferase - transferring atoms within one molecule
- reductase or oxidase - electron transfer reaction
- hydrogenase or dehydrogenase - proton addition or removal
- ligase - condensation reactions with formation of C-C, C-S, C-O, or C-N bond.

Enzymes can function only under certain (defined) conditions which include the concentration of substrates and products (typically low), temperature, and pH. Specific conditions are required for microorganism growth. These conditions also include specific nutrients which can stimulate microorganism growth.

The enzymatic reaction is a two-stage process given by the equation:



in which E - enzyme, S - substrate, and P - product. The enzyme must form a complex, ES, which is the rate controlling step. Product formation is kinetically an unimolecular reaction. Michaelis-Menten constant, K_M , characterizes the reaction rate. As shown in the following equation:

$$V_o = \frac{V_{\max} [S]}{K_M + [S]}$$

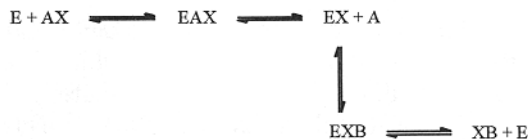
where: V_o initial rate
 V_{\max} maximum rate
 $[S]$ substrate concentration.

From this equation, K_M decreases when enzyme efficiency increases. A constant K_M applies only to a given reaction and to the defined set of conditions under which it was measured.

Enzymes also participate also in bimolecular reactions (e.g., hydrolysis in which water and polymer molecules are involved). There are two possible processes involved in bimolecular reactions: single and double displacements. The sequence of reactions in the single displacement is given by the following equation:



Substrates (A and B) are bound to the enzyme one after the other, then the complex EAB undergoes a unimolecular reaction with the formation of two products (C and D) and liberation of the enzyme. In the double displacement reaction, the sequence of reactions is as follows:



In the first stage, some segment, X, of substrate A is extracted and subsequently combined (transferred) to substrate B with the formation of the product, XB.

The above reactions are essential for understanding the two most important principles of enzymatic reactions - their specificity and their kinetics. The kinetics of the enzymatic reactions is obvious from the above equations. Each of these sequences of reactions is controlled by unimolecular kinetics in which enzyme molecules are involved. The reaction can be sped up by an increased supply of enzyme which will depend on how well the microorganism adapts to the environment. The enzyme output and its properties are the factors which essentially control the reaction.⁴ Specificity can be de-

rived from the fact that the enzyme must combine with the substrate. The most obvious conclusion from this is that the substrate molecule must have the exact chemical structure expected by the enzyme. Some enzymes have a broad activity (e.g., chymotrypsin) which can catalyze reactions of many chemicals which contain a particular functional group (in the case of chymotrypsin amides and esters). In most cases, enzymes are so specific that they cannot catalyze the reaction of the *cis*-form if they are specific to the *trans* configuration. The specificity is not only restricted to chemical composition and stereoregularity but also extends to the elasticity of the molecule. It is elasticity which allows a molecule to attain the appropriate arrangement before a complex can be formed. These two principles apply to the specific examples given below. An enzyme catalyzed reaction requires a close fit of the polymer chain into the active site on the enzyme therefore conformational flexibility generally leads to biodegradability.⁵

One more aspect also relates to specificity. Since enzymes are so specific there seems to be little chance that they would be able to act on man-made materials since enzymes have evolved to interact with the common nutrients available in nature. This would be true if not for the fact that microorganisms are very adaptive. The action of enzymes on herbicides is the most well known example of adaptation which has already occurred. Herbicides are synthetic materials but there are many microorganism which can utilize them. It is known from laboratory experiments that the same microorganism, after an adaptation period, can boost its reaction rate 1000 times.

There are chemical substances which are not biodegradable but it may be that they have just not yet encountered the right biotic environment. There is no incentive for a microorganism to adapt if it has a sufficient supply of nutrients from other sources.

19.3 BIODEGRADATION OF MATERIALS

As can be expected, natural products are most prone to biological degradation. Humus presents an interesting example because it is so durable. It can survive in a soil environment for a very long time due to its complex composition. Several different types of microorganisms are needed for its full reabsorption into the environment.

Cellulose is the most abundant biopolymer and many microorganisms are capable to digest it. Aerobic bacteria, anaerobic bacteria, and fungi can biodegrade cellulose over a wide range of temperature (up to 85°C) and pH (up to 9). Three types of fungi are involved in the process of wood biodegradation:

- white-rot fungi degrade lignin and polysaccharides to simple sugars
- brown-rot fungi degrade cellulose and hemicelluloses
- soft-rot fungi also degrade cellulose and hemicelluloses.

Two enzymes are most involved: one degrades the chain (1,4- β -glucosidic bonds) to polymers of lower molecular weight. The other hydrolyses the chain ends to monomeric and dimeric units. Some fungi have enzymes which operate on a different principle.

They produce peroxides which then oxidize glucosic chain elements. This causes the chain to split into lesser fragments to form low molecular weight components. The final products are CO₂, hydrogen, methane, and ammonia. With an abundance of microorganisms which can biodegrade cellulose there are still numerous examples of wooden objects which have survived thousands of years (e.g., in Egyptian tombs) which shows that particular conditions must be present to biodegrade material.

Starch degradation is of interest since it is frequently added to polymers in order to make them “environmentally friendly”. It should be noted that starch similar to cellulose has very high molecular weight but still there are enzymes (amylases) which can reduce starch to simple sugars such as glucose, maltose, maltotriose, etc. If starch is added to a synthetic polymer, the subsequent starch degradation produces a spongy structure consisting of man-made polymer which becomes easier to attack by microorganisms because the polymer surface area has been increased and it is accessible to the enzymes. The contact between polymer and enzyme is a key factor in the process kinetics.

Different polyesters have a varying probability of biodegradation. Polycaprolactone is known to be the most responsive to fungal growth. Poly(glycolic acid) and poly(lactic acid), both of which have very low crystallinity, are also easily biodegradable.⁶ The typical signs of the degradation progress are a loss of weight, a reduction in elongation and a reduced tensile strength. Biodegradation is mostly restricted to the amorphous regions. After these have been degraded, the biological processes continue at the edges of the crystallites and continue inward. It is frequently observed that the molecular weight of the polymer does not change, meaning that degradation consists of the subtraction of chain-end units. These split-off units are dissolved in the surrounding aqueous medium. A comparison of bottle grade PET and cinematographic film grade PET shows that the film grade PET is more durable because of its orientation.⁷ Enzymes act more readily on polyesters with the longest chain length.⁵ More rigid aromatic polymers degrade at slower rates than more flexible aliphatic polymers. Degradation of polyesters by hydrolysis occurs without the participation of microorganisms.⁸ The presence of acids and bases (especially bases) is a sufficient condition for the process to proceed. There are similarities between the chemical and biological degradation of polyester. Polymer morphology, crystallinity, water concentration, chemical structure, hydrophilicity, molecular weight, chemical modification by copolymerization have a similar effect in both chemical degradation and in biological process.

Polyethers biodegradation has been studied for over 30 years. It has been proven that poly(ethylene glycol) up to a molecular weight of 20,000 is degraded. Typical mechanisms include enzymatic dehydrogenation and oxidation. The terminal alcohol group in PEG is metabolized to aldehyde and carboxylic acid.⁹ The sequence is repeated, ultimately yielding depolymerized PEG. Typically, several microorganisms participate in these reactions in a symbiotic mechanism in which metabolites are exchanged between bacteria. This mechanism is key since various microorganisms are known to be affected

(and inhibited) by the products of reaction which they themselves produce. Such symbiosis reduces this possibility. Some microorganisms utilize glyoxylic acid as a carbon source (removing its excess). Glyoxylic acid is produced by other bacteria which obtain energy from the degradation of PEG to glyoxylic acid. Also, poly(propylene glycol) of molecular weight up to 4,000 is utilized by bacteria. These bacteria can utilize both diols and triols but are not capable of degrading PEG. PPG is not metabolized by extracellular enzymes. Only intracellular enzymes take part in the conversion which requires that PPG be in solution. This restricts the molecular weight which can be used. Secondary hydroxyl groups are preferentially used. Poly(tetramethylene glycol) can also be metabolized by bacteria in an oxidation process linked to an electron transport. All three polyethers are metabolized by the same mechanism which involves the degradation of terminal units.

Biodegradation of hydrocarbons is caused by oxidation, dehydrogenation, and C-C bond breaking. UV or thermal degradation of PE prior to biodegradation rapidly increases the biodegradation rate.¹⁰ Low molecular hydrocarbons are biodegraded by various microorganisms but an increase in molecular weight inhibits this process. Linear hydrocarbons having 12 to 32 carbon atoms were digested by fungi but these containing 36 and 40 carbon atoms were not. Within the group of digestible hydrocarbons (12 to 32 carbon atoms), the rate of reaction decreased with molecular weight. Chloroparaffins having a molecular weight higher than 500 do not support fungal growth. Branched paraffins are even more stable. Branched paraffins having 15 to 30 carbon atoms did not support fungal growth. Unmodified polyethylene of high molecular weight was found not to be degraded by microorganisms. PE, partially degraded either by UV or by a thermal process, degrades when its molecular weight is reduced to about 500. In PE, branching also reduces its susceptibility to biological degradation. Polypropylene, due to its branched structure, is even more stable. The introduction of ketone groups, followed by extensive UV degradation, affected the biodegradability of polypropylene only slightly. The degradability of polyolefins can be increased by the copolymerization with monomers known to be biodegradable such as derivatives of various oils (castor, linseed, soybean, etc.). Also, copolymerization with vinyl acetate creates copolymers which support fungal growth.

Polyvinyl alcohol, PVAL, is a water soluble material which has an important influence on biodegradation. At least 55 species were found to participate in PVAL biodegradation.³ Even polymers having a molecular weight of 100,000 were completely degraded. It was found that peroxidase produces hydroxyl radicals which then participate in PVAL degradation. Poly(enol-ketone) is even more readily degraded than PVAL.⁶

Polyurethanes, PU, were biodegraded by fungi and yeast. PUs which contain polyester and caprolactone are affected by biodegradation. Polymer biodegradability was enhanced by increasing the ester chain length (soft block).⁵ Photolysis prior to biodegradation had an effect on biodegradation kinetics. If, as the result of

photodegradation, the molecular weight was decreased (chain scission) then biodegradation proceeded faster. If crosslinking occurred (the opposite of chain scission) or crystallinity was increased in the course of degradation, then the biodegradation rate was decreased. Stress cracking of polyurethanes is observed in medical applications.¹¹ This process occurs due to oxidative changes caused by reactive species present in tissue fluids which preferentially affect the soft block in the course of free radical reactions leading to chain cleavage.

Polyacrylic acid is also readily soluble in water which again causes it to be easily degraded.⁶

The biodegradation rate of low molecular weight contaminants was rapidly increased by the simultaneous effect of microorganisms and UV radiation.^{12,13} Blending polymers of a low biological resistance rapidly reduced the durability of the blend.¹⁴ This process is concentration controlled by the polymer which degrades most easily, suggesting that degradation of that component allows for better penetration of the enzyme which then rapidly increases the disintegration of the structure.

Important factors which affect durability (biodegradation rate of synthetic polymers) can be derived from the above studies, as follows:

- structural uniformity - monomeric units having different chemical structures require several enzymes to degrade them
- structural similarity - certain functional groups found in natural polymers, such as amide, ester, ether, etc., are more likely to be degraded by the existing microorganisms
- molecular weight - increasing molecular weight decreases biodegradation rate. In most cases microorganisms do not degrade synthetic polymers which have a molecular weight higher than 20,000
- crosslinking - reduces crystallinity but at the same time increases packing density which inhibits penetration of enzymes
- chain flexibility - increases probability of biodegradation by facilitating formation of complexes of enzyme-substrate which require a certain configuration
- functional groups - hydrophilic groups increase the probability of enzymatic reactions because they either increase polymer solubility or at least attract water (water is needed in most biodegradation reactions)
- crystallinity - amorphous regions are preferentially degraded, crystalline material can only be degraded on a lamellar surface. Enzymes cannot easily penetrate inside densely packed crystallites
- conditions - temperature, humidity, pH, oxygen, light. Specific conditions are preferred by various microorganisms
- structure porosity - increased surface area increases the probability of contact and concentration of enzyme-substrate complexes which are rate-controlling

- time - reaction time increases conversion, microorganism adaptation increases the probability of reaction
- contact type - the best conditions exist in solution
- concentration of substrate and product - enzymes work best in dilute solutions

The above polymers (except polyethylene) can be considered as materials which can be degraded by microorganisms to their structural component units. Other polymers typically used are considerably more durable. Biodegradation is not the major cause of failure of these more durable polymers but they are affected by biological processes since they are seldom processed in a pure form. Various additives are added during polymerization and processing which are not biologically stable. In the case of PVC, it is known that some of its plasticizers and stabilizers can be attacked by microorganisms. PVC by itself does not biodegrade due to the large concentration of chlorine which gives it protection. When low molecular additives are digested by microorganisms, the homopolymer stays intact during biological exposure but it can eventually be degraded by light and thermal energy because it was stripped of its stabilizing protection. Most plasticizers can be utilized by fungi and bacteria as a source of carbon. There are about 400 plasticizers in common use today but very few conclusive studies exist regarding their biological stability, especially because it is difficult to assess stability. Some plasticizers such as phthalates, adipates, and sebacates were found to support growth of a large number of microorganisms (30-80 different species). Epoxidized soya bean oil and aliphatic polyesters are the most prone to biodegradation. Also, tricresyl phosphate supports fungal growth. Among stabilizers, epoxidized soya bean oil (both a plasticizer and a stabilizer) and epoxidized octyl stearate are classical examples of materials with low resistance to microbiological attack. Some heavy metal stearates (zinc and calcium) and dibutyltin dilaureate were also found to be biodegradable as were various paraffin waxes used as common lubricants in extrusion processes. Multicolor stains are formed on the surface of plasticized PVC followed by loss of weight and mechanical properties.

Polystyrene, PS, and polymethylmethacrylate, PMMA, seem more resistant to microbiological growth but also in the case of these polymers, fungal growth was observed in cracks previously formed in the material. At the same time, PS having a molecular weight of 600 (only 6 monomer units) did not show fungal growth. It is anticipated that, because benzoic acid, known as food preservative is produced in biodegradation, PS becomes stabilized by its own degradation products. The photooxidation of PS reduced its useful life by making it more biodegradable. Most other plastics used in industry fall into the same category. It should be noted that even if a polymer by itself does not support the growth of microorganisms, the material always has some imperfections and/or surface degradation which can accumulate nutrients which can support biological life. For a product to perform, it is important that the material does not lose its mechanical properties but in most cases the loss of its original aesthetic value may preclude its fur-

ther use. If this is an important criterion of product performance, then most materials used today are vulnerable to biodegradation and require special protection. Further discussion of this subject requires that specialized source on microbiological corrosion be consulted. Our purpose here is to show that biological degradation is facilitated by changes in the material due to the surface degradation as well as to discuss the causes of biodegradation of organic materials. The following contains some suggestions regarding the protection of materials against biological corrosion and UV light.

19.4 BIOCIDES

Products which require biocide protection include auto landau tops, awnings, backlit signs, camouflage cloth, carpet underlay, coated fabrics, ditch liners, electrical cords, floor coverings, foam gaskets, hospital sheeting, leisure furniture, marine upholstery, paint, paper boards, refrigerator gaskets, sealants, shower curtains, swimming pool liners, tarpaulins, textiles and fibers, urethane outsoles, vinyl molding, wall covering adhesive, wall coverings, waterbed liners, weather stripping, and wood. This long list contains products which either work in high humidity environment, which are affected by condensation, or which retain moisture for a prolonged period of time.

Biocide group includes a broad number of chemicals. The main representatives are listed below:

barium metaborate monohydrate	Busan 11-M1	Buckman Labs
2-n-octyl-4-isothiazolin-3-one	Vinyzene IT	Morton
10,10'-oxybisphenoarsine	Vinyzene BP	Morton
silver-hydroxyapatite complex	Apacider	Sangi Co. Ltd.
2,3,5,6-tetrachloro-4(methyl sulphonyl) pyridine	Densil	ICI
2-(thiocyanomethylthio) benzothiazole	Busan 1030	Buckman Labs

10,10'-oxybisphenoarsine is the most popular fungicide. It is estimated to have about 75% of the market. It is produced by Akcros, a worldwide venture of AKZO and other companies. 2-octyl-4-isothiazolin-3-one offered by Ferro, is also in common use. Biocides are fairly universal in their application although they should be tailored to the specific application, since many of these chemicals are not sold in a pure form but dissolved or diluted by inert materials. Current regulations continue to restrict the use of metals in chemical compounds which also affects this group of products. It is noticeable that some compounds which were very popular in the past, such as mercury compounds and copper 8-quinolate, are no longer important. It is predicted that, in the near future, 10,10'-oxybisphenoarsine will also fall out of favor. For this reason, there are many efforts being made to substitute this material by organic compounds. These efforts are in-

hibited by the slow and expensive procedures used by safety organizations to approve new materials.

Biocides for outdoor applications are typically screened for the application based on their overall efficiency as biocides. This is followed by outdoor and/or accelerated testing. Data are available which show that some of these products offer lower protection after exposure to UV radiation. Barium metaborate monohydrate is an example of a durable biocide. It is considered a multifunctional product which also offers anticorrosive and UV stabilizing effects (its one deficiency is that it has to be used in high concentrations). Its exposure to 2000 h in Weather-O-Meter did not change its protective activity. Under similar conditions of exposure, 10,10'-oxybisphenoarsine lost about 40% of its protective activity.

Polymer-bound biocides were synthesized. Binding of biocide to the polymer reduces losses associated with volatilization, photodissociation, dissolution, and transport.¹⁶ These fungicides are applicable in various areas, such as fiber, paper, latex, rubber, machine oil, wood, leather, plastics, coatings, communication and electronic instruments, and packaging materials.

19.5 METHODS OF TESTING

Several methods of testing are used to determine biodegradation of materials. Fungal and bacterial growth is determined by placing samples of materials in a carbon-deficient agar medium containing all other necessary nutrients. The sample is inoculated with fungi or bacteria and incubated for 21 days. The samples are then graded according to a scale (0 - no visible growth, 1 - less than 10% covered, 2 - 10-30% surface covered, 3 - 30-60% percent covered, and 4 - 60-100% covered). Pure polymers generally get 0 or 1 rating. Those known to degrade, such as PVC containing epoxidized soya bean oil, get 3 and polyester polyurethanes generally receive 4. In the so-called "clear zone" method a sample of polymer is suspended in nutrient agar and, after an inoculation and incubation period, the clear zone is formed and recorded. The clear zone appears due to the digestion of polymer by microorganisms.

Frequently, materials are subjected to soil burial tests either outdoors or in a laboratory environment. In this method, the microbiological population cannot be controlled and tests lack repeatability but at the same time microorganisms have a better chance of adaptation and results are often more realistic. ¹⁴C radiotracer studies produced valuable results. Labelled carbon is introduced to the monomer and polymerized. During the biodegradation process the fate of this carbon is followed. It can be detected in the microorganisms or in gaseous products if these are produced. It also helps to identify gaseous products. Oxygen uptake measurements are also popular. Warburg respirometers are typically used in this method.¹⁷ The biodegradation process is followed by determining the change in pressure in a sealed bottle as biodegradation occurs.

Several standard methods are used in biodegradation studies. The following ones are the most common:¹⁸

ISO 846	Determination of behavior under the action of fungi and bacteria
ASTM G21	Determining resistance of synthetic polymeric materials to fungi
ASTM G22	Determining the resistance of plastics to bacteria
DIN 53739	Testing of plastics, influence of fungi and bacteria
BS 1982	Methods of test for fungal resistance of manufactured building materials

REFERENCES

1. A. L. Andrady, *J. Macromol. Sci., Rev. Macromol. Chem. Phys.*, C34(1994)25.
2. B. Zyska, *Mikrobiologiczna Korozja Materialow*, WNT, Warsaw, 1977.
3. R. W. Lenz, *Adv. Polym. Sci.*, 107(1993)1.
4. J. Augusta, R. -J. Müller, H. Widdecke, *Appl. Microbiol. Biotechnol.*, 39(1993)673.
5. S. J. Huang, M. S. Roby, C. A. Macri, and J. A. Cameron, *Biodegradable Polymers and Plastics*, Eds. M. Vert, J. Feijen, A. Albertsson, G. Scott, E. Chiellini, *Royal Soc. Chem.*, Cambridge, 1992.
6. P. J. Hocking, *J. Macromol. Sci., Rev. Macromol. Chem. Phys.*, C32(1992)53.
7. M. Edge, M. Hayes, M. Mohammadian, N. S. Allen, T. S. Jewitt, K. Brems, and K. Jones, *Polym. Deg. Stab.*, 32(1991)131.
8. C. G. Pitt, *Biodegradable Polymers and Plastics*, Eds. M. Vert, J. Feijen, A. Albertsson, G. Scott, E. Chiellini, *Royal Soc. Chem.*, Cambridge, 1992.
9. F. Kawai, *Biodegradable Polymers and Plastics*, Eds. M. Vert, J. Feijen, A. Albertsson, G. Scott, E. Chiellini, *Royal Soc. Chem.*, Cambridge, 1992.
10. C. David, C. De Kesel, F. Lefebvre, and M. Weiland, *Angew. Macromol. Chem.*, 216(1994)21.
11. A. Brandwood, K. R. Noble, K. Schindhelm, G. F. Meijs, P. A. Gunatillake, R. C. Chatelier, S. J. McCarthy, and E. Rizzardo, *Biomater.-Tissue Interfaces, Adv. in Biomater.*, 10(1992)413.
12. A. Katayama and F. Matsumura, *Environ. Sci. Technol.*, 25(1991)1329.
13. N. Getoff, *Radiat. Phys. Chem.*, 37(1991)673.
14. P. Dave, R. A. Gross, C. Brucato, S. Wong, and S. P. McCarthy, *Polym. Mater. Sci. Eng.*, 62(1990)231.
15. R. P. Brown, *Polym. Test.*, 19(1991)3.
16. S. T. Oh, B. K. Min, C. S. Ha, and W. J. Cho, *J. Appl. Polym. Sci.*, 52(1994)583.
17. J. Seppala, Y. -Y. Linko, and T. Su, *Acta Polytech. Scand., Chem. Technol. Ser.*, 198, 1991.
18. R. P. Brown, *Polym. Testing*, 10(1991)3.

International Abbreviations for Polymers

aPP	Amorphous polypropylene
AAS	Copolymer of acrylonitrile, acrylate (ester) and styrene
ABA	Acrylonitrile-butadiene-acrylate copolymer
ABR	Elastomeric copolymer from an acrylate (ester) and butadiene; a rubber
ABS	Thermoplastic terpolymer, an acrylonitrile-butadiene-styrene copolymer
ABM	Copolymer of acrylonitrile-butadiene-methyl acrylate
ABMA	Copolymer of acrylonitrile-butadiene-methacrylic acid
ABSM	Graft copolymer of acrylonitrile-butadiene-styrene-methylmethacrylate
ABVC	Thermoplastic terpolymer, an acrylonitrile-butadiene-vinylchloride copolymer
ACM	Alkyl acrylate-2-chloroethyl vinyl ether copolymer, a thermoplastic elastomer
ACPES	Acrylonitrile-chlorinated polyethylene-styrene copolymer
ACRYL	Poly- or copoly- methylmethacrylate (Acrylic)
ACS	Thermoplastic blend of acrylonitrile-styrene- chlorinated PE terpolymer
AEPDM	Acrylonitrile/ethylene-propylene-diene/styrene copolymer
AES	Thermoplastic copolymer from acrylonitrile, ethylene-propylene, and styrene
AK	Alkyd resin
AMAB	Copolymer from acrylonitrile, methyl acrylate, and butadiene rubber
AMMA	Thermoplastic copolymer from acrylonitrile and methyl methacrylate
AN	Acrylonitrile
ANM	Acrylonitrile-alkyl acrylate copolymer, a thermoplastic elastomer
AP, APR	Elastomeric ethylene, propylene, unsaturated monomer copolymer; now EPDM
APP	Atactic PP
AR	Elastomeric copolymer from acrylates and olefins.
ARP	Thermoplastic polyester; polyarylterephthalate liquid crystal copolymers, also PAR,
PAT	
AS	Acrylonitrile-styrene copolymer
ASA	Thermoplastic copolymer from acrylonitrile, styrene, and acrylates
ASR	Alkylene sulfide rubber
AU	Elastomeric polyester or polyurethane with polyester segments
BAAN	Butyl acrylate-acrylonitrile copolymer
BAMM	Butyl acrylate-methylmethacrylate copolymer
BFE	Bromotrifluoroethylene polymers
BIIR	Brominated elastomer from isobutene and isoprene; bromobutyl rubber
BMMM	Butyl methacrylate-methyl methacrylate copolymer
BOPP	Biaxially oriented polypropylene film
BP or BR	Polybutadiene or an isobutene/isoprene copolymer; butyl or butadiene rubber
CA	Cellulose acetate
CAB	Cellulose acetate-butyrate
CAP	Cellulose acetate-propionate
CBR	Chlorinated butadiene rubber
CDB	Conjugated diene butyl elastomer
CE	Cellulose plastics in general
CEM	Polychlorotrifluoroethylene; see also CFM, CTFEP, PCTFE
CF	Cresol-formaldehyde resins
CFM	Polychlorotrifluoroethylene; see also CEM, CTFEP, PCTFE
CHR	Elastomeric copolymer from epichlorohydrin and ethylene oxide
CIIR	Post chlorinated elastomeric copolymer from isobutene and isoprene

CM	Chloro-polyethylene (also: Compression molding)
CMC	Carboxy methyl cellulose, (or critical micelle concentration)
CMHEC	Carboxy methyl hydroxy ethyl cellulose
CN	Cellulose nitrate
CNR	Elastomeric terpolymer from tetrafluoroethylene, tri-fluoro nitroso methane, and a small amount of an unsaturated monomer, e.g., nitroso perfluoro-butrylic acid; nitroso or carboxy nitroso rubber
CO	Polychloromethyl oxirane elastomer
CO-PAI	Copolyamideimide
CO-PI	Copolyimide
COPO	Poly(carbon monoxide-co-polyolefin)
COX	Carboxylic rubber
CP	Cellulose propionate
CP2	Alternating copolymer from vinyl ether and maleic acid
CP4	Copolymer from acrylic acid and maleic acid
CPE	Chlorinated polyethylene
CPET	Crystallizable polyethylene terephthalate
CPI	cis-Polyisoprene; also IR
CPVC	Chlorinated polyvinylchloride
CR	Chloroprene rubber
CRM	Chlorosulfonated polyethylene
CRP	Carbon fiber reinforced plastics
CS	Casein
CSM	Chlorosulfonated polyethylene (or CSR)
CSR	Chlorosulfonated polyethylene (or CSM)
CT, CTA	Cellulose triacetate
CTBN	Carboxy-terminated nitrile rubber
CTFE	Polychlorotrifluoroethylene
CTFEP	Polychlorotrifluoroethylene; see also CFM, CEM, PCTFE
CV	Viscose; see also VI
EVM	Ethylene-vinyl acetate copolymer, a thermoplastic elastomer
DAC	Diallylchloroendate
DAF	Diallylfumarate
DAIP	Diallylisophthalate
DAP	Diallylphthalate
DMC	Dough molding compound
E-PVC	Emulsion polyvinyl chloride; PVC polymerized in emulsion
E-SBR	Polymerized in emulsion styrene/butadiene copolymer
E/B	Copolymers of ethylene and 1-butene
E/P	Copolymers of ethylene and propylene
EA, EAA	Ethylene acrylic acid
EAM	Elastomeric copolymer of ethylene and vinyl acetate
EBA	Ethylene butylacrylate
EC	Ethyl cellulose
ECA	Ethylene-carbonate copolymer
ECO	Elastomeric copolymer from ethylene oxide and epichlorohydrin
ECTF, ECTFE	Poly(ethylene-co-chloro tri-fluoro ethylene)
EEA	Elastomeric copolymer from ethylene and ethyl acrylate
EEAGMA	Ethylene-ethyl acrylate-glycidyl methacrylate copolymer
EGMA	Ethylene-glycidyl methacrylate copolymer

EHEC	Hydroxy ethyl cellulose
ELAST	Elastomer
EMA	Copolymer from ethylene and maleic anhydride
EMAc	Copolymer from ethylene and methacrylic acid
EMAC	Ethylene methacrylate copolymer
EMM	Copolymer from ethylene and methylmethacrylate
EMP	Ethylene-propylene copolymers (ethylene modified polypropylene)
EP	Epoxy resins
E/P	Ethylene-propylene copolymer
EPD	Ethylene-propylene-diene copolymer
EPD, EPDM	Elastomeric terpolymer from ethylene, propylene, and a non-conjugated diene
EPE	Ester of an epoxy resin
EPM	Ethylene-propylene copolymer
EPR, EPM	Elastomeric copolymer of ethylene and propylene
EPS	Polystyrene foam; expanded PS
EPT, EPTR	Ethylene, propylene, and a non-conjugated diene terpolymer (also EPDM)
ETFE	Copolymer ethylene and tetrafluoroethylene
EVA	Ethylene-vinyl acetal copolymer
EVAc	Copolymer from ethylene and vinyl acetate
EVAc-AAc	Ethylene-vinyl acetate-acrylic acid graft copolymer
EVAc-CO	Ethylene-vinyl acetate-carbon monoxide copolymer
EVAc-MA	Copolymer from ethylene, vinyl acetate, and methacrylic acid
EVA-GMA	Ethylene-vinyl acetate-glycidyl methacrylate copolymer
EVAL, EVAL	Copolymer of ethylene and vinyl alcohol
EVAVC	Ethylene-vinyl acetate-vinyl chloride copolymer
EVC	Copolymer from ethylene and vinylene carbonate
EVOH	Ethylene vinyl alcohol copolymer
EVP	Ethylene vinyl pyrrolidinone copolymer
FE	Fluorine containing elastomer
FEP	Fluorinated EPR; tetrafluoroethylene/hexa-fluoro propylene rubber
FF	Resin from furan and formaldehyde
FK, FRP, GRP	Fiber reinforced plastic
FKM	Hexa-fluoro propylene-vinylidene fluoride copolymer
FMQ	Methyl fluoro silicone rubber
FPM	Vinylidene fluoride/hexa-fluoro propylene elastomer; rubbers with fluoro and fluoroalkyl or fluoroalkoxy groups
FPVC	Flexible PVC film
FQ	Elastomeric silicone with fluorine containing substituents
FRE	Fiber reinforced epoxy
FRP, GRP, FK	Glass fiber reinforced polyester
FVMQ	Silicone rubber with fluorine, vinyl, and methyl substituents
GEP	Glass fiber reinforced epoxy resin
GF	Glass fiber, or glass fiber reinforced plastic
GF-PF	Glass fiber reinforced phenolic resin
GF-UP	Glass fiber reinforced unsaturated polyester resin
GMA	Glycidyl methacrylate
GPO	Elastomeric copolymer from propylene oxide and allyl glycidyl ether
GPPS	General purpose polystyrene (also PS)
GPSMA	General purpose styrene-maleic anhydride copolymer (also SMA)
GR-A, GR-N	Nitrile rubber; now NBR

GR-S	Styrene/butadiene rubber
GUR	Ultra-high molecular weight polyethylene (UHMWPE)
HDPE	High density polyethylene (ca. 960 kg/m ³)
HEC	Hydroxy ethyl cellulose
HIPS	High impact polystyrene
HISMA	High impact styrene-maleic anhydride copolymer
HMWPE	Polyethylene with high molecular weight
HPC	Hydroxy propyl cellulose
HPMC	Hydroxy propyl-methyl cellulose
HTE	Hydroxyl terminated polyether
IEN	Interpenetrating elastomeric network
IHPN	Interpenetrating homopolymer network
IIR	Isobutene-isoprene rubber (butyl rubber)
IM	Polyisobutene; also PIB
IPN	Interpenetrating polymer network
IPS	Impact resistant polystyrene
IR	Synthetic cis-1,4-polyisoprene
L-SBR	Solution polymerized SBR
LCP	Liquid crystal polymer
LDPE	Low density polyethylene (ca. 918 kg/m ³)
LIPN	Latex interpenetrating polymer network
LLDPE	Linear low density polyethylene
LMDPE	Linear medium density polyethylene
LPE	Linear polyethylene
m-EPDM	Maleic anhydride-modified ethylene-propylene-diene terpolymer
M-PVC	Polymerized in bulk polyvinylchloride
MA	Maleic anhydride
MAS	Copolymer from methyl methacrylate, acrylonitrile, and styrene
MABS	Copolymer from methyl methacrylate, acrylonitrile, butadiene, and styrene
MBS	Copolymer from methylmethacrylate, butadiene, and styrene
MC	Methyl cellulose
MDPE	Medium density polyethylene (ca. 930 to 940 kg/m ³)
MF	Melamine-formaldehyde resin
MFK	Metal fiber reinforced plastic
MFQ	Silicone rubbers having both methyl and fluorine substituent groups ; also FMQ
MMA	Methylmethacrylate
MMBA	Copolymer from methyl methacrylate-butyl acrylate
MMEA	Methyl methacrylate-ethyl acrylate copolymer
MMPMI	Methylmethacrylate-co-N-phenylmaleimide copolymer
MMS	Copolymer from methyl methacrylate, and <i>a</i> -methylstyrene
MMVAc	Methyl methacrylate-vinyl acetate copolymer
MPF	Melamine/phenol-formaldehyde resin
mPP	Maleic anhydride-modified polypropylene
MPQ	Silicone rubbers having both methyl and phenyl substituent groups; also PMQ
MPS	Poly(<i>a</i> -methyl styrene)
MPVQ	Silicone rubbers with methyl, phenyl, and vinyl groups; also PVMQ
MQ	Elastomeric silicones with methyl substituents
MSABS	Methylstyrene-styrene-acrylonitrile-grafted polybutadiene
MSAN	Thermoplastic copolymer from <i>a</i> -methylstyrene and acrylonitrile
MVQ	Silicone rubbers having both methyl and vinyl substituent groups; also VMQ

NBR	Elastomeric copolymer from butadiene and acrylonitrile; nitrile rubber
NC	Cellulose nitrate; see also CN
NCR	Elastomeric copolymer from acrylonitrile and chloroprene
NDPE	Low density polyethylene; see also LDPE
NIR	Elastomeric copolymer from acrylonitrile and isoprene
NK	Natural rubber; also NR
NP	Network polymer
NR	Natural rubber; also NK
OPET	Oriented polyethyleneterephthalate
OPP	Oriented polypropylene, film or bottles; also PP
OPR	Elastomeric polymer from propylene oxide
OPS	Oriented polystyrene films
OPVC	Oriented polyvinylchloride
OSA	Olefin-modified styreneacrylonitrile
P3FE	Poly(tri-fluoro ethylene)
PA	Polyamide, the abbreviation PA is normally followed by a number
PAA	Polyacrylic acid
PAAE	Polyarylamide-polyether
PABM	Polyaminobismaleimide
PAC	Polyacrylonitrile fiber (also PAN); polyacrylate
PADC	Poly(allyl diglycol carbonate)
PAE	Polyarylether
PAEK	Polyaryletherketone
PAES	Polyarylethersulfone
PAI	Polyamide-imide
PAK	Polyester alkyd
PALL	Polyallomer, a block copolymer of propylene, ethylene (1.5-3%), butene (8%) and hexene (5%)
PAMS	Poly-a-methylstyrene
PAN	Polyacrylonitrile
PANI	Polyaniline
PAPA	Polyazelaic polyanhydride
PAPI	Polymethylenepolyphenylene isocyanate; also PMPPI
PAr	Polyarylate
PARA	Polyaryl amide (aromatic, usually amorphous polyamide)
PAS	Polyarylsulfide copolymers (esp. in German and Japanese literature)
PAS, PASU	Polyarylsulfone [-f-SO ₂ -f-O-]0.875[-f-O-]0.125
PAT	Polyaminotriazole; also polyarylterephthalate, an aromatic LCP polyester
PAUR	Polyester urethane
PB	Poly-1-butene; elastic polydiene fiber
PBA	Polybutylacrylate
PBAN	Poly(butadiene-co-acrylonitrile)
PBI	Polybenzimidazoles
PBMA	Poly-n-butyl methacrylate
PBNC	Poly(butylene-2,5-naphthalene-dicarboxylate)
PBO	Polybutyleneoxide
PBR	Copolymer from butadiene and vinyl pyridine
PBS	Copolymer from butadiene and styrene; see also GR-S, SBR
PB-SMA	Styrene-maleic anhydride-grafted polybutadiene
PBT, PBTP	Polybutyleneterephthalate

PBT-PBO	Copolymer of 1,4-butanediol-polybutylene glycol-terephthalic acid
PC	Bisphenol-A polycarbonate
PCD	Polycarbonodiimide
PCDT	Poly(1,4-cyclohexylene di-methylene terephthalate)
PCF	Polychlorotrifluoroethylene fiber
PCN	Poly(2-cyano-5-norbornene)
PC-Ph	Co-polycarbonate from phosgene with bisphenol-A and phenolphthalein
PCT	Polycyclohexyleneterephthalate, cyclohexanedimethanol-ethylene glycol terephthalic acid copolymer
PCTFE	Polychlorotrifluoroethylene; see also CEM, CFM, CTFE
PCTG	Poly(cyclohexaneterephthalate-glycol)
PCU	Polyvinyl chloride (old German literature)
PDAP	Polydiallylphthalate; also DAP, FDAP
PDCT	Poly(dicyclopentadiene)
PDMS	Polydimethylsiloxane
PE	Polyethylene
PEA	Polyethylacrylate
PEBA	Thermoplastic elastomer, polyether-block-amide
PEC	Polyestercarbonate or chlorinated polyethylene; also CPE
PeCe	Chlorinated PVC; also CPVC, PC, PVCC
PECO	Polyethylene carbonate,
PEE	Polyester ether fibers (containing diol and p-hydroxy benzoate units)
PEEK	Polyetheretherketone
PEG	Polyethyleneglycol
PEH	High density polyethylene; also HDPE
PEI	Polyetherimide
PEIm	Polyetherimine
PEK	Polyetherketone
PEL	Low density polyethylene; also LDPE
PEM	Medium density polyethylene; also MDPE
PEN	Polyethylenenaphthalate
PENDC	Poly(ethylene 2,6-naphthalenedicarboxylate)
PEP	Thermoplastic copolymer from ethylene and propylene
PEOX	Poly(2-ethyl-2-oxazoline)
PES	Polyethersulfone [-f-SO ₂ -f-O-] _n
PEST	Thermoplastic polyesters, e.g. PBT, PET, see also TPES
PET, PETP	Polyethyleneterephthalate
PETG	Polyethyleneterephthalate glycol
PEUR	Polyetherurethane
PF	Phenol-formaldehyde resin
PFA	Polyfluoroalkoxyalkane; copolymer of tetrafluoroethylene and perfluorinated alkyl vinyl ethers
PFEP	Copolymer from tetrafluoroethylene and hexa-fluoro propylene; also FEP
PFF	Phenol-furfural resin
PG	Poly-a-hydroxy acrylic acid
PGI	Polyglutarimides
PH	Phenolics
PHBA	Poly(b-hydroxybutyric acid)
PHEMA	Poly-2-hydroxyethyl methacrylate
PHIT	Poly(hexylene-isophthalate-terephthalate)

PHP	Physiological hydrophilic polymers
PHT	Polyhexamethyleneterephthalate
PI	Polyimide, but also trans-1,4-polyisoprene, gutta-percha (UK)
PIAN	Isoprene - acrylonitrile oil resistant elastomer
PIB	Polyisobutene
PIBI	Copolymer from isobutene and isoprene, butyl rubber; also Butyl, GR-I, IIR
PIBO	Polyisobuteneoxide
PIP	Synthetic cis-1,4-polyisoprene; also CPI, IR
PIR	Polyisocyanurate (foam)
PIS	Polyisobutylene
PISU	Polyimidesulfone
PKS	Polyketonesulfone [-f-SO ₂ -f-CO-] _n
PL	Polyethylene (EWG); also PE
PLA	Polylactic acid
PMA	Polymethylacrylate
PMAC	Polymethoxy acetal
PMAN	Polymethyl acrylonitrile
PMB	Polymethylenebenzoate
PMCA	Polymethyl-a-chloro acrylate
PMI	Polymethacrylimide
PMMA	Polymethylmethacrylate
PMMA-MA	Poly(methylmethacrylate-co-acrylic acid)
PMMI	Polypyromellitimide
PMP	Poly-4-methyl-1-pentene; see also TPX
PMPPI	Polymethylenepolyphenylene isocyanate; also PAPI
PMQ	Silicone rubbers with methyl and phenyl substituents
PMS	Poly-a-methylstyrene
PpMS	Poly-p-methylstyrene
PNA	Polynuclear aromatics
PNR	Polynorbornene rubber
PO	Polyolefin, but also: Elastomeric polypropylene oxide, and Phenoxy resin
POB	Poly-p-hydroxy benzoate
POCA	Poly(oxy(cyanoarylene)), or polyphthalamide
POM	Polyoxymethylene, polyformaldehyde, polyacetal or "acetal resin"
POP	Polyphenylene oxide; also PPE
POR	Elastomeric copolymer from propylene oxide and allyl glycidyl ether
PP	Polypropylene, or oriented polypropylene; see also OPP
PPA	Polyphthalamide, or Polypropyleneadipate
PPBA	Polyparabanic acid
PPC	Chlorinated PP
PPCA	Poly(polycyclic (meth)acrylate)
PPE	Poly(2,6-dimethyl 1,4-phenylene ether); see also PPO
PPG	Polypropylene glycol
PPI	Polymeric polyisocyanate
PPO	GE Co. trade name for poly(2,6-dimethyl 1,4-phenylene ether); see also PPE
PPOX	Polypropylene oxide
PPP	Poly-p-phenylene
PPS	Polyphenylsulfide
PPSS, PPS-S	Polyphenylenesulfidesulfone
PPSU	Polyphenylene sulfone; [-f-SO ₂ -f-O-f-f-O-] _n

PPT, PPTP	Polypropyleneterephthalate
PQ	Elastomeric silicone with phenyl substituents
PS	Polystyrene
PSB	Styrene-butadiene rubber
PSGMA	Styrene-glycidyl methacrylate copolymer
PS-TSG	Polystyrene foam, processed by injection (German literature)
PSAB	Copolymer from styrene and butadiene; also SB, S/B
PSAN	Thermoplastic copolymer from styrene and acrylonitrile; also SAN
PSBR	Elastomeric terpolymer from vinyl pyridine, styrene, and butadiene
PSF	Polysulfone, also PSUL, PSU, PSO
PSI	Polymethyl phenyl siloxane
PSO, PSF	Polysulfone, also PSUL, PSU, PSF
PST	Polystyrene fiber with at least 85% styrene units
PSU	Polysulfone [-f-SO ₂ -f-O-BPA-O-] _n
PSUL	Polysulfone, also PSF, PSU, PSO
PTF	Polytetrafluoroethylene fiber
PTFE	Polytetrafluoroethylene (also TFE)
PTHF	Polytetrahydrofuran
PTMA	Polytetramethyleneadipate
PTMEG	Poly(tetramethylene ether glycol)
PTMG	Polyoxytetramethylene glycol
PTMT	Poly(tetramethylene terephthalate) = polybutyleneterephthalate; also PBT
PTR	Polysulfide rubber
PU, PUR	Polyurethane elastomer
PVA	Polyvinyl acetal
PVAc, PVAC	Polyvinyl acetate
PVAl, PVAL	Polyvinyl alcohol
PVB	Polyvinyl bytyral
PVC	Polyvinyl chloride
PVCA, PVCAc	Copolymer from vinyl chloride and vinyl acetate
PVCC	Chlorinated PVC; also CPVC, PeCe
PVD	Polyvinylidene chloride fiber with 50 wt% vinylidene chloride
PVDC	Polyvinylidene chloride; also PVC2
PVDF	Polyvinylidene fluoride; also PVF2
PVF	Polyvinyl fluoride
PVFM, PVFO	Polyvinyl formal
PVI	Poly(vinyl isobutyl ether)
PVID	Polyvinylidenecyanide
PVK	Poly-N-vinylcarbazole
PVM	Copolymer from vinyl chloride and vinyl methyl ether
PVME	Polyvinylmethylether
PVMQ	Silicone rubber with methyl, phenyl, and vinyl substituents
PVOH	Polyvinyl alcohol; also PVA, PVAL
PVP	Poly-N-vinylpyrrolidone
PVSI	Polydimethyl siloxane with phenyl and vinyl substituents
PY	Unsaturated polyester resins; also UP
RF	Resorcinol/formaldehyde resin
RP, RTP	Reinforced plastics, Reinforced thermoplastic, also RP/C
RPBT	Reinforced polybutyleneterephthalate
RPET	Reinforced polyethyleneterephthalate

RPVC	Rigid PVC film
RTPO	Reactor-blended thermoplastic olefinic elastomer
RTV	Room temperature vulcanization (of silicone rubber)
RUC	Chlorinated rubber
sPP	Syndiotactic polypropylene
SAA	Styrene-acrylic acid copolymer
SAMA	Styrene-acrylonitrile-methacrylic acid copolymer
S-EPDM	Sulfonated ethylene-propylene-diene terpolymer
S-PVC	Suspension PVC
SAN	Thermoplastic copolymer from styrene and acrylonitrile; also PSAN
SANGMA	Styrene-acrylonitrile-glycidyl methacrylate copolymer
SANMA	Styrene-acrylonitrile-maleic anhydride copolymer
SB, SBR	Thermoplastic copolymer from styrene and butadiene; also PASB, S/B
SBCL	Styrene-butadiene-caprolactone copolymer
SBMA	Styrene-butadiene-maleic anhydride copolymer
SBMI	Styrene-butadiene-maleimide
SBP	Styrene-butadiene polymer
SB/BA	Styrene-butadiene-butyl acrylate copolymer
SBS	Styrene-butadiene-styrene triblock polymer
SCR	Elastomeric copolymer from styrene and chloroprene
SEBS	Styrene-ethylene/butylene-styrene triblock polymer
SEP	Styrene-ethylene-propylene block copolymer
SF	Structural foam
SHIPS	Super-high impact polystyrene
SI	Thermoplastic silicone
SIN	Simultaneous interpenetrating network or semi-interpenetrating network
SIPN	Sequential interpenetrating polymer network
SIR	Elastomeric copolymer from styrene and isoprene
SIS	Styrene-isoprene-styrene triblock polymer
SMA	Copolymer from styrene and maleic anhydride
SMA-AA	Styrene-maleic anhydride-acrylic acid copolymer
SMI	Copolymer from styrene and maleimide
SMM	Styrene-methyl methacrylate copolymer
SMM-GM	Styrene-methyl methacrylate-glycidyl methacrylate copolymer
SMM-MA	Styrene-methyl methacrylate-maleic anhydride copolymer
SMS	Copolymer from styrene and <i>a</i> -methylstyrene
SP	Saturated polyester plastics
SPPF	Solid-phase pressure forming
SPSF	Solid-phase stretch forming
SR	Synthetic rubber
SRP	Styrene-rubber plastics
SVA	Styrene-vinyl-acrylonitrile copolymer
TA	Cellulose triacetate; also CT, CTA
TC	Technically classified natural rubber
TE	Thermoplastic elastomer of any type
TEEE	Thermoplastic elastomer, ether-ester
TEO	Thermoplastic elastomer, olefinic
TES	Thermoplastic elastomer, styrenic
TFE	Polytetrafluoroethylene (also PTFE)
TGIC	Tricycidyl isocyanurate

TM	Thioplasts
TOR	trans-polyoctenamer rubber
TP	Thermoplastic
TPA, TPR	1,5-trans-poly-pentenamer
TPEL	Thermoplastic elastomer
TPES	Thermoplastic polyesters, e.g. PBT, PET, see also PEST
TPO	Thermoplastic olefinic elastomer
TPS	Toughened PS (in the UK for HIPS)
TPU, TPUR	Thermoplastic urethanes
TPX	Poly(4-methyl-1-pentene); see also PMP
TR	Thermoplastic elastomer or Thio Rubber (UK)
TS	Thermoset
TSUR	Thermoset polyurethane
UE	Polyurethane elastomer
UF	Urea-formaldehyde resin
UFS	Urea-formaldehyde foam
UHMWPE	Ultrahigh molecular weight polyethylene (over 3 Mg/mol)
ULDPE	Ultra low density polyethylene (ca. 900 to 915 kg/m ³)
UP	Unsaturated polyester
UPVC	Unplasticized PVC
UR	Polyurethane elastomers; also UP
VA	Vinylacetate
VAE	Vinylacetate-ethylene (copolymer)
VCEMA	Copolymer from vinyl chloride, ethylene, and methyl acrylate (or maleic anhydride)
VCE	Copolymer from vinyl chloride, and ethylene
VCEV	Copolymer from vinyl chloride, ethylene, and vinylacetate
VCMA	Copolymer from vinyl chloride and methyl acrylate
VCMMA	Copolymer from vinyl chloride and methylmethacrylate
VCOA	Copolymer from vinyl chloride and octyl acrylate
VCVAc	Copolymer from vinyl chloride and vinyl acetate
VCVDC	Copolymer from vinyl chloride and vinylidene chloride
VCE	Copolymer from ethylene and vinyl chloride
VCM	Vinyl chloride (monomer); also VC
VDC	Vinylidene chloride
VDC/AN	Copolymer from vinylidene chloride and acrylonitrile
VF/HFP	Copolymer from vinylidene fluoride and hexa-fluoro propylene
VLDPE	Very low density polyethylene (ca. 885 kg/m ³)
VMQ	Silicone rubber with methyl and vinyl substituents
VPE	Cross-linked polyethylene; also XLPE
VQ	Elastomeric silicone with vinyl substituents
VSI	Polydimethylsiloxane with vinyl groups
XABS	Acrylonitrile/butadiene/styrene/acidic monomer; an elastomeric copolymer
XLPE	Cross-linked polyethylene
XNBR	Acrylonitrile/butadiene/acidic monomer; an elastomeric copolymer
XSBR	Butadiene/styrene/acidic monomer; an elastomeric copolymer
YSBR	Thermoplastic block copolymer from styrene and butadiene
YXSBR	Block copolymer from styrene and butadiene containing carboxylic groups

Index

A

- AAS 242, 443
- ablation threshold 241
- abrasion 212, 257
 - resistance 212, 309, 452
- ABS 141, 220, 221, 256, 257, 378, 380, 477, 490, 512
 - absorption 380
 - carbonyl formation 380
 - color difference 172
 - degradation depth 168
 - double bonds 381
 - elongation 174
 - IR 378
 - yellowing 378
- absolute viscosity detector 258
- absorbing species 239
- absorption
 - altitude 43
 - coefficient 499
 - maxima 234
 - spectra 227
- acceleration 165
- acid rain 57, 218, 222, 242, 247
- acrylics 221, 228, 236, 300
 - chain scission 300
 - changes and properties 303
 - data 304
 - depolymerization 303
 - effect of temperature 303
 - effect of thermal history 303
 - elongation 304
 - mechanism of degradation 300
 - monomer concentration 304, 305
 - residual monomer 302
 - side groups 301
 - volatiles 302, 303
- actinomyces 523
- activation spectrum 98, 239
- additives 425
 - biodegradation 530
- adhesion 470, 482
- adhesive joints 258
- adhesives 256, 469
- adiabatic transformation 30
- afterglow 17
- agar medium 532
- aging index 474
- albedo
 - planetary and surface 45
 - seasonal variations 46
- aluminum
 - oxidation 221
- amide 228
- amide IV 440
- amorphous
 - phase 191, 243, 254
 - region 222, 242, 412
- angle of incidence 143
- anthracene 241
- anthraquinone 240, 262
- antioxidants 225, 256, 507, 512
- aphelion 41
- application standards 157
- applications
 - fusion reactors 374
 - in space 374
- aquatic environment 523
- Arizona 65
- Arrhenius plot 190
- artificial weathering 165
 - equipment 95, 105
- asphalt 472, 474
- asphaltenes 473
- asphaltic materials 238
- ASTM standards 155
- atmosphere
 - composition 47
 - density 47
 - mass 47
 - ozone 47
- atomic oxygen
 - concentration in space 462

fluence 459
ATR 228
automotive applications
 coatings 443
 dashboard 159
 engineering polymers 477
 helmets 477
 materials 477
 paints 477
 upholstery fabrics 450
 window encapsulation 256
auxochromic group 207
azo linkage 204
azo compounds 27, 31

B

backing material 182
bacteria 523
 aerobic 526
 anaerobic 526
bathochromic shift 15
beech wood 483
Beer-Lambert Law 6, 18, 25, 143, 498
benzophenone 29, 34, 212, 235, 238, 449, 452
benzotriazole 442
bimolecular reactions 525
binder
 degradation 427
 durability 219
binding energy 245
biocides 531
biocompatibility 488
biodegradation 250, 260, 523
 blends 529
 chloroparaffins 528
 crystallinity 527
 effect of branching 528
 environment 523
 hydrocarbons 528
 important factors 529
 materials 526
 methods of testing 532
 molecular weight effect 528

PE 528
polyacrylic acid 529
polyesters 527
PU 528
PVAI 528
biological studies 178
biomass burning 51
birefringence 207
bitumens 251
bituminous products 472
black-panel temperature 157
blends 97, 222, 240, 257, 385
 changes 385
 commercial 388
 photofunctionalization 385
Bohr's Formula 7
bond
 cleavage 27
 compressed 26
 dissociation 191
 double 32
 extended 26
 interaction 14
 scission 206
Born-Oppenheimer Approximation 8, 9, 10, 22
bottles 200, 480
 crates 488
 cups 479
Box-Jenkins Analysis 219
British Standards 159, 162
building materials 221, 223, 463
 life expectancy 465
 major problems 463
 methods 464
burner 101
butyl lining 456

C

cables 199, 222, 239, 249, 479
cage escape efficiency 427
calcium carbonate 250, 485, 520
calibration curve 258
capacitors 249

- car upholstery 257
- carbon arc 100, 219
- carbon black 220, 505
- carbon dioxide 48
- carbon monoxide 55, 460
- carbonyl
 - absorption 228, 233, 254, 255
 - formation 228, 240, 250
 - rate 132
 - group 440, 472, 485
 - index 257
- carpets 490
- catalysts 228
- cavities 207
- cellulose 208, 244, 447, 526
 - diacetate 208
 - fibers 243
 - regenerated 243, 420
- chain
 - diffusion 220
 - flexibility 14
 - folds 412
 - mobility 182, 214, 242, 243
 - scission 96, 191, 227, 228, 250, 252, 258, 259, 260
- chalk value 218, 246
- chalking 447
- charcoal filters 490
- chelates 507
- chemical
 - conversion 26
 - reactivity 181, 187, 194
 - shift 209
- chemiluminescence 239
- chlorinated rubber 244
- chromatography, thin-layer 208
- chromophores 8, 15, 17, 432
- chromosphere 41
- chymotrypsin 526
- CIE
 - scale 224
 - standard radiation 62
- clearcoats 246
- cleavage
 - heterocyclic 28
 - photoreductive 204
- climatic conditions 61
 - in Australia 91
 - in Austria 91
 - in Canada 67
 - in Great Britain 90
 - in Greece 83
 - in Hong Kong 85
 - in India 87
 - in Japan 84
 - in Kuwait 86
 - in Nigeria 88
 - in Singapore 85
 - in Sri Lanka 85
 - in Sudan 89
 - in Switzerland 86
 - in Trinidad 83
 - in Tunisia 89
 - in Turkey 90
 - in USA 70
- climatological categories 149
- clouds 39, 43, 45
 - transmittance 44
- coated fabrics 453
- coating 429
 - degradation depth 228
- coatings 142, 178, 199, 223, 228, 235, 237, 256, 431, 437, 441
 - acrylic 241
 - automotive 235, 443
 - binder durability 441
 - chlorinated rubber 244
 - clearcoat 443
 - degradants 437
 - ESR 440
 - function 437
 - gloss 440, 443
 - internal stress 443
 - IR 438, 443
 - measurement methods 437
 - moisture effect 440
 - pollutants effect 443
 - protective 241

- spectral absorption 443
 - top coat 441
 - UV absorbers in 241
 - coil coating 157
 - collisions 506
 - color
 - change 170, 218, 223, 225
 - difference 171, 223, 224
 - fading 203
 - fastness 203
 - compatibilizer 222
 - composites 222, 226, 246, 256, 456, 458, 462
 - mass loss 246
 - compost 523
 - compounded products 437
 - concentrated natural daylight 157
 - condensation 181
 - conditions of weathering 160
 - configuration 411, 412
 - configurational changes 26
 - conformation 185, 412, 419, 420
 - conformational
 - energy 188
 - flexibility 526
 - conjugation number 226, 227
 - contact angle 247
 - cooling 243
 - rate 131
 - copolymer, graft 222
 - copper complex 212
 - corona 41
 - correlation 165, 175, 177, 224, 225, 228
 - corrosion 244
 - cotton 210, 211, 225, 228
 - cover plates 225
 - cracks 207, 243
 - formation 182, 222
 - growth 184
 - initiation 222
 - orientation 222
 - pre-existing 222
 - primary 222
 - "speed effect" 188, 253
 - tip 222
 - cracking 222, 470, 472, 476, 477, 483
 - creep 251, 257, 419
 - crosslink density 252
 - crosslinking 191, 252, 258, 260
 - cryogenical grinding 261
 - crystalline structure 183, 221
 - crystallinity 181, 200, 417, 480
 - change 242, 250
 - crystallite
 - monolayered 414
 - size 411, 418
 - crystallization 181
 - in amorphous phase 243
 - cyclic movement 470
- ## D
- damage 222
 - dark cycle 211
 - dashboard cracking 159
 - daylight
 - illumination 122
 - mean intensity 3
 - de Broglie Law 6
 - defect removal 513
 - defects 222
 - deformation, angular 184, 185
 - degradation
 - accelerators 275
 - depth 170, 220, 240
 - hydrothermal 257
 - initiators 275
 - layer thickness 220
 - principle 10
 - thermal history effect on 275
 - under stress 235, 238
 - degraded layer thickness 220
 - dehydrochlorination 262, 433
 - delayed fluorescence 12, 21
 - denitrification 51, 52
 - densification 182
 - density 181, 193, 246
 - change 246
 - optical 208

depth profiling 232, 234, 360
depth profile 260
detector
 photoelectron 122
 photoionization 122
 sensitivity 122
Diels-Adler reaction 30, 34
diffusion 181, 191, 246
 coefficient 192, 248
 constant 262
 gas 248
 path 37
 rate 192
dilatometer 249
dimeric excited species 12
dipole
 formation 4
 moment 184
dipole-dipole transfer 19
dissipation factor 249
DMS 250
double bond formation 238, 250
dry/wet cycles 157
DSC 134, 190, 250, 415
DTA 250
DTG 250
dyes 223, 451
 affinity 211
 aggregation 208
 alizarin 206, 208, 209
 anthraquinone 205
 azo 203, 207, 208
 bonding 208
 cation 206
 classification 211
 color 209, 212
 disperse 203, 208
 distribution 208
 durability 203
 excited 207
 fading 227
 fastness 212
 lightfastness 208
 loss 208

 monodisperse 208
 photodegradant 213
 photofading 207
 poly 212
 premetallized 210, 451
 protective 212, 213
 quenching 211
 reactive 208, 210, 211
 retention 207
 shade 207
 trimethylmethane 206
 vat 212

E

Earth's axis tilt 41
Earth's orbit 41
elastic properties 183
elasticity index 473
electron
 ejection 206
 transfer 207
electron energy 8
electronic state 25
elliptical orbit 41
elongation 135, 175, 228, 254, 430, 456, 479
 retention 254
emission
 intensity 239
 spontaneous 26
 spectra 6, 14, 415
emitting species 239
EMMAQUA 131
enamel 439
energy
 absorption 1
 conversion 1
 dissipation 1, 500
 distribution 143
 elastic 222
 excitation 2
 flow rate 213
 migration 18
 sources 3

- enthalpy of fusion 250
- environmental
 - conditions 39
 - stress cracking 251
- enzymatic reactions 524
 - kinetics 525
- enzymes 524
 - adaptation period 526
- EP 429
- EPDM 382, 383, 384
- EPM 341
- epoxidized soya bean oil 530
- epoxy group
 - formation 235
- epoxy resins 227, 228, 246, 250, 322, 439
 - amide growth 327
 - carbonyl growth 327
 - chain scission 323
 - effect of thermal history 326
 - functional groups 326
 - mechanism of degradation 322
 - products of corrosion 323
 - T_g 326, 327
 - water effect on 328
- EPR 382, 384, 386
- EPR/HDPE 386
- equipment
 - control parameters 105
 - suitability 175, 177
- erythema 487
- ESCA 241, 243, 244, 439
- ESR 26, 98, 191, 217, 218, 235, 236, 237, 276, 289, 295, 300, 343, 429, 432, 446, 474, 510
- EVA 390
- excimer 19
 - emission 12
 - fluorescence 12
- exciplex emission 12
- excitation
 - multiphoton 25
 - non-resonant 25
 - resonant 25
- excited molecule 26
- excited species, geometry of 31
- excited states 4, 26
 - deactivation 506
 - density 14
 - quenchers 240
- exciton 12
- expansion coefficient 130
- exposure
 - angle 144, 150
 - beginning 145
 - carbon arc 224
 - effect of latitude 65
 - EMMAQUA 257
 - in Alps 485
 - in Arizona 61, 62, 443, 478
 - in Australia 177, 468
 - in black box 439
 - in California 457
 - in Central Europe 175
 - in England 465
 - in Florida 61, 176, 210, 213, 252, 443, 478, 489, 516
 - in Hong Kong 455
 - in India 466
 - in Japan 141, 166, 243, 246, 253, 441, 475
 - in Jordan 479
 - in Middle East 465
 - in New Jersey 478
 - in Ohio 478
 - in Panama 395
 - in QUV 176, 177, 518
 - in Saudi Arabia 244, 472
 - in Slovakia 345
 - in South Africa 455
 - in space 459
 - in Thailand 479
 - in Weather-O-Meter 254, 356, 483, 484, 485, 518
 - in Xenotest 176, 208, 450, 511
 - mercury lamp 97, 220, 247, 251, 259, 262
 - month 213
 - outdoor 97, 141, 220, 224, 225, 226, 244, 251, 257
 - relative humidity 142
 - service providers 149

- site 149
 - special rack 443
 - standard 149
 - standards 152
 - sulfur dioxide 249
 - summer effect on 213
 - sun-tracking 152
 - temperature 142
 - tilt effect 62
 - winter 213
 - with spray 151
 - xenon lamp 97
- extinction coefficient 499
- extrusion reaction 27
- F**
- fabric 210, 212, 258
 - jute 225
 - fading 225
 - time 213
 - units 223
 - fatigue properties 257
 - ferrocenes 238
 - fibers 129, 214, 221, 235, 244, 431, 450, 511
 - aramide 309
 - carbon 252
 - chalking 218
 - degradation 222
 - dimensions 222
 - dull 207
 - dyed 228
 - filament cracking 416
 - glass 226
 - mechanical properties 418
 - necking 222
 - reinforcing 222
 - tester 257
 - fiberglass 458
 - filament shrinkage 418
 - filaments 416, 417
 - fillers 235, 242, 443
 - film 207, 208, 211, 213, 244, 479
 - filters 103
 - transmittance 122
 - fire resistance 250
 - flexural
 - modulus 458
 - strength 255, 256
 - Florida 65
 - fluorescence 17, 239, 506
 - decay 415
 - emission 240
 - foam 433
 - Foerster transfer process 506
 - folds 413
 - surface 413
 - forbidden transition 9
 - Franck-Condon Principle 9, 22, 32
 - free monomer 19
 - free volume 181, 192
 - fringed-micelle model 411, 413
 - fungi 523
 - brown-rot 526
 - soft-rot 526
 - white-rot 526
 - fungicides 531
- G**
- gas solubility 414
 - GC 241, 260
 - GC-IR 260
 - GC-MS 246, 260
 - gel
 - content 262
 - fraction 261
 - insoluble 261
 - geomembranes 455
 - geosynthetics 454
 - geotextiles 454, 455
 - German Standards 162
 - glazing 221, 225
 - global radiation 65
 - gloss 237, 431, 441, 442
 - illumination angle 219
 - measurement accuracy 219
 - retention 219

standards 219
glycols 344
goniometer 247
GPC 217, 258
grating 122
greenhouse film 479, 488, 520
Grotthus-Draper Principle 1

H

HALS 235, 239, 261, 507, 509
 basicity 508
 free electron exchange 510
 mechanism of action 508
 molecular mobility 519
 peroxide decomposition 510
 stable radicals 510
HAN 237

hardness 257, 470

 Barcol 257
 Rockwell 257
 Shore 257
 Vicker 135, 257

hardwoods 481

HCl 261

HDPE 135, 228, 489

heat capacity 46

heat of combustion 184, 185

Heisenberg Principle 7

helmets 222

hemicelluloses 480

HIPS 235

holders 104

horizontal mixing 48

HPLC 260, 479, 516

humidity 65, 199

 control 106
 effect 170, 222

humus 526

hydrazo-compound 204

hydrogen

 abstraction 28, 206, 238
 bonding 411
 tertiary 239

hydrolytic stability 246
hydroperoxides 206, 228, 238

 concentration 235
 deactivators 507
 decomposition 512
 dissociation 228
 formation 214, 227
 titration 261

hydrophilic 247

hydrophobic 247

hydroquinone 212

hydroxyl radicals 54

hypsochromic shift 15

I

ideal elastomer concept 253

image

 acquisition 223
 analysis 222, 447
 capture 222

impact 222

 strength 512

impedance 249

impurities 16, 228

 luminescent 211

increased irradiance 178

initiator 431

injection molding 222, 242, 260

interface 221

intermolecular

 collision 14
 process 28
 rearrangement 33

internal

 conversion 22, 26
 hydrogen transfer 502
 marker 258
 reflection 5
 stress 159, 443
 transmission 143

intersystem crossing 10, 15, 21, 211

intramolecular

 abstraction 28

- collision 14
 - intrinsic viscosity 473
 - ionization 4
 - ionosphere 48
 - IR 217, 228, 235, 244, 246, 250, 262, 358, 480, 481
 - ATR 228
 - derivatization 100, 234
 - detector 258
 - micro 228
 - micro-ATR 234
 - photoacoustical 228
 - reference band 233
 - specimen preparation 234
 - time-lapse 228
 - iron oxide 236
 - ISO Standards 156
 - isomerization 27
 - isomers
 - structural 30
 - valence-bond 30
 - isorefractive system 499
- J**
- Jablonski diagram 10, 22
 - jute 448
- K**
- keratitis solaris 485
 - ketone 28
 - concentration 235
 - end-groups 235
 - Kevlar 222, 450, 458
- L**
- lamellae 413
 - lamellar
 - thickness 413
 - width 413
 - lamp
 - cooling 101
 - energy 105
 - fluorescent 101
 - HPUV 101
 - metal halide 101
 - stability 102
 - landfill 523
 - lap shear 258
 - laser
 - ablation 220, 241
 - beam width 3
 - degradation 240
 - electric field 4
 - energy 3
 - etching 3
 - irradiance 3
 - monochromacity 3
 - latitudinal variations 121
 - LC 241, 260
 - LDPE 200, 222, 228, 254, 479, 520
 - LDPE/ABS 387
 - LDPE/EVA 390
 - leaching 213
 - Lewis-Calvin plot 226
 - lifetimes of excited species 13
 - light
 - concentrating devices 152
 - dosimeter 226
 - penetration
 - particle size effect on 504
 - pigment loading effect on 503
 - sources 95, 100
 - lightning 39, 51
 - lignins 241, 480
 - degradation 221
 - linear thermal expansion coefficient 249
 - LLDPE/LDPE 388
 - load 181, 183, 196, 287, 449
 - effect 458
 - luminescence 275
- M**
- magnetic moment 26
 - Mark-Houwink constant 258
 - mass

- change 245
 - loss 218, 426, 445, 462
 - transfer 191
- materials
 - selection 476
 - semicrystalline 222
- Maxwell Theory 1
- medical applications 443, 485
- melamine 236, 244
- membranes 472
 - osmometry 258
- memory 415
- mesomorphic structure 242
- mesosphere 48, 49, 52
- metal complexes 508
- metals 228
- Michaelis-Menten constant 524
- Mie scattering 5, 42
- Mie's Theory 498
- moisture
 - effect 147, 457
 - uptake 147
- molar mass 250
- molecular
 - collision 26
 - energy 8
 - fragments migration 182
 - mobility 14, 181, 188
 - size effect on extinction 499
 - weight 132, 145, 181, 234, 241, 252, 253, 258, 259, 260
 - depth profiling 260
- monochromator 123
- monoclinic form 418
- Monte Carlo simulation 14
- morphology 207, 411
- motion picture film 479
- movement 184
- MS 241, 260
 - time-of-flight 241
- multistress aging 479
- museum textiles 452

N

- n-hexane 238
- NASA studies 459
- nitrogen oxides 51
- nitrous oxide 50, 244
- nitroxide decay assay 237
- NMR 189, 209, 217, 234, 235, 246, 250
 - magic angle 235
 - peak resonance 235
 - pulsed 235
 - solid state 235
- Nomex 450
- nonvalence interactions 184
- Norrish I 26, 27, 187
- Norrish II 26, 28, 187
- Norrish I & II 418
- nuclear distance 26

O

- obliquity 41
- orbitals 8
 - antibonding 10
 - bonding 9
 - symmetry 9, 30
 - variations 41
- organotins 512
- orientation 4, 181, 194, 222, 242, 257
 - distribution 242
- oscillation energy 8
- oxidation
 - degree 244
 - extent 251
 - plasma 244
- oxygen
 - absorption range 52
 - analysis 243
 - atomic 245, 462
 - diffusion 192, 207, 240
 - diffusion coefficient 132
 - elemental 50, 52
 - elemental - absorption range 52
 - molecular 21, 36, 52, 244

- photodissociation 52
 - singlet 36, 52, 204, 211, 225, 277
 - singlet lifetime 36
 - spin change 36
 - triplet 36
 - uptake 262, 532
 - ozone 48, 50, 52, 206, 209, 394, 470, 486, 487
 - absorption range 52
 - concentration 51, 52
 - depletion 53
 - diffusion 414
 - ground level 53
 - holes 52
 - layer 47
 - resistance 208
 - seasonal concentration 53
 - WHO guidelines 53
- P**
- PA 33, 193, 196, 208, 213, 214, 222, 225, 228, 236, 239, 305, 507
 - acid rain effect on 310
 - carbonyl groups 310
 - chain scission 306
 - changes and properties 310
 - conjugated structures 310
 - crosslinking 307
 - crystalline structure 307
 - data 312
 - diffusion coefficient 311
 - effect of thermal history 310
 - emission spectra 306
 - fibers 452
 - gas diffusion 310
 - hydroperoxides 307, 310
 - mechanical properties 310, 311
 - mechanism of degradation 305
 - models 305
 - molecular weight 311
 - oxidation 307
 - photo-Fries rearrangement 309
 - radicals 306
 - tensile strength 311
 - thermal degradation 310
 - yellowing 308
 - PA-6 98, 212, 213, 417
 - cracking 416
 - PA-66 210, 211, 212, 252
 - packing density 412
 - paints 130, 218, 219, 223, 242, 247, 249, 256, 444, 445
 - adhesion 218, 484
 - chalking 218
 - chlorinated rubber 447
 - corrosion effect 245
 - cracking 218, 446
 - degradants 445
 - deposition of chemicals 477
 - erosion 218
 - ESR 446
 - flaking 218
 - gloss 219
 - image analysis 447
 - mass loss 245
 - mechanism of degradation 444
 - pigments 444
 - pitting 218
 - testing 446
 - titanium dioxide 444
 - UV absorbers 446
 - white rusting 218
 - PAN 299
 - conjugated double bonds 299
 - hydroperoxides 300
 - mechanism of degradation 299
 - radicals 299
 - volatiles 299
 - paper 485, 489
 - particles 58
 - Pauli Exclusion Principle 10, 26
 - PB 235, 471
 - PBT 357, 362
 - PC 96, 97, 146, 226, 227, 228, 241, 244, 253, 257, 351, 430, 477, 518
 - absorbance 355
 - bisphenol A 351
 - chain scission 355

- effect of thermal history 354
- elongation 356
- hydrolysis 351
- mechanism of degradation 351
- models 351
- molecular weight 355
- photo-Fries rearrangement 351, 354
- yellowness index 356
- PC/PMMA 386
- PCTFE 257
- PDMS 188, 235, 241
- PE 132, 135, 175, 188, 194, 221, 222, 227, 228, 235, 238, 240, 244, 246, 249, 257, 258, 261, 262, 328, 432, 471, 479
 - biodegradation 528
 - carbonyl formation 335, 419
 - chain scission 331
 - color difference 173
 - crosslinking 331
 - crystallinity 328, 333, 419
 - degradation depth 169
 - degree of branching 330
 - density 328, 334
 - effect of thermal history 333
 - functional groups 335
 - gas solubility 414
 - mechanism of degradation 329
 - models 329
 - molecular oxygen complexes 330
 - Norrish I and II 329, 332
 - optical density 336
 - oxidation 335, 419
 - oxygen diffusion 334
 - ozone 414
 - products of photolysis 333
 - tensile strength 336
 - titanium dioxide 419
 - unsaturations 331
- peak response shift 123
- PEG, biodegradation 527
- penetrometer 257
- PEO 250
- perfect black body 1
- perihelion 41
- periodic structures 221
- permeability 181
- peroxidase 528
- peroxide decomposition 212
- Perrin's Equation 506
- Perrin's Model 20
- PEST 128, 210, 225, 226, 235, 357, 454
 - biodegradation 527
 - chain scission 357
 - degradation depth 360
 - effect of thermal history 360
 - enzymatic degradation 360
 - hydroperoxides 359
 - mechanism of degradation 357
 - Norrish I and II 358
 - optical density 362
 - structure 129
 - volatiles 358
 - weight change 362
- PET 200, 207, 208, 227, 243, 262, 357, 363, 420, 480
 - biodegradation 527
- phenoxy resins 363
- phosphites 236, 512, 513
- phosphorescence 17, 21, 211, 239
- photo-Fries rearrangement 32, 96, 415
- photoaddition 30
- photochemical reaction probability 3
- photochemical rearrangement 30
- photochemistry 25
- photodimerization 34
- photographic paper 218
- photographic standards 218
- photoinitiators 240, 262
- photoionization 44
- photoisomerism 30
- photolysis products of 275
- photomultiplier 123
- photon energy 95
- photooxidation products of 275
- photophysics 1
- photoreactions 35
 - primary 26
 - secondary 35

- photoreduction 240
- photosensitizer 29
- photosphere 41
- phototendering 203, 209
- PI 374
 - ablation 375
 - models 374
 - volatiles 375
 - weight loss 376
- pigments 228, 235, 242, 245, 426, 429, 430
 - artists 223
 - flocculation 428
 - light shielding 504
 - load 428
 - photocatalytic activity 445
 - screening 502
- pipes 222, 471
- Planck's constant 1
- Planck's Law 1, 6, 39
- plastic deformation 183
- plasticizers 433, 530
- PMMA 97, 188, 191, 194, 220, 221, 227, 238, 240, 241, 245, 246, 251, 252, 257, 259, 303, 431, 466, 468, 488, 518
 - biodegradation 530
 - degradation depth 168
 - molecular weight 304
- pollutants 43, 196, 248, 455, 458
 - ammonia 50, 52
 - carbon dioxide 55
 - carbon monoxide 55
 - chlorinated fluorocarbons 57
 - fuel combustion 51
 - hydrogen chloride 58
 - hydrogen species 53
 - methane 55
 - nitric oxide 51
 - nitrogen oxide 51
 - nitrous oxide 50
 - oxides of nitrogen 50
 - particulate 39
 - particulate materials 58
 - sulfur dioxide 56
- polyacetylene 244
- polyacrylic acid 529
- polyacrylophenone 235, 241
- polyalkylsilane 226, 227
- polybutadiene 394
- polybutene 472
- polydispersity 132
- polyene formation 226
- polyethers, biodegradation 527
- polyisoprene 235, 393
- polymer
 - absorptivity 502
 - amorphous 208
 - lifetime 145
 - morphology 208, 213
 - packing 207
- polymerization 181
- polyol 432, 433
- polyolefins 128, 193, 511
- polyorganosilanes 227
- polysulfide 469
- POM 221, 228, 235, 257, 343
 - cage reaction 344
 - carbonyl groups 344
 - color difference 172
 - crystallinity 242
 - degradation depth 169
 - effect of thermal history 345
 - elongation 346
 - hydroperoxides 344
 - impurities 343
 - mechanism of degradation 343
 - radicals 343
 - tensile strength 345
 - volatiles 343
 - weight loss 345
- "pop-in" 183, 253
- positive holes 425
- PP 183, 192, 194, 220, 228, 236, 239, 242, 249, 260, 261, 338, 431, 454, 455, 511, 520
 - atactic 240
 - carbonyl groups 342
 - crystalline structure 239
 - crystallinity 419
 - effect of thermal history 340

- EPM 338
- fiber 511
- functional groups 341
- hydroperoxides 338, 341
- ketones 341
- mechanical properties 339
- mechanism of degradation 338
- models 338
- nonwoven fabric 448
- orientation 422
- texture 420
- X-ray 421
- PP/PE 390
- PPE 244, 346
 - chain scission 347
 - crosslinking 347
 - effect of thermal degradation 349
 - electron transfer mechanism 348
 - mechanism of degradation 346
 - models 346
 - molecular weight 349
 - oxygen uptake 349
- PPS 366, 369
- primer 481, 482
- printing inks 489
- properties, mechanical 222
- proton migration 27
- PS 19, 132, 133, 200, 221, 227, 228, 234, 235, 236, 238, 239, 241, 244, 247, 250, 253, 255, 257, 258, 259, 288, 490, 499, 507, 518
 - anthracene 295
 - benzene formation 288
 - biodegradation 530
 - carbonyl groups 294, 295, 297
 - chain scission 290, 294
 - changes and properties 294
 - color difference 171
 - crosslinking 290, 294
 - degradation depth 167
 - effect of wavelength 288
 - elongation 294
 - gel fraction 296
 - hydroperoxides 290, 295
 - impact modifiers 295
 - impurities 291
 - initiation 291
 - mechanism of degradation 288
 - models 288
 - molecular weight 296, 297
 - Norrish I and II 293
 - Norrish II 288
 - oxidation 297
 - radical decay 294
 - radicals 289
 - reprocessing 294
 - temperature effect 294, 295
 - tensile strength 298
 - tetroxide 292
 - volatiles 292
 - yellowing 292, 295, 297
- PS/PMMA 385, 386
- PS/PPE 387
- PS/PVME 387
- PSF 227, 235, 239, 244, 366, 369, 370
- PTFE 239, 245, 377
 - atomic oxygen 377
 - mechanism of degradation 377
- PTMG, biodegradation 528
- PU 27, 33, 99, 199, 222, 225, 226, 227, 228, 235, 239, 244, 246, 247, 250, 261, 312, 416, 433, 440, 442, 506, 520
 - absorption 317
 - aliphatic 99
 - automotive clearcoats 252
 - biodegradation 318, 528, 532
 - chain flexibility 320, 321
 - change of mechanical properties 315
 - changes and properties 319
 - color change 316
 - crystalline structure 319
 - crystallinity 318
 - data 319
 - discoloration 314
 - effect of thermal history 318
 - flexibility 319
 - fluorescence 317, 415, 416
 - gel formation 321
 - hard block 319

- hydrolysis rate 320
 - hydrolytic stability 320
 - mechanism of degradation 313
 - metals 319, 321
 - models 313
 - Norrish I 316
 - photo-Fries rearrangement 313, 319
 - photooxidation 313
 - polyol 318, 319
 - polyols 322
 - radicals 319
 - soft block 416
 - spectral sensitivity 322
 - volatiles 318
 - PU-acrylate 246
 - PVAI 194, 226, 236, 284
 - biodegradation 285, 528
 - carbonyl 285
 - changes and properties 286
 - data 286
 - effect of thermal history 286
 - initiators 286
 - load 287
 - mechanism of degradation 284
 - oxidation 287
 - photobleaching 285, 286
 - polyenes 285, 286
 - radicals 284
 - UV absorption 287
 - PVC 99, 132, 148, 221, 226, 236, 246, 257, 261, 275, 420, 429, 430, 433, 453, 467, 472, 478, 513
 - benzene formation 279
 - biodegradation 530, 532
 - branching 276
 - carbonyl group 282, 283
 - changes and properties 281
 - chlorine radical 278
 - color difference 171
 - conformation 280
 - crosslinking 279
 - crystalline structure 280
 - cyclohexadiene formation 280
 - data 284
 - degradation depth 167
 - dehydrochlorination 146, 177, 279
 - effect of solvent 283
 - effect of temperature 281, 282
 - effect of thermal history 283
 - elongation 174
 - head-to-head structures 276
 - hydrogen abstraction 278
 - hydroperoxide 282
 - hydroxyl radical 278
 - initiation 280
 - models 276
 - molecular weight 283
 - oxygen effect 280
 - polyene migration 279
 - polyene sequences 279
 - polyenes 282
 - radical concentration 281
 - radicals 276
 - sample thickness 282
 - solvent effect 276
 - stabilizers 512
 - thermal degradation 282
 - unsaturations 277
 - PVC/SAN 387
 - PVDF 245
 - PVME/PS 387
 - pyranometer 121
- ## Q
- quantum yield 18, 20, 96
 - quenchers 13, 497, 507
 - singlet oxygen 225
 - quenching 227
 - quinone 212
 - QUV 157, 237
- ## R
- racks 104
 - for dry exposure 151
 - standard 150
 - temperature distribution 148

- under glass 150
- with black box 150
- radiation
 - absorbed 144
 - absorption 6
 - angle of incidence 5
 - at 340 nm 63
 - consumption 238
 - cosmic 459
 - daily global 145, 146
 - decay 236
 - electromagnetic 1
 - energy 4, 141
 - flux 39, 42
 - daily variation 45
 - density 122
 - geographic variation 45
 - latitudinal variations 45
 - seasonal 45
 - seasonal variation 45
 - frequency 1
 - global solar 64, 121, 122
 - intensity 3, 102
 - lifetime 26
 - measurement 121
 - net 122
 - reflected 122
 - reflection 4
 - scattering 4, 42
 - seasonal distribution 144, 145
 - seasonal variations 41
 - sky 122
 - terrestrial 44
 - wavelength 40, 213, 221
 - wavelength shift 44
- radicals 26
 - concentration 238
 - formation 235
 - rate 181, 237
 - hydroperoxyl 54
 - hydroxyl 53, 54
 - concentration 54
 - in EPD 238
 - in PS 238
 - in wood 238
 - lifetime 236
 - mobility 239
 - nitroxide 237
 - paramagnetic property 26
 - peroxide 238
 - peroxy 238
 - phenoxy 237
 - polystyryl 236
 - recombination 15, 27, 242
 - secondary recombination 29
 - short-lived 238
 - stability 26
 - stable 237
 - tropospheric 50
 - type 236
- radiometer 121
 - detector 124
 - Eppley 123
 - narrow band 122, 124
 - spectral response 122
 - spectral sensitivity 123
 - wide band 123
- rain control 106
- random walk 14
- ranking 166, 170
- Rayleigh's Law 42
- Rayleigh's scattering 5
- reflectance spectra 209
- refractive index 5, 143, 258
- reinforcement 222
- residence time 48
- residual
 - absorption 505
 - monomer 238
 - stress 443
- rheology 251
- RIM 256, 489
- roofing 249, 472, 473, 474
- rotational state 8
- rubber 391
 - mechanism of degradation 391
 - natural 396

Rydberg's Law 40
Rydberg's state 30

S

sample

choice 125
color 131
composition 126
contamination removal 137
dust elimination 137
effect of heat on 128
evaluation 125
morphology of 129
preparation 125, 126
solvent effect on 127
state 127
storage 137
substrates for 129
surface contamination 130, 137, 460
surface erosion 137
thickness 131, 240

SAN 379, 490

SAXS 242, 243

SBS 251, 473

Schrödinger's Equation 8

sealants 218, 253, 256, 468

adhesion 219

polysulfide 257

pores 221

silicone 221

sealed vials 261

seasonal variations 121, 213

selection rules 9

SEM 221, 451, 482

sensitizer 13

sensitizer-quencher collision 14

shear strength 256, 458

sheets 226

shopping bags 479

SI 371, 383

bond strength 371

mechanism of degradation 371

phenyl group effect 373

tensile strength 373

siding 478

silica gel 208, 209

silicon photodiode 123, 124

silicone 469

siloxane copolymers 245

SIMS 241, 244

time-of-flight 241

singlet oxygen 448

energy 13

singlet state 10

skin layer 242

skylights 221

Snell's Law 4

softwoods 480

soil 523

burial test 532

solar collectors 225, 475

solar radiative emission 39

solvent 238, 432

evaporation 181

radical formation 239

sorption 181, 193

sources, acceleration factor 103

space

conditions of exposure 459

cracking 243

environment 222, 245

space applications 459

composites 459, 461

metal laminates 461

paints 460

polymers 460

space program 137

space transfer 14

specimen

thickness 254

spectroradiometer 123

spectrum

carbon arc 109

enclosed carbon arc 110

fluorescent lamp 117

indoor actinic lamp 119

metal halide lamp 118

- window glass daylight 112
 - xenon arc 109
 - spherulites 243
 - spin multiplicity 9
 - spin overlap integral 9
 - spin-orbit coupling 9
 - spruce 483
 - stabilization 497
 - stabilizers 275
 - starch 527
 - Stefan-Boltzmann Law 40
 - steric exclusion chromatography 260
 - steric hindrance 28, 411
 - steric repulsion 188
 - Stern-Volmer Equation 506
 - stimulated emission 7
 - strain, critical 228
 - stratosphere 47, 48, 52
 - composition 48
 - stress 130, 181
 - direction 182
 - distribution 182, 184, 222
 - energy 184
 - excess energy 185
 - formation 181
 - in surface layers 182
 - internal 181, 182, 222
 - measurement 199
 - moisture effect 147
 - molecular 184, 187
 - relaxation 181, 257
 - residual 443
 - structural stress 181
 - styrene monomer 241
 - sulfur-containing compounds 56
 - sun
 - composition 40
 - emission distribution 41
 - formation 40
 - temperature 40
 - thermonuclear fusion 40
 - zenith angle 45
 - sun tracking 144
 - sunspots 41
 - surface
 - albedo 45
 - composition 247
 - contamination 241
 - crystallinity 242
 - depth profile 219
 - deterioration 166, 255
 - energy 247
 - erosion 222
 - etching 3
 - layer thickness 244
 - layers 228
 - modification 244
 - molecular reorientation 245
 - oxidation 244
 - permissivity 249
 - photoreduction 244
 - resistivity 249
 - roughness 219, 220, 221, 224, 228
 - temperature 46
 - swelling 214
- T**
- tacticity 188, 413
 - talc 220
 - tapes 188, 258, 479, 511
 - tautomeric forms 500
 - Taylor-Hobson Profilometer 220
 - tear strength 256
 - TEM 222, 450, 451
 - temperature 181, 188
 - altitude 44
 - black panel 65
 - color effect on 46, 47
 - control 106
 - distribution 148, 182
 - effect 178, 214, 222, 238, 259
 - effect of latitude 46
 - exposure angle 147
 - gradient 182
 - horizontal variations 41
 - seasonal variations 46

- tensile strength 142, 210, 213, 249, 252, 253, 260, 449
- textile materials 447
- dye-sensitization 447
 - IR 448, 450
 - nonwoven 448
 - photobleaching 448
 - temperature effect 448
 - UV absorbers 448
 - wool 448
 - yellowing 448
- textiles 203, 223, 309
- museum 223, 225
- texture 413
- T_g 182, 188, 192, 250, 457
- change 182
- TGRG 250
- thermal
- conductivity 46
 - diffusivity 46
 - expansion 181
 - expansion coefficient 188
- thermojunction 122
- thermopile 122
- thermosphere 48, 49
- thickness of degraded layer 502
- thickness of protective layer 248
- Tinuvin 327 446
- Tinuvin 770 516
- Tinuvin 900 237
- TiO_2 207, 425, 426, 429, 444
- testing method 446
- titration 235
- conductometric 261
 - potentiometric 261
- TMA 250, 417
- torsional stress 184
- total energy
- absorbed 499
 - emitted 40
- transition
- forbidden 26
 - moment 9
- triazine 449
- triplet 21
- energy 13, 506
 - formation 211
 - lifetime 240
 - sensitizer 227
 - state 10
- tristimulus values 224
- tropopause 48
- troposphere 43, 44, 48, 52
- ## U
- ultrasonic degradation 432
- universal calibration 258
- upholstery fabrics 450, 451
- UV
- absorbers 212, 225, 238, 241, 500
 - chemical structure 501
 - effect of concentration 502
 - effect of pigment 503
 - excitation 502
 - molar absorptivity 503
 - protective efficiency 505
 - retention 227
- absorption 226
- detector 258
- effect of ozone 47
- emission 41
- laser 221
- spectrophotometry 217, 226
- stabilizers 260
- UV radiation, temperature effect 2
- UV stabilizers 453
- loss 517
 - loss kinetics 517
 - retention 517
 - stability 514
 - UV spectra 514
 - vapor pressures 515
- ## V
- valence angles 184
- vertical mixing 48

vibrational energy 8, 28
vibrational energy level 25
vibrational mode 25
vibrational overlap 9
viscosity 211, 238
 intrinsic 250, 251, 252
 number 211
 relative 212
visible spectrophotometry 225
visual evaluation 218
volatile components 239, 261
volcanoes 39, 58
voltage breakdown 249

W

water
 diffusion coefficient 248
 effect 214
 evaporation 47
 latitudinal difference 47
 lifetime 47
 sorption 248
 uptake 246
 vapor concentration 48
 vapor transmission 248
wavelength
 absorption 45
 control 105
 cut-off 95
 effect on scattering 43
 shift 27
 summer 95
 temperature effect on 40
 winter 95
WAXS 242, 420, 421

Weather-O-Meter 4
weathering
 choice of parameters 160
 cycles 155
weight loss 451, 467
wet period 147
Wien's Law 40
wind 39, 147, 183
wood 130, 218, 238, 480
 chromic acid 221
 coatings 256
 erosion 256
 ferric chloride 221
 finishes 218
 middle lamellae 221
 pits 221
 pulp 243
Woodward-Hoffmann Rule 30
wool 210, 225, 256, 448, 449, 452

X

X-ray analysis 415
X-ray diffraction 411
xenon arc 100
XPS 142, 222, 243

Y

yellowness index 223, 224, 448, 449
Young modulus 257

Z

ZnO 429, 430